

DYNAMIQUE VEHICULE

Ce document compile des notes personnelles prises au cours du temps sur le sujet de la dynamique véhicules « générale ». Le sujet pneu n'y est pas traité, un document spécifique lui étant consacré.

E. Cabrol

Création 05/09/2016

Dernière MAJ 12/04/2022

Number of pages : 361

<u>1 LES MEILLEURES RESSOURCES</u>	<u>3</u>
<u>2 INTRODUCTION</u>	<u>4</u>
<u>3 CONVENTIONS / DEFINITIONS</u>	<u>10</u>
<u>4 LEXIQUE</u>	<u>13</u>
<u>5 DYNAMIQUE LONGITUDINALE</u>	<u>23</u>
<u>6 DYNAMIQUE VERTICALE - CONFORT</u>	<u>46</u>
<u>7 DYNAMIQUE EN VIRAGE</u>	<u>60</u>
<u>8 AERO</u>	<u>111</u>
<u>9 MANŒUVRES</u>	<u>118</u>
<u>10 SYNTHESE PRESTATION</u>	<u>139</u>
<u>11 OBJECTIVATION DES PRESTATIONS</u>	<u>159</u>
<u>12 MODELISATION DU VEHICULE</u>	<u>170</u>

<u>13</u>	<u>MODELES VEHICULE OPEN-SOURCE + MATLAB</u>	<u>195</u>
<u>14</u>	<u>MODELISATION DU CONDUCTEUR</u>	<u>197</u>
<u>15</u>	<u>MODELISATION DE LA ROUTE</u>	<u>202</u>
<u>16</u>	<u>DIRECTION</u>	<u>203</u>
<u>17</u>	<u>SUSPENSION</u>	<u>210</u>
<u>18</u>	<u>COMPORTEMENT A LA LIMITE ET/OU SUR FAIBLE ADHERENCE</u>	<u>227</u>
<u>19</u>	<u>SYSTEMES DE CONTROLE ELECTRONIQUE (ABS, ESP, ESC ...)</u>	<u>228</u>
<u>20</u>	<u>MESURE</u>	<u>254</u>
<u>21</u>	<u>ESTIMATION</u>	<u>256</u>
<u>22</u>	<u>CONTROLE (THEORIE)</u>	<u>262</u>
<u>23</u>	<u>CONTROLE OPTIMAL ET OPTIMISATION DE TRAJECTOIRE</u>	<u>283</u>
<u>24</u>	<u>LAP TIME SIMULATION</u>	<u>288</u>
<u>25</u>	<u>LOGICIELS COMMERCIAUX</u>	<u>293</u>
<u>26</u>	<u>DONNEES VEHICULE</u>	<u>323</u>
<u>27</u>	<u>RESSOURCES</u>	<u>326</u>
<u>28</u>	<u>PERSONNALITÉS</u>	<u>344</u>
<u>29</u>	<u>REFERENCES</u>	<u>348</u>
<u>30</u>	<u>MISC.</u>	<u>350</u>

1 LES MEILLEURES RESSOURCES

Andrea Quintarelli : <https://drracing.wordpress.com/>

Les articles d'OptimumG

<https://optimumg.com/technical-papers/>

<https://optimumg.com/news/>

Kelvin Tse : <https://kktse.github.io/>

Jonathan Vogel : <https://www.jovogel.com/>

Jahee Campbell

<https://www.waveydynamics.com/articles>

ainsi que la série publiée sur Racecar Engineering

<https://www.racecar-engineering.com/tech-explained/racecar-vehicle-dynamics-explained/>

Articles validés par des juges de Formula SAE : <https://www.designjudges.com/>

Thomas Fermi, Algorithms for Automated Driving

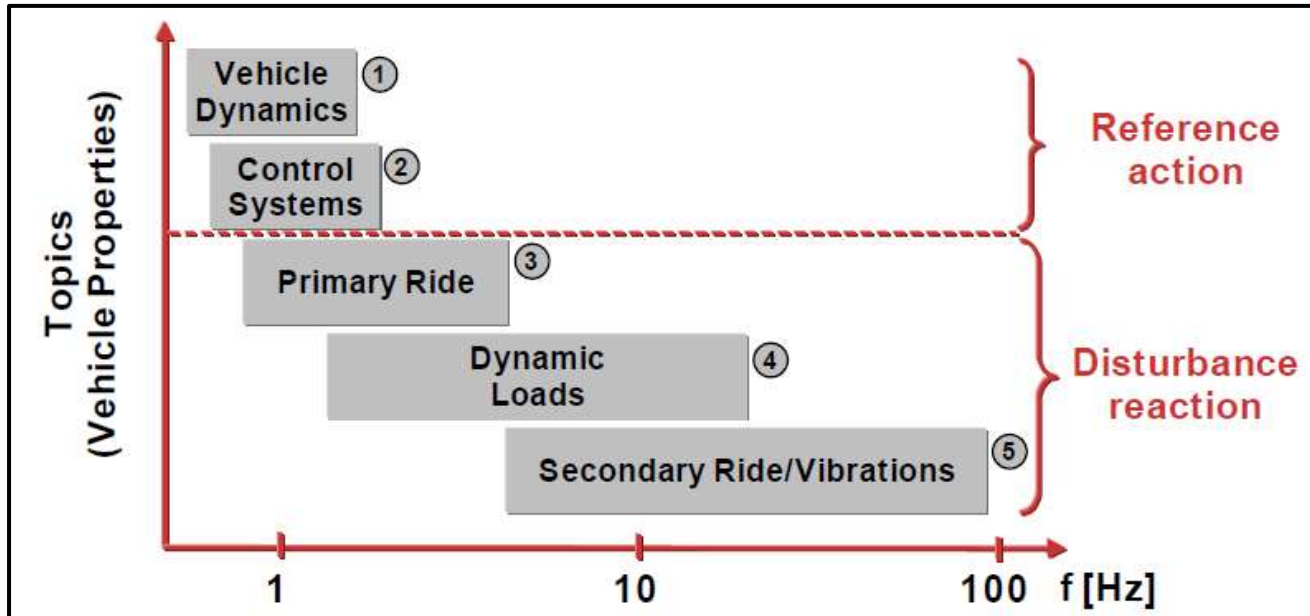
<https://thomasfermi.github.io/Algorithms-for-Automated-Driving/Introduction/intro.html>

Vehicle Dynamics Compendium (Chalmers)

<https://research.chalmers.se/en/publication/513850>

2 INTRODUCTION

2.1 CLASSIFICATION FREQUENTIELLE



[source](#)

Jusqu'à 2 Hz, c'est le domaine du **comportement**, là où on évalue la réponse du véhicule à des inputs du conducteur (2 Hz c'est à peu près la bande passante dudit conducteur, quand il est humain).

Au-delà, on étudie la réponse du véhicule à des perturbations (balourd de roue, rugosité de la route, etc ...). Entre 2 et 4 Hz, on parle de **primary ride**, où les ressorts déterminent les modes de caisse. Pour contrôler ces modes on spécifie des amortisseurs. Ce domaine correspond aux sollicitations « BF », haute amplitude / basse fréquence, en gros correspondant à des perturbations que l'on peut voir (ralentisseur ...).

La prestation **secondary ride** est liée à des sollicitations de moindre amplitude mais plus haute fréquence, comme des fripures de la route, joints de bitume, etc ... Les propriétés des pneus, et des articulations de suspension deviennent d'ordre 1.

Entre 8 et 15 Hz on trouve les modes de GMP, alors qu'entre 10 et 40 Hz on trouve les modes de masses non-suspendues, en vertical puis en longitudinal.

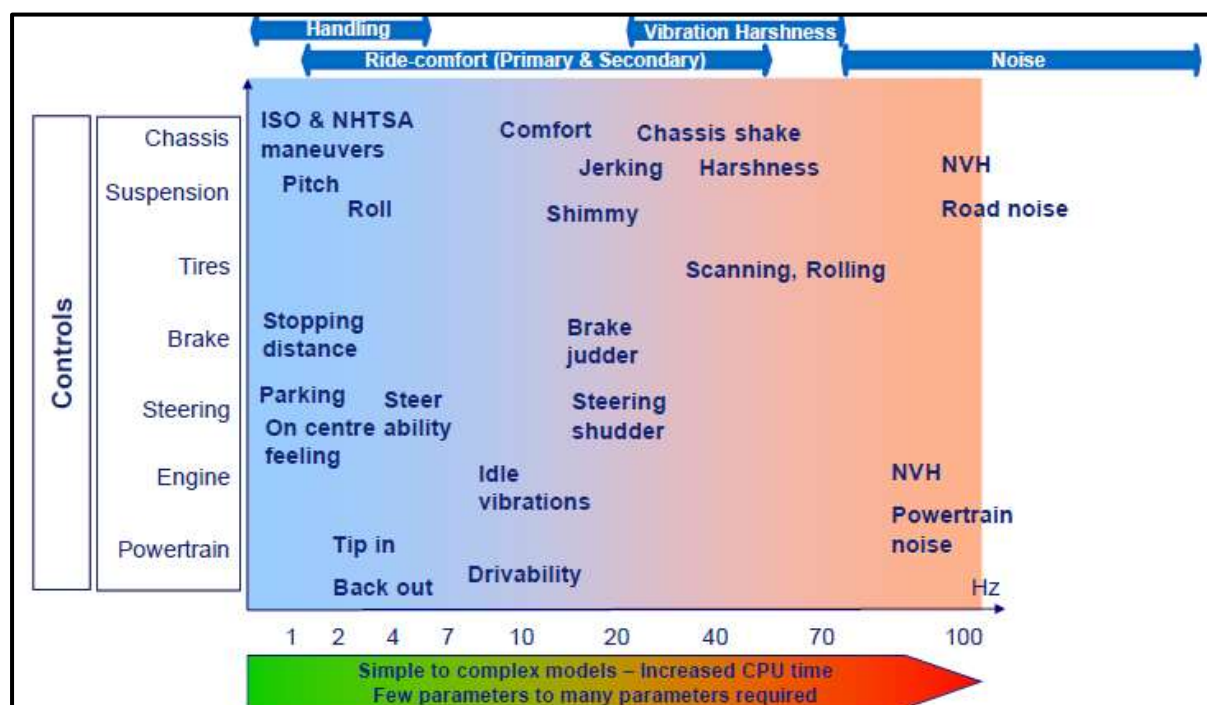
Les **efforts dynamiques** sont critiques pour l'estimation de la durée de vie des pièces de châssis. L'essentiel du contenu énergétique se situe sous 20 Hz.

▪ Handling	0 – 2 Hz
- Reaction of the vehicle to steering inputs (lateral dynamics), braking (longitudinal dynamics), ...	
- Constant radius cornering, step steer and release, ISO lane change, constant radius cornering, sweep input, brake in turn, rollover, ... all ISO & NHTSA manoeuvres!	
▪ Primary Ride	1 – 5 Hz
- The car body moves rigidly on the main springs (bounce, roll, ...)	
▪ Secondary Ride	5 – 15 Hz
- Suspension (wheel hop, axle tramp, fore-aft, ...) and powertrain (bounce, roll, ...) modes amplify excitations from road, wheel unbalance, engine idling, ...	
- Road shake, steering shimmy, impact harshness,	
▪ Drivability	5 – 15 Hz
- Suspension (hop, tramp, fore-aft, ...) and powertrain (bounce, roll, ...) and driveline (torsional) modes amplify excitations from throttle input	
- Tip-in/out, key-on/off, gear shift, idle regulation/engine control	
▪ Vibration Comfort	15 – 50 Hz
- Excitations from P/T are amplified by resonances of vehicle body or auxiliaries	
- Steering shake, floor vibrations, durability ...	
▪ Acoustic Comfort	20 – 10k Hz
- Airborne and structure borne excitation from road, P/T or auxiliaries	
- P/T boom, gear whine, rolling noise, wind noise, HVAC noise, ...	

Unrestricted © Siemens AG 2017

Page 6 2017 MM/DD

Siemens PLM Software



(doc [LMS](#))

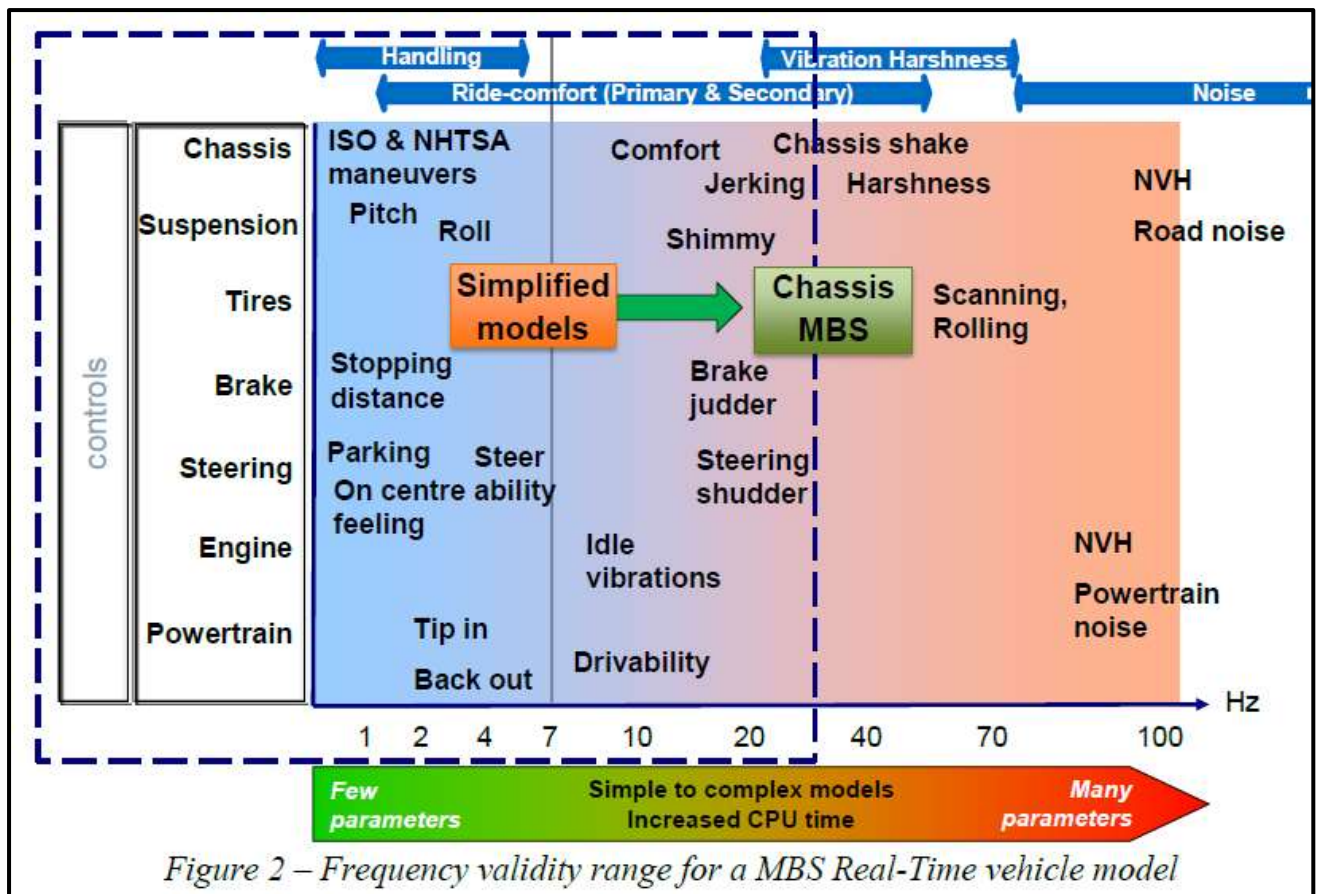
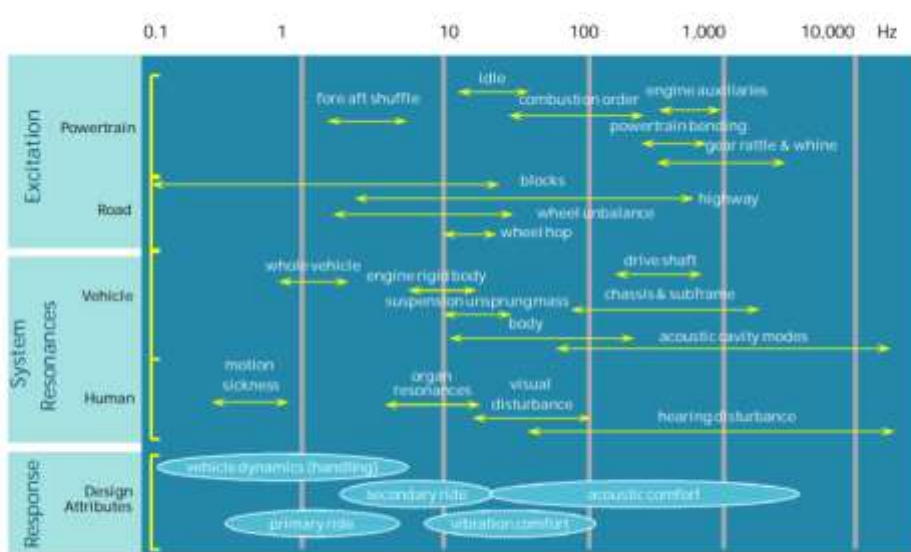


Figure 2 – Frequency validity range for a MBS Real-Time vehicle model

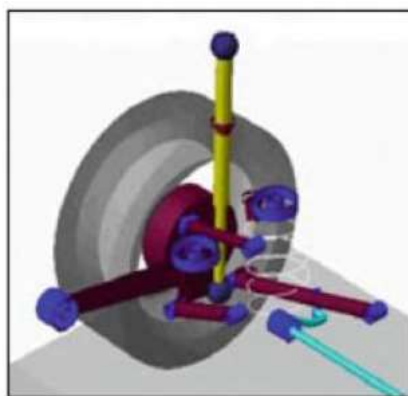
[Source](#)

Maneuvers Frequency Range

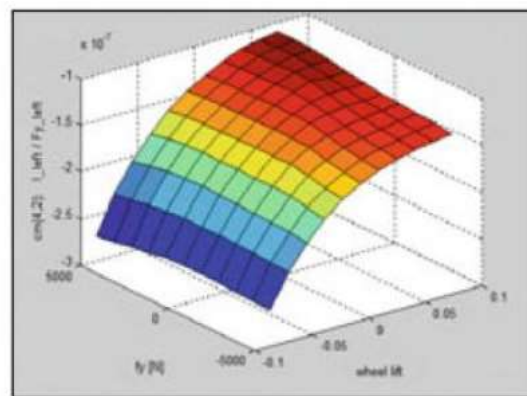
SIEMENS
Ingenuity for life



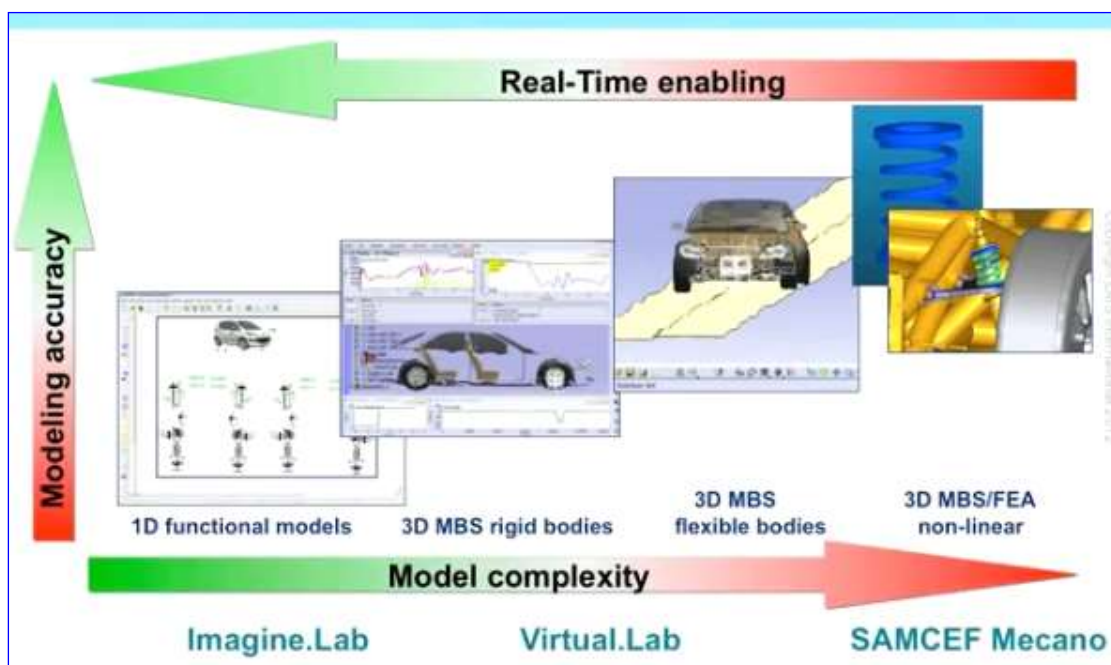
2.2 DU MULTICORPS VERS LES MODELES FONCTIONNELS



- multi-body representation
- very detailed and accurate
- suspension easily modifiable
- relatively slow in simulation



- characteristic curves
- less complex, still accurate
- limited modifiability
- fast in simulation



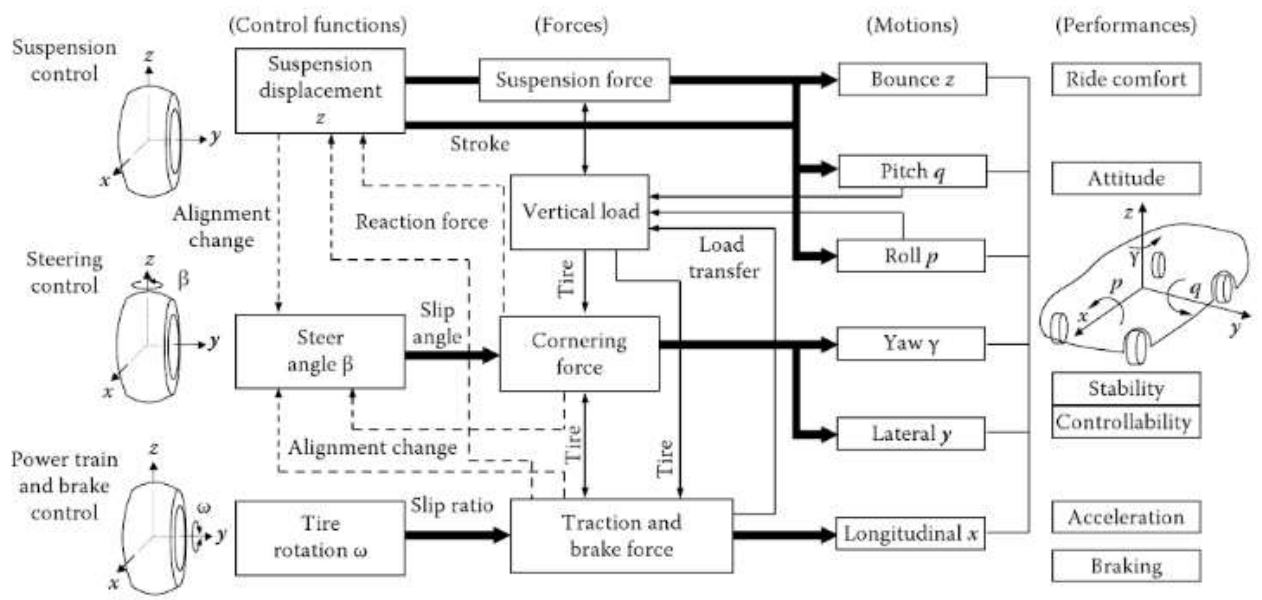


FIGURE 1.2 Conceptual diagram of vehicle dynamics and control. (From Kizu, R. et al., Electronic control of car chassis—Present status and future perspective, *IEEE International Congress on Transportation Electronics*, 88CH2533-8, 1988, pp. 173–188.)

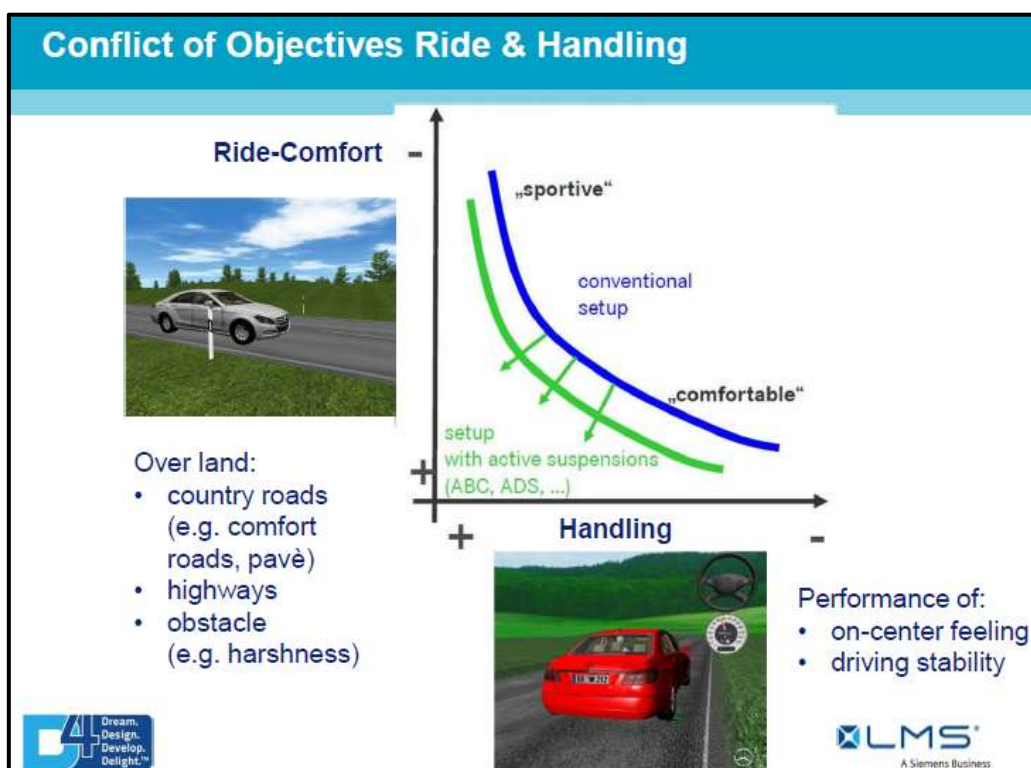
2.3 CRITERES DE JUGEMENT

En virage :

- équilibre en virage
- appui arrière
- placement en virage
- efforts de direction
- réactions de direction
- stabilité au freinage
- motricité

En ligne droite :

- tenue de cap
- effort de direction autour de la ligne droite
- réactions de direction (sur obstacles et mauvaises routes)
- collage de direction
- motricité
- sensibilité au vent latéral
- sensibilité au dévers de route



3 CONVENTIONS / DEFINITIONS

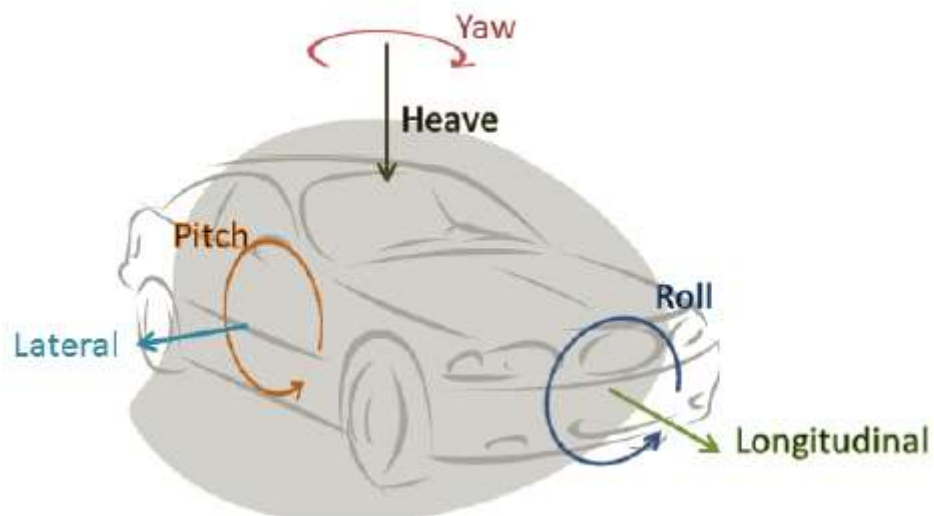
3.1 LES MOUVEMENTS (MODES) DE CAISSE

	Translation	Rotation
X	Avancement	Roulis
Y	Ripage	Tangage
Z	Pompage	Lacet

Pour les moments de tangage, on parle parfois de plongée, salut, cabrage ...

Pour les moments de pompage, on parle de (mouvement vers le) choc et rebond

Dans l'illustration ci-dessous la convention SAE est utilisée (cf § suivant)

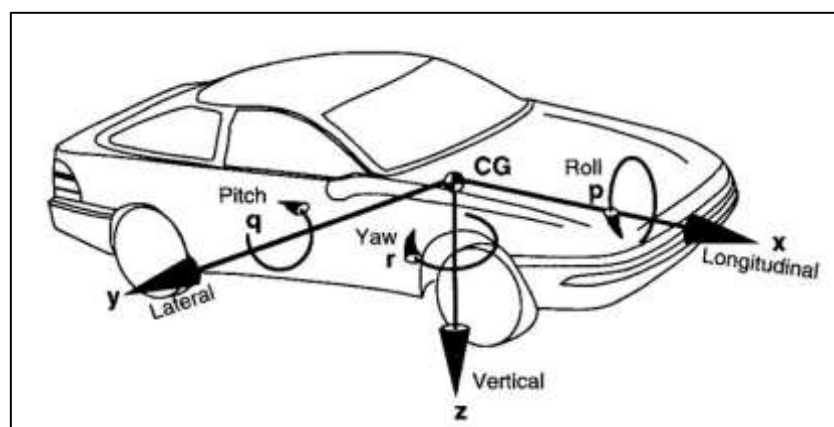
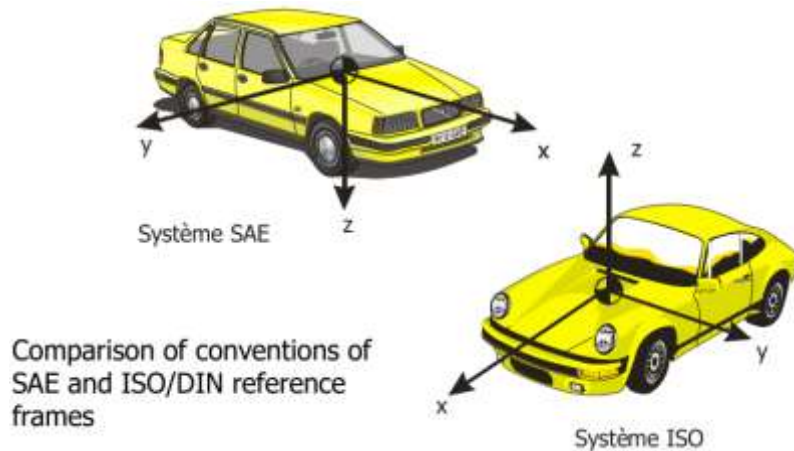


3.2 SYSTEMES DE COORDONNEES (SAE, ISO ...)

Ca peut valoir le coup de commencer par cette vidéo de M. Sayers (le "père" de CarSim)

[Vehicle Coordinate Systems](#) (2020)

Les repères SAE et ISO sont différents

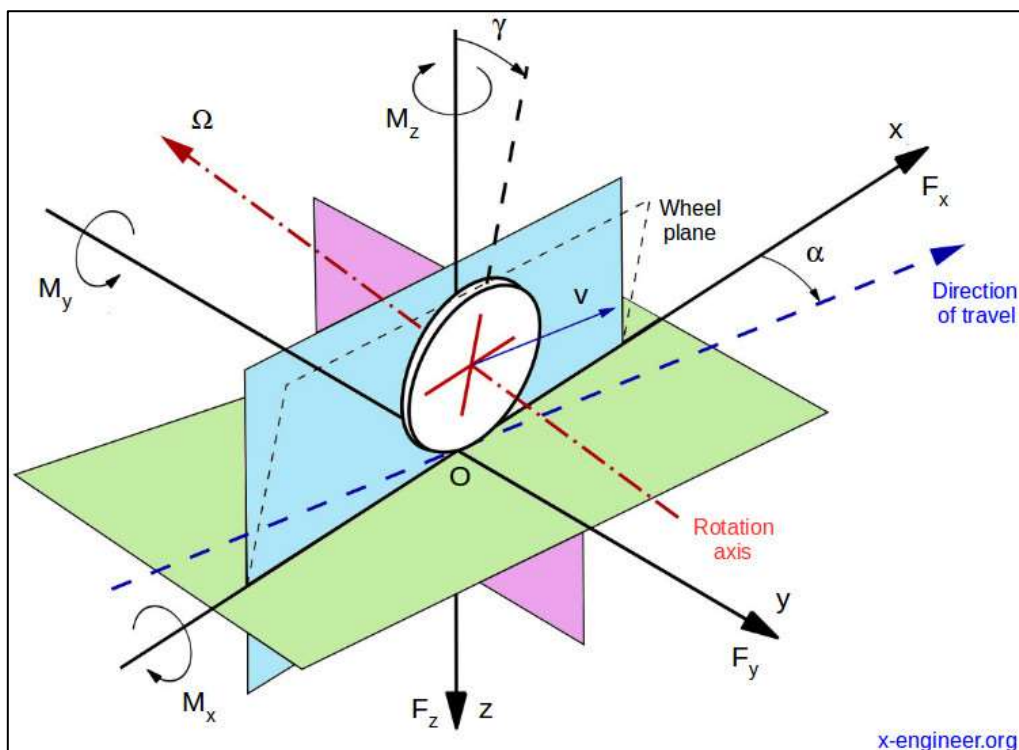


SAE J670e (1976)

NB : il y a eu une révision en 2008 (https://www.sae.org/standards/content/j670_200801/), mais il est peu probable que la convention ait changé 😊

Revision History	Related Info		
J670_200801	2008-01-24	Latest	Revised
J670_197607	1976-07-01	Historical	Revised
J670E_197607	1976-07-01	Historical	Revised

3.3 SAE



<https://x-engineer.org/automotive-engineering/chassis/vehicle-dynamics/tire-axis-system-and-terminology-defined-by-sae-standards/>

4 LEXIQUE

4.1 FRANÇAIS

Comportement: Appréciation de la facilité à faire suivre au véhicule la trajectoire voulue.

Confort: Etat de bien-être physique et psychique en réaction à un environnement ou à une situation.

Copage : Tendance du véhicule à copier les irrégularités droite & gauche de la route.

4.2 LEXIQUE COMPORTEMENT (DELPHI)

Turn-in response : Initial steering response as the car turns into a corner at different vehicle speeds.

- **Sharpness** : Over-sharp is for a car turning more and quicker than the driver would expect, sluggish is the opposite.
- **Yaw gain** : Amount of yaw built for a given SW input.
- **Phase** : Describes whether the car is responding in phase with the SW input, or with a delay.

Off-center response : Proportion of the lateral acceleration increase as a function of the steering torque increase, once in a curve.

- **Linearity** : Progressive yaw rate generated by a progressive increase of the SW input.
- **Understeer** : (Opp. Oversteer) : If the car tends to plow instead of turning more into the corner and follow the driver's request.

Handling balance : Sort of overall judgment of how a car behaves in a corner, whether its dominant behaviour is understeer, oversteer or neutral.

- **Consistency** : Balance pretty much kept the same with different payload, vehicle speed, and aggressiveness.

Yaw stability

Yaw stability, steady-state : Constant steering angle, constant radius curve.

Yaw stability, transient : High steering inputs, engine torque fluctuations and braking in a curve.

Yaw stability, lift off : The reaction of the vehicle when the gas pedal is released in mid corner when the vehicle is driven at a constant radius through a curve.

Braking-in-a-turn : As above, but also applying brakes after the gas pedal is released.

Acceleration-in-a-turn : The reaction of the vehicle when the gas pedal is pressed in a corner. Gear level, RPM, vehicle speed and amplitude of the SW input are important.

Crosswind stability : The response of the vehicle to lateral wind gusts and/or truck draughts. The driver should be able to maintain directional control of the vehicle with only minor steering correction.

For all these evaluation criteria of the yaw stability, the following key words can be used :

- **Understeer** : (Opp. Oversteer) : The vehicle runs wider in a curve than expected. For oversteer, quantify the risk of spinning out.
- **Steering correction** : Amount of correction of the SW angle required to maintain the desired path. Note if counter-steering is necessary.

- **Yaw gain** : Amount of yaw built for a given SW input.
- **Response time** : Delay between the yaw built and the steering input.
- **Yaw disturbance**

Progressiveness at limit of adhesion : Quantifies how the car reacts when the limit of adhesion is reached. The sharpness of the loss of adhesion, as well as which axle is loosing grip first, have to be evaluated.

- **Linear** : Evaluate the linearity, or smoothness, of the loss of adhesion.
- **Predictable, ease of control** : How easy it is to recover from the loss of lateral grip, and how easy it is to feel that the limit is reached, through the steering wheel.

Road grip : The amount of expected grip, wet and dry, the vehicle has. This is not just a subjective assessment of lateral acceleration, but is an indication of how the car performs on different surfaces.

Tracking : Ability of the vehicle to run straight without steering correction. Tracking has to be evaluated on smooth roads as well as uneven, bumpy roads, or roads with varying camber changes, surface repairs, longitudinal bumps,...

The driver will feel more or less confident at driving at high speeds on such roads.

- **Stability** : Stability of the vehicle in terms of body motion and yaw disturbance.
- **On-center correction** : Necessity for the driver to correct the SW on-center while driving straight ahead.

Safety feel : Feeling of confidence that the driver can have in all driving situations. This comes more from the ease of control and predictability, than from the overall level of grip or ultimate cornering capabilities.

4.3 LEXIQUE DIRECTION (DELPHI)

On-center feel : Force increase across on-center steering wheel position.

- **Valley feel** : Characterization of a sharp increase of SW torque at very small SW angle.
- **Dead band** : Amplitude of SW angle with no increase of torque, around the zero position.
- **Linearity** : Assessment of the linearity of the change of SW torque with SW angle, across the zero position.

Self centering / returnability : Ability of the steering wheel to return to zero position after a turn. This is assessed throughout the speed range.

- **Hysteresis** : Quantifies the error of SW angle remaining. 10 ° can be acceptable at parking speeds, but must be less at higher speeds.
- **Friction** : Friction will create damping in the system and will degrade the returnability.
- **Overshoot** : Quantifies how much the SW is crossing the on-center position when it oscillates back to steady zero position.

Damping (steering flick) : Ability of the car to recover its straight line stability when a flick steer input is applied. This is checked by applying a flick steer input, greater and greater and for higher and higher vehicle speeds.

- **Convergent** : (Opp. Divergent) Applies to a yaw disturbance diminishing with time. Divergence is for the oscillatory instability becoming greater and greater, up to a point where the driver must catch the SW and force it to settle down the oscillations.

- **Overshoot** : Quantifies how much the SW is crossing the on-center position when it oscillates back to steady zero position.

Wall effect : Increase of the SW torque with the SW velocity, in a hard dynamic manoeuvre, such as collision avoidance.

- **Torque gradient** : Quantifies the increase of SW torque, when the SW is turned quickly away from its on-center position.
- **Ease of control** : Describes whether the car becomes difficult to control because of the steering become too heavy.

Kick-back : Untoward shock transmitted through the steering wheel.

- **Wheel fight** : A rotary disturbance of the steering wheel produced by forces acting on the steerable wheels.

Torque gradient : Evolution of the SW torque with SW angle. This can be variable with vehicle speed, or can have several settings the driver can select through a switch on the dashboard.

- **Fluctuation** : Describes how the SW torque evolves with the increase of the angle. It can have a peak corresponding to a certain position of the SW.
- **Change with speed** : Quantifies how much the torque gradient is changing with vehicle speed, due to either the speed variable-assist, or to the change of compliance and self-aligning torque characteristics of the front suspension, with speed.

Torque steer : Yaw disturbance created by the steering reaction of the engine torque applied to the front wheels of a FWD vehicle.

- **Wander, yaw disturbance** : Vehicle hard to maintain on a straight path, if the throttle is pressed on a smooth straight road. Quantify the SW correction needed.

4.4 LEXIQUE NVH (DELPHI)

Harshness : Higher frequency vibrations of the structure or components of the vehicle that are perceived tactually and/or audibly (typically 25-100Hz).

- **Road contact feel** : Feeling to be in contact with the road through steering and tires.

Road noise : Establish the level of noise transmitted into the vehicle on different surfaces, as heard by the driver or passengers.

- **Smooth road** : Smooth texture asphalt or when bitumen covers most of reinforcing particles of the road. Also surfaced where the road has worn or melted in hot weather to form a smooth surface.
- **Coarse road** : Coarse textured asphalt with granite reinforcing particles measuring about 15mm in size bound together with bitumen. Typically this is where rumbling is most important.
- **Rough road** : Rough terrain, used concrete or asphalt, with uneven obstacles such as potholes, ridges, ... Typical example is the Piste Intérieure at Mortefontaine Proving Ground.

4.5 STANDARD TERMINOLOGY

Standard Terminology for Vehicle Dynamics Simulations (Sayers, 1996)

<https://hosting.umons.ac.be/html/mecara/grasmech/standardterminologyforvehicledynamicssimulation.pdf>

Kerb weight is the total weight of a vehicle with standard equipment, all necessary operating consumables (e.g., motor oil and coolant), a full tank of fuel, while not loaded with either passengers or cargo. Kerb weight definition differs between different governmental regulatory agencies and similar organizations. For example, many European Union manufacturers include a 75 kilogram driver to follow European Directive 95/48/EC.

Payload is the weight of carrying capacity of vehicle. Depending on the nature of the mission, the payload of a vehicle may include cargo, passengers or other equipment. In a commercial context, payload may refer only to revenue-generating cargo or paying passengers.

Gross Vehicle Mass (GVM) is the maximum operating weight/mass of a vehicle as specified by the manufacturer including the vehicle's chassis, body, engine, engine fluids, fuel, accessories, driver, passengers and cargo but excluding that of any trailers.

Other load definitions exist, such as:

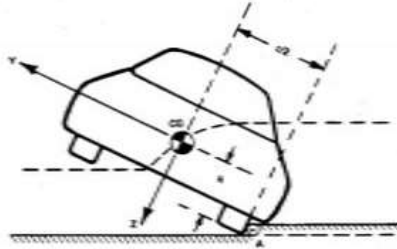
- “**Design Weight**” (typically Kerb with 1 driver and 1 passenger, 75 kg each, in front seats)
- “**Instrumented Vehicle Weight**” (includes equipment for testing, e.g. out-riggers)

from Chalmers compendium

4.6 CRITICAL SLIDING VELOCITY (CSV)

Critical Sliding Velocity (CSV)

- Theoretical lowest speed at which sliding sideways into a curb causes rollover.



$$\text{Critical Sliding Velocity} = \sqrt{\frac{2gI_{ox}}{MH^2} \left(\sqrt{\left(\frac{T^2}{4} + H^2\right)} - H \right)}$$

where,

g gravitational constant

M vehicle mass

T vehicle track width

H vehicle center of gravity height

I_{ox} roll moment of inertia of the vehicle about a pivot point at the outside of the tires, computed using the parallel axis theorem

$$I_{ox} = I_{xx} + M \left(\frac{T^2}{4} + H^2 \right)$$

where,

I_{xx} roll moment of inertia of the vehicle about the vehicle center of gravity

Dans **Measured Vehicle Inertial Parameters-NHTSA's Data Through November 1998**

▷ <https://www.sae.org/publications/technical-papers/content/1999-01-1336/>

on voit une corrélation nette entre CSV et SSF :

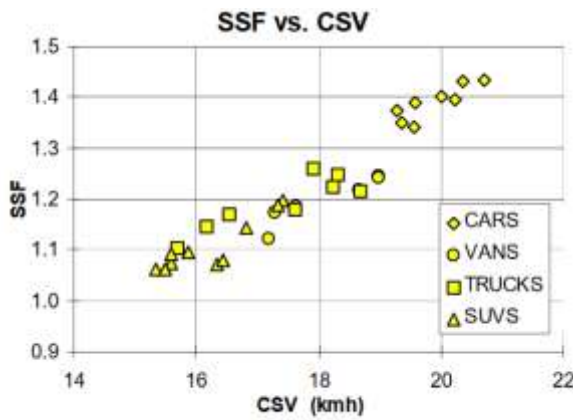


Figure 3: Driver Only SSF vs. CSV

4.7 STATIC STABILITY FACTOR (SSF)

$$SSF = T/(2H)$$

avec

T vehicle track width

H vehicle center of gravity height

4.8 TILT TABLE RATIO (TTR)

Tilt Table Ratio (TTR)

29

- Minimum table angle at which a vehicle on the table will tip over.

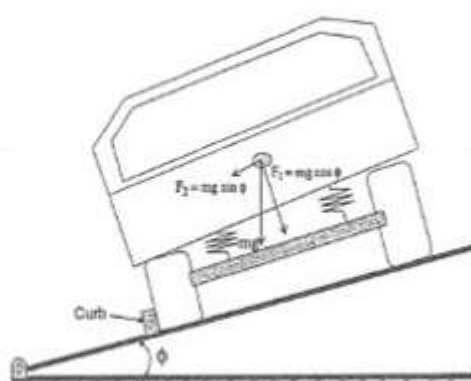
$$F_1 = m_s g = mg \cos \phi$$

$$F_2 = m_s a_s = mg \sin \phi$$

m_s :-simulated weight

a_s :-simulated lateral acceleration

$$TTR = \frac{a_s}{g} = \tan \phi$$



During the test, the tilt of the table is increased slowly until the tire at the high side loses contact with the surface of the table. The angle at which this occurs is called the tip-over angle.

Dividing above Eq., the tilt table ratio (TTR), Its used to estimate the rollover of unstable vehicles, where there is a small tilt angle, than stable vehicles.

4/23/2012

4.9 STABILITY DERIVATIVES

Elles sont définies dans (Kiefer, 1996)

The stability derivatives are the rates of change of the external forces or external moments acting on the vehicle with respect to β , r , or δ .

$Y_\beta = C_f + C_r$	Damping-in-Sideslip
$Y_r = \frac{aC_f - bC_r}{V}$	Lateral Force/Yaw Coupling
$Y_\delta = -C_f$	Control Force
$N_\beta = aC_f - bC_r$	Directional Stability
$N_r = \frac{a^2C_f + b^2C_r}{V}$	Yaw Damping
$N_\delta = -aC_f$	Control Moment

NB : chez Kiefer, les rigidités de dérive sont négatives

Ces stability derivatives permettent de réécrire ces équations

$$\begin{aligned} (C_f + C_r)\dot{\beta} + \frac{aC_f - bC_r}{V}r - C_f\dot{\delta} + F_{ya} + mg\theta &= mV\dot{\beta} + mVr \\ (aC_f - bC_r)\dot{\beta} + \frac{a^2C_f + b^2C_r}{V}r - aC_f\dot{\delta} - (c-a)F_{ya} &= I_{zz}\dot{r} \end{aligned} \quad (4.24)$$

sous la forme

$$\begin{aligned} Y_\beta\dot{\beta} + Y_r r + Y_\delta\dot{\delta} + F_{ya} + mg\theta &= mV\dot{\beta} + mVr \\ N_\beta\dot{\beta} + N_r r + N_\delta\dot{\delta} - (c-a)F_{ya} &= I_{zz}\dot{r} \end{aligned} \quad (4.25)$$

NB :

F_{ya} = aerodynamic side force

c = distance from front axle to aerodynamic side force

(et $mg\theta$ doit être un terme de dévers ...)

On retrouve en fait cette définition dans (Milliken & Milliken, 1995)

The Derivative Notation

The derivative notation comes from aeronautical practice. It was used in the earliest linear analyses of aircraft stability and control and was initially applied to the automobile by Segel in 1956 (Ref. 144). The derivatives are slopes of force/moment curves against motion variables β , r and δ . They relate the forces and moments to small excursions of these variables. In this linear system they can be considered separately; as a group they define the unbalanced forces and moments due to the tires. In the aeronautical case, the individual derivatives have been measured in specialized wind tunnel and flight tests; aero engineers think about stability and control in “derivative” terms. In both the auto and aero cases the derivatives have a physical significance.

The lateral tire force and yawing moment are linear functions of β , r and δ (since C_F , C_R , a , b , V are constants). In a linear situation such as this, the principle of superposition holds and the components due to β , r and δ are additive. Expressed mathematically, Y and N can be written

$$Y = f(\beta, r, \delta) = \left(\frac{\partial Y}{\partial \beta} \right) \beta + \left(\frac{\partial Y}{\partial r} \right) r + \left(\frac{\partial Y}{\partial \delta} \right) \delta$$

$$Y = Y_\beta \beta + Y_r r + Y_\delta \delta \quad (5.7)$$

$$N = f(\beta, r, \delta) = \left(\frac{\partial N}{\partial \beta} \right) \beta + \left(\frac{\partial N}{\partial r} \right) r + \left(\frac{\partial N}{\partial \delta} \right) \delta$$

$$N = N_\beta \beta + N_r r + N_\delta \delta \quad (5.8)$$

The constant partial derivative slopes, $\partial Y / \partial \beta$, $\partial Y / \partial r$, $\partial Y / \partial \delta$, $\partial N / \partial \beta$, $\partial N / \partial r$, $\partial N / \partial \delta$, are the *stability and control derivatives*, usually expressed in the short-hand notation, Y_β , Y_r , Y_δ , N_β , N_r , N_δ .

La signification physique de ces grandeurs est bien expliquée dans les pages 151 et suivantes de l'ouvrage de Milliken : à relire !

Dans <https://link.springer.com/content/pdf/10.1007/s11012-021-01317-3.pdf>
on trouve

$M_{z,SSC}$ is based on a Linear Quadratic Regulator (LQR). The reference vehicle model is the single track model [40]:

$$\begin{cases} mV(\dot{\beta} + r) = Y_\beta\beta + Y_r r + C_1\delta \\ J_z\dot{r} = N_\beta\beta + N_r r + aC_1\delta + M_z \end{cases} \quad (11)$$

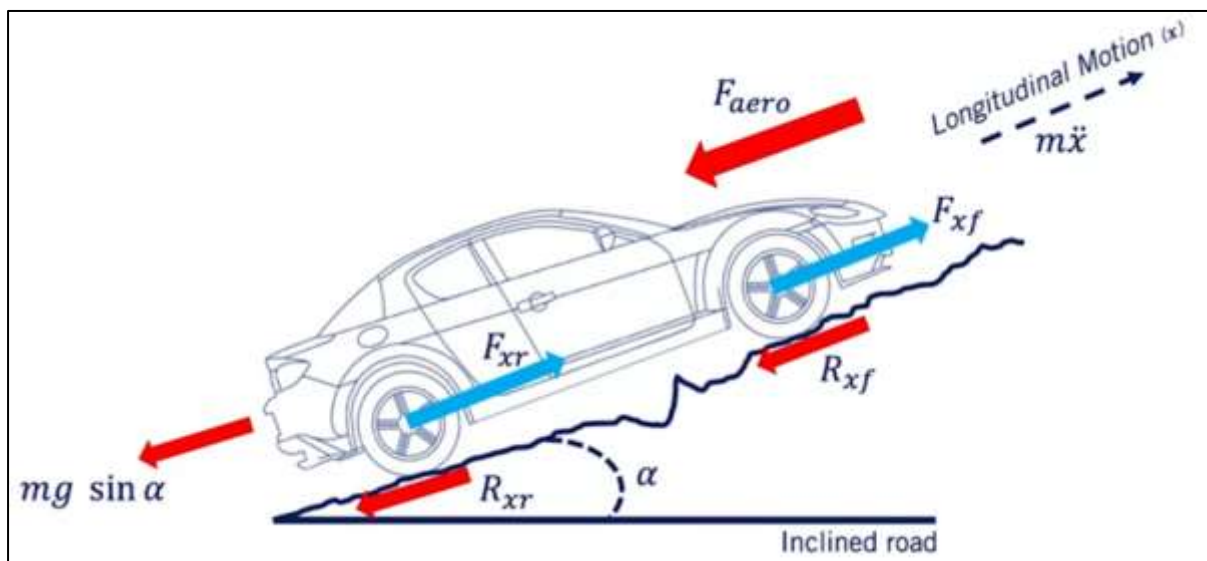
where J_z is the vehicle mass moment of inertia with respect to a vertical axis, the stability derivatives Y_β , Y_r , N_β and N_r are defined as:

$$\begin{aligned} Y_\beta &= -(C_1 + C_2) \\ Y_r &= -\frac{(aC_1 - bC_2)}{V} \\ N_\beta &= -(aC_1 - bC_2) \\ N_r &= -\frac{(a^2C_1 + b^2C_2)}{V} \end{aligned} \quad (12)$$

and C_1 and C_2 are, respectively, the cornering stiffness of the front and rear axle.

5 DYNAMIQUE LONGITUDINALE

5.1 INTRO



- The full longitudinal dynamics

$$m\ddot{x} = F_{xf} + F_{xr} - F_{aero} - R_{xf} - R_{xr} - mg \sin \alpha$$

- Let F_x - total longitudinal force: $F_x = F_{xf} + F_{xr}$
- Let R_x - total rolling resistance: $R_x = R_{xf} + R_{xr}$
- Assume α is a small angle: $\sin \alpha = \alpha$

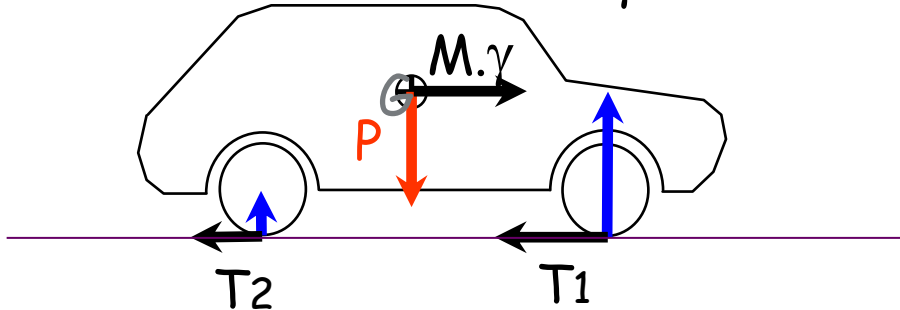
- Then the simplified longitudinal dynamics become

$$m\ddot{x} = F_x - [F_{aero} - R_x - mg\alpha]$$

Inertial Term Traction Force Total Resistant Forces (F_{Load})

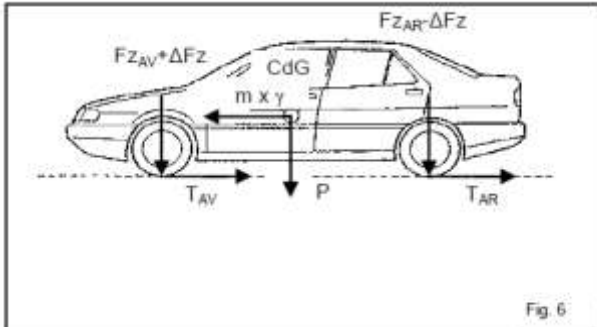
5.2 THEORIE DU FREINAGE

$$M \cdot \gamma + T_1 + T_2 = 0$$



$$D_{\text{arrêt}} = V_0 \cdot t_r + V_0^2 / 2\gamma$$

5.2.1 REPORT DE CHARGE

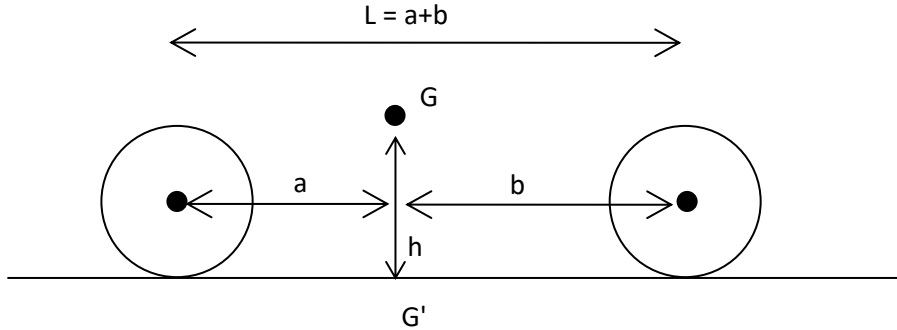


Avec :

CdG : Centre de gravité du véhicule,
 p : Poids du véhicule (N),
 ΔFz : Transfert dynamique de charge (N),
 FzAV + ΔFz : Charge dynamique sur l'essieu AV,
 FzAR - ΔFz : Charge dynamique sur l'essieu AR ,
 TAV : Force de freinage essieu AV,
 TAR : Force de freinage essieu AR,
 m x γ : Force d'inertie (N),
 m : Masse du véhicule (kg),
 γ : Décélération du véhicule (m/s^2).

$$\Delta Fz = m \cdot \gamma \cdot h_{CdG} / E$$

On écrit l'équilibre des moments par rapport à G' , projection du centre de gravité au sol



$$m\gamma h = F_{av} \cdot a - F_{ar} \cdot b \quad (1)$$

$$m \cdot g = F_{av} + F_{ar} \quad (2)$$

$$(2) \Rightarrow F_{ar} = m \cdot g - F_{av}$$

$$\begin{aligned} (1) \Rightarrow m\gamma h &= F_{av} \cdot a - (m \cdot g - F_{av}) \cdot b \\ &= F_{av} \cdot (a+b) - m \cdot g \cdot b \end{aligned}$$

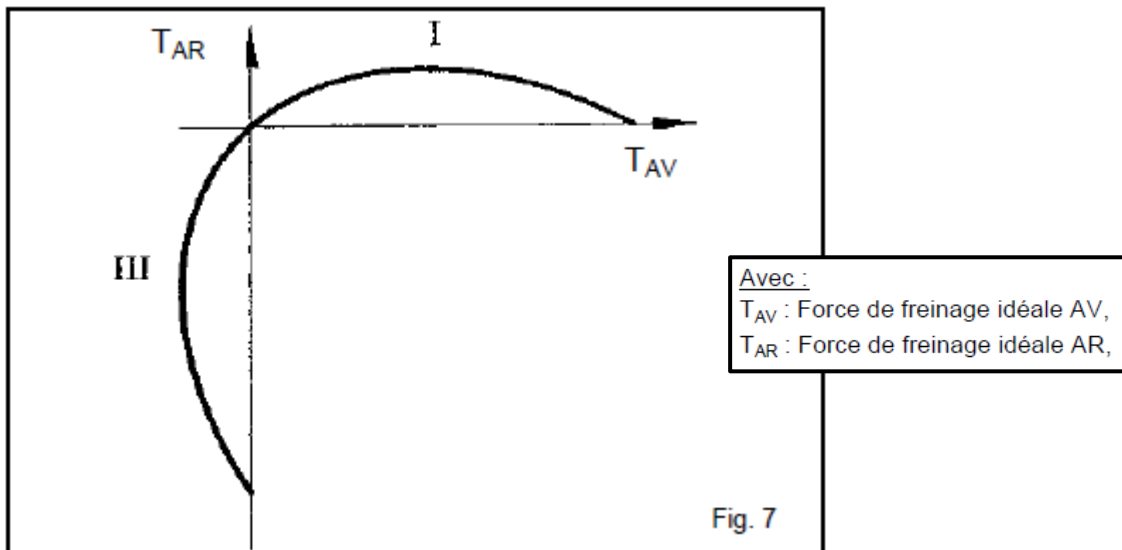
$$\Rightarrow F_{av} = mgb/L + m\gamma h/L$$

On reconnaît :

- la charge statique sur le train avant mgb/L
- le transfert de charge $m\gamma h/L$

5.2.2 PARABOLE D'ÉQUIADHÉRENCE

A l'aide d'une décélération donnée et des rapports "charges sur essieux", il est possible d'obtenir la parabole d'équiadhérence pour un véhicule donné dont l'empattement et la position du centre de gravité sont connus.

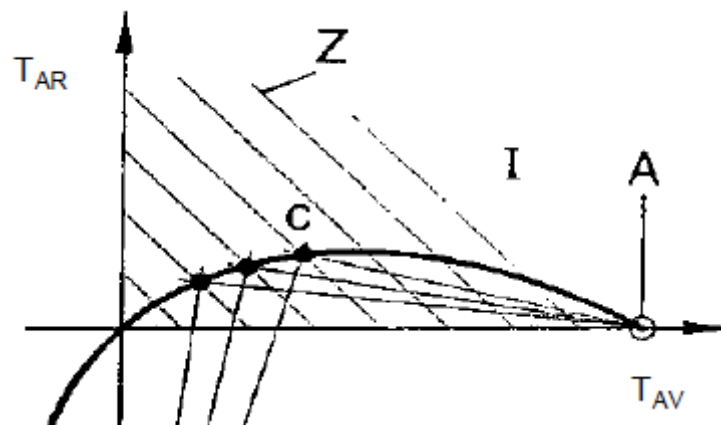


La parabole d'équiadhérence représente l'utilisation maximale (idéale) de l'adhérence des roues avant et arrière du véhicule durant le freinage (secteur I) et l'accélération (secteur III).

Lorsque la courbe de répartition des forces tangentielles (ou traînées) de freinage (T_{AV} et T_{AR}) vient couper la parabole, ceci indique que pour la décélération γ au point d'intersection, le coefficient d'adhérence maximal sera dépassé sur les roues arrière en premier. Ces roues seront donc bloquées en premier.

5.2.3 DROITES DE DÉCÉLÉRATION CONSTANTE

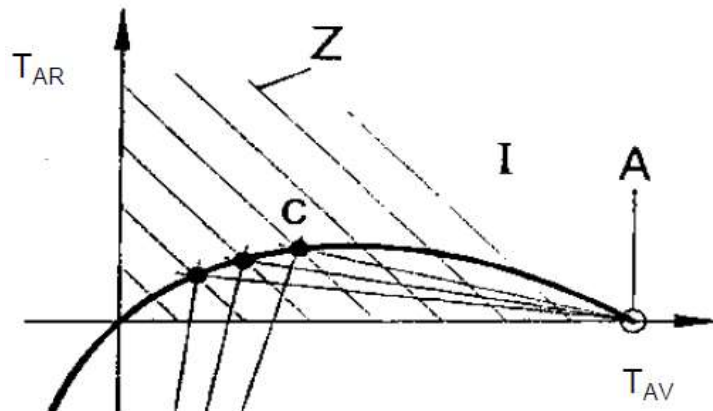
Ce sont les courbes Z sur la figure ci-dessous :



5.2.4 COURBES DES COEFFICIENTS D'ADHÉRENCE PNEU-CHAUSSÉE

Comme il existe un rapport linéaire entre la force de freinage transmissible par une roue et la charge appliquée sur celle-ci (loi de Coulomb), les courbes des coefficients constants d'adhérence seront donc des droites. Pour déterminer la position d'une droite, deux points sont nécessaires.

Le 1^e point, identifié par A, vient du moment de décollement des roues AR :



Le deuxième point correspond à l'intersection C des diverses droites de décélération constante et de la parabole d'équiadhérence.

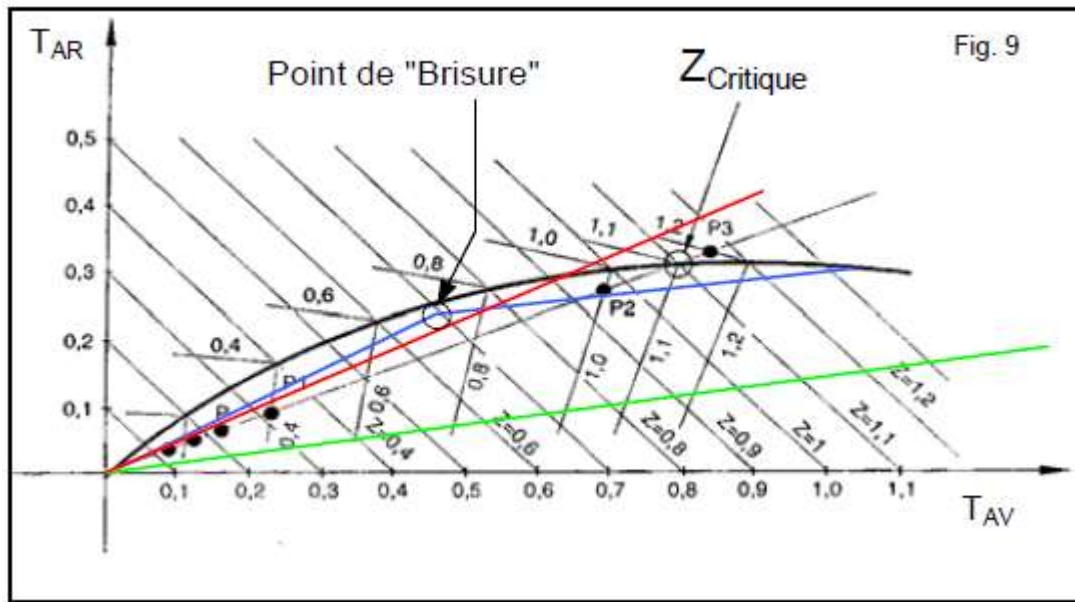
5.2.5 FREINAGE OPTIMUM

Afin de répartir au mieux les forces de freinage des essieux avant et arrière (d'utiliser au maximum l'adhérence de chaque essieu), il s'agit d'exploiter au maximum la parabole d'équiadhérence, c'est-à-dire que la droite de répartition des forces de freinage doit "coller" le plus possible à la parabole, ce qui est impossible.

a. Soit on a une répartition des forces de freinage trop prononcée sur les roues avant (la droite de répartition est donc quasi horizontale, elle ne colle plus à la parabole, et les freins arrière ne sont quasi pas sollicités), à contrario, le Zcritique est très élevé et le point de blocage des roues arrière est hors d'atteinte (décélération y trop élevée par rapport à la performance du système de freinage) (courbe verte).

b. Soit on a une répartition des forces de freinage moins prononcée sur les roues avant (la droite de répartition est plus proche de la parabole, et devrait la couper à une décélération g comprise entre 0 et 10 m/s²), (courbe rouge). Les freins arrière sont bien utilisés mais le véhicule n'est plus stable, lorsque la droite de répartition passe au dessus de la parabole, suite au blocage des roues arrière en premier.

Il faudra alors limiter la pression dans les freins arrière afin de "briser" la droite de répartition des forces de freinage avant qu'elle ne coupe la parabole. Le second segment de répartition sera lui aussi très proche de la parabole, tout en restant en dessous de celle-ci (courbes bleues).

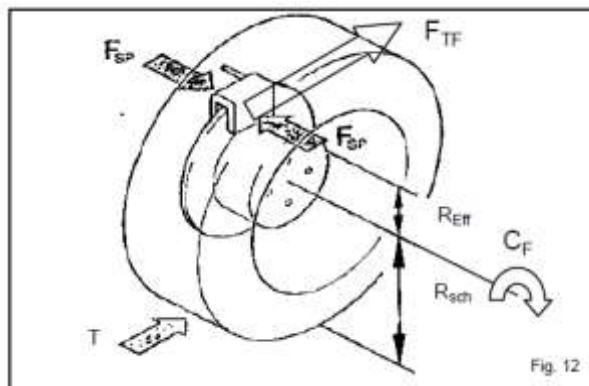


On définit donc un 1^{er} paramètre, $K=T_{AV}/T_{AR}$, qui est le coefficient de répartition de la force de freinage (la pente de la 1^e droite bleue).

On peut également l'exprimer sous forme d'un pourcentage de répartition :

$$K' = T_{AV} / (T_{AV} + T_{AR})$$

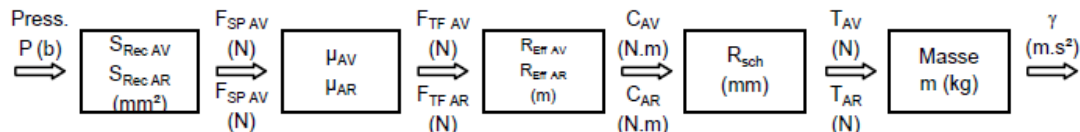
5.2.6 NOTION DE C/P



Avec :

F_{SP} : Force de pincement (N),
 F_{TF} : Force Tangentielle de Freinage (N),
 C_F : Couple de Freinage (N.m),
 T : Force de freinage tangentielle (Traînée), (N),
 R_{Eff} : Rayon efficace (m),
 R_{sch} : Rayon sous charge du pneumatique (m).

Une trainée se calcule de la manière suivante :



Comme on l'a vu précédemment, la pression P reçue par les récepteurs AV et AR est identique. Le rayon sous charge des pneumatiques AV et AR est, généralement identique également (sauf cas exceptionnel).

Les paramètres permettant de moduler le coefficient de répartition de la force de freinage sont donc :

- Les **surfaces de piston** des étriers AV/AR (force de pincement $F_{SP AV/AR}$),
- Les **caractéristiques des garnitures** de frein (coefficients de frottement entre les garnitures AV/AR et les disques, μ_{AV}/μ_{AR}),
- Les **rayons des disques** AV et AR ($R_{Eff AV/AR}$).

Pour simplifier les échanges et le choix des composants de freinage, ces trois paramètres sont compilés en un seul, appelé **l'efficacité d'un frein** (c'est-à-dire le rapport Couple de freinage / Pression de freinage), et noté : C/P.

Le coefficient de répartition des forces de freinage peut donc s'exprimer ainsi :

$$K = (C/P)_{AV} / (C/P)_{AR}$$

Le calcul des traînées se simplifie alors :



5.2.7 NOTION DE Z CRITIQUE

D'après les caractéristiques d'un véhicule donné, on détermine l'efficacité nécessaire pour chaque frein (AV et AR). La pente de la droite de répartition des forces de freinage est donc connue et implique un $Z_{critique}$.

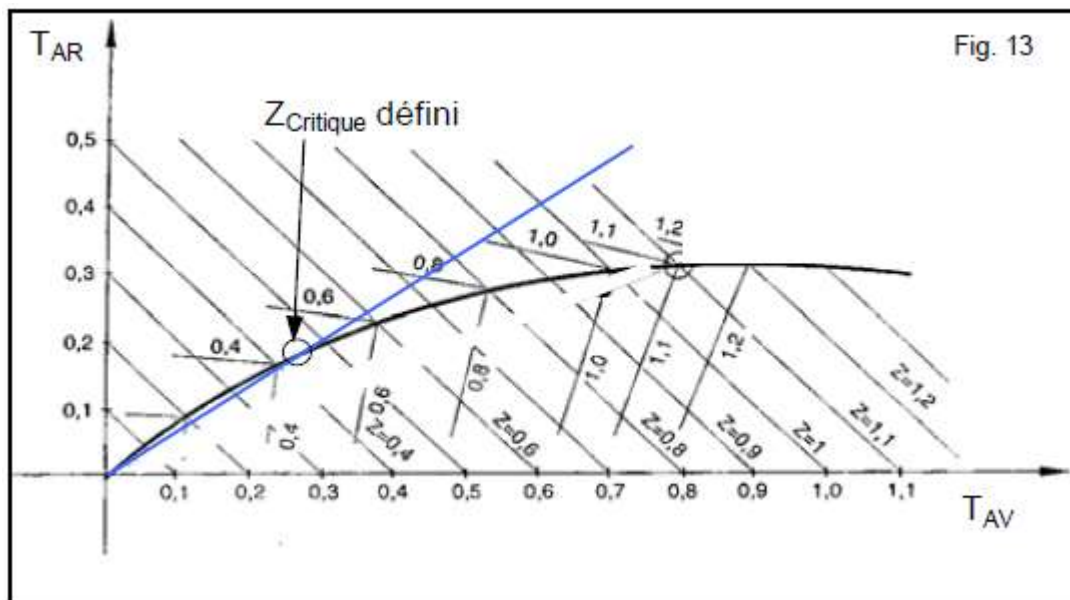


Fig. 13

5.3 STABILITE AU FREINAGE

Aidée par un déport au sol négatif

5.4 PERFORMANCE DU SYSTEME DE FREINAGE

La performance "pure" d'un système de freinage est donnée par **la décélération γ (m/s^2)** que celui-ci peut procurer à un véhicule donné dont sont connus :

- la masse véhicule (M , exprimée en kg)
- le rayon s/s charge des roues ($Rsch$, exprimé en mm)
- la pression du circuit de freinage (P , exprimée en bars)

$$\gamma = ((C/P)_{AV} + (C/P)_{AR}) \times P \times 1/Rsch \times 1/M$$

5.5 MODELISATION DU FREINAGE

Voir :

- [ASU Racing Team Brake System Development](#) sur Matlab Central
- [Modeling an Anti-Lock Braking System](#), doc Simulink

Brakes Modelling

Investing in your future
European Regional Development Fund
Surrey University

Advantage West Midlands
www.advantagewm.co.uk

Matlab Control & Dymola Plant Model



Simulation has been used extensively to examine the consequences on vehicle stability of regenerative braking control algorithms.

- Impact of brake system architecture on potential energy recovery & vehicle stability.
- Critical interactions during ABS/ESP events.
- Effects of stochastic signal propagation delay over CAN.

Carmaker Interface



- Simulation platform extended from existing longitudinal forward dynamic HEV model WARPSTAR 2+.
- Powertrain & brakes model implemented in acausal physical modelling package Dymola & embedded into MATLAB/Simulink.
- Simulink model integrated with IPG CarMaker suspension, tyre & driver + environment models.

5.6 DYNAMIQUE SYSTEME DE FREINAGE

Accumulateur hydraulique ABS

http://tesi.cab.unipd.it/46106/1/Nicola_Geromel_2014.pdf

§3.2, page 28 du pdf

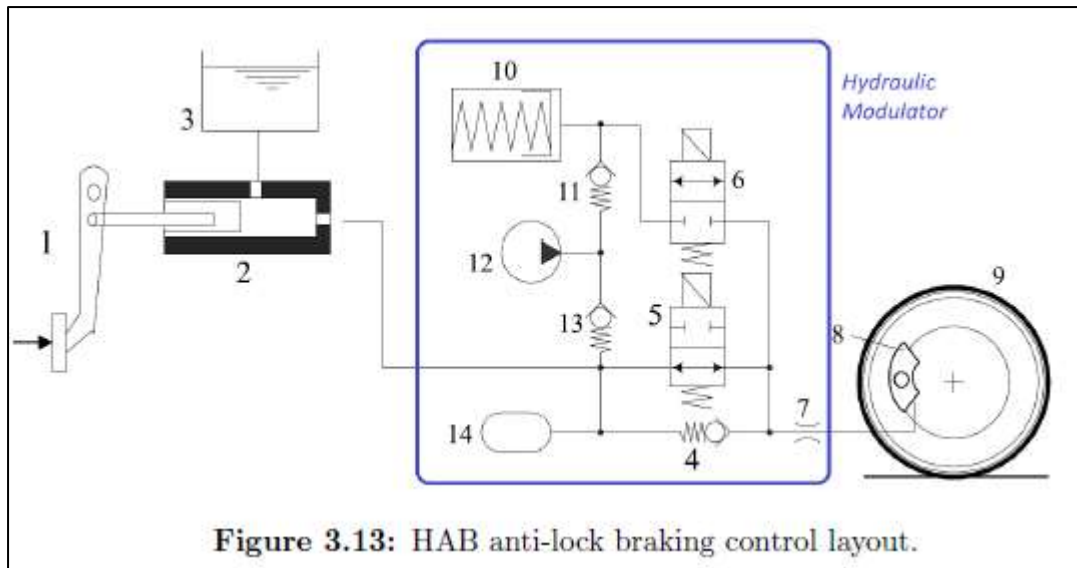


Figure 3.13: HAB anti-lock braking control layout.

The dynamic of such modulator is quite complex but the governing equation can be written. The complete model, however, can not be completed because some parameters identification should be done in order to get the proper values for the system coefficients (this can be done when the required hardware will be installed on the vehicle). In this work, a simpler model for the hydraulic modulator is built. A similar work has been done in [41]. Here some system identification work of the hydraulic dynamics model in the laboratory is presented. They also use a simplify model low pass filter, and the identified results of these two models almost the same, so we can simplify the dynamics into a low pass filter. A rough identification of the characteristics gives a pure time delay $\tau = 7 \text{ ms}$, a pressure rate limit between $r_{max} = +750 \text{ bar/s}$ and $r_{min} = -500 \text{ bar/s}$ and a second order dynamics with a cut-off frequency of 60 Hz and a damping coefficient $\xi = 0.33$.

5.7 ABS, AEB, ETC ...

Voir §19

5.8 PERFOS FREINAGE

5.8.1 TEMPS DE RÉACTION DU CONDUCTEUR

<https://thebrakereport.com/tbr-technical-corner-braking-requirements-for-optimizing-autonomous-emergency-braking-aeb-performance-part-1-out-of-3/>

Stopping distance tests from 5 different (pro) drivers and 3 different cars have been selected in this study and the brake jerk and deceleration were analyzed. The average brake deceleration is around 10.5 m/s² and the mean brake jerk is 80 m/s³.

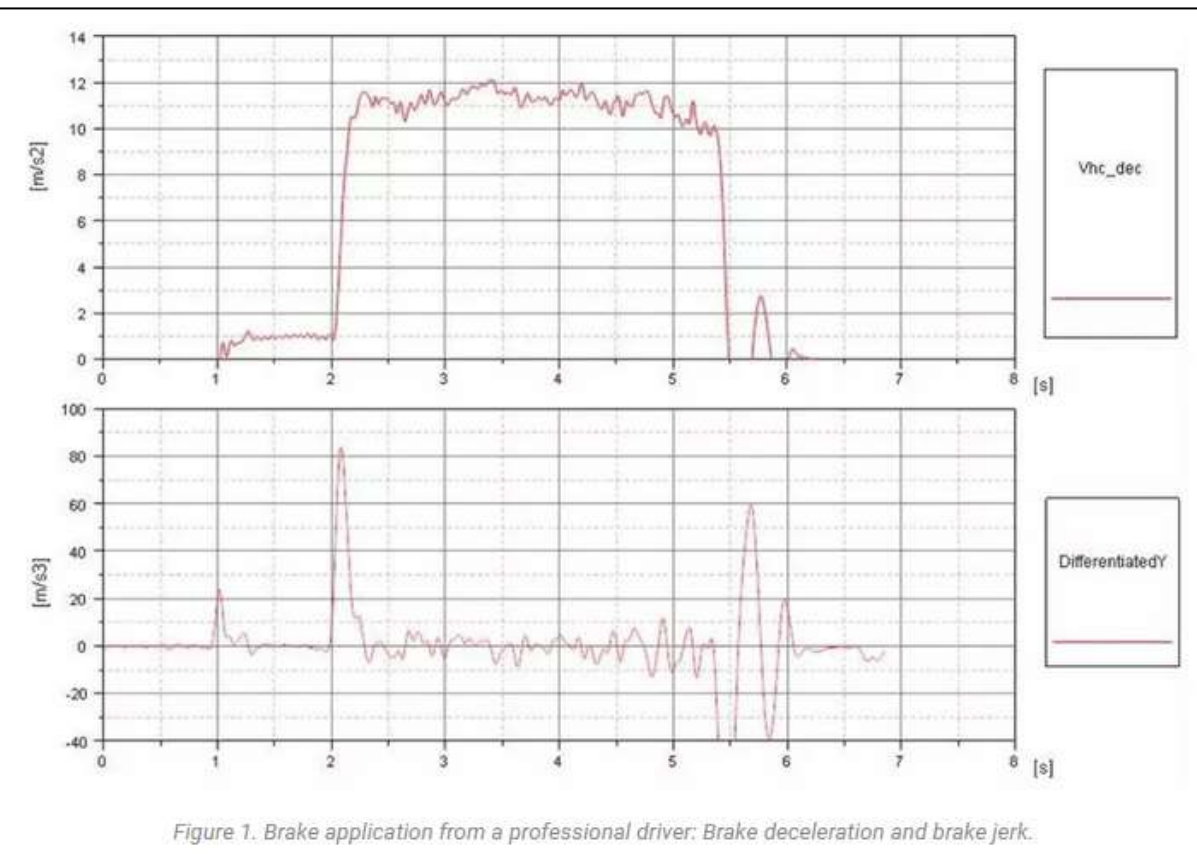


Figure 1. Brake application from a professional driver: Brake deceleration and brake jerk.

5.8.2 MOTO

ABS Comparison Test | Absolutely Brilliant Stopping (2011)

<http://www.sportrider.com/sportbikes/abs-comparison-test-absolutely-brilliant-stopping?image=13>

In order to fully test the braking systems on each bike, we used our Racepak G2X data acquisition system to record a series of stops with Kento at the controls, and looked at stopping distances as well as braking deceleration (in G) for each stop. In addition to pointing out performance differences between the three bikes, it's also worthwhile pointing out some details about braking in general that is shown in the data.

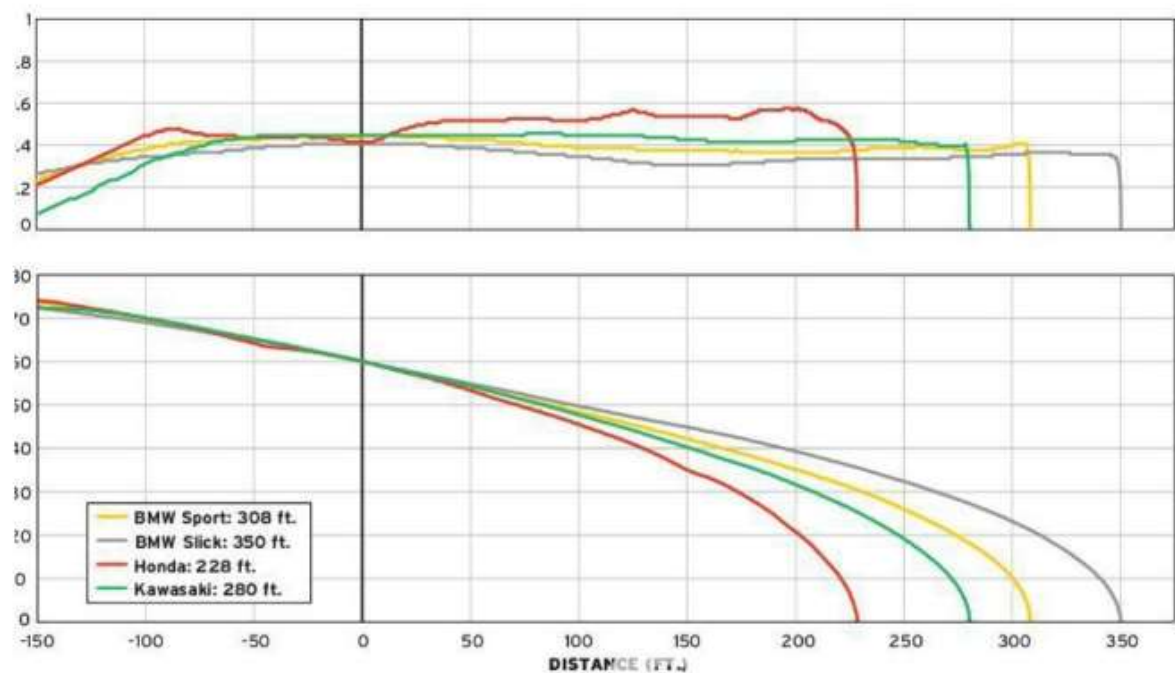
Note that the stopping data is shown here relative to distance, and the speed traces drop sharply as speed approaches zero. Here you can see an important aspect: Even at maximum braking, it takes exponentially more distance to slow from a higher speed than a lower speed. This is why it is critical in any sudden stop to get to maximum braking as quickly as possible. Note also that it takes a certain amount of time (and distance) to get to maximum deceleration, as shown in the braking G plots. This is a function partly of the rider's ability to get to maximum braking, but also how quickly weight is transferred to the front wheel without it going into a skid. ABS can help somewhat in this aspect, but the rider's skill also plays a big part.

Again, this shows how important it is to master all aspects of braking, both for quick lap times on the track and safety on the street.

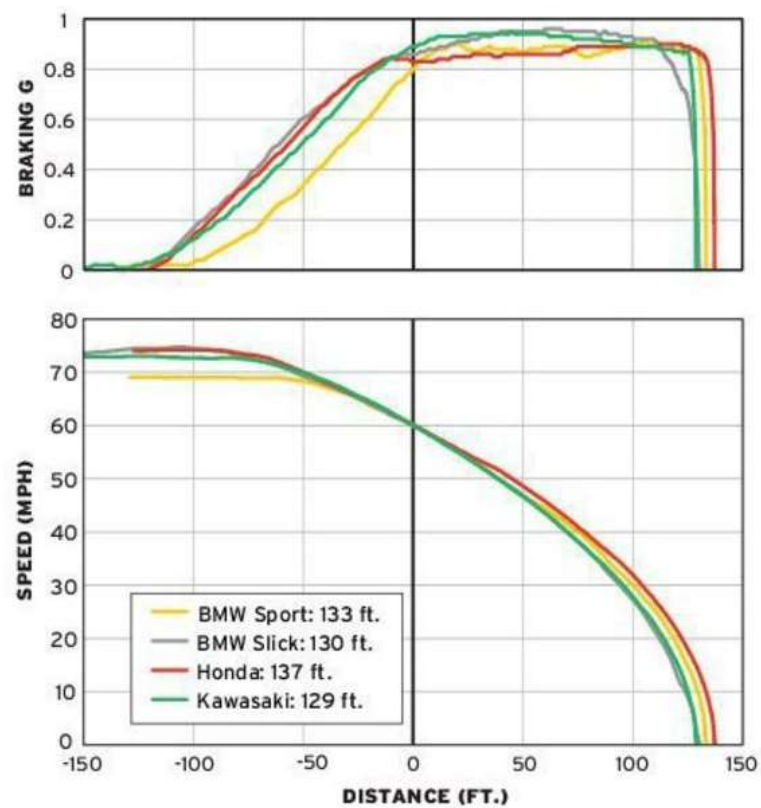
For each bike, we had Kent perform three sets of three stops: one stop with the rear brake only, one with the front brake only and one with both; that sequence was repeated three times. The best stops using rear-only, front-only and both brakes are shown here displayed as speed over distance and braking force over distance. Because it's practically impossible to begin each test from an identical speed, we lined all the data up at 60 mph and calculated stopping distance from that point, as is typical in the industry. Note that the deceleration diagrams (Braking G) begin ramping up at different points, not because of any performance discrepancy, but because the starting speed of each test is slightly different.

To ensure that braking performance with our three ABS bikes was not dependent on a tire advantage, we fit all three bikes with Bridgestone's new BT-016 Pro

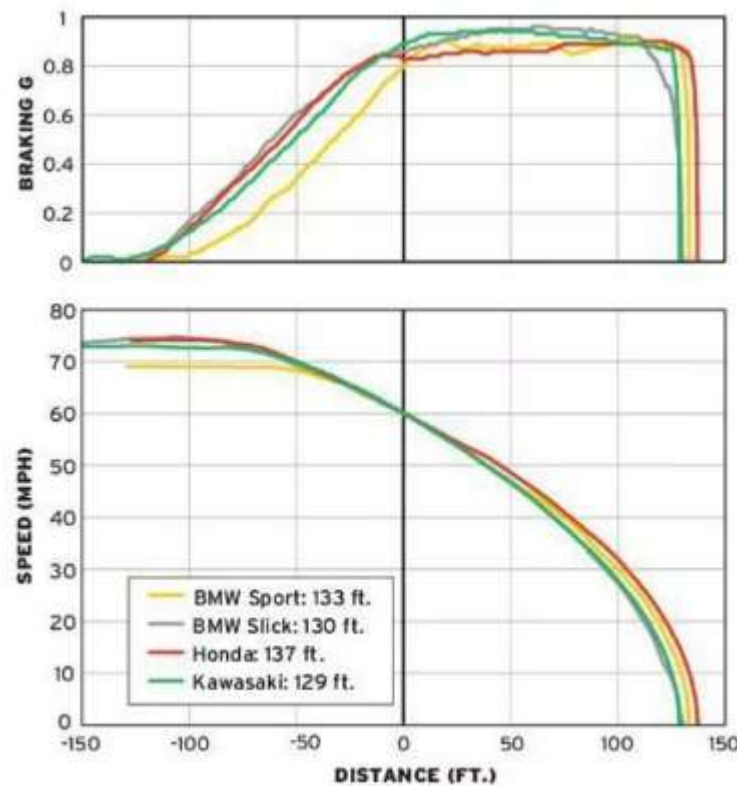
Rear brake only (the Honda is fitted with dual-brake)



Front-brake only:



Both brakes



BMW K1300S wins ABS test, beats car (12/2009)

<http://www.motorcyclenews.com/news/first-rides-tests/2009/december/dec2309-bmw-k1300s-wins-abs-test-/>

The bikes tested were:

- BMW S1000RR – has a phenomenally sophisticated ABS system that will not only stop the front wheel locking, but – in race mode – allow a certain amount of rear wheel slip so you can back it into corners. As you do
- Honda Fireblade with C-ABS – this blew MCN away when we tested it last year. It's incredibly smooth and allows ordinary riders to brake like national level racers.
- BMW's K1300S – the ABS is a generation behind the S1000RR's, but MCN's testers say it has phenomenal braking performance because of its long, low chassis and Duolever front end.
- Yamaha XJ6 ABS – budget, older generation ABS system
- Harley Electra Glide Ultra Limited – heavy bike with older-generation ABS

The car was a Honda Civic diesel – typical family hatchback with typical car ABS.

Conditions were cold and damp.

The shock result was that the BMW K1300S beat everything, including the car.

In fact the big BM's stopping distance was 4.8 metres less from 60mph than the car

5.8.2.1 AVEC OU SANS ABS

<https://www.youtube.com/watch?v=X6kO6ltk3a0>

Honda Fireblade: ABS v non-ABS (MCN)

5.8.3 AUTO

Dans un Auto-Plus qui doit dater de 2002, ont été mesurées les distances de freinage suivantes :

		STOP	50 à 0 km/h	90 à 0 km/h	130 à 0 km/h
Les meilleures					
1 ^e	Seat Ibiza 1900 TDI 110		11 m	34 m	67 m
2 ^e	Seat Arosa 1.4 16V		11 m	33 m	69 m
3 ^{me}	Opel Corsa 1.7 DTI		11 m	33 m	70 m
3 ^{me}	Toyota Yaris 1.3i		11 m	33 m	70 m
5 ^e	Seat Ibiza 1900 TDI 90		10 m	34 m	70 m
6 ^e	Toyota Yaris 1.0i		11 m	35 m	70 m
7 ^e	Renault Clio 1.6 16V		11 m	35 m	72 m
8 ^e	Rover 25 1.4		12 m	35 m	72 m
9 ^e	Fiat Punto 80 16V		12 m	37 m	72 m
10 ^e	Peugeot 206 1.4		12 m	34 m	73 m
Les pires					
50 ^e	Citroën Saxo 1.4		11 m	37 m	78 m
52 ^e	Fiat Punto 60		12 m	37 m	80 m
53 ^e	Opel Agila 1.2		12 m	38 m	81 m
54 ^e	Renault Clio 1.9 D		12 m	38 m	82 m
55 ^e	Volkswagen Polo 1.4 16V		12 m	40 m	83 m

Citadines

		STOP	50 à 0 km/h	90 à 0 km/h	130 à 0 km/h
Les meilleures					
1 ^e	Volkswagen Golf GTI TDI 150		10 m	32 m	60 m
2 ^e	Audi A3 S3 Quattro		10 m	32 m	64 m
3 ^{me}	Volkswagen Golf 1.6 16V		10 m	33 m	65 m
4 ^e	Audi A3 1.9 TDI 110		10 m	33 m	67 m
5 ^e	Citroën Xsara 1.6i 16V		11 m	33 m	67 m
6 ^e	Opel Astra OPC		11 m	34 m	67 m
7 ^e	Volkswagen Golf V5 4Motion		10 m	33 m	68 m
8 ^{me}	Audi A3 1.6		11 m	33 m	68 m
9 ^{me}	Fiat Bravo 155 20V HGT		11 m	33 m	68 m
10 ^e	Ford Focus 1800		11 m	34 m	68 m
Les pires					
50 ^e	Fiat Bravo TD 75		12 m	37 m	79 m
52 ^e	Toyota Corolla D		11 m	37 m	80 m
53 ^e	Nissan Almera 2.0 D		13 m	41 m	80 m
54 ^e	Opel Astra 2.0 DI 16V		12 m	40 m	81 m
55 ^e	Mazda 323 2000 D		13 m	44 m	81 m

Compacts

5.8.3.1 458 ITALIA, 911 GT2, MP4-12C (2011)

[Car and Driver](#)

VEHICLE	Ferrari 458 Italia	McLaren MP4-12C	Porsche 911 GT2 RS
PRICE BASE	\$230,275	\$233,500*	\$245,950
PRICE AS TESTED	\$332,032	\$303,690*	\$249,090
DIMENSIONS			
LENGTH	178.2 inches	177.4 inches	175.9 inches
WIDTH	76.3 inches	75.2 inches	72.9 inches
HEIGHT	47.8 inches	47.2 inches	50.6 inches
WHEELBASE	104.3 inches	105.1 inches	92.5 inches
FRONT TRACK	65.8 inches	65.2 inches	59.4 inches
REAR TRACK	63.2 inches	62.3 inches	61.2 inches
INTERIOR VOLUME	52 cubic feet*	51 cubic feet	48 cubic feet
CARGO	8 cubic feet	7 cubic feet	11 cubic feet

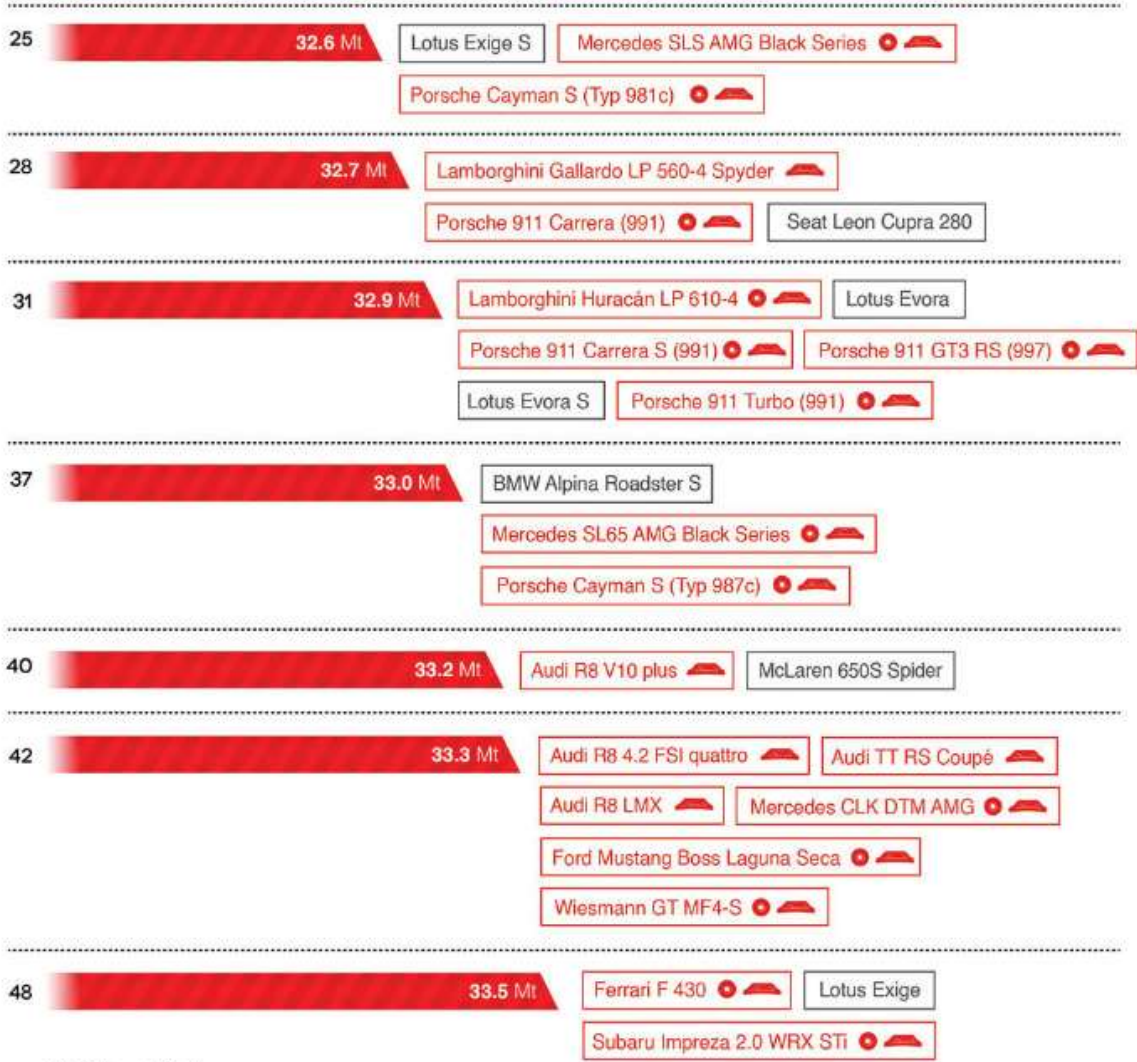
C/D TEST RESULTS			
ACCELERATION			
0-30 MPH	1.4 sec	1.3 sec	1.3 sec
0-60 MPH	3.0 sec	2.9 sec	3.3 sec
0-100 MPH	6.5 sec	6.1 sec	6.6 sec
0-150 MPH	15.0 sec	13.9 sec	14.4 sec
1/4-MILE @ MPH	11.0 sec @ 131	10.7 sec @ 134	11.1 sec @ 133
ROLLING 5-60 MPH	3.5 sec	3.6 sec	4.3 sec
TOP GEAR 30-50 MPH	2.2 sec	2.3 sec	7.8 sec
TOP GEAR 50-70 MPH	2.5 sec	2.8 sec	6.3 sec
TOP SPEED	210 mph (redline ltd, C/D est)	205 mph (drag ltd, mfr's claim)	209 mph (redline ltd, C/D est)
CHASSIS			
BRAKING 70-0 MPH	146 feet	145 feet	145 feet
ROADHOLDING, 120-FT-DIA SKIDPAD	1.01 g	1.02 g	1.07 g
610-FT SLALOM	48.2 mph	47.4 mph	49.3 mph
WEIGHT			
CURB	3325 pounds	3187 pounds	3085 pounds
%FRONT/%REAR	42.6/57.4	42.0/58.0	36.9/63.1

5.8.3.2 AUTO, MOTOR UND SPORT (2017)

<http://www.brembo.com/fr/company/news/50-special>

Dans le classement des 50 voitures qui offrent les meilleures performances de freinage, établi par la revue allemande Auto Motor und Sport, 40 modèles sont équipés de disques et/ou d'étriers de frein Brembo. Les symboles du disque rouge (●) et des étriers de frein (■) à côté de chaque véhicule signalent la présence du produit Brembo correspondant.

1	30.7 Mt	Porsche 911 GT3 (991) ● ■
2	31.0 Mt	Chevrolet Corvette C6 Z06
3	31.3 Mt	Ferrari F12 Berlinetta ● ■ KTM X-Bow GT ● ■
5	31.4 Mt	Porsche 918 Spyder ● ■
6	31.6 Mt	Lexus LFA ● ■ Pagani Zonda F ● ■
8	31.9 Mt	Dodge SRT Viper ● ■ Lamborghini Gallardo LP 570-4 Squadra Corse ● ■ Lamborghini Aventador LP 700-4 ● ■ Porsche 911 Turbo S (991) ● ■
12	32.1 Mt	Artega GT ● ■ Porsche 911 Sport Classic (997) ● ■
14	32.2 Mt	Corvette ZR1 ● ■ Lamborghini Gallardo LP 570-4 Superleggera ■ Ferrari 430 Scuderia ● ■ Porsche 911 Carrera S (997) ● ■ Porsche 911 GT2 RS (997) ● ■
19	32.3 Mt	Mini John Cooper Works GP ● ■
20	32.4 Mt	Audi RS 4 ■ BMW M3 CSL E46 Lotus Elise Club Racer ■ Porsche 911 Targa 4S (991) ● ■
24	32.5 Mt	Alfa Romeo 4C ■



5.8.4 COMPARAISON AUTO-MOTO

<https://www.pistonheads.com/gassing/topic.asp?t=378965> (2007)

From Road & Track 0-100-0 (1994) just the braking:

Toyota Supra = 372ft

Porsche 993TT = 351ft

Kawasaki ZX9R= 320ft

(...)

I've got some figures from the 27th April 2004 Autocar magazine:

Suzuki GSX-R 1000: 100mph - 0 in 5.63 seconds

Lotus Elise 111R - 4.09 seconds

Peugeot 206 Gti 180 - 4.39 seconds

Porsche 911 GT3 - 4.00 seconds

https://www.reddit.com/r/motorcycles/comments/1nhqx3/an_excellent_illustration_of_motorcycle_vs_car/ (2014)

60-0 braking distances:

- MCN Performance index 12/13: S1000RR '12 = 119.3 feet
- Edmunds 2012 Camry test: 129 feet
- Motor Trend 2011 BMW 1 Series M: 107 feet
- or: Edmunds 2011 BMW 1 Series M: 103 feet

It's not that motorcycles in general are especially bad at braking. It's that the new BMW M1 has one of the shortest braking distances of any production car ever. [Consumer Reports](#) doesn't even test any vehicles that stop that fast (their best was the Boxster, at 112 feet). Previously Motor Trend only found [22 cars](#) that do 60-0 in under 100 feet, and it's mostly Porsches and Ferraris.

5.9 REGLEMENTATION

5.9.1 ECE 13H

Distance d'arrêt et MFDD (Mean Fully Developed Deceleration), notée J_m dans les tableaux ci-dessous

Test en condition chargée et non chargée

NB : catégorie M1 = VP (pas plus de 8 sièges), et N1 = VU légers (<3.5t)

On distingue les tests type 0 (freinage unique) et type 1 (avec répétition)

Table 8.3(a): Summary of Test Conditions and Minimum Service and Secondary Braking System Performance Requirements for Type-0 Tests for Category M₁ and N₁ Vehicles in UN Regulation 13H

		Service Braking	Secondary Braking
Type-0 test with engine disconnected	V	100 km/h	100 km/h
	s ≤	0.1V + 0.0060V ² (m)	0.1V + 0.0158V ² (m)
	J _m ≥	6.43 m/s ²	2.44 m/s ²
Type-0 test with engine connected	V	80% V _{max} ≤ 160 km/h	
	s ≤	0.1V + 0.0067V ² (m)	
	J _m ≥	5.76 m/s ²	
	F _d	6.5–50 daN	6.5–50 daN

Table 8.3(b): Summary of Test Conditions and Minimum Service and Secondary Braking System Performance Requirements for Type-I Tests for Category M₁ and N₁ Vehicles in UN Regulation 13H

Type-I Test (Fade and Recovery Test)	V_1 (km/h)	V_2 (km/h)	Number of Brake Applications (n)
	$80\% V_{max} \leq 120 \text{ km/h}$	$0.5V_1$	15

V = vehicle road (test) speed (km/h).

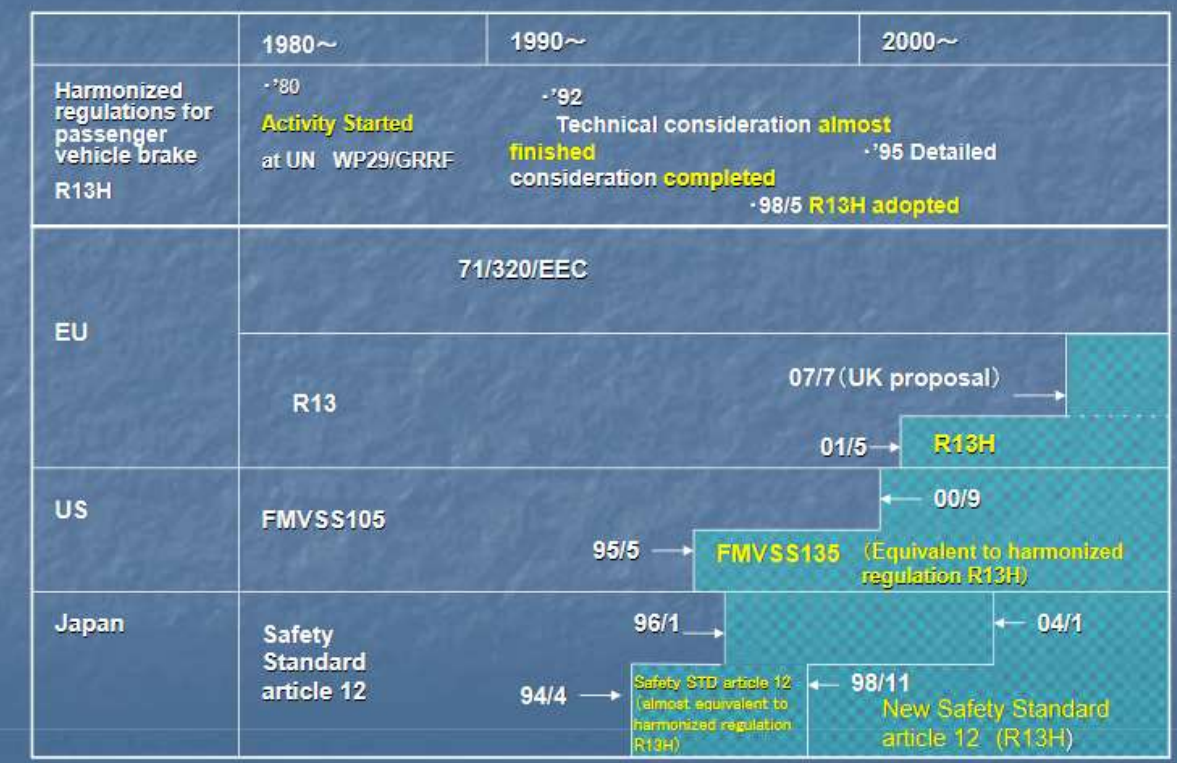
s = stopping distance (m).

j_m = mean fully developed deceleration (m/s^2).

F_d = Force applied by the driver to the brake pedal, also termed force applied to foot control (daN).

V_{max} = maximum vehicle road speed (km/h).

(1) History of harmonized brake regulations for passenger vehicles



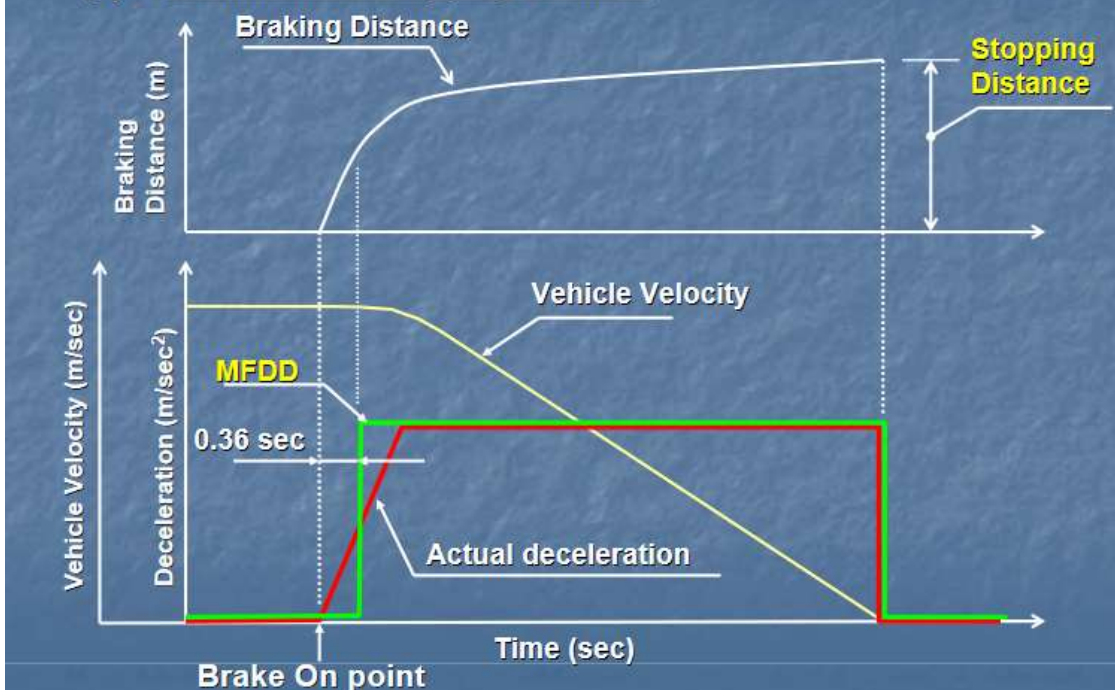
source https://www.jasic.org/j/07_wp29/pdf/2005/3rd_Expert_Meeting_j.pdf

5. Terminology in Brake Regulations

9

(1) Stopping distance / MFDD

(1)-1. Definition of Stopping distance

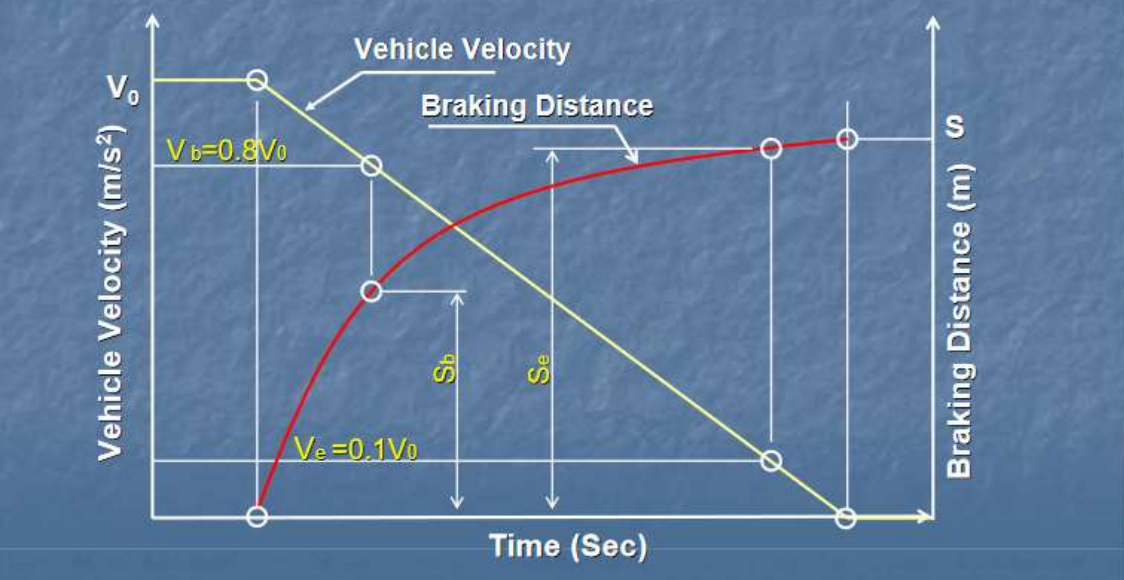


(5) Terminology in Brake Regulations

10

(1)-2. Definition of MFDD (Mean Fully Developed Deceleration)

$$MFDD \quad d_m = \frac{v_b^2 - v_e^2}{25.92 (S_e - S_b)} \quad m / s^2$$



5. Terminology in Brake Regulations

11

(1)-3. Conversion of MFDD to Stopping distance

$$d_m = \frac{0.0386 V_0^2}{S - 0.10 V_0}$$

$$S = 0.01 V_0 + \frac{0.0386 V_0^2}{0.60 (d_m)}$$

d_m = MFDD Mean Fully Developed Deceleration (m/sec^2)

S=Stopping distance (m)

V_0 =Initial vehicle speed (km/h)

5. Terminology in Brake Regulations

12

(2) Brake/Steering operation

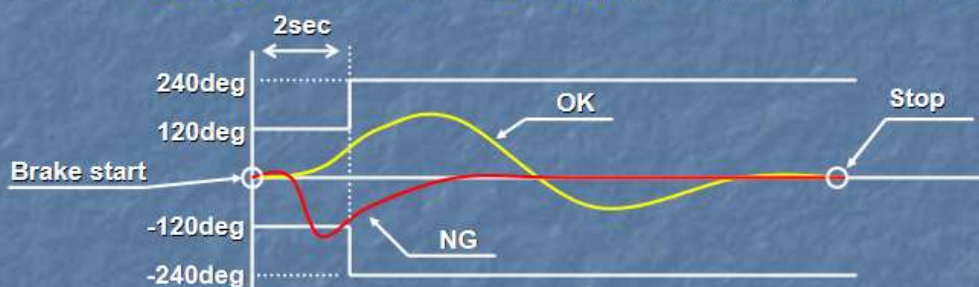
(2) -1. Pedal effort

It is permitted until Max. 500N with no wheel locking

(2) -2. Steering correction

It is permitted under following condition

- 120 deg at first 2 sec
- 240 deg in total until vehicle stop



(2) -3. Wheel lock

- Wheel lock is not allowed over 15km/h vehicle speed

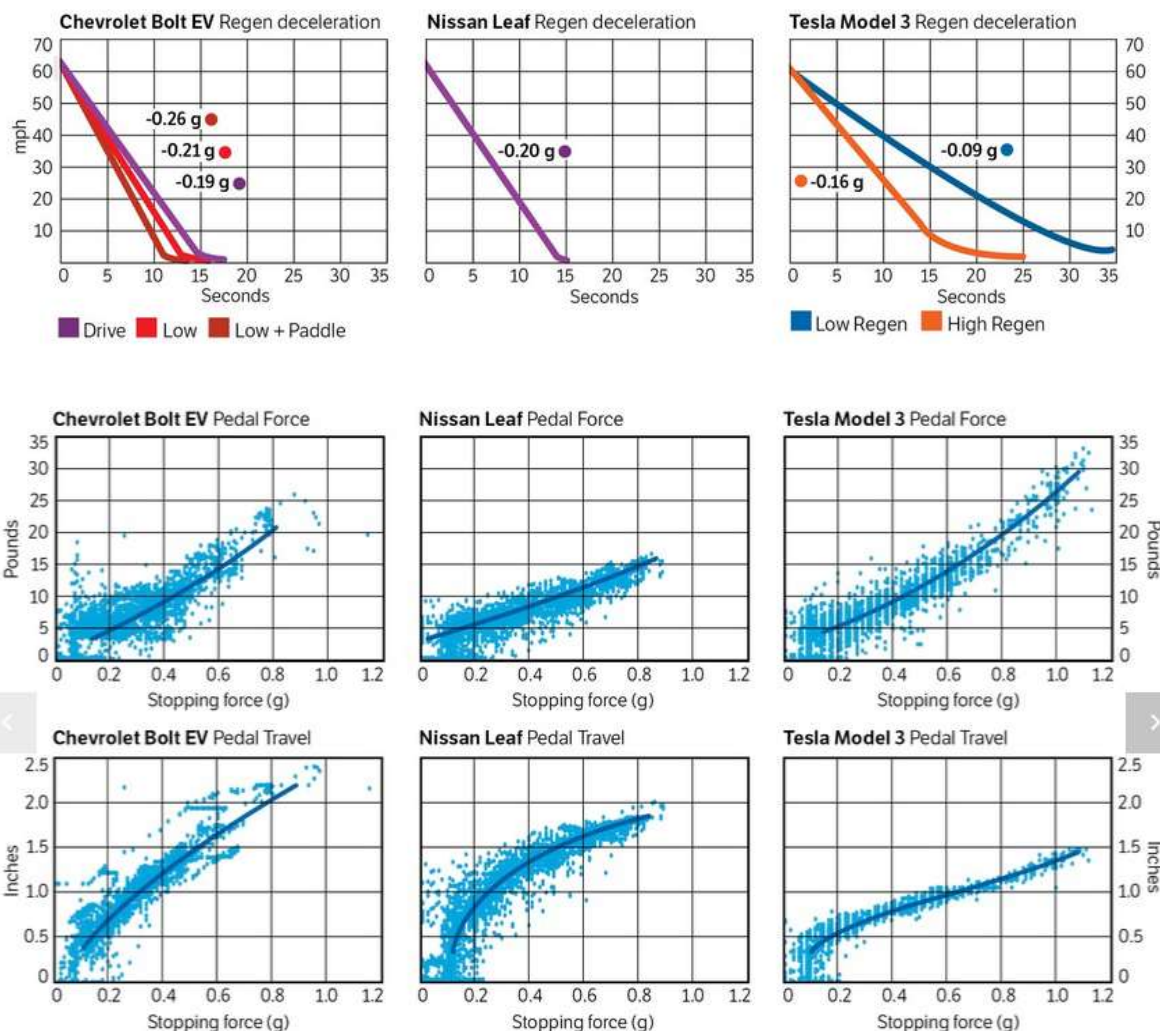
5.10 FREINAGE REGENERATIF VE

Vehicle Dynamics and Traction control for Maximum Energy Recovery

http://www2.warwick.ac.uk/fac/sci/wmg/research/lcvtp/news/hevc11/ws8_review_may11.pdf

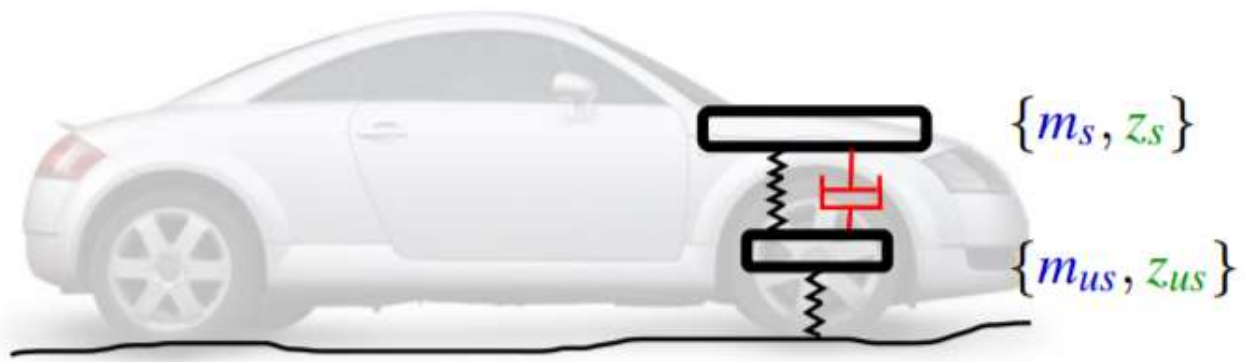
1. Implémentation powertrain + freins dans Dymola
2. Intégration dans Matlab/Simulink
3. Mise en œuvre du modèle Simulink dans CarMaker

<https://www.motortrend.com/cars/tesla/model-3/2017/the-automobile-2-0-chevrolet-bolt-ev-premier-vs-nissan-leaf-sl-vs-tesla-model-3-long-range/>



6 DYNAMIQUE VERTICALE - CONFORT

6.1 ILLUSTRATION



6.2 RESSOURCES

En introduction, ces deux articles de Julian Edgar sur autospeed :

1. https://www.autospeed.com/cms/a_111836/article.html@populararticle
2. https://www.autospeed.com/cms/a_111837/article

Une thèse avec une biblio très riche :

Bennett, L J (2012) **Ride and handling assessment of vehicles using four-post rig testing and simulation** PhD, Oxford Brookes University

▷ <https://radar.brookes.ac.uk/radar/items/7fc3dce7-8da4-4362-a5dc-df16a19c1683/1/>

[Passive and Active Control of Road Vehicle Heave and Pitch Motion](#) (Karnopp, 1987)

6.3 NORMES

ISO 2631-1 : Vibrations et chocs mécaniques - Évaluation de l'exposition des individus à des vibrations globales du corps

<https://www.iso.org/fr/standard/45604.html>

ISO 5805:1997(en)

Mechanical vibration and shock — Human exposure — Vocabulary

6.4 PLAGES DE FREQUENCE

0-25 Hz : ride & handling

0-100 Hz : comfort & harshness

50-1000 Hz : structure borne noise

In 2002, Vanhees and Maes [39] wrote a paper describing the test and evaluation methods used by Tenneco Automotive to characterise a vehicle on a four-post rig. The paper explains how the NVH behaviour of vehicles is divided into three main areas. The 0-25 Hz range is the Ride and Handling range, the 0-100 Hz is the Comfort and Harshness range and the 50-1000Hz range is the concerned with Structure Borne Noise from the vehicle. The authors explain the

(Bennett, 2012)

6.5 PRIMARY RIDE / SECONDARY RIDE

https://www.fev.com/fileadmin/user_upload/Media/TechnicalPublications/Chassis/V0815_FISITA2008_Objective_Evaluation_F20080319-Paper_01.pdf

Primary ride is generally associated with rigid body movements in the frequency range from 0–4 Hz, whereas **secondary ride** is defined as vibrations >4 Hz exposed to the driver. The item secondary ride is chosen since this relates the most to what normal customers define as ride comfort. Moreover the secondary ride does not have the contradiction of comfort and (body) control, which is well known from primary ride

6.6 PRINCIPAUX MODES 0-30 Hz

Les ordres de grandeur des fréquences ci-dessous sont issues d'une note de 1983 (!).

A remettre d'actualité, donc ...

Fréquence (Hz)	Description	Raideurs	Masses et inerties

1	pompage TAV	raideur verticale du ressort AV	masse TAV
1.4	tangage caisse	raideurs verticales TAV+TAR	inertie en tangage de la caisse
1.9	oscillation longi lors d'un à-coup de couple en 1e	raideur en torsion de la transmission (du moteur aux roues) + raideurs longis du TAV et du pneu AV	Inertie en rotation volant moteur + masse caisse
2.7	roulis caisse	raideurs antiroulis TAV+TAR	inertie en roulis de la caisse
2.8	transversal caisse	raideur de ballant des 4 pneus	masse caisse
3	tassemement de siège	raideur verticale siège	masse passager
3.2	oscillation longi lors d'un à-coup de couple en 2nde	idem 1.9 Hz avec une nuance : la raideur en torsion entre le volant moteur et les roues augmente lorsqu'on monte les rapports, donc la fréquence propre de la torsion de boite également (prise isolément). Elle se rapproche des premières fréquences de la suspension moteur.	Idem 1.9 Hz avec une nuance : la démultiplication étant plus faible, l'inertie du volant moteur diminue
3.4	lacet caisse	raideur de ballant des 4 pneus	inertie en lacet de la caisse
4.3	oscillation longi lors d'un à-coup de couple en 3e	cf modes à 1.9 et 3.2	cf modes à 1.9 et 3.2
4.7	tangage caisse (trains bloqués)	raideurs verticales des pneus	inertie en tangage de la caisse
4 à 5	oscillation buste sur dossier	raideur longi dossier	masse buste

5	oscillation longi lors d'un à-coup de couple en 4 ^e		
6	roulis caisse (trains bloqués)	raideurs verticales des pneus	inertie en roulis de la caisse
9	longi moteur	somme des raideurs longis des tampons moteur	masse moteur + inertie tangage
14	hachis moteur	raideur verticale des tampons	masse moteur + inertie tangage
14	échappement	flexion	masse ligne échappement
15	battement de roue AV	raideur verticale pneu + raideur verticale du train partiellement figé	MNS AV
16	battement de roue AR	raideur verticale pneu + raideur verticale du train partiellement figé	MNS AR

Données tirées d'une conférence LMS en 2013 :

Positionnement des modes du moteur

Tamis : 5 à 8 Hz
Ballant : 6 à 9
Hachis : 7 12
Galop : 13 20
roulis : 8 11
lacet : 11 20

6.7 POMPAGE-TANGAGE (< 2HZ)

6.7.1 FREQUENCE DE POMPAGE

1.5 Hz bien toléré (~ fréquence marche à pied)

2.0 Hz trop raide

6.7.2 EQUILIBRE EN POMPAGE

un véhicule homogène avec un bon accord AV/AR est un véhicule qui pompe à plat avec des mouvements soft et bien freinés afin d'éviter les tassements.

6.7.3 EQUILIBRE EN TANGAGE

L'équilibre en tangage est fortement lié à l'équilibre en pompage. Au cours de la MAP, nous cherchons à éviter tout mouvement de tangage, car ceux-ci rendent le véhicule peu confortable, il est en effet préférable d'avoir un mouvement de pompage que de tangage.

Un véhicule bien équilibré en tangage est un véhicule qui « transforme » un mouvement de tangage en un mouvement de pompage.

Au passage d'un obstacle, le train arrière est sollicité après le train avant (l'écart dépend de la vitesse et du l'empattement).

Les écarts de fréquence propre permettent de rephaser les 2 trains rapidement et limiter la durée où les trains sont en opposition de phase (tangage)

6.7.4 FLAT RIDE

Cet équilibre en tangage a été popularisé par Maurice Olley dès 1930

Cependant, dans (Crolla, 1999), l'auteur montre que le respect des précos de M.Oolley sur le rapport de raideur des suspensions av/ar n'a d'impact que sur l'amplitude du mouvement de tangage, qui peut jouer un rôle subjectif mais ne fait généralement pas partie des critères objectifs de mesure du confort.

Il rappelle également que la préconisation d'Olley n'est valable que pour une vitesse donnée

6.8 COMPROMIS

- une raideur de suspension importante favorise la tenue de la caisse mais dégrade l'isolation vibratoire (dilemme tenue de caisse – isolation vibratoire) ;
- une raideur de suspension importante réduit les variations de l'effort vertical du pneumatique donc améliore la tenue de route mais augmente l'accélération verticale de la caisse lors des franchissements d'obstacles (dilemme confort - tenue de route) ;
- un coefficient de frottement visqueux important diminue le battement de roue et améliore le confort visuel mais accroît l'accélération verticale.

http://autospeed.com.au/cms/title_Ride-Quality-Part-1/A_111836/article.html

The oscillation frequency of the car body is determined by front and rear spring (dampers provide damping), wheelbase, pitch inertia and velocity (wheel excitation). All these parameters go into a differential equation which can be solved to 2 "motion" centers of the body movement - so called "Bounce Center" and Pitch Center - and one of these motion centers is outside of the wheelbase (bounce) and one is within the wheel base. You can find more of this on www.dynatune-xl.com with some indications on how to tune.

Ideally one would like the bounce center to be as "far" as possible from the car (parallel heave) and the pitch center as near as possible to the front axle (since the driver usually sits there) and miraculously this combination happens usually when the rear frequency is higher. Typically this method of working is for the utmost importance of wing cars since they are pitch sensitive and any changes in down-force distribution does immediately affect performance. Yet, to come back to your question I do not agree with Milliken that generally on a RWD car the front ride frequency should be higher than the rear.

Paul Fickers ("Ride Frequency: Front greater than rear? Why?" sur LinkedIn)

6.9 MODELISATION AMESIM SIMPLIFIEE

http://unit-amesim.insa-rouen.fr/co/analyse_1.html

Suspensions
Introduction
Suspension mécanique
Modélisation d'une suspension mécanique
Critères de confort et de tenue de route
Recherche des valeurs propres du modèle monoroue
Exploitation du modèle avec AMESim
Analyse du confort et de la tenue de route
Conclusion
Suspension hydraulique
Suspension hydropneumatique Citroën

Critères de confort et de tenue de route

Qualité d'une suspension

On peut introduire deux critères qui permettent de « juger » de la qualité d'une suspension.

- une bonne suspension doit permettre au véhicule de suivre les ondulations de la route afin d'assurer une bonne manœuvrabilité du véhicule ;
- en ce qui concerne le confort des passagers, une bonne suspension est sensée isoler au maximum les passagers des perturbations verticales issues de la route (entrées sol).

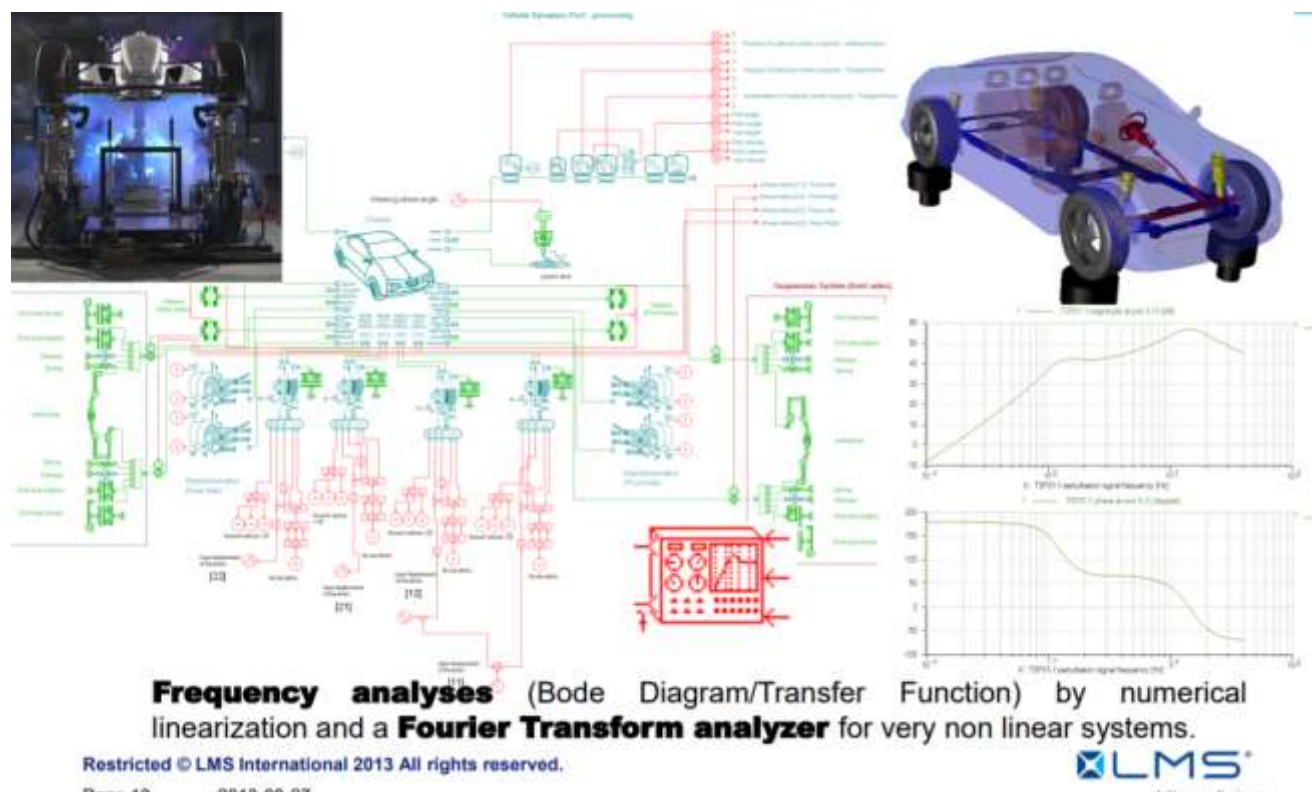
Ces deux critères sont souvent représentés par des fonctions de transfert typiques. En effet, les entrées sol peuvent être perçues comme des perturbations sinusoïdales de fréquences variables : une même bosse, franchie à différentes vitesses induit une entrée de fréquence différente mais d'amplitude en déplacement toujours identique. C'est pour cela que l'on utilise des réponses en fréquence.

6.10 CONFORT – VIBRATIONS

6.10.1 SHIMMY

[Tyre models for shimmy analysis : from linear to nonlinear \(pdf\)](#)

6.10.1.1 ANALYSE FOURIER SOUS AMESIM



6.10.2 CRITÈRES

Critères de confort pour simu semi-active

https://www.researchgate.net/publication/260290013_Performance_Measures_of_Comfort_and_Reliable_Space_Usage_for_Limited-Stroke_Vehicle_Suspension_Systems

Privilégie le jerk plutôt que l'accélération RMS

Utilise une fonction sigmoïde pour contraindre les débattements de suspension

Voir la thèse de Ian Storey

https://www.researchgate.net/publication/260290319_Performance_Measures_and_Control_Laws_for_Active_and_Semi-Active_Suspensions_Acknowledgements

6.10.3 ESSAI BANC 4 VÉRINS

Road profile excitation on a vehicle measurements and indoor testing using a four-post rig

<http://www.theoryinpracticeengineering.com/resources/7-post/four-post%20test%20rig.pdf>

6.11 PROFIL DE ROUTE

6.11.1 STANDARDS

British Standards Institution, 1996, Mechanical vibration – Road surface profiles – Reporting of measured data BS 7853:1996 ISO 8608:1995, London: BSI

6.11.2 IRI (INTERNATIONAL ROUGHNESS INDEX)

Sayers, M.W. (1995), On the Calculation of International Roughness Index from Longitudinal Road Profile, Transportation Research Record 1501, pp. 1-12.

The IRI is a measure of cumulative suspension displacement of the vehicle normalised by the length of the profile, in units of mm/m.

6.11.3 QUANTIFICATION

$$G_q(n) = C_{sp} n^{-W}$$

where $G_q(n)$ is the power spectral density (PSD) of the road profile, n is the spatial frequency in m^{-1} , C_{sp} and W are two constants representing the excitation energy and PSD slope, respectively.

Table 2. Parameters for six representative road types.

No.	Description	W	C _{sp}
1	Smooth Runway (SR)	3.8	4.3 × 10 ⁻¹¹
2	Smooth Highway (SH)	2.6	1.9 × 10 ⁻⁸
3	ISO-Level B (ISO-B)	2	6.4 × 10 ⁻⁷
4	Highway with Gravel (HG)	2.1	4.4 × 10 ⁻⁶
5	ISO-Level E (ISO-E)	2	4.1 × 10 ⁻⁵
6	Pasture (PA)	1.6	3 × 10 ⁻⁴

La relation ci-dessus est parfois écrite

$$G_d(n) = G_d(n_0) \times \left(\frac{n}{n_0} \right)^{-w}$$

avec

G_d – Displacement PSD

n – Spatial frequency (cycles/m)

n₀ – Reference spatial frequency (0.1 cycles/m)

w – Exponent

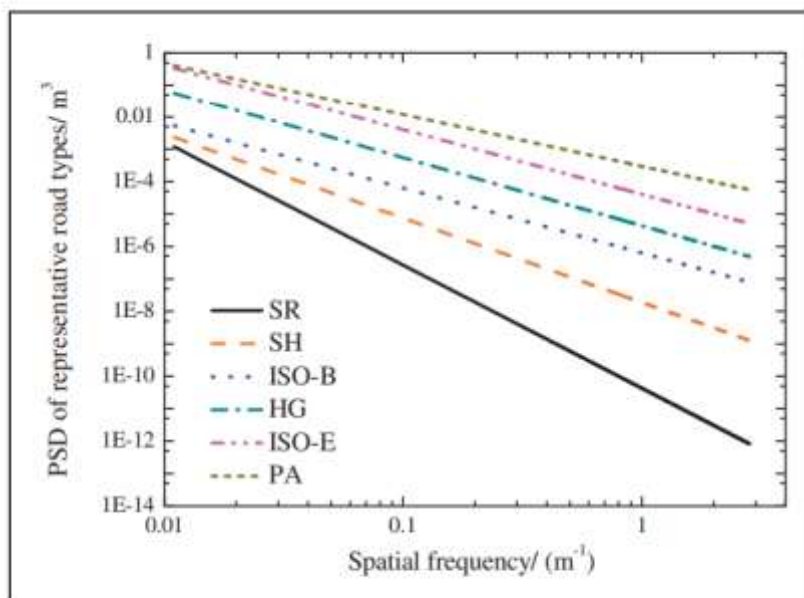


Figure 3. PSD (power spectral density) of six representative road types.

origine et légende inconnues

The standard explains that in the case where the exponent is equal to 2, the velocity PSD is constant along both frequency and spatial frequency domains. The standard presents a classification of road surfaces A to H which all have an exponent of 2. The profiles A to E represent: 'Very Good', 'Good', 'Average', 'Poor', and 'Very Poor' roads respectively :

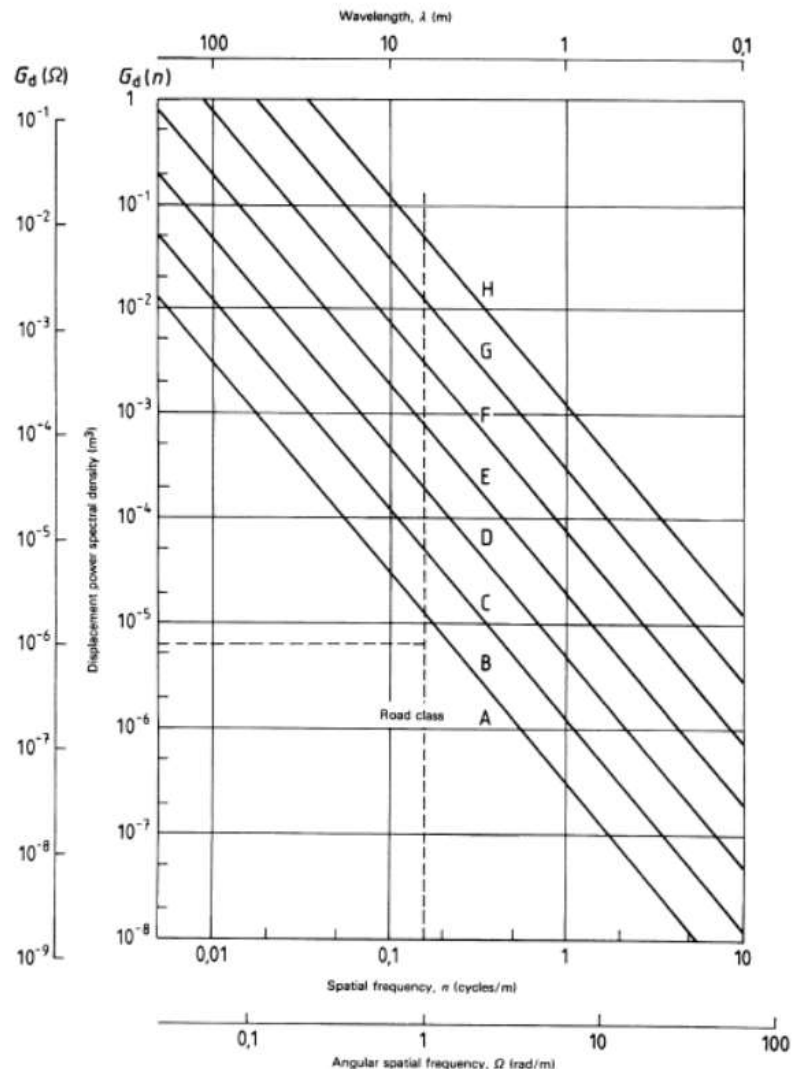


Figure 2-2 – Road profile classification – ISO 8608 [4]

6.11.4 ESTIMATION

Road profile estimation and classification

https://www.researchgate.net/publication/312057858_Road_Excitation_Classification_for_Semi-Active_Suspension_System_Based_on_System_Response

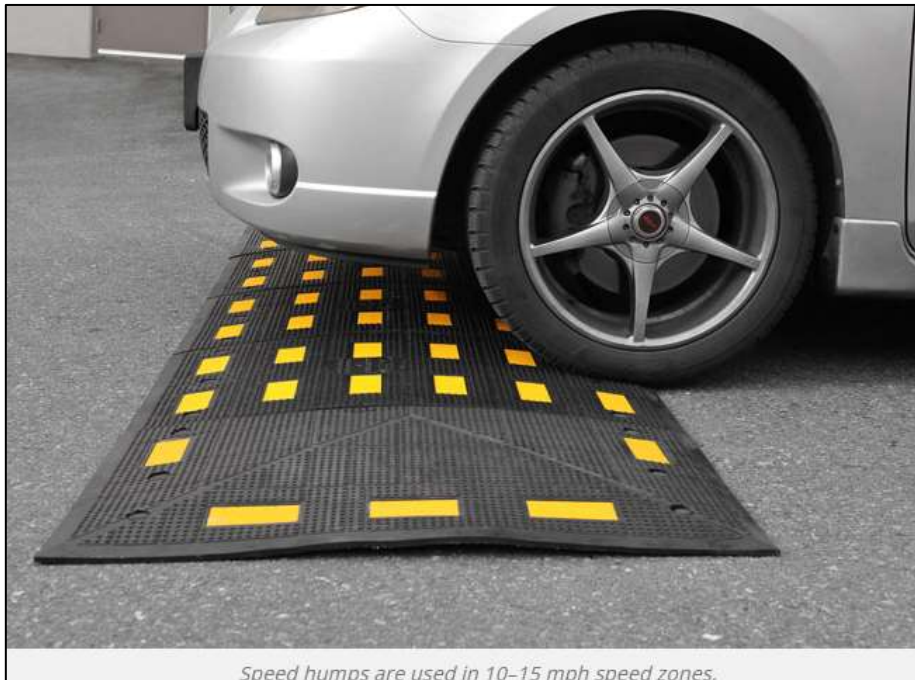
6.11.5 GÉNÉRATION DE PROFIL DE ROUTE PAR IA

Plutôt orienté endurance :

Artificial road input data generation tool for vehicle durability assessment using artificial intelligence (2015)

<https://etheses.bham.ac.uk/id/eprint/6156/1/Ogunoiki15PhD.pdf>

6.11.6 OBSTACLES ROUTIERS



Speed humps are used in 10–15 mph speed zones.

Speed hump



Speed bumps encourage speed reduction to 2–10 mph.

Speed bump



Speed cushion / coussin berlinois



Speed table

6.11.7 COMPARAISON DE FFT PAR PROFIL DE ROUTE

Dans <https://journals.sagepub.com/doi/pdf/10.1177/1687814017726004>



Table 3. Test performed.

Test	Surface/stress	Speed (km/h)
1	Asphalt	50
2	Gravel (raw)	15
3	Pavé	30
4	Speed hump	20

Figure 6. Proving surfaces – 1: asphalt; 2: gravel; 3: pave; 4: speed hump.

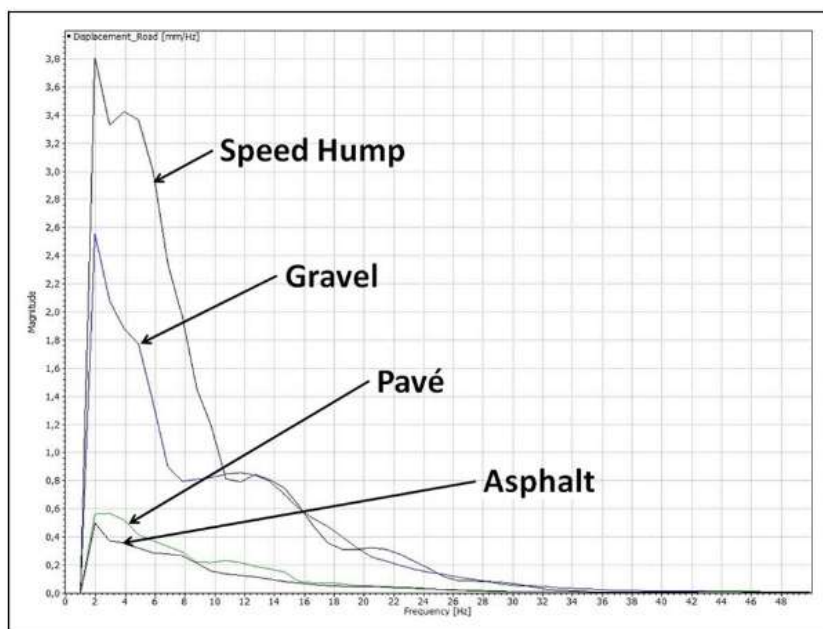


Figure 7. FFT plot for each surface.

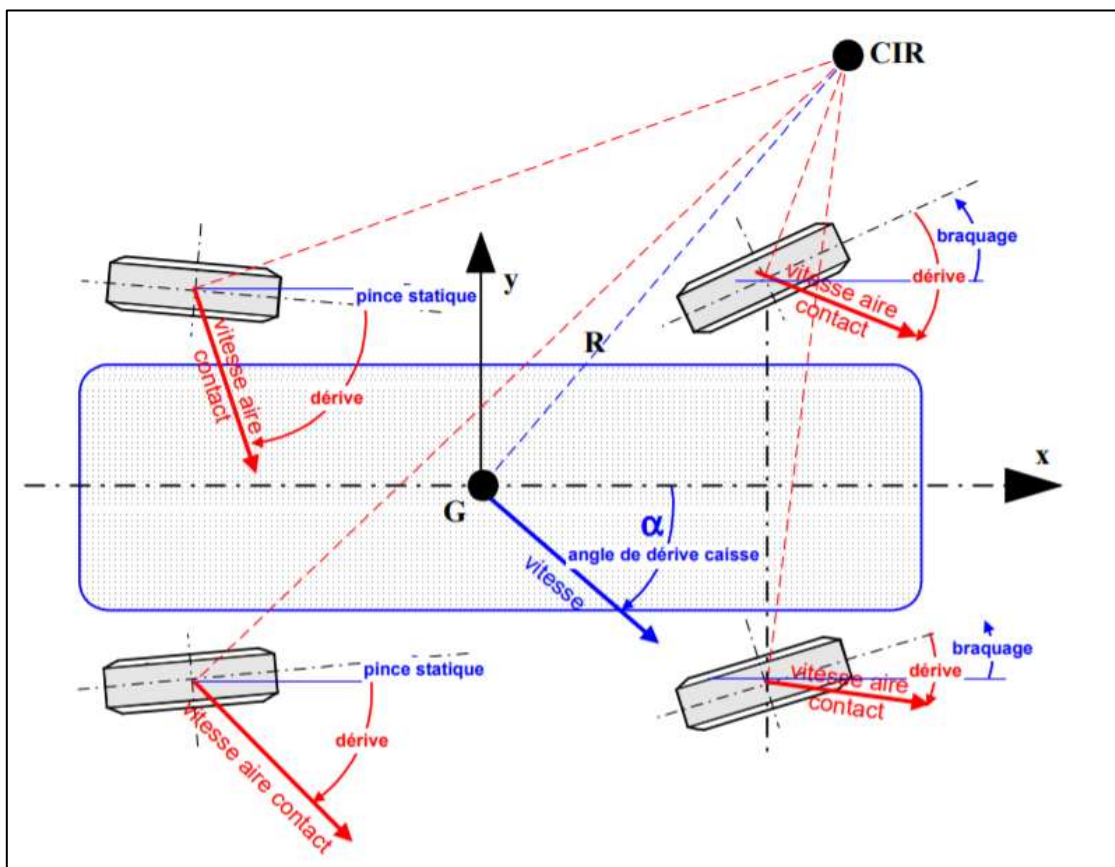
6.12 FRONT-REAR INTERCONNECTION

Packard, Citroen and BMC products with Hydrolastic and Hydragas systems

7 DYNAMIQUE EN VIRAGE

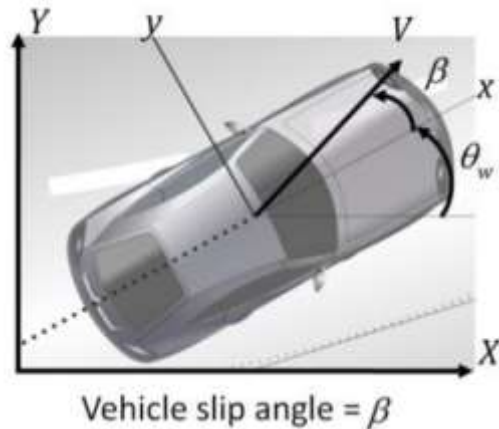
7.1 ANGLES DE DERIVE

Nota : la figure ci-dessous ne correspond évidemment pas à une situation de conduite réaliste ☺



7.1.1 DERIVE VEHICULE

La dérive véhicules est définie par l'angle entre son axe longi et son vecteur vitesse



A lire ! <https://www.oxts.com/app/uploads/2014/11/Slip-Angle-Accuracy-120802.pdf>

A faible vitesse, l'angle de dérive est "positif" (vers l'intérieur du virage).

A vitesse plus élevée, du fait des dérives pneumatique, l'angle de dérive véhicule devient négatif (vers l'extérieur du virage).

La vitesse à laquelle l'angle de dérive est nul est parfois appelée "vitesse tangente".

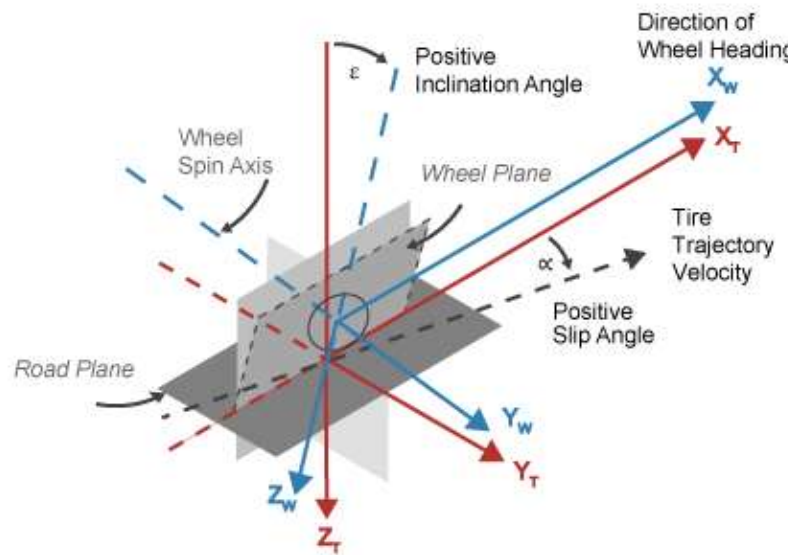
7.1.2 DERIVE PNEU

L'angle de dérive pneu est également donné par l'angle formé entre le plan médian de la roue, et le vecteur vitesse porté par la trajectoire.

Le signe de la dérive pneu est évidemment dépendant des conventions globales utilisées (ISO vs SAE, cf §3)

Dans la convention SAE, le vecteur Z étant vers le bas, un angle de dérive (positif vers la droite) correspond à une roue braquée à gauche par rapport au vecteur vitesse, et donc à un virage à gauche

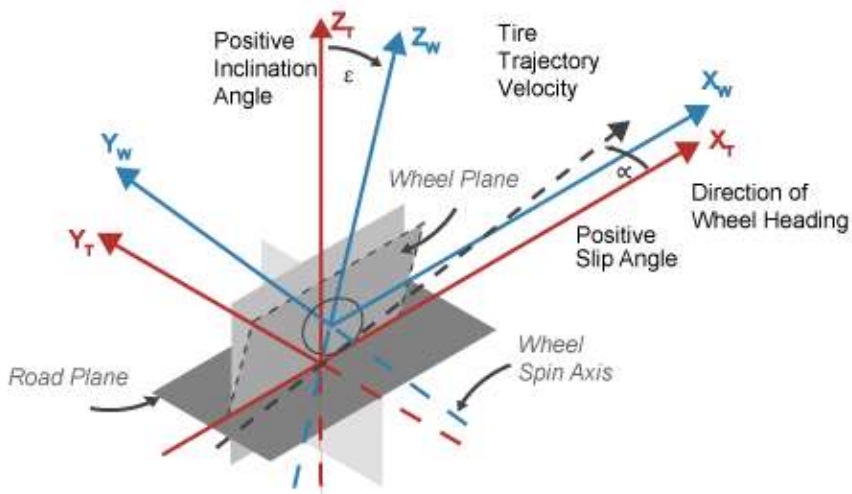
Z-Down Orientation



<https://www.mathworks.com/help/vdynblk/ug/coordinate-systems-in-vehicle-dynamics-blockset.html>

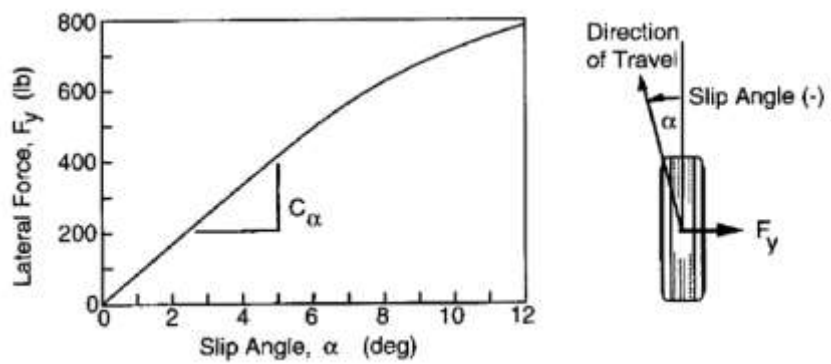
C'est évidemment l'inverse dans la convention ISO. Ci-dessous l'angle positif correspond à un plan de roue sur "la droite" du vecteur vitesse, donc à un braquage à droite.

Z-Up Orientation^[1]



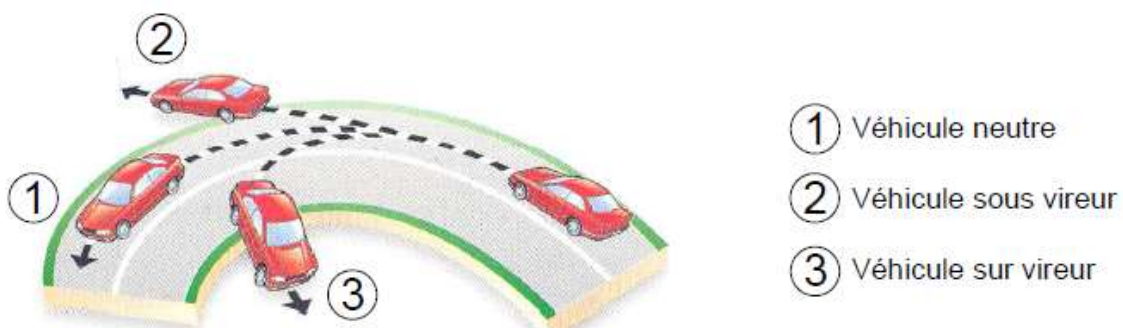
Ayant lu le passage ci-dessous ([ici](#), Schlueter 2012), du coup, je ne comprends pas le passage mis en gras :

Tire lateral forces are created as lateral slip angle is increased. At small slip angles, the relationship is linear, and is characterized by the cornering stiffness, C_a , or the slope of the lateral force curve vs. slip angle at $\alpha = 0$ (or small slip angles). **A negative slip angle produces a positive lateral force (to the right).** SAE convention defines the cornering stiffness as the negative of the lateral force slope, thus C_a is positive.



7.2 VIRAGE EN REGIME PERMANENT

7.2.1 DEFINITION SOUS-VIRAGE / SURVIRAGE



Sous-vireur : la dérive avant est supérieure à la dérive arrière, le véhicule a tendance à sortir de sa trajectoire. Un sur- braquage peut être nécessaire.

Survireur : (comportement souvent jugé « instable »)

la dérive avant est inférieure à la dérive arrière, trop de dérive du train arrière, le véhicule rentre trop dans sa trajectoire par rapport au rayon initialement demandé. Un contre-braquage au volant peut être nécessaire.

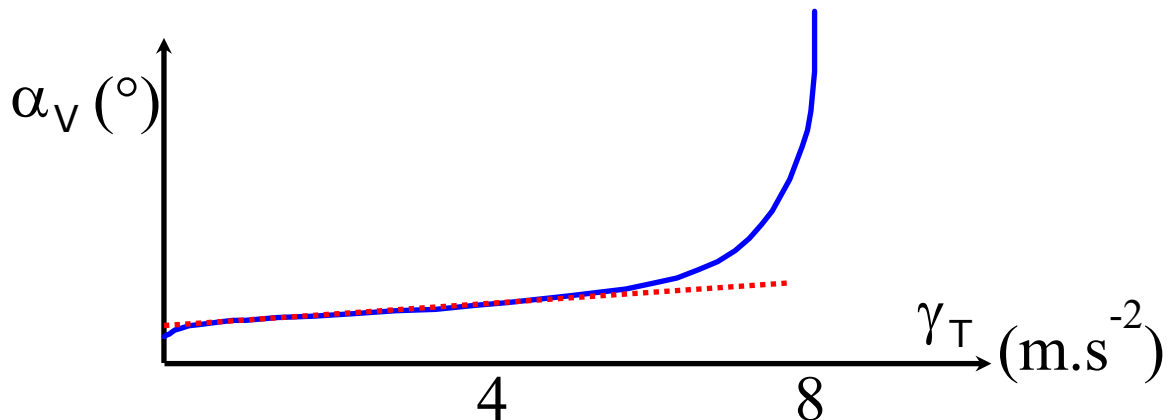
Vehicle dynamics and self-steering behaviour were first systematically studied in the nineteen-thirties. The term *understeering*, which had been introduced by Lanchester, was complemented with the terms *oversteering* and *neutral behaviour*. These terms were first published by Maurice Olley in 1938 (Fig. 1.5), although he had already investigated vehicle dynamics at General Motors for many years before. As early as 1931 he had studied the importance of roll steer and the influence of tire pressure on vehicle stability. Later he established the definition of under- and oversteering, depending on the slip angles occurring at the front and rear axles. If these slip angles were greater at the front axle than at the rear axle, this was described as understeering, while the opposite was defined as oversteering. When these angles were similar at both axles, the vehicle behaviour was described as neutral. Nowadays, this definition is no longer used and has been replaced by a definition based on the occurring steering wheel angle gradient in relation to the lateral acceleration (see Chap. 5).

7.2.2 GRADIENT DE SOUS-VIRAGE

Le comportement du véhicule peut être quantifié par une grandeur, qu'on appelle gradient de sous-virage / understeer gradient (et "dynamique angulaire" chez Renault), et qui représente la variation d'angle volant, dans un virage à rayon constant), en fonction de l'accélération latérale.

$$da = \frac{\partial \alpha_v}{\partial \gamma_t} \Big|_{R=cste}$$

Cette quantité reste quasi-constante sur une bonne partie de la plage de fonctionnement d'un véhicule, tant que le pneu fonctionne dans sa partie linéaire principalement.



En partant d'un modèle bicyclette, on montre que l'angle de braquage à la roue évolue avec la vitesse comme suit :

$$\delta = \frac{L}{R} + \left(\frac{m_f}{C_f} - \frac{m_r}{C_r} \right) \frac{v^2}{R}$$

où

- δ angle de braquage à la roue (radians)
- L empattement (m)
- R rayon du virage (m)
- m_f masse train avant (kg)
- m_r masse train arrière (kg)
- C_f rigidité de dérive du train avant (N/rad)
- C_r rigidité de dérive du train arrière (N/rad)
- v vitesse (m/s)

On peut réécrire simplement

$$\delta = \frac{L}{R} + K \cdot a_y$$

où K est le gradient de sous-virage et a_y l'accélération latérale.

Si les rigidités de dérive sont en $N/\text{°}$, alors les termes $\frac{m_f}{C_f}$ et $\frac{m_r}{C_r}$ sont en $\frac{kg}{N/\text{°}}$ soit en $\frac{\text{°}}{m/s^2}$

Selon les habitudes K peut également être exprimé en $\text{°}/g$

On peut aussi l'exprimer en degrés de braquage au volant en le multipliant par la démultiplication de direction.

Les mélanges de genre sont fréquents : chez Kelvin Tse on voit par exemple un gradient de sous-virage tout d'abord défini en $\text{rad}/(\text{m}/\text{s}^2)$ [ici](#)

The tendency for a vehicle to require more (or less) steering input relative to the Ackermann steer angle is a measure of understeer. The gain due to lateral acceleration is the understeer gradient.

$$\delta = \frac{L}{R} + K a_y$$

Where:

- δ is the steering angle [rad]
- L is the wheelbase of the car [m]
- R is the radius of the turn [m]
- a_y is the lateral acceleration [m/s^2]
- K is the understeer gradient [$\text{rad}/\text{m}/\text{s}^2$]

puis dans le [billet suivant](#) K passe en rad/g :

In our [last article](#), we defined understeer as the tendency for a vehicle to require more (or less) steering input relative to the Ackermann steer angle. The gain due to lateral acceleration is the understeer gradient.

$$\delta = \frac{L}{R} + K a_y$$

Where:

- δ is the steering angle [rad]
- L is the wheelbase of the car [m]
- R is the radius of the turn [m]
- a_y is the lateral acceleration [m/s^2]
- K is the understeer gradient [rad/g]

7.2.3 FLEXIBILITE DE DERIVE (CORNERING COMPLIANCE)

On trouve aussi parfois, notamment chez les auteurs anglo-saxons, avec $W=m.g$

$$\delta = \frac{L}{R} + \left(\frac{W_f}{C_f} - \frac{W_r}{C_r} \right) \frac{v^2}{Rg}$$

où W_f et W_r sont les poids avant et arrière en N.

Le gradient de sous-virage peut être réécrit en introduisant les flexibilités de dérive (cornering compliances) "par g d'accélération", notées D. On repart de :

$$\begin{aligned}\delta &= \frac{L}{R} + K \cdot a_y \\ \delta &= \frac{L}{R} + K \cdot g \cdot \frac{a_y}{g} \\ \delta &= \frac{L}{R} + \left(\frac{m_f}{C_f} - \frac{m_r}{C_r} \right) g \frac{a_y}{g}\end{aligned}$$

or using the weight on each axle $W = mg$:

$$\delta = \frac{L}{R} + \left(\frac{W_f}{C_f} - \frac{W_r}{C_r} \right) \frac{a_y}{g}$$

Then we introduce the cornering compliances

$$D = \frac{W}{gC}$$

so that

$$\delta = \frac{L}{R} + (D_f - D_r)a_y$$

Since W is in N, and C in N/°, we have W/C in ° and then D in °/g

Ces flexibilités peuvent être exprimées en rad/g ou en °/g.

Ordre de grandeur pour la flexibilité des pneus : 1 à 3 °/g

Descendre sous la valeur de 1° est difficile pour les manufacturiers. Plus la dérive spécifique demandée est faible, plus le coût de fabrication du pneu augmente.

Pour un pneu avec une charge verticale de 400kg, et une rigidité de dérive de 1400 N/°, on a

$$D_r = \frac{m_r g}{C_r} = \frac{400 * 9.8}{1400} = 2.8^\circ/g$$

Dans (Milliken & Milliken, 1995), page 172, on lit :

where F_F and F_R and F are lateral forces
 W is the gross weight
 C_F, C_R are the respective cornering slopes

Since
$$-\ell K \left(\frac{V^2}{R} \right) = -\ell K \left(\frac{V^2}{gR} \right) g = -\ell K A_Y g$$

$$\ell K = - \left(\frac{W_F/C_F}{g} - \frac{W_R/C_R}{g} \right)$$

$$57.3 (\ell K) = D_F - D_R \quad (5.53)$$

where D_F and D_R are the Bundorf cornering compliances (Ref. 28) at the front and rear, respectively, in deg./g.

Warning : chez Milliken K désigne le stability factor et pas le gradient de sous-virage

04/2021 : discussion avec Kelvin Tse sur ce qu'il a écrit sur

<https://kktse.github.io/jekyll/update/2019/01/06/cornering-compliance-identification.html>

Normalizing the acceleration by g yields the cornering compliance definition of the understeer gradient:

$$K = \frac{m_f g}{C_f} - \frac{m_r g}{C_r} = D_f - D_r$$

Where:

- D_f represents the front axle cornering compliance [$\frac{\text{rad}}{g}$]
- D_r represents the rear axle cornering compliance [$\frac{\text{rad}}{g}$]

Les termes en mg/C sont étranges, puisqu'homogènes à du ° (ou du rad), et pas du °/g.

7.2.4 CONTRÔLE VS STABILITÉ

7.2.5 MARGE STATIQUE / STATIC MARGIN

Claude Rouelle (01/2022)

For me static margin is about "what end of the car prevents you to go faster ?".

A vérifier (Tim Wright) :

The Milliken formulation is (from memory) $SM = -(aC_f - bC_r)/(C_f + C_r)/\text{Wheelbase}$

With the Miliken formulation it's normalised by the wheelbase which means you get similar numbers from a Smart and an S-Class.

Chez Duysinx (qui pour rappel note b et c les demi-empattements, alors que tout le monde utilise a et b :

$$e = \frac{b C_{\alpha_f} - c C_{\alpha_r}}{C_{\alpha_f} + C_{\alpha_r}}$$

7.2.6 STABILITY INDEX

Chez Danny Nowlan : <https://www.youtube.com/watch?v=0dGfDXo3nLQ> (10/2021)

$$STBI = \frac{aC_f - bC_r}{C_T L} - \frac{a^2 C_f + b^2 C_r}{V_x C_T L}$$

où L est l'empattement (noté wb dans la vidéo), et $C_T = C_f + C_r$

On a donc $STBI = SM/L$, où SM est la marge statique.

NB : attention à cette vidéo, où d'un côté du tableau C_f désigne la rigidité de dérive, et de l'autre (à [t=5'50](#)) l'effort latéral normalisé.

7.2.7 LES COURS DE DUYNSINX

<http://www.ingveh.ulg.ac.be/>

Voir [MECA0525](#) et notamment [MECA0525/11_MECA0525_VEHODYN1_SSTURN_2020-2021.pdf](#)

7.2.8 EXERCICE ENG-TIPS

Message du 05 Nov 2018 en fin de page sur <https://www.eng-tips.com/viewthread.cfm?qid=445691>

(NB : cibachrome = Bill Cobb)

OK, so make up a table as an array of Front Cornering Compliance (DF), Rear Cornering Compliance (DR) plus Lateral Response Time and Yaw Velocity Overshoot as key metrics for your issues. Since understeer (K) is simply the scalar difference between DR and DR, you can talk it all you want but your crew chief will have to guess which end of the car is THE problem if all you can say is that "Its understeering".

so:

DF DR K T_Ay and R_po is your score card. T_Ay is Ay response time (time to reach 90% of steady

state) and R_{po} is the yaw velocity overshoot during a quasi step steer input. Wheelbase is typical of a mid-sized car with a slight forward weight distribution. The model is linear, which is best to educate the masses.

DF	DR	K	T_Ay	R_po
3	2	1	.27	4.2
6	3	3	.30	18.1
4	3	1	.38	5.9
4	2	2	.24	8.7
3	3	0	.50	0
2	2	0	.33	0

So if you have a heavy understeering car (6,3), response time is good but the overshoot is NFG. So, you 'fix' the front by tightening it up (4,3) and the overshoot backs down but the response times (think bandwidth) are horrible (think fully loaded P/U truck). So now you 'fix' the rear down to 2 (tires, wheels, air pressure, compliance, axle weight) and drop the front to 4 and you have a maybe decent car (the 8% overshoot may take getting use to).

If all you can do is play instead of design, then all your magazine buddies will call for that famous 'NEUTRAL' car ($K=0.0$), Yes the overshoot is zero, but the response times are worse than a fully loaded armor plated hearse (which may be convenient for you at a track). Sure, getting the neutral steer really low front (and rear) cornering compliance car could be a player for you but there's no forgiveness by the car as your tires go on vacation, fuel tank is filled and some damage occurs to your aero package.

7.2.9 LES CONTRIBUTIONS AU SOUS-VIRAGE

<i>Understeer Component</i>	<i>Source</i>
$K_{tires} = \frac{W_f}{C_{af}} - \frac{W_r}{C_{ar}}$	<i>Tire cornering stiffness</i>
$K_{camber} = \left(\frac{C_{\gamma f}}{C_{af}} \frac{\partial \gamma_f}{\partial \phi} - \frac{C_{\gamma r}}{C_{ar}} \frac{\partial \gamma_r}{\partial \phi} \right) \frac{\partial \phi}{\partial a_y}$	<i>Camber thrust</i>
$K_{roll steer} = (\varepsilon_f - \varepsilon_r) \frac{d\phi}{da_y}$	<i>Roll steer</i>
$K_{lfc_s} = A_f W_f - A_r W_r$	<i>Lateral force compliance steer</i>
$K_{at} = W \frac{p}{L} \frac{C_{af} + C_{ar}}{C_{af} C_{ar}}$	<i>Aligning torque</i>
$K_{llt} = \frac{W_f}{C_{af}} \frac{2b\Delta F_{zf}^2}{C_{af}} - \frac{W_r}{C_{ar}} \frac{2b\Delta F_{zr}^2}{C_{ar}}$	<i>Lateral load transfer</i>
$K_{strg} = W_f \frac{rv + p}{K_{ss}}$	<i>Steering system</i>

-Gillespie, Thomas D., "Fundamentals of Vehicle Dynamics." Society of Automotive Engineers, Inc: Warrendale, PA. 1992. [13]

Exemples d'application numérique

- Contribution du roll steer

$$K_{rs} = (\varepsilon_f - \varepsilon_r) \frac{d\phi}{da_y} \quad (6.6)$$

Where ε_f - front roll steer coefficient = 0.033 deg/deg

ε_r - rear roll steer coefficient = -0.025 deg/deg

$\frac{d\phi}{da_y}$ - roll angle gradient with respect to lateral acceleration = 4.56 deg/g

Therefore,

$$K_{rs} = 0.26 \text{ deg/g}$$

- Contribution de la flexibilité latérale des trains

Lateral Force Compliance Steer:

$$K_{lfs} = A_f W_f - A_r W_r \quad (6.7)$$

Where A_f - front lateral force compliance steer coefficient = 5.42 e-04
 A_r - front lateral force compliance steer coefficient = -1.67 e-04

Therefore,

$$K_{lfs} = 1.02 \text{ deg/g}$$

- Contribution de la poussée de carrossage

$$K_{camber} = \left(\frac{C_{\gamma f}}{C_{\alpha f}} \frac{\partial \gamma_f}{\partial \phi} - \frac{C_{\gamma r}}{C_{\alpha r}} \frac{\partial \gamma_r}{\partial \phi} \right) \frac{\partial \phi}{\partial \alpha_y} \quad (6.8)$$

Where,

$$F_y = C_\alpha \alpha + C_\gamma \gamma$$

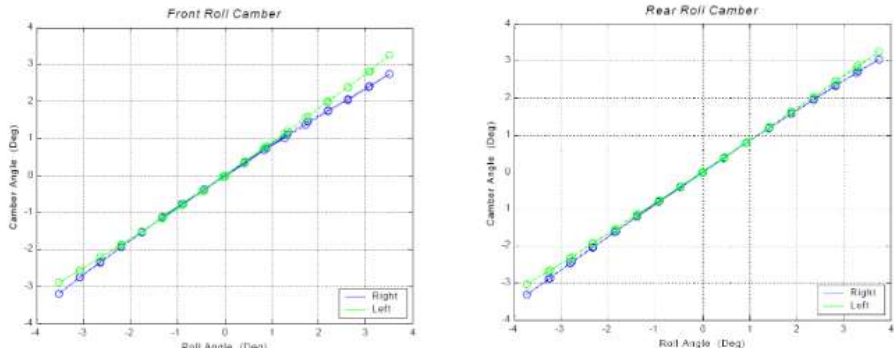


Figure 82: Camber Gradient

Where $C_{\gamma f}$ - front camber stiffness = 20.99 lb/deg

$C_{\gamma r}$ - rear camber stiffness = 20.46 lb/deg

$\frac{\partial \gamma_f}{\partial \phi}$ - front camber gradient = 0.8 deg/deg

$\frac{\partial \gamma_r}{\partial \phi}$ - rear camber gradient = 0.833 deg/deg

Therefore,

$$K_{camber} = -2.37 \text{e-004 deg/g}$$

- Contribution de la direction

$$K_{strg} = W_f \frac{rv + p}{K_{ss}} \quad (6.9)$$

Where
 r - wheel radius = 0.373 m
 v - caster angle = 0.129 rad
 p - pneumatic trail = 0.048 m
 K_{ss} - steering stiffness = 3690 N-m/deg

Therefore,

$$K_{strg} = 0.34 \text{ deg/ } g$$

- Contribution du moment d'alignement

Aligning Torque:

$$K_{at} = W \frac{p}{L} \frac{C_{af} + C_{ar}}{C_{af}C_{ar}} \quad (6.10)$$

Therefore,

$$K_{at} = 0.28 \text{ deg/ } g$$

- Contribution du transfert de charge

Lateral Load Transfer:

$$K_{llt} = \frac{W_f}{C_{af}} 2b \frac{\Delta F_{zf}^2}{C_{af}} - \frac{W_r}{C_{ar}} 2b \frac{\Delta F_{zr}^2}{C_{ar}} \quad (6.3)$$

Where

$$F_{zf} = [C_{af} - 2b\Delta F_{zf}^2]\alpha_f \quad (6.4)$$

And

$$F_{zr} = [C_{ar} - 2b\Delta F_{zr}^2]\alpha_r \quad (6.5)$$

Where
 ΔF_{zf} - front lateral load transfer = 188.24 lb
 ΔF_{zr} - rear lateral load transfer = 145.27 lb
 b - second coefficient in the cornering stiffness polynomial = 7.67 e-05 1/lb-deg
 F_{zf} - front lateral force lb
 F_{zr} - rear lateral force lb

Therefore,

$$K_{llt} = 0.01 \text{ deg/ } g$$

7.2.10 ANALYSE DE BUNDORF

Etude de la contribution des systèmes à l'équilibre quasi-statique du véhicule

https://en.wikipedia.org/wiki/Bundorf_analysis

An imaginary example [edit]

	Front	Rear
	deg/g	deg/g
Load transfer effect and cornering stiffness of tire	8.0	7.0
Aligning torque	0.2	-0.2
Roll camber	1.2	0.0
Roll steer	0.6	-0.4
Fy Compliance steer	0.3	-0.1
SAT compliance steer	0.7	0.6
Total Axle Cornering compliance	11.0	6.9

Hence the total under-steer is 11.0 deg/g minus 6.9 deg/g, or 4.1 deg/g.

Negative values are over-steering, positive values are under-steering, for that axle. If the under-steer contribution of the rear axle is greater than that of the front axle you get negative under-steer, which is known as oversteer. The analysis is only applicable while the parameters remain constant, and thus only up to about 0.4 g.

Explanation of terms

Load transfer effect and cornering stiffness of tire. As load transfers across the vehicle the tire's ability to provide cornering force for a given slip angle changes. The latter is known as the cornering stiffness of the tire. See also Tire load sensitivity

Aligning torque. The tire does not just generate a lateral force, it generates a torque as well. This tends to rotate the vehicle as a whole.

Roll camber. As the vehicle rolls the kinematics of the suspension provide a change in the camber of the tire. This generates a force known as camber thrust.

Roll steer. As the vehicle rolls the kinematics of the suspension provide a change in the steer angle of the tire. This generates a cornering force in the normal way.

Fy compliance steer. The lateral force at the contact patch causes the wheel to rotate about the steer axis, generating a steer angle.

SAT compliance steer. The aligning torque directly twists the wheel on the compliances in the suspension, generating a steer angle.

Under-steer. In this case, the tendency for an axle or vehicle to turn outwards from a corner.

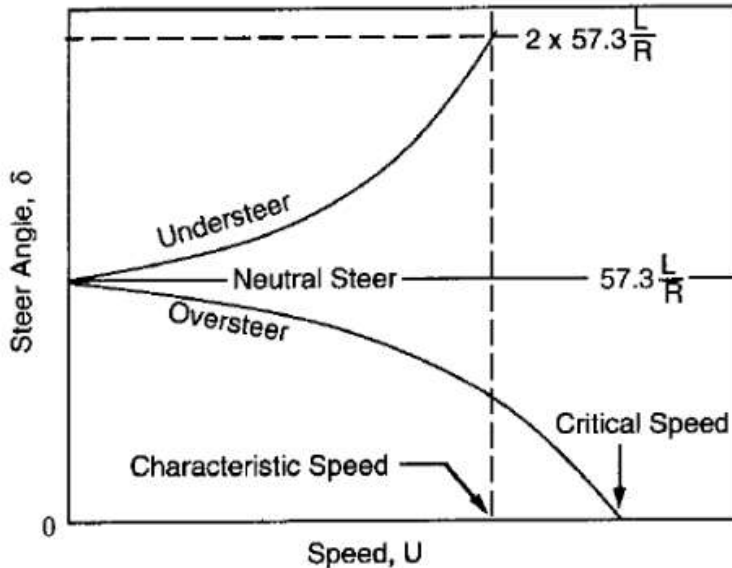
Comme le dit Bill Cobb (aka cibachrome) [ici](#) :

These days, front values for any decent car are 3.5 to 4.5 deg/g and rears are 2.0 to 3.0 deg/g

◇ Bundorf, R. T., & Leffert, R. L. (1976). *The Cornering Compliance Concept for Description of Vehicle Directional Control Properties*. SAE Technical Paper Series. doi:10.4271/760713

7.2.11 VITESSE CARACTÉRISTIQUE

Dans Gillespie, la vitesse caractéristique est définie comme celle pour laquelle l'angle de braquage est égal au double de l'angle d'Ackerman



NB : c'est aussi la vitesse pour laquelle la réponse en vitesse de lacet passe par un maximum

Lorsque le gradient de sous-virage K est exprimé dans les unités SI, à savoir rad/(m/s²), on montre que

$$V_{ch} = \sqrt{\frac{L}{K}}$$

The characteristic velocity stability indicator for passenger cars (2006)

<https://www.tandfonline.com/doi/abs/10.1080/0042311042000266793>

Elle se dérive de l'écriture des équations dans l'espace d'état :

$$\dot{x} = A \cdot x + B \cdot u$$

$$y = C \cdot x$$

avec

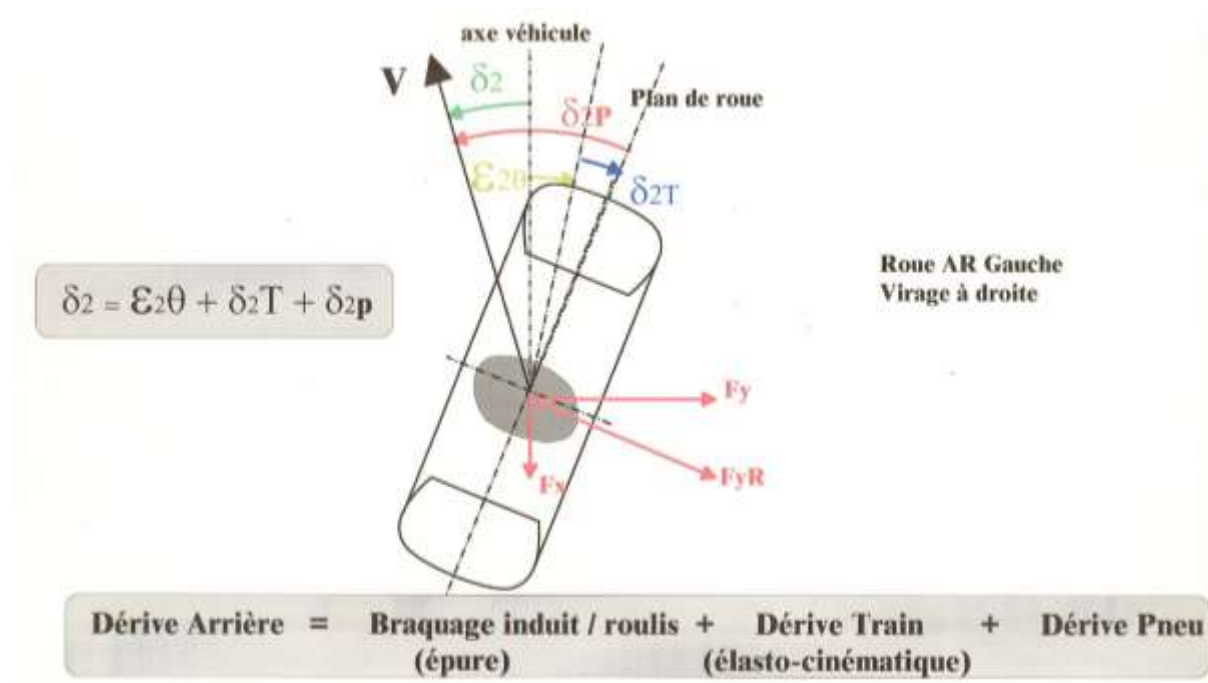
$$x = \begin{pmatrix} \dot{y} \\ \dot{\psi} \end{pmatrix}$$

$$C = \begin{pmatrix} 1 & 0 \\ 0 & 1 \end{pmatrix}$$

(à suivre ...)

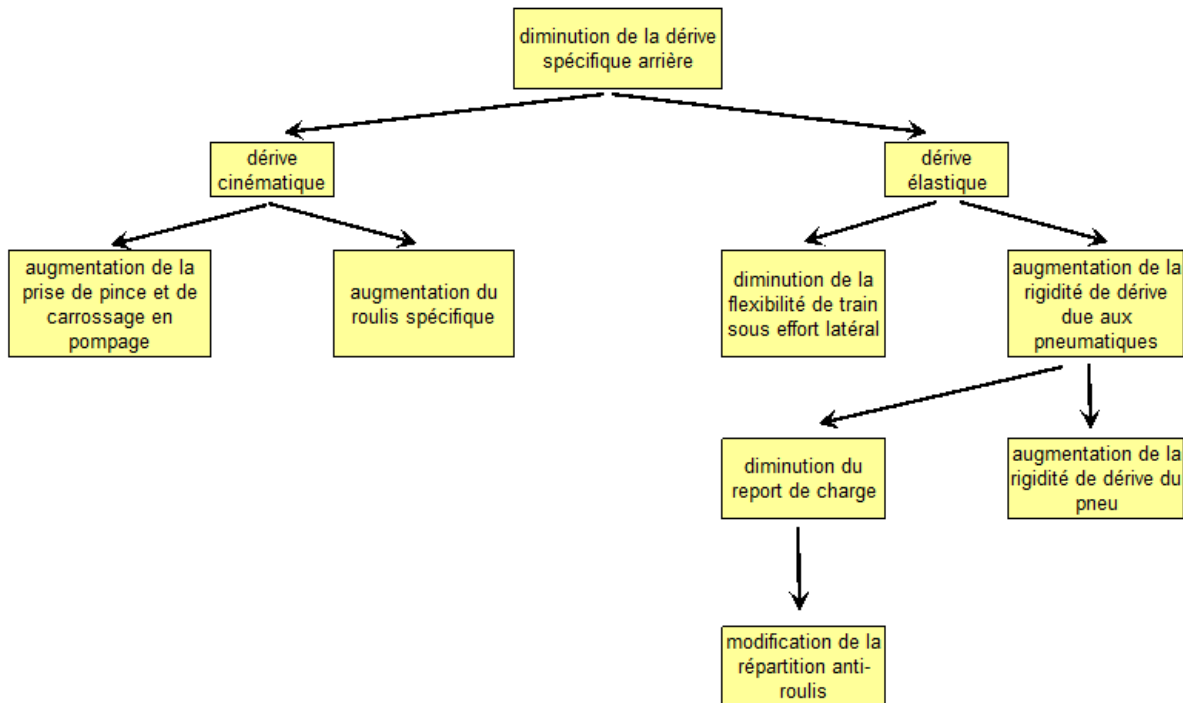
7.2.12 DERIVE ARRIERE / REAR AXLE SIDESLIP STIFFNESS

La dérive arrière caractérise la qualité de l'appui arrière : plus le centre de la trajectoire est proche du train arrière meilleur semble le comportement du véhicule



analyse des dépendances de la dérive spécifique arrière

Imaginons que l'on souhaite diminuer la dérive spécifique arrière d'un véhicule



Bill Cobb, sur [Vehicle Dynamics Professionals](#)

if you can measure Ay, yaw velocity and speed, get the rear cornering compliances easily from a frequency response test. Don't even need to calibrate the equipment. The difference in phase angle slope between Yawrate and Ay vs. frequency is the sideslip gain.

<https://www.eng-tips.com/viewthread.cfm?qid=445691>

It's the gradient of the curve of rear axle slip angle vs lateral acceleration. Strongly related to your understeer gradient and yaw delay time. Less is good. I don't ever remember having a development engineer complaining about too little rear sideslip

(...)

The "rear axle sideslip stiffness" is the generic term for the Rear Cornering Compliance. It is the summation of tire Fz, Fy, Mx and Mz slip and camber effects, rear roll steer and camber, and all sorts of the compliances associated with the rear suspension (which can include multiple axles). It describes this action over the full range of lateral acceleration up to the limit of control. There is a corresponding "front axle sideslip stiffness" named: Front Cornering Compliance, which describes the very same characteristics at the front of a vehicle. Appropriate ISO tests measure Understeer (K) as the derivative of [(steering wheel angle/overall steering ratio)] minus the Ackermann Gradient by lateral acceleration. Then, by means of several techniques including a precision sideslip angle sensor, the sideslip at the rear axle is determined, producing the Rear Cornering Compliance (DR). Adding the Understeer (K) function to the Rear Cornering Compliance (DR) function produces the Front Cornering Compliance (DF). DF = DR + K .

Simple or complex analysis makes it obvious that the lower the DR value is, the lower (better and subjectively more favorable) the lateral acceleration, yaw velocity and body sideslip angle response times are. Think of it in frequency response terms as lower DR produces higher bandwidth. So, DF - DR is the Understeer, while DF + DR is proportional to the damping in the 3 modes (actually Ay response is a combination of yaw velocity and body sideslip states, so its really only 2 modes). Increasing K usually means adding overshoot and longer settling times to vehicle response in order to produce improved response times. But the obvious way to improve the lateral dynamics is to have as low a DR as you can tolerate. This usually means tires with high cornering stiffness. However there is a big price to pay for the ride quality, rolling resistance and the cost of tires in order to get a low DR. This includes very low lateral force suspension compliance etc. meaning hard suspension bushings, oversized tires, cost of replacement tires and other packaging dilemmas. Many vehicles now have much larger rear tires or simply wider wheel rims than fronts if they think they need a 50/50 or more rearward weight distribution. (Think F1, Luxo Rides, big trucks, etc).

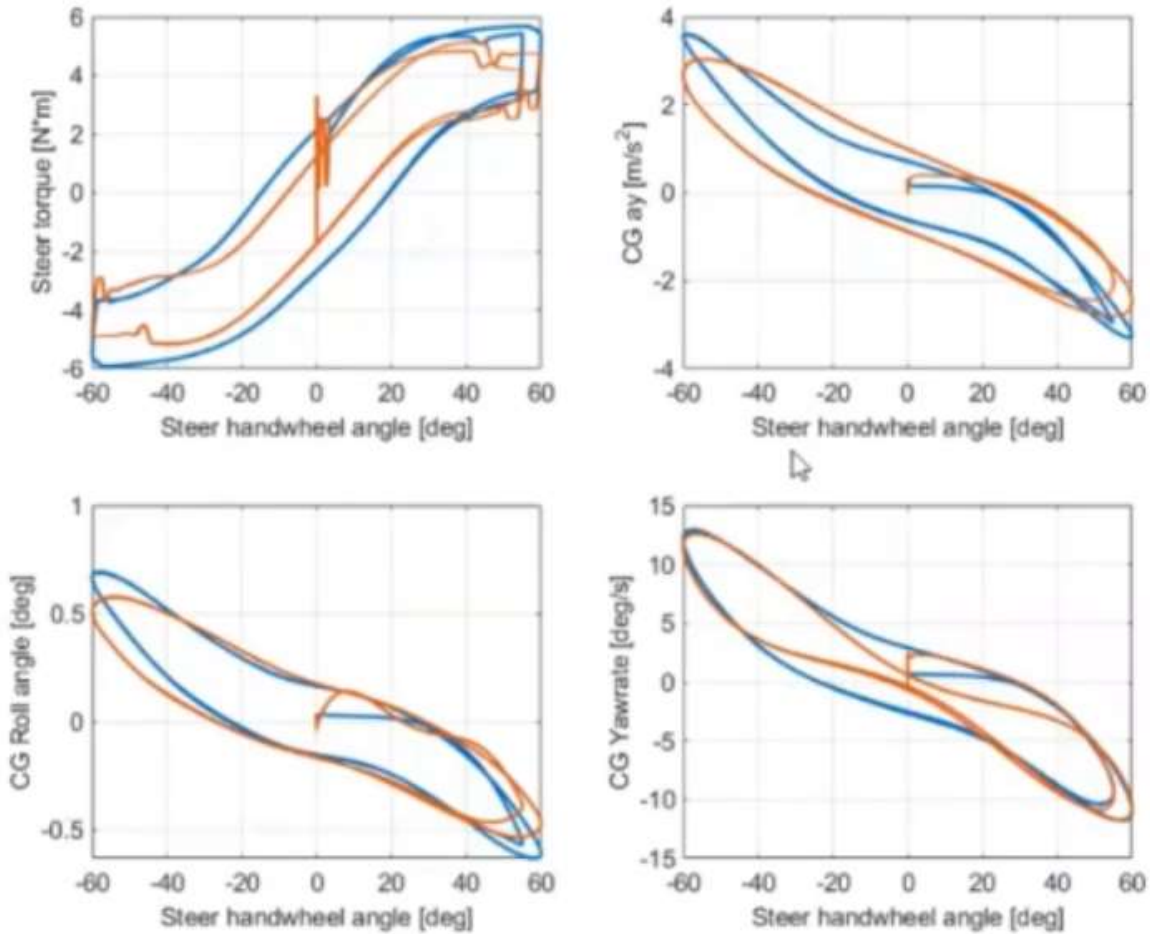
A practical handling teaching tool is to make a carpet plot of DF, DR and Ay Response time for any architecture with lines also for constant understeer. DR lines have a steep descent.

(...)

For a very large sample of production cars and light duty trucks, DR ranges from about 1.5 deg/g to 4.0 deg/g (values taken at 0.15 g), with K ranging from 1.0 to 5.0 deg/g. These numbers cover 1 passenger to GVW payloads. For all this you will find Ay response times from about 0.28 sec to 0.50 seconds. These are computed from the 50% steer input to 90% of final response at the 0.30 g's level of a step test sequence.

Short response times from high understeer feel squirelly. From a low DR, feel wonderful!

7.3 GRAPHS COUPLE VOLANT / ACCEL / VIT.LACET



source (57') : <https://fr.mathworks.com/videos/vehicle-powertrain-modeling-and-full-vehicle-simulation-using-matlab-and-simulink-for-student-competitions-1637606624013.html>

7.4 MILLIKEN (OR YAW) MOMENT DIAGRAM (MMD/YMD)

7.4.1 INTRO

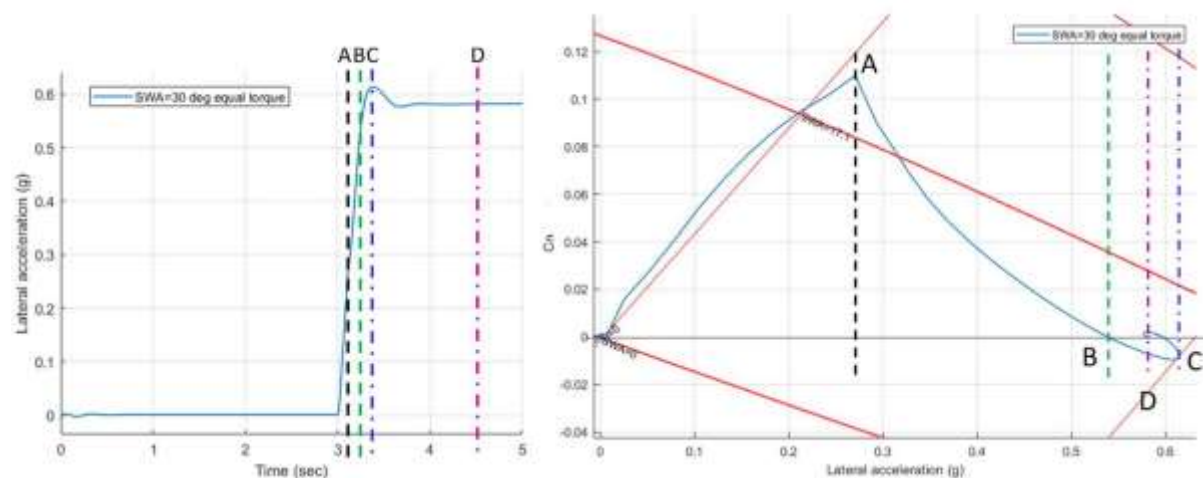
Correspondent à une situation quasi-statique

Chaque diagramme correspond à un rayon donné (ou à une vitesse de passage).

Le § ci-dessous sur la thèse de Chris Patton donne une explication assez visuelle.

Le yaw moment, c'est l'inertie de lacet multipliée par la dérivée (en rad/s) de l'indication d'un gyro. On trace ensuite ce moment de lacet en fonction de l'accel latérale dans un graphe 2D.

Illustration sur une mise en virage :



A – Max SWA, Max yaw moment

B – yaw moment = 0

C – max lateral acceleration, negative yaw moment

D – steady state

7.4.2 CHRIS PATTON PHD

Development of vehicle dynamics tools for motorsports (2013)

▷ https://ir.library.oregonstate.edu/concern/graduate_thesis_or_dissertations/tx31qm51z

3.2.1. C_N - A_Y Diagrams

There are two types of MMDs presented in [11]. The first is constructed at a constant speed, and all lateral force created by the tires is used to hold the vehicle in steady state equilibrium without any outside disturbances. The yaw rate varies across the diagram with lateral acceleration and satisfies the steady state condition of (47). This type of diagram is referred to as a C_N - A_Y diagram, as it is a plot of the yaw moment coefficient C_N vs. lateral acceleration A_Y as defined in (48, 49). Figure 34 is an example of a C_N - A_Y diagram.

$$\omega = \frac{A_y}{V} \quad (47)$$

$$C_N = \frac{M_z}{mgl} \quad (48)$$

$$A_Y = \frac{F_y}{mg} \quad (49)$$

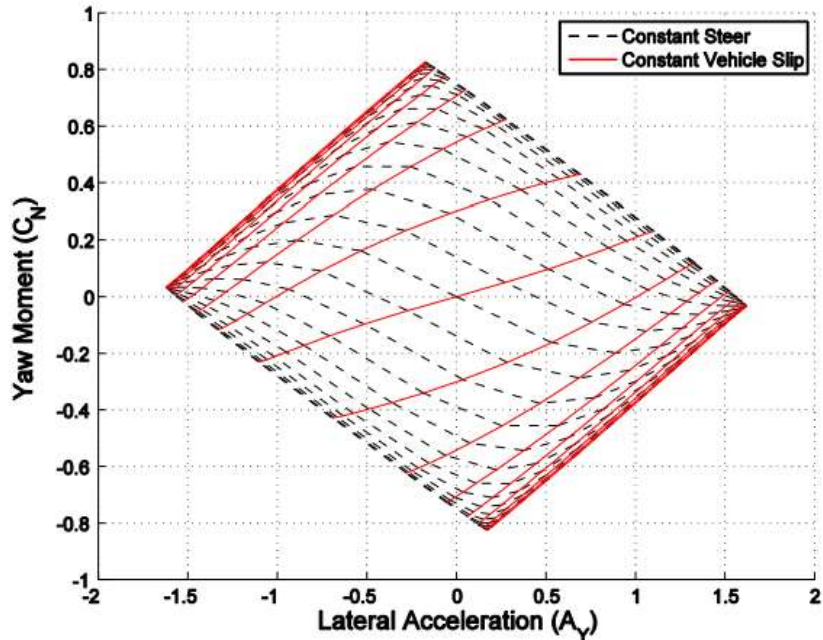
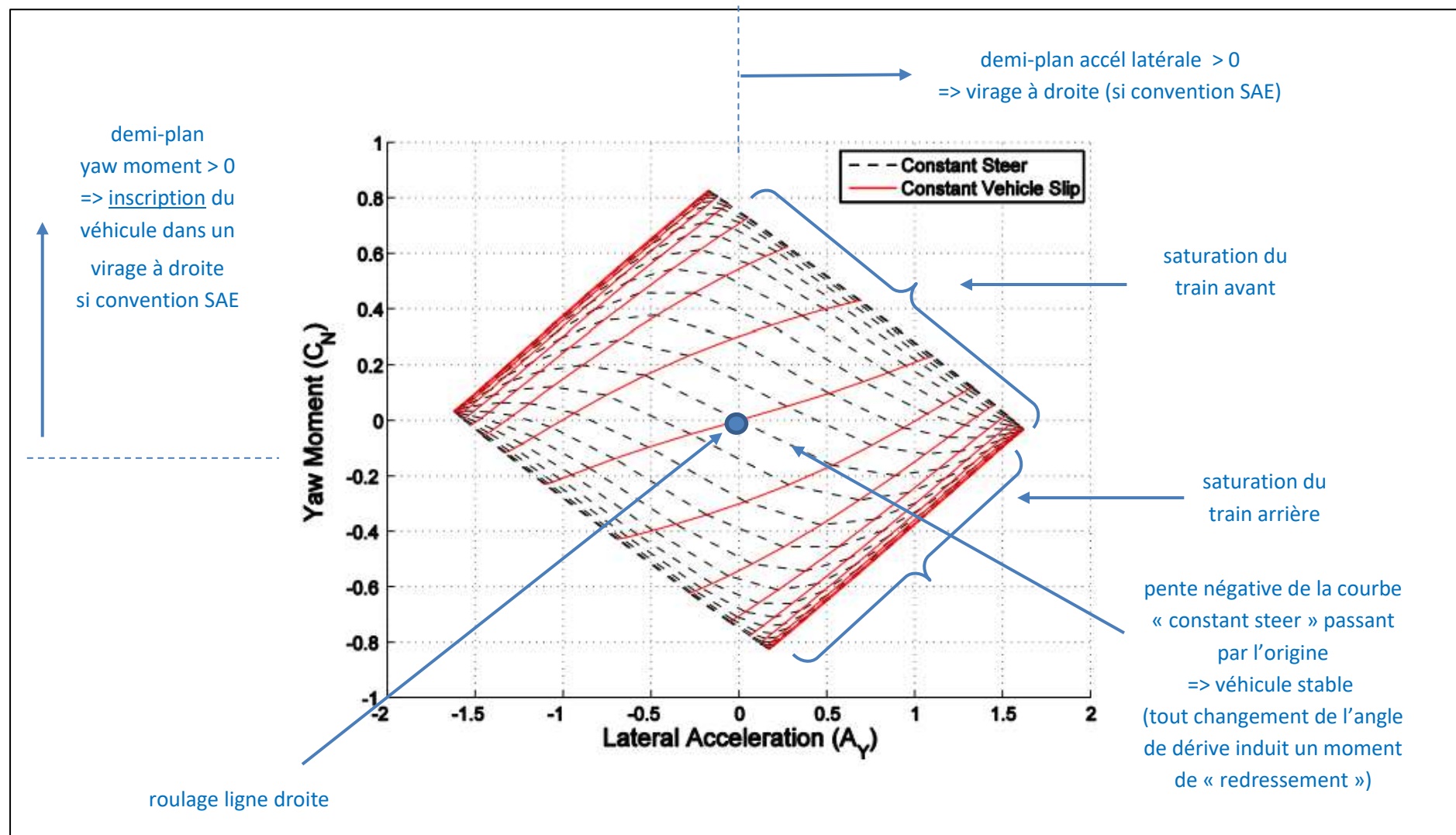
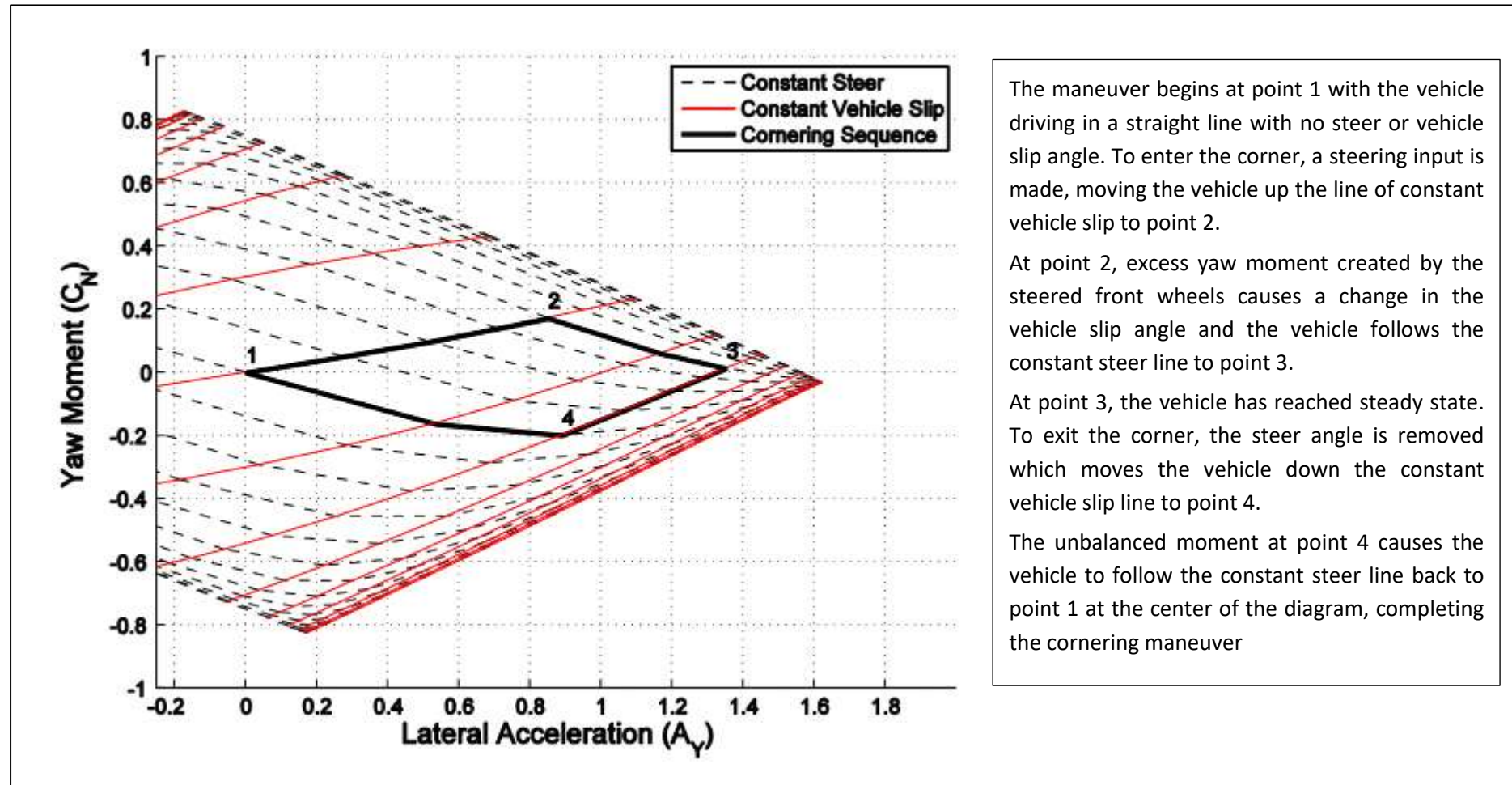


Figure 34: Milliken Moment Diagram – C_N - A_Y – 30 m/s

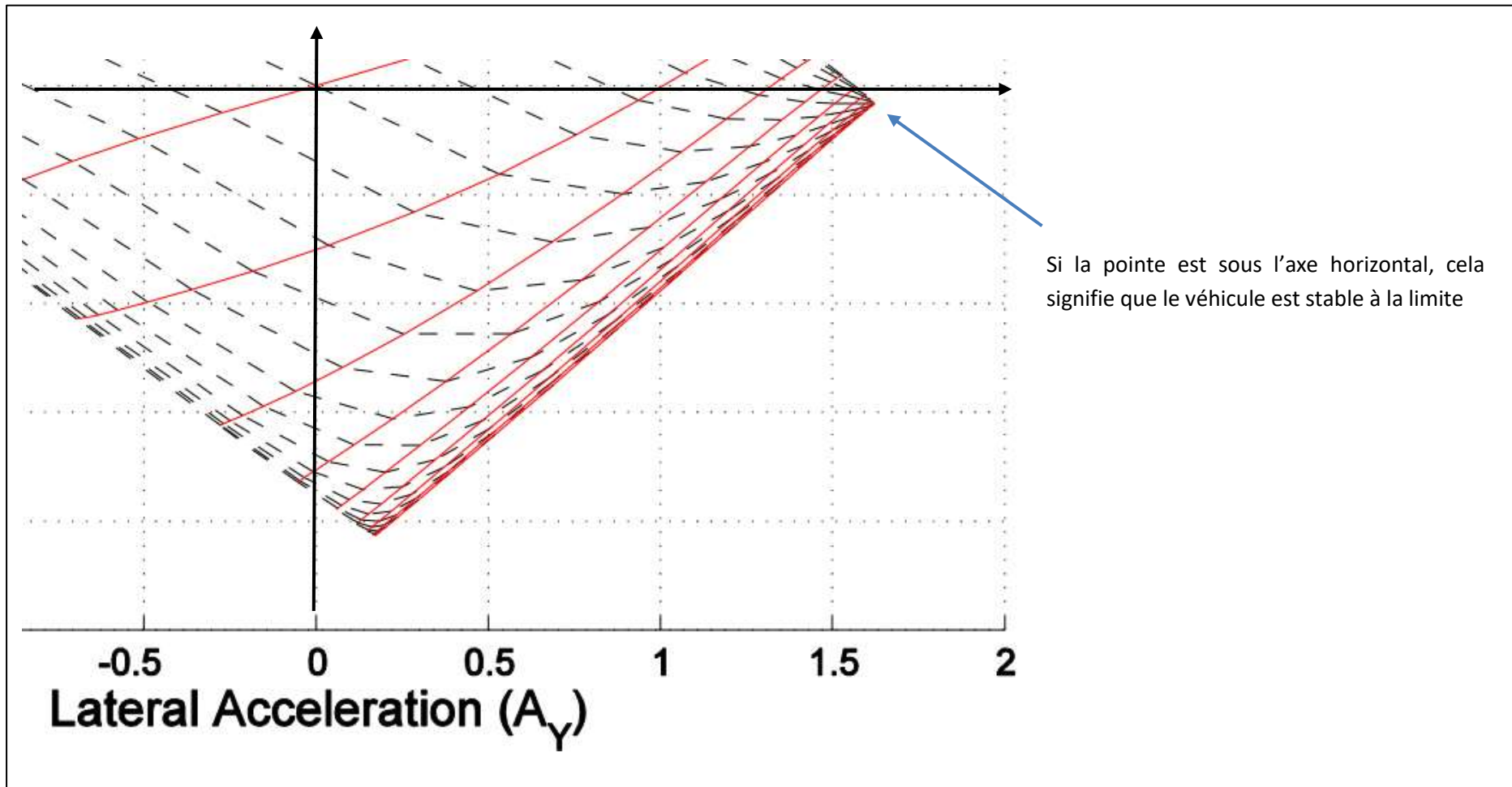
Explication :



Séquence virage à vitesse constante :



Zoom sur la pointe du diagramme :



7.4.3 CLAUDE ROUELLE

A écrit plusieurs articles sur le sujet

[Getting to grips with your yaw moments](#) (05/2017)

[Slide rules: analysing an oversteering car](#) (07/2017)

[Getting more from your yaw diagrams](#) (09/2017)

[The four secrets for chassis happiness](#) (11/2017)

Claude Rouelle (03/2021)

Transient simulation will do better than the yaw moment Vs lateral acceleration diagram

(...)

Another thing that I think (again tell me if I am wrong) that the yaw moment method provides (and that is not described in the articles I wrote) is that you can make a 3D Yaw moment diagram: yaw moment Vs lateral vs longitudinal acceleration which allows you to understand and measure the effect that brake balance and diff settings have on the 6 "magic numbers: grip, balance, on center control and stability and at the limit control and stability.

(...)

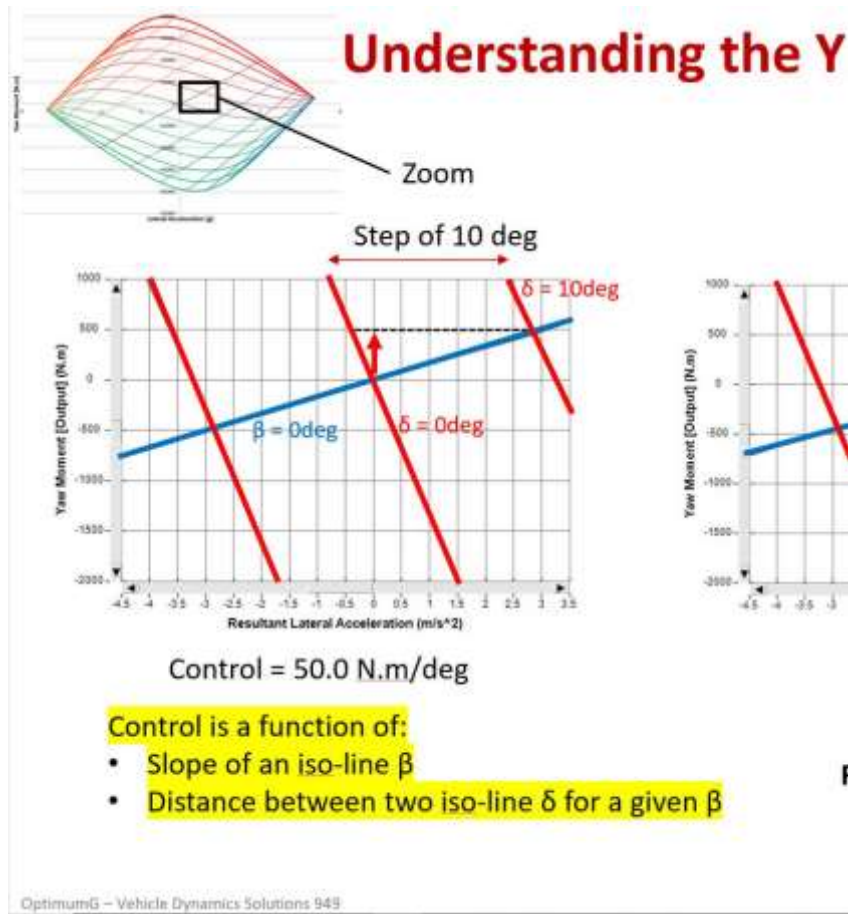
Claude Rouelle (01/2022)

For me control, in simple words is "is the car going where I want it to go ?" and stability is "does the car continue to do what it / was doing?"

Control is yaw moment created from an "within" action (steering) while stability is anti yaw moment created from an "outside" action (bump on the road, gust of wind, another car hitting - just watch some Nascar races).

Claude Rouelle (01/2022) :

for me bigger the angle between the isoline of beta and the X axis of the lateral acceleration AND the bigger the distance between the Isolines of delta the more control there is.



7.4.4 DR RACING

Un long billet sur le blog d'Andrea Quintarelli

<https://drracing.wordpress.com/2015/07/20/the-joy-of-yaw-moment-diagrams/>

The Yaw Moment Diagrams and, in general, the Milliken Moment Methods (also called Force-Moment Method) were used anyway already many years before, transferring to cars a typical aeronautical approach to stability and control studies. And, as we will see, stability and control are some of the features of a vehicle that can be investigated with this method and are, otherwise, difficult to describe and quantify.

A Yaw Moment Diagram is basically a plot which has lateral acceleration on the horizontal axis and Yaw Moment on the vertical one. To be precise, actually several versions exist with the Yaw Moment and/or lateral acceleration normalized on car mass and wheelbase, but the basic concept stays and that is what I will discuss here.

The original approach to build up such a diagram was based on a constrained vehicle test, with a car (or a car scale model) running on a flat belt and locked by two cables, one at the front of it (at a certain and known distance from the CG) and one approximately at the CG. The vehicle would be then put to several Body Slip Angles (Beta, β) while its front wheels would be steered at several Steering Angles (Delta, δ) through sweeps of one and the other, measuring each time (for example through load cells on the cables) the Lateral Force at the CG (Cornering Force) and the Yaw Moment (Force at the front cables times its distance from the CG).

Beside the possibility to build such a diagram through constrained testing, the Force Moment approach makes potentially very easy to investigate cars behavior through steady state simulations where, for each Beta value, a Delta one is picked up and Lateral Forces (and, if interested, self-aligning torques) produced by the tires are calculated.

This means, we can immediately estimate the lateral acceleration and the Yaw Moment acting on the vehicle.

As a consequence, since we investigate the vehicle status for several combinations of Beta and Delta, the Diagram itself gives a very clear picture of how the vehicle behaves more or less in its complete operational window (and inside the given boundaries, depending, for example, on speed and/or downforce).

Looking to a Yaw Moment Diagram we can anyway immediately recognize two main groups of lines: constant Delta lines and constant Beta ones. The constant Beta lines are cutting the first and third quadrant and could be more or less straight. The constant Delta ones, are normally curved and, near the origin, they normally point downward for positive lateral accelerations. Of course, everything depends on the sign conventions in use and on the tire model formulation.

7.4.5 QUELQUES RESSOURCES

Le repo Matlab/Python du TUMFTM qui permet de brancher n'importe quel modèle de dynamique véhicule
<https://github.com/TUMFTM/YawMomentDiagrams>

IHM Matlab pour visualiser les résultats obtenus avec un modèle bicyclette : Graphical User Interface to calculate the Yaw Moment Diagram and Phase Portrait of a vehicle based on the bicycle model.

<https://www.mathworks.com/matlabcentral/fileexchange/88376-vehicle-dynamics-gui>

Implementing the Milliken Moment Method using Controlled Dynamic Simulation

▷ <https://saemobilus.sae.org/content/2005-01-0417>

Mentionné ici :

http://www.iaeme.com/MasterAdmin/UploadFolder/IJMET_09_07_045/IJMET_09_07_045.pdf

The velocity that a race car can achieve during a turn is limited by the grip available for generating slip angles and yet remains a function of the lateral load transfer. The phenomenon is easily understood by the Milliken Moment diagram Fig.9 [1]. The diagram is a plot between normalized lateral acceleration and normalized yaw moments across a number of vehicle side slip angles and steer angles.

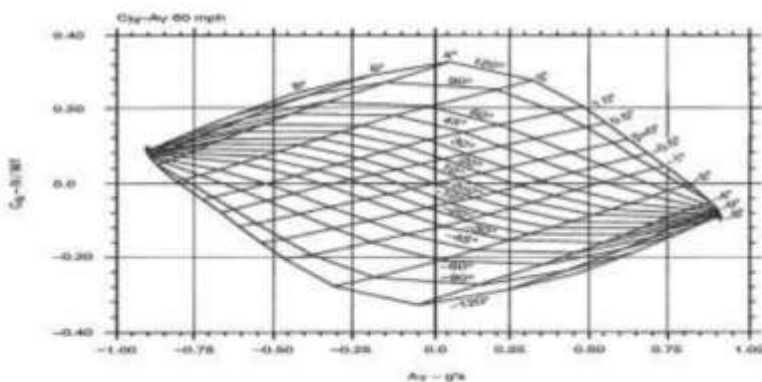
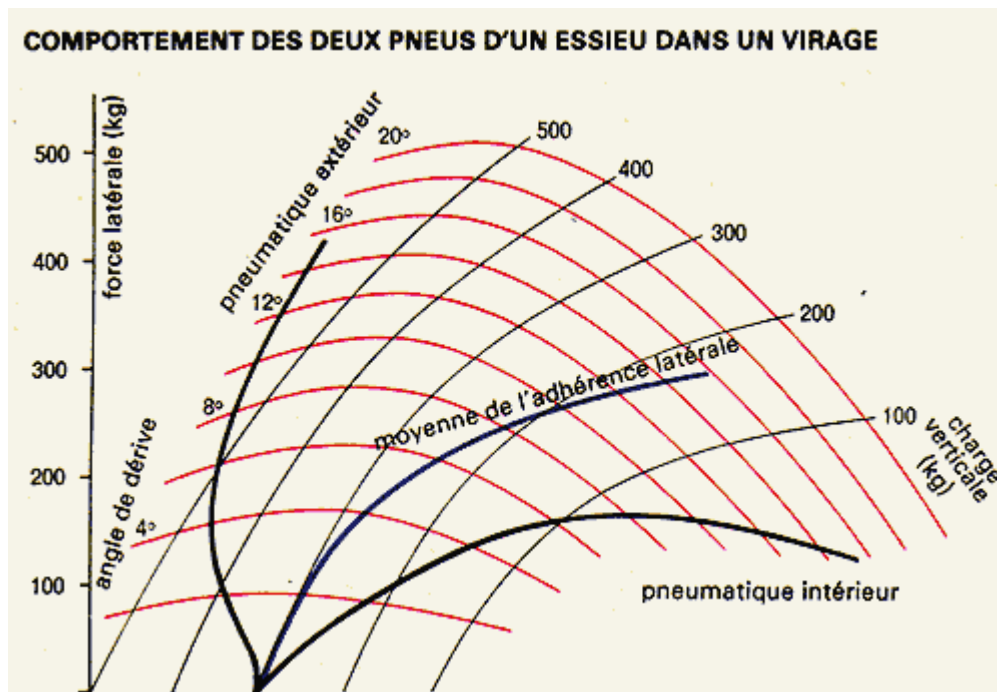


Figure 9 Milliken Moment Diagram (Cn-Ay) [1]

7.5 TRANSFERT DE CHARGE



7.5.1 TRANSFERT GEOMETRIQUE VS TRANSFERT ELASTIQUE

Le transfert de charge (de la masse suspendue) en virage vaut

$$\Delta W = \frac{m \cdot \gamma_y \cdot h_{cog}}{t}$$

m masse

t voie

γ_y accélération latérale

h_{cog} hauteur centre de gravité

On peut le décomposer en

$$\Delta W = \frac{m \cdot \gamma_y \cdot h_{cog}}{t} (h_{cog} - h_{RC} + h_{RC})$$

h_{RC} hauteur centre de roulis

soit

$$\Delta W = \Delta W_{elas} + \Delta W_{geom}$$

avec

$$\Delta W_{elas} = \frac{m \cdot \gamma_y \cdot h_{cog}}{t} (h_{cog} - h_{RC})$$

$$\Delta W_{geom} = \frac{m \cdot \gamma_y \cdot h_{cog}}{t} (h_{RC})$$

Le transfert de charge géométrique est lié à la géométrie de la suspension, qui conditionne la hauteur de centre de roulis. Les efforts associés sont repris par les bras de suspension.

Le transfert de charge élastique dépend de la distance entre centre de masse et centre de roulis. Les efforts correspondants sont repris par les éléments (élastiques) de suspension (ressorts, barre anti-roulis, butées ...)

C'est très bien illustré par Jahee Campbell-Brennan ici :

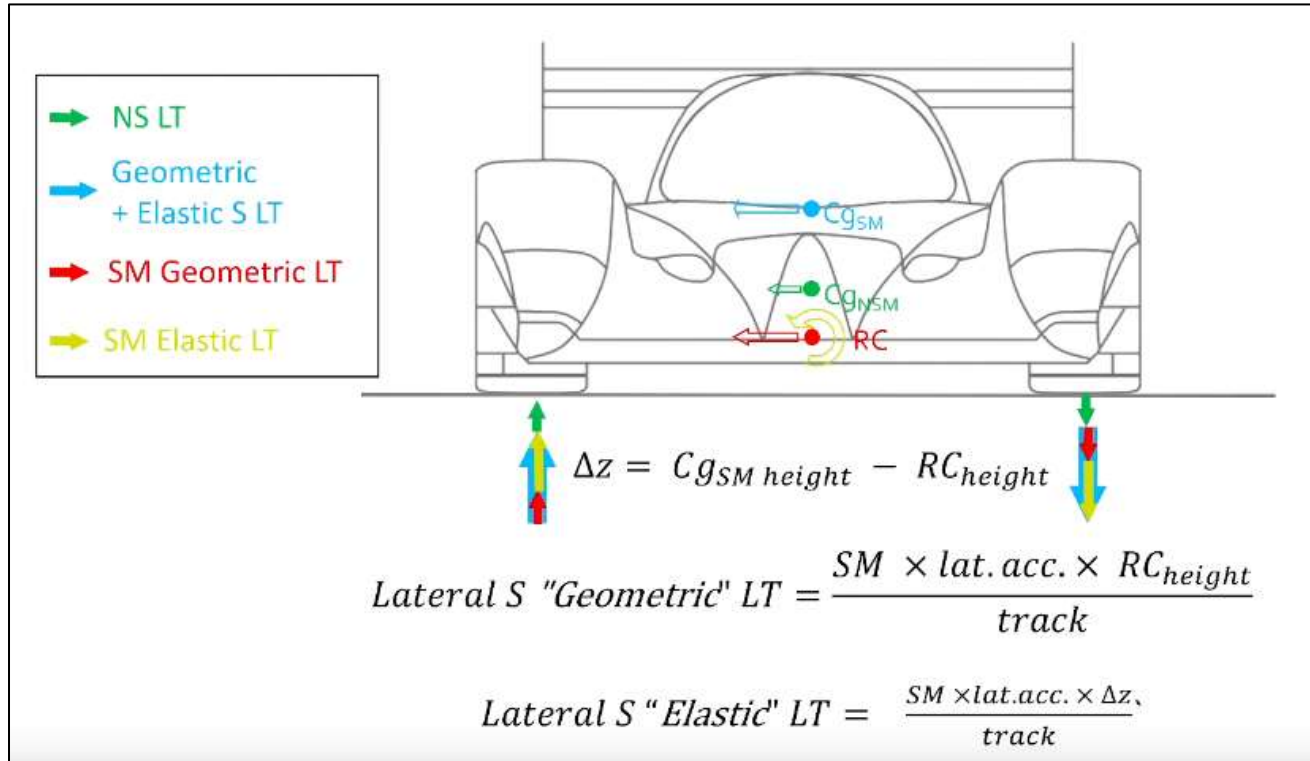
▷ <https://www.waveydynamics.com/post/weight-transfer-rc>

When the roll centre is at equal height to the CoM, there is no chassis roll moment generated and therefore no body roll.

In this condition lateral weight transfer is solely geometric, so while there's no roll, you still expect to experience weight transfer.

Et évoqué par Claude Rouelle dans cette vidéo, à t=36'

<https://www.youtube.com/watch?v=dKyhjZgQyoU>



7.5.2 REPARTITION DE REPORT DE CHARGE (RRCH)

La RRCH est un pourcentage qui exprime la part du report de charge qui s'exerce sur (en général) le train avant.

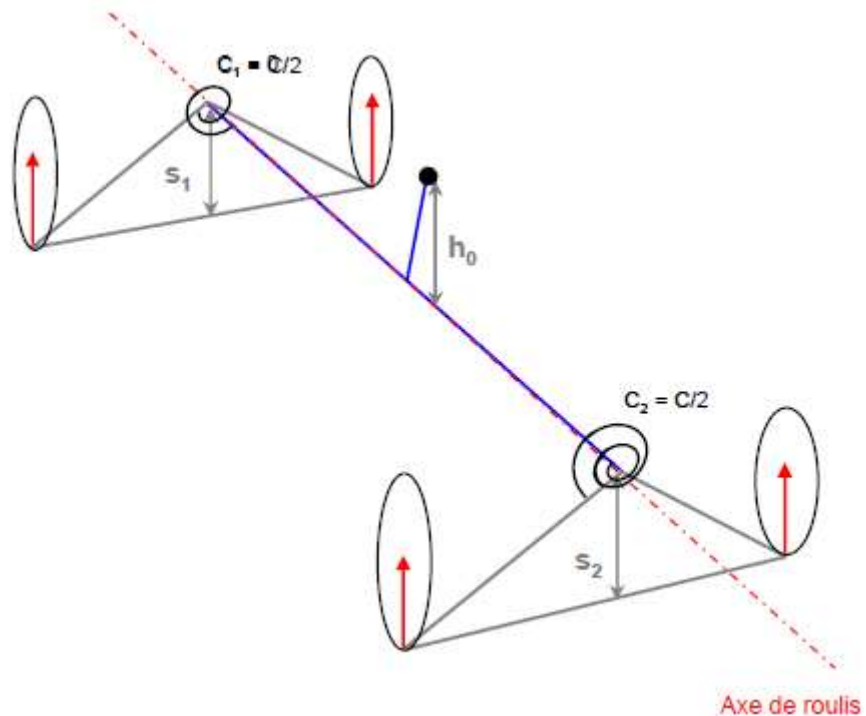
Expression répartition de report de charge:

$$rrch = \frac{\Delta Fz_1}{\Delta Fz_1 + \Delta Fz_2}$$

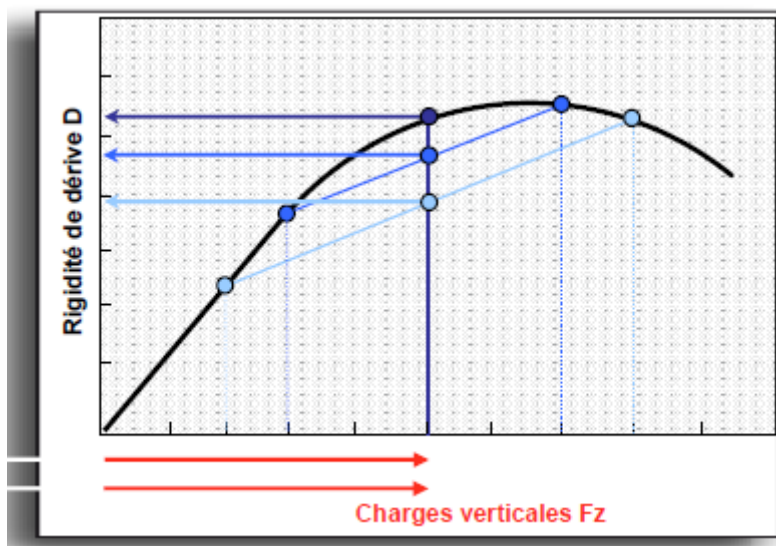
Expression charge verticale:

$$Fz_2 = \frac{M_2 g}{2} + / - \left(\frac{C_2 \theta}{E_2} + \frac{M_2 \gamma_r S_2}{E_2} \right)$$

En anglais : FLLTD pour Front Lateral load transfer distribution (ou TTLTD : Total Lateral Load ...)



Axe de roulis



Plusieurs règles empiriques coexistent dans la littérature :

- Rechercher une RRCH proche de la répartition de masse
- Biaiser légèrement la RRCH vers l'avant et/ou vers l'essieu non moteur

Greg Locock :

A good rule of thumb for RWD road cars would be LLTD on front axle = WD+5%

Un peu plus bas dans le thread, on peut lire par un autre contributeur :

On FWD Honda's, they worked best at around 46% LLTD when the WD was around 62%

Plus la RRCH est élevée (i.e sur l'avant), plus la tendance est sous-vireuse : l'essieu le plus raide voit un transfert de charge plus rapide, avec donc une dégradation plus rapide du potentiel d'adhérence latérale.

A lire :

https://blackardynamics.com/bagshopify/Chassis_Articles/Tyres_and_load_transfer.php

voir le eduauto sur le même sujet aussi

Parameter to Analyse

- Front Roll Rate Distribution (FRRD)
- Rear Roll Rate Distribution (RRRD)
- Front Total Lateral Load Transfer Distribution (FTLLTD)
- Rear Total Lateral Load Transfer Distribution (RTLLTD)

$$FRRD = \frac{K_f}{K_f + K_r}$$

$$RRRD = \frac{K_r}{K_f + K_r}$$

$$FTLLTD = \frac{\Delta W_f}{\Delta W_f + \Delta W_r}$$

$$RTLLTD = \frac{\Delta W_r}{\Delta W_f + \Delta W_r}$$

Load Transfer

$$\frac{\Delta W_f}{A_y} = \frac{W}{l} \times \left[\left(\frac{H \times K_f}{K_f + K_r} \right) + \left(\frac{b}{l} \times z_{rf} \right) \right]$$

$$\frac{\Delta W_r}{A_y} = \frac{W}{l} \times \left[\left(\frac{H \times K_r}{K_f + K_r} \right) + \left(\frac{a}{l} \times z_{rr} \right) \right]$$

	Model_v03_0	Model_v03_14	Model_v03_16	Model_v03_18	Model_v03_20	
Lateral Load Transfer						
DWF	164.98	184.75	200.84	217.05	231.82	N/(m/s²)
DWR	203.89	184.13	168.04	151.82	137.06	N/(m/s²)
Roll Rate Distribution						
Front	45.06	52.07	57.77	63.52	68.76	%
Rear	54.94	47.93	42.23	36.48	31.24	%
Total Lateral Load Transfer Distribution						
Front	44.72	50.08	54.45	58.84	62.85	%
Rear	55.27	49.92	45.55	41.16	37.15	%

$$\frac{\Delta W_f}{A_y} = \frac{W}{t_f} \times \left[\left(\frac{H \times K_f}{K_f + K_r} \right) + \left(\frac{b}{l} \times z_{rf} \right) \right]$$

$$\frac{\Delta W_r}{A_y} = \frac{W}{t_r} \times \left[\left(\frac{H \times K_r}{K_f + K_r} \right) + \left(\frac{a}{l} \times z_{rr} \right) \right]$$

z _{rf}	Front Roll Centre Height	130	mm
z _{rr}	Rear Roll Centre Height	140	mm
H	Height between CG and NRA axis	440	mm
t _f = t _r	Track (front/rear)	1404	mm
l	Wheelbase	1900	mm
a	CG distance from front axle	1036	mm
W	Total Vehicle Weight	900	kg

7.6 INFLUENCE DU ROULIS

7.6.1 INFLUENCE SUR LE COMPORTEMENT

http://www.formula1-dictionary.net/roll_center.html

If the axis runs nose-down, the car tends to oversteer. If the axis runs nose-up, the car tends to understeer.

<http://www.fsaecommunity.com/forums/showthread.php?12183-Roll-Center-height&p=125022&viewfull=1#post125022>

RC Height divides your weight transfer into "elastic" and "geometric".

- 1) Low Roll Centre -> Little track width variation, less tire temperature, bigger Roll Moment is acting on your springs and dampers ("elastic weight transfer") therefore you've got more inertia in roll and car responds slower
- 2) High Roll Centre -> Big track width variation, more tire temperature, lesser Roll Moment is acting on your springs and dampers and you have more responsive car

As grip is generated by the front axle, weight transfer starts from there. That causes a time gap between front and rear axles weight transfer. In order to decrease this gap many designers increase the amount of "geometric" weight transfer on the rear (which acts faster - isn't damped) by setting higher RC on that axle.

http://www.thecartech.com/subjects/auto_eng2/roll_center.htm

Rolling produces more grip

(...)

Effects of Front Roll Center Adjustment

Front roll center has most effect on on-throttle steering during mid-corner and corner exit.

LOWER front roll center

- * More on-throttle steering
- * Car is less responsive
- * Better on smooth, high grip tracks with long fast corners

HIGHER front roll center

- * Less on-throttle steering
- * Car is more responsive
- * Use in high grip conditions to avoid traction rolling
- * Use on tracks with quick direction changes (chicanes)

Effects of Rear Roll Center Adjustment

Rear roll center affects on- and off-throttle situations in all cornering stages (entry, mid, exit)

LOWER rear roll center

- * More on-throttle grip
- * Less grip under braking
- * Use to avoid traction rolling at corner entry (increases rear grip)
- * Use under low traction conditions
- * Increases traction, reduces rear tire wear

HIGHER rear roll center

- * Less on-throttle steering
- * Car is more responsive
- * Use in high grip conditions to avoid traction rolling
- * Use on tracks with quick direction changes (chicanes)

<https://www.eng-tips.com/viewthread.cfm?qid=431615>

Raising the front roll centre certainly improves on centre steering feel (Greg Locock)

https://site.petitrc.com/setup/associated/RayMunday_RollCentreTuningQuickReferenceGuide/

Generally when tuning roll centres, we usually lower them on a hard / slick track and raise them on a soft /wet track (to help the tyre dig in a little more). Each tyre and surface likes a slightly different roll centre but this is the general rule of thumb we follow. At the rear, a lower roll centre usually gives you more mid and exit traction, but if you go too low the car will feel to 'dump over' and can spin on exit. Sometimes when you lower the roll centre you need to run a slightly stiffer spring or move the shock out on the tower slightly to compensate.

Attention : rabaisser un véhicule a généralement plus d'impact sur la position du centre de roulis que sur celle du centre de gravité, et peut donc avoir l'effet inverse de celui escompté, puisqu'ayant pour résultat d'augmenter le moment de roulis.

<https://motoiq.com/the-ultimate-guide-to-suspension-and-handling-its-all-in-the-geometry-part-one-the-roll-center/3/>

The often-overlooked disadvantage to lowering is that roll center drops more radically than the center of gravity on most cars. Although lowering the center of gravity and increasing the track width are the two most effective ways to reduce weight transfer, over lowering increases the roll couple and dynamic weight transfer.

7.6.2 DANS QUEL ORDRE FAIRE LE TUNING D'UN VÉHICULE ?

<https://www.eng-tips.com/viewthread.cfm?qid=431615>

(Cibachrome, 27/10/2017)

1) Ride balance at a designated speed demands that there be a rear to front ride frequency ratio. For hiway driving this number is often set at 1.2 for 'flat ride'.

(2) Once the chassis is defined, 3 levels of suspension are usually offered: Base (Level I) handling, level II with a base tire and a rear bar to reduce the roll gradient from 6.5 - 7 deg/g to 5 - 6 deg/g, and a Level III car with Summer Tires, stiffer springs (same R/F ride ratio) and a roll gradient of 3.5 - 4.5 deg/g (just for the sake of argument). So: pick roll centers which simultaneously achieve the ride balance and the TLLTD with a small front bar and no rear bar. Without changing trim heights or wheelhouse clearances, add a rear bar with only slight ride frequency changes (suspension bushings most likely and taking into account a larger motor (maybe 2 more cylinders)). Drop the TLLTD maybe down to 3 points over the weight distribution. Then there is the level III car, with much stiffer suspension (springs and bars all around) with a Summer class tire on wider and larger wheels, maybe split tires, TLLTD dropped to within a point or 2 of weight distribution. All this without re-configuring the body line at the plant and without a lot of extra holes or slots (net build, please). The simultaneous solution to delivering ride frequencies (structural and wheel travel windows, plus roll gradients at several tune-able TLLTDs hands you roll center locations. Its called synthesis: Spec what performance you want, compute the hardware you need with specific constraints. From my perspective, many car makers grab a crate of parts, build up a car, patch and play car-car until start of production and then quit. This is followed by next year's "refined, modified and optimized" suspension packages. Then they use the same words to describe the ding chassis as a new and improved model is prepared.

3) Paying attention to body (sprung mass) inertia defined by power-train mounting and accessory locations plus passenger, payload and fuel mass properties also gives you something to think about in terms of the roll axis location. Want roll or roll with lateral translation ?

Once you tell the computers what you are after, its just 'turn the crank'.

7.7 VIRAGE TRANSITOIRE / FREQUENTIEL

7.7.1 MISE EN VIRAGE

La caractérisation du comportement d'un véhicule en transitoire peut se faire principalement en étudiant la façon dont il rejoint la trajectoire qu'on veut lui imposer (prise de virage, manœuvre de dépassement,...), ou la faculté qu'il a de garder la trajectoire souhaitée (coup de vent latéral, lâcher de pied,...).

Petite analyse de la mise en virage :

1- tout d'abord le volant/la roue tourne.

2-Quasi-instantanément, le train avant dérive, crée un effort transversal, et l'accélération transversale apparaît donc.

3-Suit le mouvement de lacet résultant de la rotation du train avant ; le train arrière, lui, continue à aller tout droit (pas de dérive). Les courbes de lacet et de roulis sont très plates à l'origine (effet de l'inertie de lacet et de roulis).

4-Le roulis suit lentement l'accélération.

5-arrive enfin la dérive du train arrière.

Vivacité de roulis (aptitude du mouvement de roulis à accompagner l'angle volant)

7.7.2 REPONSE A UN ECHELON VOLANT

Damian Harty (01/2022)

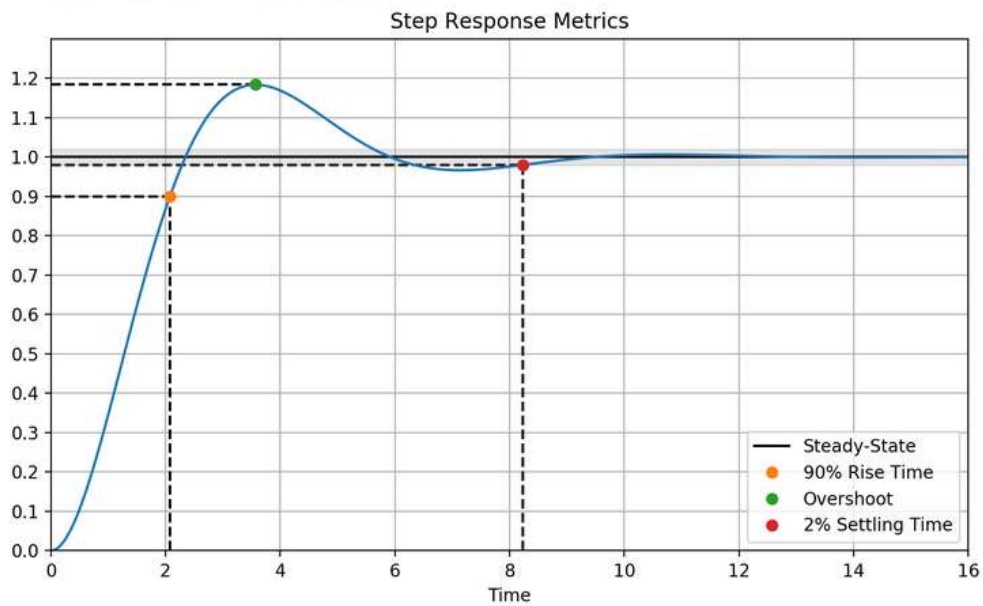
What humans hate most are delays. Inside about about 100msec, humans see events as simultaneous (we've learned this from aviation, where initial responses inside 100msec are strongly correlated with a score of 1 on the Cooper-Harper scale). Beyond about 500msec, humans see events as quite separate unless they are very practised. This is why normal humans absolutely can't catch a spinning car through a lane change the first time they try it - the delay in response to a steering reversal is outside what an untrained human regards as a "viable" response. Trained humans have learned they need a fast and large reaction, and need to wait for it to take effect.

Between 100msec and 500msec is some kind of uncanny valley, and any changes you make that pull responses back towards 100msec are regarded as improving "control". Since not many (sic) cars have a 5Hz bandwidth, basically anything that speeds the response of the car is taken as a win.

<https://kktse.github.io/jekyll/update/2019/02/13/on-centre-handling-metrics.html>

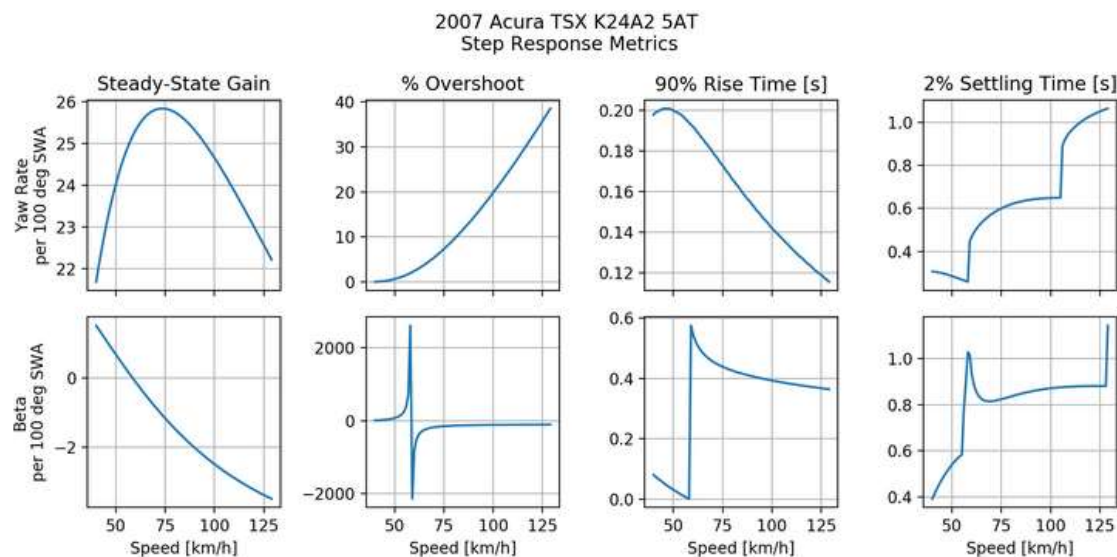
- **Rise Time** - time to achieve 90% of steady-state
- **Overshoot** - maximum percentage over the steady-state value
- **Settling Time** - time taken for the signal to stay within a $\pm 2\%$ band of steady-state
- **Steady-State Gain** - the magnitude of the output over input when the signal is no longer changing

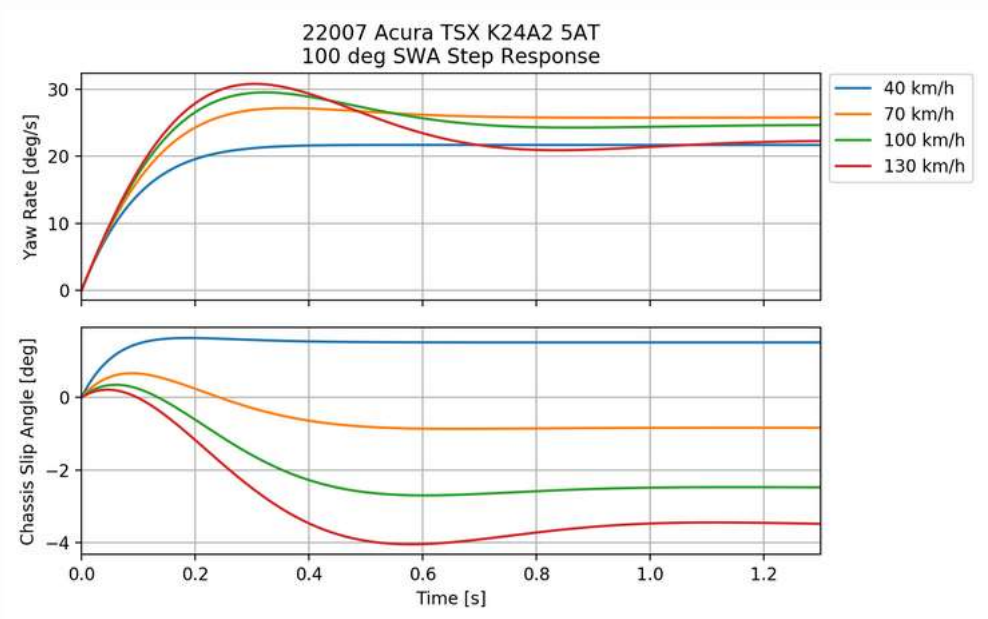
These metrics are visualized in the figure below:



Quelques exemples mesurés sur une Honda Acura

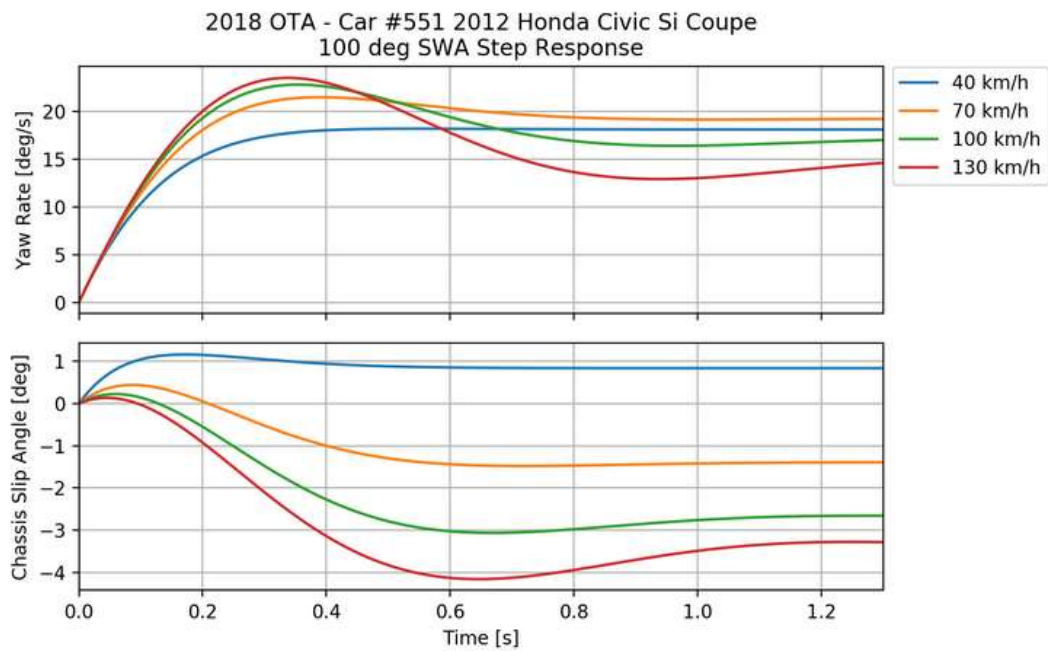
<https://kktse.github.io/jekyll/update/2019/06/01/typical-cornering-compliances.html>



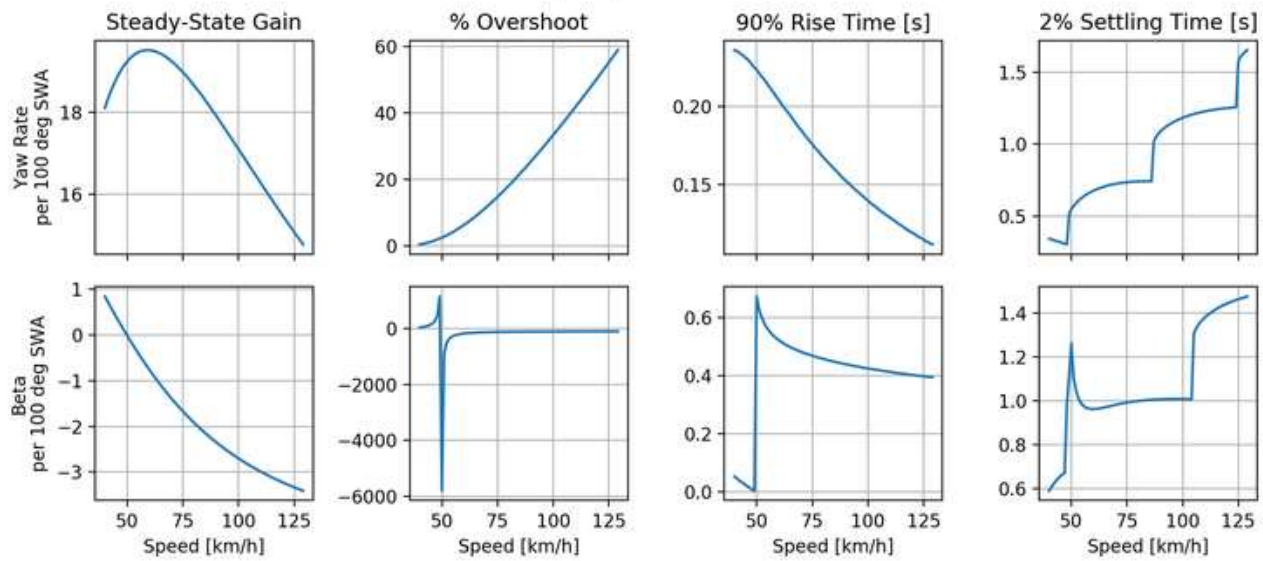


ou ici sur une Honda Civic

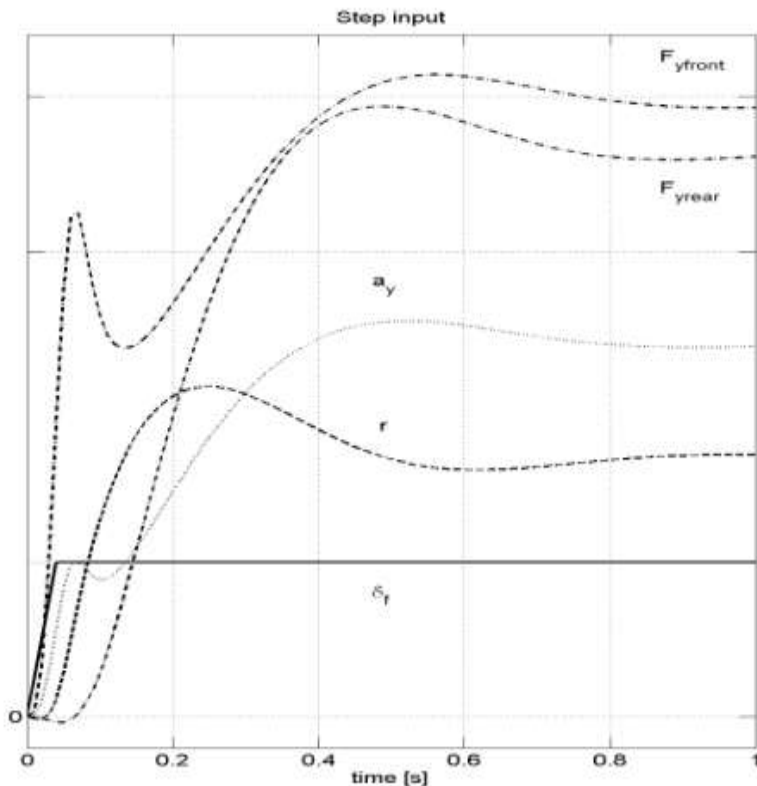
<https://kktse.github.io/jekyll/update/2019/02/13/on-centre-handling-metrics.html>



2018 OTA - Car #551 2012 Honda Civic Si Coupe
Step Response Metrics

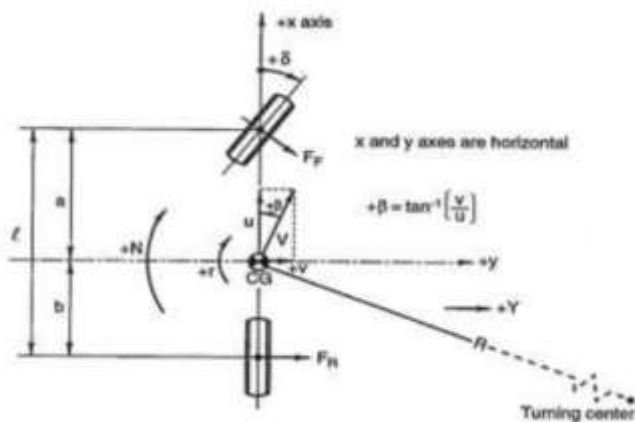


Chez (Groenendijk, 2009) on trouve les courbes suivantes qui détaillent la réponse des efforts latéraux par train :



So, as the vehicle enters a curve it travels along the constant beta line ($\beta=0$) which is the vehicle side slip angle as illustrated in figure below. Vehicle side slip angle is defined by the angle included between the vehicle

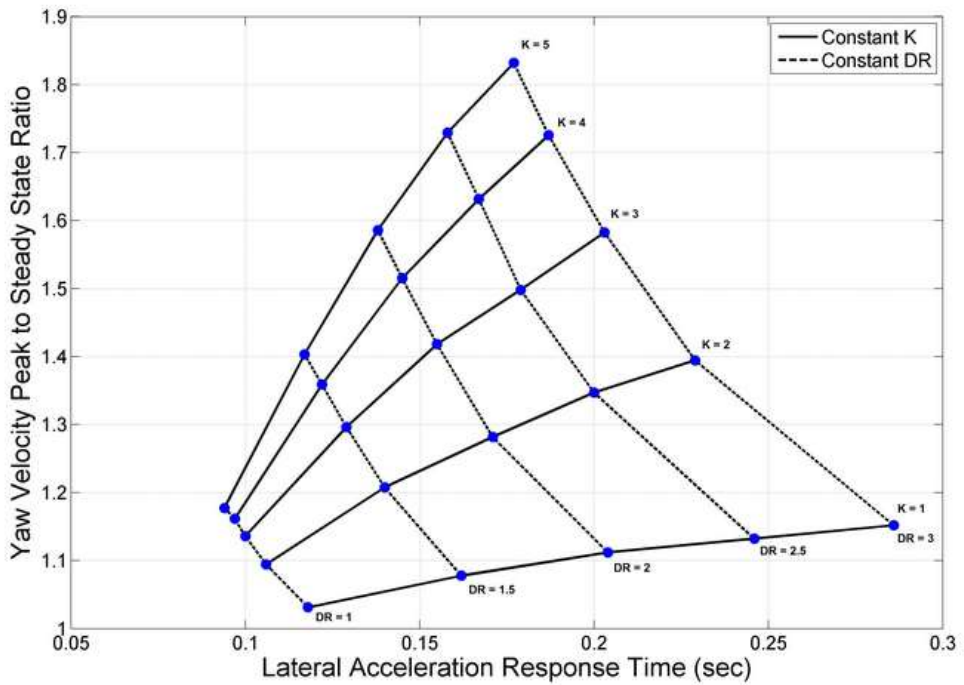
heading direction and its actual direction of travel which is dictated by the path it follows. When the vehicle just enters a turn there is no side slip because right now only the front wheels have been steered. As the front wheels are steered a moment as well as acceleration is generated. Then increasing the steer gives rise to the moment start giving an effect, the side slip is generated which varies across a constant steer line to reach a steady-state value where there is no yaw moment. Thus, the grip available and the corresponding force generated on each end depend on the way the vehicle is modelled. The whole modelling process revolves around the modified bicycle model.



(Groenendijk, 2009)

The rear axle cannot establish a tyre slip angle until the vehicle acquires a yaw angle. After a delay associated with the rear tyre relaxation lengths, side force is applied at the rear of the vehicle. In what follows, lateral acceleration is increased, yaw acceleration is reduced to zero thus leading to steady state cornering. One can see that the rear lateral force begins negative, delaying the lateral forces. A solution to reduce this is to increase the wheelbase (more weight and bad maneuverability) or steer the rear wheels to achieve quicker establishment of the lateral force. Using the rear wheels, one can also decrease the overshoot of lateral acceleration and yaw velocity. The overshoot is undesirable since it can lead to dangerous situations, an overshoot on the lateral acceleration can lead to a spin of the vehicle.

7.7.3 CARPET PLOT

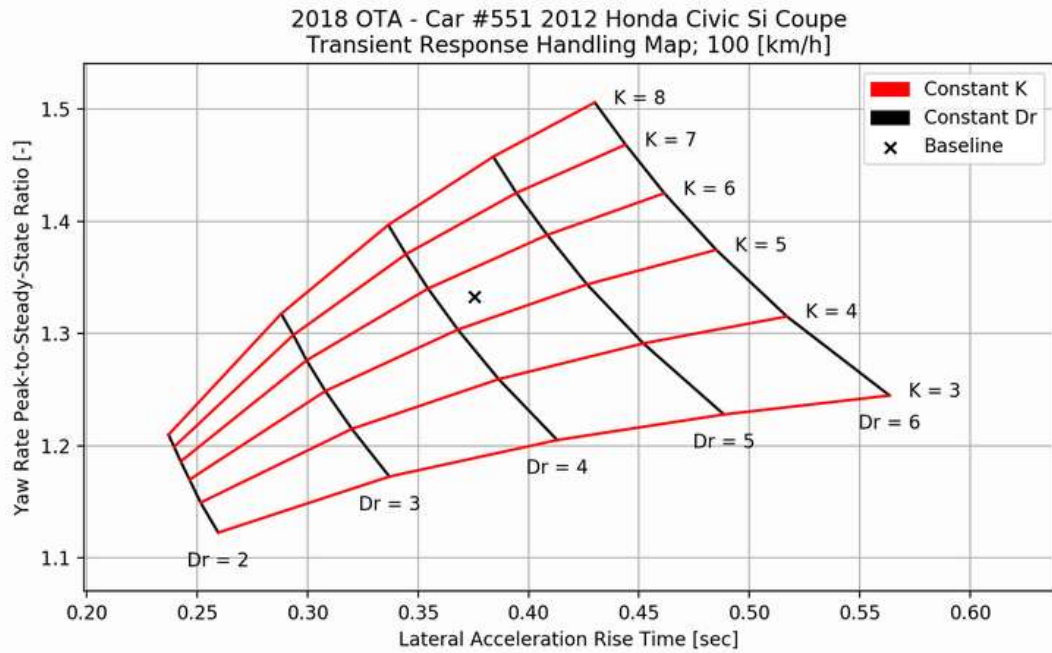


source <http://www.fsaе.com/forums/showthread.php?12204-Testing-Testing-1-2-.../page2>

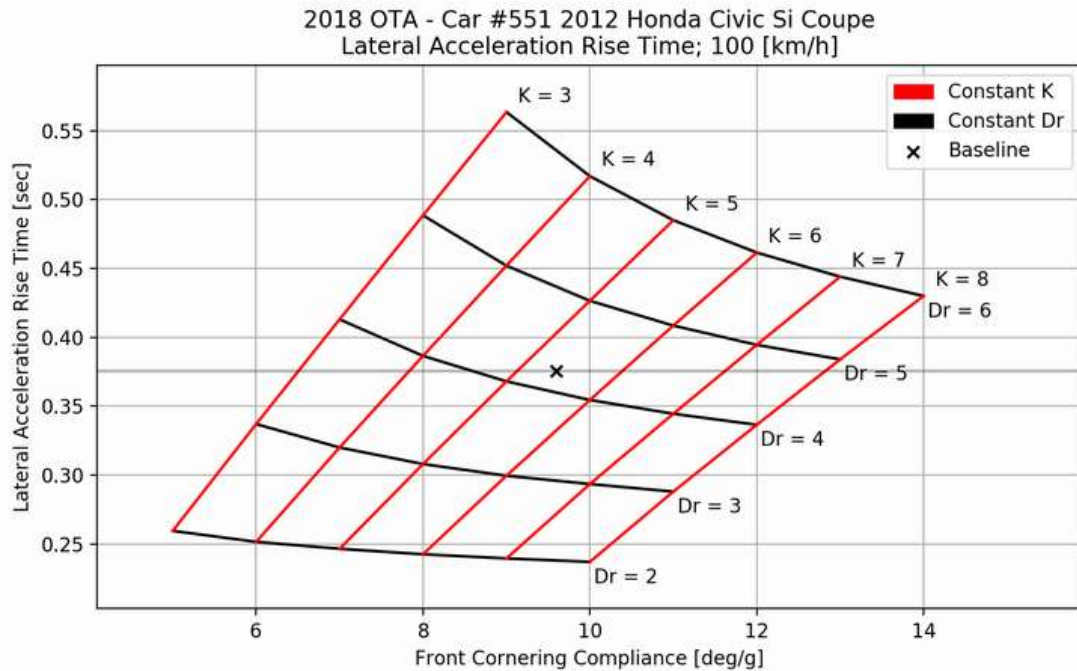
Plot of vehicle yaw damping and lateral acceleration response time for various rear cornering compliance (DR) and understeer (K) values. The yaw velocity peak to steady state ratio is from the same old frequency response stuff and the lateral acceleration response time is from a step steer input (calculated from 50% steer to 90% steady state lateral acceleration).

L'inclinaison des courbes d'iso dérive arrière montre que le fait de réduire le gradient de sous-virage (à iso dérive arrière) permet de réduire l'overshoot de vitesse de lacet, mais augmente le temps de réponse de l'accélération latérale.

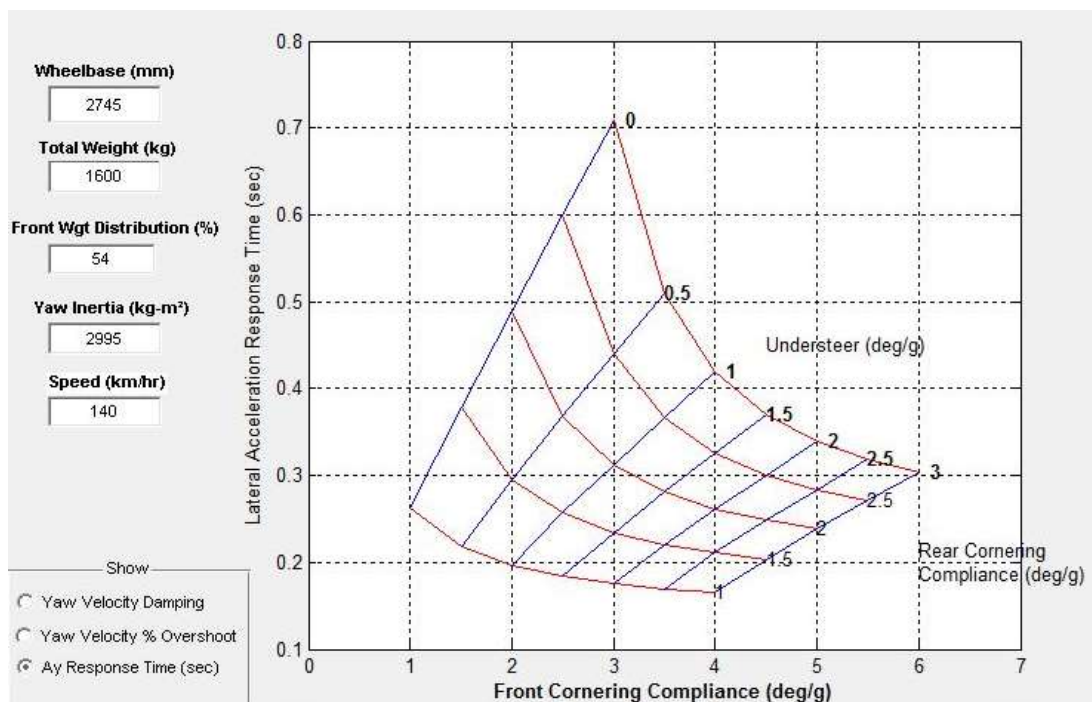
Sur <https://kktse.github.io/jekyll/update/2019/03/17/parameter-sensitivity-analysis.html> (à relire !) , Kelvin Tse trace le même genre de plot



puis étudie l'influence de la dérive avant :



Par Bill Cobb, la même chose :



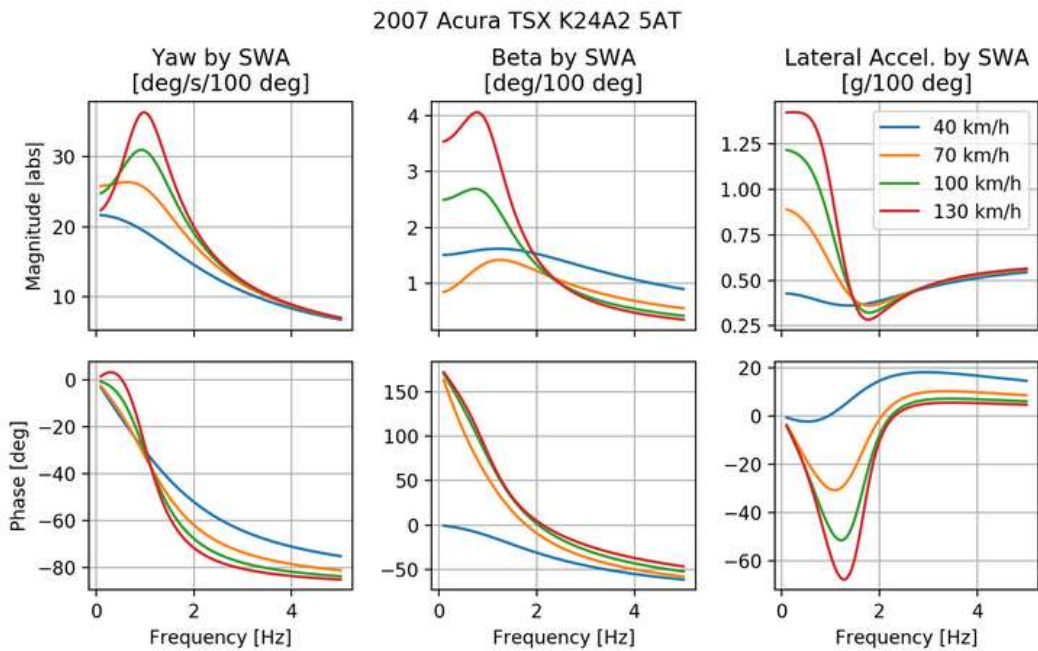
7.7.4 LINÉARITÉ

La linéarité correspond, lors de la mise en virage, à la conformité entre l'entrée du conducteur (angle au volant) et la réponse du véhicule (vitesse de lacet). Le début de la courbe de vitesse de lacet dépend essentiellement du train avant (rigidité de dérive, braquage sous efforts) et de l'inertie en lacet du véhicule. Ce qui est important, c'est la vitesse à laquelle le lacet rattrape son retard par rapport à l'angle au volant (progressive vs réponse en 2 temps).

7.7.5 CARACTÉRISATION FRÉQUENTIELLE

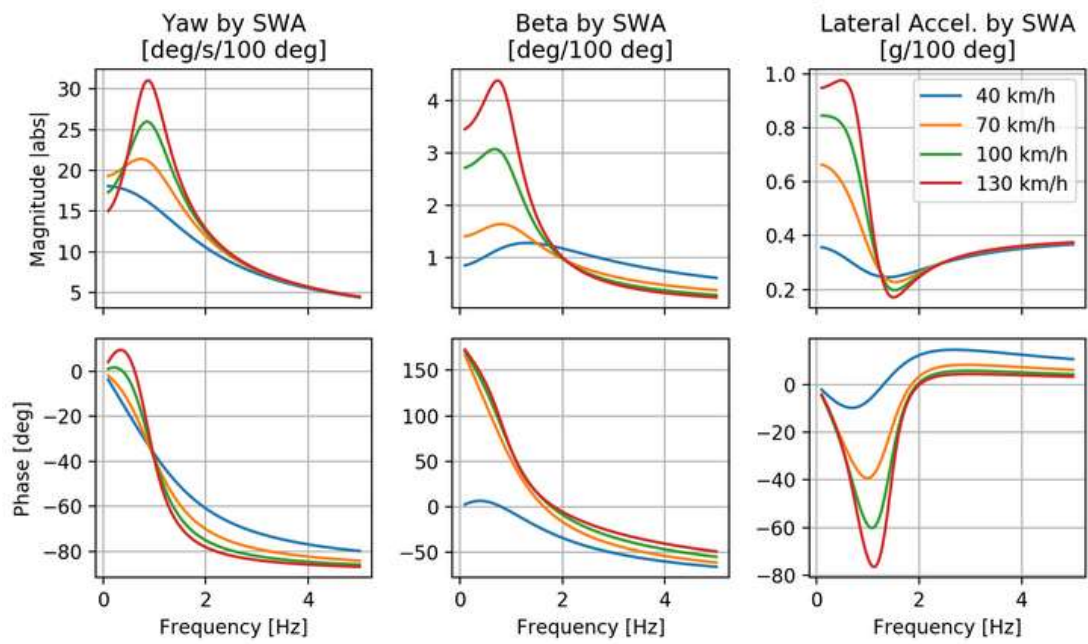
Toujours chez Kelvin Tse

<https://kktse.github.io/jekyll/update/2019/06/01/typical-cornering-compliances.html>

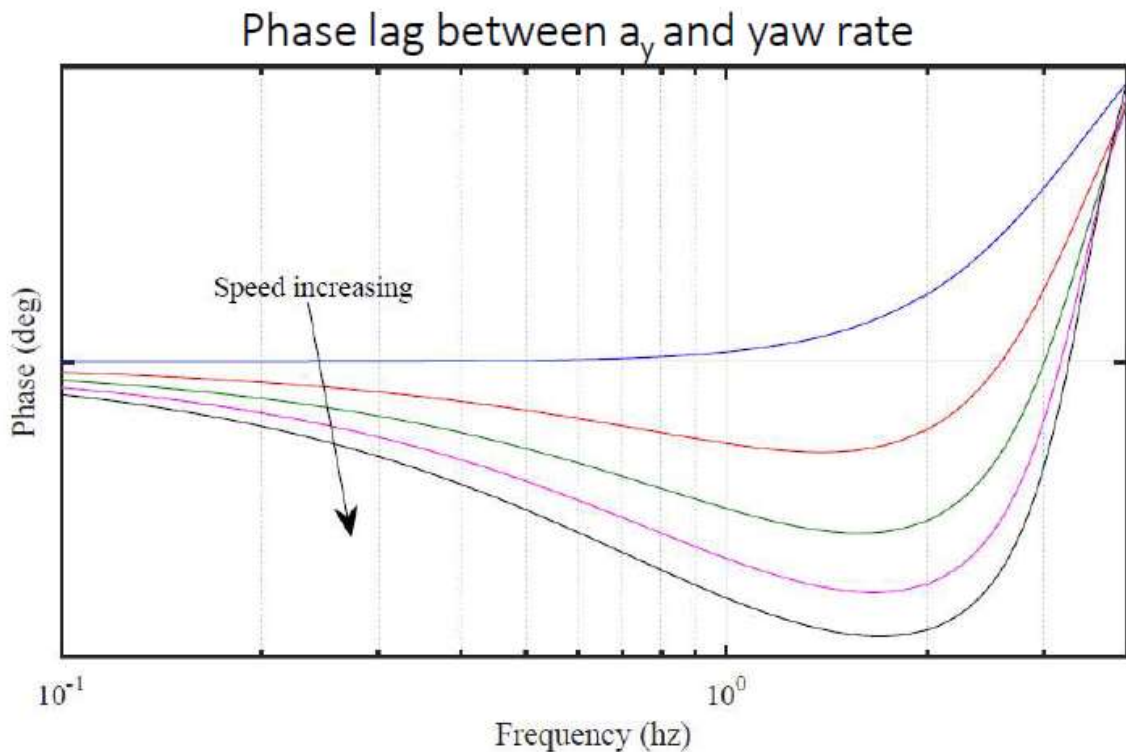


et <https://kktse.github.io/jekyll/update/2019/02/13/on-centre-handling-metrics.html>

2018 OTA - Car #551 2012 Honda Civic Si Coupe



7.7.6 DÉPHASAGE LACET / ACCEL LATÉRALE

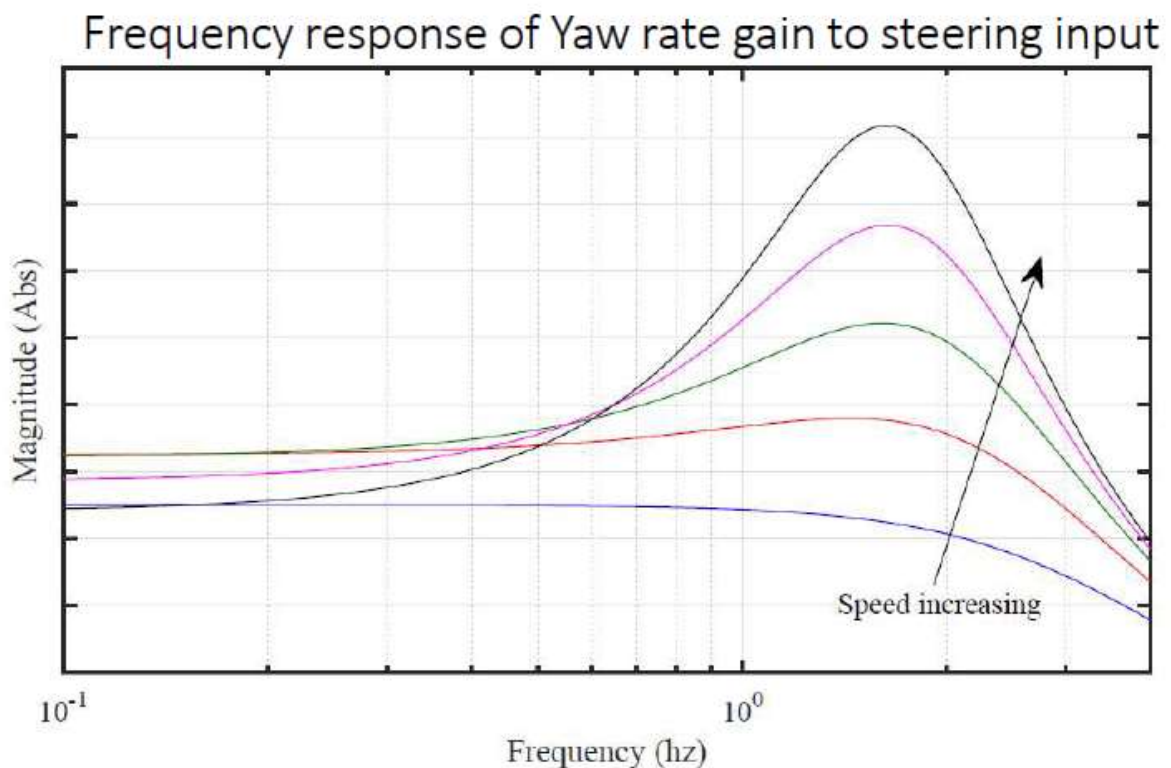


7.7.7 VIDEO ILLUSTRATION DEPHASAGE

Pour illustrer le déphasage entre l'angle volant et la réponse en lacet :

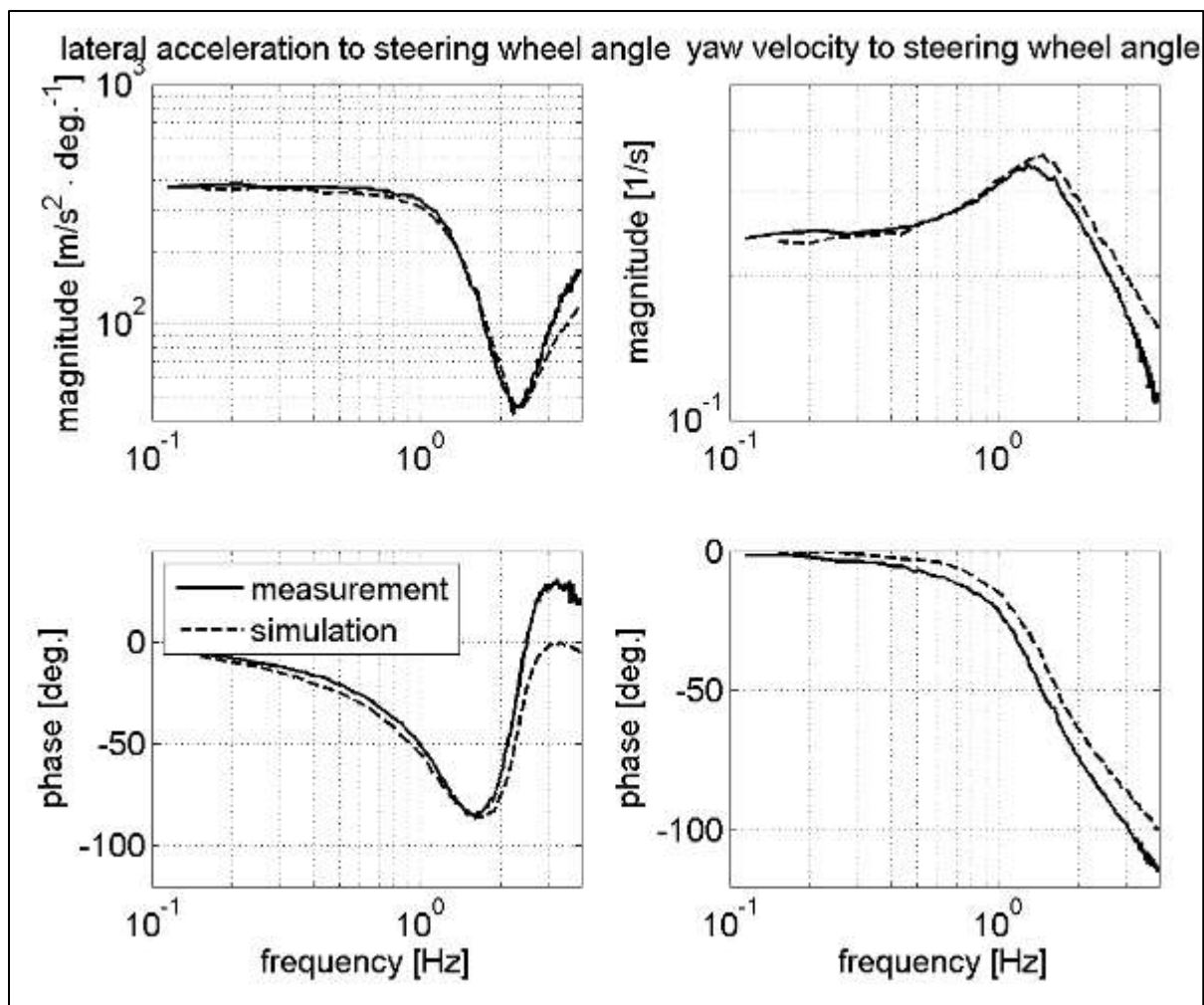
[Slalom with a car at increasing frequency](#) (G. Schaefer)

7.7.8 GAIN EN VITESSE DE LACET



7.7.9 ANTIRÉSONANCE

Phénomène bien visible sur ces courbes tirées de (Groenendijk, 2009) pour une BMW série 5



7.8 INFLUENCE DU DÉVERS

Voir (Kiefer, 1996)

7.9 ANTI-ACKERMANN ?

L'article suivant de Jonathan Vogel illustre le fait que, lorsque le pic d'effort maxi augmente avec l'angle de dérive, il serait préférable de faire en sorte que la roue extérieure dérive plus que la roue intérieure, et donc d'avoir un réglage "anti-Ackermann" (en compétition seulement)

<https://www.racecar-engineering.com/articles/tech-explained-ackermann-steering-geometry>

The higher the vertical load on the tyre, the greater peak lateral force it can produce. At higher vertical loads, the peak lateral force arrives at a higher slip angle. This trend is expected but not necessarily present in all tyres and may depend on compound or construction.

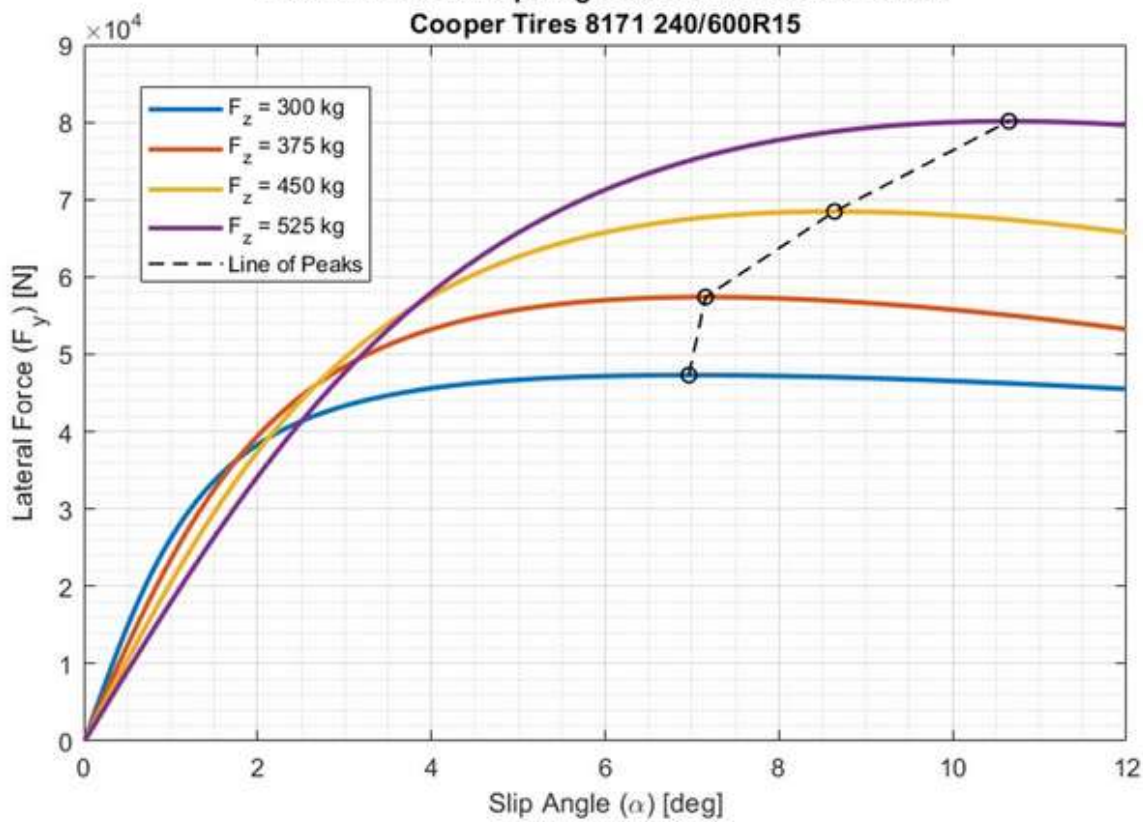
The relationship between vertical load and peak slip angle is known as the Line of Peaks. Characterising the Line of Peaks is essential due to the onset of lateral load transfer during a cornering manoeuvre, transferring vertical load from the inside tyres to the outside tyres.

It is critical to make sure both tyres operate at their peak slip angles simultaneously to maximise performance. In the case of the Indy Lights tyre, this means that the more heavily loaded outside tyre should be at a higher slip angle than the inside tyre. Steering the outside tyre more than the inside for a given steering wheel input achieves this.

The result is the exact opposite of Ackermann Steering and is known as reverse Ackermann or anti-Ackermann. Many race cars fitted with Anti-Ackermann exploit the peak operating conditions of the individual tyres.

Lateral Force vs Slip Angle at Various Vertical Loads

Cooper Tires 8171 240/600R15



8 AERO

8.1 TRAÎNÉE

La traînée mesurée expérimentalement permet de définir un coefficient appelé généralement C_x qui caractérise la qualité aérodynamique d'un véhicule du point de vue résistance à l'avancement. La traînée est un élément important dans le calcul des performances d'un véhicule et en particulier dans la détermination de la vitesse maximum. C_x est un coefficient sans dimension

8.2 PORTANCE

La portance est généralement décomposée en 2 efforts verticaux, sur les trains avant et arrière. Ces efforts modifient l'équilibre statique du véhicule, en diminuant les charges sur chaque train, on peut de la même façon que pour la traînée définir un coefficient de portance C_z .

8.3 MESURE

Les essais en soufflerie permettent d'obtenir les caractéristiques aérodynamiques sous un vent d'incidence variable. On mesure, en fonction de l'angle de dérapage, le torseur des efforts aérodynamiques rapporté en un point O du sol, situé à mi-voie et mi-empattement, avec :

F_x	:	effort de traînée
F_y	:	effort de dérapage
F_z	:	effort de portance
M_x	:	moment de roulis aérodynamique en O
M_y	:	moment de tangage aérodynamique en O
M_z	:	moment de lacet aérodynamique en O

En général l'angle de dérapage ne dépasse pas 20 degré, valeur maximum donnée par la largeur de la veine d'air de la soufflerie dans laquelle le véhicule est mesuré. Au delà il apparaît des effets de bord, qui ne permettent plus une mesure représentative.

On obtient ainsi les courbes d'essai en dérapage qui expriment les coefficients SCX , SCY , SCZ , SCL , SCM , SCN en fonction du dérapage b , avec :

$$\begin{aligned} Fx &= \frac{1}{2} \cdot \rho \cdot V_0^2 \cdot SCX \\ Fy &= \frac{1}{2} \cdot \rho \cdot V_0^2 \cdot SCY \\ Fz &= \frac{1}{2} \cdot \rho \cdot V_0^2 \cdot SCZ \\ Mx &= \frac{1}{2} \cdot \rho \cdot V_0^2 \cdot L \cdot SCL \\ My &= \frac{1}{2} \cdot \rho \cdot V_0^2 \cdot L \cdot SCM \\ Mz &= \frac{1}{2} \cdot \rho \cdot V_0^2 \cdot L \cdot SCN \end{aligned}$$

avec,

ρ = Masse volumique de l'air.

V_0 = Vitesse du vent résultant.

L = Longueur de référence (empattement du véhicule).

S = Surface de référence (maître couple ou projection de la surface frontale).

8.4 RÉPONSE EN LACET

A partir d'un modèle simplifié de véhicule lacet-dérive (sans roulis, ni braquage), on fait une étude de la réponse en lacet à une sollicitation transversale en coup de vent latéral, permettant d'obtenir la valeur du rapport ψ'/F , donnant la sensibilité en lacet du véhicule à un coup de vent latéral (rapport de la vitesse de lacet stabilisée sur l'effort aérodynamique s'appliquant en un point **Ca**, centre de poussée latérale situé à la distance **a** du centre de gravité **G**).

Les détails relatifs à ce modèle simplifié d'étude du comportement sous vent latéral sont explicités dans la note N° **3484/86/0861** de T. Landreau, qui a développé ce modèle.

Tous calculs effectués on obtient la formulation suivante :

$$\frac{\psi'}{F} = \frac{V \cdot (D1 + D2) \cdot (a - d)}{L'^2 \cdot D1 \cdot D2 \left(1 + V^2 \cdot \frac{dr}{L'} \right)}$$

qui donne en exprimant la dynamique angulaire simplifiée à la roue (termes de dérive seuls),

$$dr = \frac{M.(D_2.l'2 - D_1.l'1)}{L'.D_1D_2}$$

la valeur finale du rapport ψ'/F ,

$$\boxed{\frac{\psi'}{F} = \frac{V}{M} \left(1 - \frac{a}{d}\right) \frac{dr}{L' + V^2 \cdot dr}}$$

avec,

ψ' = Vitesse de lacet stabilisée du véhicule

F = Effort aérodynamique s'appliquant au point Ca (centre de poussée latérale)

V = Vitesse du véhicule

M = Masse totale du véhicule

D_1 = Rigidité de dérive du train avant (pneus+train)

D_2 = Rigidité de dérive du train arrière (pneus+train)

l_1 = Distance du centre de gravité au train avant $\rightarrow l'1 = l_1 - a_1$

l_2 = Distance du centre de gravité au train arrière $\rightarrow l'2 = l_2 + a_2$

L = Empattement du véhicule avec $L = l_1 + l_2 \rightarrow L' = l'1 + l'2$

a_1 = Bras de levier du moment d'auto-alignement pour le pneu avant

a_2 = Bras de levier du moment d'auto-alignement pour le pneu arrière

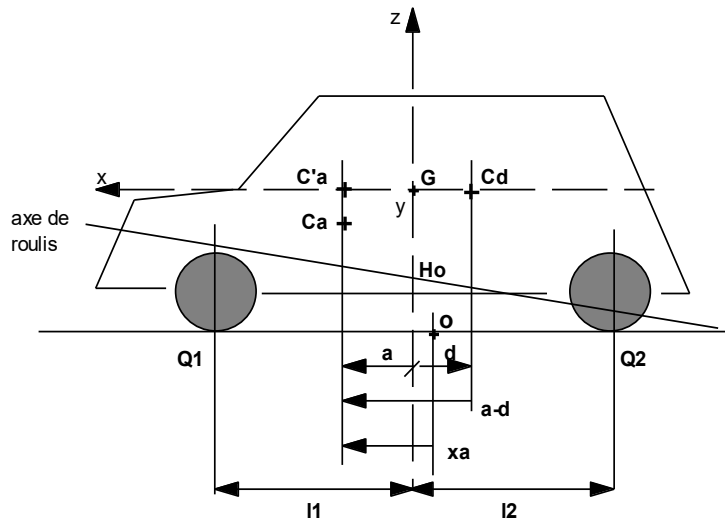
dr = Dynamique angulaire simplifiée à la roue (termes de dérive seuls)

a = Distance de la projection du centre de poussée latérale C'a au centre de gravité G

d = Distance du centre équidérive Cd au centre de gravité G

Remarques : Bien sûr ce modèle simplifié de comportement sous vent latéral ne répond pas à toutes les questions du fait de sa trop grande simplicité, mais il permet dans une phase amont d'un projet, de comparer un véhicule en cours d'étude à un véhicule existant que l'on connaît bien. On peut ainsi analyser les paramètres qui participent à "la tenue de cap" sous vent latéral, comme le rapport SCN/SCY, la répartition des masses, la rigidité de dérive du train arrière, la dynamique angulaire, etc, ...

8.5 PARAMÈTRES DU LACET



- G = Centre de gravité du véhicule
 O = Point du sol où s'exprime le torseur des efforts aérodynamiques
 (point situé à mi-voie et mi-empattement)
 Ca = Centre de poussée latérale (point d'application de l'effort F_y)
 C'a = Projection du centre de poussée latérale sur l'axe \vec{x}
 Cd = Centre équidérive, c'est le point où un effort transversal ne produit aucun lacet
 a = Distance de la projection du centre de poussée latérale C'a au centre de gravité G

$$a = \overline{G} \overline{C}'a$$

$$a = \frac{l_1 - l_2}{2} + xa$$

- d = Distance du centre équidérive Cd au centre de gravité G

$$d = \overline{G} \overline{C}d$$

$$d = \frac{(D_1.l'_1 - D_2.l'_2)}{D_1 + D_2}$$

□ En général, on a $a > 0$ et $d < 0$, le terme $(a-d)$ représente donc le bras de levier par lequel un effort aérodynamique de dérapage induit une vitesse de lacet, d'où l'importance de celui-ci dans la réponse du véhicule. Toutefois la valeur $|a/d|$ rend mieux compte de la sensibilité au vent latéral.

- xa = Bras de levier de Mz, moment de lacet aérodynamique

$$Mz = Fy \cdot xa$$

$$xa = L \cdot \frac{SCN}{SCY}$$

Mz = Moment de lacet aérodynamique

$$Mz = \frac{l}{2} \cdot \rho \cdot V_0^2 \cdot L \cdot SCN$$

Fy = Effort de dérapage aérodynamique

$$Fy = \frac{l}{2} \cdot \rho \cdot V_0^2 \cdot SCY$$

SCN = Coefficient du moment de lacet aérodynamique

SCY = Coefficient de l'effort de dérapage aérodynamique

8.6 SENSIBILITÉ AU VENT LATÉRAL

Dans nos études effectuées nous montrions que certains véhicules pouvaient présenter une plus grande sensibilité en lacet au vent latéral, par rapport à d'autres véhicules de la gamme ou par rapport à la concurrence, due principalement à :

- un rapport SCN/SCY défavorable (trop grand),
- une moins bonne répartition des masses (G pas assez avancé),
- une rigidité de dérive du train arrière D2 plus petite,
- une dynamique angulaire **da** plus faible.

Pour diminuer cette sensibilité au vent latéral, il faut donc réduire le rapport SCN/SCY, qui est le paramètre principal, c'est à dire travailler sur l'aérodynamique du véhicule, mais aussi chercher à réduire le rapport ψ'/F qui intègre également les caractéristiques statico-dynamiques (dynamique angulaire et donc rigidités de dérive totales aux trains D1 et D2).

La valeur du terme $|a/d|$ (distance du centre de gravité G au centre de poussée latérale aérodynamique Ca, sur la distance du centre de gravité G au centre équidérive Cd) rend bien compte de l'évolution de ψ'/F pour les véhicules sous-vireurs classiques (dynamique angulaire **da** de 3 degré à 5 degré au volant). Pour des véhicules sur-vireurs ou peu sous-vireurs, réduire ψ'/F à la valeur $|a/d|$ serait toutefois hasardeux.

La valeur de **d** est liée à la dynamique angulaire par le fait qu'elle prend en compte les rigidités de dérive totales des trains avant et arrière, et dire qu'il faut diminuer $|a/d|$, revient à dire qu'il faut d'autant plus

*reculer le centre de poussée latérale **Ca** que la dynamique angulaire est faible, donc que le véhicule est moins stable, ce qui semble cohérent avec le bon sens physique.*

Les recommandations pour **réduire cette sensibilité au vent latéral** peuvent se résumer ci-dessous :

<u>effet</u>	<u>responsable</u>
F aéro le plus petit possible	1
C a le plus reculé possible	1
C d le plus reculé possible	dr ↗ a/d ↘ 2 + 3 + 1
G le plus avancé possible	3

avec

- 1** Aérodynamique (style)
- 2** Trains
- 3** Architecture

Ca : centre de poussée aérodynamique

Cd : centre équidérive

G : centre de gravité

8.7 INFLUENCE DES DIFFERENTS PARAMETRES

Un coup de vent latéral a tendance à provoquer un mouvement de lacet. Si le centre de poussée latérale aérodynamique est situé au-dessus de l'axe de roulis, comme les braquages induits par le roulis sont sous-vireurs, ils vont avoir tendance à amplifier l'effet du moment de lacet dû au coup de vent.

Le rapport vitesse de lacet/effort dû au vent varie comme le rapport b/d , avec b la projection sur x de la distance du centre de gravité au centre de poussée aérodynamique et d la projection selon x de la distance du centre de gravité au centre équidérive. Pour diminuer la valeur du premier rapport, il faut donc augmenter la valeur de d . Les braquages initiaux et induits par le roulis sont un moyen de le faire (d est grand si la dynamique angulaire est importante).

8.8 F1



source <https://www.youtube.com/watch?v=dKyhiZgQyoU>

9 MANŒUVRES

9.1 NORMES ISO

Generalities	ISO test norm	ISO simulation norm
Road vehicles -- Types -- Terms and definitions	3833	
General conditions for passenger cars	15037	
Vehicle dynamics and road-holding ability -- Vocabulary	8855	
Masses -- Vocabulary and codes	1176	
Manoeuvre		
Steady-state	4138	19364
Sine with dwell	ECE-13H / FMVSS 126	19365
Lateral transient	7401	
Double lane change	3888	
Power-off reaction of a vehicle in a turn	9816	
Braking in a turn	7975	
Sensitivity to lateral wind	12021	
Quantification of on-center handling : weave test + transition test	13674	
Straight line braking	DIN 70028	
Mu-split braking	14512	
Steering swing (Steering-release open-loop test method)	17288	
Trailer Stability	9815	

Côté confort, on peut également noter l'ISO 2631, avec par exemple la 2631-4 mais qui est plutôt dédiée au transport ferroviaire.

Dans [Blundell & Harty](#) :

Vehicle handling simulations are intended to recreate the manoeuvres and tests that vehicle engineers carry out using prototype vehicles on the test track or proving ground. Some are defined by the International Standards Organization (ISO), which outlines recommended tests in order to substantiate the handling performance of a new vehicle:

ISO 3888-1:1999	Passenger cars – Test track for a severe lane-change manoeuvre – Part 1: Double lane-change.
ISO 3888-2:2002	Passenger cars – Test track for a severe lane-change manoeuvre – Part 2: Obstacle avoidance
ISO 4138:1996	Passenger cars – Steady-state circular driving behaviour – Open-loop test procedure
ISO 7401:2003	Road vehicles – Lateral transient response test methods – Open-loop test methods
ISO 7975:1996	Passenger cars – Braking in a turn – Open-loop test procedure
ISO/TR 8725:1988	Road vehicles – Transient open-loop response test method with one period of sinusoidal input
ISO/TR 8726:1988	Road vehicles – Transient open-loop response test method with pseudo-random steering input
ISO 9815:2003	Road vehicles – Passenger-car and trailer combinations – Lateral stability test
ISO 9816:1993	Passenger cars – Power-off reactions of a vehicle in a turn – Open-loop test method
ISO 12021-1:1996	Road vehicles – Sensitivity to lateral wind – Part 1: Open-loop test method using wind generator input
ISO 13674-1:2003	Road vehicles – Test method for the quantification of on-centre handling – Part 1: Weave test
ISO 14512:1999	Passenger cars – Straight-ahead braking on surfaces with split coefficient of friction – Open-loop test procedure
ISO 15037-1:1998	Road vehicles – Vehicle dynamics test methods – Part 1: General conditions for passenger cars
ISO 15037-2:2002	Road vehicles – Vehicle dynamics test methods – Part 2: General conditions for heavy vehicles and buses
ISO 17288-1:2002	Passenger cars – Free-steer behaviour – Part 1: Steering-release open-loop test method
ISO/TS 20119:2002	Road vehicles – Test method for the quantification of on-centre handling – Determination of dispersion metrics for straight-line driving

719

On trouve également :

[ISO 1176:1990, Road vehicles — Masses — Vocabulary and codes.](#)

[ISO 3833:1977, Road vehicles — Types — Terms and definitions.](#)

[ISO 4138:1996, Passenger cars — Steady-state circular driving behaviour — Open-loop test procedure.](#)

[ISO 8855:1991, Road vehicles — Vehicle dynamics and road-holding ability — Vocabulary](#)

9.2 NORMES FVSS

https://en.wikipedia.org/wiki/Federal_Motor_Vehicle_Safety_Standards

9.3 NORMES NHTSA

Tiré d'un papier NHTSA de 2003

- **Characterization**
 - Constant Speed, Slowly Increasing Steer (SAE J266)
- **Rollover Resistance Assessment**
 - NHTSA J-Turn
 - Fishhooks
 - .. Fixed Timing Fishhook (Fixed Dwell Time)*
 - .. Roll Rate Feedback Fishhook (Variable Dwell Time)*
 - .. Nissan Fishhook
 - Double Lane Changes
 - .. Ford Path-Corrected Limit Lane Change (PCL LC)
 - .. Consumers Union Short Course*
 - .. ISO 3888 Part 2*
 - .. Open-loop Pseudo Double Lane Change

Criteria	J-Turn	FT Fishhook	RRF Fishhook	ISO 3888-2
Drivers Required	<i>One</i>	<i>One</i>	<i>One</i>	<i>Multiple</i>
Steering Input	<i>Controller</i>	<i>Controller</i>	<i>Controller</i>	<i>Driver</i>
Steering Repeatability	<i>High</i>	<i>High</i>	<i>High</i>	<i>Driver-Dependent</i>
Precise Reproducibility	<i>High</i>	<i>High</i>	<i>High</i>	<i>Low</i>
Rating	<i>Excellent</i>	<i>Excellent</i>	<i>Excellent</i>	<i>Bad</i>

- Slowly Increasing Steer
- NHTSA J-Turn (Dry, Wet)
- NHTSA Fishhook (Dry, Wet)
- Closing Radius Turn
- Pulse Steer (500 deg/s, 700 deg/s)
- Sine Steer (0.5 Hz, 0.6 Hz, 0.7 Hz, 0.8 Hz)
- Increasing Amplitude Sine Steer (0.5 Hz, 0.6 Hz, 0.7 Hz) (2ième lobe *1.3)
- Sine with Dwell (0.5 Hz, 0.7 Hz)
- Yaw Acceleration Steering Reversal(500 deg/s, 720 deg/s)
- Increasing Amplitude YASR (500 deg/s, 720 deg/s)

9.4 MAIS AUSSI ...

<https://www.measx.com/en/products/software/moses/maneuvres>

9.5 STEADY-STATE DYNAMICS (ISO 4138)

<http://www.driveability-testing-alliance.com/download/datasheets/DTA-Steady-State-Circular-Test-DE-B090603e.pdf>

Parameters for the Steady-State Circular Test

At increasing vehicle speed the **slip angle difference** between the front and rear axle is of major significance with a one-track model. In case of a positive difference $\alpha_v - \alpha_h$ the steering wheel angle must be increased, in case of negative difference decreased. The **following definitions** have been established:

$\alpha_v - \alpha_h \geq 0$ understeer self-steering effect

$\alpha_v - \alpha_h = 0$ neutral self-steering effect

$\alpha_v - \alpha_h \leq 0$ oversteer self-steering effect

The same definitions apply to the self-steering gradient.

In **steady-state driving mode** each axle has to build up lateral forces to support the inertial force $m \cdot a_{quer}$. The axle with the higher slip angle shows greater motion in the lateral direction. In case of **understeer** the higher slip angles occur on the front axle. The vehicle pushes outward over the front axle. When a vehicle **oversteers** the higher slip angles occur on the rear wheels and, in case of high values, can lead to instability.

$$EG = \frac{d\delta_H}{da_{quer}} \cdot \frac{l}{i_s}$$

l = axle distance, i_s = steering ratio

The **self-steering gradient** equates to the incline of the curve $\delta_H = f(a_{quer})$. In the linear vehicle dynamics range up to 4 m/s^2 the self-steering gradient is a constant, above this value it changes, depending on lateral acceleration.

For yaw speed, the following applies:

$$\frac{\dot{\psi}}{\delta_H} = \frac{v}{i_s \cdot l + i_s \cdot EG \cdot v^2}$$

The **DTA measurement vehicle** has understeering characteristics ($EG > 0$), displaying the typical behavior of yaw intensification initially increasing as speed increases, then reaching a maximum and ultimately decreasing again. The speed equating to the maximum is called characteristic speed.

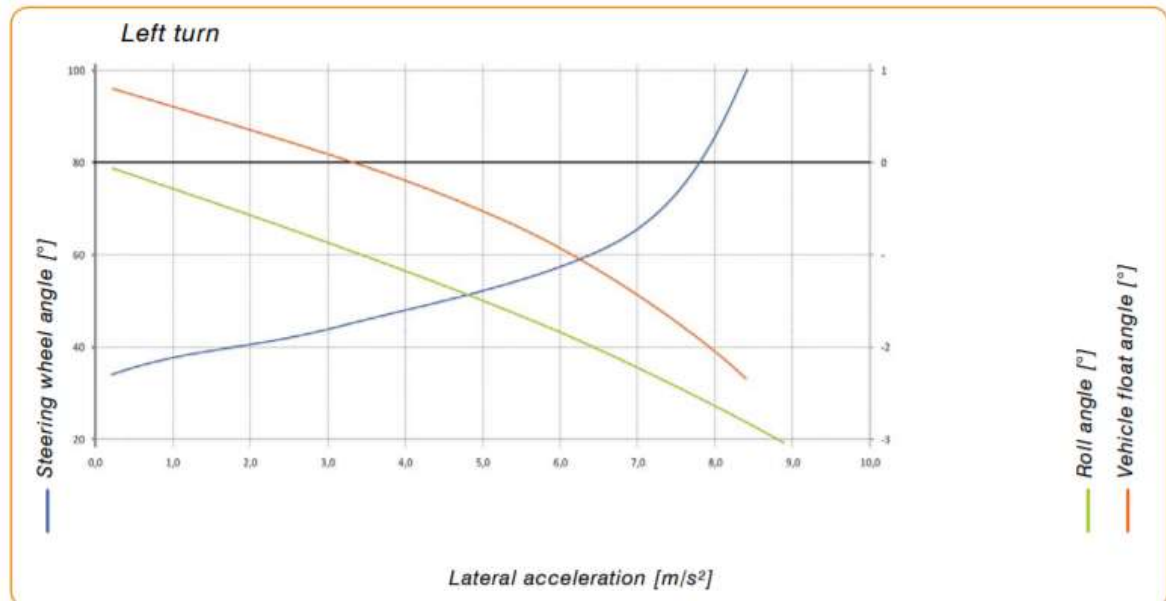
$$v_{ch} = \sqrt{\frac{l^2 \cdot C_v \cdot C_h}{m \cdot (C_h \cdot l_h - C_v \cdot l_v)}}$$

C_v, C_h = slip stiffness front axle, rear axle; l_v, l_h = distances of center of gravity to front axle, rear axle; m = mass

Yaw intensification substantially characterizes the steady-state qualities of a vehicle and is a measure of how intensively the vehicle responds to steering angle changes.

Data Analysis

To analyze the **quasi-steady-state circular test**, TÜV SÜD has developed a routine which, based on existing criteria, serves to identify the respective steady-state conditions set up and to deliver the values for the steering wheel angle and lateral acceleration as averaged values over the measurement period. These individual parameters are plotted using a mathematical interpolation function.



Based on the **positive incline value** of the curve obtained during the counter-clockwise test, for the steady-state range up to 4 m/s^2 , a positive value for the self-steering gradient $EG = 3.35 \frac{\text{rad/s}^2}{\text{m}}$ is calculated, which means **understeering**. From a lateral acceleration of 5 m/s^2 the amount of steering angle required to maintain the constant cornering radius (100 m) notably increases. At the same time, the steering torque (not plotted here) decreases. The roll angle continually increases with increasing lateral acceleration. The characteristic speed is 112 km/h .

The **float angle** can be used to characterize the vehicle's orientation relative to its trajectory tangent as well as to evaluate the **vehicle's stability and controllability** up to the limit. In the counter-clockwise test shown here the float angle displays positive values up to a lateral acceleration of 3.5 m/s^2 , which means that the vehicle is oriented toward the outside of the corner with its longitudinal axis. According to the one-track model the float angle has been determined at

$$\beta = \frac{l_h}{R} - \alpha_h$$

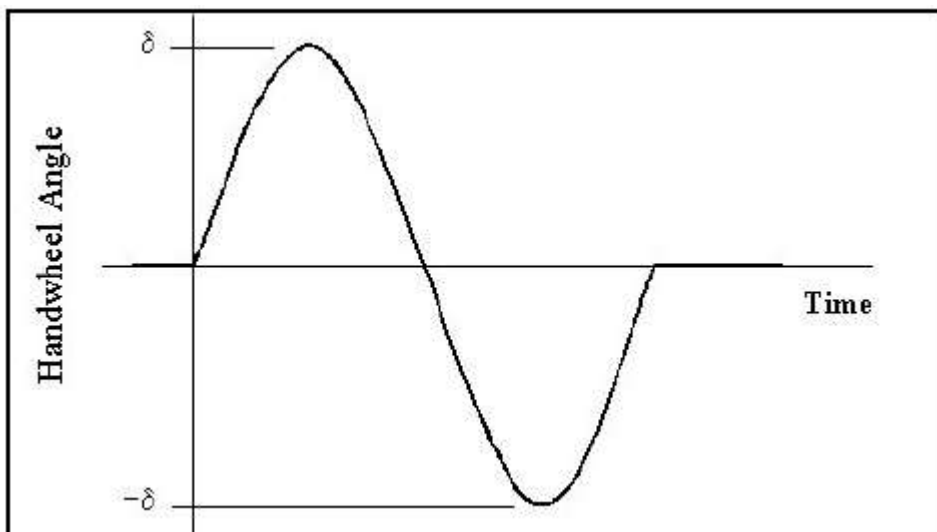
l_h = distance between center of gravity and rear axle; α_h = slip angle rear axle

During the **test on a constant radius** the float angle continues to decrease as the slip angle keeps increasing and assumes negative values after a zero crossing. The negative float angle means that the longitudinal vehicle axle now points inward. This behavior does not depend on the self-steering effect but only on the slip angle on the rear axle, which means that understeering vehicles display this characteristic as well.



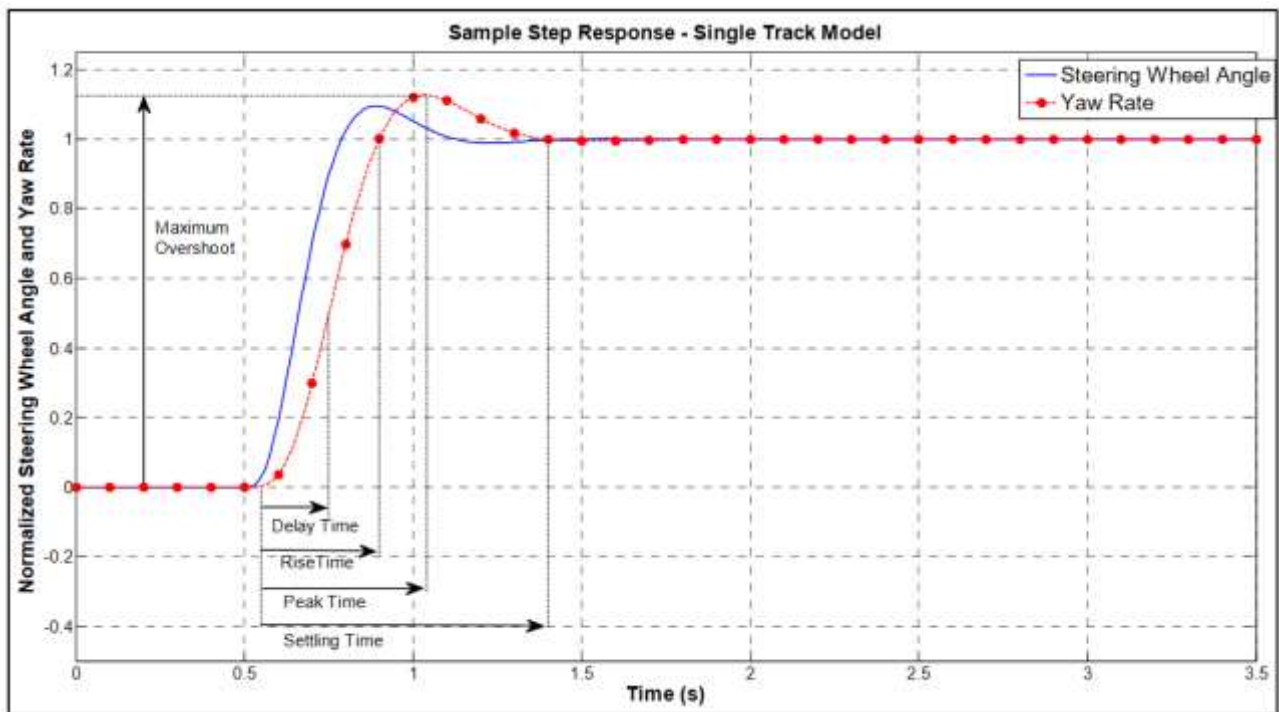
9.6 SIS : SLOWLY INCREASING STEER

9.7 SINE STEER



Fréquences de 0.5 à 0.8 Hz

9.8 STEP STEER (ISO 7401)



Commonly used performance metrics, which can be seen in Figure 4.4 are:¹²⁸

- Delay time, t_d
- Rise time, t_r
- Peak time (provided that the system is underdamped), t_p
- Settling time, t_s
- Maximum overshoot ratio (provided that the system is underdamped), M_{os}

Dans (Pauwelussen, 2014), p.128

TABLE 5.2 Test Methods, Included in ISO 7401

Test Method	Description	Performance Metrics
Time Domain		
Step input	Rapid change (ramp) of steering angle δ	Response time, peak response time, overshoot values for vehicle motion response (yaw rate a_y)
Sinusoidal input (one period)	One period steering wheel input (0.5 Hz, 1 [Hz] optional) at $a_y = 4 [\text{m/s}^2]$ (2 or 6 [m/s^2] optional)	First peak values of a_y , yaw rate r , time lags of a_y , r to δ , gains (a_y , r) w.r.t. steering input δ
Frequency Domain		
Random input	Continuous inputs covering a frequency area, for $a_y < 4 [\text{m/s}^2]$ ($2 [\text{m/s}^2]$ recommended)	Steady-state gains (a_y , r) w.r.t. steering input δ , bandwidth, peak ratio, equivalent time
Pulse input	Triangular wave form steering input of 0.3–0.5 s width, with δ_{\max} cf. $a_y = 4 [\text{m/s}^2]$ steady state	Similar to random input
Continuous sinusoidal input	Three successive periods in δ , with increasing frequency and $a_y < 4 [\text{m/s}^2]$	Amplitudes (a_y , r), gains (a_y , r) w.r.t. steering input δ , phase shifts between a_y , r , and steering angle δ

<http://www.driveability-testing-alliance.com/download/datasheets/DTA-Step-Steering-Input-DE-B090601e.pdf>

Objective of the Driving Maneuver

According to ISO 7401 this test serves the main objective of describing the **transverse dynamic behavior** of a vehicle. It defines characteristic values and functions required for both the time range and the frequency range.

Key criteria in the **time range** include, among others:

- Time shift between steering wheel angle, lateral acceleration and yaw speed
- Gain factor of yaw speed ($\frac{\psi}{\delta_H}$)

Key criteria in the **frequency range** include, among others:

- Lateral acceleration related to steering wheel angle
- Yaw speed related to steering speed

Test Procedures

From straight-line driving at a constant speed of approx. 80 km/h the steering wheel is moved as fast as possible to the angle position that will result in a **lateral acceleration** of 4 m/s² as the vehicle now begins to corner. This angle position was previously measured during steady-state circular motion. To facilitate the requisite steering precision for the driver a limit stop may be used, however, actuation by a steering robot is preferable in order to ensure the repeatability of the tests. On the DTA test vehicle an actuation speed for the steering wheel angle was fixed at 500 °/s by a **steering robot**. To determine the aforementioned characteristic values and functions, three tests in counter-clockwise and three in clockwise direction are analyzed. The lowest deviations between the individual tests are a measure for the quality of performing the test.

Measurands

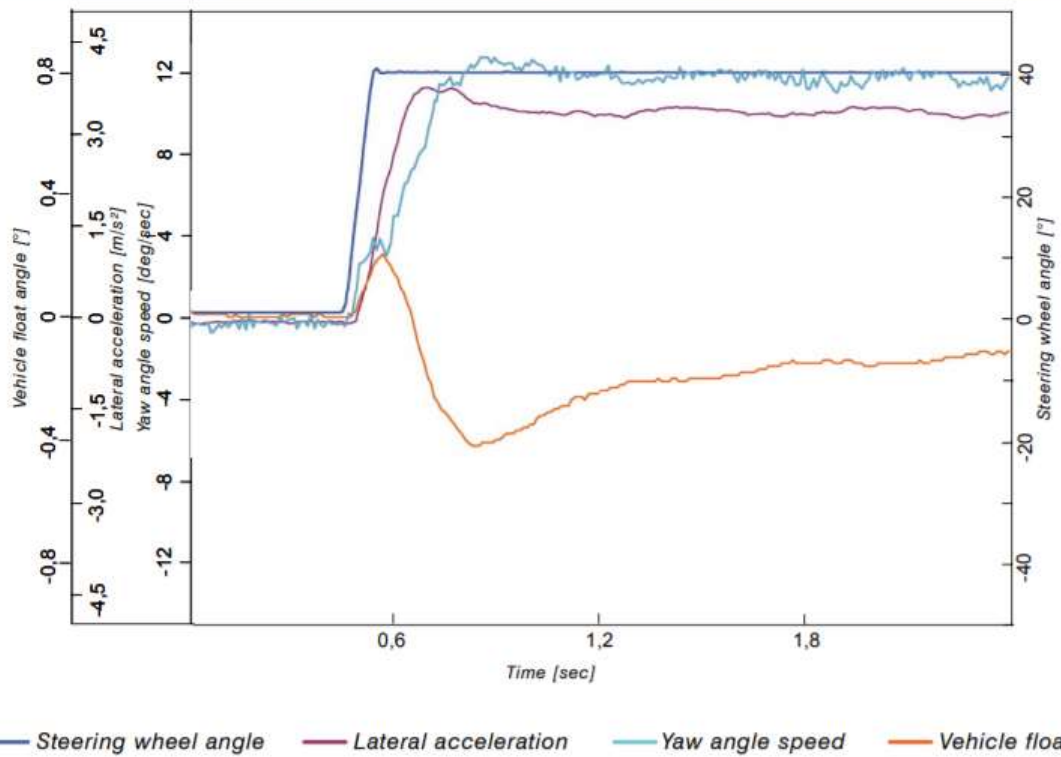
According to ISO 7491 the following "**mandatory measurands**" must be logged:

- Steering wheel angle
- Lateral acceleration
- Yaw speed
- Steady-state float angle
- Longitudinal speed

In addition, logging of the following "**optional measurands**" is recommended:

- Lateral speed or unsteady float angle
- Roll angle
- Steering wheel torque
- Forces and moments acting on the wheels
- Slip angle on the wheels

Data Analysis



At the beginning of the step steering input at $t = 0$, due to the turn-in, the **lateral force** is initially generated only at the front axle which tends to push the vehicle toward the outside of the corner as a result of **inertia** $m \cdot a_y$. As a consequence of this effect an **increasing slip angle** acts on the rear axle with correspondingly increasing lateral force. The slip angle on the rear axle is generated with a time delay vis-à-vis the front axle. When the steady-state driving conditions have been achieved the lateral forces at the wheels and the vehicle's inertia are in balance.

In accordance with the – initially very small – slip angle at the rear axle the values of the float angle in counter-clockwise motion are positive at first. However, as the slip angle at the rear axle increases the float angle decreases continually and, after a zero crossing, reaches negative steady-state values. Steering angle and lateral force are exactly in phase, a slight phase delay exists for the slip and roll angles.

The table below shows the characteristic values obtained for step steering input:

Parameter	Symbol	Unit	Counter-clockwise Tests			Clockwise Tests		
			1	2	3	1	2	3
Stat. yaw gain factor	$(\frac{\psi}{\delta_H})_{ss}$	s^{-1}	0.25	0.25	0.25	0.27	0.27	0.27
Response time of a_{lat}	$T_{a\gamma}$	s	0.24	0.24	0.24	0.24	0.24	0.24
Response time of ψ	T_ψ	s	0.12	0.12	0.12	0.13	0.13	0.12
Time until maximum a_{lat}	$T_{a\gamma, max}$	s	0.40	0.43	0.40	0.43	0.43	0.43
Time until maximum ψ	$T_{\psi, max}$	s	0.22	0.24	0.21	0.22	0.22	0.21
Overshoot value of a_{lat}	$U_{a\gamma}$	-	0.08	0.09	0.05	0.06	0.05	0.05
Overshoot value of ψ	U_ψ	-	0.12	0.12	0.10	0.11	0.12	0.10

Summary

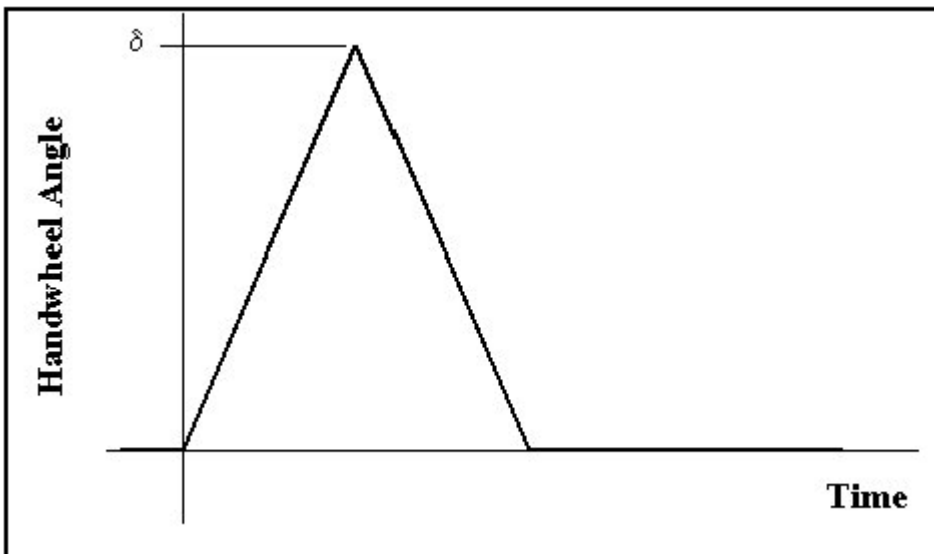
The vehicle's response to sudden step steering input enables statements to be made about the speed of response, vehicle stability under the existing conditions as well as for the precision of the steering system. In case of a **major phase delay** between steering wheel input and yaw speed the **vehicle can be perceived as inert and possessing poor cornering ability**.

If during the change from the unsteady to the steady-state phase of the step steering input yaw speed and lateral acceleration exhibit **large amplitudes** and **long transient periods**, then **vehicle stability may be jeopardized**.

The **gain factor**, the quotient of yaw speed and the steering wheel angle, is a measure of how much steering angle the driver needs in order to generate a certain yaw response. A precise steering system is characterized by a large **gain factor**.

9.9 PULSE STEER

Vitesse volant de 500 ou 700°/sec



9.10 ON-CENTER HANDLING (ISO 13674)

<https://www.iso.org/standard/54302.html>

ISO 13674-1:2010

QUANTIFICATION DU CENTRAGE -- PARTIE 1: ESSAI EN PETITE SINUSOÏDE AU VOLANT / Weave test

Publications liées :

- K.D. Norman Objective evaluation of on-center handling performance. SAE1 Technical Paper 840069, 1984
- D.G. Farrer An objective measurement technique for the quantification of on-centre handling quality. SAE Technical Paper 930827, 1993
- J. Sommerville, D.G. Farrer, J.P. Whitehead Improvements in the quantification of on-centre handling quality. Paper C466/049/93, Institution of Mechanical Engineers, London, 1993

9.11 SINE WITH DWELL (ECE-13H / FMVSS 126)

<https://www.sis.se/api/document/preview/8022897/>

**Passenger cars – Validation of vehicle dynamic simulation –
Sine with dwell stability control testing (ISO 19365:2016, IDT)**

This document specifies a method for comparing computer simulation results from a vehicle mathematical model to test data measured for an existing vehicle undergoing sine with dwell tests that are typically used to evaluate the performance of an electronic stability control (ESC) system. The comparison is made for the purpose of validating the simulation tool for this type of test when applied to variants of the tested vehicle.

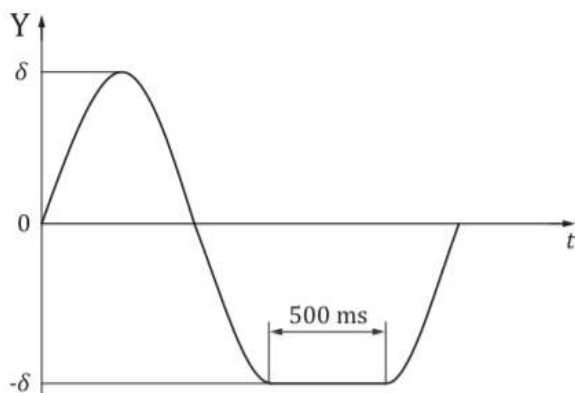
It is applicable to passenger cars as defined in ISO 3833.

NOTE The sine with dwell test method described in this document is based on the test method specified in regulations USA FMVSS 126 and UN/ECE Regulation No. 13-H.

sine with dwell test

test in which the vehicle is steered by a robot using a steering pattern of a sine wave at a frequency of 0,7 Hz with a delay of 500 ms beginning at the second peak amplitude

Note 1 to entry: See [Figure 1](#).



Key

Y steering-wheel angle

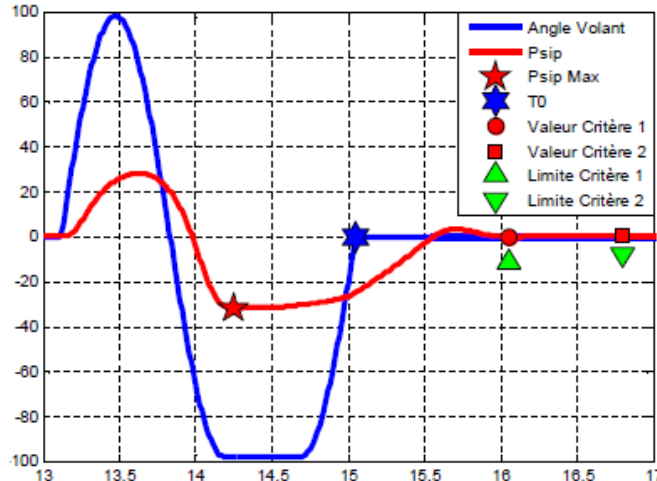
t time

Figure 1 — Steering-wheel input for a sine with dwell test

BOS = beginning of steer

COS = completion of steer

Le test SineDwell consiste en une période de sinus en angle volant à 0.7 Hz, coupé par une pause de 500 ms. Les valeurs crêtes de l'angle volant dépendent d'un angle de référence, qui est l'angle volant donnant une **accélération transversale de 0.3g à 80 km/h**. On applique un angle volant variant de 1.5 à 6.5 fois cet angle de référence, par pas de 0.5



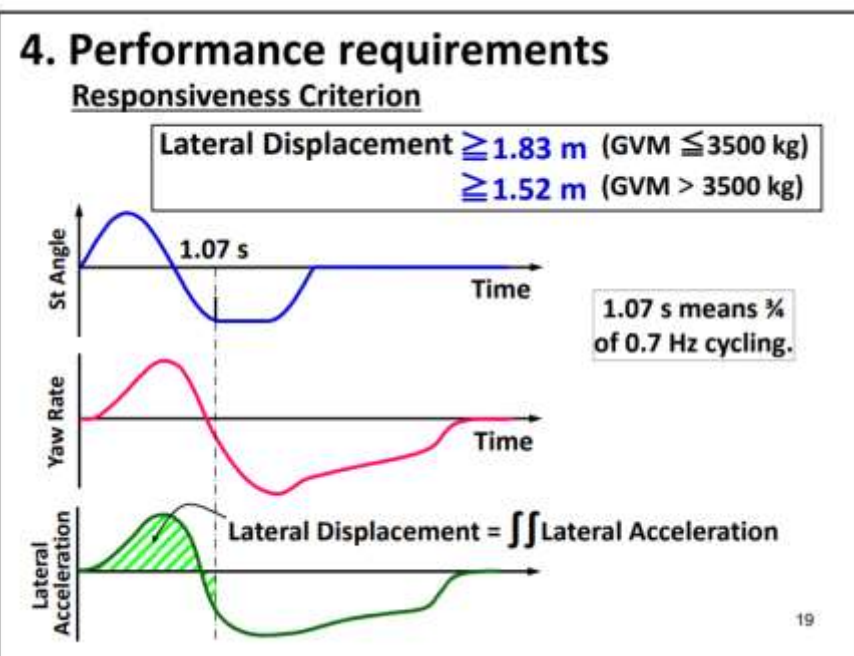
Le test échoue si l'un des deux critères suivants n'est pas respecté :

$$\dot{\Psi}(t_0 + 1.00) / \dot{\Psi}_{Pic} \leq 35\%$$

$$\dot{\Psi}(t_0 + 1.75) / \dot{\Psi}_{Pic} \leq 25\%$$

L'exemple ci-contre est pour la B91 avec un multiplicateur de 3.5, sans ESC. Dans ces conditions, le test échoue pour un multiplicateur de 4.

On trouve aussi ([ici](#)) les critères suivants :



A theoretical justification of the sine with dwell manoeuvre

<https://doi.org/10.1080/00423114.2014.1002794>

The paper at hand uses optimal control theory to theoretically justify the use of the SWD manoeuvre to produce a severe lateral motion and over-steering based on steering input. It is shown that a manoeuvre similar to the SWD manoeuvre can be obtained from an optimal control problem using simple vehicle dynamics models. The optimal control method is further used to analyse the manoeuvre's robustness with respect to vehicle dimensions and tyre

properties. It is shown that the manoeuvre is robust in dimensions, which theoretically motivates its application for various sizes of vehicles.

Cet article montre qu'en utilisant un modèle simplifié et une approche de type contrôle optimal, la commande en angle volant qui maximise la vitesse de lacet est assez proche de celle adoptée dans les manœuvres de SwD.

[What Is FMVSS No. 126? And Why You Should Care... \(11/2018\)](#)

(...)

NHTSA defines “spinout” as a situation where the vehicle’s final heading angle is greater than or equal to 90 degrees from the initial heading after a symmetric steering maneuver, in which the magnitude of right and left steering is equal. During the required test, the vehicle is not permitted to lose lateral stability. In addition to being required to satisfy the standard’s lateral stability criteria, the standard requires an ESC equipped vehicle also must satisfy responsiveness criteria to preserve the ability of the vehicle to adequately respond to a driver’s steering inputs during ESC intervention.

Together, the lateral stability and responsiveness criteria ensure that an ESC system achieves acceptable stability performance, but not at the expense of the vehicle responding to the drivers steering inputs. Note that the agency is still conducting research to develop an appropriate understeering intervention test. Thus, the final rule does not specify any understeering performance criteria.

The lateral stability criteria can be represented in the mathematical notations as follows:

$$\frac{\dot{\psi}_{(t_0+1.00)}}{\dot{\psi}_{Peak}} \times 100 \leq 35\% \text{ (Criterion #1), and}$$

$$\frac{\dot{\psi}_{(t_0+1.75)}}{\dot{\psi}_{Peak}} \times 100 \leq 20\% \text{ (Criterion #2)}$$

Where,

$\dot{\psi}_t$ = Yaw rate at time t (in seconds)

$\dot{\psi}_{Peak}$ = First local peak yaw rate generated by the 0.7 Hz Sine with Dwell steering input

t_0 = Time to completion of steering input

A noter que pour le 2^e critère on trouve une variation, puisque la borne est fixée ici à 20%, contre 25% un peu plus haut dans ce même paragraphe.

9.12 FMVSS 126 FOR AUTONOMOUS VEHICLES

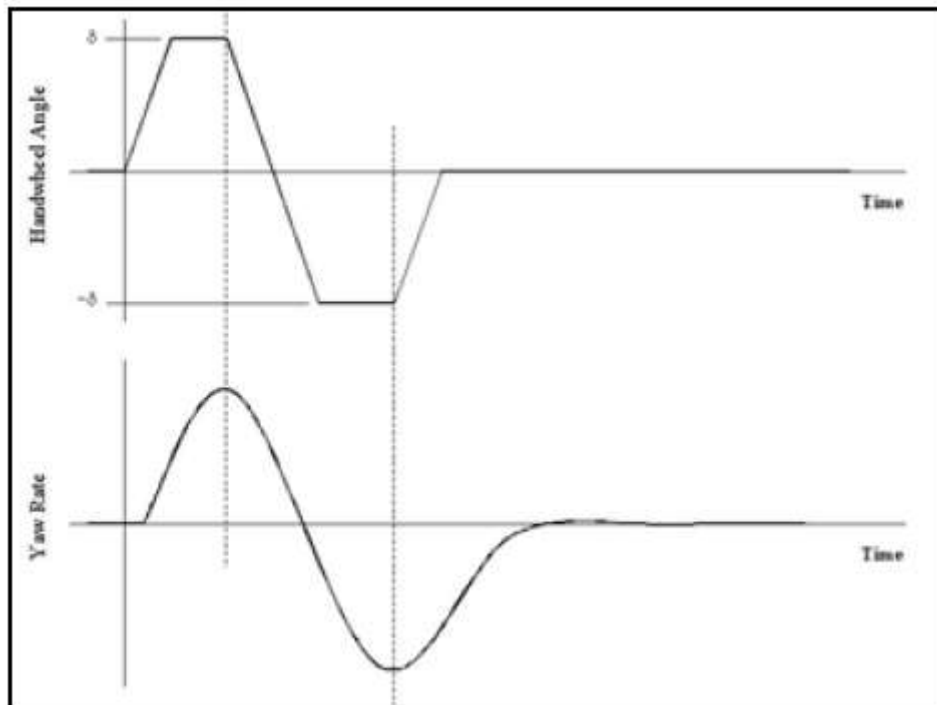
<https://www.sae.org/publications/technical-papers/content/2019-01-1011/>

Autonomous cars have sensors and control systems which can be used to improve ESC, where commercial standard vehicles do not. In this manuscript, we explored how an autonomous vehicle could complete the FMVSS 126

regulation, on its own, without a human driver, and discussed whether the FMVSS 126 (also called Sine with Dwell) test remains a useful regulation for autonomous cars. Additionally, we described a potential general obstacle avoidance capability assessment (GOACA) which could be a better system-level regulation applied to assure the safety of autonomous cars in avoiding obstacles. This proposed assessment would test the sensing and recognition of obstacles in the car's path, in addition to its control and handling ability to maneuver safely around the object. The summary of potential maneuvers and metrics for this GOACA are enumerated in this manuscript, while details for application are saved for future work.

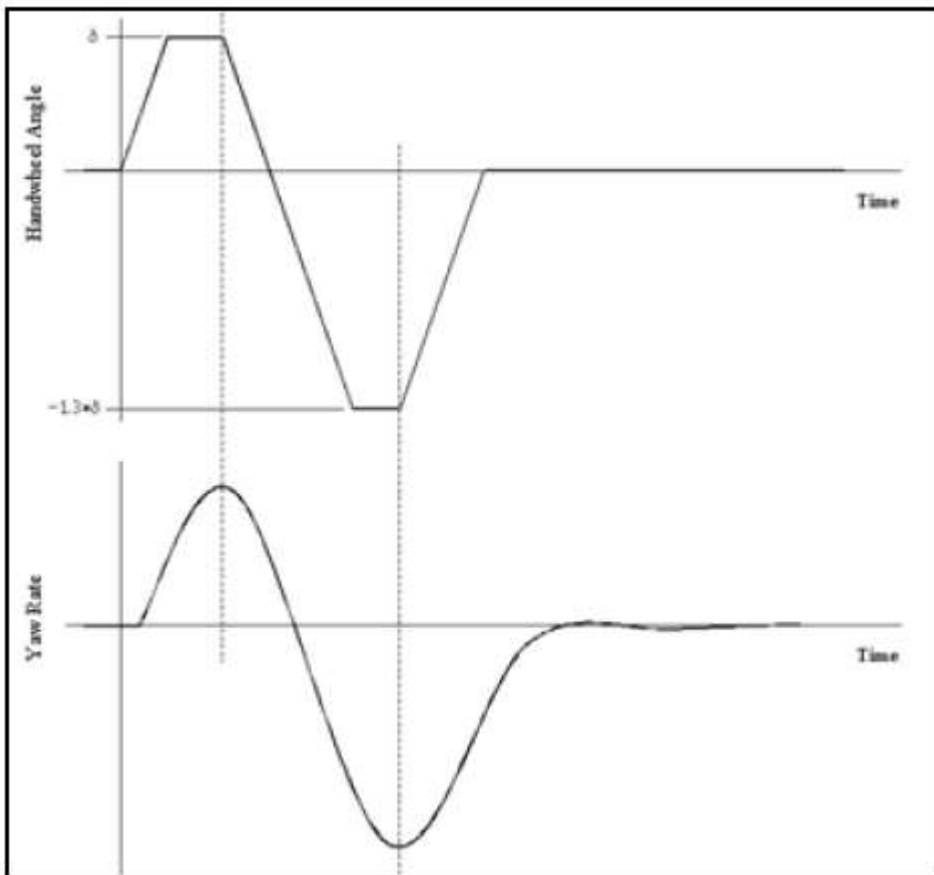
9.13 YAW ACCELERATION STEERING REVERSAL (YASR)

The Yaw Acceleration Steering Reversal (YASR) maneuver was designed to trigger changes in direction of steer at maximum yaw rate. In theory, this timing should maximize maneuver severity by allowing each vehicle to seek out its own yaw natural frequency. The maneuver was comprised of three steering ramps: an initial steer, a steering reversal, and a return back to zero.



9.14 INCREASING AMPLITUDE YAW ACCELERATION STEERING REVERSAL (IAYASR)

The key difference between this maneuver and the YASR maneuver is the magnitude of the initial steer, as it is 1.3 times less than the peak reversal magnitude.



9.15 ISO 7975:2006 (BRAKING IN A TURN)

ISO 7975:2006 specifies an open-loop test procedure to examine the effect of braking on course holding and directional behaviour of a vehicle. Specifically, the procedure determines how the steady-state circular response of a vehicle is altered by a braking action only. ISO 7975:2006 applies to passenger cars as defined in ISO 3833 and to light trucks.

The open-loop manoeuvre specified in this test procedure is not representative of real driving conditions but is useful to obtain measures of vehicle braking behaviour resulting from control inputs under closely controlled test conditions.

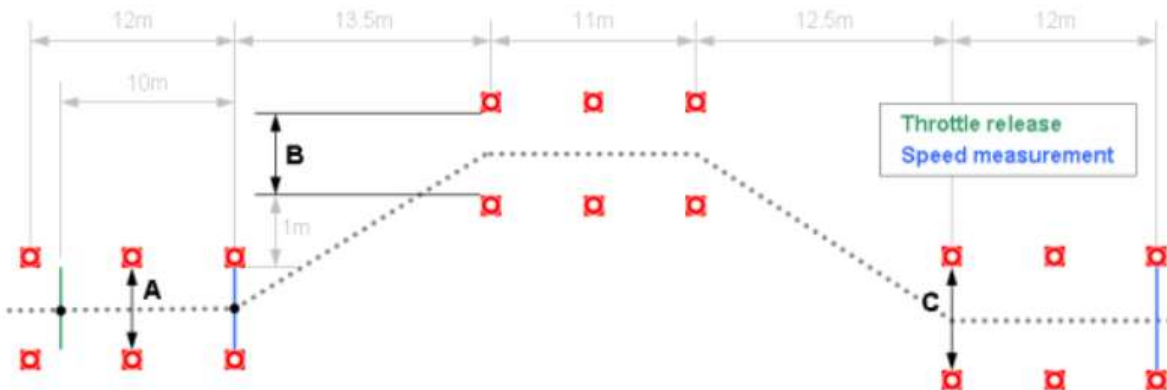
On peut trouver le texte de la version 1996 ici :

<https://www.sis.se/api/document/preview/20382/>

9.16 ISO 3888-2 : DOUBLE LANE CHANGE

9.16.1 PRESENTATION

Initialement connue sous le nom de manœuvre de l'élan (*elk test* ou *moose test*¹), elle a ensuite été revue par l'organisme allemand VDA², et standardisée dans la norme ISO 3888



$$A = 1.1 \times \text{vehicle_width} + 0.25\text{m}$$

$$B = \text{vehicle_width} + 1.0\text{ m}$$

La pédale d'accélérateur est relâchée 2m après l'entrée dans la zone de test (repère vert)

La vitesse est mesurée en fin des voies d'entrée et de sortie (repères bleus)

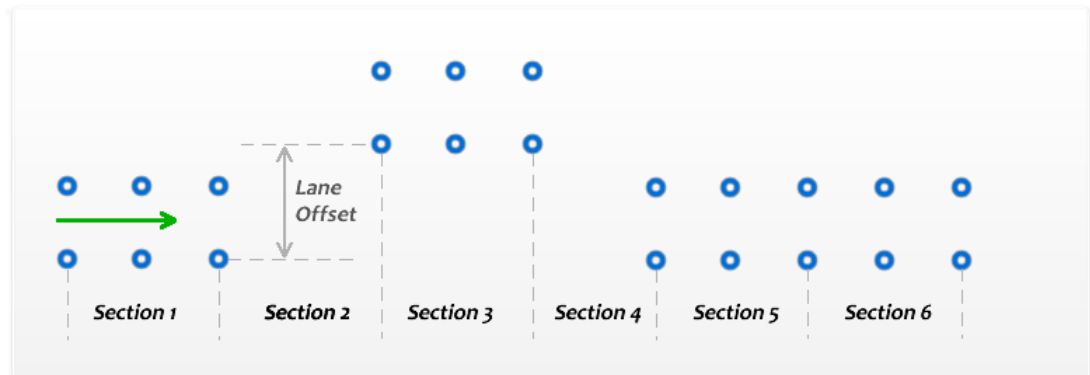
Le conducteur ne doit pas toucher au frein.

Sur <http://www.car-engineer.com/the-moose-test-or-vda-test/> on peut trouver les dimensions suivantes (??) :

¹ https://en.wikipedia.org/wiki/Moose_test

² Verband der Automobilindustrie, soit Union de l'industrie automobile

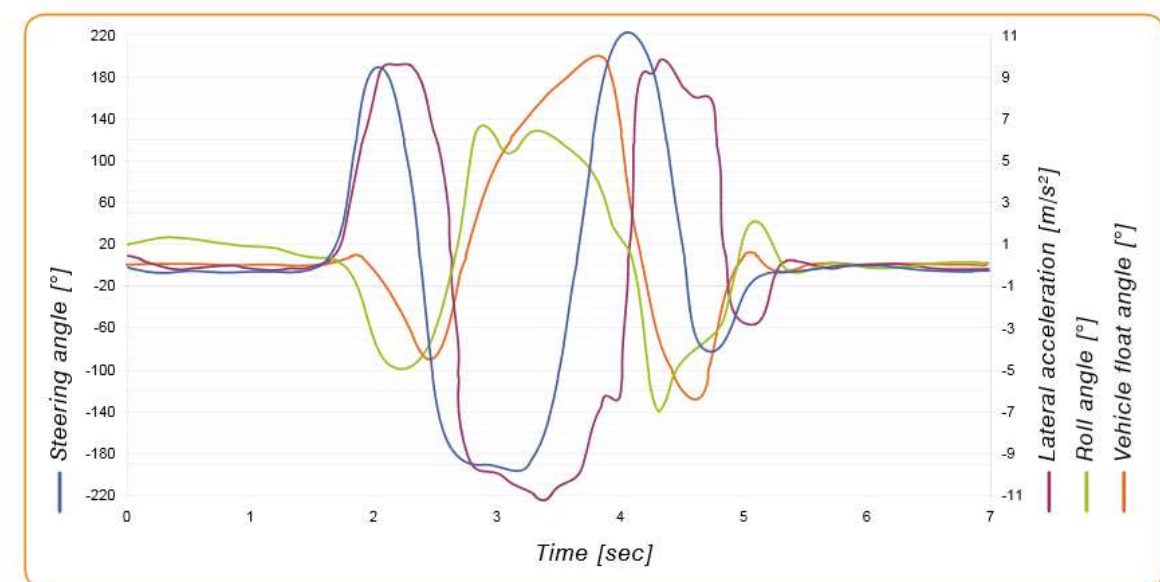
VDA Test track dimensions

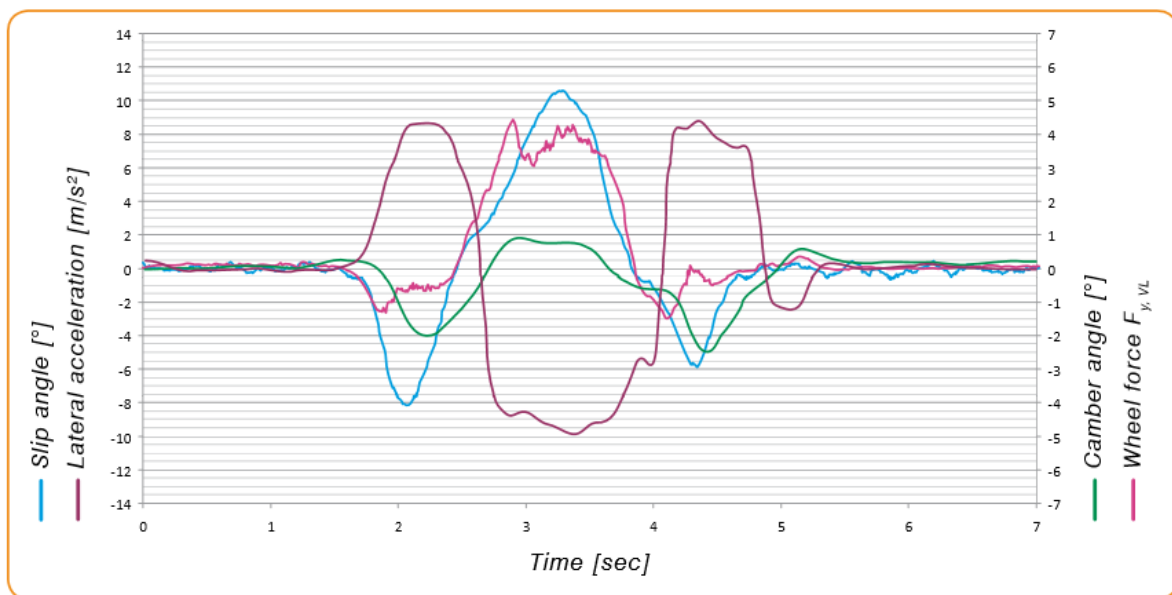


SECTION	LENGTH OF SECTION	SECTION WIDTH
1	15.0 m	$1.1 \times \text{vehicle width} + 0.25 \text{ m}$
2	30.0 m	
3	25.0 m	$1.2 \times \text{vehicle width} + 0.25 \text{ m}$
4	25.0 m	
5	15.0 m	$1.3 \times \text{vehicle width} + 0.25 \text{ m}$

Lane offset = 3.5 m

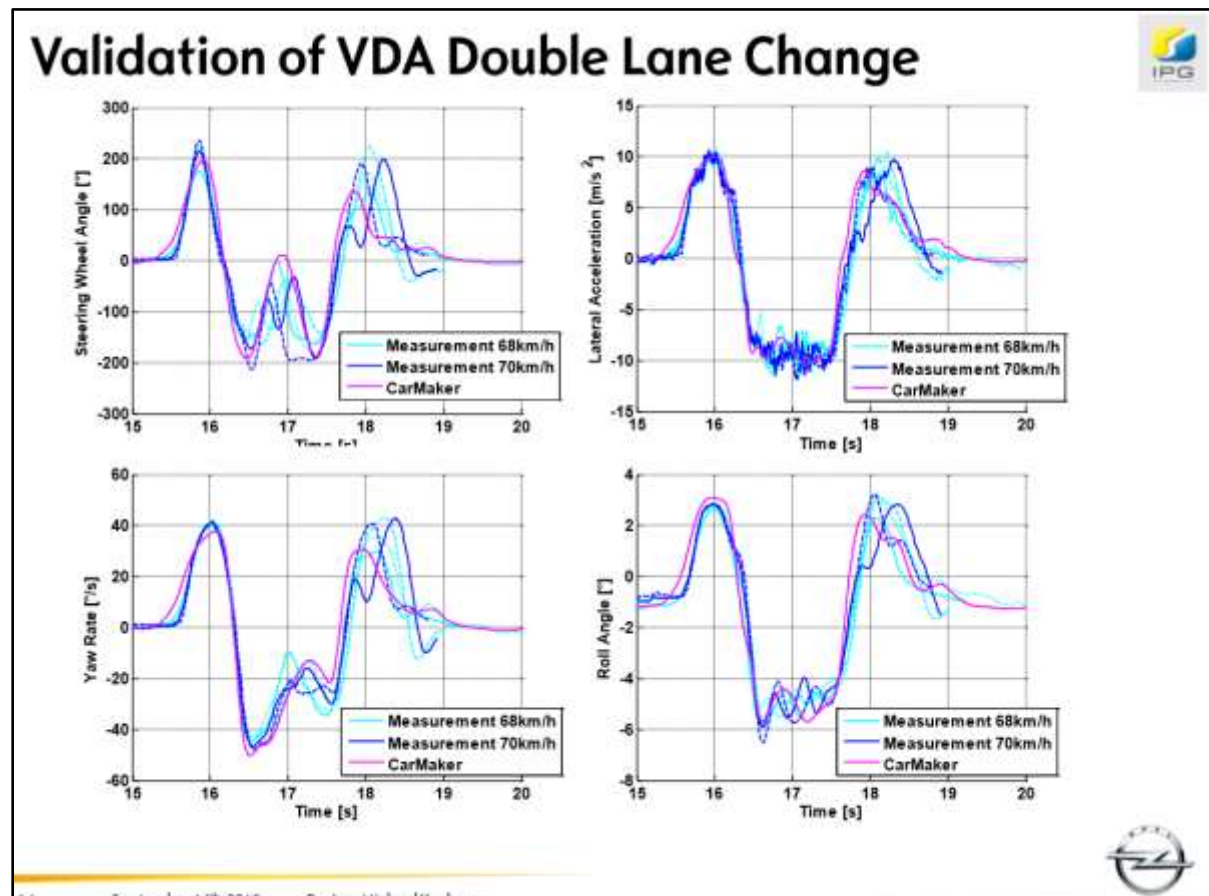
9.16.2 REPONSE DYNAMIQUE TYPE





<http://driveability-testing-alliance.com/download/datasheets/DTA-VDA-Lane-Change-DE-B090602e.pdf>

Et côté simulation :



Source [HiLsimulation of closed-loop-driving maneuvers](#)

9.16.3 CRITIQUES

Les vitesses de rotation volant nécessaires pour passer le test ne sont pas représentatives de l'usage d'un conducteur classique.

En outre la non-utilisation de la pédale de frein ne correspond pas à la réaction de la plupart des conducteurs. La vitesse de passage est fortement dépendante de la maîtrise technique de l'essayeur. Cette critique peut être levée par l'utilisation d'un robot-volant (cf § ci-dessous)

9.16.4 MOOSE TEST – DRIVER VEHICLE INTERACTIONS

Analysis of driver-vehicle-interactions in an evasive manoeuvre - results of "moose test" studies (Daimler)

<https://pdfs.semanticscholar.org/5723/752bbc290bfb3e4302749e4afd215ed92669.pdf>

On y trouve une étude avec un échantillon conséquent sur les performances (vitesse volant, accélération latérale ...) que peuvent atteindre des conducteurs (semi-spécialisés puisqu'il s'agit de journalistes) :

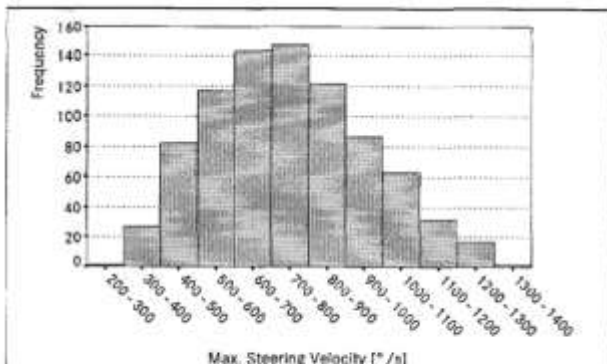


Figure 5. Frequency Distribution of Maximum Steering Velocity (841 Valid "Moose-Tests" by 399 Journalists).

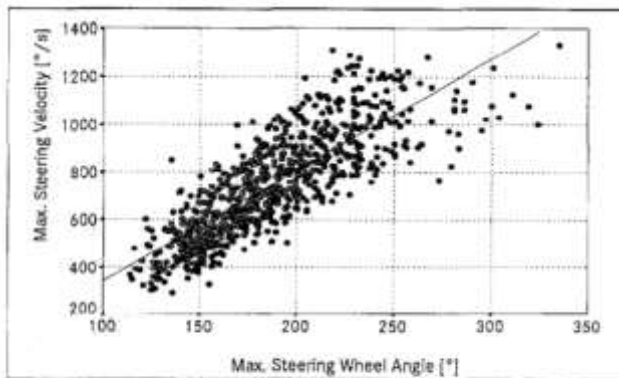


Figure 6. Maximum Steering Velocity as a Function of Maximum Steering Wheel Angle (841 valid "Moose-Tests" without ESP-Interference, Linear Regression: $r^2 = 0,67$).

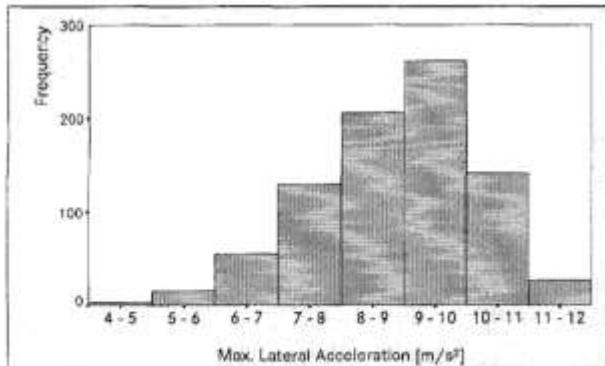
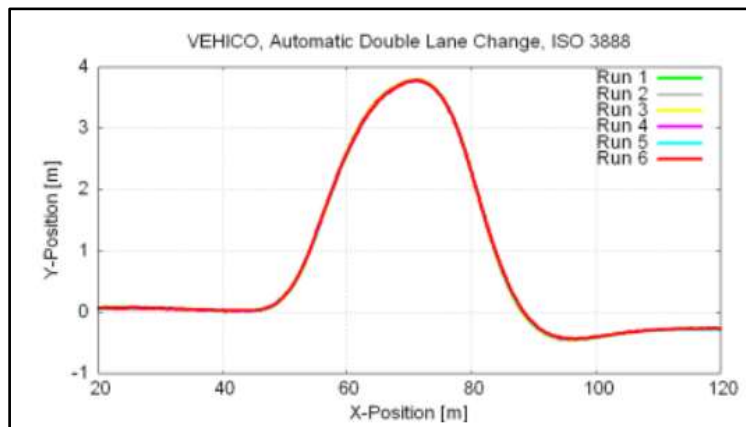


Figure 8. Frequency Distribution of Maximum Lateral Acceleration (841 Valid "Moose-Tests" by 399 Journalists).

9.16.5 UTILISATION D'UN ROBOT-VOLANT

<http://www.vehico.com/index.php/en/applications/iso-lane-change-test>

⇒ très bonne répétabilité (il y a plusieurs courbes sous le trait rouge, sisi)



9.16.6 QUELQUES LIENS SUR LE SUJET

<http://www.vehico.com/index.php/en/applications/iso-lane-change-test>

<http://www.car-engineer.com/the-moose-test-or-vda-test/>

Opel : [HiLsimulation of closed-loop-driving maneuvers](#)

10 SYNTHESE PRESTATION

10.1 FACTEURS INFLUENTS

10.1.1 SYNTHESE (BIBLE EXCEL)

voir **bible_dynamique_vehicule.xlsx**

10.1.2 INFLUENCE DES ANGLES INITIAUX

Table 2.1: Overview of driving situations and toe setting, [9, 10]

Toe set-up	Front	Rear	Remark
lateral force	toe-out	toe-in	
traction force (cornering)	toe-out	toe-out	understeering toe-in with power change
braking/driving straight	toe-in	toe-in	
μ -split braking	toe-in	toe-out	
power-off/braking in a turn	toe-out	toe-in	obtain an opposite yaw moment
crosswind	toe-in	toe-out	
in reality, under braking	toe-out	toe-in	

source (Groenendijk, 2009)

Pourquoi est-ce que l'ouverture initiale aide améliore l'inscription en virage ? (alors que ça semble contre-intuitif)

On trouve un bout d'explication ici, citant un numéro de Racecar Magazine de 2011 :

<https://www.f1technical.net/forum/viewtopic.php?t=10528>

Essentially When the inside wheel turns in it creates a lateral force and drag force -both of which create positive yaw moment into the corner...

When the outside wheel turns in it creates a lateral force (which adds a yaw moment into the corner), but also a drag force which has yaw moment out of the corner...

So the toe out case removes the yaw moment out of the corner caused by the drag of the outside front wheel.. hence aids turn in...

(mais le commentaire suivant n'est pas d'accord)

<https://www.tirerack.com/tires/tiretech/techpage.jsp?techid=4>

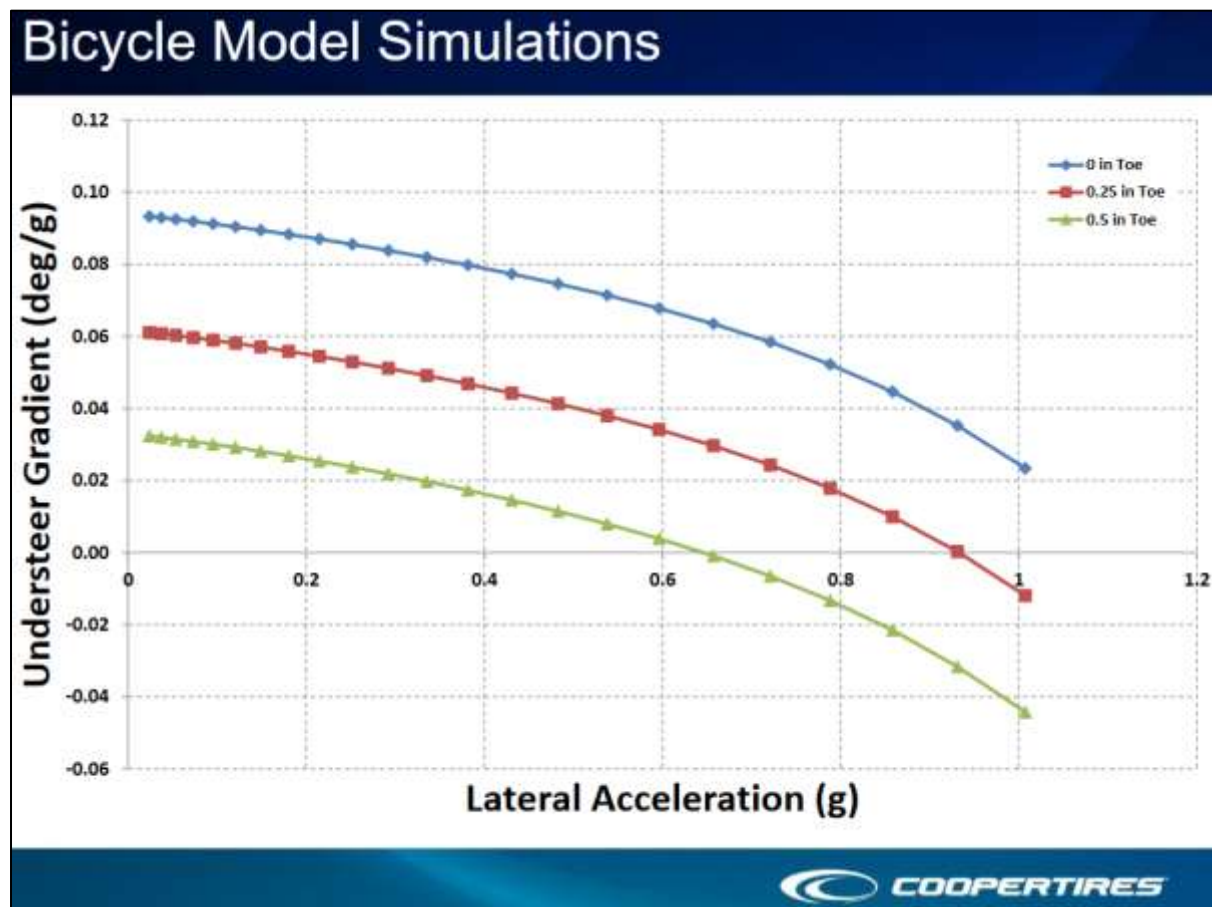
Toe can also be used to alter a vehicle's handling traits. Increased toe-in will typically result in reduced oversteer, help steady the car and enhance high-speed stability. Increased toe-out will typically result in reduced understeer, helping free up the car, especially during initial turn-in while entering a corner.

<https://dsportmag.com/the-tech/extracting-handling-performance-alignment-settings/>

Using Toe plates for Alignment TechWhen driving at high speeds, you're looking for as little resistance as possible. Four wheels pointed perfectly straight prevent the car from wandering and causing excessive tire wear. However, with the exception of drag racing, the car will have to turn sooner or later. Most drivers prefer a small amount of toe-out on the front wheels for their track setup. This type of setup, if not overdone, assists in the vehicle's turn-in capabilities. When turning the wheel of a vehicle with toe-out, the inside wheel is angled more aggressively than the outside wheel, providing an advantage in turning response since the inside and outside wheels travel around a different length radius through a corner.

Toe-in delivers an opposite effect, improving straight-line stability at the sacrifice of turn-in responsiveness. To that end, many racers set up their RWD cars with a small amount of toe-in on the rear wheels if the suspension arms allow for changes. Running toe-out on the front end and toe-in on the rear delivers the best of both worlds, with front-end responsiveness and rear-end stability

Sur la dynamique angulaire, on trouve ([ici](#)) cette planche obtenue avec un modèle bicyclette (ndec : comment fait-on pour introduire la pince dans un tel modèle ?)



10.1.3 INFLUENCE DES ANGLES INITIAUX (PINCE)

Tenue de cap :

Augmenter la pince initiale à l'arrière et l'ouverture initiale à l'avant rend le véhicule plus sous-vireur et permet d'augmenter l'impression de stabilité. Ils ne doivent cependant pas être trop élevés sous peine de causer une surconsommation en carburant et une usure inégale et rapide des pneumatiques.

Equilibre du véhicule en virage, dynamique angulaire

Les roues extérieures étant les plus chargées, celles-ci auront la rigidité de dérive la plus importante. Pour qu'elles aient un effet sous-vireur, il faut de l'ouverture à l'avant et de la pince à l'arrière. Il en est de même pour les braquages induits par le roulis, qui pour être sous-vireurs doivent braquer les roues avant vers l'extérieur du virage (valeur négative de ϵ_{p1}), et les roues arrières vers l'intérieur du virage (valeur positive de ϵ_{p2}).

Note : Il faut noter que l'influence des braquages initiaux (et en pompage/roulis) sur la dérive spécifique et la dynamique angulaire n'est pas nécessairement importante, et peut même avoir l'effet inverse de celui escompté. Il ne faut pas oublier, pour le train considéré de vérifier en fonction du pneumatique utilisé et de la charge sur celui-ci, si on n'a pas déjà atteint la zone de saturation du pneu en dérive. Si cette zone est dépassée (cas des pneus sous-dimensionnés?) le pneu "guidant" le train n'est plus l'extérieur mais l'intérieur. De plus, l'influence peut ne pas être la même quand la charge sur ce train évolue, par exemple entre vide (1 personne) et charge (5 personnes), puisqu'en fonction de la charge on se déplace sur la courbe de rigidité $D_y = f(F_z)$.

10.1.4 INFLUENCE DU CARROSSAGE

La thèse de Koenigs 2008 montre l'influence du carrossage sur la dynamique angulaire

Rôle du carrossage initial

Le but du carrossage initial est de maximiser la surface de contact au sol en virage. Il a pour but aussi (voire même surtout) d'homogénéiser l'usure due au pincement. Pour ce faire, il faudrait selon Michelin 5 fois plus de carrossage que de pince (nous on en met que 4 !!!).

Sur un véhicule particulier non sportif, on met au maximum 1° de contre-carrossage au train arrière et un carrossage nul à l'avant. En virage, le roulis aidant, il peut atteindre 10°, en tenant compte des déformations des trains sous effort.

10.1.5 INFLUENCE DE LA CHASSE

La chasse linéaire permet de donner à la direction du rappel en courbe, c'est-à-dire un effort de résistance au virage, d'où découle une stabilité naturelle.

Les réactions de direction augmentent avec l'angle de chasse.

L'inconvénient de l'angle de chasse est qu'il induit un contre-rappel gravitaire. S'il l'emporte, la direction braque toute seule (on dit qu'elle enroule) à faible allure, quand la force centrifuge est négligeable (?)

Augmenter l'angle de chasse améliore le plan de roue en grand braquage : la chasse se transforme en carrossage favorable.

Augmenter l'angle de chasse en pompage (vers le choc) permet d'améliorer le plan de roue sous fortes accélérations transversales.

La chasse au sol :

- participe au rappel de direction
- permet d'améliorer la tenue de cap et la stabilité en ligne droite.
- augmente la sensibilité au vent latéral (couplage roulis-lacet) - ??
- rend le train sensible au tirage en dévers
- influence la dynamique angulaire par augmentation des déformations du système de direction (contribution sous-vireuse).

En résumé :

	↗ Angle de chasse	↗ Chasse au sol
Carrossage en braquage	+	
Efforts de direction	-	
Tenue de cap, stabilité haute vitesse		+
Rappel de direction	- (à basse vitesse)	+
Réactions de direction		-
Sensibilité au vent latéral		-
Gradient de sous-virage		+ (sous-vireur)

L'angle de chasse permet d'obtenir la chasse linéaire sur une traction, car l'axe de fusée et de pivot sont concourants pour éviter que le braquage induise un allongement des arbres de transmission.

Ceci dit ce coulissolement de transmission induit par un éventuel déport de chasse peut s'accompagner d'effets bénéfiques : Il permet en effet de diminuer la chasse au sol (direction moins « lourde », moins de couplage roulis-lacet, moins de sensibilité au dévers et au vent latéral,...) tout en conservant un angle de chasse élevé (plan de roue extérieure favorable en braquage,...).

Measured in degrees, caster plays a large role in determining both steering feel and high-speed stability. The goal of proper caster alignment is to achieve optimal balance between low-speed steering effort and high-speed stability. An increasingly positive caster enhances high-speed stability, but increases low-speed steering effort. An increasingly negative caster decreases low-speed steering effort and high-speed stability. For cars with power steering, an increase in low-speed steering effort increases the rate of wear in the power steering system. With most suspension designs, there is a trade-off between caster and camber angles at the extreme limits.

10.1.6 INFLUENCE DU DEPORT AU SOL

Un déport au sol négatif génère un braquage compensateur (pince) en cas de dissymétrie de traînée de freinage avant.

Le déport au sol participe au rappel de direction (moment formé par la force verticale appliquée sur le pneu, le déport au sol et l'angle de pivot).

10.1.7 INFLUENCE DE L'ANGLE DE PIVOT

Son effet est de donner à la direction un rappel gravitaire et de faire prendre aux roues du carrossage lors du braquage.

Son augmentation "durcit" la direction.

The king pin angle has an influence on the geometric variations of the wheel plan when steering and the forces transmitted to the chassis. Combined with the caster angle, it affects the steering stability. The king pin angle must be positive to allow a better steering feedback but should not be too high to limit the camber gain when steering. In fact, when a steering wheel angle is applied it induces a negative camber gain on the outer wheel and a positive camber gain on the inside wheel.

10.1.8 INFLUENCE DE LA RAIDEUR DE RESSORTS SUR LE SOUS-VIRAGE

Greg Locock, de l'influence de la raideur des ressorts sur le sous-virage :

On a given axle on a sprung car, increasing the spring rate will increase the load transfer to the outside wheel on that axle, and lessen it on the other axle.

Generally that will cause that axle to understeer more.

But not always. As it reduces the roll gain of that axle, and if the axle was set up with a lot of roll steer, that will reduce, or even negate the understeer change caused by the weight transfer. Also, some tires are more resistant to load sensitivity than others

10.1.9 INFLUENCE DE LA RAIDEUR DE CAISSE EN TORSION

Chassis Torsional Rigidity Analysis for a Formula SAE Racecar

<https://pdfs.semanticscholar.org/926b/94cdacedb55170ae032665fd3ae63dc99127.pdf>

Studies have been carried out to investigate the effects that the torsional stiffness (resistance to distortion about the longitudinal axis) of a vehicle chassis has on the handling and performance of the vehicle. Although physical testing has shown that vehicles with higher stiffnesses perform better, the exact effects that torsional stiffness has on performance is not entirely known [3]. CAE simulations on the other hand have shown torsional stiffness to not affect the lateral acceleration, yaw rate, or other critical characteristics, during steady state turns [2][3]. The biggest effect of torsional deflection has been found to be the effect it has on lateral load transfer distribution between the front and rear axle [3]. During a steady state turn an infinitely rigid chassis will cause the front and rear roll angle to be identical, as is assumed when suspension

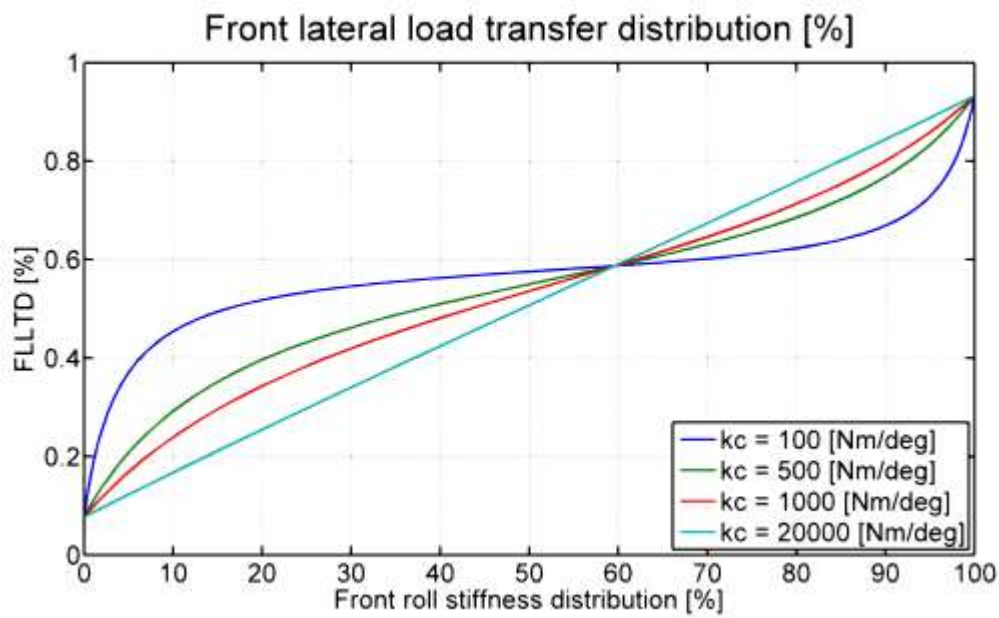
[2] Research of chassis torsional stiffness on vehicle handling performance, Pang, Shu-yi

[3] Influence of Body Stiffness on Vehicle Dynamics Characteristics in Passenger Cars, Danielsson, Oskar

Influence of Body Stiffness on Vehicle Dynamics Characteristics in Passenger Cars (2015)

◇ <https://publications.lib.chalmers.se/records/fulltext/219391/219391.pdf>

Previous studies have been carried out to investigate the effects of various body stiffeners on vehicle dynamics characteristics. They have found gains in both objective and subjective physical tests [3] & [14]. However the effect of increased torsional stiffness on overall vehicle performance is not completely known [4]. CAE assessments of body stiffness have been performed but they are not showing any big differences in the metrics used to objectively assess the handling, steering and ride characteristics of a vehicle [4]. Nevertheless during subjective vehicle assessments it is found that the stiffer car performs better. Studies performed by Volvo Cars Corporation have shown an influence from body stiffness on subjective measurements taken during physical tests. However the CAE analysis performed are not able to capture the influence from body stiffness on vehicle dynamics characteristics seen in the subjective assessments where the car was described as more solid and premium. According to Milliken [15], excessive chassis flexibility induces problems in the field of lateral load transfer, suspension kinematics and it results in unwanted vibrations. For a race vehicle, Milliken [15] states that the chassis torsional stiffness can be approximately designed to be 3-5 times the total suspension roll stiffness. This cannot be directly transposed to a passenger car but it gives an approximation of the influence of the body stiffness in the vehicle dynamics characteristics. Typical values for torsional stiffness in a passenger car are in the range of 17000 to 40000 Nm/deg, with a roll stiffness of 1000-2500 Nm/deg per axle. Meaning a chassis/roll stiffness ratio of 6,8-40 [7]. Regarding the vehicle dynamics properties, the overall response of the vehicle is improved with a stiffer chassis due to the better synchronization between front and rear according to subjective tests and objective measurements [14]. Up to 14% of improvement in the phase lags of the vehicle for steering input frequencies (0,5 Hz) through increasing the global torsional stiffness of the car is found. Regarding local stiffness, it is found that increasing the local stiffness in the front lower arm also shows an improvement in the overall vehicle response [3]



10.1.10 INFLUENCE DE LA VOIE

Une augmentation de la voie :

- augmente le diamètre de braquage
- diminue le roulis spécifique
- augmente le report de charge sur le train considéré
- augmente par conséquent la dérive spécifique, et impacte le gradient de sous-virage

10.1.11 INFLUENCE DE LA RÉPARTITION DE ROULIS AV/AR

Equilibre du véhicule en virage, dynamique angulaire

A anti-roulis total constant, augmenter l'anti-roulis d'un train le rendra moins efficace. Attention ceci n'est valable que pour des accélérations transversales inférieures à 3 m.s^{-2} . Au delà la tendance s'inverse, à cause de la convexité de la courbe rigidité de dérive=f(Fz). Cette influence de la répartition anti-roulis sur la dynamique angulaire s'explique à partir de la courbe donnant la rigidité de dérive en fonction de la charge verticale. A cause de la saturation de la courbe de rigidité en fonction de la charge verticale, quand on augmente le report de charge sur un train, la roue la plus chargée voit sa rigidité de dérive moins augmenter que ne diminue celle de la roue la moins chargée, d'où une augmentation de la dérive moyenne du train.

Motricité

Afin d'augmenter la motricité en virage, il faut augmenter l'effort vertical sur la roue intérieure motrice, donc limiter le transfert de charge sur la roue extérieure : diminution de l'anti-roulis du train moteur. À anti-roulis

total constant, on pourra mettre plus d'anti-roulis sur l'arrière, c'est le cas pour un véhicule à caractère sportif traction, ou sur l'avant dans le cas d'un véhicule propulsion.

10.1.12 INFLUENCE DE LA HAUTEUR DE CENTRE DE ROULIS

Tenue de cap : mauvaises routes

Un centre de roulis haut provoque des variations de voie en pompage et donc l'apparition de forces latérales exercées au point de contact roue/sol.

Copage

Une HCR basse permet de diminuer les variations de voie en pompage mais diminue la raideur de roulis du train. On doit alors augmenter la contribution de la barre anti-dévers, ce qui favorise l'apparition de copage

Roulis spécifique

Un centre de roulis élevé permet de diminuer le roulis spécifique.

10.1.13 INFLUENCE DES BRAQUAGES INDUITS PAR LE POMPAGE

Tenue de cap

Afin d'assurer une bonne tenue de cap, les braquages induits par le pompage doivent être sous-vireurs, mais cependant limités, afin de limiter le couplage roulis-lacet.

Stabilité au freinage en ligne droite

En tenant compte des effets Brouilhet limitant les débattements, on aura intérêt à ce que les variations de braquage en pompage donnent de l'ouverture sur l'avant (vers le choc) et de la pince vers l'arrière (vers le rebond). On peut remarquer que ces mouvements sont compatibles avec ceux souhaités en roulis.

10.1.14 INFLUENCE DES BRAQUAGES INDUITS PAR LE ROULIS

Tenue de cap

Braquages induits par le roulis/le pompage pas trop élevés. Si ces braquages sont trop importants, les dérives au niveau des pneumatiques génèrent des efforts latéraux déviant le véhicule sa trajectoire. Ceci donne un véhicule sensible aux perturbations de la chaussée, même si la correction peut rester aisée, grâce à une dynamique angulaire élevée donnant une impression de stabilité

Dynamique angulaire, équilibre du véhicule en virage

Les roues extérieures étant les plus chargées, celles-ci auront la rigidité de dérive la plus importante. Pour qu'elles aient un effet sous-vireur, il faut de l'ouverture à l'avant et de la pince à l'arrière. Il en est de même pour les braquages induits par le roulis, qui pour être sous-vireurs doivent braquer les roues avant vers l'extérieur du virage (valeur négative de ϵ_1), et les roues arrière vers l'intérieur du virage (valeur positive de ϵ_2).

Note : Il faut noter que l'influence des braquages initiaux (et en pompage/roulis) sur la dérive spécifique et la dynamique angulaire n'est pas nécessairement importante, et peut même avoir l'effet inverse de celui escompté. Il ne faut pas oublier, pour le train considéré de vérifier en fonction du pneumatique utilisé et de la charge sur celui-ci, si on n'a pas déjà atteint la zone de saturation du pneu en dérive. Si cette zone est dépassée (cas des pneus sous-dimensionnés?) le pneu "guidant" le train n'est plus l'extérieur mais l'intérieur. De plus, l'influence peut ne pas être la même quand la charge sur ce train évolue, par exemple entre vide (1 personne) et charge (5 personnes), puisqu'en fonction de la charge on se déplace sur la courbe de rigidité $D_y = f(F_z)$.

Réponse en transitoire

Les braquages induits par le roulis ne doivent pas être trop importants, sous peine d'avoir un effet désamortissant sur la réponse en transitoire.

10.1.15 INFLUENCE DES BRAQUAGES INDUITS SOUS EFFORT DE FREINAGE

Sous effort de freinage, l'épure cinématique amène généralement de l'ouverture (en pompage, vers le choc). Afin de ne pas accentuer ce phénomène, on peut plutôt chercher à obtenir de la pince sous effort freineur.

10.1.16 INFLUENCE DE LA FLEXIBILITÉ DE DÉRIVE SOUS EFFORT TRANSVERSE

- Tenue de cap

Diminuer la flexibilité de dérive due aux déformations des trains (F_t)

- Équilibre en virage, dynamique angulaire

La flexibilité de para sous effort transversal contribue, par la déformation du train, à des braquages impactant fondamentalement l'équilibre du véhicule en virage. Contrairement aux épures, FT n'entraîne pas de variation de para avec la course, donc avec la charge. Pas de compromis avec l'usure. Le sous-virage "élastique" serait mieux perçu que le sous-virage cinématique.

A la prise en compte de l'élasto des trains il faut ajouter l'éventuelle élasto du berceau par rapport à la caisse, et ne pas négliger les répercussions du train sollicité sur le train non-sollicité : on peut affecter 85 % des répercussions à la flexibilité propre de la colonne (flector, colonne, barreau de valve) et 15 % aux autres flexibilités : déformation de la crémaillère, élasticité de la fixation de la crémaillère sur le berceau...

Déploiement

La valeur de la dynamique angulaire est une fonction de la différence des dérives spécifiques avant et arrière. Donc pour obtenir un véhicule sous-vireur il faut au niveau de l'élasto-cinématique avant avoir une $Ft=0,5*[(Fmrns-fmrs).a+(Ftrns-Ftrs)]$ supérieure à celle de l'arrière. Ceci peut donner une borne inférieure pour Ft1. Cependant les prestations de tenue de cap et sensibilité au vent latéral exigent une flexibilité réduite sur les trains, ce qui induit une borne supérieure pour Ft1 et Ft2. Les valeurs des bornes Ftinf et Ftsup dépendent du type de prestations désirées (véhicule sportif : éventuellement plus de survirage) et des autres caractéristiques (pneus, trains,...) qui conditionnent la dérive spécifique et la dynamique angulaire.

10.1.17 INFLUENCE DU BALLANT DE TRAIN

Le ballant de train participe à la perception du comportement en transitoire. On cherchera donc à le minimiser. Dans le cas d'un essieu souple, cela oblige à un déploiement délicat de la gestion des saturations transversales. On cherche à minimiser le ballant (pour le transitoire), ce qui est souvent contradictoire avec optimiser le FT2-30 (dynamique angulaire).

10.1.18 OUVERTURE OU PINCE SOUS EFFORT MOTEUR ?

Sous accélération les véhicules ont tendance à sous virer et ce d'autant plus que le couple moteur est important. Pour conserver de la vivacité en virage il faut aller vers de la pince sous effort moteur.

En revanche afin de limiter le tirage sous couple causé par une dissymétrie de couple passé à chacune des roues d'un même essieu, il faut aller chercher de l'ouverture sous effort moteur.

10.2 GRADIENT DE SOUS-VIRAGE

il est influencé par :

- Chasse au sol

- Dérive spécifique : composante de la dynamique angulaire due aux dérives avant et arrières = $n^*(\delta_{spé1}-\delta_{spé2})$
- Flexibilité de carrossage sous effort transversal
- Flexibilité de dérive due aux déformations des trains
- Parallélisme, angles initiaux
- carrossage, angles initiaux. Le carrossage a les mêmes influences que le parallélisme, ceci au travers de la poussée de carrossage. Les efforts générés sont cependant environ 10 fois moins importants.
- Parallélisme en roulis
- Carrossage en pompage/roulis : le carrossage induit par le roulis >0 exerce une contribution sous-vireuse à l'avant et sur-vireuse à l'arrière. Le but est d'obtenir un angle de carrossage proche de zéro sur la roue extérieure à accélération transversale maximum, et de compenser l'usure des pneus due aux braquages initiaux.
- Répartition anti-roulis avant/arrière
- Rigidité de dérive des pneus avant/arrière
- Portance aérodynamique : une portance aérodynamique plus forte sur l'arrière que sur l'avant permet d'augmenter la dynamique angulaire et donc la stabilité à haute vitesse sans compromettre la vivacité à vitesse plus faible. Toutefois plus de portance implique plus de traînée et donc une consommation augmentée ainsi qu'une vitesse max réduite.

10.3 TENUE DE CAP

La tenue de cap d'un véhicule est caractérisée par son aptitude à suivre une trajectoire, grâce aux commandes du conducteur au travers du système direction (hors freinage et accélération). Il s'agit donc d'un système contrôlé en boucle fermée. Pour juger la tenue de cap d'un véhicule on doit donc s'intéresser aux caractéristiques de la boucle ouverte, base d'un bon comportement en boucle fermée, lorsque le véhicule subit des perturbations du type : déformations du sol, vent latéral, dissymétries,... On s'intéresse aussi à la facilité de correction de trajectoire en boucle fermée, qui est liée :

- aux caractéristiques de la direction (précision),
- à la forme de la réponse à un coup de volant (réponse au volant pas trop vive, linéaire et non déphasée),
- à la qualité de l'information permettant d'estimer la taille de la correction de trajectoire à effectuer (information claire et non perturbée concernant entre autres l'angle de braquage des roues et la position du véhicule - angle de dérive, vitesse de lacet - par rapport à la trajectoire souhaitée).

On distingue la tenue de cap sur bonnes et mauvaises routes.

Critères influençant la prestation tenue de cap bonnes routes

- Parallélisme, angles initiaux
- Braquages induits par le pompage

- Chasse linéaire au sol
- Empattement
- Flexibilité de dérive due aux déformations du train (Ft)

Afin de permettre une correction de trajectoire facile, la direction doit être suffisamment filtrée (information non perturbée, pas de vibrations), mais pas trop afin de garder une direction précise

Critères supplémentaires influençant la prestation tenue de cap mauvaises routes

- Hauteur de centre de roulis
- Braquages induits par le roulis
- Rotation du berceau (cas d'un berceau filtré)

Caractérisation de la prestation

- Bonne route

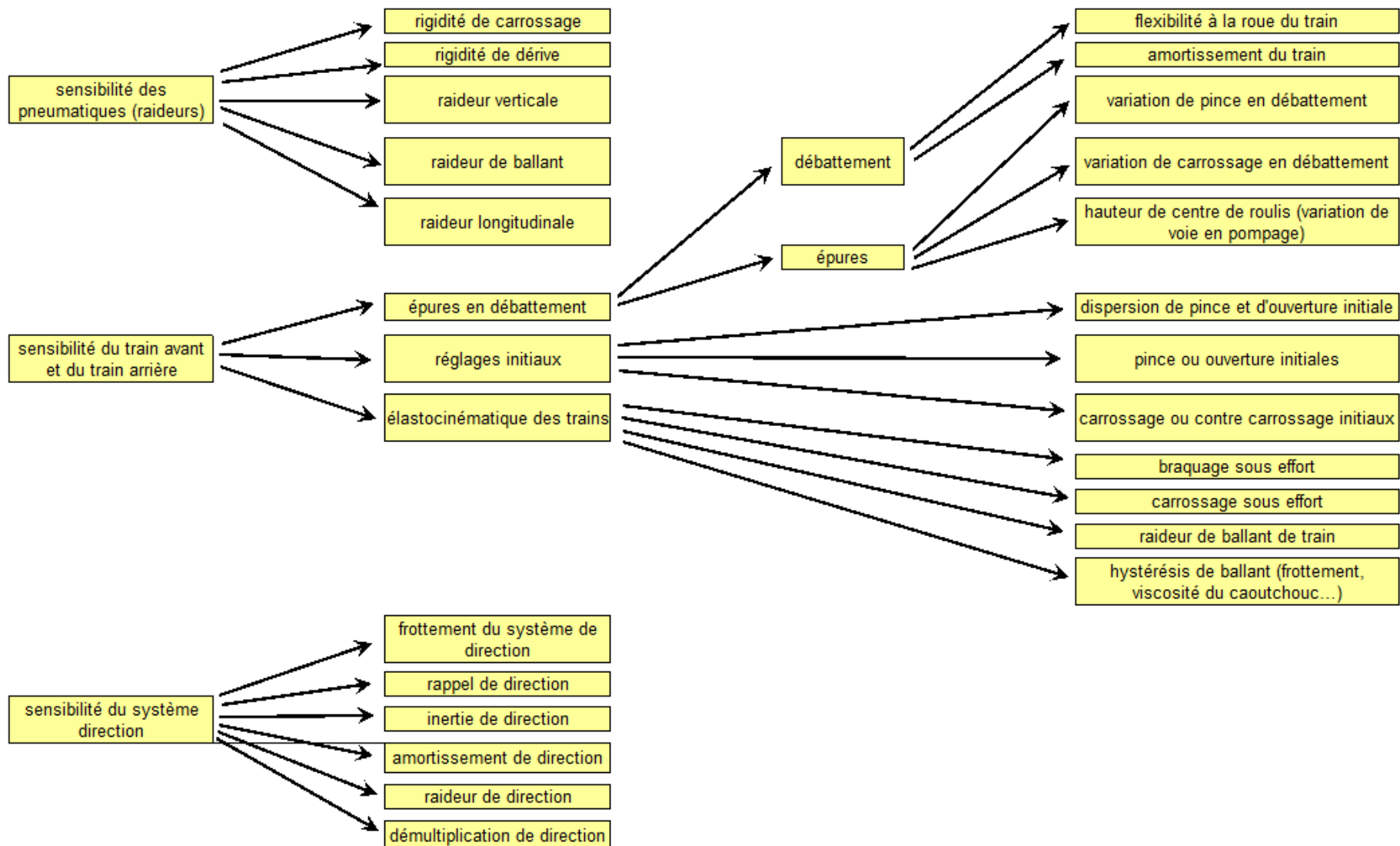
En boucle ouverte (volant bloqué) : sur route ouverte, on peut retenir la densité spectrale de puissance de la vitesse de lacet autour de 0,5Hz, et la densité spectrale du couple volant à basse fréquence (0,3, 0,4 et 0,5 Hz).

En boucle fermée (pour la facilité de correction) : le retard de phase de γ_t par rapport à α_v à 0,8 Hz (déphasage de la réponse).

- Mauvaise route

Sur une mauvaise route type, calcul de l'écart type de vitesse de lacet (0,15 à 0,6 Hz) en °/s pour ce qui concerne la stabilité de trajectoire et de l'accélération transversale (0,15 à 0,3 Hz) en m.s⁻², pour ce qui concerne la perturbation sur l'information (agitation transversale)

sensibilité aux déformations de la route, dépendances vis-à-vis des différents systèmes du véhicule



10.4 TIRAGE A L'ACCELERATION

Influencé par la flexibilité en braquage sous effort longitudinal moteur du train avant.

Les problèmes de dissymétrie se posent de la même manière qu'avec le freinage, à un niveau cependant plus faible. Afin de compenser une éventuelle dissymétrie, il faudrait aller vers de l'ouverture sous effort de traction.

Note : Sous accélération les véhicules ont tendance à sous virer et ce d'autant plus que le couple moteur est important. Pour conserver de la vivacité en virage il faut aller vers de la pince sous effort moteur. Un choix est donc nécessaire.

10.5 TIRAGE EN DEVERS

L'asymétrie de carrossage peut être d'ordre 1 !

Diminuer la chasse au sol permet de diminuer le tirage en dévers (diminution du moment causé autour de l'axe de pivot)

10.6 MOTRICITÉ

Influencée par :

- Répartition anti-roulis
- Flexibilité en braquage sous effort moteur

10.7 EQUILIBRE EN VIRAGE

Les conducteurs ayant une tendance naturelle à freiner plutôt qu'à contrebraquer en cas de conduite à la limite, on cherche à obtenir un véhicule avec une tendance au sous-virage.

Sur haute adhérence, cette prestation est décrite au travers du déploiement de la dynamique angulaire en régime établi. Les mesures sur banc d'élasto-cinématique permettent de confirmer.

On cherche à avoir un véhicule sous vireur sur toute la plage d'accélération transversale tout en cherchant à maximiser le potentiel d'accélération transversale.

Sur basse adhérence, l'accélération transversale étant plus faible, l'angle de roulis et les efforts mis en jeu sont moindres. C'est l'antiroulis naturel et les pneumatiques qui sont prépondérants dans l'équilibre en virage.

C'est dans les conditions de faible adhérence et à vide que le risque de survirage est maximal. C'est pour cette raison que les essais mouillés sont réalisés à vide.

En virage établi, le fait de lever le pied de l'accélérateur, voire de faire une légère décélération génère un transfert de charge vers le train avant et donc un mouvement de lacet pouvant faire apparaître une tendance au survirage.

Dans ces situations, nous cherchons à avoir un véhicule passif et une dérive arrière linéaire et progressive.

10.8 EQUILIBRE EN ROULIS

La mise au point de l'équilibre en roulis consiste à éviter le roulis diagonal, et à avoir une sensation de bonne tenu de la caisse en charge.

Pour équilibrer un véhicule en roulis, nous modifions la répartition anti-roulis. Les LEV d'amortisseur peuvent être un facteur limitant à cette étape.

10.9 MISE EN VIRAGE (COUP DE VOLANT)

Critères influents :

- Ballant de train
- Ballant du pneumatique/rigidité de ballant du pneumatique
- Braquages induits par le roulis
- hystérésis de ballant de train suffisante

Caractérisation de la prestation en transitoire

Mise en virage du véhicule, coup de volant brusque : (rayon = 125m (12 degrés/s), échelon=1/3s, rayon=125m (12 degrés/s), échelon=1/6s, rayon=250m (6 degrés/s), échelon=1/3s). Mesure de la vitesse de lacet, de l'accélération transversale, de la dérive du centre de gravité, et calcul pour chacun de la (sous/surtension)/valeur stabilisée, et du temps de stabilisation. Le coup de volant est donné par un vérin, réglé afin de comparer les véhicules à iso-vitesse de lacet stabilisée. Ce test est réalisé en échelon de braquage (direction bloquée). On pourrait imaginer une simulation en échelon de couple (direction libre), ce qui introduirait une équation supplémentaire prenant en compte le rappel de direction, l'amortissement de direction et l'inertie du volant ramenée à la roue. Ce type de simulation a un côté artificiel, car on ne conduit jamais en échelon de couple, mais elle permet d'éviter de négliger des facteurs importants pouvant influer sur la réponse du véhicule en transitoire. On peut tracer les principales variables de comportement au début de la réponse rendues adimensionnelles en les rapportant à leur valeur stabilisée.

Analyse des retards des courbes citées ci-dessus. On cherchera à minimiser la sous-tension en vitesse de lacet, la sous-tension en accélération transversale, la durée de la sous-tension en vitesse de lacet (temps total pendant lequel la vitesse de lacet est en retard sur l'angle de braquage) et la durée de la sous-tension en accélération transversale. Ceci traduit la capacité du véhicule à suivre la consigne (ici l'angle de braquage permettant d'obtenir la trajectoire souhaitée). On cherchera à maintenir la surtension de vitesse de lacet entre certaines limites, sachant que l'on a intérêt à augmenter la sur-tension plutôt qu'à la diminuer, en ne dépassant pas toutefois une valeur qui aurait tendance à donner une réponse oscillante. On cherchera enfin à obtenir une surtension en dérive et un temps de surtension en dérive faibles, car on a intérêt à ce que le véhicule trouve rapidement ses appuis et se place correctement sur sa trajectoire. Toutefois il vaut mieux une surtension importante et un temps de surtension faible que l'inverse.

Sollicitation sinusoïdale au volant, d'amplitude 0,4g et de fréquence 0,4Hz. Tracé des courbes vitesse de lacet= $f(t)$ et angle de roulis= $f(t)$, rendues adimensionnées en les rapportant à leurs valeurs de régime stabilisé. Mesure de l'écart temporel entre ces deux courbes. Tracé de la courbe écart= $f(\text{angle volant})$. On peut prendre la pente de la droite liant les points de la courbe à 20 et 70% d'angle volant comme "constante de déphasage". On souhaite minimiser au maximum cette constante

Ce qu'il est conseillé d'obtenir :

Sous-tension en lacet <30%, temps de surtension en lacet <0,3s, sur-tension en lacet comprise entre 15 et 30%, sous-tension en accélération transversale <35%, temps de sous-tension en accélération transversale <0,6s, sur-tension en dérive <40%, temps de sous-tension en dérive <0,7s.

10.10 STABILITE AU FREINAGE EN VIRAGE

Définition

Aptitude du véhicule à conserver le rayon de courbure initialement demandé par le client lors d'un freinage ou d'un lever de pied en courbe.

Caractérisation

Sur un virage, à rayon et vitesse fixée, on fait subir au véhicule une décélération définie. On mesure alors la variation de vitesse de lacet

10.11 IMPACT PRESTATION DU ROULIS

10.11.1 COMPORTEMENT

(pdf Eduauto)

- Toute diminution du rapport des raideurs antiroulis AV/AR, à antiroulis total constant, fait évoluer le comportement du véhicule vers le survirage.
- Toute réduction de la raideur antiroulis sur l'essieu moteur, à antiroulis total constant, améliore la motricité du véhicule en virage.

On arrive à la conclusion suivante pour un usage sportif, conduisant à un nécessaire compromis :

Toutes les raideurs doivent être augmentées pour réduire le roulis aux fortes accélérations atteintes mais, si l'on veut préserver la motricité, il faut éviter des valeurs trop élevées à l'avant. Par contre des valeurs importantes à l'arrière conduisent très vite à un appui intérieur nul : cette attitude en virage sur trois roues est systématique sur circuit pour ce type de véhicule.

10.11.2 CONFORT

- Maintien de caisse
- Copiage
- Fréquence de pompage

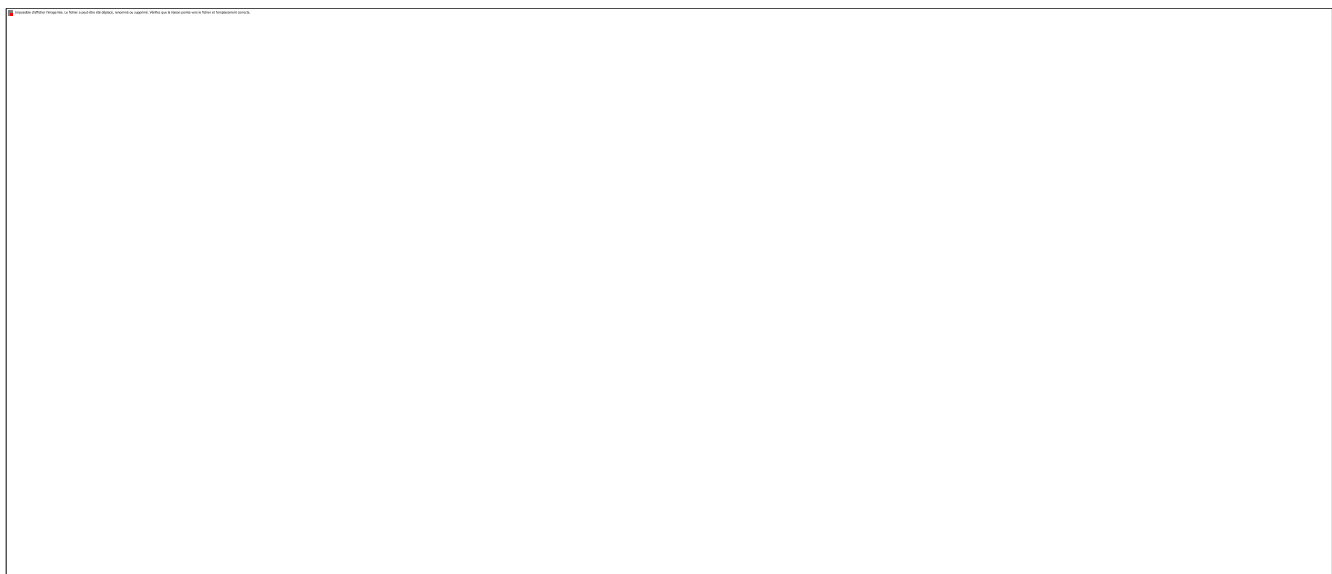
Plus le véhicule est tenu en anti – roulis, plus on a une dépendance droite / gauche, plus on a tendance à copier les aspérités de la route.

10.12 CRITERES BMW

La table 5.1 ci-dessous est extraite de la page 59 de (Eichstetter, 2017)

Traduction :

1. Gain en vitesse de lacet vs vitesse véhicule (mais extrait d'un essai réel et non pas d'un recalculation de cette courbe à partir de la DA)
2. ≈ Répartition de report de charge vs accel trans
3. Gain en vitesse de lacet vs fréquence (i.e. ce que l'on sort dans la DA générée)
4. Dérive maxi en demi-baïonnette (conditions pas très claires)
5. Charge verticale mini pneu avant et pneu arrière sur la même manœuvre
6. Roulis spécifique 7 m/s^2 (sur statico-dynamique)
7. Copiage sur mauvaise route : DSP de la vitesse de roulis entre 0 et 2.5 Hz



10.13 PERCUSSION

La percussion est une sollicitation, de type impact, telle que celle provoquée par le passage sur une plaque d'égout ou bien la jonction des plaques de béton sur autoroute. Elle est simulée à l'aide de cordes de différents diamètres. La prestation est caractérisée par la capacité à filtrer les efforts dus à l'impact, qui se traduisent par des vibrations et du bruit au niveau de la caisse.

Critères influençant la prestation

On cherchera à diminuer la fonction de transfert point de contact pneu-obstacle vers le centre roue. Le choix du pneu est important : choisir le pneu adapté donnant des efforts F_x et F_z pas trop importants, favoriser les grands diamètres de pneu et les faibles pressions. Attention toutefois : une faible pression nuit à la précision de direction, à l'adhérence maximale du pneu, au ballant pneumatique donc à la qualité du transitoire, ...

On distinguera le filtrage longitudinal et le filtrage vertical.

Percussion longitudinale

On veut diminuer la fonction de transfert point K/caisse.

- Augmenter le recul de roue : jeu sur les raideurs de bushings des points A et B, raideur des points E et F. Le déploiement des raideurs impose de prendre également en compte les flexibilités en braquage sous effort latéral, sous effort longitudinal (sous effort moteur et effort de freinage), les flexibilités en

carrossage sous effort transversal et la raideur de ballant, sous peine de dégrader la tenue de cap mauvaise route, de modifier la dynamique angulaire, de diminuer l'accélération maximale permise par le véhicule,... Une flexibilité trop élevée cause également une rafale d'oscillations après le passage de l'obstacle et perturbe la logique ABS. Il existe aussi un risque de couplage avec les modes de battement de roue

- Avoir une géométrie de train telle que la trajectoire du centre roue recule lors d'un débattement vers le choc.

Percussion verticale

- diminuer les raideurs d'attache (point F) des amortisseurs (en effet dans ce cas les efforts transitent par les amortisseurs qui aux fréquences concernées peuvent être considérés comme des solides)
- éviter le couplage des modes vertical et longitudinal en rapprochant trop les fréquences de battement de roue et le premier mode longitudinal de train.

Déploiement

Un compromis relevant de l'expérience sur de nombreux véhicules peut être trouvé en respectant les formules : $\alpha \cdot \text{Flexvert} + \beta \cdot \Delta x / F_x = \text{cste}$, avec Flexvert la flexibilité verticale au train, $\Delta x / F_x$ le recul de roue. Les valeurs retenues pour les constantes sont : $\alpha=1$, $\beta=10$ et $\text{cste}=60$

11 OBJECTIVATION DES PRESTATIONS

11.1 CRITERES SUBJECTIFS

Dans "Essentials of Vehicle Dynamics" (Pauwelussen, 2014), on trouve :

5.1 Criteria for Good Handling 127	
Good Handling Criteria	Clarification
Short time delay	Long delays between command input and vehicle response (yaw rate, lateral acceleration, etc.) should be avoided.
Gains not too large or too small	A large gain is experienced as nervous behavior with only a small input leading to a severe response. On the other hand, a significant driver input to have only a small vehicle response (low gain) is not preferable either.
Compromise between responsiveness and stability	Stability and responsiveness contradict each other. Vehicle instabilities require the driver to provide continuously stabilizing control, which is regarded as disadvantageous. Too high stability leads to delays, which one tries to avoid.
Small body slip angle	This means that the driver is looking in the direction the vehicle is moving. In other words, the heading angle and course angle coincide. On the other hand, a nonzero body slip angle is part of the feedback to the driver.
Response immunity to external disturbances	A vehicle is always subject to external disturbances, such as crosswind gusts, road disturbances, etc.
Small roll response	The best conditions for accurate sensing by the driver of the vehicle environment are obtained for minimum vehicle body roll.
Consistent vehicle behavior	Large changes in vehicle response with speed, loading, road surface conditions, lateral acceleration level, etc. are undesirable from the point of view of building up driving skills. This would lead to consistent vehicle properties over all running conditions and consequently, that the driver is not "warned" when approaching the saturation limits for the tires. Hence, consistent behavior should be limited to nonextreme vehicle behavior.

11.2 LES PRINCIPALES METRIQUES

Tiré de (Hazare, 2014)

Handling Domains	Handling Objective Metrics	Description of Metrics	Units
Steady-State Handling	Understeer Gradient	Expressed as the gradient of steering wheel angle and lateral acceleration response.	deg/G
	Yaw Rate Gain	Expressed as the sensitivity of heading angle response change per unit steering wheel angle.	1/sec
	Side-Slip Angle Gain	Expressed as the sensitivity of side-slip angle response to lateral acceleration.	deg/G
	Roll Angle Gain	Expressed as the sensitivity of roll angle response to lateral acceleration.	deg/G
Transient Handling	Yaw Rate Time Constant	Expressed as the inverse of the frequency at which the phase of the yaw rate transfer functions equals -45 degrees.	ms
	Yaw Rate Damping Ratio	Expressed as the ratio of steady-state value and peak value of yaw rate from the yaw rate transfer function.	-
	Lateral Acceleration Phase Lag	Expressed as the phase lag of lateral acceleration from lateral acceleration vs. steering wheel angle transfer functions at 1 Hz.	deg
	Roll Angle Overshoot	Expressed as the ratio of the difference between the peak and steady-state values and steady-state value of the roll angle response.	%
Steering Feedback	Steering Torque Gain	Expressed as the gradient of steering torque and steering wheel angle input.	Nm/deg
	Steering Torque Feel	Expressed as the gradient of steering torque and lateral acceleration response.	Nm/G
On-Center	Steering Torque Time Lag	Expressed as the phase lag of steering torque from steering torque vs. steering wheel angle transfer function at 0.2 Hz.	ms

Parking	Lock-to-Lock Steering Rotations	Expressed as the maximum number of steering wheel rotations required for 360 degrees of steering wheel motion.	-
	Turning Circle Diameter	Expressed as the diameter (wheel-to-wheel) of the smallest circular turn that the vehicle is capable of making.	m
	Parking Static Torque	Expressed as the magnitude of static steering wheel torque during low speed maneuvering.	Nm
Disturbance Sensitivity	Yaw Moment Sensitivity	Expressed as degree of yaw angle response per unit yaw moment disturbance input.	Deg/KN-m-sec
Coupled Dynamics	Yaw Rate Increment	Expressed as the percentage increase in yaw rate while accelerating out of a corner.	%
Road Adaptability	Yaw Rate Increment	Expressed as the percentage increase in yaw rate after cornering on single bump.	%
Straight-Line Stability	Straight-Line Stability Index	Expressed as the measure of vehicle's tendency to develop a destabilizing yaw moment while reacting to un-balanced longitudinal and lateral force inputs. Lower value of this indicates higher straight-line stability.	Nm/N
	Pitch Gradient	Expressed as the sensitivity of pitching motion per unit lateral acceleration.	Deg/G
Emergency Handling (Roll Stability)	Static Stability Factor	Expressed as the ratio of half-track width to center of gravity height.	-

11.3 VW (1973)

△ Lincke, W., Richter, B., and Schmidt, R., "Simulation and Measurement of Driver Vehicle Handling Performance," SAE Technical Paper 730489, 1973, <https://doi.org/10.4271/730489>.

... avec déjà des tests sur simulateur de conduite !

11.4 CROLLA, 1998

△ Crolla, D., Chen, D., Whitehead, J., and Alstead, C., "Vehicle Handling Assessment Using a Combined Subjective-Objective Approach," SAE Technical Paper 980226, 1998, <https://doi.org/10.4271/980226>.

Mentionné dans (Bennett, 2012) qui en fait le résumé suivant :

In 1998, Crolla, Chen, Whitehead and Alstead [59], published a paper on handling assessment using a combined subjective-objective approach. They used information from a large data set acquired through testing conducted by Leeds University and MIRA. In the test, a passenger car was used with 16 different setup configurations (tyre pressures, anti-roll bars, dampers, as well as other components), along with an identical baseline car. The study used eight professional drivers, all with experience in vehicle dynamics testing and development. 46 different metrics were analysed from three different test types in order to characterise the vehicle objectively (Figure 2-26). Subjective assessment carried out by the drivers was performed using 49 different questions (Figure 2-27). Subjective assessments were made on a scale of 1 to 7 with reference to the baseline as it had been previously found that drivers were better at rating differences rather than absolute values. The authors stated that it was important that the vehicle parameter changes resulted in sufficiently different levels of performance that the drivers could perceive the differences subjectively.

The authors found that assessments between drivers had surprisingly poor consistency with the mean answers to most subjective questions for a single setup being able to be placed 'confidently' (95% confidence level) on the 'better' or 'worse' line of the baseline setup. The authors point out that this does not imply that the mean ratings are of no value, but it does reduce their significance. A simple linear regression was used to determine a relationship between measured metrics and mean subjective assessments, with 27 of the 49 questions found to have a correlation R² value of more than 0.7. The authors found that 11 of the subjective questions were consistent reliable indicators of measured performance and that there were 17 metrics that correlated consistently well with mean subjective assessments. These were separated into three categories, as presented in Figure 2-25.

Unequivocal and Uniform Effect	Unequivocal Effect	Uniform Effect
YawGain/0.7	YawRtRespTime/0.2	Storq/0.6
YawGain/0.4	StMeanRespTime/0.6	d(storq)/0.2
Storq/0.2	YawPhase/0.4	d(storq)/0.4
SteerGain/1.0	YawRt/0.2	YawRt/0.6
d(sslip)/0.4	RollRtRespTime/0.2	RollRtRespTime/0.6
LataccGain/1.0		
SteerPhase/0.4		

Figure 2-25 – Metrics with highest levels of correlation to subjective measures – Crolla, Chen, Whitehead and Alstead (1998) [59]

Test	Description	Derived Metrics	Abbreviations
Steady state steering pad	33m radius, 0 to 6m/s ² lateral acceleration clockwise and anti-clockwise.	d(hand wheel angle)/d(lateral acceleration) at ± 2 and ± 4 m/s d(front slip)/d(Lateral acceleration) at ± 2 and ± 4 m/s d(side slip)/d(Lateral acceleration) at ± 2 and ± 4 m/s d(Torque)/d(Lateral acceleration) at ± 2 and ± 4 m/s Roll angle at ± 2 and ± 4 m/s	d(hw)/0.2, /0.4 d(fslip)/0.2, /0.4 d(sslip)/0.2, /0.4 d(Storq)/0.2, /0.4 Roll angle/ 0.2, /0.4
J-Turns (Step steer input)	2 and 6 m/s ² lateral acceleration clockwise and anti-clockwise.	Peak lateral acceleration response time Peak road wheel steer angle and response time Peak roll rate and response time Peak yaw rate and response time Peak steering torque and response time	LatacRespTime/0.2, /0.6 StMean/0.2, /0.6 StMeanRspTime/0.2, /0.6 RollRt/0.2, /0.6, RollRtRspTime/0.2, /0.6 YawRt/0.2, /0.6, YawRtRspTime/0.2, /0.6 Storq/0.2, /0.6, StorqRtRspTime/0.2, /0.6
Impulse (frequency response)	2 m/s ² impulse inputs. Time histories transformed to frequency domain using handwheel angle as input	Lateral acceleration gain and phase at 0.4, 0.7 and 1.0 Hz Road wheel steer gain and phase at 0.4, 0.7 and 1.0 Hz Yaw rate gain and phase at 0.4, 0.7 and 1.0 Hz	LatacGain/0.4, /0.7, /1.0, LatacPhase/0.4, /0.7, /1.0 StMeanGain/0.4, /0.7, /1.0, StMeanPhase/0.4, /0.7, /1.0 YawGain/0.4, /0.7, /1.0, YawPhase/0.4, /0.7, /1.0

Figure 2-26 – Derived metrics for handling assessment – Crolla and Whitehead (2001)

[60]

Heading	Subheading	Sub-Subheading	Question
Steady state Turning	Over smooth roads	Cornering behaviour	Progressive behaviour with decreasing lateral acceleration
Steady state Turning	Over smooth roads	Steering torque feedback	Indication of available grip
Steady state Turning	Over smooth roads	Steering torque feedback	Indication of magnitude of lateral acceleration
Steady state Turning	Over smooth roads	Steering torque feedback	Magnitude of torque levels- LOW lock/ HIGH lateral accel.
Steady state Turning	Over smooth roads	Steering torque feedback	Magnitude of torque levels- HIGH lock/ LOW lateral accel.
Steady state Turning	Over smooth roads	Steering torque feedback	Progression of handwheel torque levels
Steady state Turning	Over smooth roads	Steering torque feedback	Smoothness
Steady state Turning	Over smooth roads	Steering torque feedback	Symmetry
Steady state Turning	Over rough roads	Cornering behaviour	Ease with which a line is held
Steady state Turning	Over rough roads	Kickback on bumps	Kickback on bumps
Power change	Power on	Yaw response	Magnitude of response (state below whether over or under steer)
Power change	Power on	Yaw response	Progressiveness of yaw rate response
Power change	Power on	Yaw response	Yaw stability of vehicle at high lateral accel.
Power change	Power on	Steering torque feedback	Torque steer due to power change
Power change	Power off	Yaw response	Magnitude of response (state below whether over or under steer)
Power change	Power off	Yaw response	Yaw stability of vehicle at higher lateral accelerations
Sudden braking in a turn			Yaw rate response (state tendency to spin or plough below)
Sudden braking in a turn			Roll stability
Sudden braking in a turn			Wheel lift
Sudden braking in a turn			Wheel lock up
Transient cornering	Turn in response		Turn in response and precision on smooth surfaces (low lateral accel.)
Transient cornering	Turn in response		Turn in response and precision on smooth surfaces (medium lateral accel.)
Transient cornering	Turn in response		Turn in response and precision on smooth surfaces (higher lateral accel.)
Transient cornering	Turn in response		Body roll angle
Transient cornering	Turn in response		Body roll rate
Transient cornering	Steering torque feedback		Steering catch-up
Straight line directional stability	Constant throttle		Bump steer
Straight line directional stability	Constant throttle		Steer kickback
Straight line directional stability	Constant throttle		Over changing surface camber (state whether car wanders or pulls)
Straight line directional stability	Constant throttle		Over changing surface composition: ease with which a line is held
Straight line directional stability	Under acceleration		Torque steer
Straight line directional stability	Under acceleration		Tendency to pull to one side
Straight line directional stability	Under braking		Tendency to pull or weave
Obstacle avoidance	Single lane change	Trailing throttle	Turn in response
Obstacle avoidance	Single lane change	Trailing throttle	Recovery
Obstacle avoidance	Single lane change	Trailing throttle	Controllability
Obstacle avoidance	Single lane change	Trailing throttle	Limiting factor (state below whether stability, grip, steering ratio)
Obstacle avoidance	Single lane change	Balanced throttle	Turn in response
Obstacle avoidance	Single lane change	Balanced throttle	Recovery
Obstacle avoidance	Single lane change	Balanced throttle	Controllability
Obstacle avoidance	Balanced throttle		Limiting factor (state below whether stability, grip, steering ratio)
Obstacle avoidance			Double lane change
Response to steering impulse			Oscillation of vehicle
Response to steering impulse			Oscillation of handwheel
Response to steering impulse			Level of damping

Figure 2-27 – Driver subjective assessment questions – Crolla et al (2001/2002) [60], [61]

11.5 OBJECTIVATION COMPORTEMENT ON-CENTER (TOYOTA, 2001)

△ Higuchi, A. and Sakai, H., "Objective Evaluation Method of On-Center Handling Characteristics," SAE Technical Paper 2001-01-0481, 2001, <https://doi.org/10.4271/2001-01-0481>

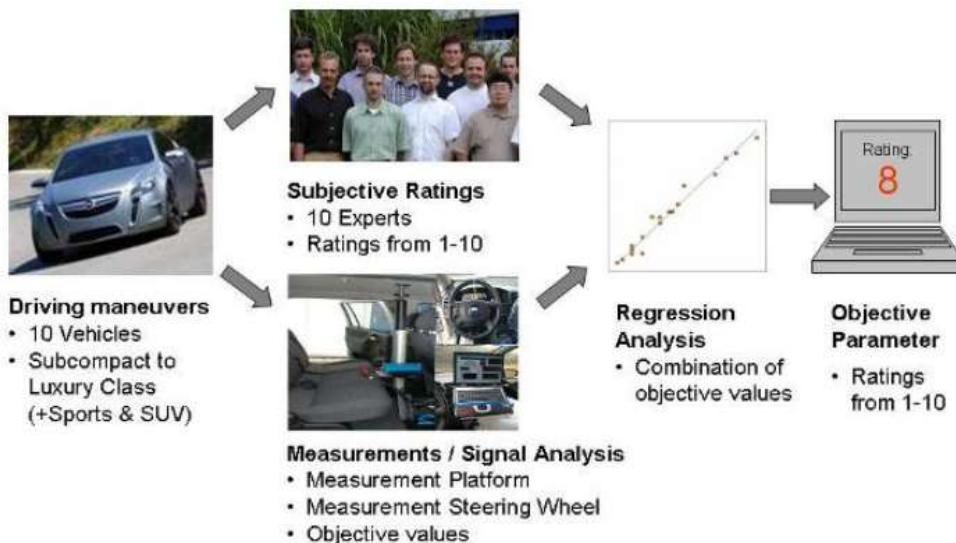
This paper introduces vehicle test method, data processing and result parameters of an objective evaluation method to quantify on-center handling at freeway driving. Vehicle test is conducted on a flat straight road with a low frequency sinusoidal steering angle input. The result consists of eleven parameters that describe relations of two quantities such as gain, non-linearity and lag time.

11.6 ETUDE FEV (2008)

OBJECTIVE EVALUATION OF SUBJECTIVE DRIVING IMPRESSIONS (FEV, 2008)

https://www.fev.com/fileadmin/user_upload/Media/TechnicalPublications/Chassis/V0815_FISITA2008_Objective_Evaluation_F20080319-Paper_01.pdf

Methodology to develop Objective Parameters



11.7 GASPAR GIL GOMEZ (VOLVO)

Voir les travaux de Gaspar Gil Gomez (§30.3.1)

Towards efficient vehicle dynamics evaluation using correlations of objective metrics and subjective assessments

- [Licentiate thesis \(2015\)](#)
- [Doctoral thesis \(2017\)](#)

Correlations of subjective assessments and objective metrics for vehicle handling and steering: a walk through history

▷ <https://www.inderscience.com/info/inarticle.php?artid=79191>

Sont mentionnés les papiers suivants :

Although not the first research in the field but probably the first extensive work aiming to identifying the correlation between OM and SA was performed by Chen (1997), Chen and Crolla (1998) and Crolla et al. (1998).

- Chen, D.C. (1997) **Subjective and Objective Vehicle Handling Behaviour**, PhD Thesis, University of Leeds, UK.
- Chen, D.C. and Crolla, D.A. (1998) '**Subjective and objective measures of vehicle handling: drivers & experiments**', Vehicle System Dynamics, Vol. 29, pp.576-597.
- Crolla, D.A., Chen, D.C., Whitehead, J.P. and Alstead, C. (1998) '**Vehicle handling assessment using a combined subjective-objective approach**', International Congress and Exposition, 23-26 February, Detroit, Michigan, Society of Automotive Engineers, Warrendale, Pa., doi:10.4271/980226.

11.8 ETUDE SCANIA-KTH SUR SIMULATEUR (CAMION REMORQUE)

Finding correlation between handling values and the drivers' performance using a moving base driving simulator <http://kth.diva-portal.org/smash/record.jsf?pid=diva2%3A499233&dswid=9093> (2011)

A moving base driving simulator was used to examine 16 truck-trailer-combinations. The driving of 28 test drivers in a special developed manoeuvre resulted in characteristic driver performance values evaluated of vehicle system quantities measured while driving. Stationary and dynamical ISO-handling tests resulted in handling quantities. The correlation by means of regression analysis between these driver performance values and the quantities of the ISO-handling tests are presented here as a step towards the mapping of steering feel.

On trouve les références suivantes dans l'intro :

Steering feel is a very complex perception. Several studies have already investigated the drivers' experience of steering feel. The most comprehensive work is probably done by Chen and Crolla [1]. In a test with 16 different vehicle set-ups in five manoeuvres they linked 49 subjective ratings to 46 objective vehicle handling metrics. Norman [2] performed an evaluation of objective quantities regarding on-centre handling of passenger cars and mapped a wide area of vehicles. Van Randwijk et al. [3] found indications for correlation between driver judgements and the measuring results from open- and closed-loop-tests with medium heavy trucks. Riedel et al. [4] investigated drivings in a double lane change and found correlations between a subjective rating and a combination of a driver individual performance quantity (unsymmetry in steering wheel angle) and a vehicle specific quantity (time delay between steering wheel angle and yaw rate). Hiramatsu et al. [5] found correlations between the steering ratio and feeling items (static steering, parking, steering effort, returning, ...) and related this to steering comprehensive appraisal items of the drivers. Harrer et al. [6] searched for correlations between objective ratings due to an own developed questionnaire and handling quantities of an ISO weave test [7]. The investigation was done by linear correlation as well as by multiple linear regression analysis. Zschocke and Albers [8] differed the subjective domain into description and liking. This could be correlated to open loop handling values by evaluating ten different cars.

References

- [1] D. C. Chen & D. A. Crolla: *Vehicle Handling Behaviour: Subjective v. Objective Comparisons*, F98T210, FISITA World Automotive Congress, Paris, 1998
- [2] K. D. Norman: *Objective Evaluation of On-Center Handling Performance*, SAE 840069, SAE Technical Paper Series, 1984
- [3] M. J. van Randwijk, J. Godhjelp, W. D. Käppler & P. A. J. Ruys: *Correlation of driver judgements and vehicle directional data to evaluate and predict truck handling*, 3rd EAEC International Conference, Strasbourg, France, 1991
- [4] A. Riedel et al.: *Bewertungskriterien zur Fahrverhaltensanalyse in Versuch und Simulation (Ermittlung neuer Kennwerte für den ISO-Spurwechsel)*, VDI Berichte Nr. 1007, Düsseldorf, 1992
- [5] K. Hiramatsu, S. Inoue & S. Iwamoto: *Quantification Analysis of Driver's Feeling on Manual Steering Vehicle*, VDI-Berichte Nr. 368, Düsseldorf, 1980
- [6] M. Harrer, P. E. Pfeffer & D. N. Johnston: *Steering feel - objective assessment of passenger cars analysis of steering feel and vehicle handling* F2006V165, FISITA World Automotive Congress, Yokohama, 2006
- [7] ISO 13674-1: *Road vehicles – Test method for the quantification of on-centre handling – Part 1: Weave test*, 2003
- [8] A. K. Zschocke & A. Albers: *Links between subjective and objective evaluations regarding the steering character of automobiles*, International Journal of Automotive Technology, Vol. 9, No. 4, pp. 473-481, 2008
- [9] M. Rothhämel, J. IJkeima & L. Drugge: *On a method to generate a word pool for the description of steering feel*, Proceedings of the 10th International Symposium on Advanced Vehicle Control (AVEC 10), Loughborough, UK, 2010
- [10] M. Rothhämel: *Capturing Steering Feel - a step towards the implementation of active steering in heavy vehicles*, TRITA-AVE 2010:57, Licentiate thesis, Royal Institute of Technology, Stockholm, 2010

Des "Driver Performance Quantities" sont définies :

$$Unsymmetry_1 = \frac{\delta_{SW_{max}}(Curve_2)}{\delta_{SW_{max}}(Curve_1)} \quad (1)$$

$$Unsymmetry_2 = \frac{\delta_{SW_{max}}(Curve_3)}{\delta_{SW_{max}}(Curve_2)} \quad (2)$$

$$Unsymmetry_3 = \frac{\delta_{SW_{max}}(Curve_3)}{\delta_{SW_{max}}(Curve_1)} \quad (3)$$

$$\delta_{SW_{Changes}} = \sum_i n_i \quad n_i = 1 \quad \text{for each} \quad \ddot{\delta}_{SW}(x) = 0 \quad (4)$$

$$\delta_{SW_{max}} = \max(\delta_{SW}) \quad (5)$$

$$\delta_{SW_{IIPS,PSD}} = \int |F(j\omega)| \, d\omega \quad (6)$$

$$\delta_{SW_{IFPS,FFT}} = \int |F(j\omega)| \omega^2 \, d\omega \quad (7)$$

$$M_{SW_{max}} = \max(M_{SW}) \quad (8)$$

$$M_{SW_{mean}} = \overline{M_{SW}} \quad (9)$$

$$M_{SW_{IFPS,PSD}} = \int |F(j\omega)| \omega \, d\omega \quad (10)$$

$$a_{y_{RMS}} = \sqrt{\sum_{i=1}^n \frac{a_{y,i}^2}{n}} \quad (11)$$

$$\omega_{z_{IF2PS,FFT}} = \int |F(j\omega)| \omega^2 \, d\omega \quad (12)$$

$$\Delta t(\delta_{SW}, \omega_z) = \frac{S_{\max(R_{\delta_{SW}\omega_z})} - S_N}{f_s} \quad \text{with} \quad R_{\delta_{SW}\omega_z}(\tau) = \lim_{T_F \rightarrow \infty} \frac{1}{T_F} \int_{-\frac{T_F}{2}}^{\frac{T_F}{2}} \delta_{SW}(t) \times \omega_z(t + \tau) \, dx \quad (13)$$

Une étude de corrélation est menée :

Table 2: Regression analysis results showing the coefficients and R^2 p-values of the analysis with averaged DPQ explained by handling values.

DPQ	explained by	Coefficients	p	R^2
$Unsymmetry_3$	Bandwidth Time delay Torque gradient (off center)	$b_0 = 0.899$ $b_1 = -0.0800$ $b_2 = 0.0691$ $b_3 = 0.0530$	0.0332%	78%
$\delta_{SW_{max}}$	Time delay Torque gradient (off center) Response deadband	$b_0 = 1.08$ $b_1 = -0.0858$ $b_2 = -0.0339$ $b_3 = 0.0241$	0.00924%	82%
$\delta_{SW_{IFPS,PSD}}$	Understeer gradient Time delay Torque gradient (off center)	$b_0 = 0.123$ $b_1 = 0.0074$ $b_2 = -0.0172$ $b_3 = -0.0151$	2.39%	53%
$\delta_{SW_{IF2PS,FFT}}$	Understeer gradient Bandwidth Time delay	$b_0 = 289$ $b_1 = 23.3$ $b_2 = -62.6$ $b_3 = -77.1$	1.32%	58%
$M_{SW_{max}}$	Torque magnitude	$b_0 = 3.11$ $b_1 = -1.46$	0.51%	44%
$M_{SW_{mean}}$	Understeer gradient Bandwidth Time delay Torque gradient (off center)	$b_0 = -0.275$ $b_1 = 0.370$ $b_2 = -0.982$ $b_3 = -0.574$ $b_4 = -0.349$	0.0306%	83%
$M_{SW_{IFPS,PSD}}$	Torque gradient Response deadband	$b_0 = 29.2$ $b_1 = -188$ $b_2 = 162$	0.19%	62%
$a_{y_{RMS}}$	Bandwidth Time delay Response deadband	$b_0 = 1.30$ $b_1 = -0.0357$ $b_2 = -0.0587$ $b_3 = -0.0328$	2.90%	51%
$\omega_{z_{IF2PS,FFT}}$	Understeer gradient Bandwidth Response deadband	$b_0 = 5.66$ $b_1 = 0.883$ $b_2 = -1.28$ $b_3 = 0.548$	1.35%	58%

An integrated systems engineering methodology for design of vehicle handling dynamics

◇ https://tigerprints.clemson.edu/all_dissertations/1451/

(Hazare, 2014)

Table 1. Vehicle Handling Domains and Objective Metrics.

Handling Domains	Description of Handling Domains	Handling Objective Metrics
Steady State Handling	Scenarios of constant speed; constant steer angles with vehicle turning along a constant radius of curvature	Understeer gradient, yaw rate gain, roll gain, side-slip angle gain
Transient Handling	Scenarios of changing yaw velocity, side-slip velocity, and path curvature; represents vehicle's response during dynamic situations (i.e., turn-entry and turn-exit); evaluated with metrics: agility, responsiveness and damping	Yaw rate time constant, lateral acceleration phase lag, yaw rate damping ratio, roll angle overshoot, roll angle response time
Steering Feedback (Off-Center)	Steering system response, described in terms of steering-wheel torque feedback, of vehicle during normal driving scenarios	Steering torque feel (torque vs. angle, torque vs. lateral acceleration gradient)
On-Center Steering	Steering system response during straight-line driving at highway speeds	Steering torque time lag (vs. steering angle) at low lateral accelerations and low steering frequencies
Emergency (Limit) Handling	Vehicle's response during critical maneuvers such as obstacle avoidance	Yaw stability, roll stability
Parking	Ease of vehicle maneuverability during low-speed, high-steer angle maneuvers	Static parking torque, turn circle diameter, lock-to-lock steering turns
Coupled Dynamics	Vehicle's directional stability in scenarios where cornering is coupled with other dynamic motions such as braking or acceleration	Yaw rate increment
Road Adaptability	Handling behavior of vehicle on different road surfaces (i.e., rough roads, bumps, or low friction surfaces).	Yaw rate increment
Straight-Line Stability	Pull and drift behavior of vehicle (i.e., tendency of vehicle to deviate from intended path during straight-line cruising, acceleration, and braking scenarios); vehicle's response during acceleration and braking on split-mu surfaces.	Pitch gradient, straight-line stability index
Disturbance Sensitivity	Vehicle's straight-line performance in presence of external environmental disturbances such as winds, road crown, and road roughness.	Yaw moment sensitivity

11.10 DIVERS

Classification supervisée en grande dimension. Application à l'agrément de conduite automobile (2006)

(Labo Maths Orsay)

Liens :

<https://hal.archives-ouvertes.fr/hal-00530349>

http://archive.numdam.org/item/RSA_2006__54_4_41_0

<https://math.unice.fr/~malot/Montpellier04I.pdf>

12 MODELISATION DU VEHICULE

12.1 UN PEU D'HISTOIRE

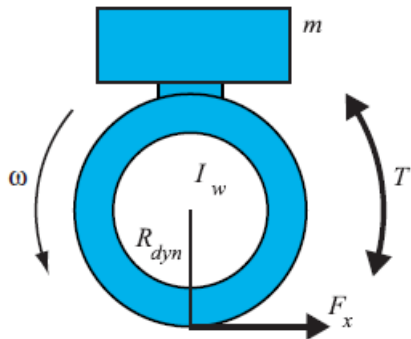
[Road and Off-Road Vehicle System Dynamics Handbook](#)

In modeling vehicle motion, a road vehicle treated as a rigid body has six degrees of freedom, which are lateral, longitudinal, vertical, yawing, pitching, rolling directions. However, in order to analyze characteristics of vehicle motion, a simpler model is more attractive to employ. Segel presented a three-degree-of-freedom model considering lateral, yawing, and rolling motion to describe vehicle-cornering characteristics in 1956 [2]. Moreover, Whitcomb and Milliken presented a well-known two-wheel vehicle model in 1956 neglecting rolling motion and this is a useful model in theoretical analysis of lateral motion and control until now [3]. A quarter car model for analyzing characteristics of a suspension system was also presented around the same time. Gillespie presented a vehicle ride model in 1985 for simulating dynamic tire forces [4]. Besides four-wheel motor vehicles, in 1978, Sharp presented a four-degree-of-freedom model of a motorcycle considering rolling motion in the two-wheel model and also explained the theory of steering behavior of motorcycles by calculating eigenvectors for (straight-line) weave and wobble modes, etc. [5,6]. Modeling of an articulated vehi-

Les modèles de véhicule sont développés depuis les années 1950 [2], les équations étant écrites à la main et comportant peu de degrés de liberté (ddl). Puis le développement des ordinateurs dans les années 1960 à 1980 a permis d'augmenter la complexité des modèles [3] (de 10 à 20 ddl). Les améliorations portaient principalement sur la prise en compte des non-linéarités et sur la modélisation de la cinématique des suspensions. Les équations étaient toujours écrites à la main mais la résolution se faisait par ordinateur. Le milieu des années 1980 a vu l'apparition de programmes de simulation multicorps, permettant aux ingénieurs de développer des modèles élément par élément [4]. L'avantage de cette modélisation est que l'on n'a plus à écrire les équations générales. On peut alors intégrer autant d'éléments que désirés, la seule limite étant fixée par le temps de calcul nécessaire à la résolution. On comprend l'avantage de cette démarche pour les constructeurs automobiles, qui peuvent rapidement connaître l'influence de nombreux paramètres sur le comportement du véhicule. Mais bien souvent seuls les constructeurs ont accès aux données géométriques nécessaires. De plus ces programmes sont plus lents que des modèles écrits à la main développés spécifiquement pour un besoin, et pas toujours plus précis.

http://sari.ifsttar.fr/livrables/radarr/RADARR_1.3.2.pdf

12.2 MODELE "UNE ROUE"

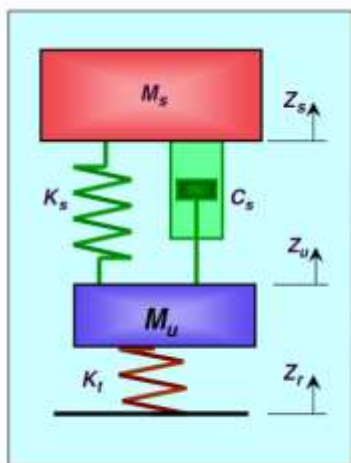


$$\begin{cases} m(\ddot{x}) = F_x \\ I_w\ddot{\omega} = -R_{dyn}F_x + T \end{cases} \quad (1.1)$$

Où m représente la masse supportée par la roue, T est le couple résultant (freinage ou moteur) appliqué à la roue et F_x la force d'interaction longitudinale entre le pneumatique et la chaussée.

12.3 MODELE QUART DE VEHICULE

12.3.1 PRESENTATION



$$M_s \cdot \ddot{Z}_s = F_{st}$$

$$M_u \cdot \ddot{Z}_u = F_t - F_{st}$$

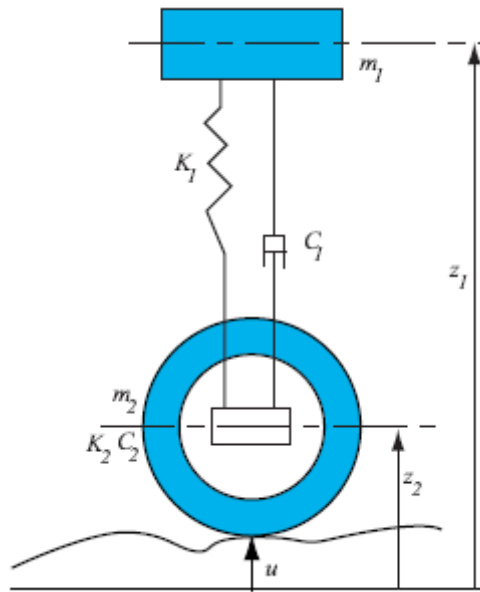
$$F_t = K_t \cdot (Z_r - Z_u)$$

$$F_{st} = (K_s + C_s) \cdot (Z_u - Z_s)$$

$$ApparentMass = \frac{F_{suspension}}{\ddot{Z}_s}$$

$$ComfortIndex = SF \cdot \int_{0.5Hz}^{30Hz} ISO_comfort_filter\left(\frac{\ddot{Z}_s}{\ddot{Z}_r}\right)$$

$$HubAccelerationRatio = \frac{\ddot{Z}_u}{\ddot{Z}_r}$$



Le modèle d'évolution qui lie les différentes variables présentées sur la figure 1.3 est le suivant :

$$\begin{cases} m_1 \ddot{z}_1 + C_1 \dot{z}_1 + K_1 z_1 = C_1 \dot{z}_2 + K_1 z_2 \\ m_2 \ddot{z}_2 + (C_1 + C_2) \dot{z}_2 + (K_1 + K_2) z_2 = C_1 \dot{z}_1 + K_1 z_1 + C_2 \dot{u} + K_2 u \end{cases} \quad (1.2)$$

avec :

K_1 : raideur de la suspension $N.m^{-1}$;

K_2 : raideur verticale du pneumatique $N.m^{-1}$;

C_1 : coefficient d'amortissement de la suspension $N.s.m^{-1}$;

C_2 : coefficient d'amortissement du pneumatique $N.s.m^{-1}$;

m_1 : masse suspendue (masse suspendue véhicule/4) kg ;

m_2 : masse de l'ensemble "roue" kg ;

z_1 : hauteur de la masse suspendue m ;

z_2 : hauteur du centre de roue m ;

u : profil de la chaussée m .

Une représentation d'état qui correspond à cet ensemble d'équation est :

$$\begin{cases} \dot{\mathbf{X}} = \mathbf{AX} + \mathbf{Bu} \\ \mathbf{Z} = \mathbf{CX} + \mathbf{Du} \end{cases}$$

avec :

$$\mathbf{X} = \left(z_1 \ z_2 \ \dot{z}_1 \ (\dot{z}_2 - \frac{C_2}{m_2} \dot{u}) \right)^T$$

$$\mathbf{Z} = (z_1 \ \ddot{z}_1)^T$$

$$\mathbf{A} = \begin{pmatrix} 0 & 0 & 1 & 0 \\ 0 & 0 & 0 & 1 \\ -\frac{K_1}{m_1} & \frac{K_1}{m_1} & -\frac{C_1}{m_1} & \frac{C_1}{m_1} \\ \frac{K_1}{m_2} & -\frac{K_1+K_2}{m_2} & \frac{C_1}{m_2} & -\frac{C_1+C_2}{m_2} \end{pmatrix}$$

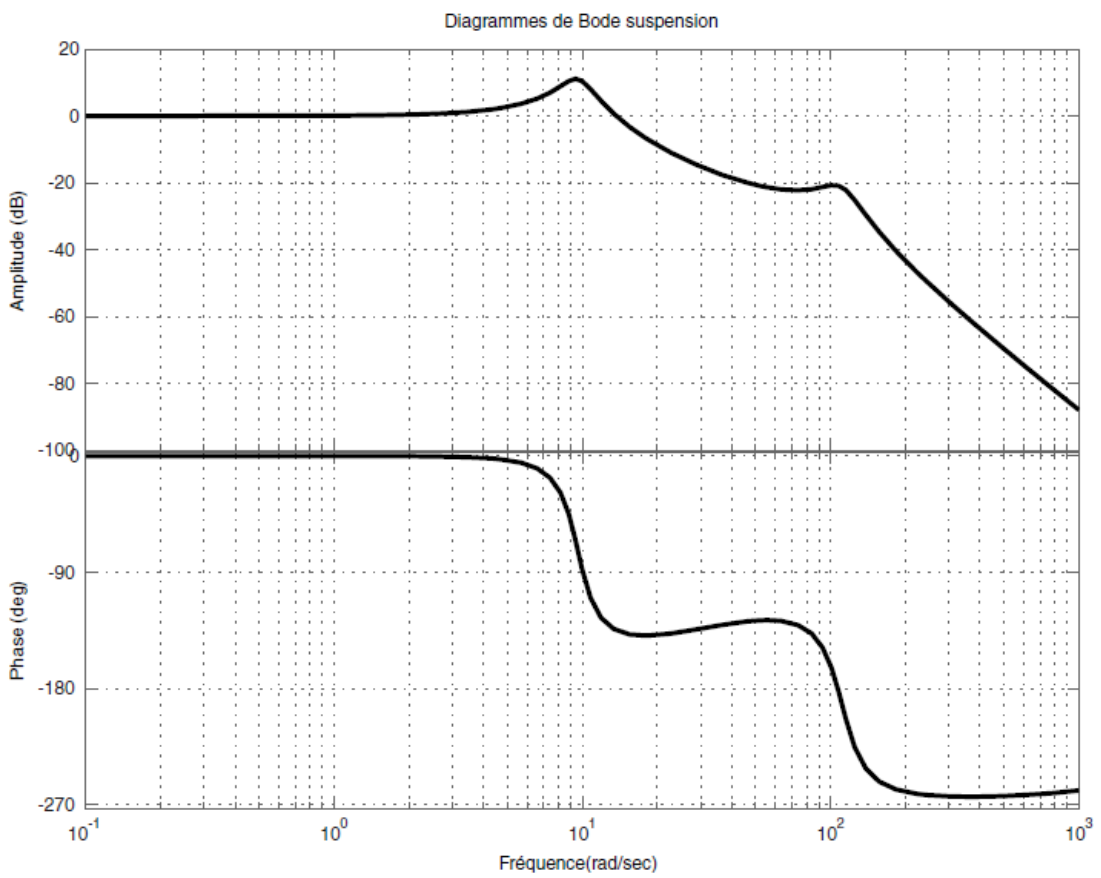
$$\mathbf{B} = \left(0 \ \frac{C_2}{m_2} \ \frac{C_1 C_2}{m_1 m_2} \ \frac{1}{m_2} \left(\frac{K_2 - C_2(C_1 + C_2)}{m_2} \right) \right)^T$$

$$\mathbf{C} = \begin{pmatrix} 1 & 0 & 0 & 0 \\ -\frac{K_1}{m_1} & \frac{K_1}{m_1} & -\frac{C_1}{m_1} & \frac{C_1}{m_1} \end{pmatrix}$$

$$\mathbf{D} = \left(0 \ \frac{C_1 C_2}{m_1 m_2} \right)^T$$

La suspension agit sur deux modes vibratoires : le plus lent caractérise les mouvements de la masse suspendue, le plus rapide concerne les imperfections de la route

Avec des valeurs typiques de masse/raideur/amortissement on peut reconstruire des diagrammes de Bode qui ressemblent à ceci :



12.3.2 LES CONTRIBUTIONS DE JAMES ALLISON

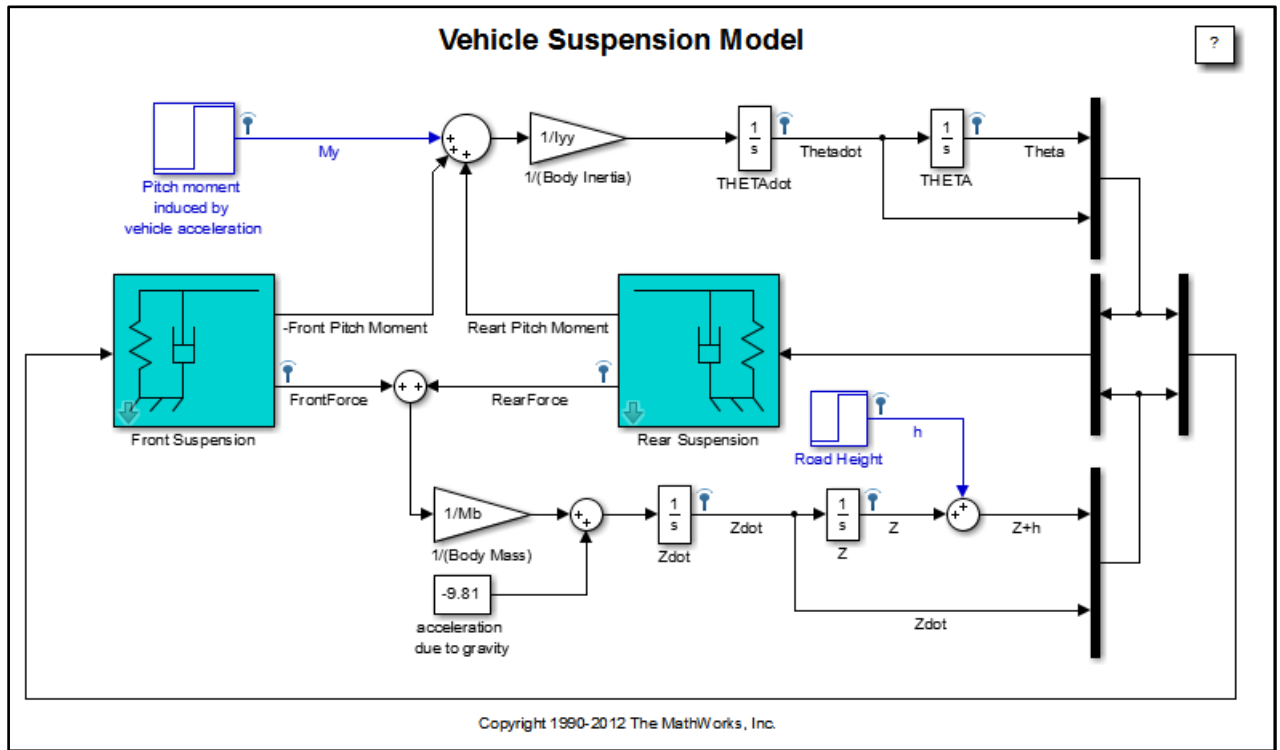
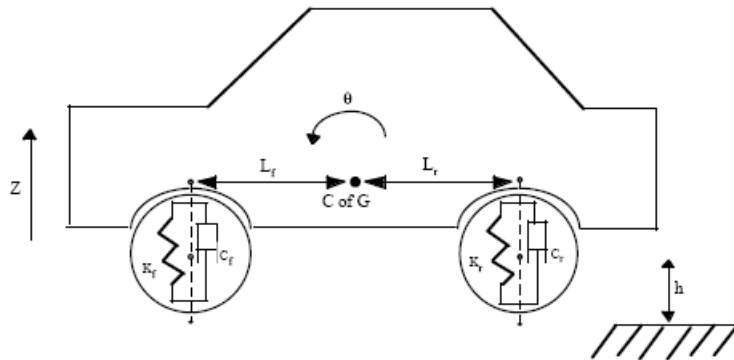
<https://www.mathworks.com/matlabcentral/profile/authors/2913545>

12.4 MODELE DEMI-VEHICULE

On peut découper le véhicule longitudinalement, en négligeant le roulis, ou bien transversalement pour faire une étude essieu par essieu, en négligeant le tangage.

12.4.1 DEMO MATLAB VEHICLE SUSPENSION

Un exemple du premier cas se trouve dans la démo Simulink **sldemo_suspn**



- initialisation : `sldemo_suspdat.m`
- structure de sortie : `sldemo_suspn_output`
- graphes : `sldemo_suspgraph.m`

The front and rear suspension are modeled as spring/damper systems. A more detailed model would include a tire model, and damper nonlinearities such as velocity-dependent damping (with greater damping during

rebound than compression). The vehicle body has pitch and bounce degrees of freedom. They are represented in the model by four states: vertical displacement, vertical velocity, pitch angular displacement, and pitch angular velocity. A full model with six degrees of freedom can be implemented using vector algebra blocks to perform axis transformations and force/displacement/velocity calculations.

The front suspension influences the bounce (i.e. vertical degree of freedom) according to **Equation 1** :

$$F_{front} = 2K_f(L_f\theta - z) + 2C_f(L_f\dot{\theta} - \dot{z})$$

F_{front}, F_{rear} = upward force on body from front/rear suspension

K_f, K_r = front and rear suspension spring constant

C_f, C_r = front and rear suspension damping rate

L_f, L_r = horizontal distance from gravity center to front/rear suspension

$\theta, \dot{\theta}$ = pitch (rotational) angle and its rate of change

z, \dot{z} = bounce (vertical) distance and its rate of change

The pitch contribution to the front suspension is given by **Equation 2** :

$$M_{front} = -L_f F_{front}$$
 (pitch moment due to front suspension)

Equation 3 contains expressions for the rear suspension :

$$F_{rear} = -2K_r(L_r\theta + z) - 2C_r(L_r\dot{\theta} + \dot{z})$$

$M_{rear} = L_r F_{rear}$ pitch moment due to rear suspension

The forces and moments result in body motion according to Newton's Second Law (see **Equation 4**)

$$m_b \ddot{z} = F_{front} + F_{rear} - m_b g$$

$$I_{yy} \ddot{\theta} = M_{front} + M_{rear} + M_y$$

m_b = body mass

M_y = pitch moment induced by vehicle acceleration

I_{yy} = body moment of inertia about gravity center

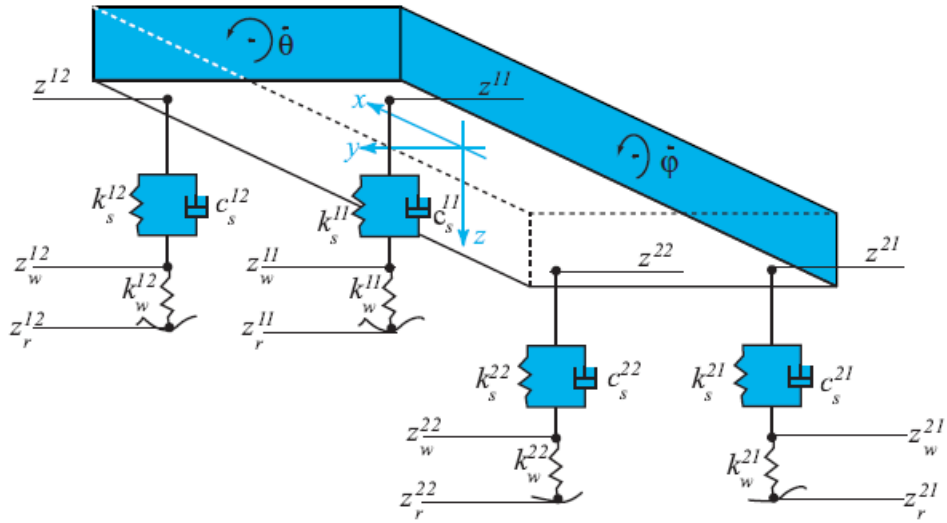
Valeurs d'initialisation :

```

Lf = 0.9;      % front hub displacement from body gravity center (m)
Lr = 1.2;      % rear hub displacement from body gravity center (m)
Mb = 1200;     % body mass (kg)
Iyy = 2100;    % body moment of inertia about y-axis in (kg m^2)
kf = 28000;    % front suspension stiffness in (N/m)
kr = 21000;    % rear suspension stiffness in (N/m)
cf = 2500;     % front suspension damping in (N sec/m)
cr = 2000;     % rear suspension damping in (N sec/m)

```

12.5 MODELE "QUATRE ROUES" VERTICAL



On utilise généralement de simples ressorts pour modéliser les pneumatiques

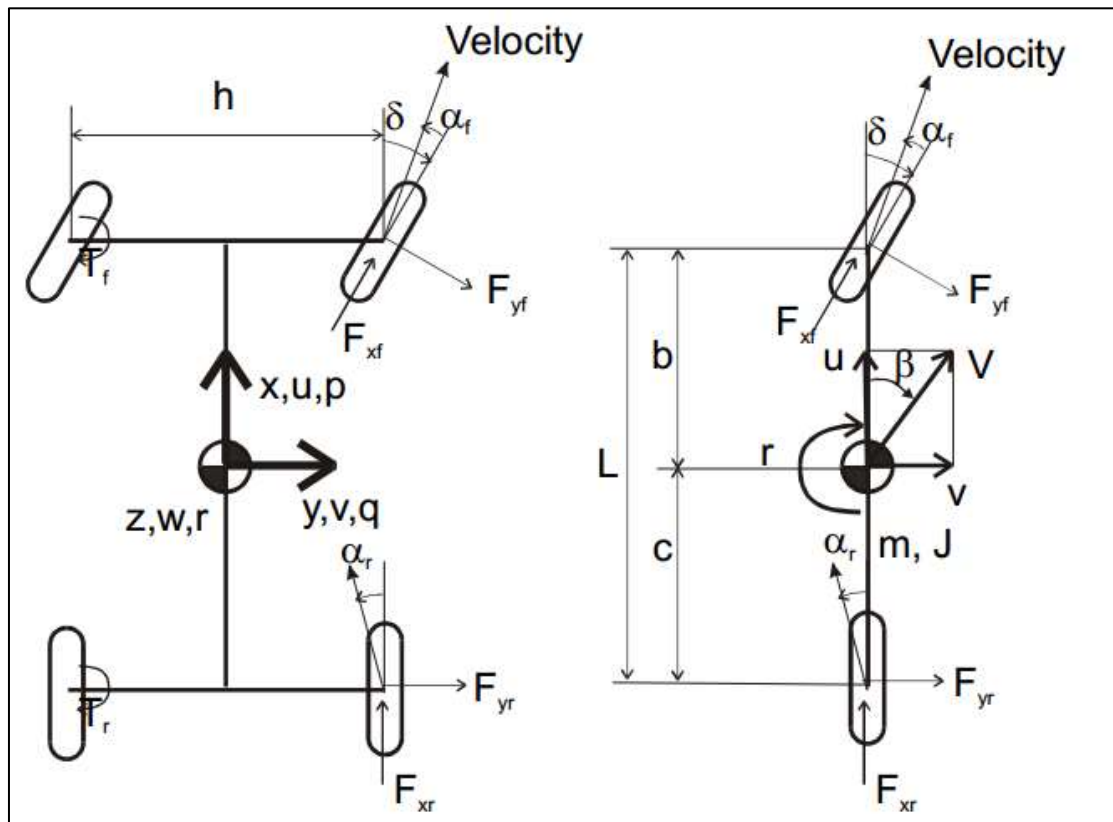
Données pour une Laguna GT (Aubouet, 2010)

Parameter/variable	Description	Value
m_s	Sprung mass	1450kg
$m_{us1,2}$	Front unsprung masses	39kg
$m_{us3,4}$	Rear unsprung masses	32kg
$k_{1,2}$	Front suspension stiffnesses	30000N/m
$k_{3,4}$	Rear suspension stiffnesses	18000N/m
$c_{1,2}$	Front linear damping rate	4000Ns/m
$c_{3,4}$	Rear linear damping rate	3000Ns/m
$k_{t1,2,3,4}$	Tire stiffnesses	200000N/m
I_x, I_y	Roll and pitch inertia	610, 2750kg.m ²
t_f	Distance COG ¹ - front left tire	0.75m
t_r	Distance COG - rear left tire	0.75m
l_f	Distance COG - front	1.06m
l_r	Distance COG - rear	1.7m

12.6 MODELE "BICYCLETTE"

Modèle à 2 degrés de liberté:

- r , vitesse de lacet
- β , angle de dérive du véhicule



12.6.1 FORMULATION CINEMATIQUE

Sources utilisées :

<https://www.coursera.org/learn/intro-self-driving-cars>

2D Kinematic Modeling

- The kinematic constraint is nonholonomic
 - A constraint on rate of change of degrees of freedom
 - Vehicle velocity always tangent to current path

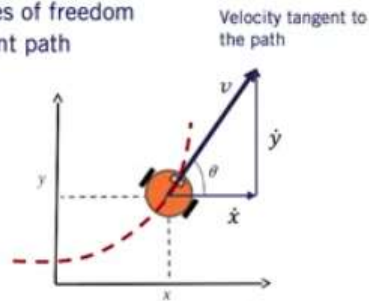
$$\frac{dy}{dx} = \tan \theta = \frac{\sin \theta}{\cos \theta}$$

- Nonholonomic constraint
- $$\dot{y} \cos \theta - \dot{x} \sin \theta = 0$$

- Velocity components

$$\dot{x} = v \cos \theta$$

$$\dot{y} = v \sin \theta$$



On peut écrire plusieurs formulations différentes selon le point de référence que l'on prend. Si on le choisit à la roue arrière on a :

- Rear Wheel Reference Point
 - Apply Instantaneous Center of Rotation (ICR)

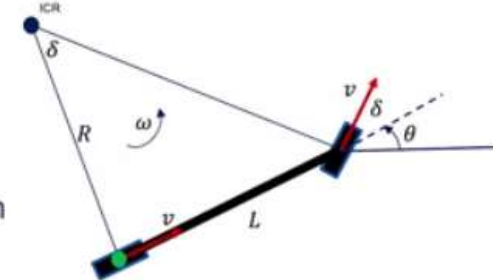
$$\dot{\theta} = \omega = \frac{v}{R}$$

- Similar triangles

$$\tan \delta = \frac{L}{R}$$

- Rotation rate equation

$$\dot{\theta} = \omega = \frac{v}{R} = \frac{v \tan \delta}{L}$$



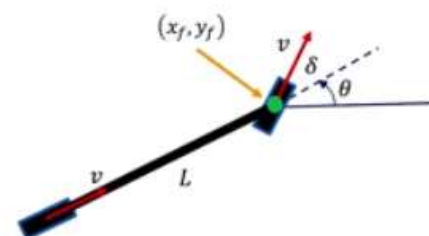
Si on le prend à la roue avant :

- If the desired point is at the center of the front axle

$$\dot{x}_f = v \cos(\theta + \delta)$$

$$\dot{y}_f = v \sin(\theta + \delta)$$

$$\dot{\theta} = \frac{v \sin \delta}{L}$$



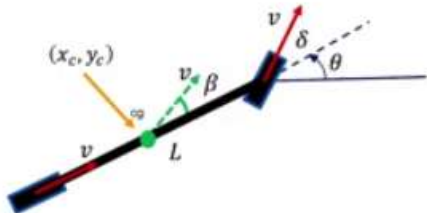
Enfin au centre de gravité, on fait apparaître l'angle de dérive du véhicule, lié au fait qu'on impose une contrainte de non-glissement des pneus. On utilise généralement cette formulation car elle simplifie la mise en œuvre du principe fondamental de la dynamique.

- If the desired point is at the center of the gravity (cg)

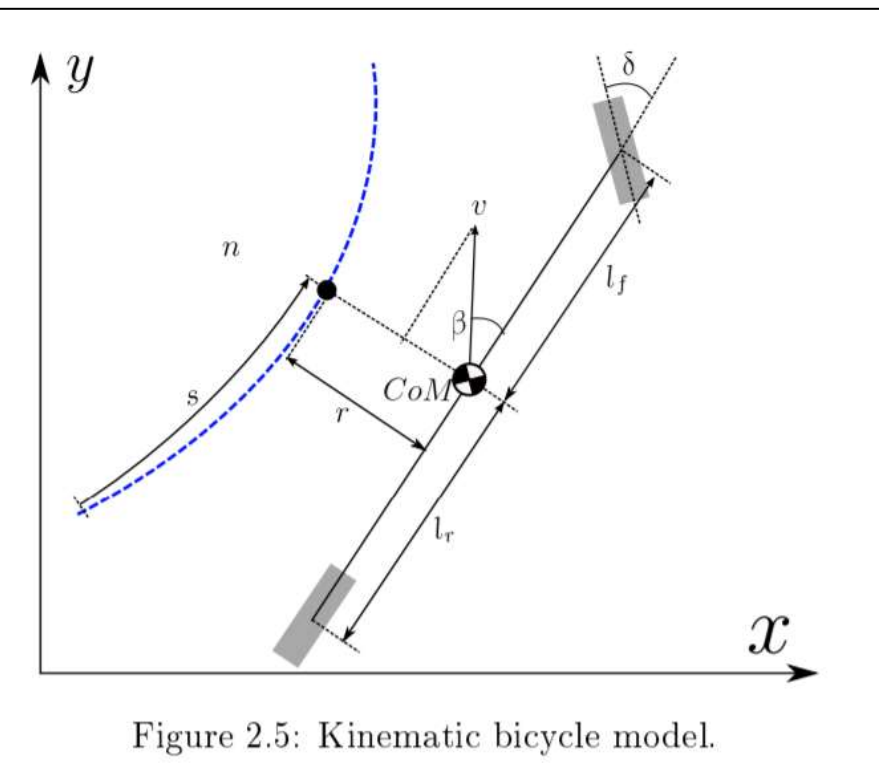
$$\dot{x}_c = v \cos(\theta + \beta)$$

$$\dot{y}_c = v \sin(\theta + \beta)$$

$$\dot{\theta} = \frac{v \cos \beta \tan \delta}{L}$$



Les illustrations suivantes sont tirées de <https://pastel.archives-ouvertes.fr/tel-01635261/document>



$$\dot{x} = v \cos(\theta + \beta), \quad (2.11a)$$

$$\dot{y} = v \sin(\theta + \beta), \quad (2.11b)$$

$$\dot{v} = a, \quad (2.11c)$$

$$\dot{\theta} = \frac{v}{l_r} \sin(\beta), \quad (2.11d)$$

$$\dot{\phi} = \psi, \quad (2.11e)$$

$$\beta = \tan^{-1} \left(\frac{l_r}{l_f + l_r} \tan(\phi) \right), \quad (2.11f)$$

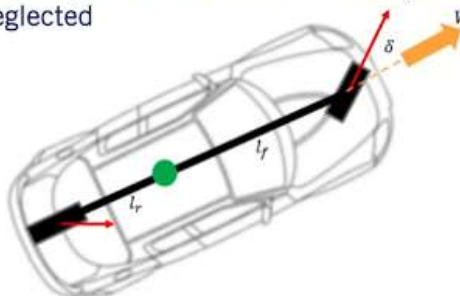
where x and y are the coordinates of the center of mass. v , θ and ϕ are respectively the speed, heading and the steering angle of the front wheel. β is the side-slip angle, a and ψ are respectively the acceleration and the steering angular velocity. Eq. (2.11f) is an algebraic equation connecting β and ϕ . l_r and l_f are respectively the distance of the center of mass to the rear wheel and to the front wheel.

12.6.2 HYPOTHESES

Vehicle Model to Bicycle Model

- Assumptions

- Longitudinal velocity is constant
- Left and right axle are lumped into a single wheel (bicycle model)
- Suspension movement, road inclination and aerodynamic influences are neglected



- Pas de transfert de charge latéral, d'où véhicule compressé en une seule trace
- Pas de transfert longitudinal
- Pas de mouvement de roulis ou de tangage
- Pneus en régime linéaire
- Vitesse d'avance V constante
- Pas d'effets aérodynamiques
- Contrôle en position
- Pas d'effet de souplesse de la suspension et du châssis

Implications des hypothèses

- Régime linéaire des pneumatiques : accélération < 0.4 g
- Petits angles de braquage, de dérive, etc.
- Sol lisse, pas de débattement de suspension
- Contrôle en position: mouvement du véhicule avec contraintes sur les entrées du système (ex. direction) sous forme de déplacements imposés, indépendamment des forces à mettre en œuvre
- Braquage de la direction = seule entrée

Steering Handbook :

By the end of the nineteen-thirties the theoretical treatment of stationary driving conditions had already been established. Our understanding of the transient vehicle behaviour was significantly enhanced by Riekert and Schunck (1940) in their ground-breaking study on the driving mechanics of rubber-tired motor vehicles. For the first time, they analytically solved the motion equations of a simplified vehicle model, which today is referred to as the single-track model. The two degrees of freedom used for the equation were the yaw and the sideslip angle, and even the aerodynamics were taken into account. Interestingly, their analysis concluded that all the vehicles of that time were unstable, even at low speeds.

But these instabilities occurred only at high lateral acceleration and were produced by the saturation of the lateral traction of the tires. This paradox was only solved with the introduction of steering elasticity into the theoretical examination of vehicle behaviour by Fiala (1960). The reduction of lateral tire stiffness by the steering elasticity had already been recognised by Fujii (1956). Based on the findings of Riekert and Schunck, many other practical and theoretical studies followed in the nineteen-forties. The first basic theory of the pneumatic tire was formulated by Von Schlippe and Dietrich (1942). This theory describes the relationship between cornering stiffness, lateral tire stiffness, and the chronological sequence of the lateral forces subject to the slip angle.

12.6.3 EQUATIONS

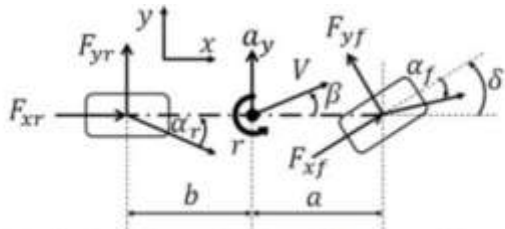


Figure 2 Single track model for vehicle lateral dynamics [3]

The 2 DOF model of the vehicle lateral dynamics as shown in Figure 2 consists of the lateral translation and the yaw rate of the vehicle. The nonlinear vehicle lateral dynamics can be formulated as

$$m a_y = m(\ddot{y} + r u_x) = F_{yf} + F_{yr} \quad (51)$$

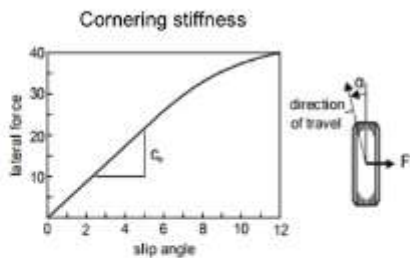
$$I_z \dot{r} = a F_{yf} - b F_{yr} \quad (52)$$

where m is the mass of the vehicle, a_y is the lateral acceleration, y is the lateral translation, r is the yaw rate, u_x is the longitudinal velocity, F_{yf} and F_{yr} are the lateral tire forces of the front and rear wheels respectively, I_z is vehicle inertia, and a and b are the distances of the front and rear tires respectively from the c.g. of the vehicle.

<https://hal.archives-ouvertes.fr/hal-01541110/document>

Les efforts délivrés par les pneus dépendent de leurs angles de dérive, ce qui permet de les réécrire en fonction des inputs δ et V , et du vecteur d'état du véhicule par le biais de β et $d\psi/dt$.

Front and Rear Tire Forces



- C_f : linearized cornering stiffness of the front wheel

$$F_{yf} = C_f \alpha_f = C_f \left(\delta - \beta - \frac{l_f \dot{\psi}}{V} \right)$$

- C_r : linearized cornering stiffness of the rear wheel

$$F_{yr} = C_r \alpha_r = C_r \left(-\beta + \frac{l_r \dot{\psi}}{V} \right)$$

On arrive à ce système couplé d'EDO :

Lateral and Yaw Dynamics

- From the previous slide formulations:

$$F_{yf} = C_f \alpha_f = C_f \left(\delta - \beta - \frac{l_f \dot{\psi}}{V} \right)$$

$$F_{yr} = C_r \alpha_r = C_r \left(-\beta + \frac{l_r \dot{\psi}}{V} \right)$$

Substitute the lateral forces

$$mV(\dot{\beta} + \dot{\psi}) = F_{yf} + F_{yr}$$

$$I_z \ddot{\psi} = l_f F_{yf} - l_r F_{yr}$$

Rearranging the equations

$$\dot{\beta} = \frac{-(C_r + C_f)}{mV} \beta + \left(\frac{C_r l_r - C_f l_f}{mV^2} - 1 \right) \dot{\psi} + \frac{C_f}{mV} \delta$$

$$\ddot{\psi} = \frac{C_r l_r - C_f l_f}{I_z} \beta - \frac{C_r l_r^2 + C_f l_f^2}{I_z V} \dot{\psi} + \frac{C_f l_f}{I_z} \delta$$

12.6.4 FORMULATIONS STATE SPACE

Il est possible de dériver plusieurs formulations selon les variables d'état que l'on souhaite prendre.

Voir par exemple le cours en vidéo de Georg Schildbach (Univ. of Luebeck), et notamment

[Vehicle Dynamics & Control - 09 Dynamic bicycle model with linear tires](#)

En repartant du système ci-dessus avec β et $\dot{\psi}$ on obtient :

$$\begin{bmatrix} \dot{\beta} \\ \ddot{\psi} \end{bmatrix} = \begin{bmatrix} -\frac{(C_r + C_f)}{mV} & \frac{C_r l_r - C_f l_f}{mV^2} - 1 \\ \frac{C_r l_r - C_f l_f}{I_z} & -\frac{C_r l_r^2 + C_f l_f^2}{I_z V} \end{bmatrix} \begin{bmatrix} \beta \\ \dot{\psi} \end{bmatrix} + \begin{bmatrix} \frac{C_f}{mV} \\ \frac{C_f l_f}{I_z} \end{bmatrix} \delta$$

qu'on retrouve écrit presque sous la même forme [ici](#) par exemple :

$$\begin{bmatrix} \dot{\beta} \\ \dot{r} \end{bmatrix} = \begin{bmatrix} -\frac{C_{af} + C_{ar}}{mu_o} & -\frac{(aC_{af} - bC_{ar})}{mu_o^2} - 1 \\ -\frac{(aC_{af} - bC_{ar})}{I_z} & -\frac{(C_{af}a^2 + C_{ar}b^2)}{I_z u_o} \end{bmatrix} \begin{bmatrix} \beta \\ r \end{bmatrix} + \begin{bmatrix} \frac{C_{af}}{mu_o} \\ \frac{aC_{af}}{I_z} \end{bmatrix} \delta$$

Il est souvent utile d'ajouter le déplacement latéral y , sachant que

$$\begin{aligned}\dot{y} &= v + V\psi \\ \ddot{y} &= \dot{v} + V\dot{\psi}\end{aligned}$$

On peut par exemple écrire

$$\begin{bmatrix} \dot{y} \\ \dot{v} \\ \dot{\psi} \\ \ddot{y} \end{bmatrix} = \begin{bmatrix} 0 & 1 & V & 0 \\ 0 & -\frac{(C_r + C_f)}{mV} & 0 & \frac{C_r l_r - C_f l_f}{mV} - V \\ 0 & 0 & 0 & 1 \\ 0 & \frac{C_r l_r - C_f l_f}{I_z V} & 0 & -\frac{C_r l_r^2 + C_f l_f^2}{I_z V} \end{bmatrix} \begin{bmatrix} y \\ v \\ \psi \\ \dot{\psi} \end{bmatrix} + \begin{bmatrix} 0 \\ \frac{C_f}{m} \\ 0 \\ \frac{C_f l_f}{I_z} \end{bmatrix} \delta$$

[source](#)

En version courte, avec seulement \dot{v} et \dot{r} :

$$\begin{bmatrix} \dot{v} \\ \ddot{\psi} \end{bmatrix} = \begin{bmatrix} -\frac{(C_r + C_f)}{mV} & \frac{C_r l_r - C_f l_f}{mV} - V \\ \frac{C_r l_r - C_f l_f}{I_z V} & -\frac{C_r l_r^2 + C_f l_f^2}{I_z V} \end{bmatrix} \begin{bmatrix} v \\ \dot{\psi} \end{bmatrix} + \begin{bmatrix} \frac{C_f}{m} \\ \frac{C_f l_f}{I_z} \end{bmatrix} \delta$$

[source K.Tse](#)

Si on utilise y, \dot{y}, ψ et $\dot{\psi}$ on a

$$\begin{bmatrix} \dot{y} \\ \ddot{y} \\ \dot{\psi} \\ \ddot{y} \end{bmatrix} = \begin{bmatrix} 0 & 1 & 0 & 0 \\ 0 & -\frac{(C_r + C_f)}{mV} & 0 & \frac{C_r l_r - C_f l_f}{mV} - V \\ 0 & 0 & 0 & 1 \\ 0 & \frac{C_r l_r - C_f l_f}{I_z V} & 0 & -\frac{C_r l_r^2 + C_f l_f^2}{I_z V} \end{bmatrix} \begin{bmatrix} y \\ \dot{y} \\ \psi \\ \dot{\psi} \end{bmatrix} + \begin{bmatrix} 0 \\ \frac{C_f}{m} \\ 0 \\ \frac{C_f l_f}{I_z} \end{bmatrix} \delta$$

[source](#)

Dans <https://www.coursera.org/learn/intro-self-driving-cars> est utilisé l'argument que l'angle de braquage lui-même ne peut être utilisé comme input car il ne peut varier instantanément, et qu'il est donc préférable d'utiliser la dérivée de l'angle de braquage (notée ϕ), conduisant à la formulation suivante :

- Modify CG kinematic bicycle model to use steering rate input

○ State: $[x, y, \theta, \delta]^T$

Inputs: $[v, \varphi]^T$

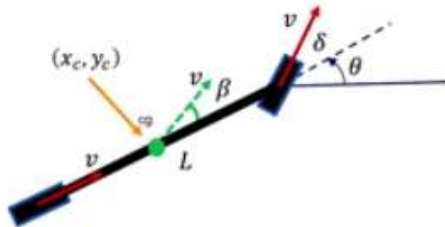
$$\dot{x}_c = v \cos(\theta + \beta)$$

$$\dot{y}_c = v \sin(\theta + \beta)$$

$$\dot{\theta} = \frac{v \cos \beta \tan \delta}{L}$$

$$\dot{\delta} = \varphi$$

Modified Input: rate of change of steering angle



On peut réécrire le système obtenu ci-dessus sous la forme :

- State Vector: $X_{lat} = [y \quad \beta \quad \psi \quad \dot{\psi}]^T$

lateral position
 side slip angle
 yaw angle
 yaw rate

$$A_{lat} = \begin{bmatrix} 0 & V & V & 0 \\ 0 & -\frac{C_r + C_f}{mV} & 0 & \frac{C_r l_r - C_f l_f}{mV^2} - 1 \\ 0 & 0 & 0 & 1 \\ 0 & \frac{C_r l_r - C_f l_f}{l_z} & 0 & -\frac{C_r l_r^2 + C_f l_f^2}{l_z V} \end{bmatrix}$$

$$\dot{X}_{lat} = A_{lat} X_{lat} + B_{lat} \delta$$

$$B_{lat} = \begin{bmatrix} 0 \\ \frac{C_f}{mV} \\ 0 \\ \frac{C_f l_f}{l_z} \end{bmatrix}$$

12.6.5 MOMENTS DES RIGIDITES DE DERIVE

Dans Vehicle Dynamics of Modern Passenger Cars (Lugner, 2019) est introduite (p.209) la notion de moments d'ordre p, construits à partir des rigidités de dérive

$$\begin{aligned} L_0 &= C_{af} + C_{ar} \\ L_1 &= l_f C_{af} - l_r C_{ar} \\ L_2 &= l_f^2 C_{af} + l_r^2 C_{ar} \end{aligned}$$

sous la forme générique

$$L_p = \sum_i x_i^p C_{\alpha i}$$

Comme ces termes se retrouvent de manière récurrente dans les équations du mouvement, écrites chez lui sous la forme suivante

$$MU \frac{d\beta}{dt} + (C_{af} + C_{ar})\beta + MUr + \frac{(l_f C_{af} - l_r C_{ar})}{U} r = C_{af} \delta_f \quad (7)$$

$$I \frac{dr}{dt} + (l_f C_{af} - l_r C_{ar})\beta + \frac{(l_f^2 C_{af} + l_r^2 C_{ar})}{U} r = l_f C_{af} \delta_f \quad (8)$$

cela permet d'alléger l'écriture et d'obtenir la formulation state space suivante (en β et r) :

$$A = - \begin{pmatrix} L_0/MU & 1 + L_1/MU^2 \\ L_1/I & L_2/IU \end{pmatrix}$$

$$B = \begin{pmatrix} C_{af}/MU \\ l_f C_{af}/I \end{pmatrix}$$

On retrouve une expression similaire à ce que j'ai écrit plus tôt :

$$\begin{bmatrix} \dot{\beta} \\ \ddot{\psi} \end{bmatrix} = \begin{bmatrix} -\frac{(C_r + C_f)}{mV} & \frac{C_r l_r - C_f l_f}{mV^2} - 1 \\ \frac{C_r l_r - C_f l_f}{I_z} & -\frac{C_r l_r^2 + C_f l_f^2}{I_z V} \end{bmatrix} \begin{bmatrix} \beta \\ \dot{r} \end{bmatrix} + \begin{bmatrix} \frac{C_f}{mV} \\ \frac{C_f l_f}{I_z} \end{bmatrix} \delta$$

On retrouve le même concept dans le cours de David Bevly (Auburn Univ.), où les moments sont notés C_0 , C_1 , C_2 :

$$\begin{bmatrix} \dot{\beta} \\ \dot{r} \end{bmatrix} = \begin{bmatrix} \frac{-C_0}{mV} & -\left(1 + \frac{C_1}{mV^2}\right) \\ \frac{-C_1}{I_z} & \frac{-C_2}{I_z V} \end{bmatrix} \begin{bmatrix} \beta \\ r \end{bmatrix} + \begin{bmatrix} \frac{C_{af}}{mV} \\ \frac{aC_{af}}{I_z} \end{bmatrix} \delta$$

https://www.eng.auburn.edu/~dmbevly/mech4420/State_Space_Control.pdf

12.6.6 FONCTIONS DE TRANSFERT

Toujours dans le cours de David Bevly (Auburn Univ.), on retrouve

Bicycle Model

$$\frac{R(s)}{\delta(s)} = \frac{aC_{\alpha f}s + \frac{aC_{\alpha f} - c_1C_{\alpha f}}{mV}}{I_zs^2 + \frac{c_0I_z + mc_2}{mV}s + \left(\frac{c_0c_2 - c_1mV^2 - c_1^2}{mV^2} \right)}$$

https://www.eng.auburn.edu/~dmbevly/mec4420/VD_Lecture_1_Classical_Control.pdf

où c_0 , c_1 et c_2 sont les moments introduits ci-dessus.

Chez Kelvin Tse on retrouve l'expression plus directe :

<https://kktse.github.io/jekyll/update/2018/09/18/single-track-bicycle.html>

$$\frac{R(s)}{\delta(s)} = \frac{\frac{C_f l_a}{I} s + \frac{C_f C_r (l_a + l_b)}{I m u}}{s^2 + \left(\frac{C_f + C_r}{m u} + \frac{C_f l_a^2 + C_r l_b^2}{I u} \right) s + \frac{C_f C_r (l_a + l_b)^2}{I m u^2} + \frac{-C_f l_a + C_r l_b}{I}}$$

En multipliant par I pour retomber sur une formulation similaire à celle de D. Bevly on arrive à :

```
% (a1.s+a0) / (b2.s^2+b1.s+b0)
a1 = a*Cf;
a0 = Cf*Cr*(a+b)/m/V;
b2 = I;
b1 = (Cf+Cr)*I/(m*V) + (Cf*a^2+Cr*b^2)/(V);
b0 = Cf*Cr*(a+b)^2/m/V^2 + (-Cf*a+Cr*b);
```

$$G_\delta^\psi = K_\psi \frac{T_\psi s + 1}{\frac{1}{\omega_0^2} s^2 + \frac{2\zeta}{\omega_0} s + 1}$$

$$G_\delta^{v_y} = K_{v_y} \frac{T_{v_y} s + 1}{\frac{1}{\omega_0^2} s^2 + \frac{2\zeta}{\omega_0} s + 1}$$

$$G_\delta^{a_y} = (K_\psi v_x) \frac{\frac{K_{v_y} T_{v_y}}{K_\psi v_x} s^2 + \left(\frac{K_{v_y} T_{v_y}}{K_\psi v_x} + T_\psi \right) s + 1}{\frac{1}{\omega_0^2} s^2 + \frac{2\zeta}{\omega_0} s + 1}$$

$$K_{\dot{\psi}} = \frac{v_x}{L + K_{us}v_x^2}$$

$$K_{v_y} = \frac{v_x}{L + K_{us}v_x^2} \left(b - \frac{f m v_x^2}{L C_r} \right)$$

$$K_{a_y} = \frac{v_x^2}{L + K_{us}v_x^2}$$

$$T_{\dot{\psi}} = \frac{f m v_x}{L C_r}$$

$$T_{v_y} = \frac{I_z v_x}{b L C_r - f m v_x}$$

$$\omega_0^2 = \frac{L C_f C_r (K_{us} v_x^2 + L)}{I_z m v_x^2}$$

$$\zeta \omega_0 = \frac{m(C_f f^2 + C_r b^2) + I_z(C_f + C_r)}{2 I_z m v_x}$$

Where f and b are the distances between the CoG and front and rear axles respectively, and L is the wheelbase of the vehicle such that $f + b = L$. K_{us} is the understeer gradient, and C_f and C_r are the effective cornering stiffness of the front and rear axles.

<https://www.diva-portal.org/smash/get/diva2:1285767/FULLTEXT01.pdf>

Table 1: Analysis of the single-track model

Symbol	Description	Analytical representation	Parameter variation		
			C_f	C_r	$\lambda = f/L$
$K_{\dot{\psi}}$	$\dot{\psi}$ - S-S gain	$\frac{v_x}{L + K_{us} v_x^2}$	+	-	+
K_{v_y}	v_y - S-S gain	$\frac{v_x}{L + K_{us} v_x^2} \left(b - \frac{f m v_x^2}{L C_r}, \right)$	/	+	- (low v_x) + (high v_x)
K_{a_y}	a_y - S-S gain	$\frac{v_x^2}{L + K_{us} v_x^2}$	+	-	+
$T_{\dot{\psi}}$	$\dot{\psi}$ - effect of zero location	$\frac{f m v_x}{L C_r}$	/	-	+
T_{v_y}	v_y - effect of zero location	$\frac{I_z v_x}{b L C_r - f m v_x}$	/	+	-
ω_{0,a_y}^2	a_y - effect of zeros location	$\frac{I_z}{L C_r}$	/	+	/
$\zeta_{a_y} \omega_{0,a_y}$	a_y - numerator damping term	$\frac{b}{v_x}$	/	/	-
ω_0^2	effect of poles location	$\frac{C_f C_r L (K_{us} v_x^2 + L)}{I_z m v_x^2}$	+	+	-
$\zeta \omega_0$	denominator damping term	$\frac{m(C_f f^2 + C_r b^2) + I_z (C_f + C_r)}{I_z m v_x}$	/	+	+

12.6.7 VITESSE DE LACET = F(ANGLE BRAUQUAGE)

Dans [An energy efficient intelligent torque vectoring approach](#) (2020), on trouve

This reference is calculated based on the well-known *bicycle model*, as it provides a good balance between performance and computational cost, providing optimal accuracy in demanding situation for vehicle dynamics. This way, the yaw rate reference equation is calculated as proposed in [8]:

$$\dot{r}_{\text{ref}} = \frac{V}{L + \frac{m}{L} \left(\frac{b}{C_{\alpha F}} - \frac{a}{C_{\alpha R}} \right) V^2} \delta \quad (1)$$

where m is the total mass of the vehicle located in the centre of gravity (CoG), a and b are the distances to the CoG of the front and rear axles, respectively, L is the distance between axles (or wheelbase), δ is the angle of rotation of the front wheels, $C_{\alpha F}$ and $C_{\alpha R}$ are the lateral stiffness coefficients of the front and rear tires, respectively, and V is the longitudinal vehicle speed.

On retrouve l'expression du gain quasi-statique en vitesse de lacet (par ex. [ici](#))

$$R_{ss} = \frac{V_x}{L + K_{us} V_x^2} \delta$$

12.6.8 KELVIN TSE

On trouve aussi bien sur cet article

<https://kktse.github.io/jekyll/update/2018/09/18/single-track-bicycle.html>

que sur le notebook associé

<https://gist.github.com/kktse/7e27c9669c971112cc3e1eca49a3ddf7>

une dérivation complète du modèle, sous plusieurs formes

12.6.9 OPENPILOT (G. HOTZ)

Le code d'OpenPilot est sur github :

https://github.com/commiai/openpilot/blob/master/selfdrive/controls/lib/vehicle_model.py

Le modèle est inspiré du livre de Guiggiani : "The Science of Vehicle Dynamics (2014), M. Guiggiani"

```
x_dot = A*x + B*u
```

La matrice d'état dynamique est construite comme suit :

```
def create_dyn_state_matrices(u: float, VM: VehicleModel) -> Tuple[np.ndarray,
np.ndarray]:
    """Returns the A and B matrix for the dynamics system
    Args:
        u: Vehicle speed [m/s]
        VM: Vehicle model
    Returns:
        A tuple with the 2x2 A matrix, and 2x1 B matrix
    Parameters in the vehicle model:
        cF: Tire stiffness Front [N/rad]
        cR: Tire stiffness Front [N/rad]
        aF: Distance from CG to front wheels [m]
        aR: Distance from CG to rear wheels [m]
        m: Mass [kg]
        j: Rotational inertia [kg m^2]
        sR: Steering ratio [-]
        chi: Steer ratio rear [-]
    """
    A = np.zeros((2, 2))
    B = np.zeros((2, 1))
    A[0, 0] = - (VM.cF + VM.cR) / (VM.m * u)
    A[0, 1] = - (VM.cF * VM.aF - VM.cR * VM.aR) / (VM.m * u) - u
    A[1, 0] = - (VM.cF * VM.aF - VM.cR * VM.aR) / (VM.j * u)
    A[1, 1] = - (VM.cF * VM.aF**2 + VM.cR * VM.aR**2) / (VM.j * u)
    B[0, 0] = (VM.cF + VM.chi * VM.cR) / VM.m / VM.sR
    B[1, 0] = (VM.cF * VM.aF - VM.chi * VM.cR * VM.aR) / VM.j / VM.sR
    return A, B
```

Tirées de (Groenendijk, 2009)

Table B.1: *Vehicle parameters*

vehicle parameter	symbol	value
vehicle mass	m	1659 kg
yaw moment of inertia	I_{zz}	2259 kgm^2
wheelbase	l	2.83 m
distance CG to front	a	1.42 m
cornering stiffness front	$C_{F\alpha,1}$	3030 N/deg (2 tyres)
cornering stiffness rear	$C_{F\alpha,2}$	3038 N/deg (2 tyres)
relaxation length front	σ_1	0.45 m
relaxation length rear	σ_2	0.45 m
steering compliance front	c_1	0.35 deg/kN
steering compliance rear	c_2	0.05 deg/kN
steering ratio	i_s	19.2

BMW 523i, 1996

13 MODELES VEHICULE OPEN-SOURCE + MATLAB

13.1 ANDRES MENDES

Open source simulation package for Octave/Matlab

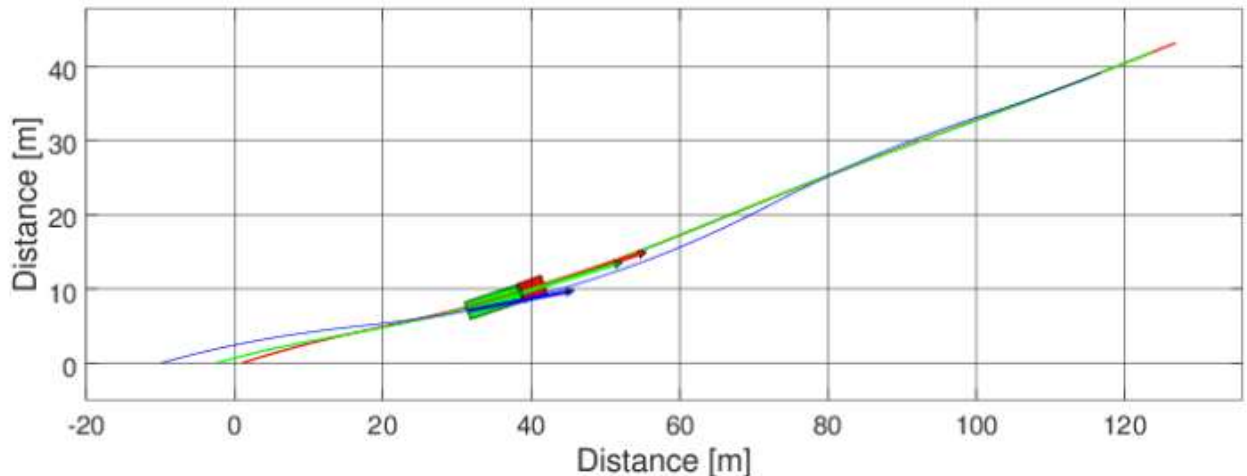
S'appuie sur du code orienté-objet

<https://github.com/andresmendes/openvd>

<http://andresmendes.github.io/Vehicle-Dynamics-Lateral/>

<https://www.mathworks.com/matlabcentral/fileexchange/58683-vehicle-dynamics-lateral>

Lateral is an open source initiative that provides vehicle models and graphics features for yaw dynamics simulation of simple and articulated vehicles.



13.2 BRUCE MINAKER (EOM)

<https://github.com/BPMinaker>

Portage Julia

13.3 TEAM VDSE

<https://www.mathworks.com/matlabcentral/fileexchange/89574-vehicle-dynamics-simulation-environment/>

VDSE (Vehicle Dynamics Simulation Environment) is a tool that predicts the acceleration, braking, cornering and ride behaviour of four-wheeled vehicles with independent suspension. The tool includes a 14 Degrees of Freedom (DoF) sprung/unsprung vehicle model, including three different tyre formulations, a driver model, powertrain model, brakes model and road input. The tool is developed under MATLAB and Simulink and aimed at being user friendly and modular by allowing the user to easily modify or change any of the provided equations and subsystems. Furthermore, the inherent modularity of the model makes it ideal for testing active systems (such as active aerodynamics, 4WS, torque vectoring, ESP, ABS etc.), implementing different suspension models (air springs, adaptive damping, hydropneumatic suspension etc.), implementing different powertrain models (hybrid, electric, fuel cell etc.) and more. This tool has been created with the goal for it to be fast to run making it suitable to be used as a plant for controller design and running design of experiments or optimization of a specific subsystem or even the whole vehicle.

PS : on retrouve Marco Furlan dans cette équipe

13.4 TUMFTM

https://github.com/TUMFTM/sim_vehicle_dynamics

14 MODELISATION DU CONDUCTEUR

14.1 INTRO

Un article fondateur

◇ **Understanding and Modeling the Human Driver** (Macadam, 2003)

Vehicle System Dynamics - 2003, Vol. 40, Nos. 1–3, pp. 101–134

Plutôt orienté perfo-conso :

◇ Setareh Javanmardi, Eric Bideaux, Jean-François Trégouët, Rochdi Trigui, Hélène Tattegrain, et al..

Driving Style Modelling for Eco-driving Applications. *The 20th World Congress of the International Federation of Automatic Control*, Jul 2017, Toulouse, France. 50 (1), pp.13866 - 13871, 2017, [⟨10.1016/j.ifacol.2017.08.2233⟩](https://doi.org/10.1016/j.ifacol.2017.08.2233) . [⟨hal-01624447⟩](https://hal.inria.fr/hal-01624447)

Road and Off-Road Vehicle System Dynamics Handbook

The concept that the human driver must look ahead becomes the first representative concept in modeling the lateral driver model. Kondo and Ajimine's work focused on measuring the driver "sight point" ahead of the vehicle and developed steering based on deviations between the sight point and the desired course [18]. Yoshimoto included a "second prediction term" into the preview driver model to represent driver anticipation when entering a curve [19]. To model the adaptive control behavior of the human driver, McRuer and Jex offered the now well-known crossover model for automobile drivers [20]. Ploechl and Lugner proposed the three-level driver model, anticipatory control, compensatory control, and local control, and explained its application to driving simulations [21]. There is also an attempt to develop a driver model capability applicable to nonlinear, near-limit operating conditions, for example, when a tire blows out, as in the GM/UMTRI (General Motors/The University of Michigan, Transportation Research Institute) driver model presented by MacAdam [22].

Examination of technical papers related to the longitudinal driver model reveals that models and associated studies of driver braking/acceleration control behavior are relatively sparse when compared to work related to lateral steering control. Pipes suggested a linear follow-the-leader model, in which the driver accelerates the vehicle in proportion to the speed difference between the leading vehicle and the following vehicle, in 1953 [23]. Gipps proposed a switching vehicle speed model based on two competing considerations: to keep a safe distance from the lead vehicle and to converge to the desired free flow speed [24]. Newcomb and McLean provide examples of modeling of the driver–vehicle system during longitudinal braking [25]. As for the development of adaptive cruise control (ACC), researchers employ a longitudinal vehicle model to design and analyze the behavior. The works of Fancher et al. are primarily concerned with the headway control behavior of typical drivers and their interaction with ACC systems during highway driving [26]. Peng's recent work using a modified version of Gipps' model is likewise advancing the modeling effort in the headway control area and accurately represents traffic flow behavior of human drivers [27].

14.2 INTERACTION CONDUCTEUR-VEHICULE

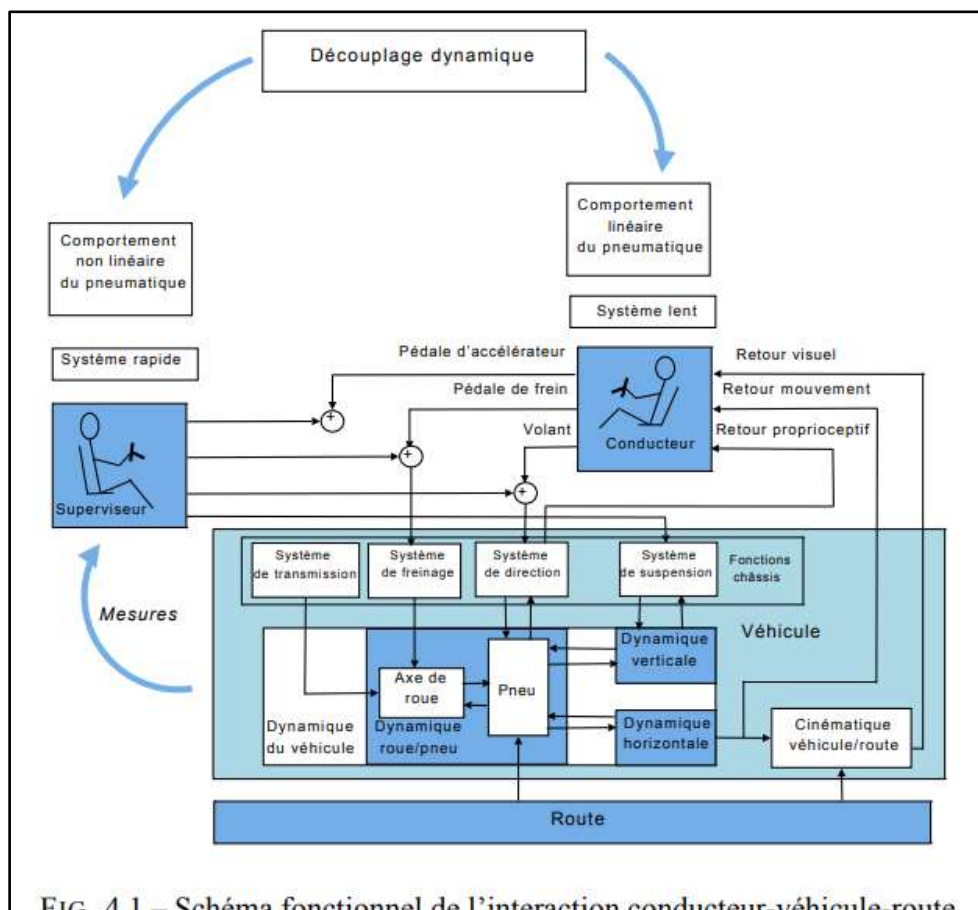


FIG. 4.1 – Schéma fonctionnel de l’interaction conducteur-véhicule-route

14.3 GROENENDIJK (2009)

Improving Vehicle Handling Behaviour with ActiveToe-control

<http://www.mate.tue.nl/mate/pdfs/11254.pdf>

In this paper a reference is made to Weir and McRuer [6], they conclude that it is reasonable to assume that a driver controls the vehicle based on the perception of lateral-position error and yaw-angle.

From the tests they performed the following conclusions are taken, [6]:

- In a lane change task, the handling qualities are affected more significantly by the characteristics of lateral acceleration response than by those of yaw rate response. This means that a faster lateral acceleration response is effective in improving the handling qualities in a lane change.
- As the speed of the lateral acceleration response increases, the driver aims his attention to lateral position error, whereas as the speed of the yaw rate response increases, the driver aims his attention to the yaw angle.
- A slower vehicle response results in an increased mental workload of the driver. This implies that a faster vehicle response is effective in reducing the driver his mental workload.

14.4 DENOUAL (2012)

(Denoual, 2012)

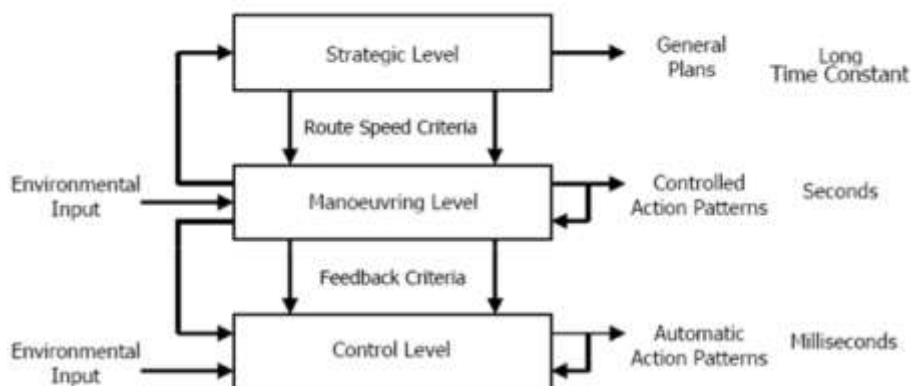


Figure 1.4 Découpage de l'activité de conduite (Michon, 1985)

Le niveau stratégique (Strategic level) correspond aux tâches cognitives les plus fortes. C'est le niveau le plus haut dans la hiérarchie. Ce niveau agit sur la planification à long terme du trajet (itinéraire).

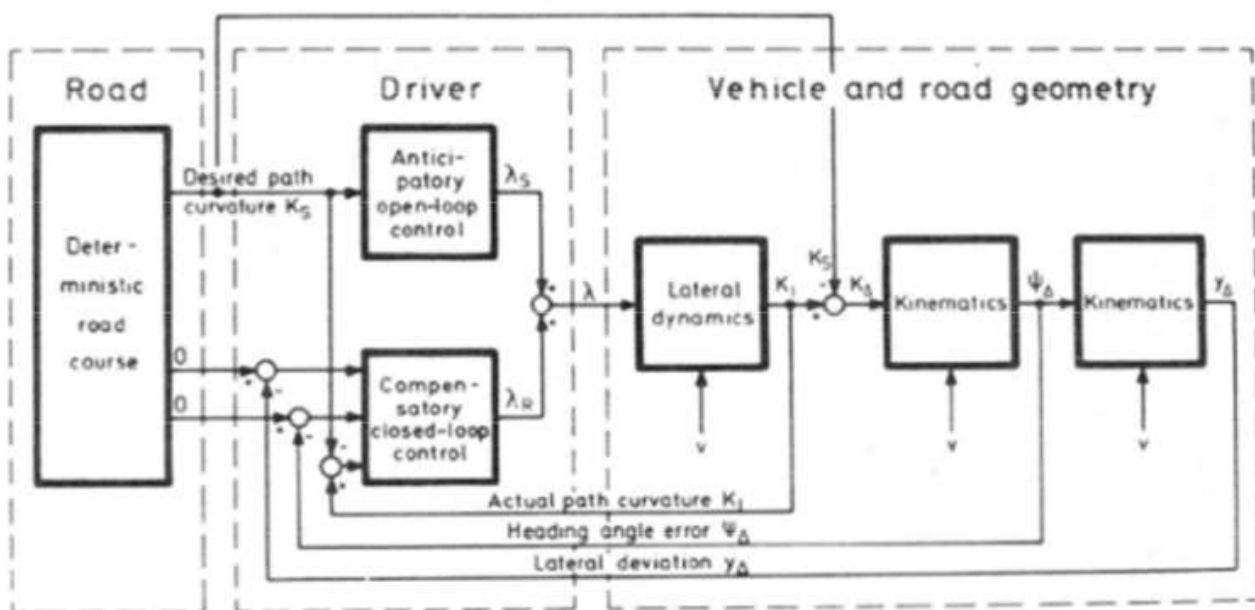
Le niveau tactique (Manoeuvring level) a une exigence cognitive moins importante mais requiert une décision avec une plus forte contrainte temporelle. Un bon exemple est l'approche d'un virage. Un conducteur pressé pourra par exemple décider, pour gagner du temps, de couper l'intérieur du virage.

Au niveau opérationnel (Control Level), l'exigence cognitive est très faible mais la contrainte temporelle est très élevée. Le conducteur fait plutôt ici appel à des modèles internes de contrôle sensori-moteur du volant ou des pédales par exemple. Les actions de régulation de la vitesse ou de contrôle latéral réalisés à ce niveau

sont presque totalement automatisées (angle du volant en fonction de la lecture des changements de courbure du virage, par exemple).

Modèle de Donges

Le modèle classique de contrôle de trajectoire proposé par Donges (1978) est découpé selon deux niveaux opérant en parallèle. Un contrôle lointain de la trajectoire est réalisé en boucle ouverte et permet d'anticiper sur les actions à venir. Le second niveau concerne le traitement des informations proches et permet de corriger rapidement un écart de la position latérale du véhicule.



Modèle « Time to lane crossing »

Le modèle de Donges est un modèle continu qui implique que le conducteur contrôle en permanence sa trajectoire. Cependant, il existe des moments où le volant est maintenu fixe par le conducteur. Pour tenir compte de cet état, Goedthelp et al. (1984) ont proposé un modèle discret de même type prédicteur-correcteur. Le critère permettant de changer de mode, volant fixe ou compensation, est un temps appelé TLC (Time to Lane Crossing). Ce critère représente le temps nécessaire au véhicule pour atteindre le bord de la voie si le volant restait fixe.

14.5 MODEL-PREDICTIVE CONTROL

Applications

[Applications Of Model Predictive Control To Vehicle Dynamics For Active Safety And Stability \(pdf\)](#)

Craig Beal, PHD, 2011

[Model Predictive Control for Autonomous Driving of a Truck](#)

<https://kth.diva-portal.org/smash/get/diva2:930995/FULLTEXT01.pdf>

Günther Prokop (2001) **Modeling Human Vehicle Driving by Model Predictive Online Optimization**,
Vehicle System Dynamics, 35:1, 19-53, DOI: [10.1076/vesd.35.1.19.5614](https://doi.org/10.1076/vesd.35.1.19.5614)

14.6 MODÉLISATION NON-ENTIÈRE

cf le §4 de la thèse de Firas Khemane « Modélisation entière et non entière de la dynamique du conducteur par approche classique et ensembliste »:

http://ori-oai.u-bordeaux1.fr/pdf/2011/KHEMANE_FIRAS_2011.pdf

Le nombre d'études concernant l'interaction homme-machine est en progression, notamment dans le secteur de l'automobile [MacAdam, 1981], [Hess et Modjtahedzadeh, 1989], [Fukui *et al.*, 2004], [Yu *et al.*, 2004], [Amberkar *et al.*, 2004], [Speich *et al.*, 2005] et [MacAdam, 2006]. En effet, le développement des lois de commande permettant de garantir la sécurité du conducteur et du véhicule ont gagné de l'importance, d'où la nécessité de se focaliser de plus en plus sur le comportement du conducteur. Parmi les limites observées dans ce cadre, les retards liés à la perception de l'information, à son traitement et à sa transmission occupent une place importante. Par ailleurs, la capacité de l'être humain à pré-visualiser une scène aide à réduire le temps de réponse (le canal visuel représente 90% des informations reçues par le conducteur [Speich *et al.*, 2005]). Cependant, dans le cas où la prévisualisation n'est pas possible comme lors d'une rafale de vent, d'autre sens interviennent à la place de la vision. Des études en simulateur ont montré que l'être humain est sensible aux mouvements de son corps à travers l'accélération, la vitesse et le déplacement. De plus, les informations tactiles sont surtout ressenties à travers le volant [Guo et Guan, 1993], [Mostafa, 1994], les pédales de frein et d'accélérateur, le siège, le levier de vitesse ...etc. Le retour d'effort volant est particulièrement utile pour le conducteur pour détecter les changements d'adhérence pneu/route et avoir un ressenti global de son véhicule. Enfin, l'audition est plus utilisée lorsqu'il y a une somme importante d'informations à traiter. Dans certaines études, le temps de réponse auditif est aussi faible que le temps de réponse du canal visuel. C'est dans ce contexte que s'inscrivent les travaux présentés dans ce chapitre. Plus précisément, ils concernent la modélisation de la dynamique de la boucle du conducteur [Burnham *et al.*, 1974], [Renski, 2001], l'objectif étant de disposer à terme d'une bibliothèque de modèles utilisable dans le cadre du Contrôle Global du Châssis CGC (les lois de commande implantées dans le véhicule permettant de commander les organes tels que ESP, ABS, Suspension...etc) et éventuellement de détecter des comportements anormaux de conducteurs.

15 MODELISATION DE LA ROUTE

15.1 FORMATS DE ROUTE

15.1.1 INTRO

- .XML (eXtensible Markup Language or XML 3D Spline Road): allows creating a road by defining: coordinates (X, Y and Z), total width, banking and left/right friction coefficient. XML roads are only supported by Adams Car, which includes a built-in road builder to create this kind of roads.
- .RDF (Road Data File, 3D Shell): consists on a text file also created by defining the same parameters as an XML road. The best way to create or modify it is to directly edit the text file using a simple text editor. It can also be created using a specific software called Cosin. RDF files are only supported by Adams Car.
- .RGR (Regular Grid Road): very similar to RDF, but it is a binary file which has to be created using Cosin. This software allows creating road profiles by using different methods, although its interface is not very user-friendly. Also, RGR files are only supported by Adams Car.
- .CRG (Curved Regular Grid): one of the most complex kinds of road files available, which can also provide a higher level of complexity and definition. There is an open software called OpenCRG that operates with Matlab and allows to create, modify and visualize CRG roads. This road format is the only one that is supported by both Adams Car and CarMaker.
- .ROAD (ASCII file): very similar to a RDF file (consist on a text file), with the difference that it is only supported by CarMaker, and not by Adams Car. Also, left/right friction is not defined in the road file but directly in Car Maker road interface.
- .KML (Keyhole Markup Language): file obtained directly from Google Earth or Google Maps, containing the WGS-84 coordinates. It is only supported by CarMaker, which then converts the original coordinates into Cartesian coordinates.

15.1.2 CRG

CRG is a format that was initially used by Daimler AG during some years before it was officially released by the OpenCRG initiative. This initiative was born in 2008 and it established the CRG as an open format, with the support of the main German automotive manufacturers: Audi, BMW, Daimler, Mini, Porsche and Volkswagen. Its main goal was to fill the gap between the macroscopic description of road networks and the microscopic description of road surfaces.

16 DIRECTION

Voir doc LAS pour la partie techno/épure

16.1 MODELISATION

On peut envisager 3 types de modèles :

- Mapped steering relates the tyre forces to a steering torque using a lookup table which works in function of suspension travel
- Advanced steering model includes all of the internal elements in a typical assisted steering system including column joint geometry + phasing, torsion bar deflection, friction and damping in the column and rack as well as the dynamics of the power assist
- External co-simulations are used when sophisticated controls are included in the steering system such as active return, friction compensation and other non linear controls found in modern electrical power assists.

16.2 INFLUENCE DU FROTTEMENT

Le frottement de direction doit être suffisant afin de ne pas rendre la direction trop sensible aux déformations de la chaussée. Le frottement de direction ne doit toutefois pas être trop important, afin d'éviter une non linéarité de la réponse au volant.

16.3 PRESTATIONS

16.3.1 LISTE

Collage : effort de frottement lors de petites corrections volant.

Le Rappel : Retour naturel du volant lorsque cesse l'effort après un braquage

La précision de direction : Aptitude et facilité à suivre une trajectoire voulue (consigne d'angle, variation d'angle inférieure à 10° autour de la consigne) et à la modifier (placement grande courbe).

Démultiplication au Train: Rapport entre l'angle de rotation du volant et l'angle de rotation des roues (environ 18)

La Régularité (absence de modulation) : Modulation du rapport de démultiplication autour de sa valeur théorique

Le Centrage: un véhicule bien centré subit très peu de déviation et ne nécessite pas de corrections au volant

Le Pendulage: Amortissement angulaire du volant et des mouvements du véhicule sous un échelon d'angle volant.

Tenue de Cap : aptitude d'un véhicule à suivre une direction donnée sur différentes routes (BR-MR) en ligne droite + Jugement du ressenti volant associé.

Clavetage : valeur du couple à fournir au volant pour sortir de la position "ligne droite"

le clavetage de direction en ligne droite, directement lié au moment de rappel Cvol, sera dégradé si:

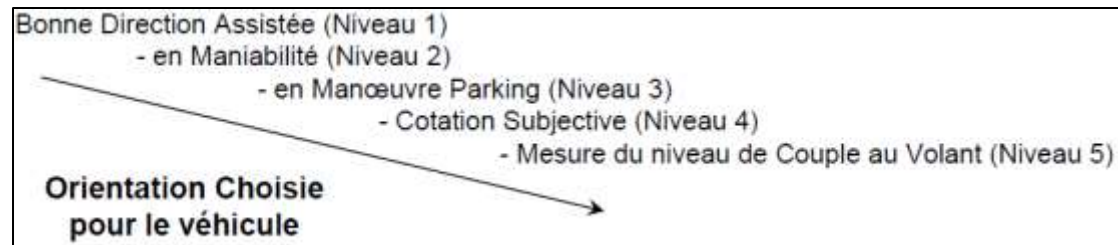
- la charge au train est diminuée
- la chasse mécanique est diminuée
- la chasse pneumatique est diminuée
- la démultiplication de direction est augmentée
- on a une direction assistée

Efforts au Volant en manœuvre à petite Vitesse : exemple, en parking ou en coin de rue => limiter les efforts au maxi en assurant la réversibilité

Diamètre de Braquage : largeur de route nécessaire à faire un demi tour => faire aussi petit que possible

La Directibilité de la direction : nombre de tour nécessaire à faire une manœuvre

Être le plus direct possible => limiter le nombre de tours



16.3.2 MANIABILITÉ

Ordre de grandeur :

- -100 mm de voie avant diminue le rayon de braquage entre trottoirs de 12 cm,
- -100 mm d'empattement de 34 cm
- +1° de braquage moyen fait gagner 23 cm

16.3.3 STEERING FEEL

Driver perception of steering feel

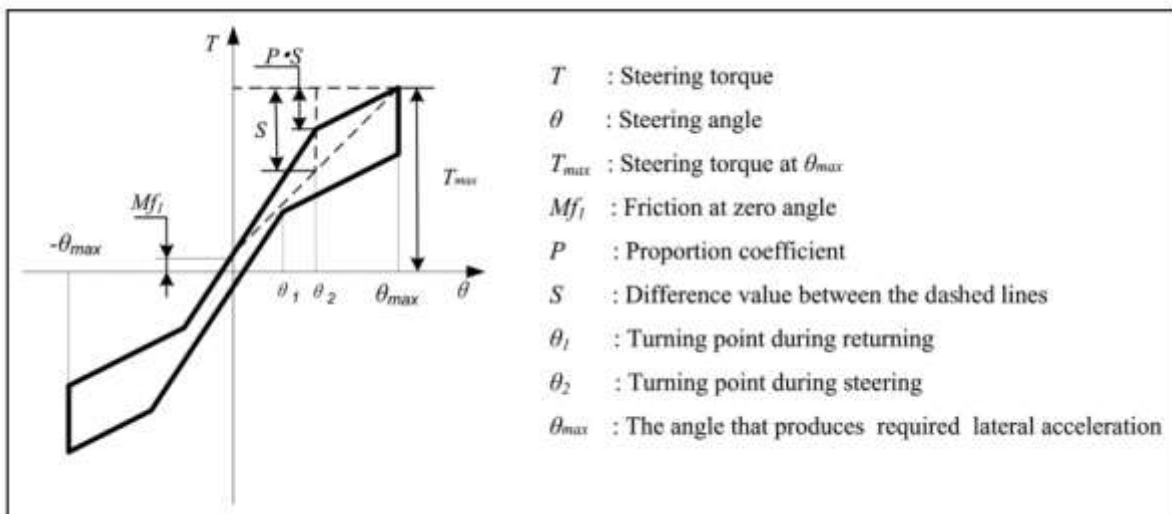
<http://resource.isvr.soton.ac.uk/staff/pubs/PubPDFs/Pub9301.pdf>

Steering feel is optimized at a late stage of vehicle development, using prototype vehicles and expert opinion. An understanding of human perception may assist the development of a good 'feel' earlier in the design process. Three psychophysical experiments have been conducted to advance understanding of factors contributing to the feel of steering systems. The first experiment, which investigated the frames of reference for describing the feel (i.e. haptic properties) of a steering wheel, indicated that subjects focused on the steady state force that they applied to the wheel rather than the steady state torque, and on the angle that they turned the wheel rather than the displacement of their hands. In a second experiment, thresholds for detecting changes in both steady state steering-wheel force and steady state steering-wheel angle were determined as about 15 per cent.

16.3.4 ON-CENTER STEERING FORCE

A method to set the target on-centre steering force characteristic

https://www.researchgate.net/publication/287109778_A_method_to_set_the_target_on-centre_steering_force_characteristic



SFC = Steering Force Characteristics

Table 5. Objective metrics.

Number	Symbol	OM	Units
1	K_1	Steering stiffness	N m/deg
2	K_2	Steering torque gradient at 10°	N m/deg
3	MF_1	Steering torque hysteresis at 0°	N m
4	MF_2	Steering torque hysteresis at 10°	N m
5	T_p	Steering torque at 10°	N m
6	AH	Angle hysteresis	deg
7	a_{y0}	Lateral acceleration at 0 N/m	m/s^2
8	T_0	Steering torque at 0 m/s^2	N m
9	T_1	Steering torque at 1 m/s^2	N m
10	G_1	Steering torque gradient at 0 m/s^2	$N\ m/(m/s^2)$
11	G_2	Steering torque gradient at 1 m/s^2	$N\ m/(m/s^2)$
12	F_r	Steering torque hysteresis at 1 m/s^2	N m
13	K_2/K_1	K_2 divided by K_1	
14	K_1/K_2	K_1 divided by K_2	

OM: objective metric; AH: angle hysteresis.

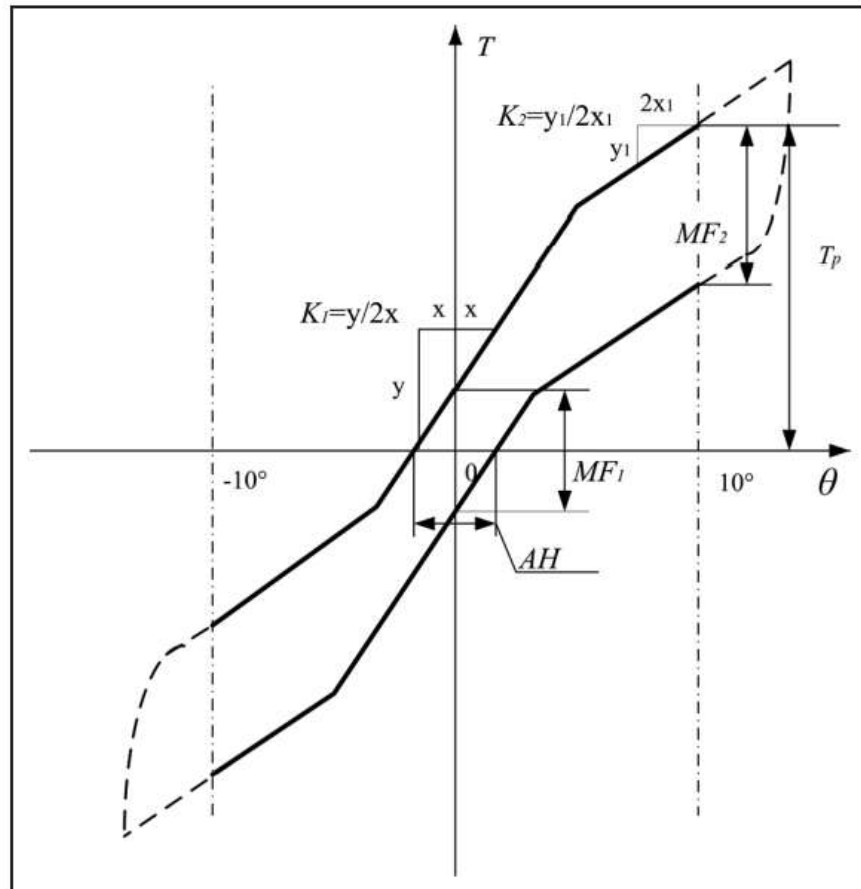


Figure 7. OM_s derived from the curve of the steering torque versus the steering angle.

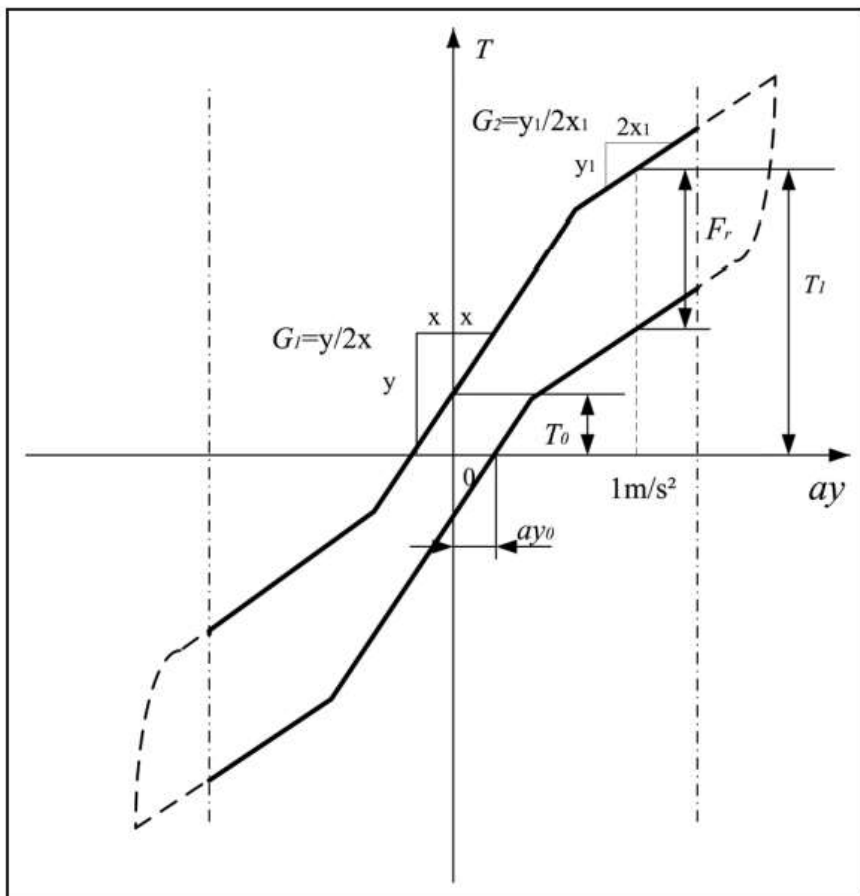


Figure 8. OM_s derived from the curve of the steering torque versus the lateral acceleration.

Table 2. Subjective evaluation items.

Item	Evaluation content
Steering effort (SE)	Whether the reaction torque over the whole steering-angle range is appropriate
Steering stiffness (SS)	Whether the steering stiffness over the whole steering-angle range is appropriate
Linearity of the steering torque (LST)	Whether the change in the steering torque with respect to the steering angle occurs smoothly Whether no uncomfortable feeling occurs
Solid feel (SF)	Whether the steering angle is foreseeable as the steering torque is increased gradually Whether it is easy to keep the steering wheel at a fixed angle and the friction is appropriate
Steering aligning torque (SAT)	Whether the steering aligning torque is appropriate
Centring feel (CF)	Whether it is possible to feel the centre position of the steering wheel according to the reaction torque
Overall evaluation (OE)	Whether the overall steering feel of this characteristic suits the driver's preference

16.4 STEER BY WIRE (SBW)

Article de Toyota qui propose une solution alternative à un capteur d'effort pour assurer le retour de force d'une direction SbW.

△ Asai, S., Kuroyanagi, H., Takeuchi, S., Takahashi, T. et al., "Development of a Steer-by-Wire System with Force Feedback Using a Disturbance Observer", SAE Technical Paper 2004-01-1100, 2004

<https://doi.org/10.4271/2004-01-1100>.

Un actionneur génère un couple qui est la somme d'un couple de référence et d'un couple de compensation. Le couple de référence est une carte fonction du couple de réaction estimé :

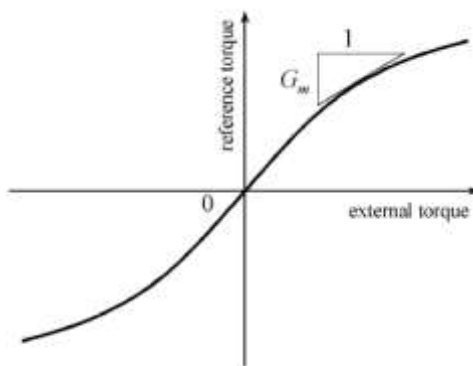


Fig. 3 Reaction torque map

Le couple de compensation permet de stabiliser le système.

The additional compensation torque is intended to stabilize the system and adjust the steering feel. The compensation torque is determined in the similar way to that in an electric power steering system. The compensation torque includes phase compensation torque, damping torque, inertia compensation torque and friction compensation torque.

The phase compensation torque is intended to reduce the vibration caused by the low stiffness torsion bar. The phase compensation torque is determined from the derivative of the reaction torque.

The damping torque is used to reduce the vibration caused by the external force and to adjust the steering "viscosity" feel. The damping torque is determined from the motor angular velocity that is obtained by differentiating the motor angle of the steering wheel actuator.

The inertia compensation torque is used to adjust the steering "inertia" feel. The inertia compensation torque is determined from the motor angular acceleration that is obtained by differentiating the angular velocity of the steering wheel actuator.

The friction compensation torque is intended to suppress the friction torque in the motor and the gear of the steering wheel actuator, adjusting the steering "friction" feel. The friction compensation torque is determined from the reaction torque, the motor current of the steering wheel actuator, etc.

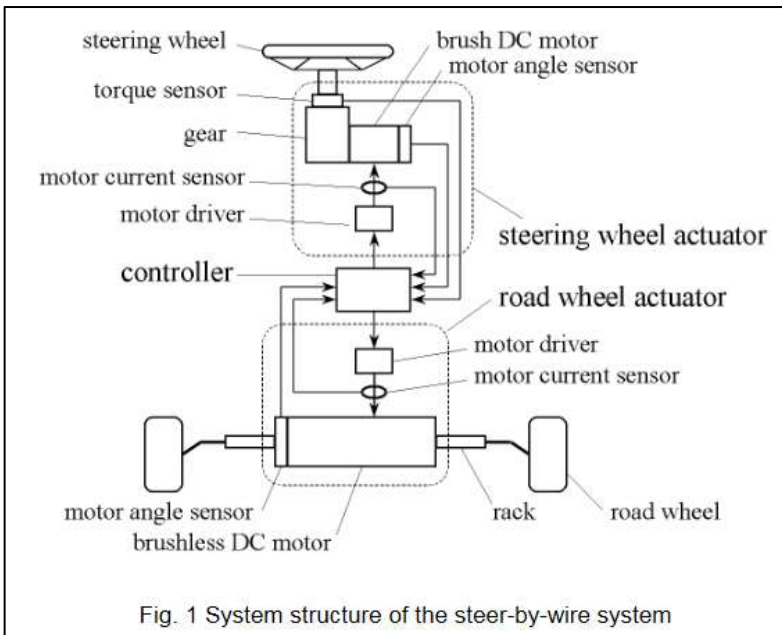


Fig. 1 System structure of the steer-by-wire system

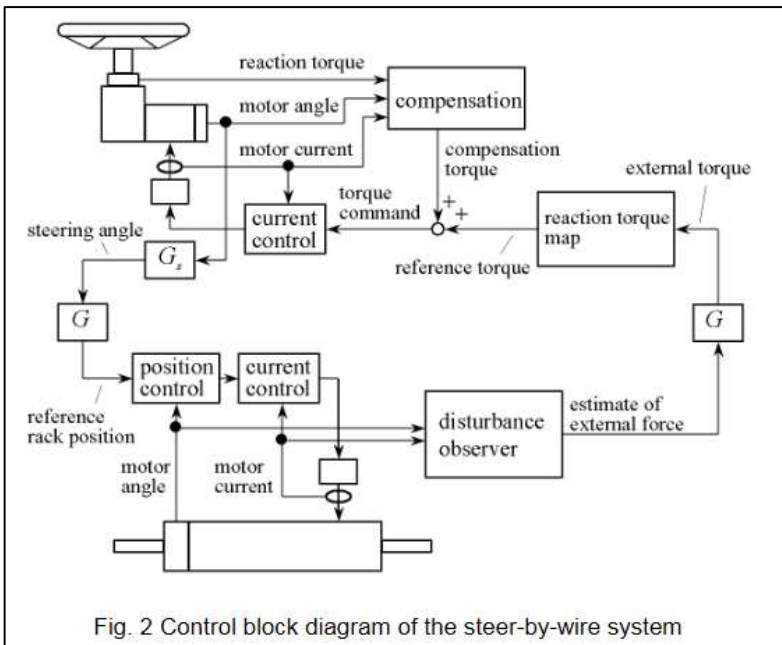


Fig. 2 Control block diagram of the steer-by-wire system

17 SUSPENSION

Voir la techno amortisseurs dans le doc LAS

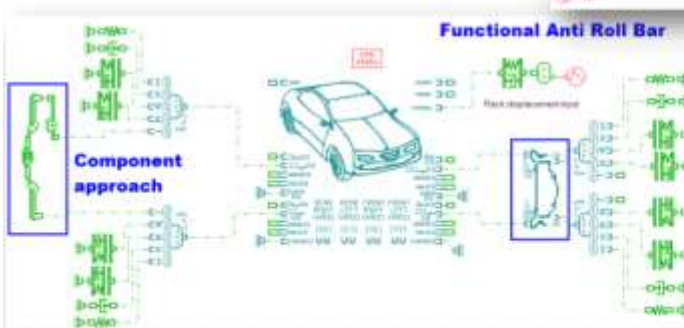
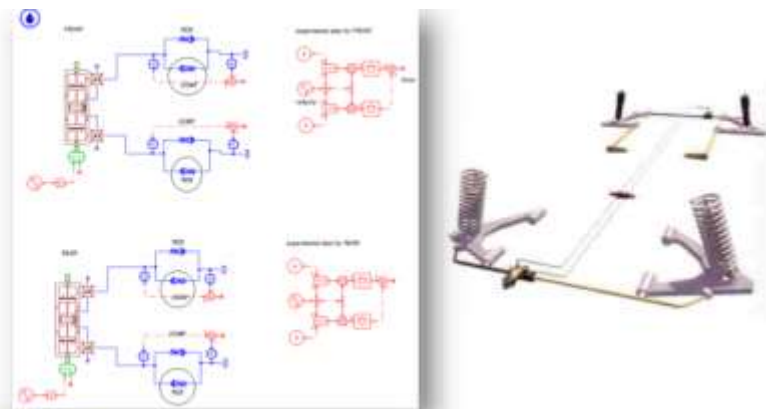
17.1 INTRODUCTION

Over the Waves - Chevrolet Suspension (1938)

https://www.youtube.com/watch?v=ej7CRAIGXow&feature=emb_logo

17.2 ANTIROULIS

- Functional modeling of the anti roll bar.
- Possibility to use the Hydraulic library to make the **anti roll bar active** (linear or rotary cylinder).
- Evaluation of the suspension system performances/design on the entire virtual vehicle model.



Restricted © LMS International 2013 All rights reserved.

Page 10 2013-08-27

LMS
A Siemens Business

17.2.1 ANTI-ROULIS ACTIF

[Enhancing the roll stability of heavy vehicles by using an active anti-roll bar system \(2017\)](#)

17.3 AMORTISSEUR

17.3.1 NOTION DE LOI EFFORT-VITESSE

L'amortisseur joue un rôle fondamental dans la tenue de route et le confort. Il est au carrefour de prestations souvent contradictoires. Sa mise au point devient, en conséquence, de plus en plus délicate.

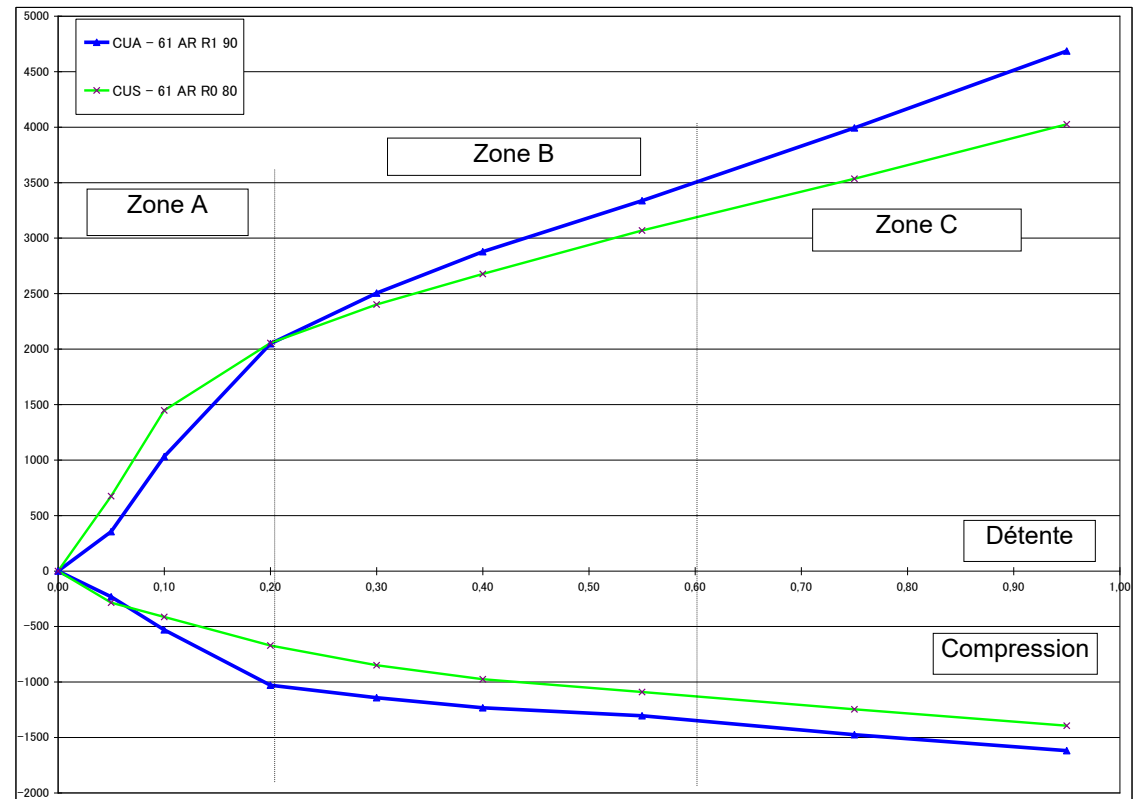
Pour la tenue de route, l'amortisseur participe activement au maintien de caisse, en particulier pour les fréquences de pompage et de tangage du véhicule. Il permet aussi de garder le contact avec le sol en amortissant le phénomène de battement de roue. Ce battement résulte de l'excitation d'un mode de vibration de la masse non suspendue prise en sandwich entre les raideurs verticales du pneumatique et de la suspension.

Les contraintes d'amortissement (maintien de caisse, battement de roue) nécessitent des efforts de dissipation d'amortisseurs, souvent trop importants pour avoir un confort vibratoire acceptable en roulage client.

La solution, aujourd'hui, passe par une Loi Effort d'amortisseur- Vitesse amortisseur, dite loi L.E.V, souvent non linéaire et dissymétrique en compression et détente. Une telle loi est aujourd'hui majoritairement déterminée par des boucles essais routiers.

La Loi effort vitesse d'un amortisseur peut être découpée en 3 secteurs :

V(m/s)	0,95	0,75	0,55	0,40	0,30	0,20	0,10	0,05	0,00	0,05	0,10	0,20	0,30	0,40	0,55	0,75	0,95
CUA - 61 AR R1 90	-1619	-1475	-1304	-1233	-1142	-1029	-531	-233	0	355	1031	2048	2505	2877	3337	3993	4686
CUS - 61 AR R0 80	-1394	-1246	-1090	-975	-849	-671	-414	-285	0	674	1447	2054	2401	2676	3069	3535	4025



A/ Vitesse de tige inférieure à 0.1m/s. Les efforts augmentent de manière parabolique. Cette partie de la LEV conditionne la tenue de la caisse en pompage, et en roulis c'est à dire à des débattements basse fréquence et de forte amplitude. Ce sont les passages permanents.

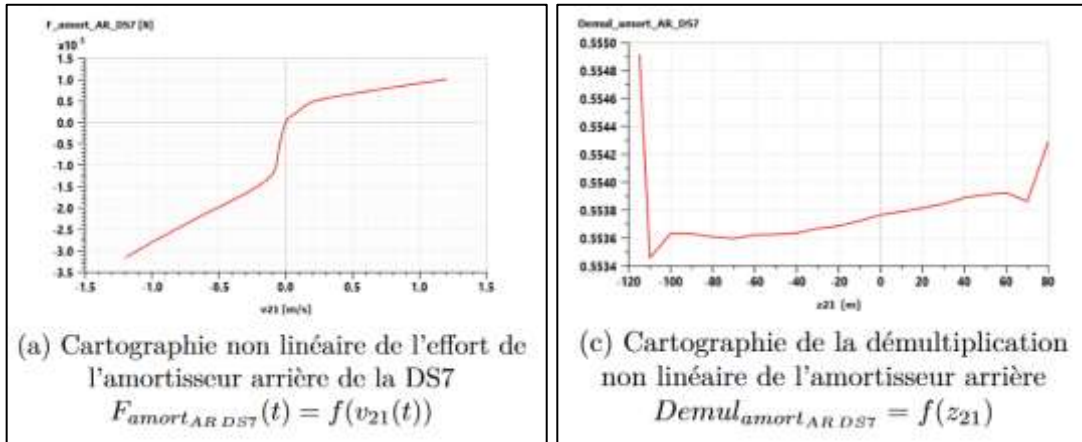
Abis/ A partir de 0,1m/s et jusqu'à 0.6m/s, les clapets commencent à s'ouvrir car le ressort est vaincu par les efforts hydrauliques. On voit une inflexion dans l'augmentation des efforts.

B/ Vitesse intermédiaire entre 0.2 et 0.6m/s correspondant aux battements de roue et aux modes de trains de moyennes fréquences et amplitudes.

C/ A partir de 0.7m/s, c'est le piston qui rentre en action correspondant aux moyenne et haute fréquence sous faible amplitude, c'est-à-dire obstacles isolés, vibrant, ...

Dans le cas d'une technologie utilisant un piston double effet, la détente et la compression sont assurées par la même pièce ce qui impose des compromis.

17.3.2 QUELQUES DONNEES DE LEV



(Hamrouni, 2021)

17.3.3 PRESTATIONS IMPORTANTES

Frottement => confort

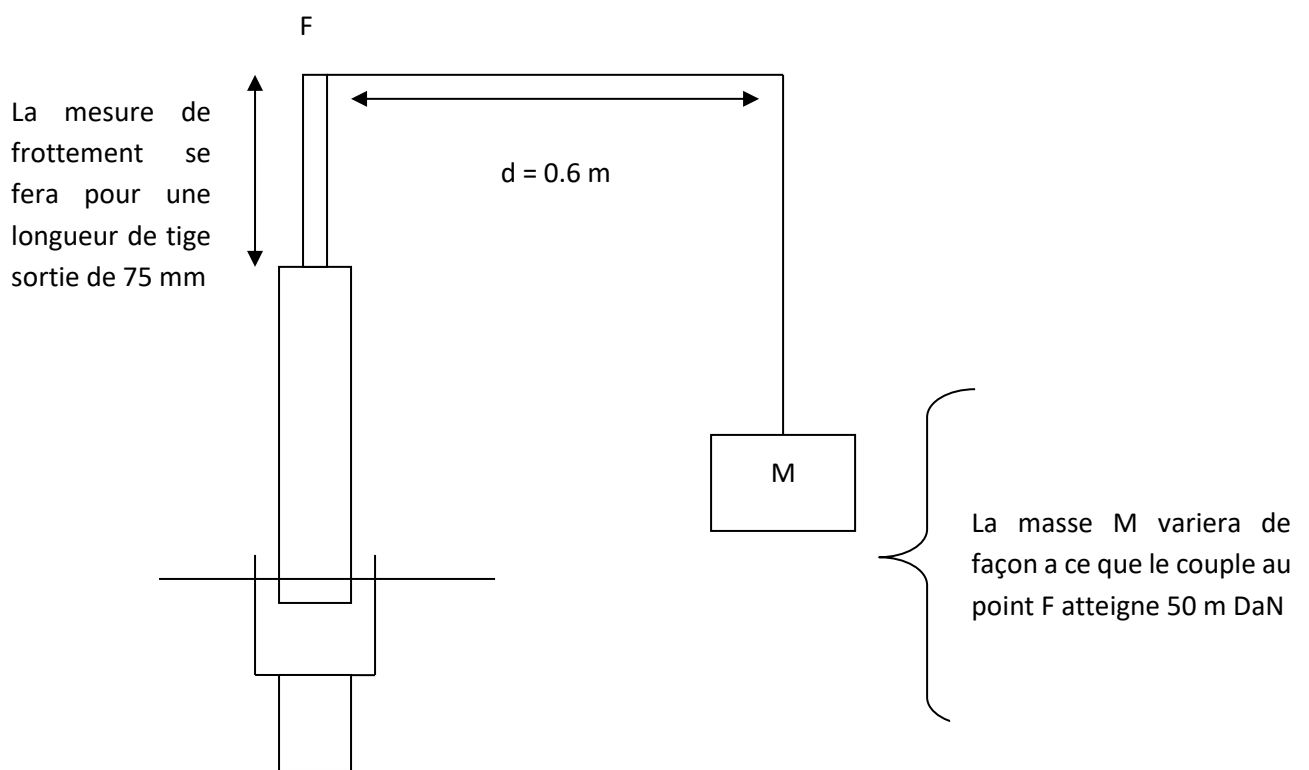
Raideur => Potentiel train avant

Frottement sous couple => motricité

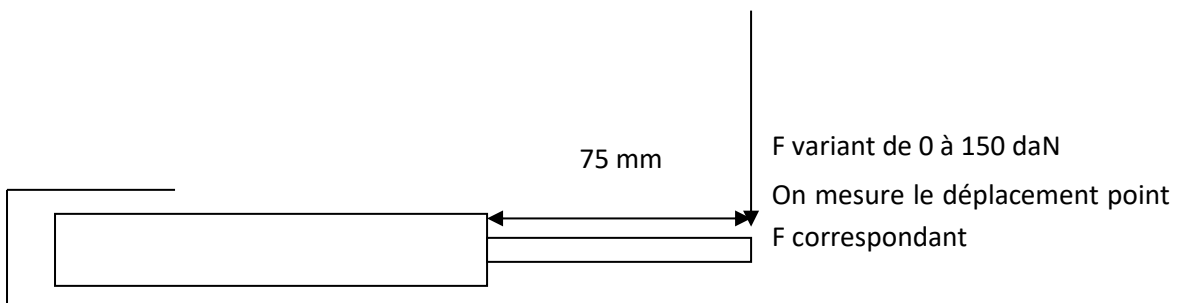
Déchéance à chaud => robustesse thermique

La raideur de la jambe de force est un important contributeur ($\sim 1/3$ sur McPherson) de la tenue en carrossage du plan de roue

Procédure de la mesure de frottement :



Procédure de la mesure raideur :



Ordre de grandeur : 2daN maxi de frottements à vide et 6daN maxi de frottements sous couple de 20 m daN.

Déchéance thermique (ordre de grandeur) : 20 à 30% à 65°

17.3.4 MODELISATION

Différents niveaux de modélisation existent :

Model type	Plus	Minus
1D Fluid dynamics	Design data related Limited need of test data	Design data availability CPU time
Empirical/Tabular	CPU time	Big amount of test data required Not accurate in extrapolation
Semi-physical/functional	Partially related to design data CPU time	Some test data required

17.3.4.1 MODELISATION FONCTIONNELLE

Dans la thèse de S. Aubouet ([Semi-active SOBEN suspensions modeling and control](#), 2010), on voit :

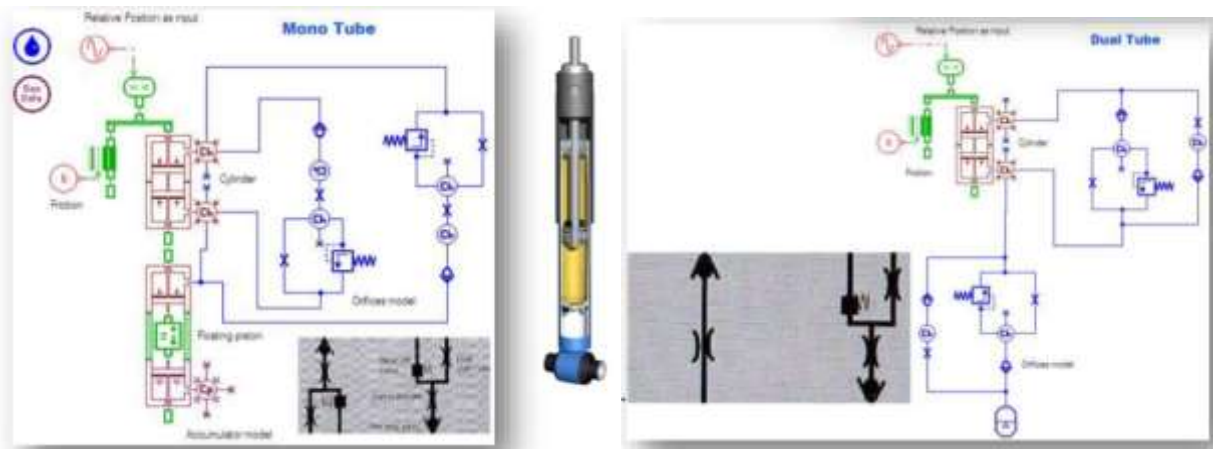
$$F(t) = (A_1 u_d + A_2) \tanh(A_3 v + A_4 x) + A_5 v + A_6 x + A_7$$

avec comme paramètres

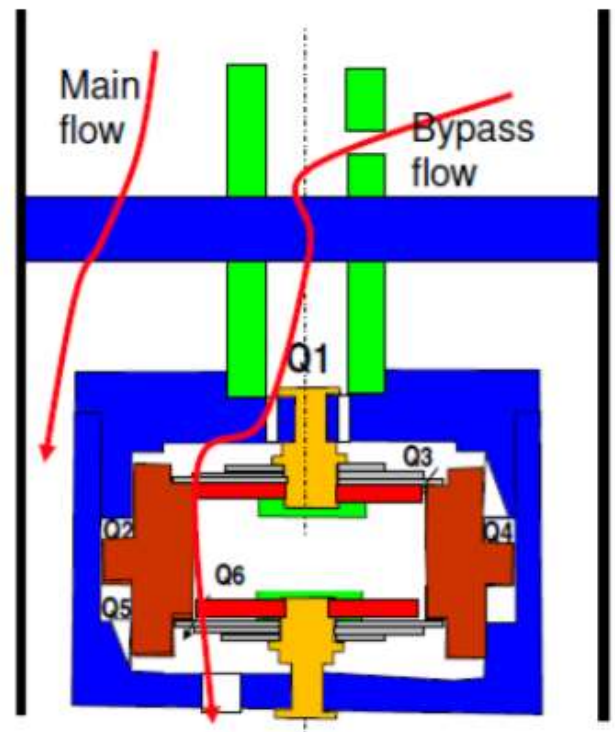
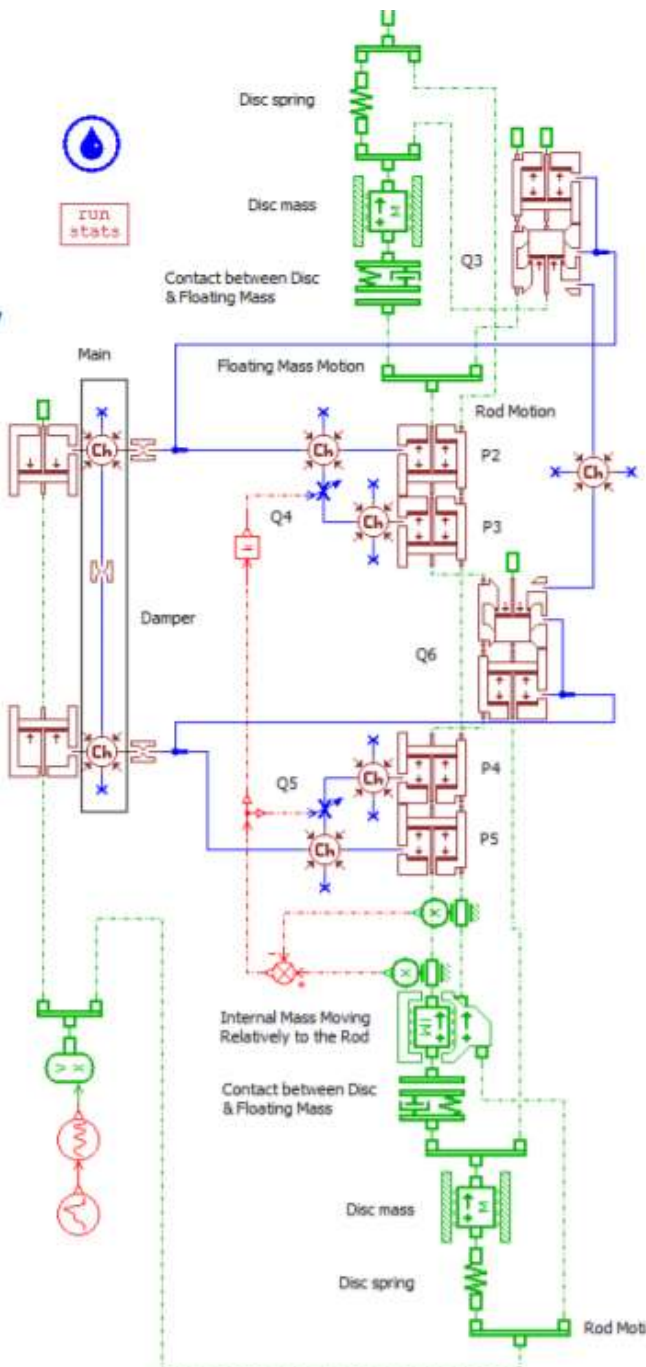
Parameter	A_1	A_2	A_3	A_4	A_5	A_6	A_7
Value	792	47	1328	10.5	1233	-0.27	4

17.3.4.2 MODELISATION SEMI-PHYSIQUE STANDARD

Doc LMS / Amesim : <http://oss.jishulink.com/caenet/forums/upload/2014/12/27/392/23680231207181.pdf>

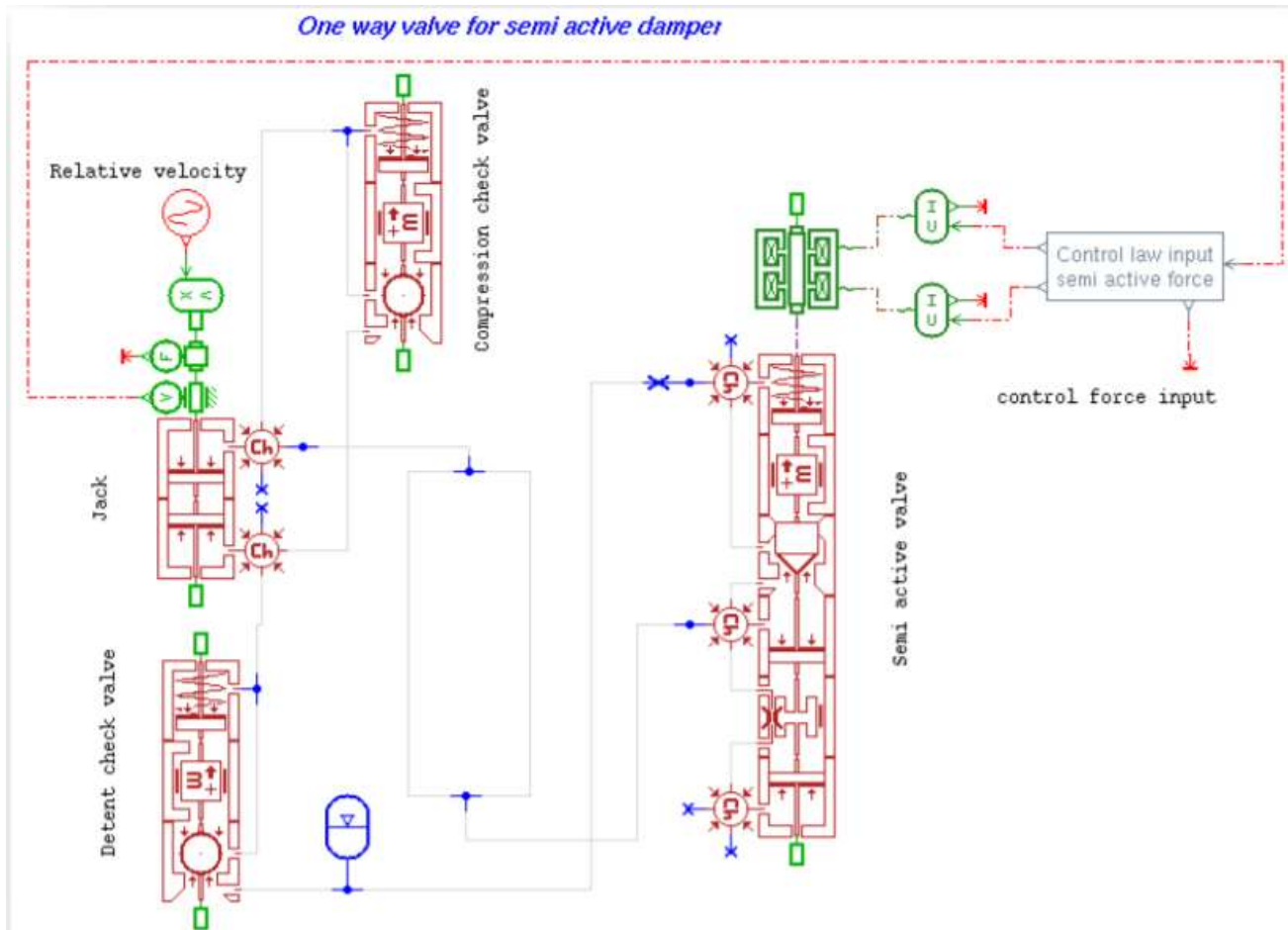


17.3.4.3 MODELISATION SEMI-PHYSIQUE AVANCEE



LMS®

17.3.4.4 SYSTEMES ACTIFS



17.3.4.5 IDENTIFICATION DU FROTTEMENT ET DE LA PRESSURISATION

Voir le papier de Brian Warner, Chrysler Corp, SAE 962548 (1996)

17.3.5 RESSOURCES

Voir la thèse de Master de (Reineh, 2012)

Keywords: Passive shock absorber, hydraulic, 1D modeling

The developed AMESim numerical model is capable of capturing the physics behind the real shock absorber damping characteristics, under both static and dynamic conditions. The model is developed mainly using the standard AMESim mechanical, hydraulic and hydraulic component design libraries and allows discovering the impact of each single hydraulic component on the TTR overall behavior. In particular, the 1D model is presented in two levels of progressive physical complexity in order to improve the dynamic damping characteristics. Several physical phenomena are considered, such as the hydraulics volumes pressure dynamics, the contribution of external spring and pressure forces to

the dynamic balance of the moving elements, the static and viscous frictions, and the elastic deformations induced by solid boundaries pressure. In this thesis, progressive model validation with different types of measurements is as well presented, covering the individual hydraulic components models as well as the entire shock absorber model. The measurements have been performed on the flow benches and dynamometers available at the Öhlins Racing measurements laboratory. These comparisons, deeply discussed in the thesis, allow discovering the impact of specific physical effects on the low and high speed hydraulic valves static performance and on the shock absorber dynamic behavior. Numerical results show good agreement, especially at low and medium frequencies and symmetric ‘click’ adjustments on compression and rebound sides. Further model development is necessary in the other areas, for example by considering more complex models of the valve dynamics and fluid flow patterns, i.e. flow forces, together with more advanced models of the sealing elements viscous friction, and thermal effects.

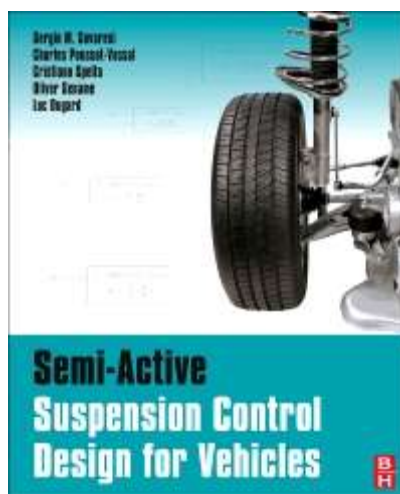
17.4 AMORTISSEMENT VARIABLE / SUSPENSION ACTIVE

17.4.1 TECHNOLOGIE : CF DOC LAS

17.4.2 RESSOURCES

[Semi-Active Suspension Control Design for Vehicles](#)

(Savaresi, Poussot-Vassal, Spelta, Dugard, & Sename, 2010)



[A Comprehensive Review of the Techniques on Regenerative Shock Absorber Systems](#)

<https://doi.org/10.3390/en11051167>

17.4.3 LES DIFFERENTES FAMILLES

Classification des suspensions à commande électronique

Classe du système de suspension	Plage de contrôle (ressort)	Plage de contrôle (amortisseur)	Bandes passantes de contrôle	Demande de puissance	Variable de contrôle
Passive			-	-	-
Adaptative			1-5 Hz	10-20 W	b (coefficients d'amortissement)
Semi-active			30-40 Hz	10-20 W	b (coefficients d'amortissement)
À compensation de charge			0,1-1 Hz	100-200 W	W (charge statique)
Active Basse Fréquence			1-5 Hz	1-2 kW	F (force)
100% active			20-30 Hz	5-10 kW	F (force)

Semi-active suspension control design for vehicles

(Savaresi, Poussot-Vassal, Spelta, Dugard, & Sename, 2010)

Table 1
Classification of suspension systems. Natural frequencies: f_B body and f_W wheel

System	System representation	Force range	Operation range	Actuator/sensor demand	Max. energy demand	Improvements compared to passive system	
						Comfort	Safety
Passive			—	—	—	—	—
Slowly variable/adaptive			$< f_B$	$4-8/\geq 1$	ca. 50 W	15-20%	10-25%
Semi-active			$f_B - f_W$	$4-8/\geq 8$	ca. 50 W	20-30%	10-25%
Active partially loaded			$0-f_B$	$4-8/\geq 12$	1-2 kW	> 30%	—
Active fully loaded			$0-f_W$	$4/\geq 12$	1.5-7 kW	> 30%	25%

source [Mechatronic semi-active and active vehicle suspensions \(2004\)](#)

17.4.4 SUSPENSION SEMI-ACTIVE

Semi-Active Suspension Control Design for Vehicles

<https://www.elsevier.com/books/semi-active-suspension-control-design-for-vehicles/savaresi/978-0-08-096678-6>

17.4.5 SUSPENSION CRONE

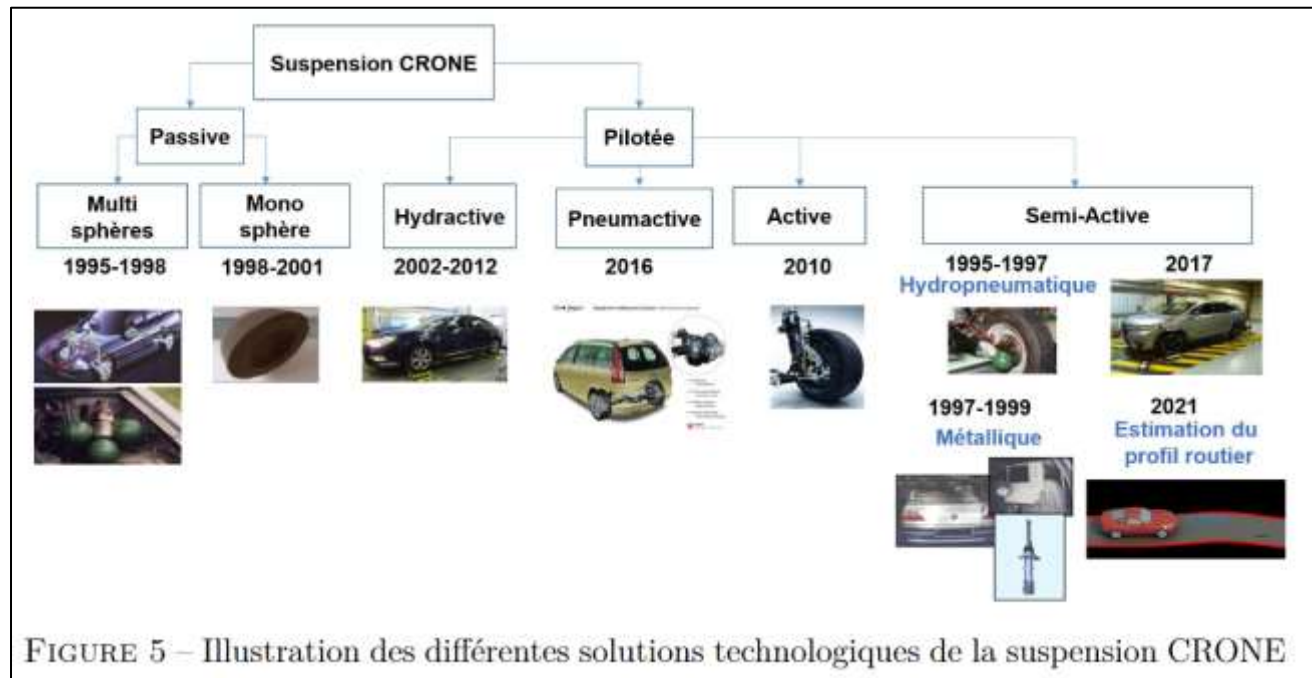


FIGURE 5 – Illustration des différentes solutions technologiques de la suspension CRONE

<https://tel.archives-ouvertes.fr/tel-03463959/document> (Hamrouni, 2021)

CRONE : <http://eric.cabrol.free.fr/dotclear/index.php/2020/04/25/Une-petite-histoire-de-la-suspension-CRONE>

Partenariat de longue durée entre la DRIA (Direction de la Recherche et de l'Innovation Automobile) de PSA et l'université de Bordeaux (laboratoire IMS), notamment Xavier Moreau et Alain Oustaloup.

On pourra consulter un listing des thèses autour de cette thématique sur <https://www.theses.fr/033265569> et <https://www.theses.fr/134532457>

A lire en particulier, les thèses suivantes :

- Analyse de l'influence des non-linéarités dans l'approche CRONE : application en isolation vibratoire ([lien](#)), soutenue par Pascal Serrier en 2008
- L'approche CRONE dans le domaine des architectures complexes des suspensions de véhicules automobiles : la suspension CRONE Hydractive ([lien](#)), soutenue en 2012 par [Audrey Rizzo](#)
- Etude de l'influence des suspensions de véhicule de tourisme sur le confort vibratoire, le comportement routier et les limites de fonctionnement : l'approche CRONE en matière de formalisation, d'analyse et de synthèse ([lien](#)), soutenue par Aurore Létévé en 2014

- Vers une version alternative à la suspension CRONE Hydractive, thèse de Jean-Louis Bouvin ([lien](#))

En 2021 une nouvelle thèse démarre, celle de Ramon Guridis

<http://www.theses.fr/s268531>

La thèse d'Emna Hamrouni (Hamrouni, 2021) évoque également ces sujets, plutôt en rapport avec les ADAS :

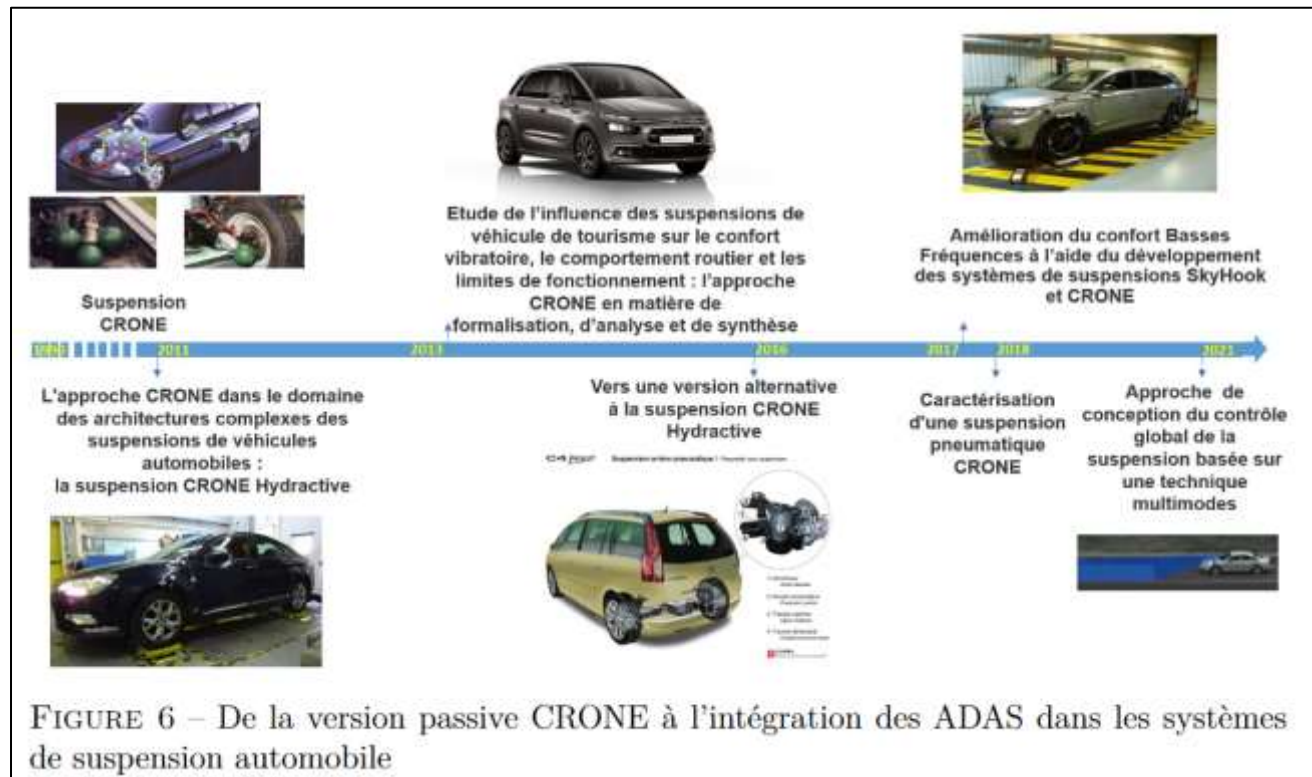


FIGURE 6 – De la version passive CRONE à l'intégration des ADAS dans les systèmes de suspension automobile

A noter : l'affaire Crone, avec comme protagonistes Benoit Bergeon

<http://perso.numericable.fr/benoit-be/>

où l'on peut notamment voir ces documents qui expliquent l'ensemble de l'affaire :

<http://perso.numericable.fr/benoit-be/site-affaire-crone/affaire%20crone.htm>

<http://perso.numericable.fr/benoit-be/site-affaire-crone/lettre%20aux%20conseils.pdf>

En résumé, Alain Oustaloup a reçu une médaille du CNRS pour des publis dont l'exactitude scientifique a été mise en cause par une équipe toulousaine. Benoit Bergeon (responsable d'une équipe au sein du labo d'Oustaloup) a été contacté pour se prononcer, a donné raison aux critiques, désavouant ainsi son directeur, et a ensuite été viré.

17.4.6 CONTRÔLE LPV

Voir le paragraphe spécifique § 0

17.4.7 A LIRE

(Sathishkumar, 2014)

Keywords : suspension – contrôle – quart véhicule

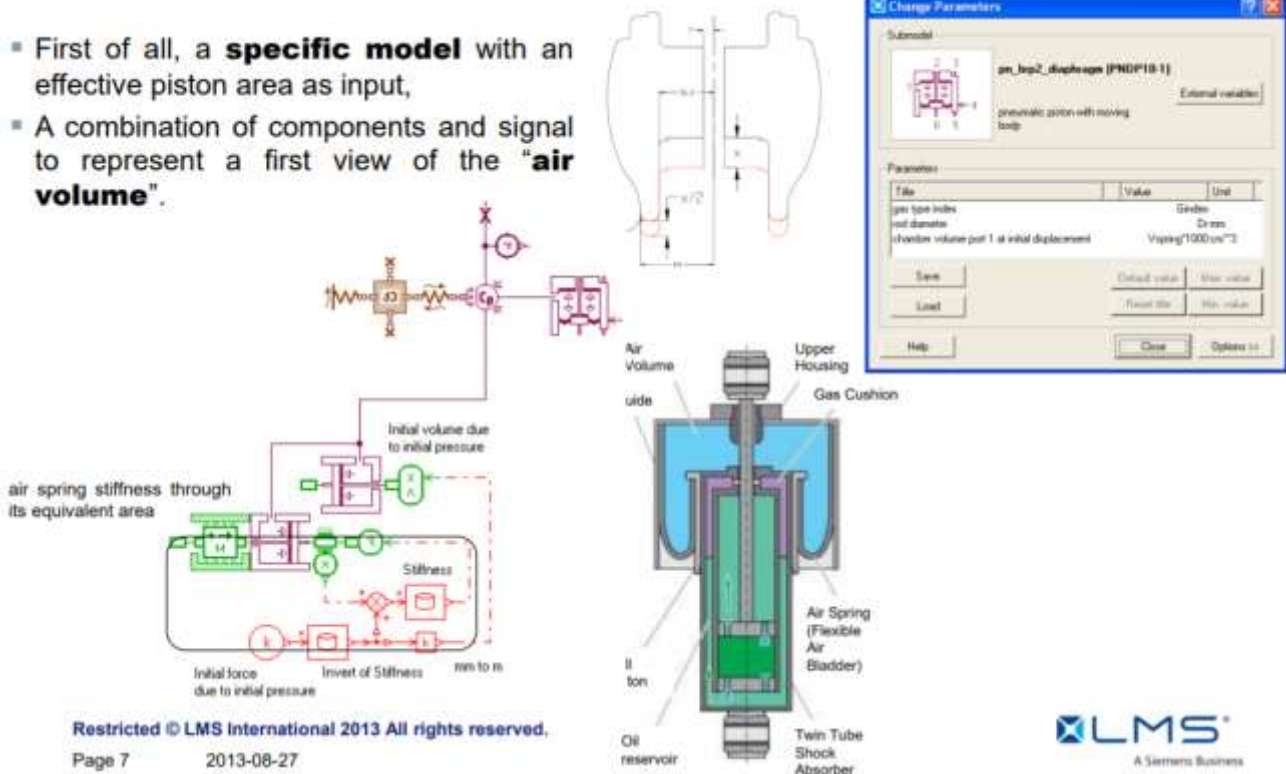
Semi-active Control of Skyhook for 1/4 Suspension System

<http://www.mathworks.com/matlabcentral/fileexchange/11118-semi-active-control-of-skyhook-for-1-4-suspension-system>

Keywords : suspension – contrôle – skyhook – quart véhicule

17.5 SUSPENSION PNEUMATIQUE

- First of all, a **specific model** with an effective piston area as input,
- A combination of components and signal to represent a first view of the “**air volume**”.



17.6 ARTICULATIONS ELASTIQUES

17.6.1 MODELISATION

Mxmountmodel

Deux articles sur le site mais qui n'en disent pas beaucoup :

<https://mdynamix.de/en/smart-test-tools/mxmountmodel/>

<https://mdynamix.de/en/smart-test-tools/mxmountdesigner/>

17.7 BUTEES

http://www.vehicledynamicsinternational.com/exclusive_articles.php?ArticleID=2294

Voir le § “Butées PU” dans le doc LAS.

18 COMPORTEMENT A LA LIMITE ET/OU SUR FAIBLE ADHERENCE

Modeling Aggressive Maneuvers on Loose Surfaces: The Cases of Trail-Braking and Pendulum-Turn

▷ <http://soliton.ae.gatech.edu/people/dcsl/papers/ecc07a.pdf>

Aggressive Maneuvers on Loose Surfaces: Data Analysis and Input Parametrization

(2007) E. Velenis, P. Tsotras and J. Lu

▷ <http://www.advantech.gr/med07/papers/T34-001-528.pdf>

Paramétrage et optimisation de l'appel / contre-appel !

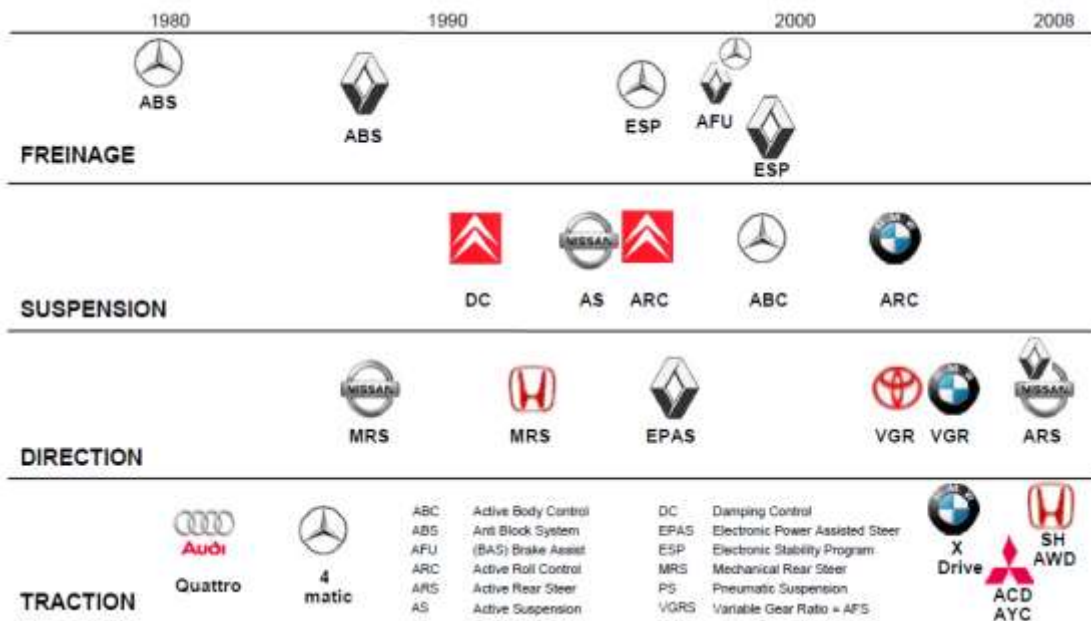
Steady-State Cornering Equilibria and Stabilization for a Vehicle During Extreme Operating Conditions

(Efstathios Velenis, Emilio Frazzoli, Panagiotis Tsotras)

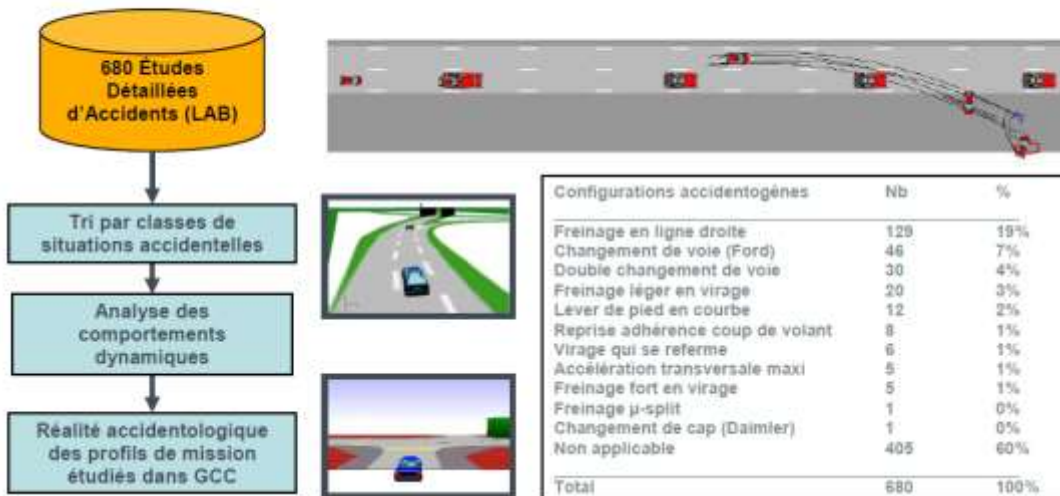
(Tavernini, 2013)

19 SYSTEMES DE CONTROLE ELECTRONIQUE (ABS, ESP, ESC ...)

19.1 HISTORIQUE

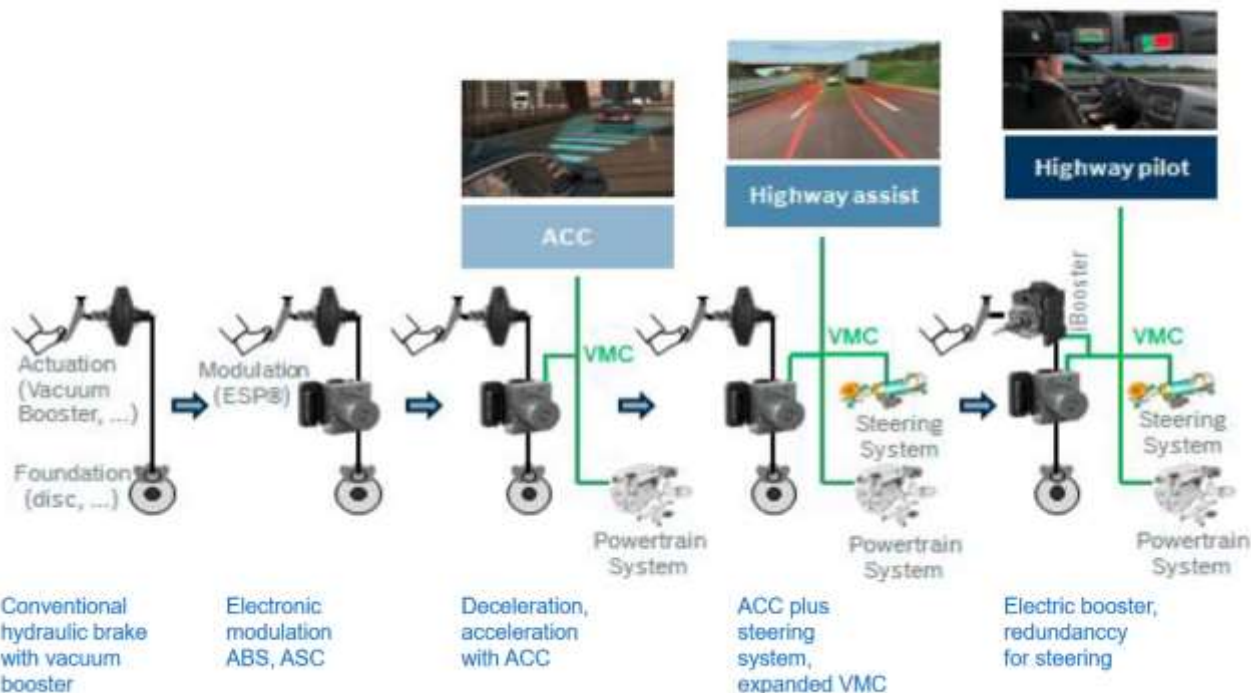


En 2005, une analyse accidentologique²⁴ a été réalisée avec le LAB pour déterminer les situations de conduites les plus représentées dans les accidents.



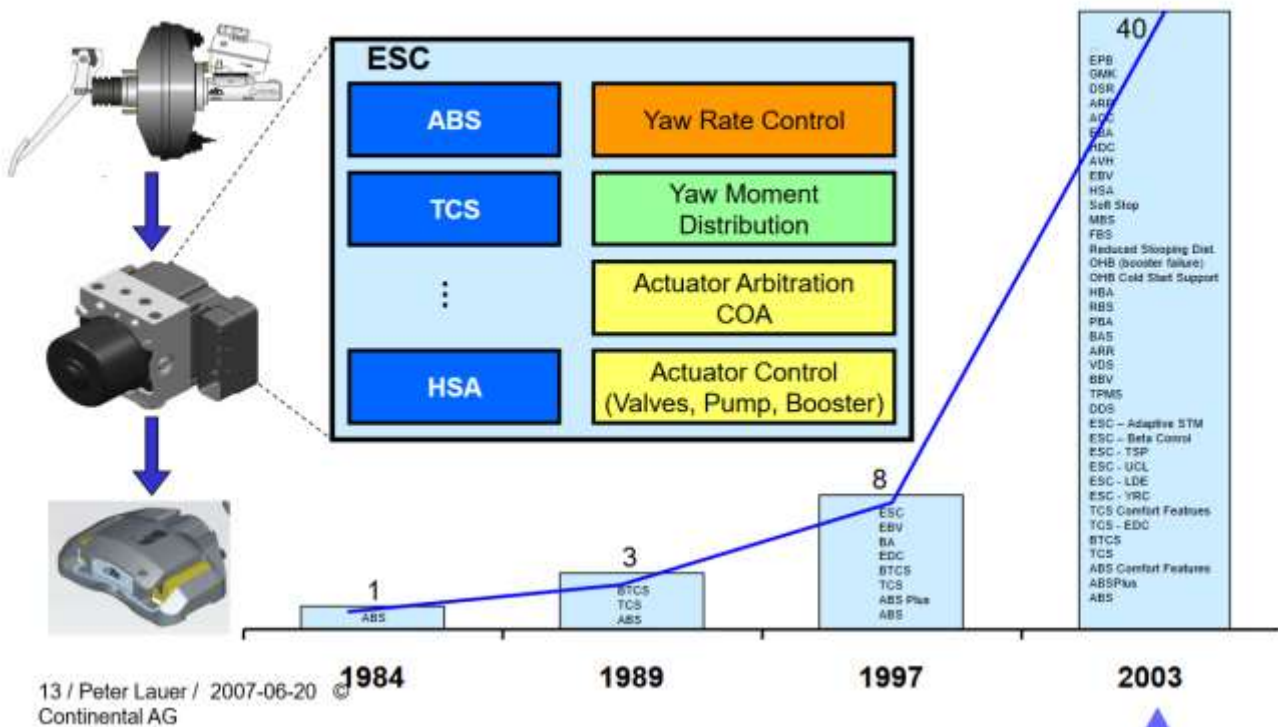
Sensors	Mechatronic components and driver-assistance systems	Actuators
wheel speed	Antilock brakes (ABS, 1979)	hydraulic pump
pedal position		magnetic switching valves
yaw rate	Traction control (TCS, 1986)	electronic throttle valve
lateral & longitudinal acceleration	Electronic stability program (ESP, 1995)	electro-pneumatic brake booster
susp. deflection	Brake assist (BA, 1996)	magnetic proportional valves
brake pressure	Electrical power steering (EPS, 1996)	semi-active shock absorbers
steering angle	Electronic air suspension control (EAS, 1998)	electromotoric actuator for active front steering
steering torque	Adaptive cruise control (ACC, 1999)	electro-hydraulic or electromotoric stabiliser
ultra sonic		
Radar system		
video camera system		
stereo camera system		
	Highly automated driving (20xxx) Anti-collision-avoidance (20xx)	
	Parking assistance (2003)	
	Dynamic drive control (DDC, 2003)	
	Active front steering (AFS, 2003)	
	Continuous damping control (CDC, 2002)	
	Electro-hydraulic brake (EHB, 2001)	
	Active body control (ABC, 1999)	

From hydraulic brake systems to mechatronic brake systems



Source: Alexander Haeussler; Bosch; Automated Driving ..., ATZ Conf. ChassisTec ,Munich 2015 VMC: Vehicle Motion Control

Brake System Software Functions



Modern chassis with actuators and advanced driver assistance systems

AFS
Active front axle steering

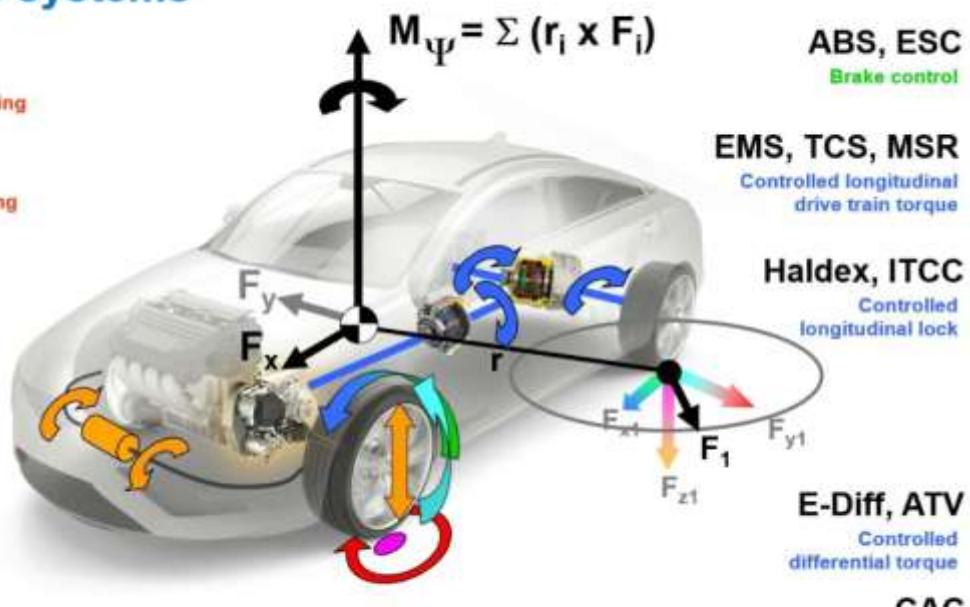
ARK
Active rear axle steering

EAS, ABC
Active suspension level control

ARS, ABC
Vertical force control

EAD, ABC
Pitch and roll control

TPMS, DDS
Tire pressure control



Source: Peter Lauer, Continental AG, Frankfurt

19.2 ABS

19.2.1 HISTOIRE

The current ABS were conceived from system that were developed for trains in the early 1900's. The first patents for ABS on cars date from 1932 'An improved safety device for preventing the jamming of running wheels of automobiles when braking' and a similar patent was filed in 1936 as a 'Apparatus for preventing wheel sliding' Anti-lock braking systems were first developed for aircraft use in 1929, by the French automobile and aircraft pioneer, Gabriel Voisin. An early system was Dunlop's Maxaret system, introduced in the 1950s and still in use on some aircraft models. These entirely mechanical control systems use a flywheel-operated pressure-limiting valve. In testing, a 30% improvement in braking performance was noted. An additional benefit was the elimination of burned or burst tires. A fully mechanical system saw limited automobile use in the 1960s in the Ferguson P99 racing car and the Jensen FF. The system was soon abandoned as it was expensive and unreliable.

Chrysler, together with the Bendix Corporation, introduced a true computerized threechannel, four sensor all-wheel antilock brake system called "Sure Brake" on the 1971 Imperial. In 1971 Nissan offered EAL (Electro Anti-lock System) as an option on the Nissan President. This became Japan's first electronic ABS (Anti-lock Braking System). Teldix, a joint venture of Bendix and Telefunken had put Tekline on the market. The electronics of these early systems was vulnerable to magnetic interference, large operating temperature variation, humidity and vibrations. Durability, reliability and most of all the associated legal concerns, has put the ABS development on hold in the US while Europe took the lead: Teldix and Daimler-Benz have been co-developing anti-lock braking technology since the early 1970s. Soon after they asked Bosch to join the ABS project for their experience in reliable mass-produce electronics, Bosch acquired Teldix in 1975.

Bosch introduced the first completely electronic 4-wheel multi-channel abs system in the Mercedes-Benz S-Class in 1978. By 1985 Mercedes, BMW and Audi had their Bosch ABS, and Ford introduced its Teves system. Today 50 years after the first appearance have become standard and mandatory by law in Europe.

A lire aussi :

Recent advances in antilock braking systems and traction control systems (2000)

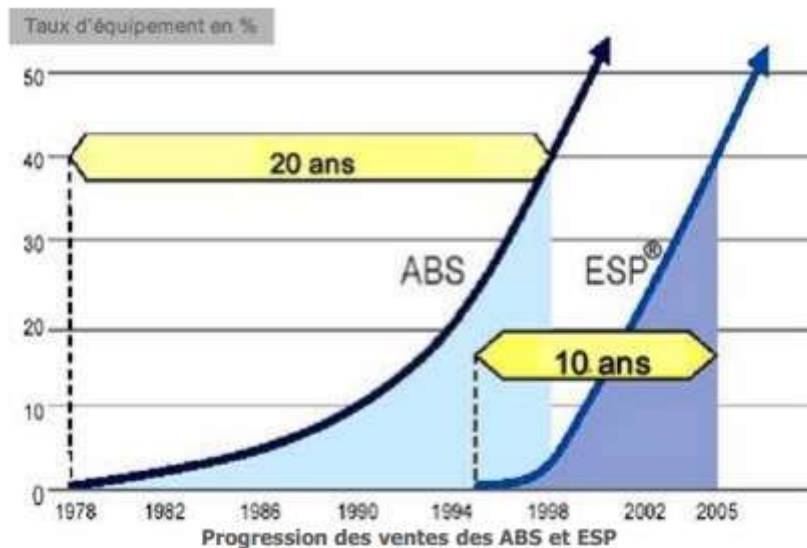
<http://journals.sagepub.com/doi/10.1243/0954407001527493>

19.2.2 FOURNISSEURS

<https://www.vehicledynamicsinternational.com/features/why-the-esc-market-will-exceed-us45-billion-by-2025.html> (01/2021)

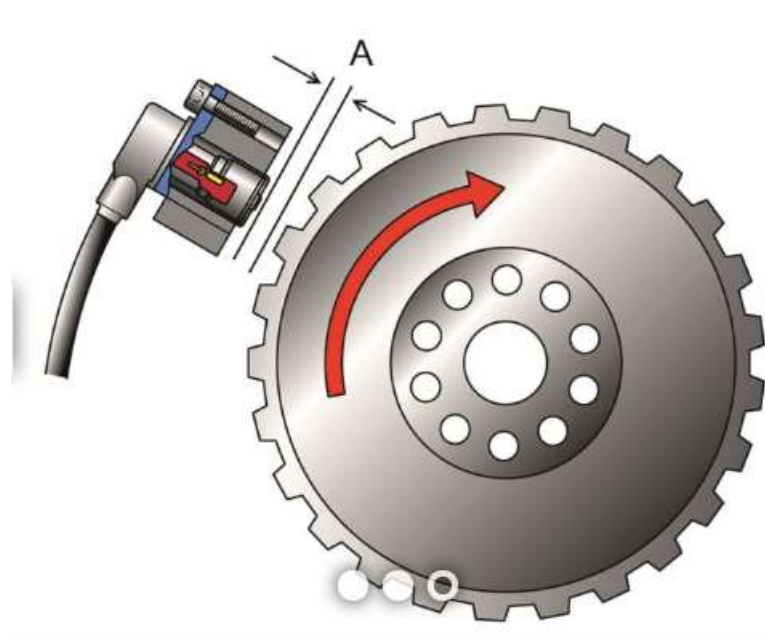
Robert Bosch GmbH, ZF Friedrichshafen, Continental AG, Autoliv, Hitachi Automotive Systems, Johnson Electric, Bendix Commercial Vehicle Systems, and WABCO are leading companies in the ESC system market

19.2.3 TAUX D'EQUIPEMENT



19.2.4 CAPTEURS ABS

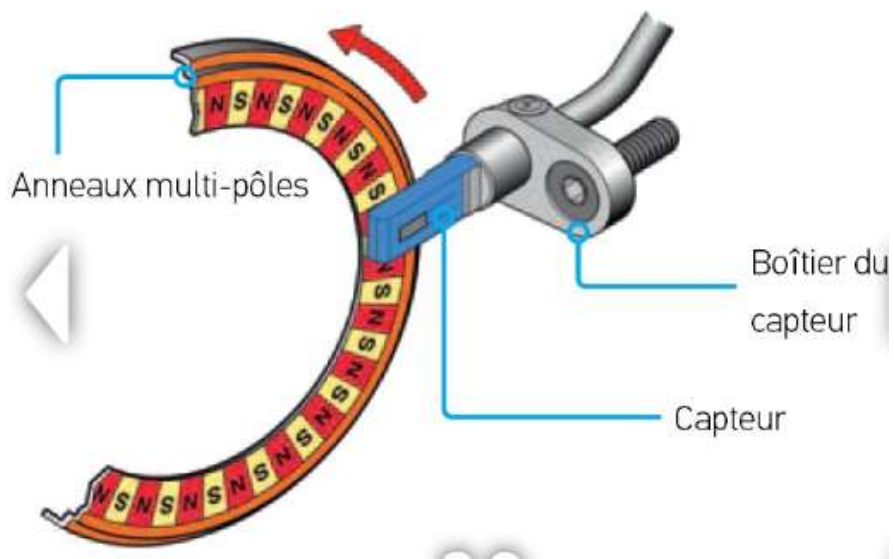
Capteurs passifs



Les capteurs de vitesse de roue sont placés directement au dessus de la roue d'impulsion qui est reliée au moyeu de roue ou à l'arbre de transmission. La broche polaire entourée d'un enroulement est reliée à un aimant permanent dont l'effet magnétique s'étend jusqu'à la roue polaire. Le mouvement rotatif de la roue d'impulsion et l'alternance entre dent et espace interdentaire qui en découle a pour effet un changement du flux magnétique à travers la broche polaire et l'enroulement. Ce champ magnétique changeant induit une tension alternative mesurable dans l'enroulement.

La fréquence et les amplitudes de cette tension alternative sont proportionnelles à la vitesse de roulement. Les capteurs inductifs passifs ne nécessitent aucune tension d'alimentation séparée par le calculateur. Étant donné que la plage de signal pour la détection du signal est définie par le calculateur, la hauteur d'amplitude doit se déplacer à l'intérieur d'une plage de tension. La distance (A) entre le capteur et la roue d'impulsion est prédefinie par la construction de l'axe.

Capteurs actifs



Le capteur actif est un capteur de proximité avec une électronique intégrée, alimentée avec une tension définie par le calculateur ABS. Un anneau multipolaire, également inséré dans la bague d'étanchéité d'un roulement de roue, peut par exemple être utilisé comme roue d'impulsion. Dans cette bague d'étanchéité sont placés des aimants dont la polarité est alternée. Les résistances magnétorésistives intégrées dans le circuit électronique du capteur détectent le champ magnétique alternant lors de la rotation de l'anneau multipolaire. Ce signal sinusoïdal est transformé en un signal numérique par l'électronique dans le capteur. La transmission vers le calculateur se fait par un signal électrique avec le procédé de modulation de largeur d'impulsions.

Le capteur est relié au calculateur par un câble de raccordement électrique à deux pôles. Le signal du capteur est transmis par la ligne d'alimentation en tension. L'autre ligne sert de masse du capteur. En plus des éléments magnétorésistifs, des éléments à effet Hall sont également utilisés aujourd'hui, ceux-ci autorisant des entrefers plus importants et réagissant aux plus petites modifications du champ magnétique. Si une roue d'impulsion en acier est installée dans un véhicule à la place d'un anneau multipolaire, un aimant est placé en plus sur l'élément capteur. Lorsque la roue d'impulsion tourne, le champ magnétique constant change dans le capteur. Le traitement du signal et le circuit intégré sont identiques à ceux du capteur magnétorésistif.

Avantages des capteurs actifs

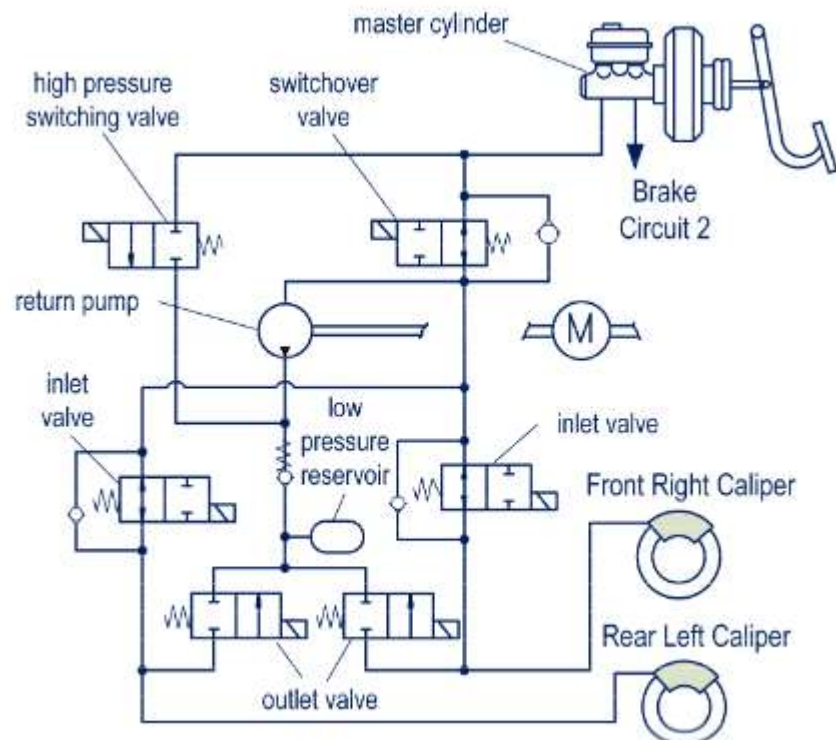
- Détection de la vitesse de rotation à partir de l'arrêt. Cela permet de mesurer la vitesse jusqu'à 0,1 km/h, ce qui est important pour les systèmes anti-patinage (ASR) au moment du démarrage.
- Les capteurs fonctionnant selon le principe de l'effet Hall détectent les mouvements d'avance et de recul.
- Le capteur est plus petit et plus léger.
- La suppression des roues d'impulsion permet de simplifier les articulations de transmission des forces.
- La sensibilité par rapport aux perturbations électromagnétiques est plus faible.
- Les variations de l'entrefer entre le capteur et l'anneau magnétique n'ont pas d'effets directs sur le signal.
- Quasiment aucune sensibilité aux vibrations et aux variations de température.

19.2.5 LES DIFFERENTES TECHNOS

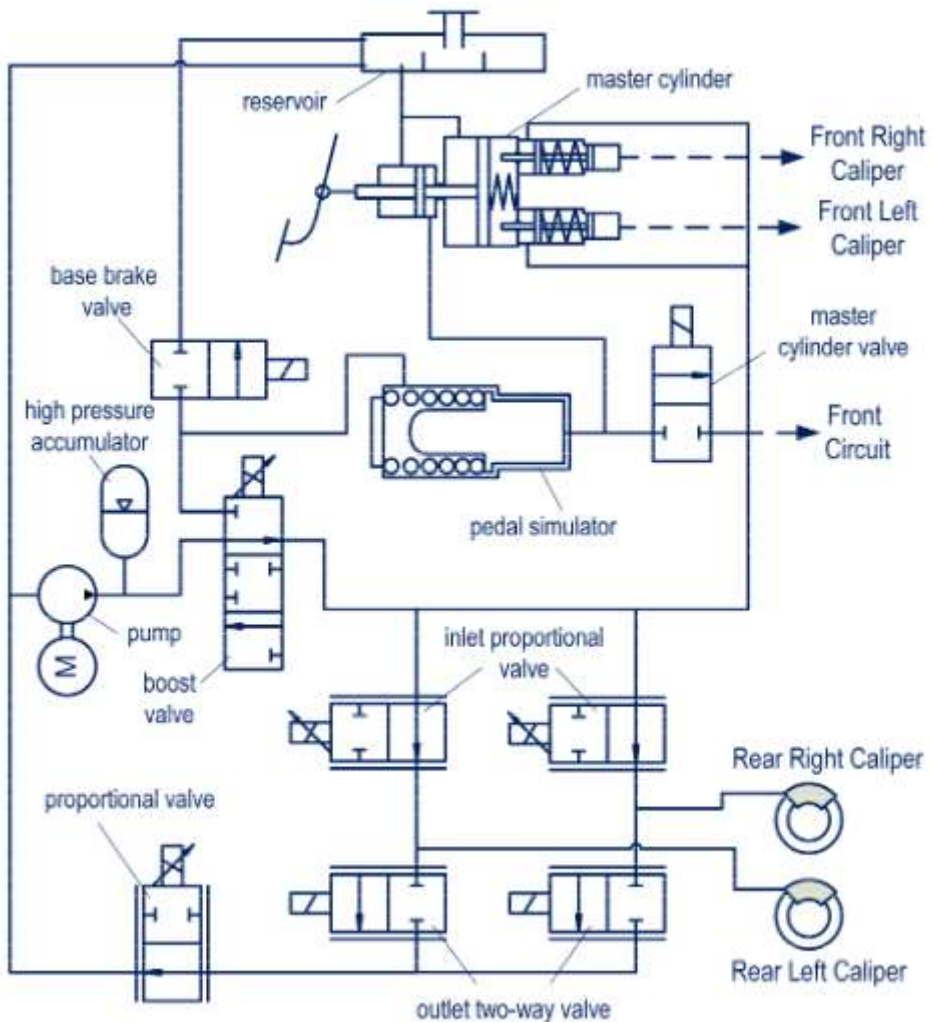
HAB : Hydraulically Applied Brakes

	HAB	EHB	EMB
Techology	Hydraulic	Electro-hydraulic	Electro-mechanical
Force modulation	Discrete (on/off)	Continuous	Continuos
Ergonomics	Pedal Vibration	No vibrations	No vibrations
Environmental issues	Toxic oils	Toxic oils	No oil

Le temps de réponse d'un système HAB est estimé entre 200 et 400ms, alors qu'un système EHB est donné entre 60 et 100ms



(a) Conventional hydraulic ABS hardware, half view (adapted from [1]).

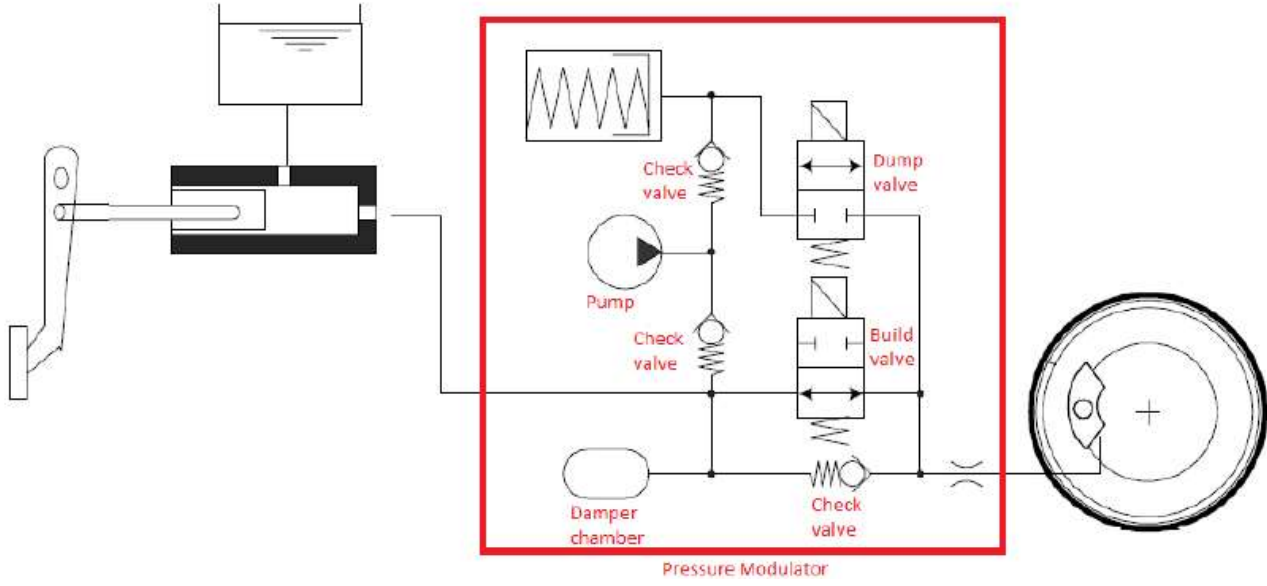


(b) Electro-hydraulic ABS hardware, half view (adapted from [21])

19.2.6 HYDRAULIC BRAKE ACTUATOR (HAB)

Un bloc ABS ne sert qu'à retirer de la pression. Si on a besoin d'en ajouter, il faut passer par le bloc ESP.

The pressure exerted by the driver on the pedal is transmitted to the hydraulic system via an inlet (or build) valve, which communicates with the brake cylinder. Moreover, the hydraulic system has a second valve, the outlet (or dump) valve, which can discharge the pressure and which is connected to a low pressure accumulator. A pump completes the overall system.



The ABS available on most passenger cars are equipped with hydraulic brake actuators (HAB) with discrete dynamics. The HAB actuator is indeed only capable of providing three different control actions :

- Increase the brake pressure: in this case the build valve is open and the dump one closed.
- Hold the brake pressure: in this case both valves are closed
- Decrease the brake pressure: in this case the build valve is closed and the dump one open

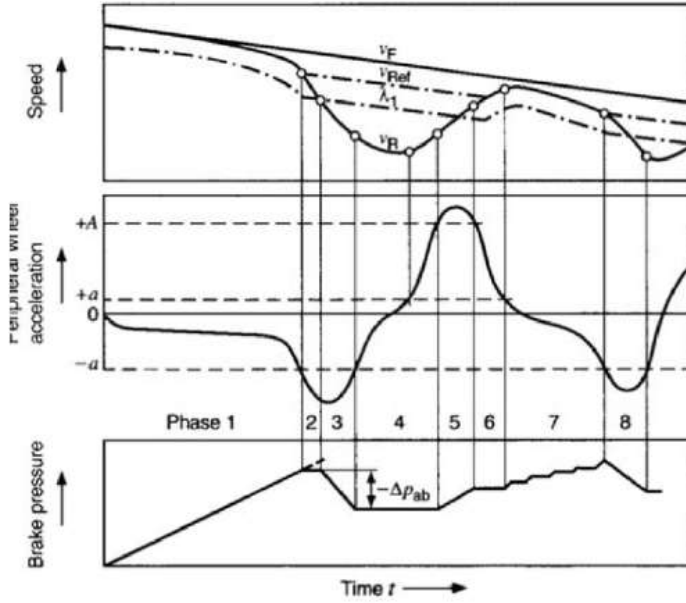
The disadvantage of HAB is related to ergonomic issues: with these brakes, in fact, the driver feels pressure vibrations on the brake pedal when the ABS is activated, due to the large pressure gradient in the hydraulic circuit.

19.2.7 TEMPS DE REPONSE

Time to lock : temps pour avoir la pression max = entre 100 et 300 ms selon technos

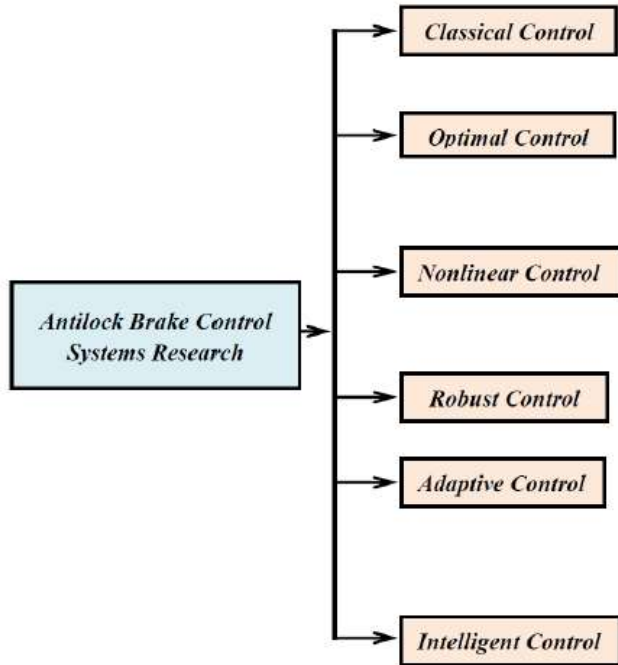
19.2.8 ALGORITHME BOSCH

The Bosch ABS system is used on many passenger cars. The algorithm is based on wheel spin acceleration and a critical tire slip threshold. Upon brake pressure application, once ABS is invoked (i.e., the thresholds are exceeded), the current brake pressure application is divided into eight phases :



1. Initial application. Output pressure is set equal to input pressure. This phase continues until the wheel angular acceleration (negative) drops below the Wheel Minimum Spin Acceleration, $-a$.
2. Maintain pressure. Output pressure is set equal to previous pressure. This phase continues until the tire longitudinal slip exceeds the slip associated with the Slip Threshold. At this time, the current tire slip is stored and used as the slip threshold criterion in later phases. This slip corresponds to the maximum slip; the tire is beginning to lock.
3. Reduce pressure. Output pressure is decreased according to the release Rate until the wheel spin acceleration becomes positive (this is a slight modification to the sequence shown above, in which the pressure is decreased until the spin acceleration exceeds $-a$)

19.2.9 STRATEGIES / LOIS DE COMMANDE



Un article de 2020 par une équipe de l'université de Delft (+un auteur de Toyota Europe) :

F. Pretagostini, L. Ferranti, G. Berardo, V. Ivanov and B. Shyrokau, "**Survey on Wheel Slip Control Design Strategies, Evaluation and Application to Antilock Braking Systems**," in IEEE Access, vol. 8, pp. 10951-10970, 2020.

▷ DOI : [10.1109/ACCESS.2020.2965644](https://doi.org/10.1109/ACCESS.2020.2965644)

Ce papier propose un contrôleur sur la base d'un nonlinear MPC.

La littérature relative au contrôle ABS s'appuie généralement sur le choix comme variable à contrôler de l'accélération de roue ou du glissement longitudinal du pneu.

L'avantage du contrôle par l'accélération est qu'on peut mesurer cette dernière directement.

En revanche le contrôle basé sur le glissement est plus simple d'un point de vue dynamique (?), et le couple appliqué converge vers une valeur fixe. Un tel contrôleur est donc moins oscillant, mais se révèle plus sensible à la valeur de consigne, qu'il faut spécifier notamment en tenant compte des conditions d'adhérence.

En outre l'estimation du glissement nécessite de disposer de la vitesse longitudinale du véhicule, qui doit elle aussi être estimée car ne pouvant être mesurée directement (du moins pour une production en série).

Dans la revue de littérature proposée, plusieurs techniques sont mentionnées pour l'estimation du glissement du pneu :

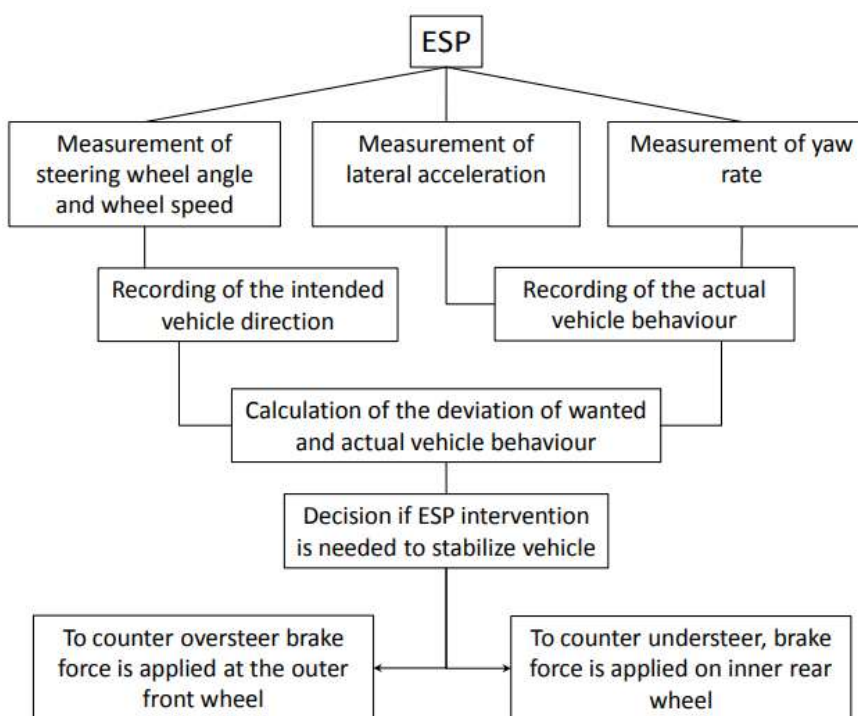
Méthode	Auteur	Année	Lien
---------	--------	-------	------

Bootstrap Rao-Blackwellized particle filter based on the signals from the wheel speed sensors, accelerometer and GPS	K. Berntorp	2015	DOI: 10.1109/TCST.2015.2470636
second-order system based on LuGre friction model	W. Wang	2008	DOI: 10.1109/TIE.2008.2009439
Feedback linearizing control	D. Nesic	2012	DOI: 10.1109/TAC.2012.2215270

Voir la thèse de Nicola Geromel : ***Modelling and control of the braking system of the electric Polaris Ranger all-terrain-vehicle***

19.3 ESC

19.3.1 PRINCIPE



19.3.2 DEFINITION

<https://modernjeeper.com/what-is-fmvss-no-126-and-why-you-should-care/>

This standard is required on all model year 2012 vehicles and newer and is also known by other trade names such as AdvanceTrac, Dynamic Stability Control (DSC), Dynamic Stability and Traction Control (DSTC), Electronic Stability Program (ESP), Vehicle Dynamic Control (VDC), Vehicle Stability Assist (VSA), Vehicle Stability Control (VSC), Vehicle Skid Control (VSC), Vehicle Stability Enhancement (VSE), StabiliTrak, and Porsche Stability Management (PSM).

(...)

The agency adopts the ESC definition based on the Society of Automotive Engineers (SAE) Surface Vehicle Information Report J2564 (revised June 2004). ESC is defined as a system that has all of the following attributes:

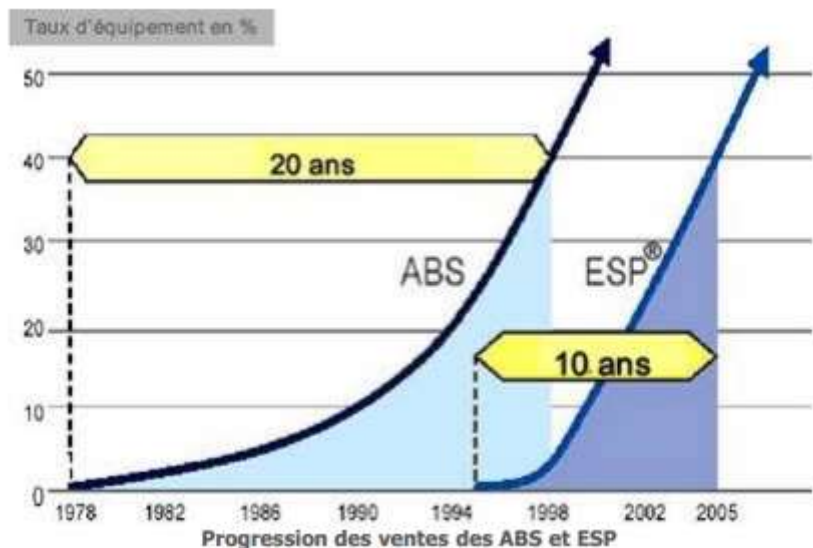
1. (a) **ESC augments vehicle directional stability by applying and adjusting the vehicle brake torques individually to induce a correcting yaw moment to the vehicle.**
2. (b) **ESC is a computer controlled system, which uses a closed loop algorithm to limit vehicle oversteer and to limit vehicle understeer. [The closed loop algorithm is a cycle of operations followed by a computer that includes automatic adjustments based on the result of previous operations or other changing conditions.]**
3. (c) **ESC has a means to determine the vehicle's yaw rate and to estimate its sideslip slip or side slip derivative with respect to time. [Yaw rate means the rate of change of the vehicle's heading angle about a vertical axis through the vehicle center of gravity. Sideslip is the arctangent of the ratio of the lateral velocity to the longitudinal velocity of the center of gravity.]**
4. (d) **ESC has a means to monitor driver steering input.**
5. (e) **ESC has an algorithm to determine the need, and a means to modify engine torque, as necessary, to assist the driver in maintaining control of the vehicle.**
6. (f) **ESC is operational over the full speed range of the vehicle (except at vehicle speeds less than 15 kph (9.3 mph) or when being driven in reverse).**

19.3.3 HISTOIRE

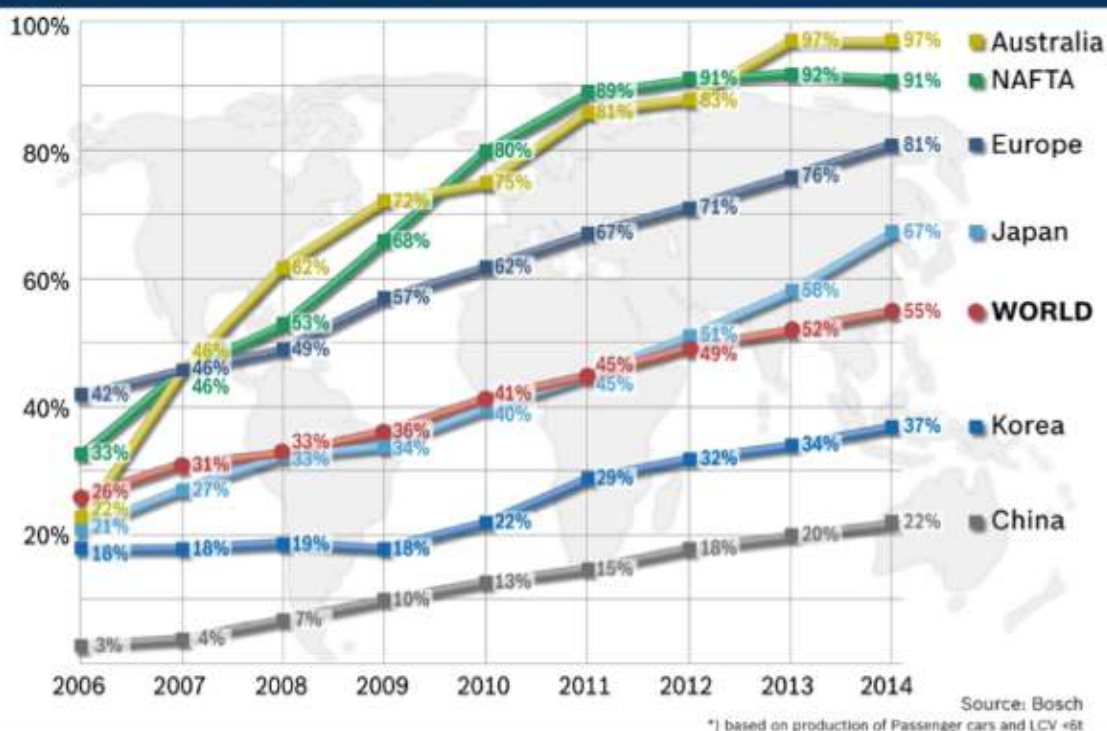
<http://206-cc.fr/ressources/Fonctionnement-ESP.pdf>

En 1995 apparut le contrôle de trajectoire, appelé de façon plus commerciale « Programme électronique de stabilité » ou ESP (Electronic Stability Program). Cet équipement a équipé 40% des véhicules vendus en Europe de l'Ouest en 2005

19.3.4 TAUX D'EQUIPEMENT



ESP® Installation Rates^{*}



source <http://www.car-engineer.com/esp-electronic-stability-program/>

<https://www.vehicledynamicsinternational.com/features/why-the-esc-market-will-exceed-us45-billion-by-2025.html> (01/2021)

The electronic stability control (ESC) system market is set to grow from its current market value of more than \$27 billion, to over \$45 billion by 2025. Vehicle stability and traction control systems have become important for

improving vehicle safety. The growing need to prevent vehicle skidding due to events such as sudden braking, slippery road surfaces, and loss of vehicle control by drivers has boosted developments in the ESC system market.

19.3.5 FONCTIONNEMENT ESC

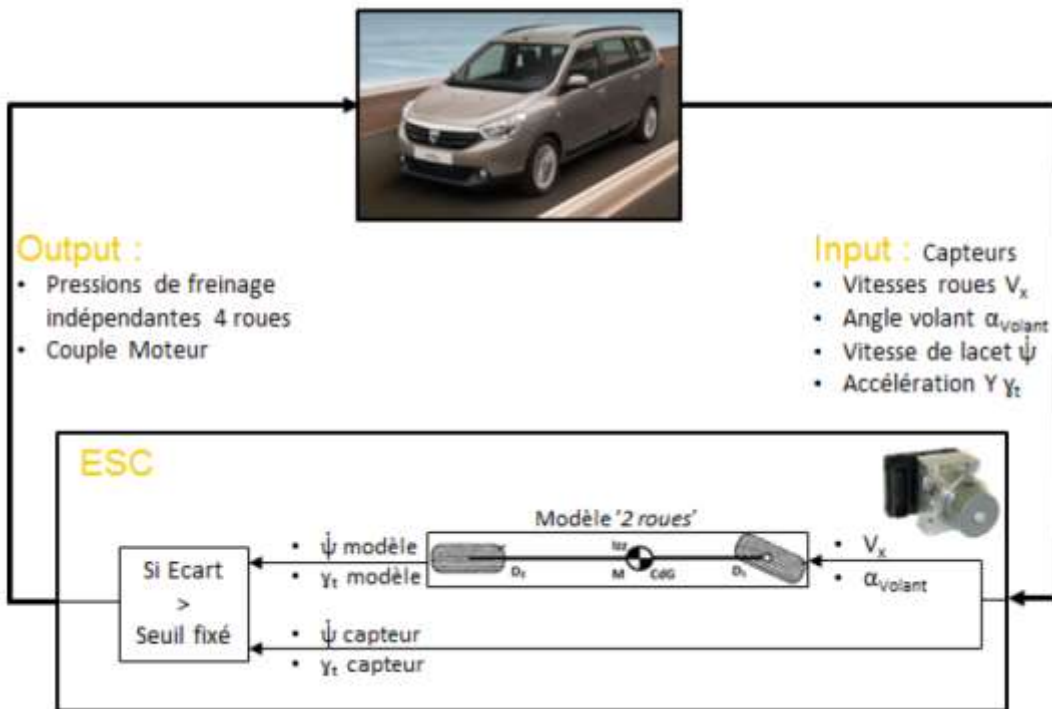
ABS et ESC constituent deux systèmes distincts, mais un bloc ESC implique 1 bloc ABS

Techno moteur pour pompe bloc ESP : courant continu

Durabilité : 500 heures

On n'a pas un bloc par véhicule : trop cher. On fonctionne donc par génération (chez Bosch, génération 9 actuellement), et plutôt par plate-forme.

Capteur de pression : pilotage très fin



Les actions d'un ESC sont globalement liées à la différence qu'il observe entre :

- Les grandeurs qu'il enregistre à l'aide de différents capteurs
- Les grandeurs théoriques qu'il calcule, à l'aide d'un modèle interne du véhicule

Lorsque l'écart entre son modèle interne, et ce qu'il enregistre devient trop important, il procède à des actions (freins et/ou moteur) afin de rapprocher le véhicule physique de son véhicule numérique théorique.

Le modèle véhicule que l'ESC utilise est donc essentiel pour la réalisation de corrections justes et au bon moment. Ce modèle de véhicule enregistré par l'ESC consiste en un «simple» modèle 2 roues, caractérisé par :

- un empattement
- une masse totale
- la position du centre de gravité
- une inertie de lacet
- une dérive spécifique avant globale véhicule
- une dérive spécifique arrière globale véhicule
- une loi ‘Angle volant – Angle roue’
- un critère quasi-statique résultant de tous ces paramètres

19.4 4RD / 4WS

Remonte à un décret déposé au Japon en 1907 !

(Groenendijk, 2009)

Hyundai motors has a system called AGCS (Active Geometry Control Suspension). This system uses toe-control to improve vehicle stability. The AGCS controller estimates the lateral acceleration based on the vehicle velocity and steer angle. Based on lateral acceleration, a map is chosen and then the ECU uses this map to calculate the stroke of the actuator.

Renault recently put its four wheel steering system in production on the Laguna GT (active chassis control). This system consists of a relatively simple rear axle with a steering actuator. The rearwheels steer in opposite direction to the front wheels with a maximum angle of 3.5 degrees, when the velocity is under 60 [km/h]. Above 60 [km/h] the steering angles are in the same direction as the front wheels

BMW introduced active front steering on the BMW 5 series in 2003. The active front steering system is developed by ZF. BMW developed the safety concept, the application and associated high level safety functions. Yaw-rate control, yaw torque and disturbance rejection function are developed and implemented by the manufacturer,

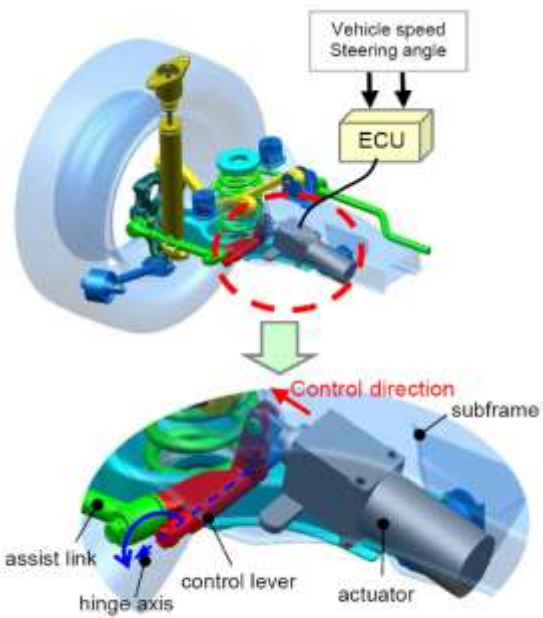


Figure 2.8: AGCS system of Hyundai, [31]

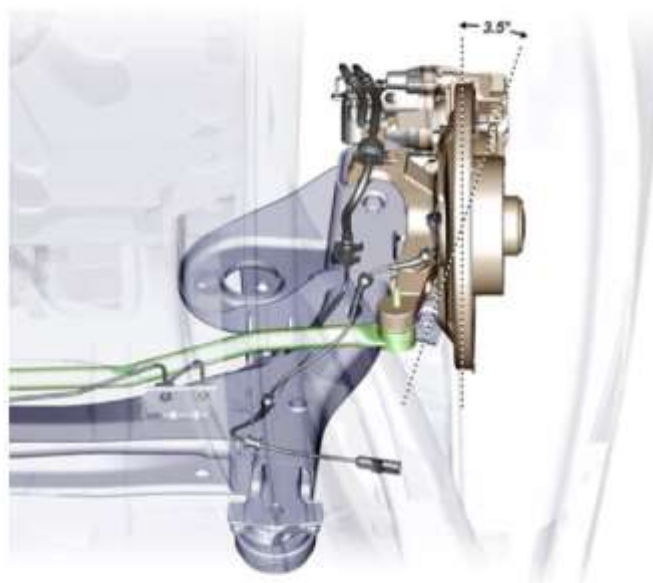


Figure 2.9: Renault active drive system, one wheel, [32]

19.5 CARROSSAGE ACTIF

Thèse sur le sujet : E. Koenigsen (cf §27.10)

Yoshino, T. and Nozaki, H., "About the Effect of Camber Control on Vehicle Dynamics," SAE Technical Paper 2014-01-2383, 2014, <https://doi.org/10.4271/2014-01-2383>.

Conclusion : this research focused on a method of ground negative camber angle control that is proportional to the steering angle as a technique to improve maneuverability and stability to support the new era of electric vehicles, and the effectiveness thereof was clarified. As a result, it was found that camber angle control can control both the yaw moment and lateral acceleration at the turning limit in the critical cornering range as well. It was also confirmed that both stability and the steering effect in the critical cornering range are improved by implementing ground negative camber angle control that is proportional to the steering angle using actuators. Dramatic improvements in cornering limit performance can be achieved by implementing ground negative camber angle control that is proportional to the steering angle.

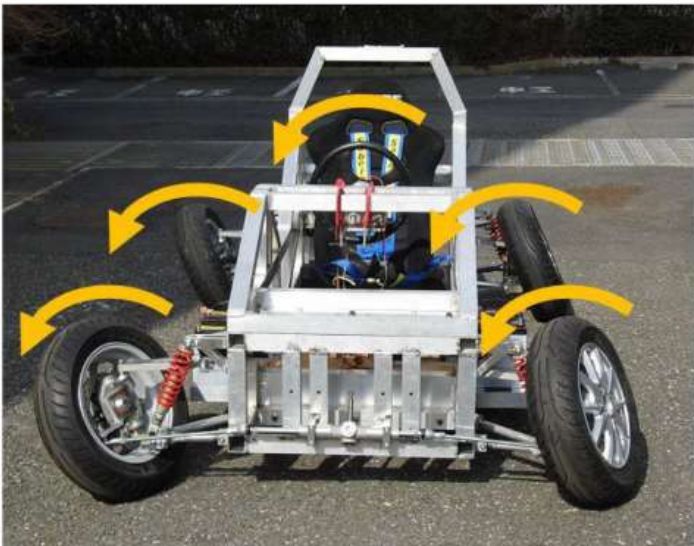


Figure 16. Large camber angle control vehicle.

19.6 CONTROLE GLOBAL CHASSIS

19.6.1 POTENTIEL DES DIFFERENTES SOLUTIONS

System Potential		AFS	ARS	ARC	ESC	TVbB	aLSD	TVD
Straight Line Driving		13.000	12.000	-	11.000	4.000	-	4.500
Handling Region	OS	17.000	5.000	600	9.000	-	1.500	3.000
	US	5.000	16.000	600	5.000	6.000	-	2.500
Max. Lateral Acceleration	OS	2.500	1.500	2.000	10.500	-	1.000	1.500
	US	-	7.000	2.300	6.000	7.500	-	1.700

Figure 2.12: Overview of additional yaw torque [Nm] produced by different systems, [40]

source (Groenendijk, 2009)

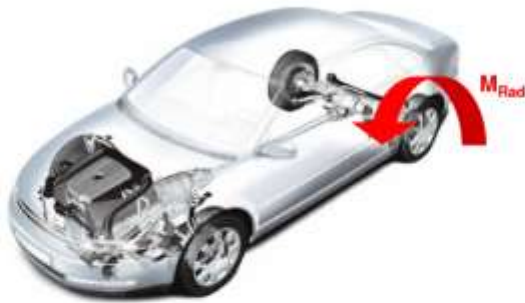
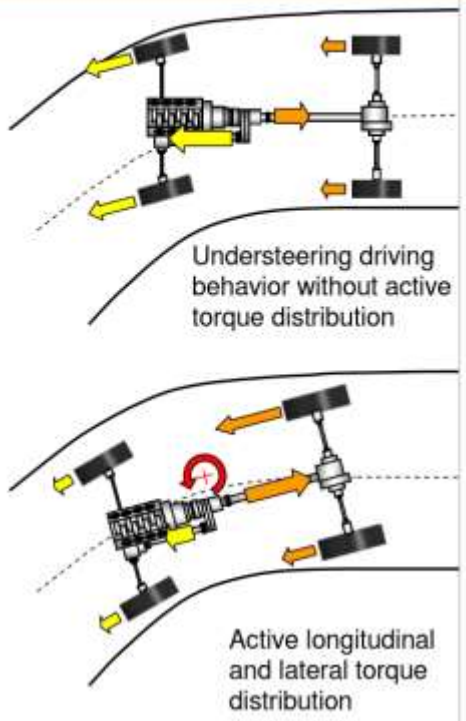
19.6.2 TORQUE VECTORING

RAD = torque vectoring Alfa

http://www.ukintpress-conferences.com/conf/09vdx_conf/pdfs/day2/15_Ruediger_Freimann.pdf

Axle differential with active torque distribution

Torque-Vectoring



Positive effect on

- Traction
- Critical cornering speed
- Self-steering response
- Handling and cornering characteristics
- Agility
- Yaw damping / yaw boosting
- Reducing brake intervention

Dans <https://d-nb.info/1071620835/34> (Gerd Kaiser, PhD, 2015), on trouve le tableau suivant :

Table 3.1: Torque vectoring implemented in serial production vehicles

Vehicle	System	Year
Mitsubishi EVO II, for WRC	Active	1994
Mitsubishi EVO IV-X [56]	Active & Passive	1996
Honda/Acura RLX, MDX, RDX [57]	Active	2005
Audi A4, A5, S4, S5, Q5, A8 [58]	Active	2008
BMW X6, X6M, X5M [59]	Active	2008
Mercedes AMG S63, S65 [60]	Passive	2009
Mitsubishi Outlander GT [61]	Active & Passive	2009
Porsche 911 Turbo, Cayenne, Macan, Cayman [62]	Active	2009
Mercedes CL, CLS, GLA, S, SL, SLK [63]	Passive	2011
McLaren MP4-12C [64]	Passive	2011
Ford Focus [65]	Passive	2012
Nissan JUKE [66]	Active	2012
Range Rover Sport [67]	Passive	2013
Holden Special Vehicles Gen-F GTS [68]	Passive	2013
Mercedes AMG SLS electric [16]	Electric	2013
Cadillac XTS [69]	Active	2014
Lexus RC F [70]	Active	2014

Il est dit quelques lignes plus loin que la plupart des systèmes contrôlent en vitesse de lacet, alors que dans de plus rares cas le contrôle est fait sur l'angle de dérive. On trouve aussi une combinaison des deux.

La sortie du contrôle "haut niveau" est un moment de lacet. Ensuite ce moment peut être réalisé de plusieurs manières différentes :

- différentiels actifs
- freinage différentiel
- moteurs électriques

19.6.3 G-VECTORING CONTROL (MAZDA)

Fonctionnalité intégrée dans le SkyActiv-Vehicle Dynamics

Lorsque le volant est tourné, une faible réduction du couple moteur est déclenchée, afin de charger le train avant :

Dynamics are key to the enjoyment of a vehicle, so why not consider them in every aspect of vehicle design and engineering? This is the approach Mazda has adopted with SkyActiv-Vehicle Dynamics, a series of vehicle motion control technologies that integrate dynamics with every key element of the driving experience, from engine and transmission, to chassis and body.

The inspiration comes from *yabusame*, the Japanese sport of mounted archery which dates back to the 12th century. Accurately firing an arrow from a cantering horse is quite a challenge, and to ensure stability and accuracy, horse and rider must work as one. The term for this sense of connectedness is *Jinba-ittai* and Mazda is applying it in its dynamics work to make drivers feel more connected with their cars.

The first stage of the SkyActiv-Vehicle Dynamics technologies is G-Vectoring Control (GVC), which is being introduced with the updated Mazda3 (known as Axela in Japan) before being rolled out across all its new-generation models.

Turning the steering wheel in a GVC-equipped car does not just rotate the wheels: steering inputs also vary engine torque – torque that is available the moment the driver asks for and expects it, due to optimized boost control and precise fuel injection – and together

they provide integrated control of lateral and longitudinal acceleration forces, optimizing the vertical load on each wheel. Better still, as GVC is a software system, it has no weight penalty.

When the steering wheel is turned, GVC adjusts engine drive torque to generate a deceleration *g*-force (usually 0.01*g* or less), thereby shifting load to the front wheels to increase front-wheel tire grip and turn-in responsiveness.

When a constant steering angle is maintained, GVC recovers engine drive torque, which transfers load to the rear wheels for vehicle stability.

As well as improving responsiveness and stability, the effect of the system is to make vehicle motion smoother, and for that motion to feel more natural and more in tune with what the body feels, thus keeping the driver – and passengers – comfortably and confidently in the saddle. An added bonus is that the control – and feeling of control – the technology provides improves everything from everyday driving to collision avoidance maneuvers, to handling on slippery or loose surfaces.

Customers that select the SkyActiv-D 2.2 engine can also opt for i-Activ AWD, an all-wheel-drive system that provides optimal distribution of torque to the front and rear wheels by anticipating road conditions, weather and the driver's intentions.



19.6.4 AYC

https://en.wikipedia.org/wiki/Active_Yaw_Control

<http://www.mitsubishi-motors-pr.ca/ca/fr/media/pressreleases/796>

La Lancer Evolution 2008 est le premier modèle Evolution nord-américain à offrir le différentiel arrière à CAL. Une innovation à l'époque, le CAL a été utilisé pour la première fois sur les Lancer Evolution IV en 1996. En 2003, Mitsubishi a remplacé le pignon conique par un différentiel central à trains planétaires, ce qui a permis de doubler le couple transmis par le CAL. La nouvelle version du CAL sur la Lancer Evolution 2008 utilise toujours un différentiel central à trains planétaires.

Le différentiel arrière à contrôle actif du lacet de Mitsubishi Motors fonctionne à l'aide d'un mécanisme de transfert du couple, situé dans le différentiel arrière. Ce dispositif contrôle la répartition du couple afin d'améliorer les performances dans les virages en réduisant les mouvements de lacet exercés sur le véhicule. Le CAL sert également de différentiel à glissement limité car il contrôle également le glissement des roues arrière afin d'améliorer la traction. Le différentiel CAL de la Lancer Evolution 2008 surveille le lacet à l'aide de capteurs et contrôle la force de freinage par le biais du contrôle actif de stabilité (CAS).

En contrôlant le montant de couple transmis aux roues arrière lorsque la traction est faible ou que les roues n'adhèrent pas avec la même force sur la route, le CAL aide aussi à améliorer l'accélération et la stabilité sur les routes glissantes. Il est également assisté par l'intégration du CAS sur la Lancer Evolution 2008. Cependant, le CAL a été principalement conçu pour offrir une meilleure stabilité lors de la prise de virages à grande vitesse et donc, l'adhérence dans les virages.

Comment fonctionne le CAL

Le différentiel à CAL sépare activement le couple entre les roues de droite et les roues de gauche. Cela modifie le moment de lacet du véhicule lors de la prise d'un virage. Comme le CAS, le CAL est contrôlé par l'ordinateur S-AWC qui surveille l'angle du volant, l'ouverture du papillon, la vitesse de rotation des roues ainsi que les mouvements longitudinaux et latéraux du véhicule.

Le CAL est composé de deux sections : le différentiel arrière et le contrôle de répartition de la puissance entre la droite et la gauche. La section de contrôle de répartition de la puissance comprend deux embrayages hydrauliques, un pour le pont de droite, et l'autre pour le pont de gauche. Dans les virages, ces deux embrayages interprètent les données de l'ordinateur S-AWC et agissent sur le différentiel afin d'accroître le couple retrasmis aux roues extérieures et de réduire le couple retrasmis aux roues intérieures. Cette intervention change le mouvement de lacet du véhicule, incite le véhicule à se diriger vers l'intérieur du virage et limite le glissement des pneus avant, ce qui réduit le sous-virage.

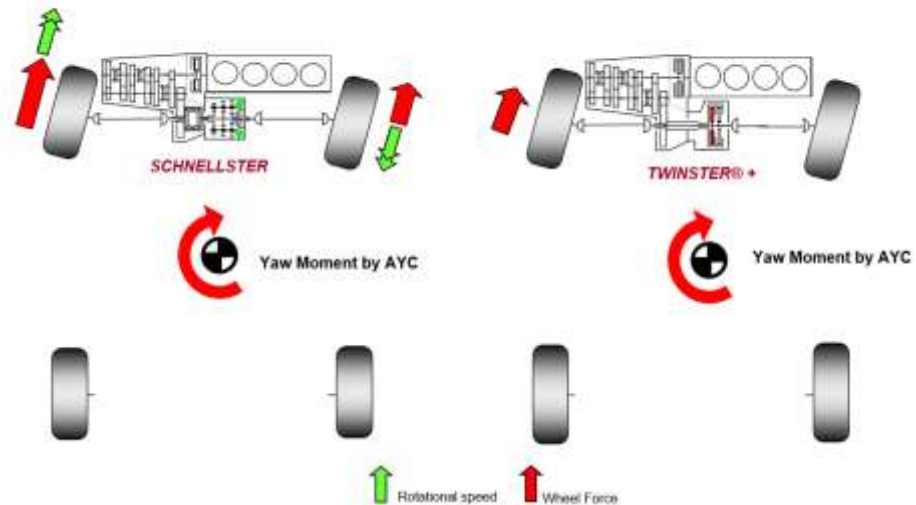
GETRAG - Active Yaw Systems: Re-experience Front Wheel Drive with SCHNELLSTER® and TWINISTER®

http://www.ukintpress-conferences.com/conf/09vdx_conf/pdfs/day1/4_Heinz-Peter_Oberguenner.pdf

SCHNELLSTER Superimposed Planetary Gear System Speed Lead

TWINISTER®+ TWIN Clutch System Torque lead

SCHNELLSTER and **TWINSTER®+**
Influence on Yaw Behavior by Different Solutions



TWINSTER®+
Overview of System Potentials

- Differential Function
 - eliminate differential (cost / weight compensation)
- Gearbox Main Clutch Function
 - eliminate main clutch including actuation (cost / weight compensation)
 - different clutch characteristic possible (normal- sport or snow mode)
- Torque Limiter Function
 - Protect driveline for overload
 - Eliminate stamping front axle (e.g. acceleration on wet asphalt)
 - Prevent for spinning front wheels
 - Provide best acceleration performance independent from friction coefficient
- Limited Slip Differential (eLSD) Function
- Active Yaw Control
 - Yaw support
 - Yaw damping
- Friction Coefficient Detector Function
 - pressure mirrors transmittable wheel torque
- Freewheel Function (sailing)
 - switch engine in coast off (fuel saving)
 - decouple while Braking or during ABS/ESP intervention
- Hybrid
 - instead of eliminated coupling this area can be used for a hybrid disc
- Cost reduction by Integration into DCT
 - one ECU
 - one hydraulic system
 - same pressure control valves

19.6.5 MCLAREN PROACTIVE CHASSIS CONTROL

The McLaren 720S Suspension Is A Complex Masterpiece

<https://www.youtube.com/watch?v=tkwL8lBo2e0>

<https://www.carscoops.com/2017/02/mclaren-details-proactive-chassis/>

Whether drivers will be selecting Comfort, Sport or Track mode, the Proactive Chassis Control II system will make sure to deliver the optimal “balance of cornering grip, dynamic response and comfort”, best suited to the individual mode as well as exterior conditions.

The new system uses 12 more sensors than it did on [previous Super Series models](#), including an accelerometer on each wheel hub, reading inputs from the road while measuring tire contact patch.

The info is then processed in milliseconds by the ‘Optimal Controller’ algorithm sitting at the core of the system, as suspension damping is optimized on the fly.

“Proactive Chassis Control II generates a significant amount of additional grip, but not at the expense of the balance and feel of the car,” said Product Development exec, Mark Vinnels. *“The depth and breadth of handling precision and ride comfort in combination with the peerless level of driver involvement in the second-generation McLaren Super Series is simply extraordinary.”*

Another new feature [to look forward to](#) is the Variable Drift Control, which is said to provide even “greater involvement” for the driver, allowing for variable Electronic Stability Control intensity.

<https://www.sae.org/news/2018/07/mclaren-720s-semi-active-suspension>

The Proactive Chassis Control II suspension system features hydraulic cross-linking (lead image) and “semi-active” dampers. The dampers’ rates are continuously adjustable by means of a needle valve and solenoid which are controlled by a computer in real time (Fig. 2). Although semi-active systems are not new in themselves, there has been a big advance in performance through use of a new algorithm developed in a PhD project at the University of Cambridge to simultaneously optimize the car’s ride and handling response.

19.6.6 A LIRE

Contrôle Global de Châssis appliqué à la sécurité active des véhicules de distribution

Yerlan Akhmetov, 2011

<https://www.theses.fr/161842305>

20 MESURE

20.1 CAPTEURS EMBARQUES SUR VEHICULE

Capteur de lacet : peut être externalisé pour des raisons vibratoires

20.2 MATERIEL

Vbox automotive

<https://www.vboxautomotive.co.uk/index.php/en/applications/handling-dynamics>

Data Loggers

<https://www.vboxautomotive.co.uk/index.php/en/products/data-loggers>

Volant instrumenté

Measurement Steering Wheel MSW

The measurement steering wheel MSW by CORRSYS-DATRON was developed for **simultaneous data acquisition** of the **steering wheel turning angle**, **steering torque** and **steering angle speed**. The steering angle and the steering angle speed derived thereof are obtained by means of a non-contact, optical steering angle sensor. The steering angle can be measured in two measurement ranges ($\pm 200^\circ$ or $\pm 1250^\circ$) at an angular dissolution of 0.05° ; for the steering angle speed a range of $\pm 1000^\circ/\text{s}$ is available. The measurement steering wheel can be easily fitted to the steering column through a center hole; the assembly depth is relatively small. CORRSYS-DATRON article number: 14256.



Capteur optique d'angle de dérive

Slip Angle Sensor SF II

The angle **between the speed vector** at the tire contact patch and **wheel plane** has been defined as the slip angle. The SFII by CORRSYS-DATRON is an optical sensor for non-contact measurements used for the simultaneous acquisition of longitudinal and transversal speeds at the wheel and the slip angle to be derived thereof. The sensor is designed for a **speed range of up to 250 km/h**. The angle range is $\pm 40^\circ$ at a resolution of 0.1° .



The **measurement principle of the correlation-optical, non-contact speed sensor** is based on the structure of the road being projected on an optical grid and a photo receiver located behind the grid. The brightness differences in the road surface lead to a frequency in the photo receiver which is proportional to the speed in the measurement direction.

Roue dynamométrique

Wheel Force Dynamometer RoaDyn P650

The wheel force dynamometer by Kistler is available in versions with DMS-applied dynamometers and stiff, biased piezoelectric measurement sensors. The RoaDyn P650 measurement system uses **piezoelectric measuring technology** and is characterized by a **high natural frequency** of up to 2 kHz and **high sensitivity** across the entire measurement range ($F_x = 45 \text{ kN}$, $F_y = 24 \text{ kN}$, $F_z = 45 \text{ kN}$). It is ageing-resistant and exhibits outstanding stability as well as high linearity. The wheel force dynamometer measures the **wheel force distribution** in circumferential, transverse and vertical directions as well as drive, camber and self-aligning torques. Data is transmitted by telemetry from the rotor to the stator and magnets inside the rotor enable the exact **determination of the wheel turning angle** by using the Hall effect. The onboard electronics system 2000 enables self-identification of the measurement wheel sensors used and performs online calculations of the aforementioned measurands. In addition, further analog signals can be connected to the wheel force dynamometer (e.g. temperature signals of the T³M measurement system by TÜV SÜD Automotive). Kistler article number: 9298B1Q03.



Acquisition synchrone

Synchronous Data Acquisition

Synchronicity of the measured data is of crucial importance in all vehicle dynamics tests. Up to now, the data obtained by different sensors and sensor systems could only be correlated with each other with major error tolerances. The special feature of the data acquisition unit is the generation of a high-precision quartz-stabilized **system cycle with 80 MHz** and a **slope accuracy of 2 ns**. With this system cycle all measurements are synchronized and provided with a real-time stamp. In addition, the internal system cycle can be coherently (in-phase) coupled with an external cycle signal in order to make absolutely synchronous measurements using, for example, the pps signal of a GPS satellite. Besides analogous and digital information, various CAN-Bus systems, LAN and other **asynchronous interfaces are synchronized with the system cycle**. The video cameras used have an external cycle input with which each individual image is accurately timed, thus achieving exact synchronicity here as well. DEWETRON article name: DEWE-501.



20.3 SOCIETES

<https://www.oxts.com/industry/vehicle-dynamics/>

Calspan

21 ESTIMATION

21.1 ESTIMATION D'EFFORTS

21.1.1 A VOIR

N. Msirdi, A. Rabhi, Nabila Zbiri, Y. Delanne. **Vehicle-road interaction modelling for estimation of contact forces.** *Vehicle System Dynamics*, Taylor & Francis, 2004, 43, pp.403--411. [⟨hal-00342867⟩](https://hal.archives-ouvertes.fr/hal-00342867)

Belgacem Jaballah, Kouider M'Sirdi, Aziz Naamane, Hassani Messaoud. **Estimation of Vehicle Longitudinal Tire Force with FOSMO & SOSMO.** *Int. J. on Sciences and Techniques of Automatic control and computer engineering*, 2011, 5 (1), pp.1516-1531. [⟨hal-01479724⟩](https://hal.archives-ouvertes.fr/hal-01479724)

https://www.sta-tn.com/IJ_STA/Papers/volume_5N1_jun_2011/P7_IJSTA_V5N1_11.pdf

Estimation of tire–road friction coefficient

<https://www.tandfonline.com/doi/pdf/10.1080/21642583.2014.985804>

21.1.2 M. DOUMIATI

Domaine de recherche : Système LPV, Commande Hirf, Observation d'état, Commande globale du châssis du véhicule

<http://www.gipsa-lab.grenoble-inp.fr/~moustapha.doumiati/>

Sa thèse

Embedded estimation of vehicle's vertical and lateral tire forces for behavior diagnosis on the road

<http://www.gipsa-lab.grenoble-inp.fr/~moustapha.doumiati/thesis.pdf>

Ses publis

<http://www.gipsa-lab.grenoble-inp.fr/~moustapha.doumiati/publications.html>

dont par exemple

Embedded estimation of the tire/road forces and validation in a laboratory vehicle (2008)

<http://www.gipsa-lab.grenoble-inp.fr/~moustapha.doumiati/Avec08.pdf>

This paper proposes a new estimation process for tire-road forces and sideslip angle. This method uses measurements from currently available standard sensors (suspension sensors, yaw rate, longitudinal/lateral accelerations, steering angle and angular wheel velocities). This estimation process is separated into three principal

blocks: the role of the first block is to estimate vertical tire forces, the second block contains an observer whose principal role is to calculate tire-road forces without a descriptive force model, while in the third block an observer estimates the sideslip angle and the cornering stiffness with an adaptive tire-force model.

These different observers are based on Kalman Filter. The estimation process was applied and compared to real experimental data, notably sideslip angle and wheel force measurements acquired using the INRETS-MA Laboratory car. Experimental results show the accuracy and potential of this approach which enables practical realization of a low cost solution for tire-road contact forces and sideslip angle calculation.

21.2 ESTIMATION DE RAIDEUR DE PNEU

Real-Time Estimation of Tire Stiffness

Max Karjalainen, Msc Thesis, 2016

▷ <http://www.diva-portal.org/smash/record.jsf?pid=diva2%3A956629&dswid=4592>

<https://liu.diva-portal.org/smash/get/diva2:956629/FULLTEXT01.pdf>

21.3 ESTIMATION PARAMETRES VEHICULE

En France, pas mal d'articles venant du labo Heudyasic, en partenariat avec l'INRETS.

Par exemple :

Guillaume Baffet, Ali Charara, Daniel Lechner. Estimation of vehicle sideslip, tire force and wheel cornering stiffness. *Control Engineering Practice*, Elsevier, 2009, 17 (vol17, n11), pp1255-1264.
<https://doi.org/10.1016/j.conengprac.2009.05.005>. [hal-00849264](https://hal.archives-ouvertes.fr/hal-00849264)

La thèse de Kun Jiang à l'UTC en 2016 : <https://tel.archives-ouvertes.fr/tel-01417660/>

Real-time estimation and diagnosis of vehicle's dynamics states with low-cost sensors in different driving conditions

Les thèses encadrées par Ali Charara : <https://www.theses.fr/081388268>

NB : Ali Charara a contribué en 2017 à la création du labo Sivalab entre Renault et Heudyasic

Beaucoup d'articles et de nombreuses thèses encadrées par N.K M'Sirdi (labo SASV au LIS, Univ. Aix-Marseille)
<https://www.theses.fr/061087823>

#PHD **Estimation de la dynamique du véhicule en interaction avec son environnement** (2005)

<http://www.theses.fr/2005VERS0033>

Nacer Kouider M'Sirdi, A. Rabhi, L. Fridman, J. Davila, Y Delanne. **Second order sliding-mode observer for estimation of vehicle dynamic parameters.** International Journal of Vehicle Design, Inderscience, 2008, 48 (3-4), pp.190-207. <10.1504/IJVD.2008.022576>. <hal-01741315>

<https://hal.archives-ouvertes.fr/hal-01741315>

#PHD **Observateurs robustes pour le diagnostic et la dynamique des véhicules** (Jaballah, 2011)

▷ <https://tel.archives-ouvertes.fr/tel-00734379>

Identification des paramètres géométriques et élastocinématiques de mécanismes de liaison au sol automobile (Meissonnier, 2006)

▷ <https://tel.archives-ouvertes.fr/tel-00702270/>

⇒ bof bof (parcouru 09/2020). Parle du système OCP de Michelin (Optimal Contact Patch)

21.4 ESTIMATION D'ANGLE DE DERIVE

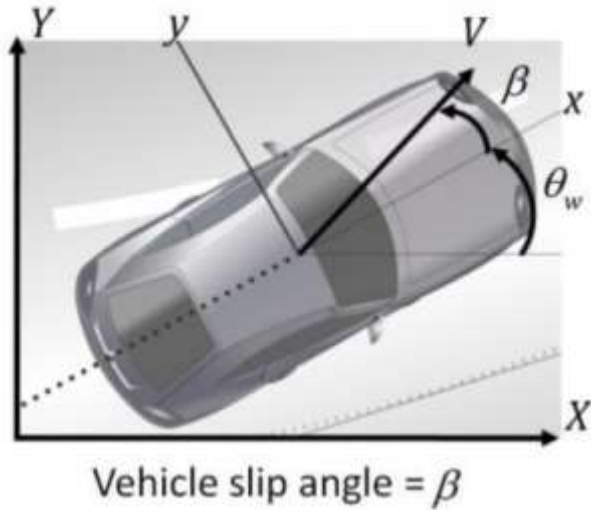
Sujet générateur de quantité d'articles, voir [vehicle sideslip angle estimation](#) sur Google

Côté français, de nombreuses publications de Joanny Stéphant

<https://scholar.google.fr/citations?user=xb9-AOIAAAJ&hl=fr>

Une review récente :

▷ [On the Vehicle Sideslip Angle Estimation: A Literature Review of Methods, Models, and Innovations](#) (2018) avec Basilio Lenzo parmi les auteurs



On peut estimer la position d'un véhicule avec un GPS simple antenne, sa vitesse de lacet avec un gyroscope, mais mesurer l'angle de dérive n'est pas accessible sans un GPS double antenne qui reste onéreux.

Plusieurs chercheurs ont essayé d'obtenir une estimation en s'appuyant sur les données d'un GPS simple antenne et d'une centrale inertie, mais le biais dans la mesure d'accélération induit une dérive dans l'estimation de vitesse qui reste problématique.

Par filtre de Kalman :

- ◇ M. Gadola, D. Chindamo, M. Romano & F. Padula (2014) **Development and validation of a Kalman filter-based model for vehicle slip angle estimation**, Vehicle System Dynamics, 52:1, 68-84, DOI: [10.1080/00423114.2013.859281](https://doi.org/10.1080/00423114.2013.859281)

Une publi plus récente, toujours sur base de filtres de Kalman :

Villano, E., Lenzo, B. & Sakhnevych, A. **Cross-combined UKF for vehicle sideslip angle estimation with a modified Dugoff tire model: design and experimental results**. Meccanica (2021).

- ◇ <https://doi.org/10.1007/s11012-021-01403-6>

<https://www.oxts.com/technical-notes/slip-angle-measurement-advanced/>

When it comes to measuring slip angle, accuracy means something very small indeed. ISO15037 recommends a maximum error of 0.5°, although most end users require much better accuracy than this because even a change of 0.5° in slip angle is significant in vehicle dynamics. But if you want to capture slip angle data with any confidence in its accuracy, it pays to understand how it's measured and what you can do to minimise the sources of error that affect all GPS or inertial navigation slip angle devices.

You should also be aware slip angle accuracy changes with speed—something that often puzzles end-users. To calculate an object's track angle, GPS and inertial measurement systems take the arctangent of the east and north velocities [$\text{atan}(\text{Ve}/\text{Vn})$]. Bearing in mind these instruments measure velocity with a relatively fixed accuracy of, say 0.1 km/h, it seems obvious a small error like this is proportionally more significant at low speeds. That's why slip angle accuracy improves with speed.

If you know the speed you want to conduct your slip angle tests at, you can calculate the expected accuracy of any system with the following function:

$$\text{slip angle accuracy} = \sqrt{\text{heading accuracy}^2 + \tan^{-1} \left(\frac{\text{velocity accuracy}}{\text{speed}} \right)^2}$$

The importance of this is clear if you consider a vehicle with a wheelbase of 3 metres. Assuming a steer angle of 3° the measuring device needs to be located within 50 centimetres horizontally of the point of interest. To achieve a slip angle accuracy of 0.1° this decreases to 10 centimetres.

The same is true vertically because the roll rate of vehicles during dynamic tests can be as high as 1 radian/s. If the vertical distance between the point you're interested in and the point you're measuring from is 1 metre, it can affect the lateral velocity by up to 1 m/s. This in turn throws the slip angle off by nearly 3° at 72 km/h. For 0.5° accuracy it's important to mount the instrument within 50 centimetres vertically of the point you wish to measure or your data will be inaccurate during dynamic tests.

Une solution peut être de construire un observateur s'appuyant sur des données déjà existantes et utilisées par le contrôle de stabilité du véhicule, c'est le cas de la publication suivante :

Gridsada Phanomchoeng, Ali Zemouche, Rajesh Rajamani. Real-time automotive slip angle estimation with extended H_∞ circle criterion observer for nonlinear output system. American Control Conference, ACC 2017, May 2017, Seattle, WA, United States

<https://hal.archives-ouvertes.fr/hal-01541110/document>

Many active vehicle safety systems such as electronic stability control (ESC), rollover prevention, and lane departure avoidance could benefit from knowledge of the vehicle slip angle. However, it is a challenge to design an observer to estimate slip angle reliably under a wide range of vehicle maneuvers and operating conditions. This is due especially to nonlinear tire characteristics and system models which have nonlinear output equations. Hence this paper develops an extended H_∞ circle criterion observer for state estimation in systems with nonlinear output equations. The observer design approach utilizes a modified Young's relation to include additional degrees of freedom in the linear matrix inequality (LMI) used for observer gain design. This enhanced LMI is less conservative than others proposed in the literature for Lipschitz nonlinear systems, both with and without nonlinear output equations. The observer is applied to slip angle estimation and utilizes inexpensive sensors available in all modern vehicles. Finally, experimental tests on a Volvo XC90 sport utility vehicle are used to evaluate the developed approach. The experimental results show that the slip angle estimates for a variety of test maneuvers on road surfaces with different friction coefficients are reliable.

(...)

Several slip angle estimation approaches have been developed, which can be categorized into two groups: kinematics-based methods and vehicle-model-based methods. **The kinematics-based approaches are very sensitive to sensor error**, particularly sensor bias error, which causes a drift. **The vehicle-model-based methods are relatively robust against sensor bias errors. However, they rely on the accuracy of the vehicle model, vehicle parameters and tire parameters and knowledge of road conditions.** Also, most of the observer-based slip angle estimation methods published in literature rely on linear vehicle models. Therefore, when the vehicle is skidding and the slip angle becomes large, these estimation methods will not be reliable.

21.5 ESTIMATION DE LA VITESSE

Low-Cost Sensor for Vehicle Speed Based on Sliding Mode Observer

<https://hal.archives-ouvertes.fr/hal-01741307>

21.6 ESTIMATION D'EFFORT AMORTISSEUR

Comparison of several robust observers for automotive damper force estimation

<https://hal.archives-ouvertes.fr/hal-02156880/document>

NB : L'observateur est construit à partir des accélérations mesurées sur un quart de véhicule

21.7 A LIRE

Estimation and prediction of vehicle dynamics states based on fusion of OpenStreetMap and vehicle dynamics models

<https://hal.archives-ouvertes.fr/hal-01310763/file/IV16KUNv6.R9SrN.pdf>

22 CONTROLE (THEORIE)

22.1 LITTERATURE

22.1.1 QUELQUES DOCS DE BASE

Introduction to vehicle dynamics control (O.Sename, 2017)

http://hal.univ-grenoble-alpes.fr/hal-01661033/file/IVSS2017_GCC_V2.pdf

Towards Global chassis control approaches

Two main approaches, one considering the vehicle as a MIMO system, the other developing a "super controller" for the local actuators. Some references : Lu and DePoyster (2002), Shibahata (2005), Chou and d'Andréa Novel (2005), Andreasson and Bunte (2006), Falcone et al. (2007a), Falcone et al. (2007b), Gáspár et al. (2008), Fergani and Sename (2016)...

Vehicle considered as a MIMO system

- This approach consists in considering the vehicle as a global MIMO system and in designing a controller that solves all the dynamical problems by directly controlling the various actuators with the available measurements. No local controller is considered (no inner loop). See, for instance Lu and DePoyster (2002), Chou and d'Andréa Novel (2005), Andreasson and Bunte (2006), Gáspár et al. (2008), Fergani et al (2016).

High level reference super controller

- The second approach consists in designing a controller which aims at providing somehow, the reference signals to local controllers, which have been previously designed to solve a local subsystem problem (e.g. ABS). Thus, this controller, more than a controller, "monitors" the local controllers. Therefore, such a controller solves the global vehicle dynamical problems, playing the role of "super controller". See also Falcone et al. (2007a).

Human Control of a Bicycle: Jason K. Moore

<http://moorepants.github.io/dissertation/#>

avec un notebook très bien illustré ici :

<https://plot.ly/python/v3/ipython-notebooks/bicycle-control-design/>

22.1.2 REVIEWS

△ Etsuo Katsuyama, Makoto Yamakado & Masato Abe (2021) **A state-of-the-art review: toward a novel vehicle dynamics control concept taking the driveline of electric vehicles into account as promising control actuators**, Vehicle System Dynamics, 59:7, 976-1025

<https://doi.org/10.1080/00423114.2021.1916048>

22.1.3 AUTEURS

Ali Charara

<https://www.hds.utc.fr/~acharara/dokuwiki/fr/recherche>

Directeur de l'UMR Heudiasyc de 2008 à 2017

Voir l'ensemble de ses publis : https://www.hds.utc.fr/~acharara/dokuwiki/fr/publis_hal

M. Doumiati

(cf §21.1.2)

Luc Dugard (Gipsa)

https://www.gipsa-lab.grenoble-inp.fr/page_pro.php?vid=217

<https://www.theses.fr/035740086>

Olivier Sename (Gipsa)

<https://www.gipsa-lab.grenoble-inp.fr/~o.sename/index.html>

<https://www.theses.fr/106980130>

Projet INOVE (avec Soben)

<http://www.gipsa-lab.fr/projet/inove/index.html>

Basilio Lenzo

<https://ieeexplore.ieee.org/author/37085461265>

Guillermo Pita Gil

Application de techniques de commande avancées dans le domaine automobile (2011)

<https://tel.archives-ouvertes.fr/tel-00591522/>

Les travaux effectués lors de cette thèse se sont focalisés sur les applications des méthodes et techniques d'Automatique avancée à des problématiques actuelles de l'automobile. Les sujets abordés ont porté sur trois axes fondamentaux en s'appuyant sur des techniques telles que la synthèse H infini LTI et q-LPV, la linéarisation par

bouclage dynamique, la retouche de correcteurs de type PI en particulier et l'optimisation des pondérations des filtres nécessaires aux synthèses H infini :

- Contrôle de la trajectoire d'un véhicule automobile. Nous avons proposé une structure de commande reprenant une démarche classiquement mise en œuvre dans le milieu aéronautique ou spatial.
- Contrôle de la chaîne d'air d'un moteur essence, turbocompressé. Nous avons proposé une formulation novatrice de type q-LPV du modèle du moteur. Cette formulation d'un nouveau modèle de commande nous a permis de synthétiser des correcteurs évolués à paramètres variables qui s'adaptent automatiquement au point de fonctionnement.
- Contrôle du freinage d'un véhicule électrique. Pour cette partie, nous avons précisé la motivation et l'intérêt des véhicules électriques, puis étudié le gain d'autonomie potentiellement accessible par la mise en œuvre d'une récupération d'énergie au freinage. Finalement, des solutions permettant de réduire les oscillations induites dans la chaîne de traction par des demandes de couple freineur à la machine électrique ont été développées.

22.1.4 THESES

Application de techniques de commande avancées dans le domaine automobile (Guillermo Pita-Gil, 2011)

Approche LPV pour la commande robuste de la dynamique des véhicules (Anh-Lam Do, 2011)

Robust multivariable control for vehicle dynamics (Fergani, 2014)

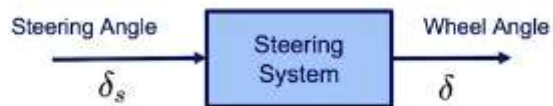
22.2 CONSTRUIRE DES MODELES SIMPLES

<https://www.coursera.org/lecture/intro-self-driving-cars/lesson-6-vehicle-actuation-fSAQG>

22.2.1 DIRECTION

L'hypothèse la plus simple fait l'affaire pour du contrôle "pas à la limite" :

Simple Steering Model



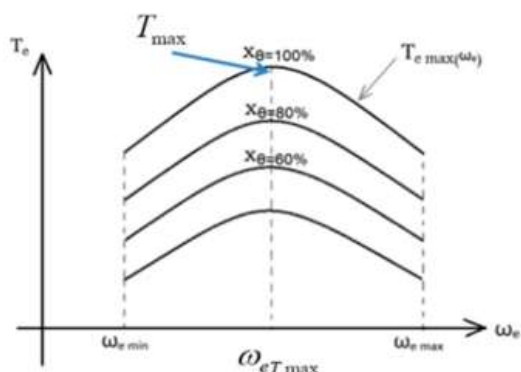
$$\delta = c\delta_s$$



22.2.2 GMP

Pour le GMP, on peut prendre un polynôme du 2nd degré pour un moteur ICE :

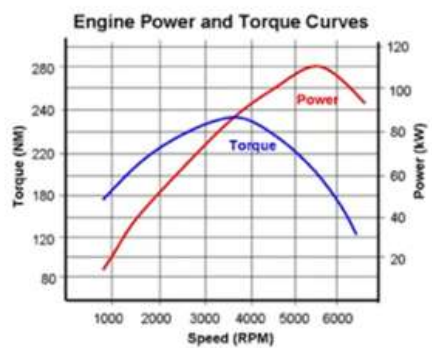
Typical Torque Curves for Gasoline Engines



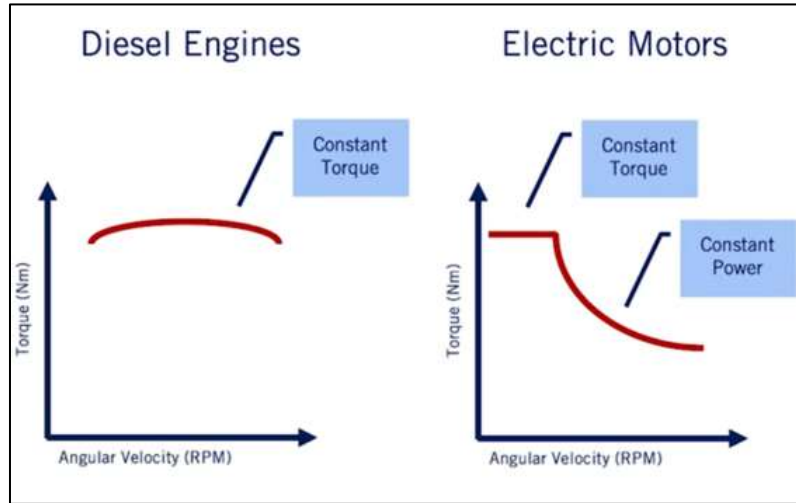
$$T_{e \max}(\omega_e) = A_0 + A_1 \omega_e + A_2 \omega_e^2$$

$$T_e(\omega_e, x_\theta) \approx x_\theta (A_0 + A_1 \omega_e + A_2 \omega_e^2)$$

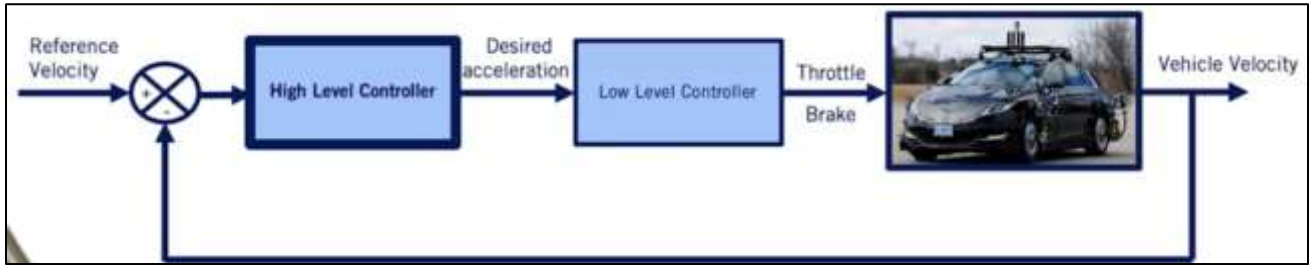
Throttle position (percentage)



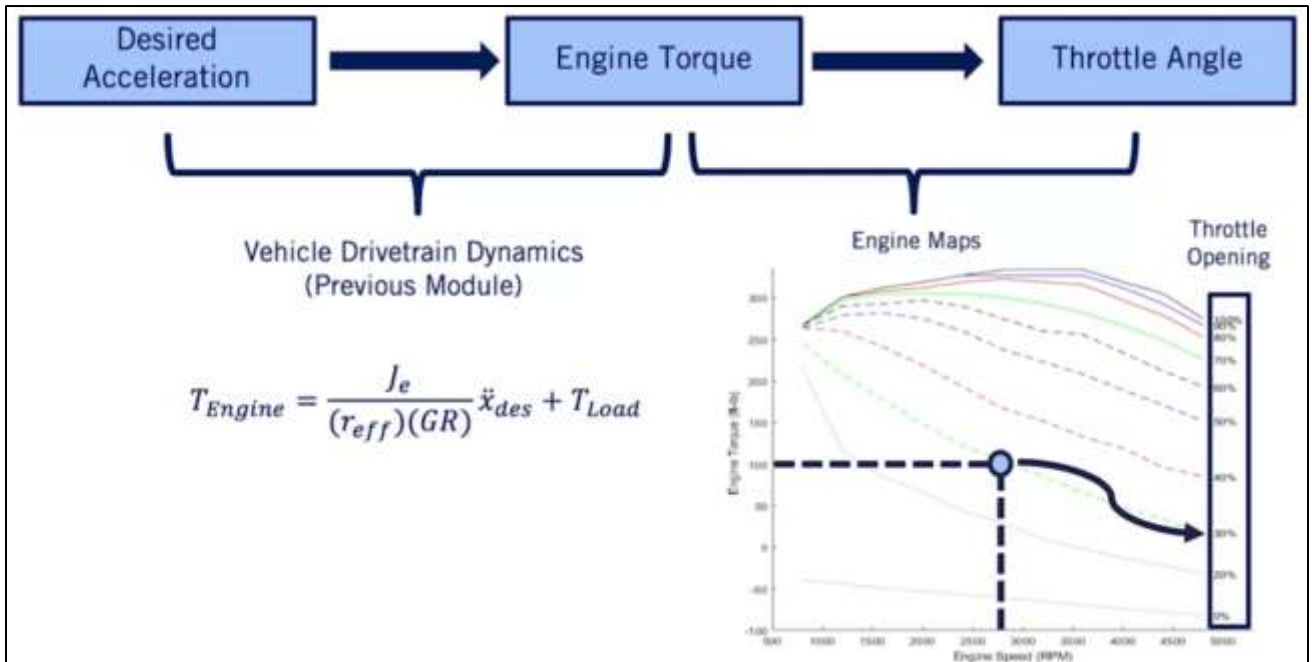
Et pour d'autres motorisations :



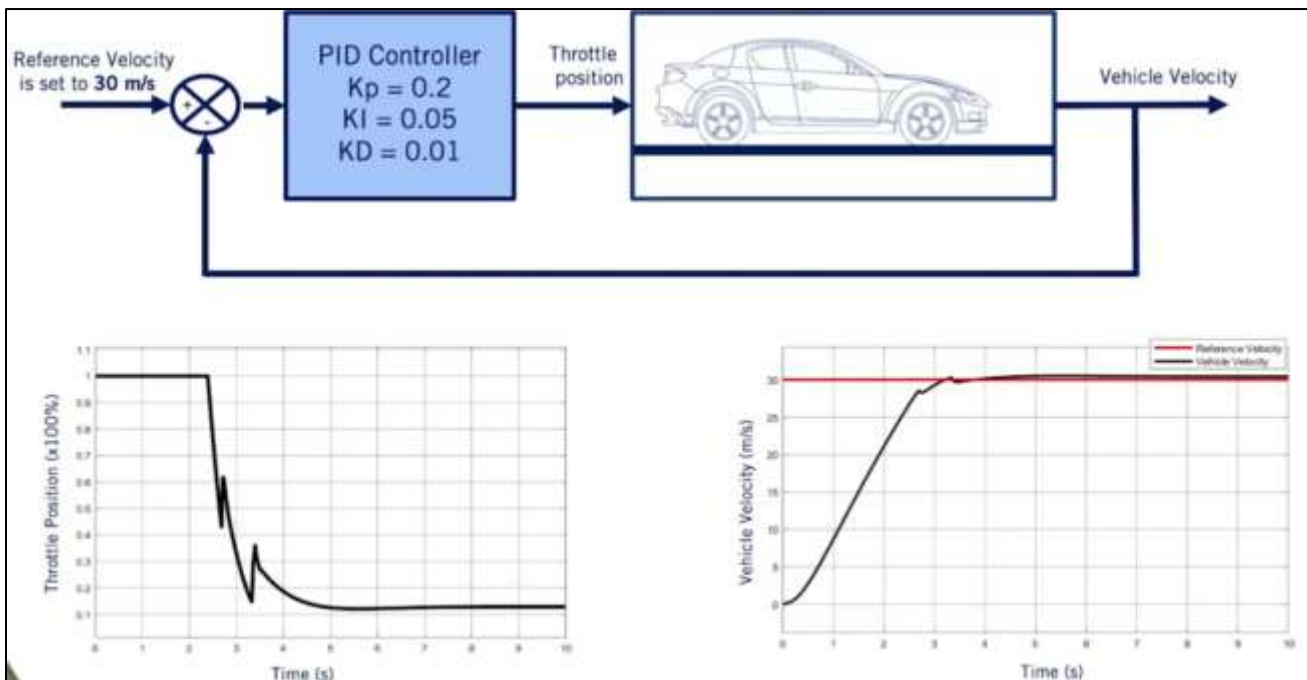
Le contrôle est ensuite généralement décomposé en deux niveaux :



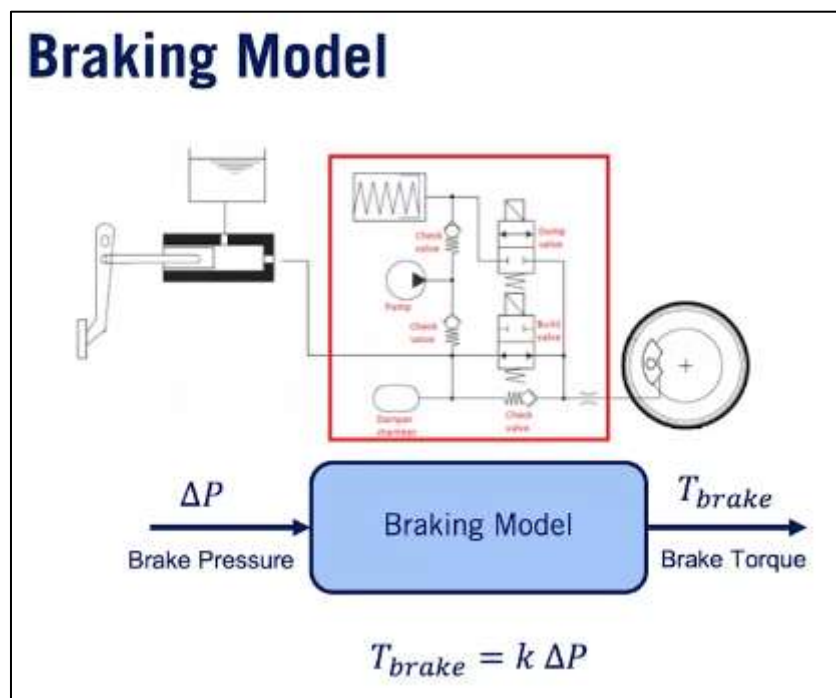
On peut utiliser un PID pour le contrôle haut niveau, et s'appuyer sur le modèle de GMP pour la partie bas niveau :



Exemple :



22.2.3 FREINAGE



22.3 CONTRÔLE LATÉRAL

22.3.1 INTRO

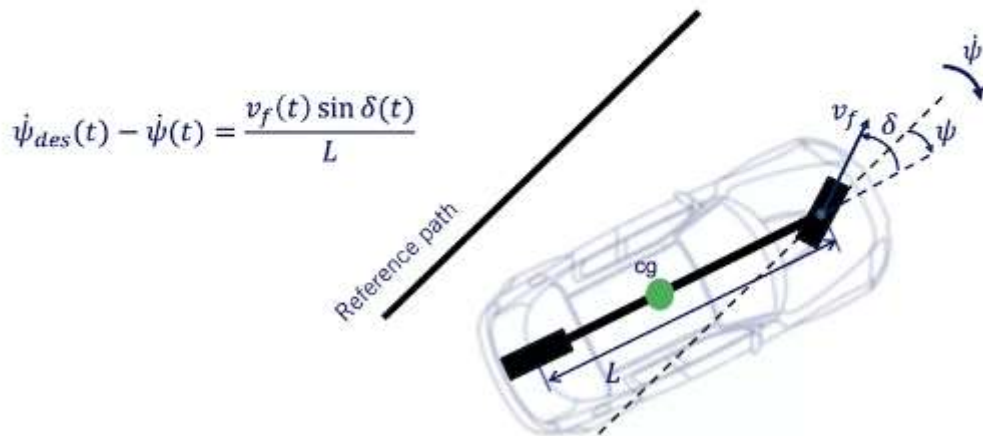
Plusieurs techniques existent :

Two Types of Control Design

- Geometric Controllers
 - Pure pursuit (carrot following)
 - Stanley
- Dynamic Controllers
 - MPC control
 - Other control systems
 - Sliding mode, feedback linearization

Heading error :

- Controller error terms
 - Heading error
 - Component of velocity perpendicular to trajectory divided by ICR radius

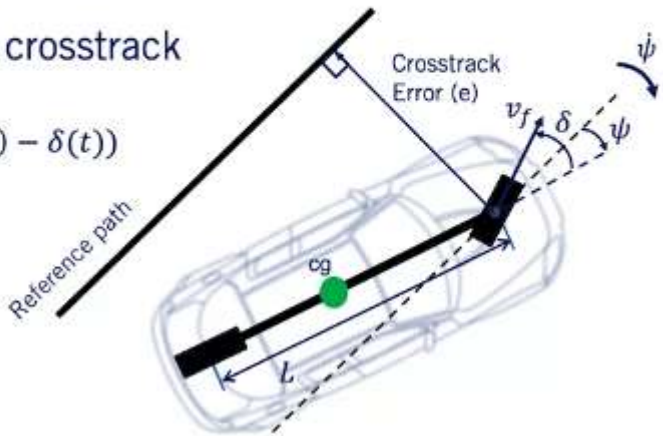


Crosstrack error :

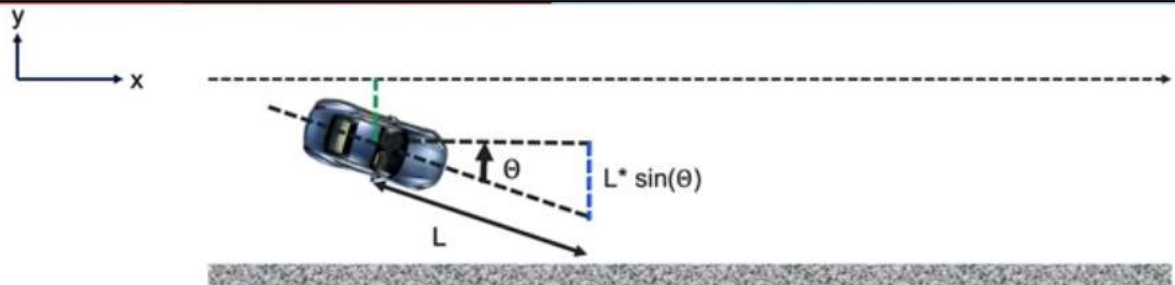
- Crosstrack error (e) :
 - Distance from center of front axle to the closest point on path

- Rate of change of crosstrack error (\dot{e})

$$\dot{e}(t) = v_f(t) \sin(\psi(t) - \delta(t))$$



Un terme d'erreur proposé ici



Goal:

- Keep the car driving along the Centerline: $y=0$
- Drive Parallel to the walls: $L \cdot \sin(\theta) = 0$

→ Error Term: $e(t) = - (y + L \cdot \sin(\theta))$

22.3.2 PURE PURSUIT MODEL

Présentation claire dans ce Jupyter Notebook découvert en 2021 :

<https://thomasfermi.github.io/Algorithms-for-Automated-Driving/Control/PurePursuit.html>

Sur la chaîne de UPenn

[ESWeek 2021 - Education Lecture - Learn to Drive \(and Race!\) Autonomous Vehicles - Part II: PP](#) (10/2021)

How do we get steering angle?

$$r = \frac{L^2}{2|y|}$$

Curvature is the inverse of radius
Steering angle should be proportional to the curvature of the arc

$$\gamma = \frac{1}{r} = \frac{2|y|}{L^2}$$

Penn Engineering

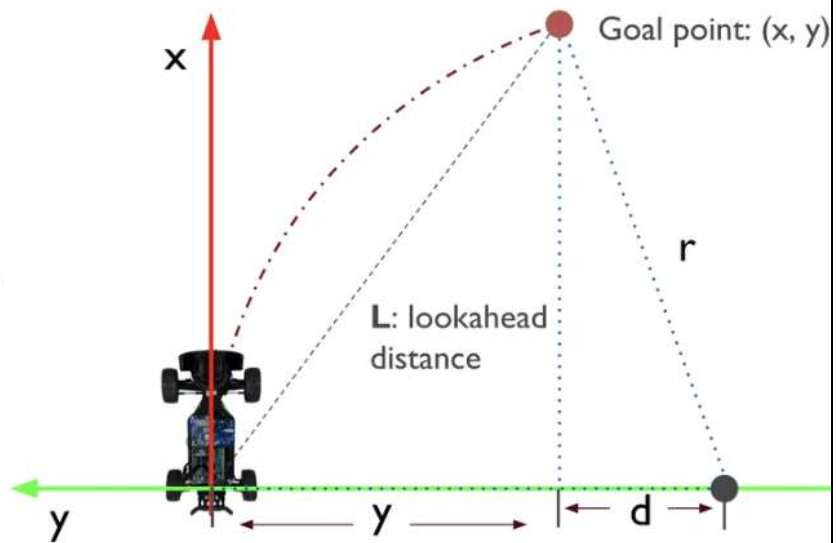
How do we get steering angle?

γ is the curvature. Using the bicycle model (defines the dynamics of the vehicle):

$$R = L / \tan(\delta)$$

So the final steering angle δ can be calculated as:

$$\delta = 1/R = 2*y / L^2$$



22.3.3 STANLEY

<https://fr.mathworks.com/help/driving/ref/lateralcontrollerstanley.html>

Présent dans Matlab depuis la 2018b, il s'agit de l'implémentation réalisée par Stanford sur le VW Touareg prénommé « Stanley » ayant concouru au Darpa Challenge en 2005.

[1] Hoffmann, Gabriel M., Claire J. Tomlin, Michael Montemerlo, and Sebastian Thrun. "Autonomous Automobile Trajectory Tracking for Off-Road Driving: Controller Design, Experimental Validation and Racing." *American Control Conference*. 2007, pp. 2296–2301. doi:10.1109/ACC.2007.4282788

https://www.researchgate.net/publication/224718332_Autonomous_Automobile_Trajectory_Tracking_for_Off-Road_Driving_Controller_Design_Experimental_Validation_and_Racing

Vehicle Path Tracking Using Stanley Controller

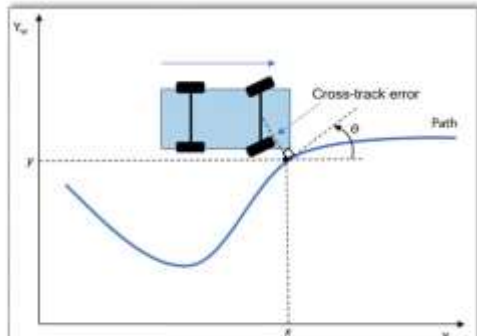
<https://www.youtube.com/watch?v=FHQFya0-JBs> (Mathworks, 10/2021)

Stanley Controller

Formulation

$$\delta(t) = \begin{cases} \psi(t) + \arctan\left(\frac{ke(t)}{v(t)}\right) & \text{if } \left|\psi(t) + \arctan\left(\frac{ke(t)}{v(t)}\right)\right| < \delta_{\max} \\ \delta_{\max} & \text{if } \left|\psi(t) + \arctan\left(\frac{ke(t)}{v(t)}\right)\right| \geq \delta_{\max} \\ -\delta_{\max} & \text{if } \left|\psi(t) + \arctan\left(\frac{ke(t)}{v(t)}\right)\right| \leq -\delta_{\max} \end{cases}$$

$\delta(t)$ = Steering angle
 $\psi(t)$ = Yaw angle
 $e(t)$ = Cross-track error



L'algorithme est détaillé dans la publication Automatic Steering Methods for Autonomous Automobile Path Tracking

△ <https://www.ri.cmu.edu/publications/automatic-steering-methods-for-autonomous-automobile-path-tracking/>

de Carnegie Mellon

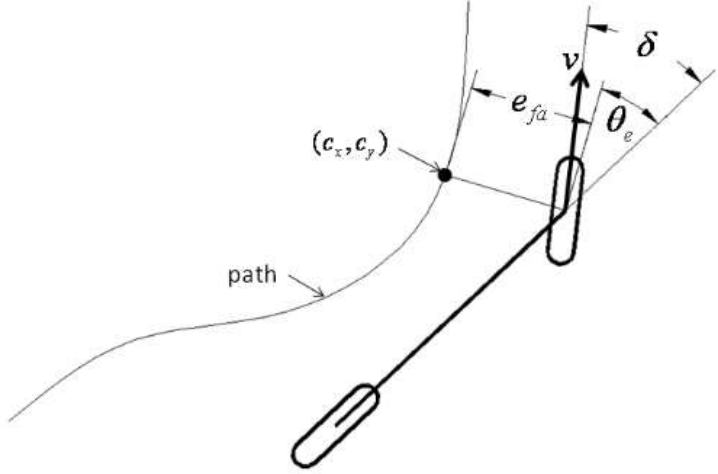


Figure 14: Stanley method geometry

The Stanley method [16] is the path tracking approach used by Stanford University's autonomous vehicle entry in the DARPA Grand Challenge, Stanley. The Stanley method is a nonlinear feedback function of the cross track error e_{fa} , measured from the center of the front axle to the nearest path point (c_x, c_y) , for which exponential convergence can be shown [16]. Co-locating the point of control with the steered front wheels allows for an intuitive control law, where the first term simply keeps the wheels aligned with the given path by setting the steering angle δ equal to the heading error

$$\theta_e = \theta - \theta_p,$$

where θ is the heading of the vehicle and θ_p is the heading of the path at (c_x, c_y) . When e_{fa} is non-zero, the second term adjusts δ such that the intended trajectory intersects the path tangent from (c_x, c_y) at $kv(t)$ units from the front axle. Figure 14 illustrates the geometric relationship of the control parameters. The resulting steering control law is given as

$$\delta(t) = \theta_e(t) + \tan^{-1} \left(\frac{ke_{fa}(t)}{v_x(t)} \right), \quad (5)$$

where k is a gain parameter. It is clear that the desired effect is achieved with this control law: As e_{fa} increases, the wheels are steered further towards the path.

22.3.4 B. DOUGLAS

Rien de fondamental dans cette vidéo, mais un rappel des notions de commandabilité et observabilité (cf bible contrôle) : <https://www.youtube.com/watch?v=BYvTEfNAi38>

Thought exercise...


$$\dot{x} = A \cdot \begin{bmatrix} P_x \\ P_y \\ \dot{P}_x \\ \dot{P}_y \\ \theta \\ \dot{\theta} \end{bmatrix} + B \cdot \begin{bmatrix} \text{steering} \\ \text{pedals} \end{bmatrix}$$
$$y = C \cdot \begin{bmatrix} P_x \\ P_y \\ \dot{P}_x \\ \dot{P}_y \\ \theta \\ \dot{\theta} \end{bmatrix} + D \cdot \begin{bmatrix} \text{steering} \\ \text{pedals} \end{bmatrix}$$

22.3.5 CONTRÔLE LATÉRAL ET DEEP LEARNING

Dans la thèse de Guillaume Devineau :

Coupled Longitudinal and Lateral Control of a Vehicle using Deep Learning

<https://www.youtube.com/watch?v=yyWy1uavIXs>

22.4 CONTRÔLE LONGI

22.4.1 FREINAGE

Application of linear optimal preview control theory to severe braking of a car (R.S Sharp, 2011)

<https://journals.sagepub.com/doi/abs/10.1177/2041298310392852>

22.4.2 ANTI-JERK

Anti-jerk controllers for automotive applications: A review (2020)

<https://www.sciencedirect.com/science/article/pii/S1367578820300237>

22.4.3 CONTRÔLE DU TANGAGE PAR LE MOTEUR

Adopté par Nissan sur Maxima, Qashqai, Micra (!) : l'Intelligent Ride Control se base sur les mesures des vitesses de roue pour en déduire l'écrasement des flancs, et déterminer cabrage ou plongée du véhicule. Lorsque le nez se soulève, le couple moteur est instantanément réduit pour limiter la tendance (ndec : ???)

22.5 INDICATEURS DE PERFORMANCE

Dans [On pre-emptive vehicle stability control](#) (2021), on trouve les indicateurs de performance suivants, pour un contrôleur type MPC qui fait du latéral et aussi du longi via du trail braking :

3.3. Performance indicators

Objective performance indicators are used to assess the performance of the vehicle configurations along the manoeuvres, namely:

- V_{crit} , i.e. the critical speed, which is the maximum entry speed – the higher the better – at which the considered vehicle configuration manages to successfully complete the obstacle avoidance. In this study, such speed is taken 20 m in advance of the standard obstacle avoidance course, to consider the effect of the predictive trail braking control actions;
- V_{fin} , i.e. the final speed at the exit point of the obstacle avoidance course. A good tuning of the controller should slow down the vehicle as little as possible;
- $RMS(e_{\dot{\psi}})$, i.e. the root mean square value (RMS) of the yaw rate error $e_{\dot{\psi}}$, which assesses the yaw rate tracking performance:

$$RMS(e_{\dot{\psi}}) = \sqrt{\frac{1}{T_{fin} - T_{in}} \int_{T_{in}}^{T_{fin}} [\dot{\psi}_{ref} - \dot{\psi}]^2 dt} \quad (48)$$

where T_{in} and T_{fin} are the initial and final times of the relevant part of the test, corresponding to the condition of the vehicle entering and exiting the obstacle avoidance course, and t is time;

- $|\alpha_{R,max}|$, i.e. the maximum absolute value of the rear axle sideslip angle during the test, which is an indicator of the level of vehicle stability;
- $IA_{\delta_{SW}}$, i.e. the normalised integral of the absolute value of the steering wheel angle δ_{SW} , which assesses the steering effort made by the virtual driver model to follow the desired path:

$$IA_{\delta_{SW}} = \frac{1}{T_{fin} - T_{in}} \int_{T_{in}}^{T_{fin}} |\delta_{SW}| dt \quad (49)$$

- $IA_{\Delta\delta_{SW}}$, i.e. the normalised integral of the absolute value of the steering wheel rate $\dot{\delta}_{SW} = d\delta_{SW}/dt$, which also assesses the level of steering effort:

$$IA_{\Delta\delta_{SW}} = \frac{1}{T_{fin} - T_{in}} \int_{T_{in}}^{T_{fin}} |\dot{\delta}_{SW}| dt \quad (50)$$

- $IA_{\Delta F_x}$, i.e. the integral of the absolute value of the longitudinal tyre force difference among the two vehicle sides, which assesses the intensity of the direct yaw moment control effort:

$$\begin{aligned} IA_{\Delta F_x} &= \frac{1}{T_{fin} - T_{in}} \int_{T_{in}}^{T_{fin}} |F_{x,FL} - F_{x,FR} + F_{x,RL} - F_{x,RR}| dt \\ &\approx \frac{1}{R_w(T_{fin} - T_{in})} \int_{T_{in}}^{T_{fin}} |\tau_L - \tau_R| dt \end{aligned} \quad (51)$$

where, in the computation of the indicator, the left and right tyre forces are approximated as the ratios of the side wheel torque, output by the controller, to the wheel radius;

- $IA_{F_{x,tot}}$, i.e. the normalised integral of the absolute value of the longitudinal tyre force reduction imposed by the controller, which provides an indication of the trail braking control effort:

$$IA_{F_{x,tot}} = \frac{1}{T_{fin} - T_{in}} \int_{T_{in}}^{T_{fin}} |F_{x,ref} - [F_{x,FL} + F_{x,FR} + F_{x,RL} + F_{x,RR}]| dt$$

$$\approx \frac{1}{T_{fin} - T_{in}} \int_{T_{in}}^{T_{fin}} \left| F_{x,ref} - \frac{1}{R_w} [\tau_L + \tau_R] \right| dt \quad (52)$$

Raksincharoensak P, Daisuke S, Lidberg M. **Direct Yaw Moment Control for Enhancing Handling Quality of Lightweight Electric Vehicles with Large Load-To-Curb Weight Ratio.** *Applied Sciences*. 2019; 9(6):1151. <https://doi.org/10.3390/app9061151>

Abstract : In this paper a vehicle dynamics control system is designed to compensate the change in vehicle handling dynamics of lightweight vehicles due to variation in loading conditions and the effectiveness of the proposed design is verified by simulations and an experimental study using a fixed-base driving simulator.

On trouve le critère suivant, utilisé pour quantifier l'efficacité d'un contrôleur sur une manœuvre de type double changement de file :

- Emergency Avoidance Performance Index, (EAPI):

Here, the index called EAPI is determined as the area which is integrated along the curve of steering angle with respect to the yaw rate. It is generally known that the better the vehicle handling quality, the smaller the value of EAPI [28].

$$S = \frac{1}{2} \int_0^T \left(\delta_{sw}^2 + r^2 \right) d \left(\tan^{-1} \left(\frac{r}{\delta_{sw}} \right) \right) = \frac{1}{2} \int_0^T \left(\delta_{sw} r - \delta_{sw} r \right) dt. \quad (38)$$

Dans une présentation de Red Cedar utilisant Heeds, on trouve :

- ▶ Define a drivability metric which considers work done by the driver:

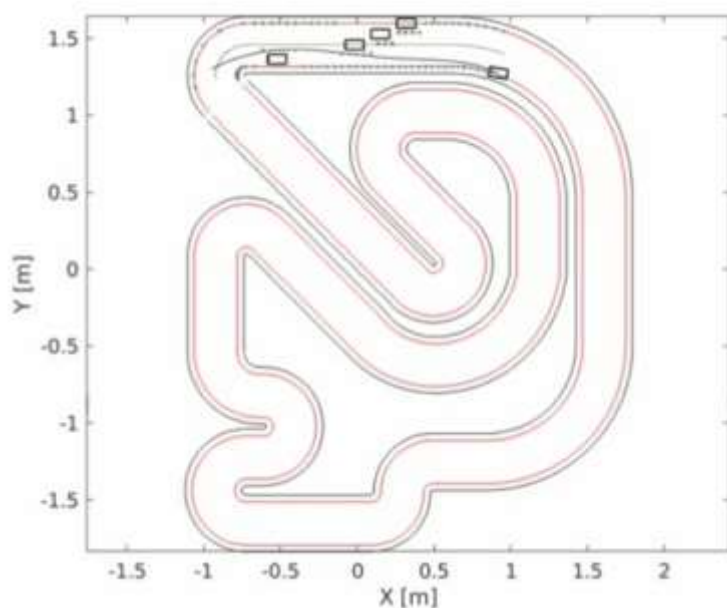
$$\text{Steering work} = \int_0^{\text{lap time}} \text{Steering Torque}(t) \times \text{Steering velocity}(t) dt$$

22.6 MODEL PREDICTIVE CONTROL

22.6.1 MPCC (ALEX LINIGER)

Model Predictive Contouring Controller (MPCC) for Autonomous Racing

<https://github.com/alexliniger/MPCC>



22.7 COMMANDE OPTIMALE / LPV

Giacomo Perantoni & David J.N. Limebeer (2014) **Optimal control for a Formula One car with variable parameters**, Vehicle System Dynamics, 52:5, 653-678, DOI: [10.1080/00423114.2014.889315](https://doi.org/10.1080/00423114.2014.889315)



ECOLE DES MINES DE NANTES

Tutoriel : La commande LPV
GR MOSAR, 20 septembre 2007 - Nantes (13)



- Paramètre variant : vitesse longitudinale du véhicule
- Le modèle bicyclette (quasi-LPV):
 - $$\begin{bmatrix} \dot{\beta} \\ \dot{r} \\ \dot{\psi}_L \\ \dot{y}_L \end{bmatrix} = \begin{bmatrix} \frac{a_{11}}{V} & -1 + \frac{a_{12}}{V^2} & 0 & 0 \\ a_{21} & \frac{a_{22}}{V} & 0 & 0 \\ 0 & 1 & 0 & 0 \\ V & I_s & V & 0 \end{bmatrix} \begin{bmatrix} \beta \\ r \\ \psi_L \\ y_L \end{bmatrix} + \begin{bmatrix} b_1 \\ b_2 \\ 0 \\ 0 \end{bmatrix} \delta_f + \begin{bmatrix} e_{11} \\ e_{22} \\ 0 \\ 0 \end{bmatrix} f_w + \begin{bmatrix} 0 \\ 0 \\ -F \\ 0 \end{bmatrix} \rho_w$$

β : angle de dérive
 r : vitesse de lacet
 ψ_L : erreur sur l'angle de cap
 y_L : déplacement latéral
 f_w : force de vent latéral
 V : vitesse longitudinale
 ■ δ_f : angle de braquage des roues avant



[source](#)

Quelques développements sur le contrôle de la dynamique de véhicule : une approche LPV du problème
<https://www.gipsa-lab.grenoble-inp.fr/~o.sename/docs/CIFA2012pl.pdf>

Quelques développements sur le contrôle de la dynamique
de véhicule : une approche LPV du problème

[Olivier Sename et Luc Dugard](#)

Gipsa-lab, UMR CNRS 5216, Département Automatique, France
[\(olivier.sename,luc.dugard@gipsa-lab.fr](mailto:(olivier.sename,luc.dugard@gipsa-lab.fr)

La thèse d'Anh-Lam Do : approche LPV pour commande robuste
<https://tel.archives-ouvertes.fr/tel-00822010>

Charles Poussot-Vassal : <https://sites.google.com/site/charlespoussotvassal/home>

Sa thèse [Commande robuste LPV multivariable de châssis automobile](#)

22.8 CONTROLE GLISSEMENT ROUE

22.8.1 SLIDING MODE

A. El Hadri, Cadiou J.C., Kouider M'Sirdi, Delanne Y.. **Wheel slip regulation based on sliding mode approach.** SAE, 2002, Transactions Journal of Passenger Cars - Mechanical Systems (ISBN 0-7680-1102--7). [⟨hal-01479755⟩](https://hal-01479755/)

22.8.2 FUZZY CONTROL

Jun, L., Jianwu, Z., and Fan, Y., "An Investigation into Fuzzy Control for Anti-Lock Braking System Based on Road Autonomous Identification," SAE Technical Paper 2001-01-0599, 2001, <https://doi.org/10.4271/2001-01-0599>.

22.9 APPLICATION VÉHICULE AUTONOME

Cohérence entre la modélisation et les objectifs de contrôle pour les véhicules autonomes (2017)

<https://hal-mines-paristech.archives-ouvertes.fr/hal-01473160/document>

Thomas Fermi, Algorithms for Automated Driving

<https://thomasfermi.github.io/Algorithms-for-Automated-Driving/Introduction/intro.html>

22.10 CONTRÔLE CHASSIS ET EFFICACITÉ ÉNERGÉTIQUE

22.10.1 BASILIO LENZO

De nombreuses publications sur le sujet

Par exemple

SFORZA, A, LENZO, Basilio and TIMPONE, F (2019). **A state-of-the-art review on torque distribution strategies aimed at enhancing energy efficiency for fully electric vehicles with independently actuated drivetrains.** International Journal of Mechanics and Control, 20 (2), 3-15.

http://shura.shu.ac.uk/25806/1/Sforza_Lenzo_Timpone.pdf

To the knowledge of the authors, for the first time this paper experimentally compares and critically analyses the

potential energy efficiency benefits achievable through the appropriate set-up of the reference understeer characteristics and wheel torque CA. Interestingly, the experiments on a four-wheel-drive EV demonstrator show that higher energy savings can be obtained through the appropriate tuning of the reference cornering response rather than with an energy-efficient CA.

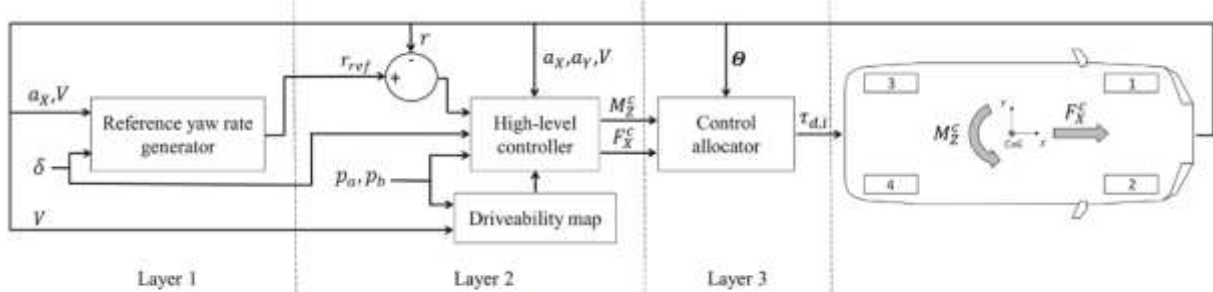


Fig. 2. Simplified schematic of the vehicle control system.

CA = Control Allocation

GRUBER, P, SORNIOTTI, A, LENZO, Basilio, DE FILIPPIS, G and FALLAH, S (2016). **Energy efficient torque vectoring control**. In: AVEC '16 : 13th International Symposium on Advanced Vehicle Control, Munich, Germany, 13-16 September, 2016. CRC Press. (In Press)

http://shura.shu.ac.uk/13974/1/Lenzo%20Energy%20efficient%20torque%20vectoring%20control_Final.pdf

DE FILIPPIS, Giovanni, LENZO, Basilio, SORNIOTTI, Aldo, GRUBER, Patrick, SANNEN, Koen and DE SMET, Jasper (2016). **On the energy efficiency of electric vehicles with multiple motors**. In: 13th IEEE Vehicle Power and Propulsion Conference, Hangzhou, China, 17-20 October, 2016. (Unpublished)

<http://shura.shu.ac.uk/13976/1/Defilippis2016energy.pdf>

22.11 CONTRÔLE À LA LIMITE

Voir également le §0

Voir la thèse de Jonathan Goh à Stanford, sur un proto base DeLorean (2019)

<https://ddl.stanford.edu/content/jonathan-goh>

Car driving at the limit by adaptive linear optimal preview control (2008)

<https://core.ac.uk/download/pdf/20365456.pdf>

The Optimality of the Handbrake Cornering Technique (2014)

Davide Tavernini, Efstathios Velenis, Roberto Lot, Matteo Massaro

<https://doi.org/10.1115/1.4026836>

22.12 SKYHOOK

Voir la thèse de (Hamrouni, 2021) notamment au §2.3.1 qui introduit le concept, puis en §5.2.1 un exemple de cosimulation Amesim-Simulink

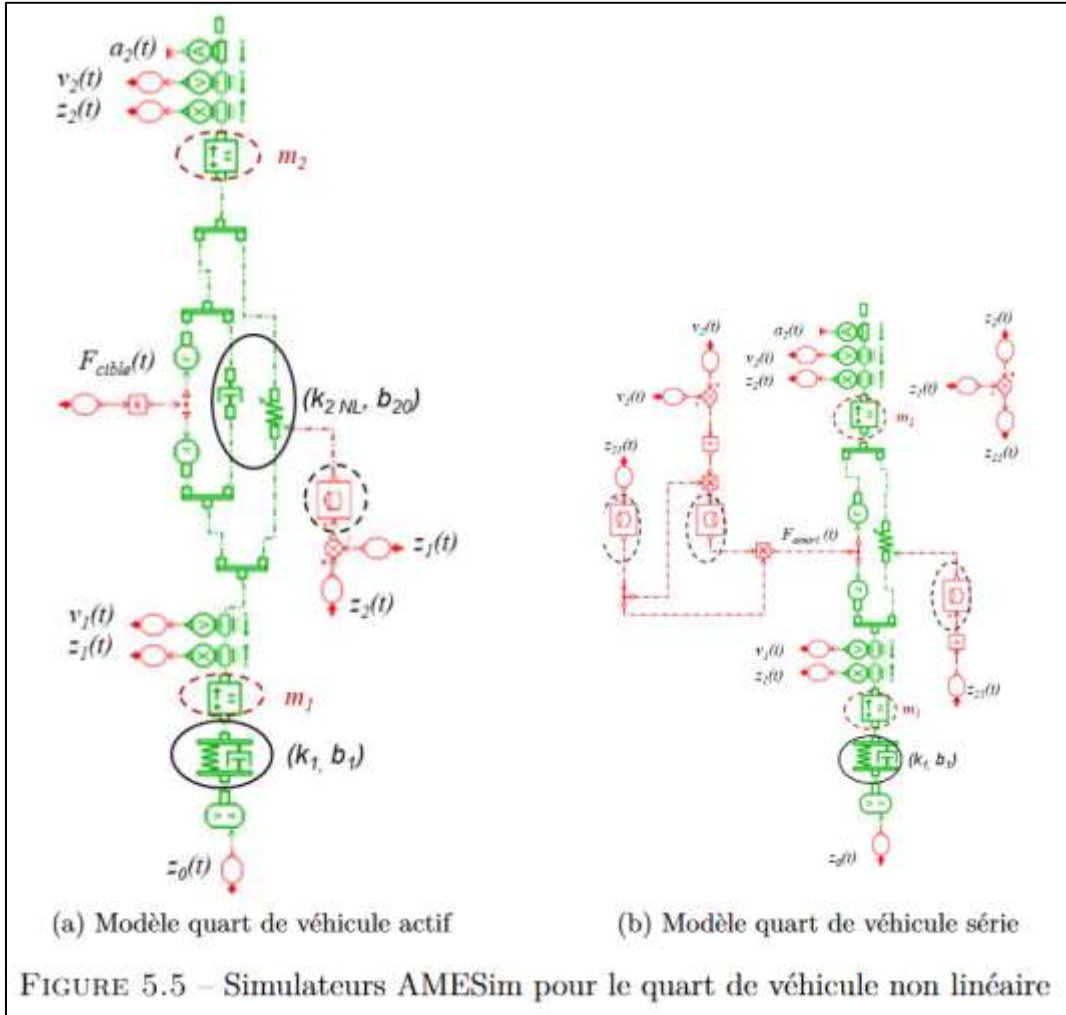


FIGURE 5.5 – Simulateurs AMESim pour le quart de véhicule non linéaire

23 CONTROLE OPTIMAL ET OPTIMISATION DE TRAJECTOIRE

23.1 BIBLIO

Optimal Vehicle Path Generator Using Optimization Methods

△ Pete Ramanata, 1998

<https://vttechworks.lib.vt.edu/handle/10919/36615>

This research explores the idea of developing an optimal path generator that can be used in conjunction with a feedback steering controller to automate track testing experiment. This study specifically concentrates on applying optimization concepts to generate paths that meet two separate objective functions; minimum time and maximum tire forces.

A three-degree-of freedom vehicle model is used to approximate the handling dynamics of the vehicle. Inputs into the vehicle model are steering angle and longitudinal force at the tire. These two variables approximate two requirements that are essential in operating a vehicle. The Third order Runge-Kutta integration routine is used to integrate vehicle dynamics equations of motion. The Optimization Toolbox of Matlab is used to evaluate the optimization algorithm. The vehicle is constrained with a series of conditions, includes, a travel within the boundaries of the track, traction force limitations at the tire, vehicle speed, and steering.

http://www.jameshakewill.com/Lap_Time_Simulation.pdf (2000)

Lap time simulation for racing car design (2002)

Blake Siegler, PhD thesis, University of Leeds.

<https://etheses.whiterose.ac.uk/1767/>

Lap time simulation with transient vehicle and tyre dynamics (2008)

Daniel P. Kelly, PhD, Univ. Cranfield

<https://dspace.lib.cranfield.ac.uk/handle/1826/4791>

Race driver model

△ F. Braghin, F. Cheli, S. Melzi, and E. Sabbioni. Comput. Struct., 86(13-14):1503–1516, 2008.

<https://www.sciencedirect.com/science/article/abs/pii/S0045794908000163>

L. Cardamone, D. Loiacono, P. L. Lanzi and A. P. Bardelli, "Searching for the optimal racing line using genetic algorithms," *Proceedings of the 2010 IEEE Conference on Computational Intelligence and Games*, 2010, pp. 388-394, doi: [10.1109/ITW.2010.5593330](https://doi.org/10.1109/ITW.2010.5593330).

The search of the best racing line is modeled as a quadratic optimization problem to compute the optimal trade-off between two conflicting objectives:

- driving fast, following the path with minimum curvature (MCP)
- following the shortest path (SP).

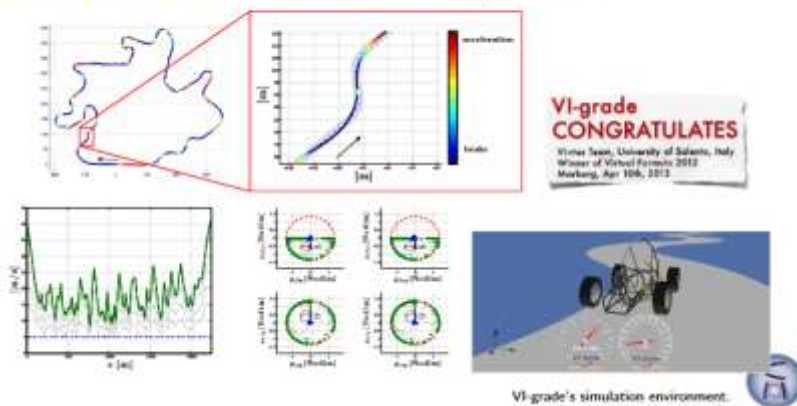
Commercial racing games typically rely on human-designed racing lines designed by domain experts. The few notable exceptions to such a hand-crafted approach include Colin McRae Rally 1 (Codemasters), where the racing line is computed with a neural network trained by domain experts ([link](#)), and the Forza Motorsport 2 series (Microsoft), where the supervised learning techniques are exploited to train the game AIs and evolutionary computation is applied to optimize their racing lines. Open-source racing games usually rely on heuristics approaches that typically combine good practices with heuristics to generate a racing line for any given track automatically. The most successful examples of such approaches include :

- the K1999 algorithm, which was developed by Remi Coulom and exploits gradient descent
- [Simplix](#), developed by Wolf-Dieter Beelitz for The Open Car Racing Simulator ([TORCS](#)), based on a simple heuristic
- the bot by Jussi Pajala for the Robot Auto Racing Simulator ([RARS](#)) applies A*
- the DougE1 bot for RARS by Doug Elenveld applies a genetic algorithm.

▷ **Optimal control methods for dynamics exploration and trajectory optimization of car vehicles** (A. Rucco, PhD, 2014)

http://cor.unisalento.it/rucco/docs/AR_PhD_31jan14.pdf

Minimum lap-time trajectory for a long race circuit: the VIRTUAL FORMULA 2012 competition



Path Planning for an Automated Vehicle Using Professional Racing Techniques (2014)

https://stacks.stanford.edu/file/druid:zn992vv3694/Theodosis_thesis-augmented.pdf

Une revue récente :

M. Massaro & D. J. N. Limebeer (2021) **Minimum-lap-time optimisation and simulation**, Vehicle System Dynamics, 59:7, 1069-1113, DOI: [10.1080/00423114.2021.1910718](https://doi.org/10.1080/00423114.2021.1910718)

23.2 SYSTEME DE COORDONNEES

Quel système adopter pour formuler le problème ?

<http://www.multibody.net/mbsymba/vehicles/curvilinear-coordinates/>

23.3 LOGICIELS

<https://python-control.readthedocs.io/en/latest/optimal.html>

Application à l'optimisation de trajectoire : voir [Dymos](#) dans le §24 (Lap time simulation)

<https://github.com/OpenMDAO/dymos/blob/master/docs/examples/racecar/racecar.ipynb>

23.3.1 OPTIMUM LAP

<http://www.optimumg.com/software/optimumlap/>

23.3.2 TUMFTM

https://github.com/TUMFTM/global_racetrjectory_optimization

23.4 RACING LOUNGE

<http://fr.mathworks.com/videos/matlab-and-simulink-racing-lounge-lap-time-simulation-essential-part-of-concept-development-98733.html>

23.5 MATTHEW KELLY

23.5.1 PUBLICATION

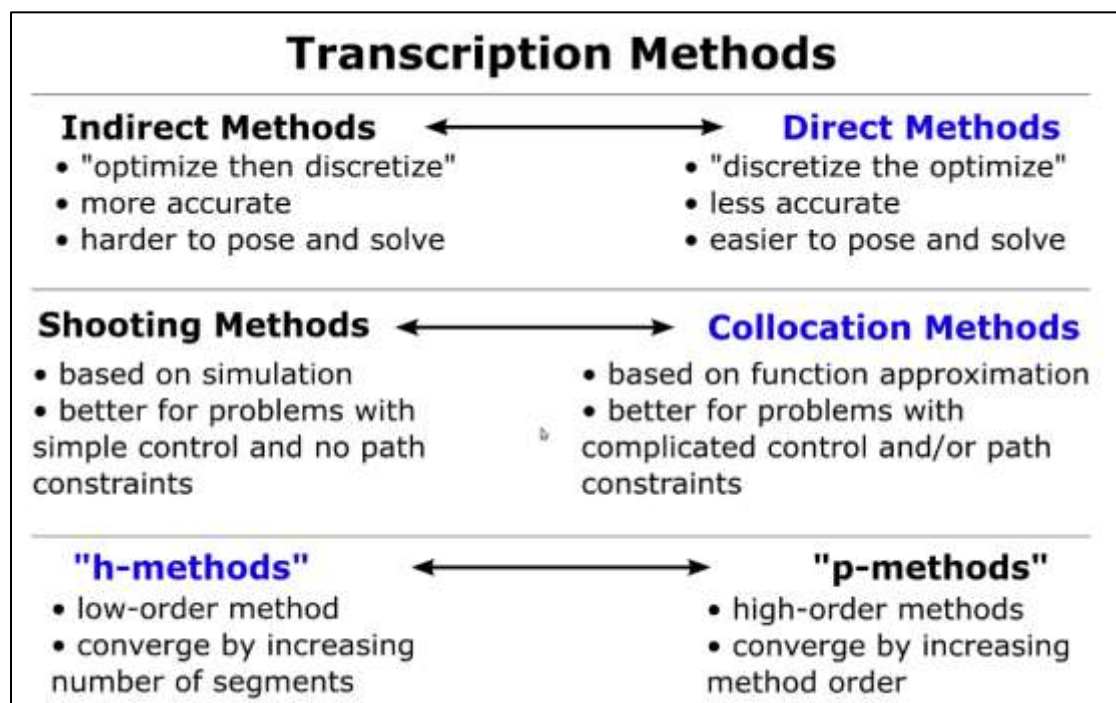
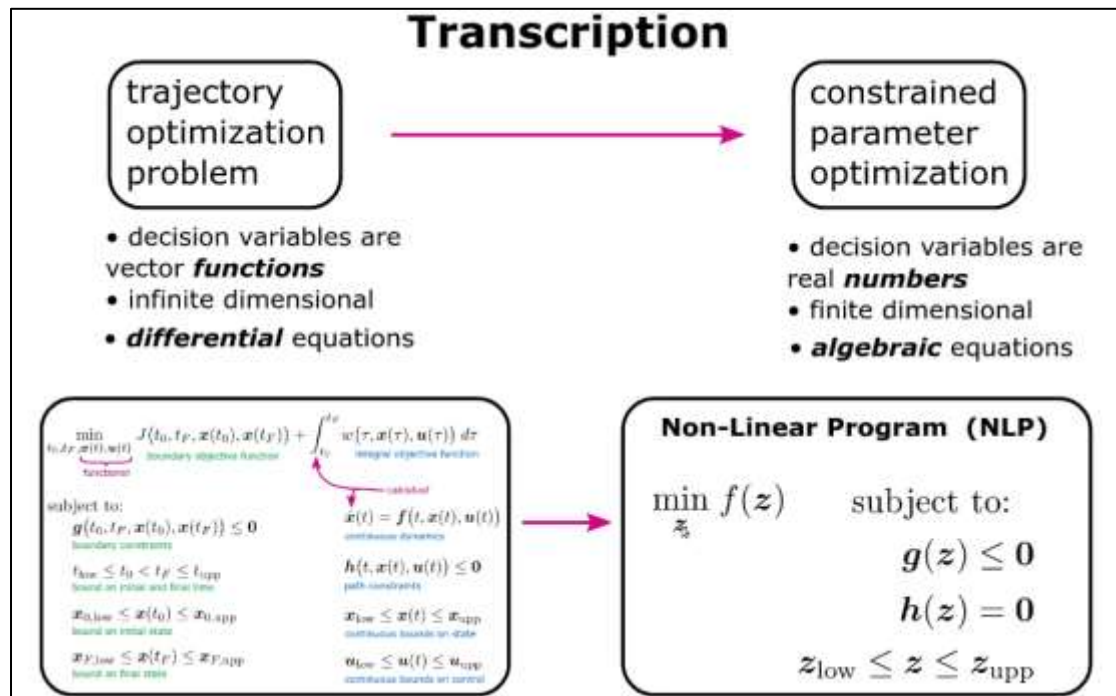
An Introduction to Trajectory Optimization (Matthew Kelly, 2017)

▷ <https://doi.org/10.1137/16M1062569>

23.5.2 YOUTUBE

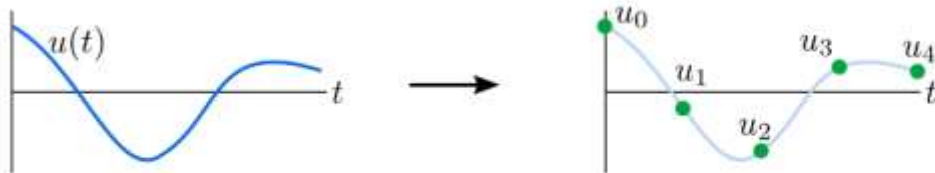
Introduction to Trajectory Optimization (2016)

<https://www.youtube.com/watch?v=wlkRYMVUZTs>



Direct Transcription:

continuous time and functions	\longrightarrow	discrete set of real numbers
$N = \text{number of grid points}$		
$x_k = x(t_k)$	$t \rightarrow [t_0, t_1, \dots, t_N]$	
$u_k = u(t_k)$	$x(t) \rightarrow [x_0, x_1, \dots, x_N]$	
	$u(t) \rightarrow [u_0, u_1, \dots, u_N]$	



Boundary Constraints:

- apply at: t_0, x_0, u_0 or t_N, x_N, u_N

Path Constraints:

- apply at: $t_k, x_k, u_k \quad k \in 1 \dots N$

References

"Practical Methods for Optimal Control and Estimation Using Nonlinear Programming"
John T. Betts, 2011, Advances in Design and Control, SIAM.

"Barycentric Lagrange Interpolation"
Jean-Paul Berrut, Lloyd Trefethen, 2004, SIAM Review.

"A survey of numerical methods for optimal control"
Anil V. Rao, 2009, Advances in the Astronautical Sciences.

"Costate Estimation in Optimal Control using Integral Gaussian Quadrature Orthogonal Collocation Methods"
Anil V. Rao, 2014, Optimal Control Applications and Methods.

"GPOPS-II: A Matlab software for solving multiple-phase optimal control problems using hp-adaptive gaussian quadrature collocation methods and sparse nonlinear programming"
Michael Patterson, Anil V. Rao, 2013, ACM Transactions on Mathematical Software, Vol 39.

"Direct Trajectory optimization using nonlinear programming and collocation"
Hargraves, Paris, et al. 1987, AIAA J. Guidance

"Direct Trajectory optimization of rigid body dynamical systems through contact"
Michael Posa and Russ Tedrake. Algorithmic Foundations of Robotics X. 2013.

23.5.3 GITHUB

<https://github.com/MatthewPeterKelly/OptimTraj>

24 LAP TIME SIMULATION

24.1 RÉCUPÉRER LE TRACÉ D'UN CIRCUIT

Voir les conseils donnés sur

<https://github.com/TUMFTM/laptimesimulation>

qui suggère d'utiliser <https://overpass-turbo.eu/>

Extracting the centerline of a race track from OpenStreetMap

- Step 1 : Open <https://overpass-turbo.eu/> This is a tool to extract map informations from OpenStreetMap.
- Step 2 : Navigate to the desired race track, e.g. the Red Bull Ring in Austria.
- Step 3 : Paste the following search into the text field and execute the search to highlight everything which is tagged as a raceway.

```
[out:json][timeout:25];
(
  node["highway"="raceway"]({{bbox}});
  way["highway"="raceway"]({{bbox}});
  relation["highway"="raceway"]({{bbox}});
);
out body;
>;
out skel qt;
```

- Step 4 : Click export and save it as a GeoJSON. Be aware that the export might include a lot of unnecessary points which must be excluded either in a separate step or during the import.

Le code est le suivant :

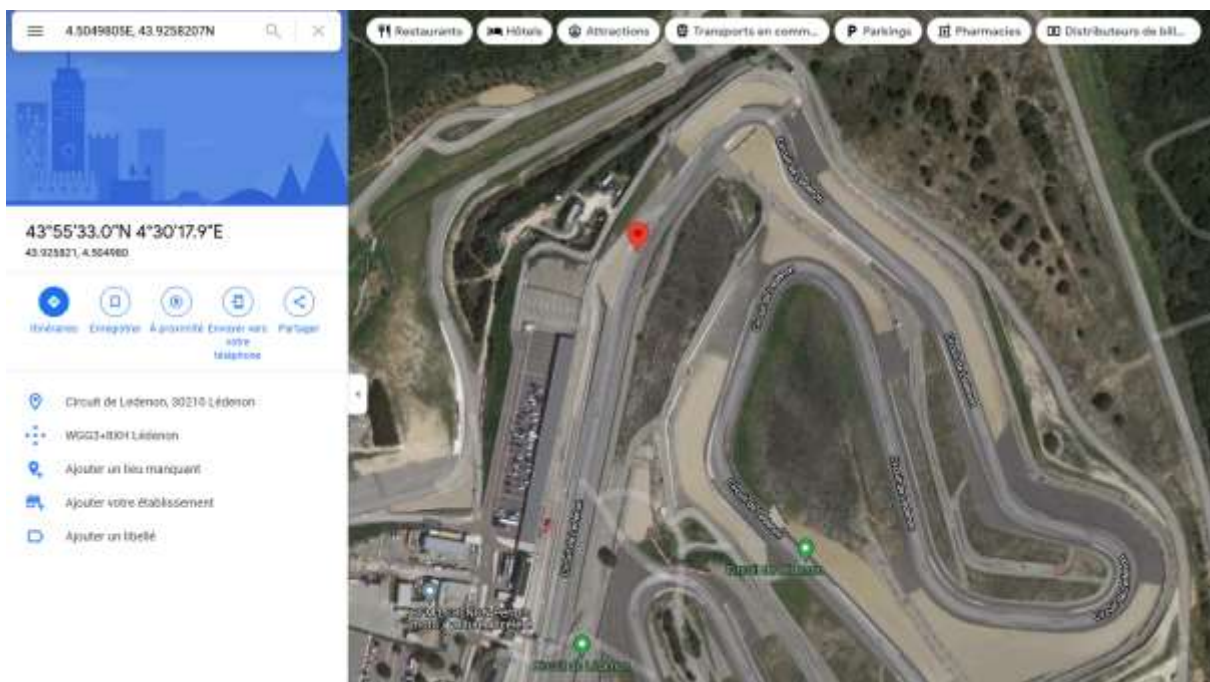
```
[out:json] [timeout:25];
(
  node["highway"="raceway"] ({{bbox}});
  way["highway"="raceway"] ({{bbox}});
  relation["highway"="raceway"] ({{bbox}});
);
out body;
>;
out skel qt;
```

On récupère les données GPS sous la forme suivante :

```
{
  "type": "FeatureCollection",
  "generator": "overpass-ide",
  "copyright": "The data included in this document is from www.openstreetmap.org. The data is made available under ODbL.",
  "timestamp": "2021-10-27T22:03:13Z",
  "features": [
    {
      "type": "Feature",
      "properties": {
        "id": "way/43165485",
        "highway": "raceway",
        "name": "Circuit Automobile de Lédenon",
        "source": "cadastre-dgi-fr source : Direction Générale des Impôts - Cadastre. Mise à jour : 2008"
      },
      "geometry": {
        "type": "LineString",
        "coordinates": [
          [
            [
              4.5049805,
              43.9258207
            ],
            [
              [
                4.5047965,
                43.9254043
              ],
              [
                4.5049805,
                43.9258207
              ]
            ]
          ]
        ]
      }
    }
  ]
}
```

Il peut être nécessaire de faire un peu de ménage pour conserver la bonne "feature" dans le json, car plusieurs tracés peuvent être présents après l'export.

On peut coller les coordonnées dans Google Maps en spécifiant E/W et N/S, par exemple pour le 1^e pt donné par 4.5049805E, 43.9258207N :

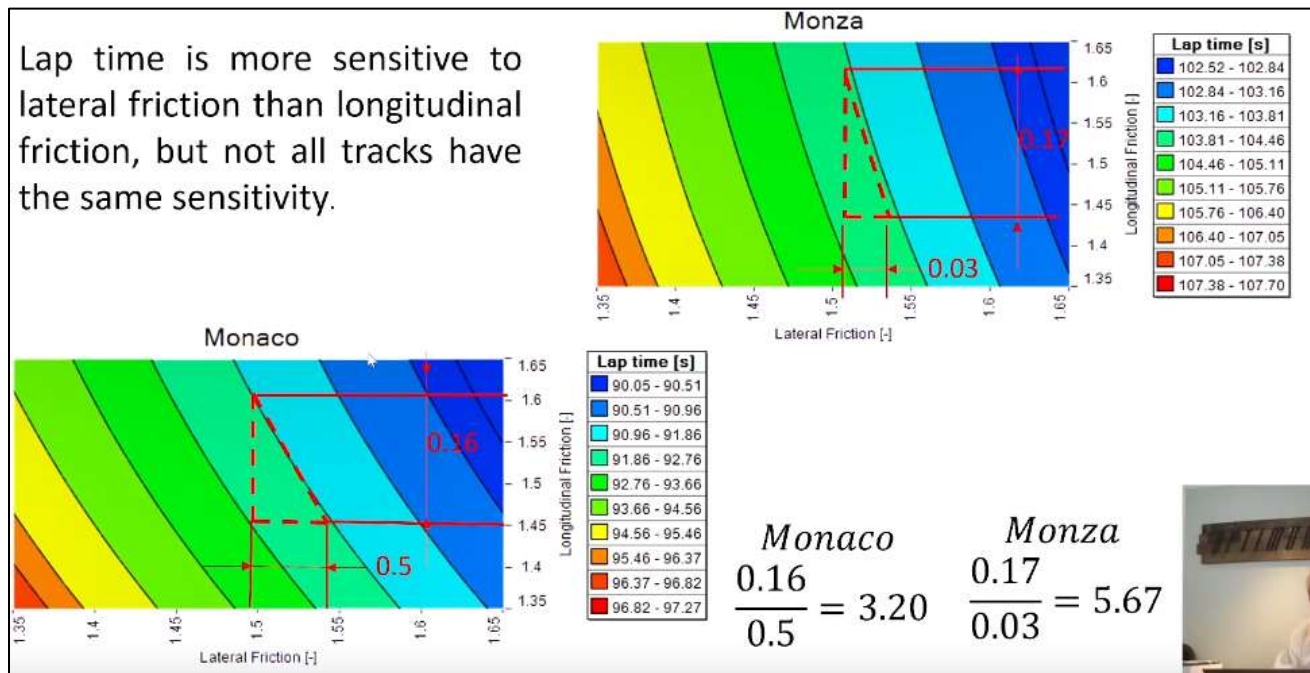


24.2 BASE DE DONNÉES DE TRACÉS DE CIRCUIT

<https://github.com/TUMFTM/racetrack-database>

24.3 INFLUENCE RELATIVE GRIP LONGI / GRIP LATÉRAL

Dans cette vidéo de Claude Rouelle, à t=31' :



Les courbes iso représentent le temps au tour. On voit que le grip latéral est environ 4 fois plus important que le grip longi sur le temps au tour.

24.4 IN EXCEL ...

Un billet de blog ici, mais l'outil n'est pour l'instant pas mis à dispo.

<https://drracing.wordpress.com/2019/01/09/lap-time-simulation-in-excel/>

I am not the first attempting a LTS in excel. Already many years ago a guy named James Hakewill published on his website a very detailed article about his attempt of doing a simple tool in excel to simulate the performance of his car around a lap.

His vehicle model was very simple, but his paper was anyway very informative and well written. More recently, OptimumG has also made a simple lap time simulator available for free for everyone, allowing basic simulations to be run by every user at no cost.

24.5 LAPSIM

<http://www.lapsim.nl/>

In 1995 Chris graduated with a Masters degree in Mechanical Engineering from Delft University, section Vehicle Dynamics, under the supervision of Professor Hans Pacejka.

At the end of his study, in 1994, Chris started his own consultancy business.

By the end of 1996 the development of the simulation package LapSim was started. In 1999, the first release of the software package appeared.

En 2021 :

Chassis License

**€ 995 for the 1st year including support and updates
€ 495 / year renewal fee**

Présenté sur [fb](#) comme "Bosch software"

24.6 JONATHAN VOGEL

<https://www.jovogel.com/lap-time-simulation>

<https://github.com/OxxoCode/Optimum-Mindstorm> (last update 07/2020)

24.7 TUMFTM

<https://github.com/TUMFTM/laptimesimulation>

Python 3.8, dispo sous W10 et Ubuntu

24.8 OPTIMUMLAP

<https://optimummg.com/product/optimumlap/>

24.9 AVL VSM

<https://www.avl.com/simulate-racing>

You can use AVL VSM (Vehicle Simulation Model) for fully dynamic lap time simulation and optimization, either locally on a PC or in the cloud, greatly amplifying the computing power. In the cloud it is possible to analyze up to 100,000 laps to find the best possible setup for race day. AVL VSM contains comprehensive models of the whole vehicle and the environment. Each parameter can be varied automatically to run big jobs efficiently.

VSM has a world-class dynamic driver model, which is capable of driving at the limit of the vehicle's capabilities with various car setups.

24.10 DYMOS

Librairie de contrôle optimal en Python

<https://openmdao.github.io/dymos/examples/racecar/racecar.html>

Race car Lap Simulation

Things you'll learn through this example

- Optimizing trajectories for cyclic events (such as race car laps)
 - Linking a phase with itself so it is ensured that start and end states are identical
 - Using an independent variable other than time

The race track problem

The race track problem is different from other dymos example problems in that it is a cyclic problem. The solution must be such that the start and end states are identical. The problem for this example is given a race track shape, what is the optimum values for the controls such that the time elapsed to complete the track is a minimum.

25 LOGICIELS COMMERCIAUX

<http://www.racingaspirations.com/apps/suspension-geometry-calculator>

25.1 IPG CARMAKER

Spin-off de l'université de Karlsruhe

Utilisé par de très nombreux constructeurs

- Jaguar Land Rover ([pdf 2016](#))

Release 9.0 (2020)

<https://ipg-automotive.com/products-services/simulation-software/carmaker-release-90/langswitch/1/>

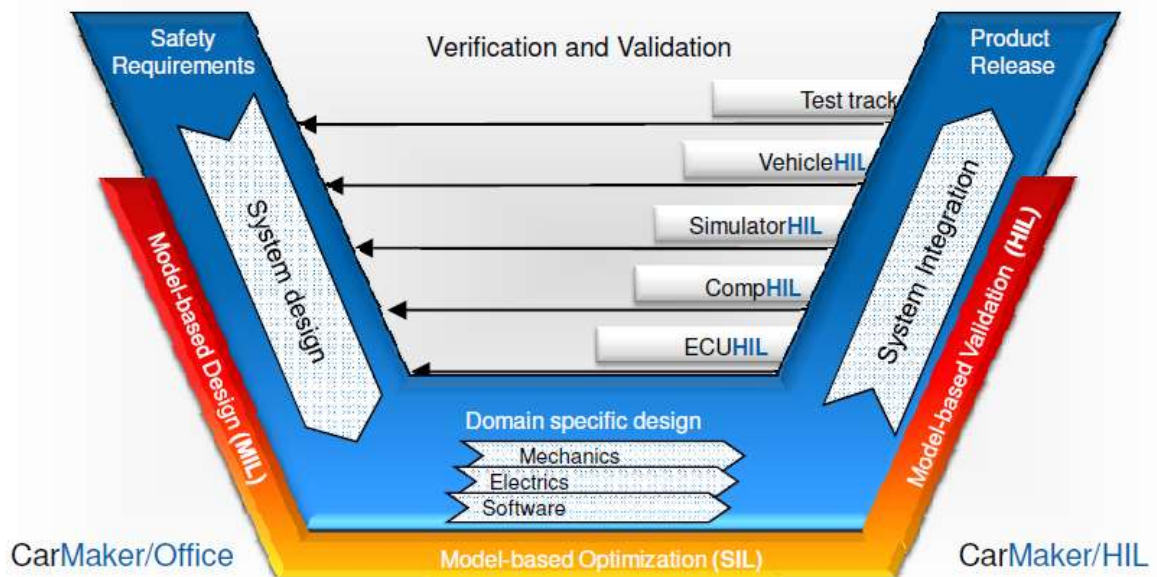
- Option to import from HERE HD Live Maps
- Option to export in OpenDRIVE format
- Cooperative driving with SimNet using co-simulation of multiple ego vehicles in a common scenario
- New camera-based HiFi sensor model
- Scalability through support of CarMaker in Docker containers
- Road users with more human-like behavior – Human Driver Model
- New Object by Lane Sensor

Optimized Vehicle Data Set Dialog & Scenario Editor (04/2020)

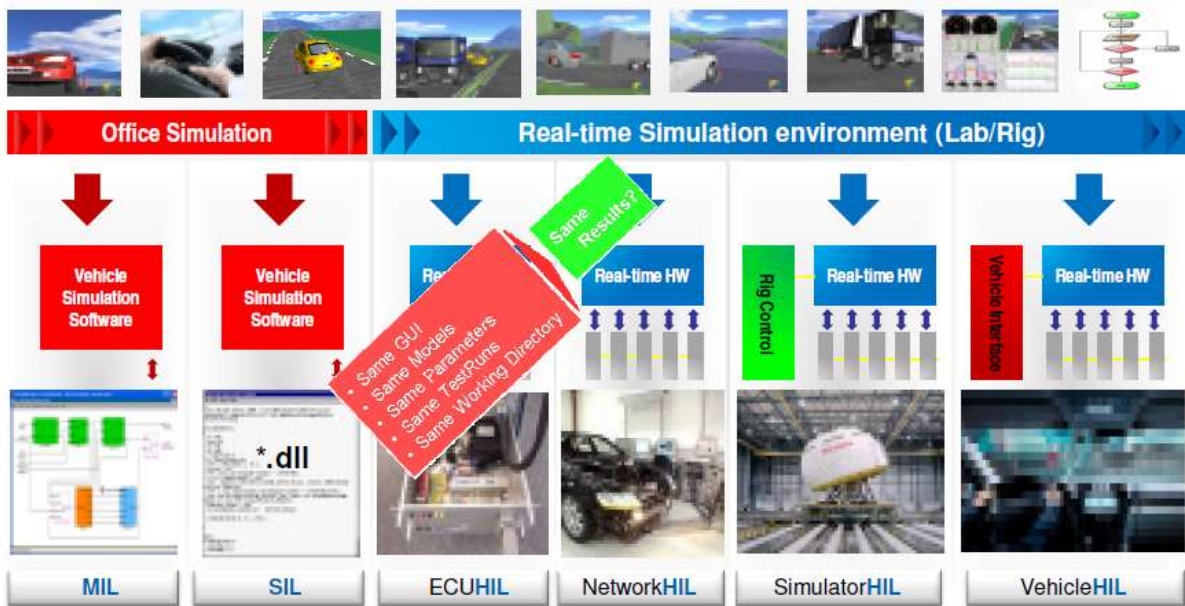
https://www.youtube.com/watch?time_continue=2&v=c4Ct-iSjiJQ

- Human Driver Model à t=10'05

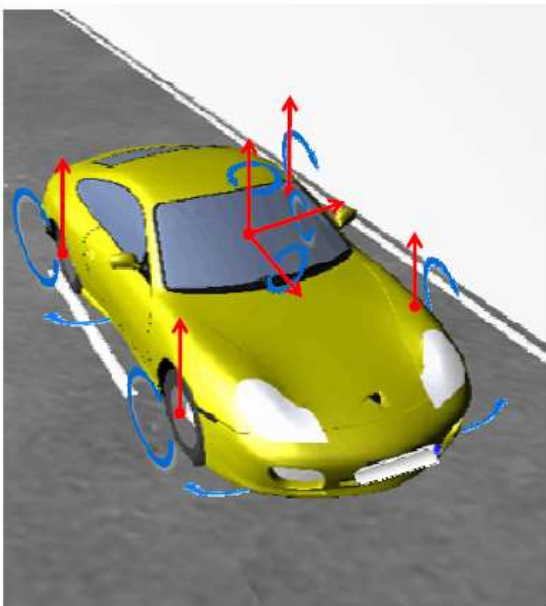
Model Based Testing within an Integrated Development Process



Integral process for functions, performance, fail safe mechanism and quality testing



IPGCar – precise and extendable



- 17 DOF - Degrees of Freedom + 20 constraints
- Mesa Verde Multi-Body Code
fully non-linear – symbolical – fast – extendable

Components

- **Body**
 - BodyFlex with 2DOF (torsion, bending)
 - sprung mass, loads, engine, trim loads
- **Suspension with linkage equation**
 - kinematics & compliance selectable
 - 2D table (map), 1D table, linear
 - Damper, spring, buffer, stabilizer, external forces
- **Steering System Front Axle**
- **Rear Axle Steering**
- **Detailed Hydraulic Model** valid for ABS/ESP
 - Booster, master and brake cylinder, pump, valves, line volume, accumulator, attenuator
- **Powertrain** (front, rear, AWD)
 - Engine, clutch, gear box, differentials
- **3D Aerodynamics**
 - drag – lift – side
 - $3 F_{x,y,z}$, $3 M_{x,y,z}$



IPGTrailer

- Full non-linear
- up to 2 axles
- free-definable geometry adjustable
- unsprung, sprung masses, trim loads
- IPG suspension model* sleeve axle, crank axle, semi-trailer arm axle
- Aerodynamics model*
- Brake model
- Tire model*
- Hitch ball model ball&trapeze, friction, damper



IPGTire

- MF 5.2 data load
 - TYDEX format
 - TIME procedure
- Additional functions
 - stop & go (hill)
 - slope parking
 - vertical damping
- 3DRoad usage
- Physically based analytical functions for
 - combined XY forces
 - Dynamic behavior
- Tire load all or single
- Automation fitting tool for IPGTire data



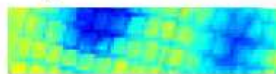
IPGRoad

- 3DRoad generator
- 3D-Track grid data load
- Friction definition
 - split, jump, sequence, line
- Markers and Pylons
- Traffic signs speed, side wind
- Obstacles wave, cone, cylinder, beam
- 3D-Track grid data load high resolution CRG

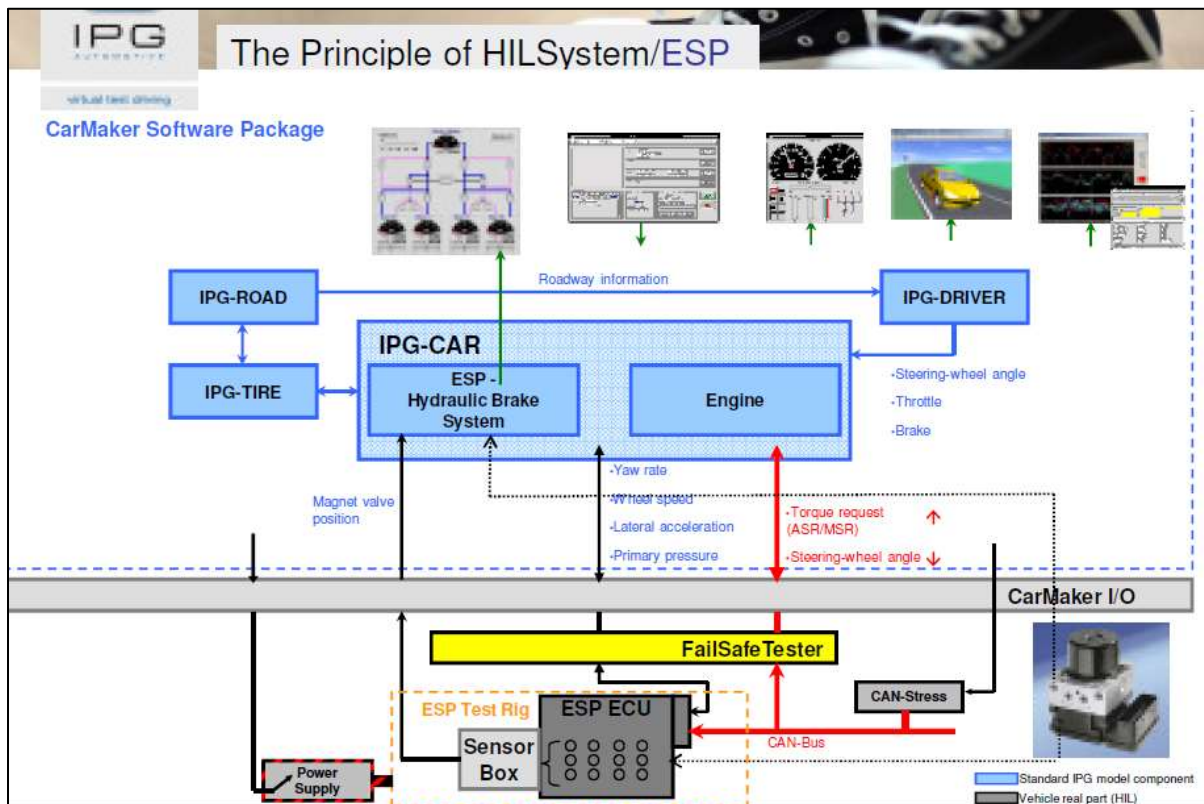
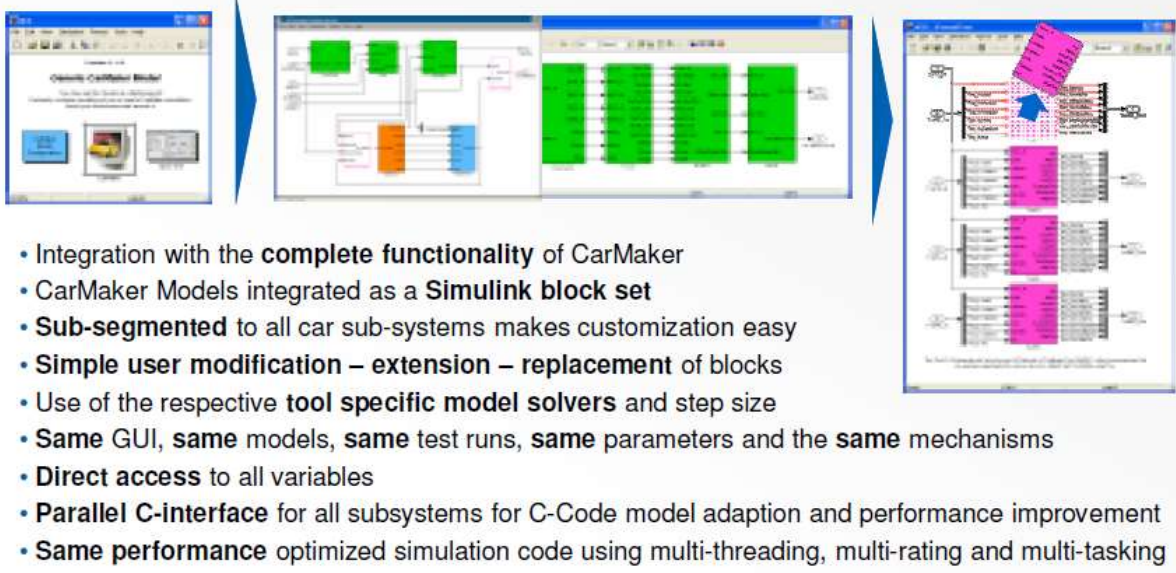


IPGTraffic

- Traffic generator longitudinal - lateral
- Different vehicle types Trucks, Vans, SUV, passenger cars, HP cars
- Maneuver definition start position, time history, speed profile (x,y), accel.
- No limits on number of vehicles
- Moving or standstill traffic
- Paired vehicles
- Traffic loop



CarMaker integration within MATLAB/SIMULINK



25.2 TESIS DYN

Société basée à Munich, rachetée par VECTOR en 2019.

Brief history of DYNA4 :

- Cornelius Chucholowski developed real-time capable vehicle models at BMW as a freelancer from 1985
- He founded TESIS in 1992
- Main products veDYNA and enDYNA with models for vehicle dynamics and engine dynamics
- Additional engineering services
- DYNA4 succeeds veDYNA and enDYNA with higher modularity and stronger simulation process support
- Ongoing model extensions and improvements
- Vector acquires TESIS in 2019

<https://www.thesis.de/en/products/>

	DYNA4 Vehicle & Environment	veDYNA Vehicle Dynamics	enDYNA Engine Dynamics
Tools & methods			
Modular model architecture in Simulink	●	(●)	(●)
Integration and interfaces	●	(●)	(●)
3D Visualization DYNAanimation	●	(●)	
Simulation data management	●		
Automation and variation	●		
Variants management	●		
Stand-alone operation for HIL and SIL	○	(○)	(○)
Vehicle dynamics models			
High-fidelity vehicle dynamics	○	●	
Tires	○	(●)	
Brake hydraulics	○	○	
Trailer	○	○	
Commercial vehicles	○	○	
Vehicle dynamics driver	○	●	
Engine and powertrain models			
Modular powertrain	○	(○)	
Electrical system	○	(○)	(○)
Engine dynamics based on mean-value	○		●
Additional components engine	○		●
Thermodynamic engine model	○		○
Cycle driver	○		●
Environment simulation			
Driving dynamics tracks	○	(○)	
OpenDRIVE road network	○		
Traffic	○	(○)	
Environment sensors	○	(○)	
Trajectory calculation	○	○	
Legend			
● Standard	(●) Standard (Limited function compared to DYNA4)		
○ Selectable	(○) Selectable (Limited function compared to DYNA4)		

https://fr.mathworks.com/products/connections/product_detail/product_38504.html

https://www.lembarque.com/automobile-vector-rachete-thesis-un-specialiste-en-simulation-dynamique-de-vehicules-virtuels_008361 (02/2019)

Les outils de simulation modulaires DYNA4, veDYNA et enDYNA de Tesis fournissent des interfaces qui assurent un couplage flexible avec des outils tiers indépendants et qui autorisent l'exécution en temps réel de la simulation dans le cadre d'une approche HIL (Hardware In the Loop).

Cette activité faisait à l'origine partie du groupe Tesis, fondé en 1992, avec trois entités : Tesis PLMware, Tesis SYSSware et Tesis DYNAware. Après les cessions des deux premières entités par le groupe (Tesis PLMware a notamment été racheté par Siemens en 2013), Tesis DYNAware, qui menait ses activités sous ce nom jusqu'en mai 2018, a acquis sa société mère pour s'appeler Tesis GmbH.

Pas mal de vidéos intéressantes :

<https://www.youtube.com/user/tesisdynaware/videos>

Utilise un solveur Euler implicite modifié, compatible temps-réel, du moins si l'on en croit la publication suivante (Rill, 2005):

A MODIFIED IMPLICIT EULER ALGORITHM FOR SOLVING VEHICLE DYNAMIC EQUATIONS 23

the implicit Euler algorithm pay off for large vehicle systems [6]. Since several years the presented algorithm is used successfully within VeDynA a commercial tool in Vehicle Dynamics [13]. VeDynA is embedded into the environment of MATLAB/SIMULINK and it is widely used for off-line and real time applications, c.f. [1].

Références :

<https://www.thesis-dynaware.com/en/expertise/vehicle-dynamics/references/browse/1.html>

25.3 CARSIM (MECHANICAL SIMULATION CORP.)

Co-fondé par Thomas D. Gillespie

<https://www.carsim.com/publications/pressreleases/gillespie.php>

Thomas D. Gillespie, Ph.D., is a research scientist and professor who has earned an international leadership position in the fields of vehicle dynamics engineering and transportation policy and safety, and who co-founded Mechanical Simulation Corporation in 1996. He authored the textbook "Fundamentals of Vehicle Dynamics," which is considered required reading for all vehicle dynamics engineers. He is frequently called upon to teach vehicle dynamics to engineers at many of the world's automotive manufacturing companies. His expertise has also thrust him into many unique, critical roles around the world.

(...)

Mechanical Simulation Corporation is a technology leader in the development and distribution of advanced software used to simulate vehicle performance under a wide variety of conditions. The company was established in 1996, and from its Ann Arbor, Mich., headquarters provides car and truck simulation packages, training and ongoing support to more than 40 OEMs and Tier 1 suppliers, and more than 50 universities and government research groups worldwide



Mechanical Simulation

- Started at University of Michigan Transportation Research Institute
- Private company since 1996
- Headquarters in Ann Arbor, Michigan
- 100+ OEMs and Tier 1 Suppliers
- 250+ Universities
- 5800+ Active Users
- Customers in over 60 countries
- Global agents provide international sales and support

Provide engineers with vehicle simulation tools (VS Solvers) for every step of the product design process

- Based on published peer reviewed work
- Precise, accurate, high-fidelity results
- Leader in computationally efficiency
- Open Interfaces/architecture
- Integrates with existing engineering and testing tools
- Allow engineers to add their own, custom, technologies
- Scalable to HiL and HPC/Cloud using the same models

<https://www.youtube.com/watch?v=Vr5uDzIg3c> (06/2021)

25.3.1 HISTORIQUE

Many of the modeling assumptions used in the CarSim math models were developed and validated at the University of Michigan Transportation Research Institute (UMTRI) and other research labs decades ago. Prior to the 1980's, most vehicle math models with a complexity approaching CarSim were written by hand for use on mainframe computers. In the late 1970's, multibody computer programs such as ADAMS® were developed and applied to the simulation of vehicles, at the expense of requiring much longer computer times. In the late 1980's symbolic multibody programs were developed that could generate computer source code for multibody systems such as ground vehicles. Perhaps the most advanced was a program called AutoSim, developed by the author (Sayers) at UMTRI. AutoSim was validated and used to replace most of the car and truck simulation programs used at UMTRI at the time. AutoSim was also licensed to the American car manufacturers and some universities and research labs around the world. The custom simulation programs generated with AutoSim have the high efficiencies associated with hand-written custom programs, with far better reliability. Since the **founding of Mechanical Simulation Corporation by Sayers, Gillespie, and others in 1996**, AutoSim has been maintained, updated, and used to create all of the math model solver programs in CarSim, TruckSim, VehSim, and BikeSim. In the early 1990's, the Simulation Graphical User Interface (SGUI) was developed by Sayers and others at UMTRI to make vehicle simulation more accessible to engineers who are not simulation specialists, and to provide a more productive software environment for all users, from novices to specialists. The SGUI has been maintained and improved over the past ten years at Mechanical Simulation, along with tools for automated plotting and 3D animation. In the late 1990's many users combined software using "co-simulation" to build models from several packages. A popular combination was CarSim and MATLAB®/Simulink® (from The Math Works). Other combinations include CarSim and real-time testing systems from companies such as dSPACE, Opal-RT, and others. CarSim models were often being extended by users with their own models in Simulink (and other software such as ASCET® and AMESim®) to simulate conditions well beyond the original scope of the CarSim models.



Company founders Tom Gillespie and Mike Sayers with "Dynamics Development Of The Year" award for CarSim, awarded by *Testing International Magazine*.

Sources :

<https://www.carsim.com/company/ourhistory.php>

https://www.carsim.com/users/pdf/release_notes/carsim/cs7_new_features_memo.pdf

<https://www.carsim.com/publications/pressreleases/sayers.php>

25.3.2 PUBLICATIONS TECHNIQUES

<https://www.carsim.com/publications/technical/modeling.php>

25.3.3 CARSIM WITH SIMULINK

Using Simulink with CarSim, TruckSim, and BikeSim

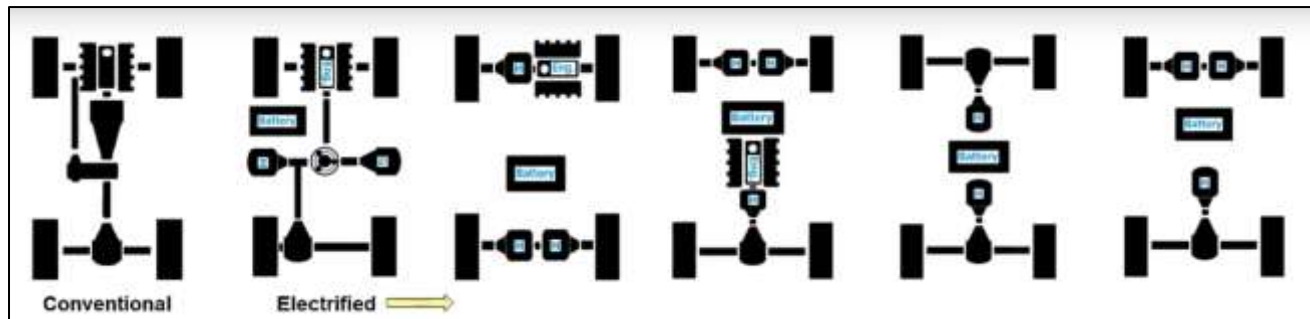
<https://www.youtube.com/watch?v=YQVUmVMtP3U>

25.3.4 SYSTÈMES DE COORDONNÉES

Vehicle Coordinate Systems

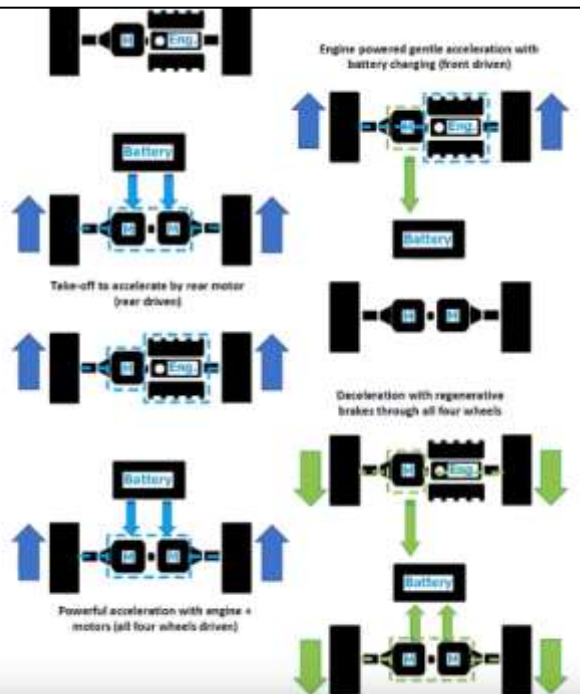
https://www.youtube.com/watch?v=p_uNMu9uhWI

25.3.5 ELECTRIFIED POWERTRAIN



2021 Electrified Powertrain

- Add the ability to drive each wheel independently
- The drive torque reaction for two-motor case can be selected to be either in-wheel or the sprung mass.
- All electric motors are involved in the battery state-of-charge calculation.



Recent Progress in Powertrain Model

- ❑ ~ 2018.0: FWD, RWD and AWD
- ❑ 2018.1: Hybrid model externally in Simulink
- ❑ 2019.0: Hybrid model internally built-in
- ❑ 2019.1: Electric model internally built-in (1 motor)
- ❑ 2020.0: Multiple motors: one on each axle
- ❑ 2021.0: Multiple motors: one on each wheel
- ❑ 2021.0: Selectable wheel motor(s) with LSD

<https://www.youtube.com/watch?v=DiMlbaROUEU> (2021)

25.3.6 VERSIONS

25.3.6.1 CARSIM 7

Nonlinear Tables

Many of the vehicle properties, controls, and road properties are described with nonlinear tables. In past versions, the form of table interpolation was determined by the developers and hard-coded into the VS solver. The new architecture supports run-time selection of one of many possible calculation methods, depending on user needs. These range from a constant, to a linear coefficient, to linear interpolation, to a spline, to 2D carpet plots. (There are currently 11 calculation options.)

Most tables include a scale factor and offset that can be used to transform a given nonlinear shape. These have keywords to help integrate with other software (DOE, sensitivity, optimization, etc.).

25.3.6.2 CARSIM 8.2 (01/2013)

https://www.carsim.com/publications/pressreleases/2013_01_02.php

"CarSim 8.2 brings spectacular visualization from the driving simulator world to engineers using basic simulation to accelerate their evaluations of vehicle performance. CarSim 8.2 provides advanced controls of the playback, heads-up displays of any variables in the models, multiple simultaneous views, and libraries of vehicles and proving ground areas developed by skilled video artists."

CarSim 8.2 also features math models extensions that have been requested by customers. Sayers notes, "...the math models have more detail in the tire model to better simulate limit conditions, more hysteresis effects in the steering, several improvements in sensor ranging and detection, and more easily configured nonlinear

table functions." He adds, "the new LINEARIZE command is a breakthrough for detailed nonlinear simulations tools such as CarSim. Although the vehicle is a complicated, nonlinear system, the new LINEARIZE command can be

applied multiple times during a simulated test to generate simplified math models that engineers can use to determine basic dynamic features, such as fundamental frequencies and stability criteria."

25.3.6.3 CARSIM 2017

https://www.carsim.com/publications/pressreleases/2016_12_22.php

- Support for multiple simulations based on a single Run Control dataset
- Rapid access to table data from large binary files
- Direct generation of Excel CSV output files
- All three VehicleSim products include support for ESC/TCS torque control requests in the powertrain
- CarSim and TruckSim have new options in the steering and braking systems
- CarSim now supports dual tires
- All of the products support live video when using Simulink
- All of the products provide more support for the open-standard functional mockup interface (FMI), including some RT systems

25.3.6.4 CARSIM 2018

https://www.carsim.com/publications/pressreleases/2017_12_20.php

The 2018 releases for CarSim and TruckSim feature a new architecture in the math models that supports simulation of almost any type of highway vehicle more efficiently, including real-time systems that might include hardware in the loop. Improved suspension and steering system features allow more realistic matching of physical vehicle behavior for a wider range of designs.

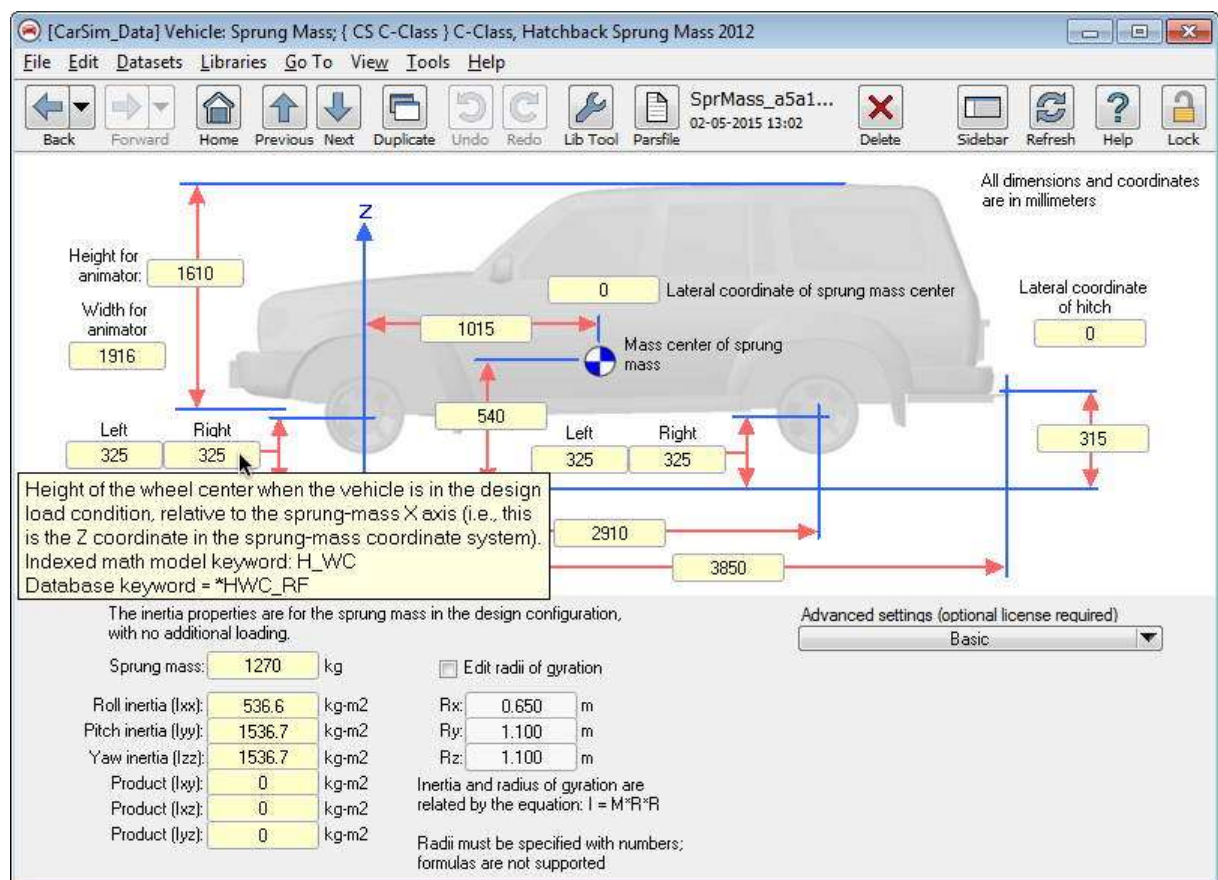
Engineers working in ADAS scenarios will appreciate improvements made to the built-in, real-time ADAS sensors and programmable moving objects (vehicles and pedestrians) in all three products. Changes were made to greatly improve the computation speed, maintaining real-time simulation even for complicated scenarios. More detection variables are provided, and control of the moving objects is more advanced. For example, when used to represent vehicles, the moving objects mimic the "offtracking" behavior of large vehicles making low-speed turns at intersections.

The vehicle math models in all three products support multiple road surfaces and paths followed by the simulated vehicle and other moving objects. Besides the existing tools for building paths with straight lines, arcs, spirals, and spline tables, three new tools have been added to make use of existing data. One is Atlas, a web tool hosted by carsim.com that obtains path and elevation data from mapping services such as Google and HERE. Version 2018 introduces the third generation of Atlas, which now includes elevation data for imported roads. Another new option is a plugin for the ADAS Research Program (RP) and database available from HERE. The third is a new interactive tool called VS Scene Builder that provides a collection of user-interface tiles that are dragged and dropped to rapidly assemble urban, rural, and highway scenes with sophisticated 3D shapes and textures that are ready for animation. Each new scene also has multiple predefined points that can be clicked to generate paths for vehicles and pedestrians.

25.3.6.5 CARSIM 2020.1

Voir présentation dans Softwares\CarSim

25.3.7 IHM



25.4 DSPACE

https://www.dspace.com/files/pdf1/ASM-VehicleDynamics_E_ebook.pdf

Automotive Simulation Models (ASM)

ASM Vehicle Dynamics

- Vehicle Dynamics Simulation
- Car, Truck and Trailer Simulation
- Brake Hydraulics and Pneumatics Simulation

25.5 MSC ADAMS/CAR

Voir le doc simulation système pour les généralités.

[Vehicle Dynamics Analysis using Adams Car \(2015\)](#)

Quelques publis :

- ADAMS Car-AT in The Chassis Development at BMW (Ewald Fischer, 11/ 2001) ([pdf](#))
- [Study of Vehicle Handing Stability Based on ADAMS/Car \(pdf\)](#) (2015, univ.)
- [Co-simulation Study of Vehicle ESP System Based on ADAMS and MATLAB \(pdf\)](#) (2011, univ.)
- [Vehicle Dynamics and Stability Analysis with Matlab and Adams Car](#) (2000)

Perfo CPU

Dans [Definition of new simulation scenarios for comfort and handling evaluation and application in a sensitivity analysis of damper characteristics](#), on trouve

Definition of new simulation scenarios for comfort and handling
evaluation and application in a sensitivity analysis of damper characteristics

Page 37

Table 2, Average simulation time with respect to real time duration

	Adams Car FTire	Adams Car MF-Tyre	CarMaker MF-Tyre
Short bump	190x	100x	Less than real time
Long bump	210x	100x	Less than real time
Badly maintained road	260x	130x	Less than real time
Cleat in a curve	200x	110x	Less than real time

25.6 AMESIM

On the correlation between a 3D high-fidelity multi-body vehicle model and a 1D 15-DOFs vehicle concept model (2014)

▷ http://past.isma-isaac.be/downloads/isma2014/papers/isma2014_0671.pdf

25.7 MODELICA VEHICLE DYNAMICS (MODELON)

<http://www.modelon.com/products/modelica-libraries/vehicle-dynamics-library/>
[Modelon's webinar on Vehicle Dynamics Library](#) (youtube, 30')

Quelques utilisateurs (2016)

Clients VDL
➤ Constructeur auto
▪ Audi – Suspension active
▪ Volvo – ADAS
▪ Tata – Véhicule complet
▪ Daimler – Groupe motopropulseur
▪ Toyota – Maniabilité et nouveaux concepts
➤ Sport auto
▪ Formula1
▪ NASCAR


Audi


Volvo


TATA


Mercedes-Benz


TOYOTA


Formula 1


NASCAR.

Et sa déclinaison pour le sport auto :

VDL Motorsports Library

<http://www.claytex.com/products/dymola/model-libraries/vdlmotorsports-library/#vdlm-features>

Lu je ne sais plus où :

Modelica is an object-oriented language for describing *multi-domain* engineering systems (i.e. systems that may contain combinations of mechanical, hydraulic, and electrical parts). The ability to model the interactions between different energy domains is noteworthy since modern vehicles are fitted with many electrical actuators, and are becoming increasingly mechatronic.

The Modelica language is intended to serve as a standard format so that models arising in different domains can be exchanged between tools and users [11]. Each component is represented as an object, which may contain differential, algebraic, and discrete equations as well as internal functions. In order for systems to be simulated, a Modelica translator must be used to assemble the component equations into a meaningful form and numerically integrate them. The most popular Modelica translator is Dymola® from DynaSim.

Dymola users are not given the option of selecting their own modeling variables. Dymola uses graph-theoretic algorithms to automatically select modeling variables, but the literature is not clear on the extent to which graph theory is used to assemble the system equations [12, 13]. If algebraic constraint equations are present, specialized techniques are used for manipulating the DAEs into a form that can be solved efficiently [7, 12, 13].

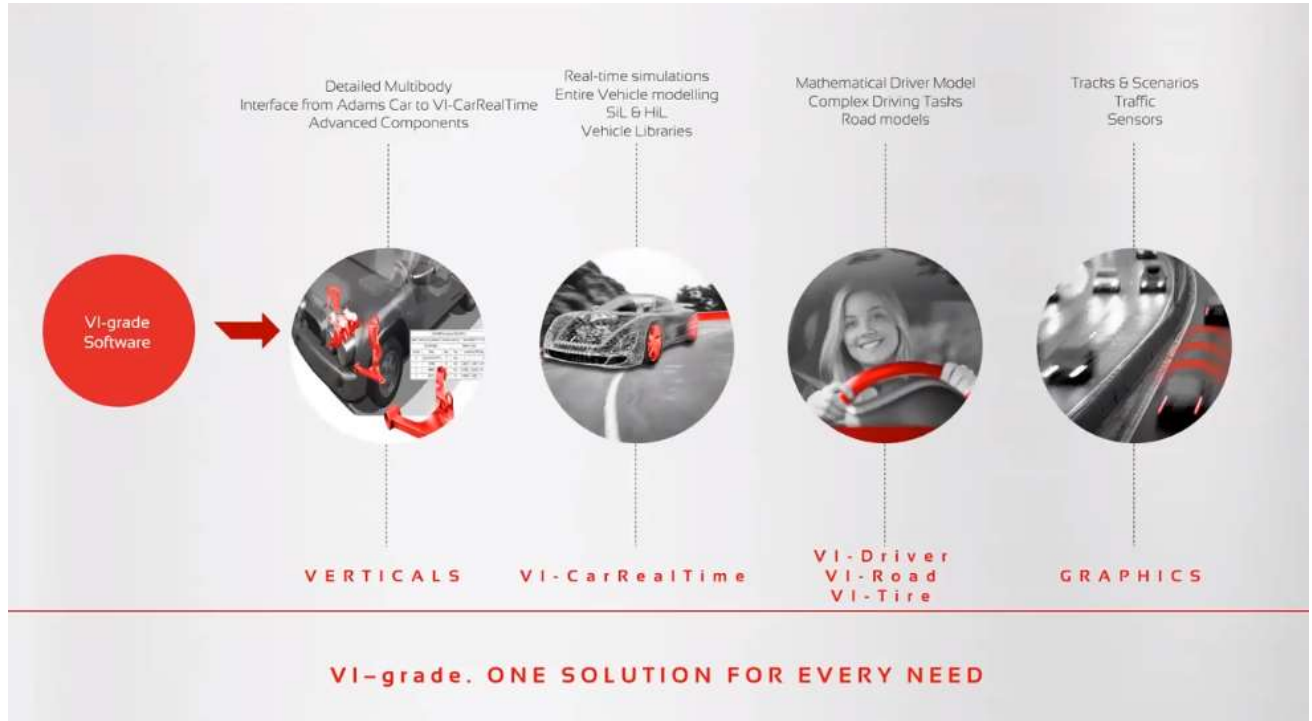
Elmqvist et al. used Dymola to construct models of various vehicle topologies [12]. One of these topologies was a generic four-wheeled vehicle with independent suspension, similar to the one described by Sayers [43], which used look-up tables to modify wheel orientation as a function of suspension deflection. This model was exported from Dymola in the form of C code, which was compiled on a real-time target machine using software from Matlab and Opal-RT. The target machine had a 3 GHz Pentium 4 processor. A double lane-change maneuver was simulated using Euler's method and a constant step size of 1 ms. The model easily ran in real-time, as only 0.1 ms of CPU time was needed to advance the solution at each time step[12]. As part of the same study, a model of a vehicle featuring MacPherson strut front suspension and trailing arm rear suspension was created. An analytic solution to the constraint equations associated with the MacPherson strut suspension is possible, and was easily incorporated into the model by using Dymola *assemblies* [12]. This eliminated the need for algebraic constraint equations and allowed the model to be described by a set of ODEs. The simulation code was exported in the same manner as before, and a double lane-change maneuver was simulated. The model ran faster than real-time, as 0.3 ms of CPU time was needed to advance the solution for each 1 ms time step [12].

25.8 DYMOLA

◇ [Modelica and Dymola for education in vehicle dynamics at KTH \(2009\)](#)

25.9 VI-GRADE

<http://www.vi-grade.com/>



Doc Audi – VI Grade de 2009 :

http://www.ukintpress-conferences.com/conf/09vdx_conf/pdfs/day2/3_wilhelm_minen.pdf

Bridging the gap between physical testing and simulation with VI-CarRealTime ([youtube](#))

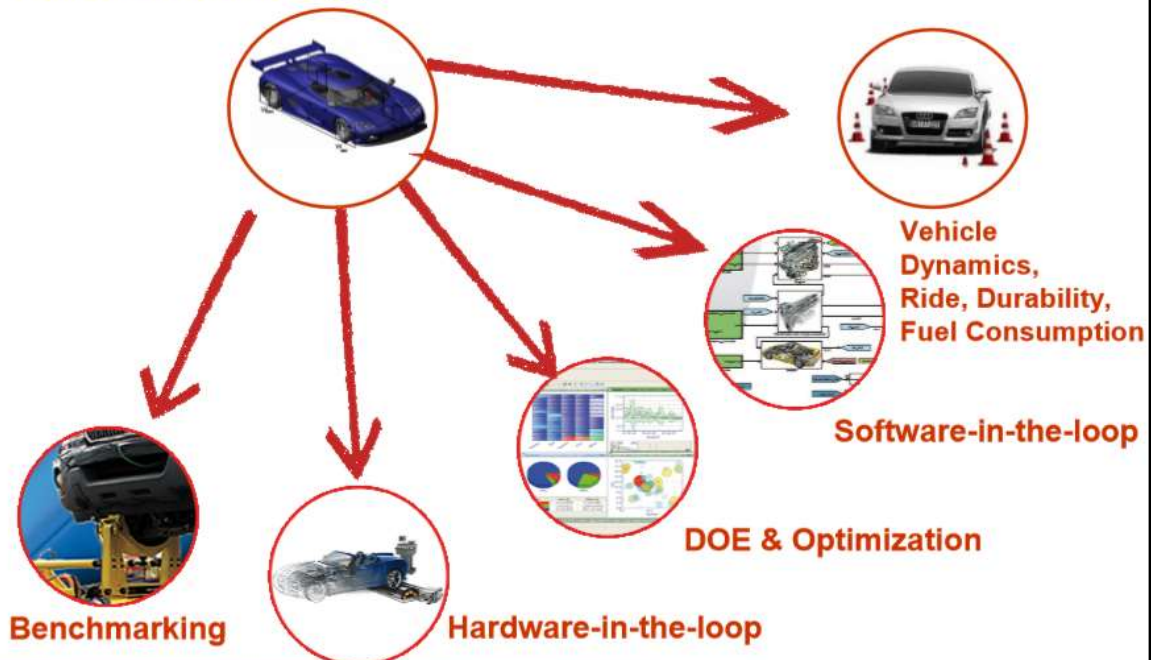
<https://www.vi-grade.com/en/products/automotive/>

Spin-out de MSC en 2005

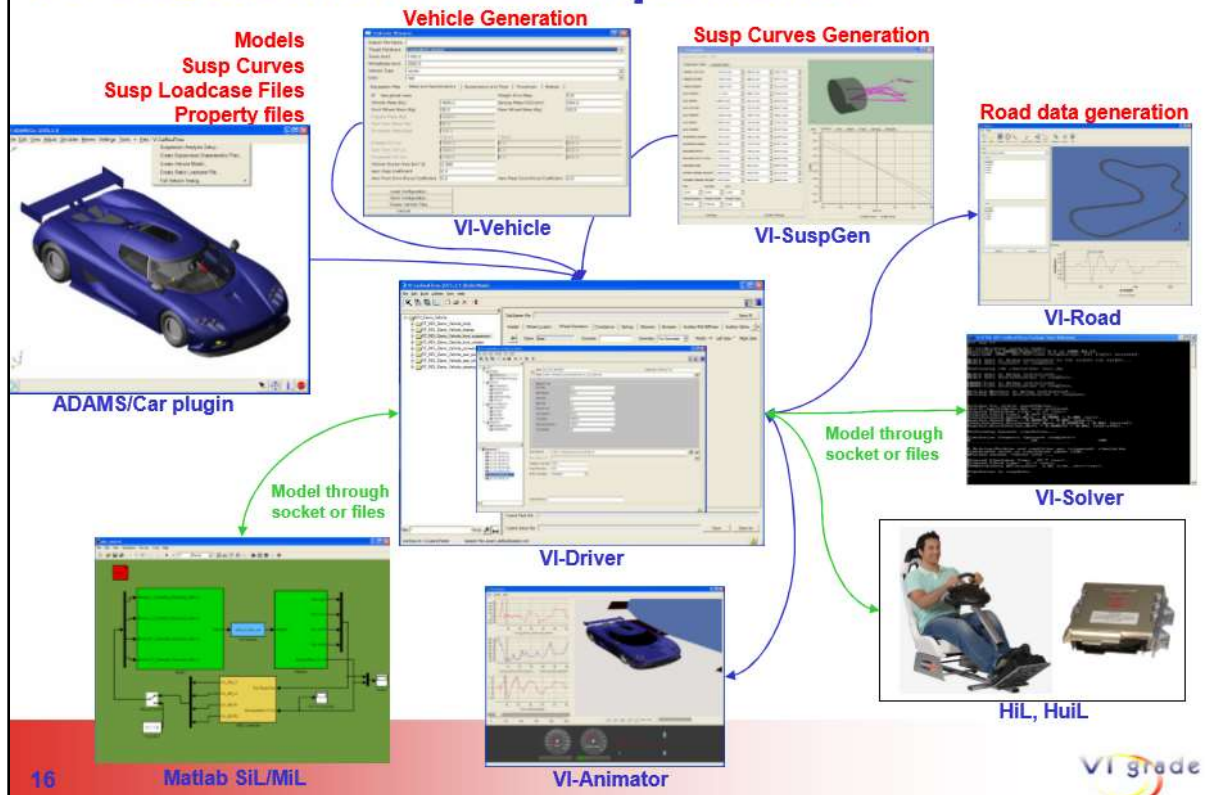
Plug-ins spécifiques

VI-CarRealTime

Product Strategy



VI-CarRealTime Components



VI-CarRealTime – It's what's inside that counts

VI-grade is committed to create an ecosystem in which one single vehicle model can be used from concept to sign-off

No data loss

Consistent model throughout the entire development cycle
(offline simulations, SIL, HIL and DIL)

One vehicle database to maintain

Interfaces with other tools

VI-CarRealTime is a real-time capable environment which provides vehicle model, driver, road and other accessories

Through VI-CarRealTime we provide openness, interfaces, processes and real-time computation

The Real-time vehicle model is the element that enables full vehicle simulation



VI-CarRealTime

Driver-in-the-loop - DIL

Driver-in-the-loop is the new way of developing vehicles and active control systems. Driving Simulators are making it possible to frontload activities in the development cycle when prototypes are not yet available.

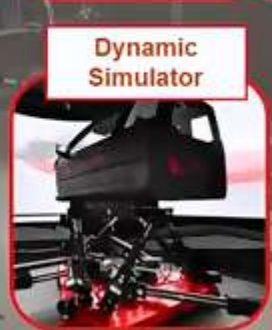
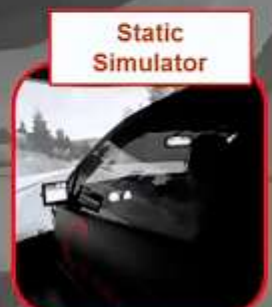
SIL and HIL applications are meeting each other when a driving simulator is used in the vehicle development process.

For DIL applications the vehicle model needs to be:

Robust (no crashes, also in highly non linear situations)

Predictive (Long driving sessions must be possible with no interruption)

Easy to modify (vehicle parameters to be modified easily)



Driver-in-the-loop activities at VI-grade

Static Simulator



Fully upgradable to Dynamic simulator

Common Software
Common Hardware

Driver-in-Motion (DiM)



Award Winning Motion Platform 2014
Development Tool of the Year, Vehicle Dynamics International



VI-DriveSim

DiM – State of the Motion Platform

- Patented 9-DOF system mimics tire dynamics and chassis dynamics separately
- Up to 50Hz content reproduction with motion
- Advanced motion cueing based on a model of the inner ear, not just filtering
- Turn Key solution provider to ensure out-of-the-box performance





Bridging the gap between physical testing and simulation

Modeling accurate road models from laser scan



Measure real tyres, and use the data in an advanced tyre model



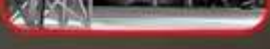
Import K&C data directly into a real-time vehicle model



Identify EPS parameters using experimental measures



Exchanging real-time vehicle model with suppliers



Measuring real sound samples and using them on a simulator



Simulating dangerous maneuvers in a virtual world



Driving your favorite test tracks on a driving simulator

All this means Bridging the Gap Between physical testing and simulation

VI développe avec Ansible Motion un nouveau type de plateforme :

VI-Simulator
Innovative Driving Simulator Platform

DESKSIDE!

PATENT PENDING

	VI-AM	Equivalent Hexapod
Base area	1	2
Volume	1	4
Power Consumption	1	2
Performance(stroke)	1	1
Performance(rate)	1	1
Weight	1	3

Comparison of VI-Simulator with an equivalent hexapod with the same active workspace

25.9.1 RELEASES

VI-Car 18.2 (07/2018)

- New variants of PressManeuver slalom event
- Drum brake model
- openCRG and advanced steering support on dSPACE SCALEXIO
- Material ID output for user defined tires
- Circular buffer option for VI-DriveSim datalogger
- Support for Adams 2017.2
- Support for TameTire 4.0
- Support for SimulationWorkbench 2017.3 and 2017.1
- Support for Matlab 2017b
- Support for SCANeR 1.7r37

25.9.2 VI-SPORTSCAR

KTM-SPORTCAR SELECTS VI-SPORTSCAR TO OPTIMIZE VEHICLE DYNAMICS AND REDUCE LAPTIME OF RACE CARS (06/2015)

VI-SportsCar will be used on the KTM X-Bow vehicle to carefully analyze vehicle dynamics and to reduce lap time by means of the sophisticated VI-grade driver controller: based on the database of the actual X-Bow, KTM will derive new models to be used either on race tracks or on roads. The software will be used for vehicle dynamics as well as

to evaluate the loads on different relevant points of the car as - together with CFD software – to perform vehicle optimization on race tracks.

25.9.3 VI-CAR REAL TIME

Information from <https://webthesis.biblio.polito.it/10615/1/tesi.pdf>

25.9.3.1 BRAKING SYSTEM

The brake model includes the following parameters:

- `master_cylinder_pressure_gain`: is the scalar relating the driver brake demand to master cylinder pressure;
- `mu (front/rear)`: friction coefficient;
- `effective_piston_radius (front/rear)`: radius for applying friction force;
- `piston_area (front/rear)`;
- `lockup_natural_frequency (front/rear)`: the brake model includes a 1DOF spring-damper system to model the wheel lockup; the parameter sets system natural frequency;
- `lockup_damping_ratio (front/rear)`: the parameter sets lockup model damping.
- `lockup_speed (front/rear)`: the parameter sets the lockup speed.

25.9.3.2 ROAD DATA FILE

```
flat.rdf - Blocco note
File Modifica Formato Visualizza ?
$--MDI_HEADER
[MDI_HEADER]
FILE_TYPE = 'RDF'
FILE_VERSION = 12
FILE_FORMAT = 'ASCII'
$--UNITS
[UNITS]
LENGTH = 'METER'
ANGLE = 'RADIAN'
FORCE = 'NEWTON'
MASS = 'KILOGRAM'
TIME = 'SECOND'
$--MODEL
[MODEL]
METHOD = 'USER'
FUNCTION_NAME = 'vitoools::vi_road'
TYPE = 'FLAT'
MODE = 'STANDARD'
FORMAT = 'STANDARD'
$--GLOBAL
[GLOBAL]
ORIGIN_X = 0
ORIGIN_Y = 0
ORIGIN_Z = 0
$--FLAT_GEOMETRY
[FLAT_GEOMETRY]
X_DIMENSION = 160.0
Y_DIMENSION = 80.0
$--FRICTION
[FRICTION]
LEFT_SIDE_MU = 1.0
RIGHT_SIDE_MU = 1.00
```

Figure 2.11 - Road data file

25.10 CALLAS / SCANER

<http://www.car-d.fr/publications.php>

CALLAS : « Couplé A La Limite d'Adhérence Au Sol »

CAR.D Creative Automotive Research & Development

Some steps of the history

- V 1 & 2 (1994-1996) : Thanks to the first customers (ETAS, Renault Sport, Nissan...) for trusting me and thanks for their patience...
- v2.3 : intensive validation with Peugeot 607 and 306,
- v3 : sensitivity check with a « wrong setting »
- v3.1 (1998) = first Real Time
- v4 : CALLAS Motorsport (F3, F3000, BTCC, JTCC F1, Le Mans)
- v4.3 (2002) opening towards external user modules, allowing namely HIL with the ETAS engine test bench
- A real time simulator inside a running car to make real time car model validation and external identification (grip, road profile, ...) research program ARCOS with PSA & INRETS.

La société SECA-CD a été créée par Charles Deutsch dans les années 1960

<https://www.leblogauto.com/2020/05/elle-na-jamais-couru-episode-25-la-cd-grac.html>

Charles Deutsch est l'un des grands artisans des 24 heures du Mans et de l'automobile française des années 30 à la fin des années 60. Né en 1911, Charles Deutsch est ingénieur Polytechnique (promo 1931) et Ponts-et-Chaussées. Dès la sortie de son école d'application, Charles Deutsch s'associe avec René Bonnet qui s'est déjà lancé dans le sport automobile plusieurs années avant. (...)

Les deux hommes se sont alors liés d'amitié et devant la complexité et la cherté des voitures de course de l'époque, ils décident de créer des voitures à partir d'élément de la Citroën Traction Avant. Ainsi naît les automobiles DB (Deutsch-Bonnet), barquettes et monoplaces. Fidèles à Citroën et Panhard, on retrouve des voitures « DB » sur les concentrations d'anciennes voitures de course(...)

Le palmarès sportif de D.B. est assez éloquent. Aux 24 Heures du Mans, les D.B. remportent des victoires à l'indice de performance, une victoire au rendement énergétique et victoires de classe. Leur meilleur classement général sera une 10e place en 1954 (11e en 1956). Deutsch et Bonnet se séparent fin 1961 et chacun va continuer de son côté.

Charles Deutsch lance alors la SECA-CD (Société d'études et de construction automobiles Charles Deutsch). La première tentative aux 24 heures du Mans sera sous la forme d'une Panhard CD Dyna. Deutsch est aérodynamicien et il avait déjà des plans pour une DB HBR 6 qui n'a jamais vu le jour

La société devient ensuite « Société d'Études et de Réalisations Automobiles » (SERA-CD)

En 2007, [Sogecclair rachète SERA-CD](#)

Sogecclair, la société d'ingénierie en haute technologie, vient d'annoncer, conformément à sa stratégie de 'développement sur des clientèles de niches à forte valeur ajoutée', la reprise des activités de Sera-CD.

Celle-ci, 'forte de l'héritage prestigieux de Charles Deutsch, dispose d'un savoir-faire de premier plan en matière de conception de véhicules et de simulation de leur comportement, depuis les véhicules légers jusqu'aux véhicules lourds, en technologie classique ou hybride', explique un communiqué de la société. 'Elle réalise des projets complets pour le compte d'une clientèle fidèle de constructeurs des secteurs civil et défense'.

Sogecclair évoque les 'complémentarités évidentes' qui existent entre ses produits et métiers et ceux de Sera-CD, et permettent de développer des 'synergies fortes'.

La partie 'Études Mécaniques' de Sera-CD rejoindra le pôle 'Ingénierie & Conseil' de Sogecclair, au sein d'une nouvelle filiale, Sera Ingénierie. La partie 'Simulation & Logiciel' rejoindra le pôle Simulation de Sogecclair, au sein de la filiale Oktal SA

25.11 MAPLECAR (MODELICA BASED)

[Meet the MapleCar – A New Topology-Based Simulation Tool in Vehicle Modeling and Control](#) (2017)

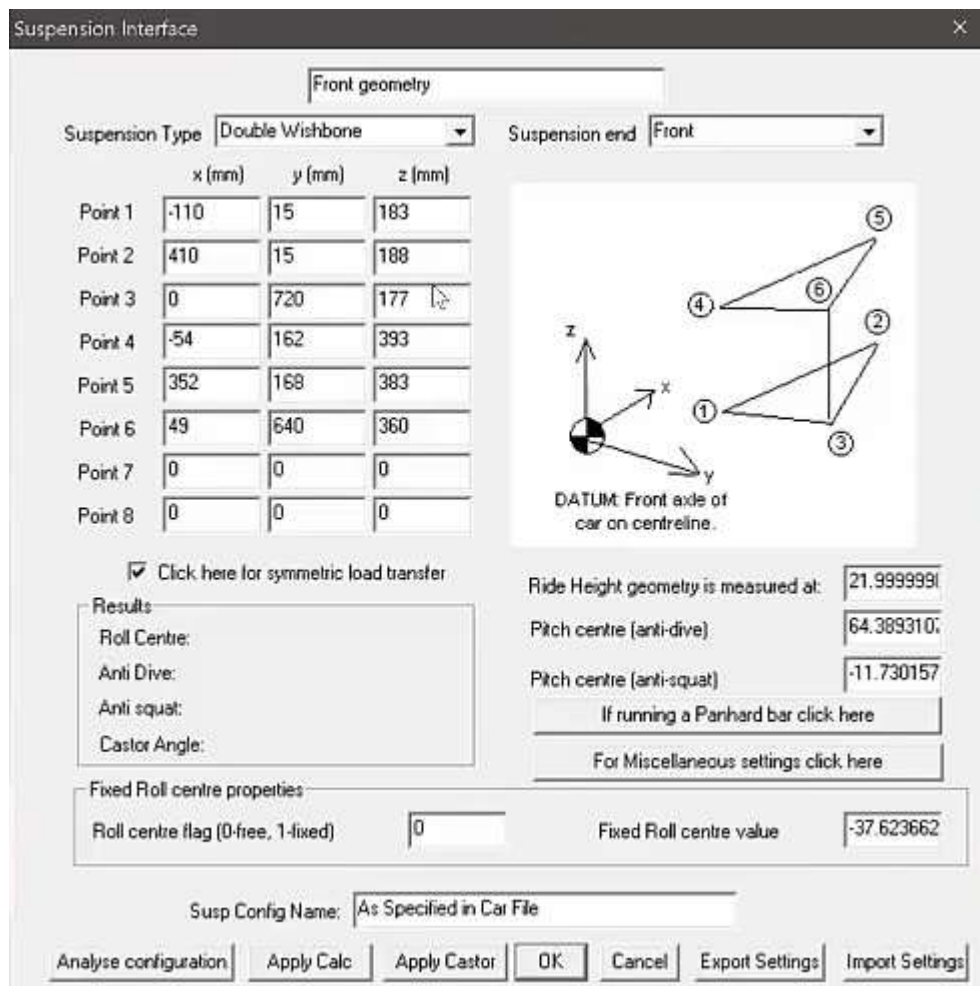
25.12 CHASSISSIM

<http://www.chassissim.com/blog/>

Version online (5\$ per simulation !)

<https://www.chassissim.com/onlinesimulation/index.php>

Suspension Geometry Viewer



25.13 REALTIME TECHNOLOGIES

<https://www.faac.com/realtime-technologies/about/>

Realtime Technologies was founded in 1998. We specialize in multibody vehicle dynamics, and graphical simulation and modeling. We offer simulation software applications, consulting services, custom engineering solutions, and software and hardware development.

We originally focused on providing consulting services in real time operator-in-the-loop simulation. During those formative years, we developed [SimCreator](#), our lead product.

<https://www.faac.com/realtime-technologies/products/simvehicle/>

SimVehicle is high-fidelity, multibody, real-time vehicle dynamics model. It can represent a variety of four-wheel vehicles. Selectable input data files are the key to how SimVehicleLT represents multiple vehicle models.

25.14 DYNACAR

DYNACAR: advanced research full electric vehicle

(PDF) Development and validation of Dynacar RT software, a new integrated solution for design of electric and hybrid vehicles ([researchgate.net](https://www.researchgate.net))

25.15 DYNAV (FREEWARE)

<http://brejaud.pascal.pagesperso-orange.fr/presentation.htm>

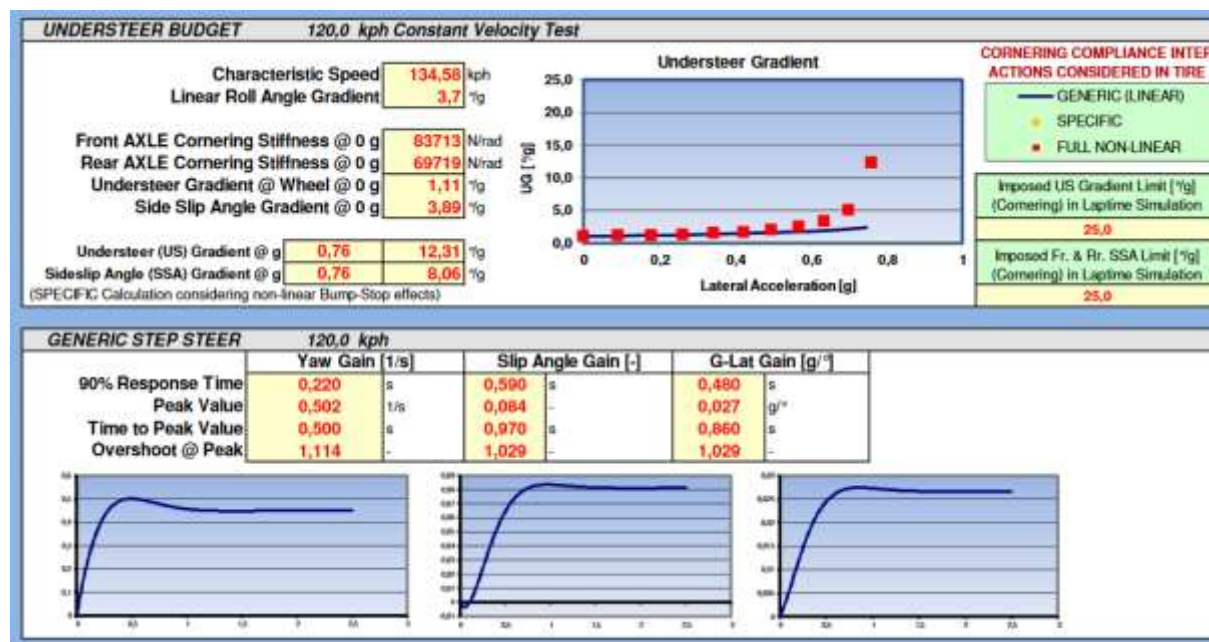
25.16 DYNATUNE

Excel tools

<http://www.dynatune-xl.com/>

<http://www.dynatune-xl.com/features-rh.html>

- [Ride & Handling](#)
- [Suspension Tuning Module](#)



25.17 MORGAN'S

Mentionné dans la thèse de D. Lechner :

https://bibli.ec-lyon.fr/exl-doc/TH_T1892_dlechner.pdf

Les modèles de véhicules réalisés dans le cadre de cette thèse ont été conçus à l'aide du logiciel de modélisation des systèmes mécaniques multicorps MORGAN'S. Je remercie donc pour cette contribution les trois concepteurs de ce logiciel : Jean-Paul MIZZI, chercheur à l'INRETS MMA à Bron jusqu'en Mai 1996, pour sa réflexion théorique, Max DURAZ (INRETS CIR) "le Magicien d'Unix" pour la solidité de ses compétences informatiques et la qualité de ses développements logiciels, et Thierry SERRE, chercheur à l'INRETS LBA à Marseille depuis 1998, après avoir effectué sa thèse en ma compagnie à MA, pour avoir enrichi MORGAN'S par une génération automatique de code C et apporté de nombreuses contributions à notre activité.

On retrouve en 2019 JP Mizzi directeur général adjoint de l'IFSTTAR. En googlant un peu on tombe sur [ça](#) :

Logiciel MORGAN'S Modélisation et simulation des systèmes mécaniques articulés : présentation générale

DURAZ,M , SERRE,T , MIZZI,JP , LECHNER,D

Morgan's est un ensemble de logiciels d'aide à la modélisation et à la simulation des systèmes mécaniques articulés ou SMA, également appelés systèmes mécaniques multi-corps, dont les caractéristiques permettent une modélisation du type corps - liaisons. La version 1.0 de Morgan's décrite ici est composée de 5 logiciels indépendants, les échanges d'informations entre eux étant assurés par des fichiers. Le procédé de calcul du logiciel principal générateur d'équations est basé sur une formulation en géométrie différentielle dans l'algèbre de lie et utilise le calcul formel, il fournit les équations sous forme symbolique. Le logiciel générateur de code produit le code informatique (en langage C) qui assure une réorganisation et une conversion des équations précédentes sous une forme permettant leur résolution. Le code source produit est optimisé de manière à assurer un fonctionnement en temps réel (sur matériel type station de travail) et peut ensuite être intégré au programme de simulation. Ces deux logiciels principaux sont complétés par des logiciels d'aide à la saisie des données géométriques et mécaniques, et à la présentation visuelle des résultats de simulation. La première partie de ce rapport est axée sur la conception et la réalisation du logiciel (rappel de la théorie, éléments sur la réalisation informatique, structures, algorithmes). Le dernier chapitre traite de l'utilisation de Morgan's (organisation générale, spécifications des différents modules). Quelques exemples typiques, dont un du domaine des transports, sont présentés en annexes.

[Les collections de l'INRETS, Outils et Méthodes OM04 - 164p - 1997](#)

ISBN : 2857825005

 Nous contacter

25.18 RACESIM



<http://www.datas-ltd.com/RaceSim.htm>

The company is a result of the collaboration of directors, vehicle dynamicist Steffen Kosuch and Formula One car designer Chris Murphy. D.A.T.A.S. Ltd. was formed when the principle product, RaceSim vehicle simulation

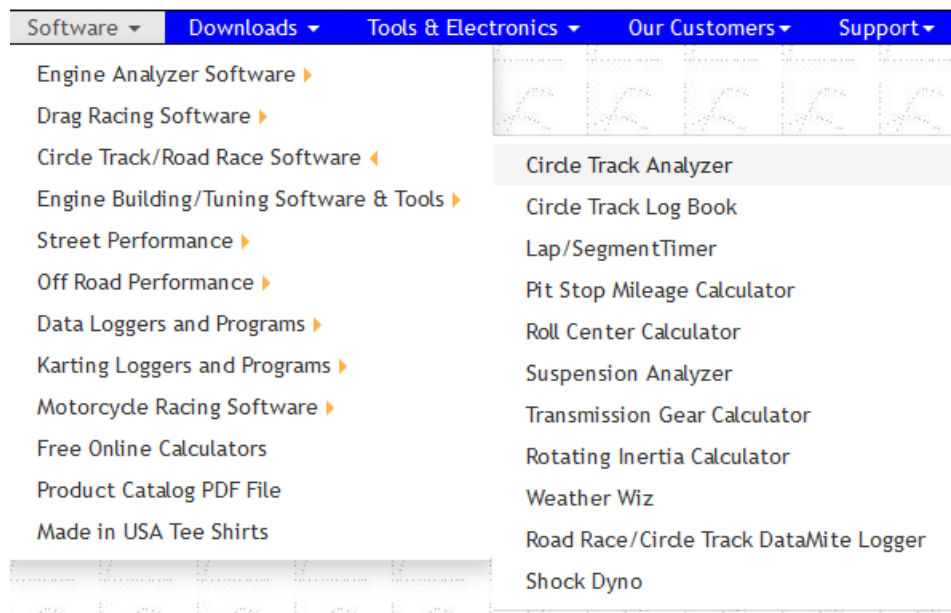
software was considered to be at a sufficiently mature stage of development to market and distribute to the motorsports industry. Following several iterations of vehicle simulation tools, the basis of the current version of **RaceSim** was initiated in 1996. Since this time, **RaceSim** has been the subject of constant development and in-field validation at the highest levels and in many categories of motorsport.

25.19 VDMS (MILLIKEN)

<https://millikenresearch.com/vdms.html>

25.20 PERFORMANCE TRENDS

- [Roll Center Calculator](#)
- [Circle Track Analyzer](#)
- ...



25.21 A VOIR EGALEMENT

Sur vterrain (<http://vterrain.org/Culture/Vehicles/>) :

Road-Vehicle Physics (Dynamics and Simulation)

- [OpenDS](#)
 - A free, EU-funded, open-source driving simulator for R&D in the automotive industry as well as scientific studies.

- Main contributor is the Automotive Group at the German Research Center for Artificial Intelligence (DFKI).
- some existing commercial software:
 - [Havok](#) (merged with Ipion)
 - "Enjoy driving full physically modeled cars!"
 - executable vehicle demos available; no price/licensing costs on their website
 - FastCar™
 - simulates vehicles, with strong claims of "speed, physical accuracy and ease of use"
 - intended to be licensed by game developers for \$5-20k
- The [Newton Game Dynamics](#) engine is closed-source but is portable and has a flexible license. There are examples available of using it for vehicle simulation.

26 DONNEES VEHICULE

26.1 DONNEES MASSES / INERTIES

Measured Vehicle Inertial Parameters-NHTSA's Data Through November 1998

▷ <https://www.sae.org/publications/technical-papers/content/1999-01-1336/>

Ca concerne le marché US, mais on trouve une analyse statistique conséquente sur près de 500 véhicules.

On en tire notamment les données suivantes :

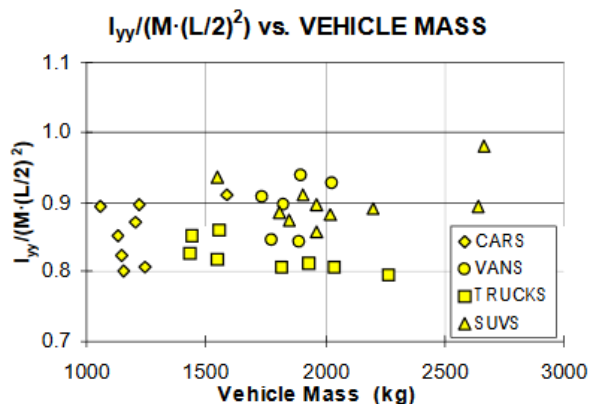


Figure 8: Driver Only Normalized Pitch Inertia

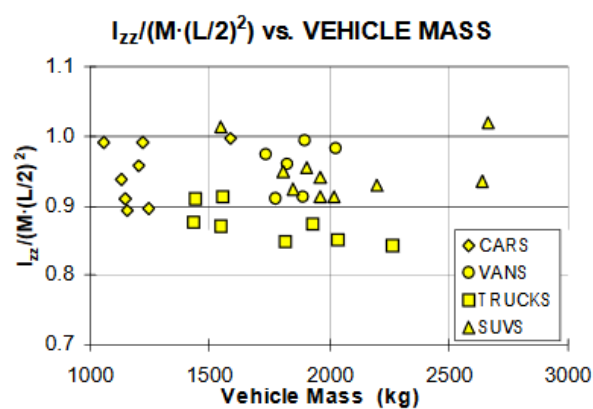


Figure 9: Driver Only Normalized Yaw Inertia

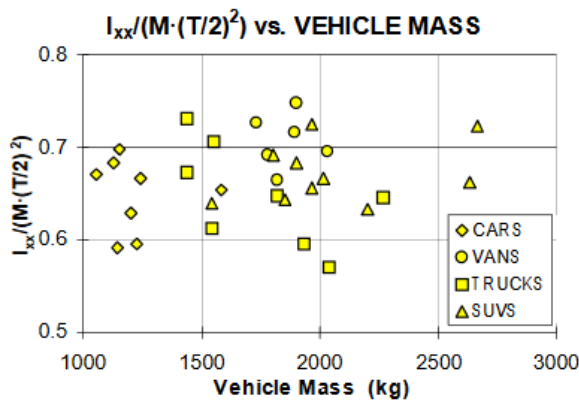


Figure 7: Driver Only Normalized Roll Inertia

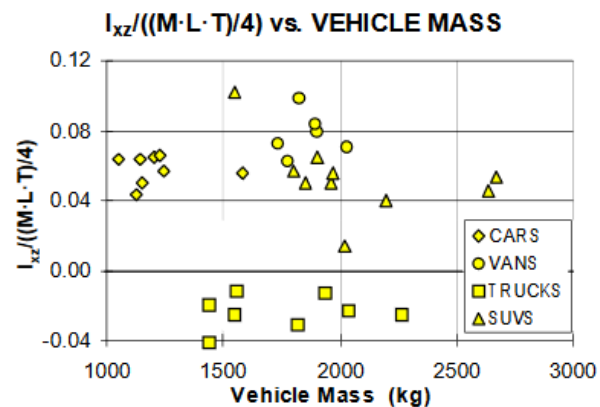


Figure 10: Driver Only Normalized Roll/Yaw Product of Inertia

26.2 RACECARS

As was previously mentioned, the vehicles used in this study are an IMSA GTP car and an Indy Lights Lola car. The parameters specific to these vehicle are listed in Table 1. The sprung mass value includes the sprung mass of the vehicle, the mass of the driver, and the mass of a full tank of gas.

Table 1
Vehicle Parameters

Vehicle Parameters	IMSA GTP	Indy Lights Lola
Sprung Mass	706 kg	503 kg
% Mass Distribution (front/rear)	42 / 58	40 / 60
Wheelbase	2.79 m	2.82 m
Pitch Inertia	718 kg - m ²	468 kg - m ²
Front Unsprung Mass (per axle)	59 kg	103 kg
Rear Unsprung Mass (per axle)	89 kg	152 kg
Front Spring Stiffness (per axle)	460,630 N/m	397,968 N/m
Rear Spring Stiffness (per axle)	538,620 N/m	582,116 N/m
Front Tire Stiffness (per axle)	761,800 N/m	603,814 N/m
Rear Tire Stiffness (per axle)	740,000 N/m	603,814 N/m
Fr. Tire Damping Rate (per axle)	1817 N/(m/s)	1967 N/(m/s)
Rr. Tire Damping Rate (per axle)	1726 N/(m/s)	2206 N/(m/s)
Distance from CG to Front Wing	2.02 m	2.09 m (est.)
Distance from CG to Rear Wing	2.00 m	1.96 m (est.)

*

Tiré de [Use of Simulation to Tune Race Car Dampers](#)

26.3 ÉLASTO-CINÉMATIQUE CATERHAM

	Front Targets	Rear Targets
Caster (deg)	5.0	2.0 to 5.0
Caster trail (mm)	30.0	5.0 to 25.0
KPI (deg)	9.0 to 11.0	<12.0
Hub offset (mm)	50.0 to 60.0	40.0 to 75.0
ground offset (mm)	8.0 to 15.0	-5.0 to 20.0
Toe (deg)	-0.10	0.17
Camber (deg)	-2.00	-1.25
Roll Centre H (mm)	30.0 to 40.0	20.0 to 40.0 > Front
RC migration @3°(mm)	-10.0 to 10.0	5.0 to 15.0 < Front
Anti-Dive (%)	20.0	-
Anti-Squat (%)	-	20.0
Anti-Lift (%)	-	40.0
Bump Steer (deg/m)	-3.0 to -5.0	1.0 to 2.5
Bump Camber (deg/m)	-10.0 to -40.0	-10.0 to -40.0
Bump Caster (deg/m)	< 20.0	Minimise
Wheel Reces. (mm/m)	> 0.0	>15.0
Roll Camber (deg/deg)	0.25 to 0.30	0.35 to 0.40
Roll Steer (deg/deg)	0.04 to 0.075	-0.01 to -0.02
Ackerman (%)	40.0%	-

source https://www.sevener.fr/fichiers_articles/caterhamsuspension.pdf

27 RESSOURCES

27.1 JOURNAUX SCIENTIFIQUES

- International Journal of Vehicle Mechanics and Mobility
- International Journal of Vehicle Systems Modelling and Testing
- Vehicle System Dynamics
- International Journal of Vehicle Design
- Journal of Automobile Engineering
- International Symposium on Advanced Vehicle Control

27.2 BLOGS

Rodrigo Santos <https://racingcardynamics.com/>
(inactif depuis 2015)

Andrea Quintarelli <https://drracing.wordpress.com/>

Sahil Gulati <https://vehicledynamics.weebly.com/>
(inactif depuis 2016)

Abel Arrieta Castro <https://aarrietac.github.io/academic/>
(co-auteur d'un livre avec Georg Rill)

<https://projectdaq.com/> KO en 2021

<https://www.monashmotorsport.com/blog>

CFD, 3D MODELLING, PROGRAMMING, THE LIFE OF A RACE ENGINEER

<https://mathieuhorsky.wordpress.com/>

27.3 CITATIONS

Claude Rouelle (03/2021)

With ISO tests you know that car A is better than car B on one specific criteria. But unless you also do several other tests like K&C, CG and inertia measurements, damper and bushing modeling, tire testing and modeling, 4 or 7 post rigs and for high performance car wind tunnel testing, hacking (bad word but everybody does it) of the ECUs of engine, diff control, ABS, ESP, power steering you do not know WHY car A is better than car B.

Charlie Ping (03/2021)

" DIL is a very interesting engineering challenge, it takes one variable out (driver model) but replaces it with a more accurate, but less consistent real human. There is potential to learn, but also potential to get very lost."

Claude Rouelle (03/2021)

A part of the answer depends on if you design a car around a tire (most often in racing) or a tire for a given car (most often in the passenger car industry)

Greg Locock (<https://www.eng-tips.com/viewthread.cfm?qid=431615>)

For racing the usual advice for a RWD is to use no rear bar, add enough front bar to keep the rear wheels stable out of corners with the power on. The usual advice for FWD is to sell it and buy a RWD.

27.4 LIVRES

27.4.1 COMPIL PERSO GITHUB

<https://github.com/EricCabrol/VehicleDynamics/blob/master/books.md>

27.4.2 LES CLASSIQUES

John C Dixon, "Tires, Suspension and Handling" ,Cambridge University Press, 1991

T. Gillespie, **Fundamentals of Vehicle Dynamics**, 1992, Society of Automotive Engineers (SAE)

W. Milliken & D. Milliken, **Race Car Vehicle Dynamics**, 1995, SAE)

G. Genta."**Motor Vehicle Dynamics. Modeling and Simulation**". World Scientific. 1997.

W. Milliken & D. Milliken, **Chassis Design - Principles and Analysis**, 2002, SAE

R. Bosch. **Automotive Handbook**, 5th edition. 2002. SAE

J.Y. Wong. **Theory of Ground Vehicles**, John Wiley & sons, 2001 (3rd edition).

Heinz Heisler, **Advanced Vehicle Technology**, Butterworth-Heinemann,Oxford,2002

Maurice Olley, **Chassis Design : Principles and Analysis**, SAE, 2002

Rajesh Rajamani, **Vehicle Dynamics and Control**, Springer, 2006

Hans B Pacejka, **Tyre and Vehicle Dynamics**, Delft University, The Netherlands

Reza N Jazar, **Vehicle Dynamics, Theory and Applications**,Springer, 2007

Julian Happien-Smith, **An Introduction to Modern Vehicle Design**,Butterworth-Heinemann, 2002

Rao V Dukkipati and others, **Road Vehicle Dynamics**, SAE, 2008

Georg Rill, **Road Vehicle Dynamics: Fundamentals and Modeling**, 2011 ([google books](#))

Voir aussi :

<https://www.eng-tips.com/faqs.cfm?fid=1327>

R/C Car Handling :

<http://users.telenet.be/elvo/> ou <http://home.scarlet.be/~be067749/58/>

27.4.3 NOUVEAUTÉS

- [Essentials of Vehicle Dynamics](#), Joop P. Pauwelussen (2014)
- [Performance Vehicle Dynamics](#), James Balkwill (2018)
- [Fundamentals of Vehicle Dynamics and Modelling](#), Bruce Minaker (2019)

- [Dynamics and Optimal Control of Road Vehicles](#), D. Limebeer (2019)
- [Vehicle Dynamics and Control - Advanced Methodologies](#), S.Azadi (2021)

27.4.4 DANS QUEL ORDRE LES LIRE ?

1. Minaker
2. Blundell/Harty
3. Pacejka

...

En dernier : Schramm ?

27.4.5 RACE CAR VEHICLE DYNAMICS (MILLIKEN, 1995)

Chapters include:	
1	The Problem Imposed By Racing
2	Tire Behavior
3	Aerodynamic Fundamentals
4	Vehicle Axis Systems
5	Simplified Steady-State Stability and Control
6	Simplified Transient Stability and Control
7	Steady-State Pair Analysis
8	Force-Moment Analysis
9	"g-g" Diagram
10	Race Car Design
11	Testing and Development
12	Chassis Set-up
13	Historical Note on Vehicle Dynamics Development
14	Tire Data Treatment
15	Applied Aerodynamics
16	Ride and Roll Rates
17	Suspension Geometry
18	Wheel Loads
19	Steering Systems
20	Driving and Braking
21	Suspension Springs
22	Dampers
23	Compliances

The book is also well-illustrated with over 450 figures and tables.

27.4.6 THE MULTIBODY SYSTEMS APPROACH TO VEHICLE DYNAMICS (BLUNDELL / HARTY)

The Multibody Systems Approach to Vehicle Dynamics – Michael Blundell, Damian Harty
[\(google books\)](#)

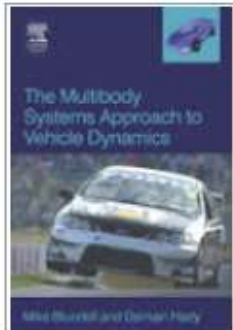
Mike Blundell is Professor of Vehicle Dynamics and Impact, Mechanical & Automotive Engineering, Coventry University, UK. He specializes in vehicle dynamics and safety teaching and research, and has worked with

multibody systems applications in vehicle dynamics in industry and academia, publishing many papers on the topic.

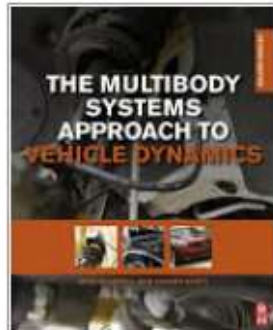
Damian Harty is a Senior Staff Engineer at Polaris Industries based in Minnesota. He was formerly Director of the Vehicle & System Dynamics Group at Coventry University, a Technical Specialist for vehicle dynamics with Prodrive on the Mini WRC, as well as a freelance consultant.

Table des matières

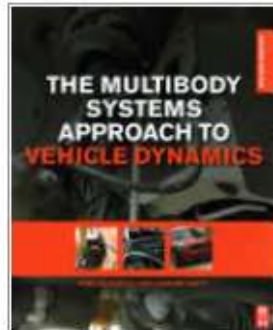
Chapter 1 Introduction	1	Appendix A Vehicle Model System Schematics and Data Sets	631
Chapter 2 Kinematics and Dynamics of Rigid Bodies	27	Appendix B Fortran Tyre Model Subroutines	653
Chapter 3 Multibody Systems Simulation Software	87	Appendix C Glossary of Terms	697
Chapter 4 Modelling and Analysis of Suspension Systems	185	Appendix D Standards for Proving Ground Tests	719
Chapter 5 Tyre Characteristics and Modelling	335	References	721
Chapter 6 Modelling and Assembly of the Full Vehicle	461	Index	729
Chapter 7 Simulation Output and Interpretation	535	Droits d'auteur	
Chapter 8 Active Systems	603		



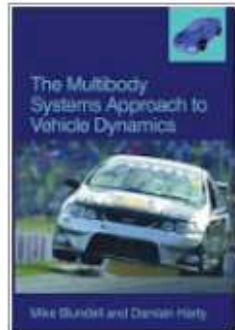
21 août 2004



18 sept. 2014

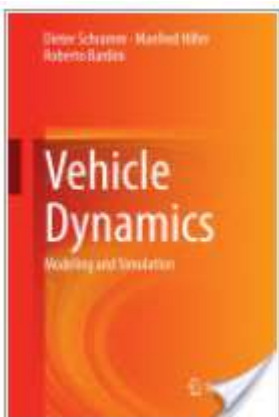


2014



2004

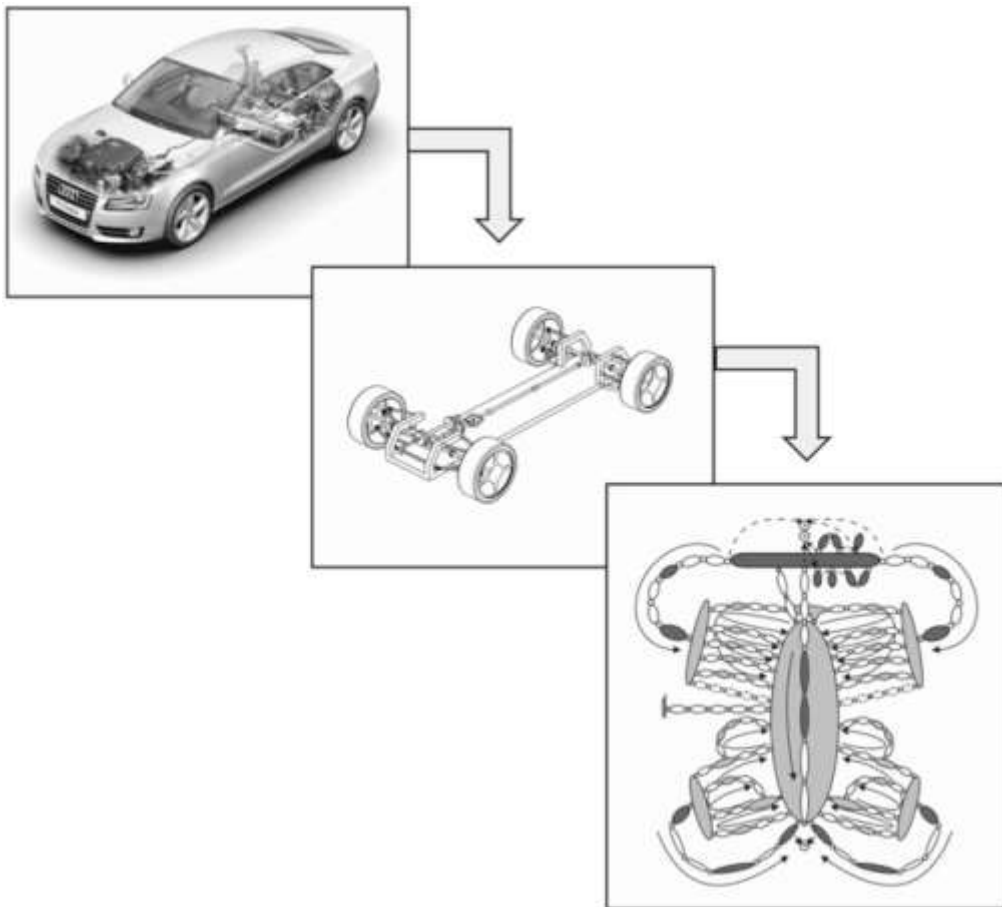
27.4.7 VEHICLE DYNAMICS : MODELING AND SIMULATION (SCHRAMM, 2014)



Début très théorique, avec une longue section sur les fondamentaux en cinématique et cinématique des systèmes multicorps. Doit être utile pour comprendre la notion de chaîne cinématique, mais bon ...

Et en fait ça continue presque jusqu'au bout : le livre passe très rapidement sur la "physique", mais est peut-être utile pour ceux qui veulent se recoder un logiciel de simulation.

Je ne compte plus (30 ? 40 dans le livre ?) les schémas de chaînes cinématiques ... qui ont un petit air de saucisses (ou de crabes) :



27.4.8 VEHICLE DYNAMICS (JAZAR, 2013)

2013

27.4.9 TIRE AND VEHICLE DYNAMICS (PACEJKA, 2012)

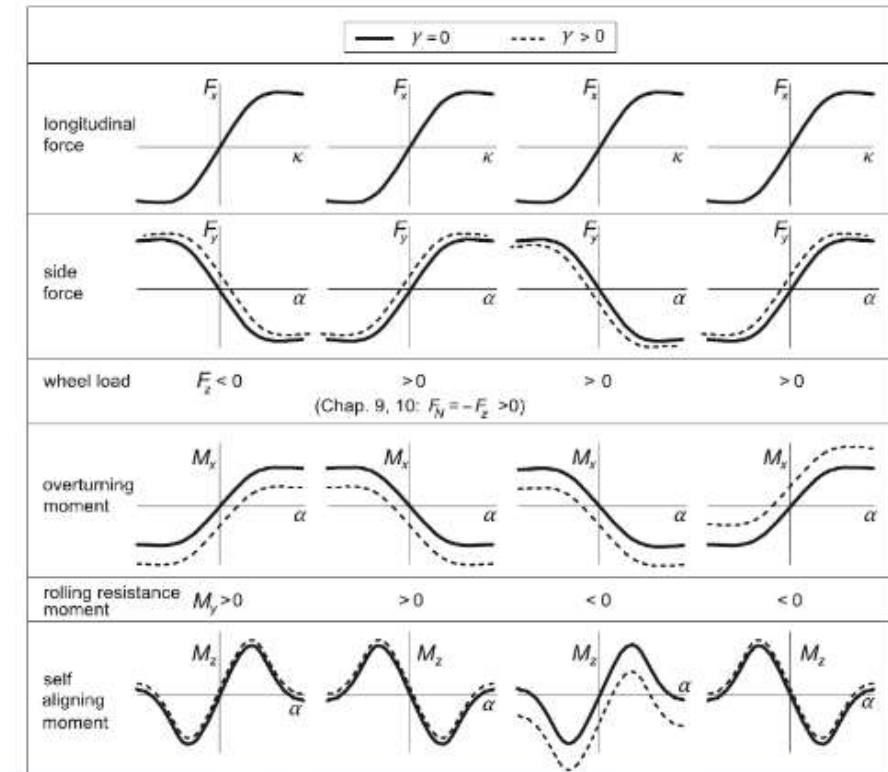
Editions en 2002-2006-2012

Table des matières

Chapter 2 Basic Tire Modeling Considerations	59	Chapter 12 Tire Steady-State and Dynamic Test Facilities	567
Chapter 3 Theory of Steady-State Slip Force and Moment Generation	117	Chapter 13 Outlines of Three Advanced Dynamic Tire Models	577
Chapter 4 Semi-Empirical Tire Models	149	References	593
Chapter 5 Non-Steady-State Cutoff Plane String-Based Tire Model	211	List of Symbols	603
Chapter 6 Theory of the Wheel Shimmie Phenomenon	287	Appendix 1 Sign Conventions for Force and Moment and Wheel Slip	609
Chapter 7 Single-Contact-Point Transient Tire Model	329	Appendix 2 Online Information	611
Chapter 8 Applications of Transient Tire Models	355	Appendix 3 MF-TireMF-Batt Parameters and Estimation Methods	613
Chapter 9 Short Wavelength Intermediate Frequency Tire Model	403	Index	627
10 Dynamic Tire Response to Short Road Irregularities	475	Droits d'auteur	
Chapter 11 Motorcycle Dynamics	505		

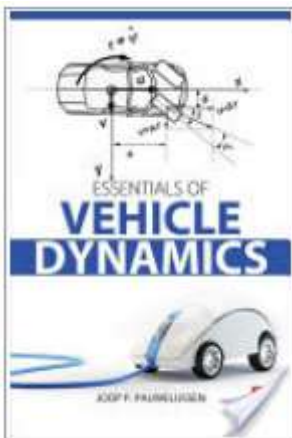
Sign Conventions for Force and Moment and Wheel Slip

$(V_x > 0)$	SAE (Pacejka, this book)	adapted SAE (Pacejka, this book)	ISO (Besselink 2000)
side angle (top view)			
inclination/camber angle (rear view)			
side slip	$\tan \alpha = \frac{V_{sy}}{V_x}$	$\tan \alpha = -\frac{V_{sy}}{V_x}$	$\tan \alpha = \frac{V_{sy}}{V_x}$
longitudinal slip	$\kappa = -\frac{V_{sx}}{V_x}$	$\kappa = -\frac{V_{sx}}{V_x}$	$\kappa = -\frac{V_{sx}}{V_x}$
turn slip	not defined	$\varphi = -\frac{\dot{\psi}}{V}$	not defined
			$\varphi = -\frac{\dot{\psi}}{V}$



27.4.10 ESSENTIALS OF VEHICLE DYNAMICS (PAUWELUSSEN, 2014)

2014



1 Introduction	1	Bode Diagram	275
2 Fundamentals of Tire Behavior	7	Lagrange Equations	283
3 Nonsteady State Tire Behavior	75	Vehicle Data	285
4 Kinematic Steering	111	Empirical Magic: Formula Tire Model	289
5 Vehicle Handling Performance	123	The Power Spectral Density	291
6 The Vehicle-Driver Interface	195	List of Symbols	295
7 Exercises	239	References	299
State Space Format	257	Index	303
System Dynamics	261	Croiss d'auteur	
Root Locus Plot	271		

Dr. Pauwelussen has 20 years' experience in vehicle dynamics and currently teaches vehicle technology with a special interest in tires and driver behavior. He worked as Research Manager for vehicle dynamics at TNO for 11 years prior to his current position, where he managed a number of high profile research projects. At HAN University of Applied Sciences, he established a professional master's automotive program covering structural mechanics, vehicle dynamics and vehicle control. With a background in mathematics and mechanics, his research and teaching are focused on balancing practical engineering with a thorough, mathematical treatment.

Un début assez pédagogique sur le pneu. A suivre ...

27.4.11 THE SCIENCE OF VEHICLE DYNAMICS (GUIGGIANI, 2018)

A noter des figures interactives avec Wolfram CDF

<http://www.dimnp.unipi.it/guiggiani-m/interactive.html>

27.4.12 MINAKER (2019)

[Fundamentals of Vehicle Dynamics and Modelling](#), Bruce Minaker, éd. Wiley

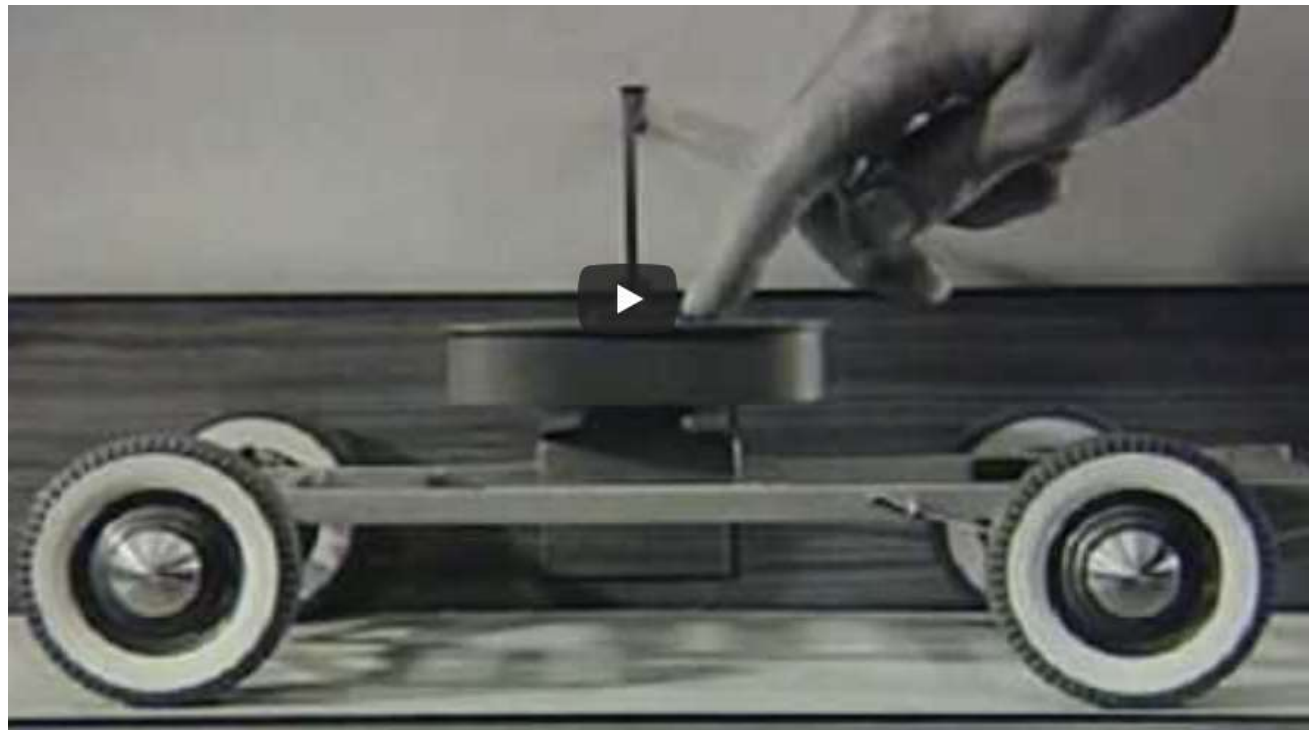
Ma [revue sur github](#)

1 Introduction 1	4 Linear Dynamic Models 31
1.1 Past, present, and future 2	4.1 .e yaw plane model 31
References 4	4.1.1 Steady state analysis 35
2 Tire Modelling 5	4.1.2 Transient analysis 42
2.1 Rolling losses 5	4.1.3 Frequency response 48
2.2 Longitudinal force 7	4.1.4 Time history solution 52
2.3 Lateral force 9	4.2 .e truck and trailer model 53
2.4 Vertical moments 11	4.2.1 Steady state analysis 56
2.5 Normal force 12	4.2.2 Transient analysis 57
References 14	4.3 .e quarter car model 60
3 Longitudinal Dynamics 15	4.3.1 Transient analysis 63
3.1 Acceleration performance 16	4.3.2 Frequency response 68
3.1.1 Engine limited performance 16	4.4 .e bounce-pitch model 73
3.1.2 Tire limited acceleration 21	4.4.1 Transient analysis 75
3.1.3 Grade performance 23	4.4.2 Frequency response 82
3.2 Braking performance 23	References 91
	References 119
6 Multibody Dynamics 121	7 Mathematics 157
6.1 Generating the governing equations 121	7.1 Algebraic equations 157
6.1.1 Preliminary definitions 122	7.1.1 Nonlinear algebraic equations 157
6.2 Definition of coordinates 123	7.1.2 Linear algebraic equations 158
6.3 Kinematic differential equations 125	7.2 Differential equations 159
6.4 Newton-Euler equations 128	7.2.1 Nonlinear differential equations 160
6.4.1 Inertial forces 129	7.2.2 Linear first order ODEs 160
6.4.2 Elastic forces 130	7.2.3 Eigen analysis 161
6.4.3 Linear spring 132	7.2.4 Linear second order ODEs 164
6.5 Constraint equations 137	7.2.5 Frequency response analysis 167
6.5.1 Spherical joint 139	7.3 Differential algebraic equations 172
6.6 State space form 141	7.3.1 Differential equation approach 172
6.7 Example systems 144	7.3.2 Algebraic equation approach 173
6.7.1 Rigid-rider bicycle 144	7.3.3 Linear differential algebraic equations 174
6.7.2 Multibody quarter car 150	A Appendix A 177
References 155	A.1 Algebraic equations 177
	A.2 Differential equations 178
	Index 183

27.5 VIDEOS

Over the Waves - Chevrolet Suspension (1938)

https://www.youtube.com/watch?v=ej7CRAIGXow&feature=emb_logo



27.6 CONFERENCES

27.6.1 IAVSD SYMPOSIUM ON DYNAMICS OF VEHICLES ON ROADS AND TRACKS

2015 (Autriche) : <https://www.crcpress.com/The-Dynamics-of-Vehicles-on-Roads-and-Tracks-...>

2017 (Australie) : <https://www.crcpress.com/Dynamics-of-Vehicles-on-Roads-and-Tracks-Proceedings-...>

2019 (Suède) : <https://iavsd2019.se/>

Workshop Connected and Automated Vehicles

<http://cav2019.engin.umich.edu/>

27.6.2 INTERNATIONAL TYRE COLLOQUIUM

The International Tyre Colloquium has a successful history in discussing the latest progress in the understanding and simulation of tyre-road-vehicle interactions. The first Tyre Colloquium was organised by Prof Pacejka in 1991 (Delft), the second one was in Berlin in 1997, organised by Prof Böhm and Prof Willumeit, and the third one was in Vienna in 2004, organised by Prof Lugner and Prof Plöchl.

Et donc le 4^e a eu lieu en 2015, organisé par l'université du Surrey.

27.6.2.1 2015

<https://www.surrey.ac.uk/mes/news/events/tyre2015//>

27.6.3 VEHICLE DYNAMICS EXPO

2009 http://www.ukintpress-conferences.com/conf/09vdx_conf/

Day 1

RIDE & HANDLING

10.30: Reactive Suspension System - The electronic damping performs for the new Lancia Delta
Fiat Automobiles Group & Magneti Marelli - Philippe Krief,
chassis & vehicle dynamics responsible - engineering &
design -FGA & Dr. Michele Spina, product development
director

10.55: Research on a transparent damper - a deeper look
into the secrets of dampers and shock absorber fluids
Fuchs Europe Schmierstoffe - Arno Wentz, product
management - OEM

11.20: Ride quality objective evaluation of heavy
commercial vehicles
Centro Ricerche Fiat/ IVECO - Massimo Caudano,
vehicle dynamics engineer



11.45: Active yaw systems - re-experience front-
wheel drive with Schnellster and Twinster+
Getrag Driveline Systems - Heinz-Peter Obergünner,
vehicle dynamics engineer



cf §19.6.4



12.10: The customization of vehicle dynamics by means of
innovative human and machine interface
Magneti Marelli - Dr Giordano Greco, control engineer

12.35: Multiplatform instrumentation for ride analysis
UPV - Dr Liborio Bortoni-Anzures, professor



SUSPENSION

13.30: Steel springs or air springs, hydropneumatic or active
– Which suspension-damper system is best?
Continental AG – Dr. Andreas Rohde, director electronic
suspension systems segment

14.00: Effective materials usage and materials
properties utilization in automotive damper design
Delphi Poland SA – Dr Tomasz Pabin, ME expert



14.25: Optimal ride height – an overview of leveling
technologies, focusing on air suspension and Wabco's new
compressor series
WABCO (BU Car Systems) – Helge Westerkamp, sales and
marketing leader

14.50: Suspension system for semi lowfloor bus
Ashok Leyland – VijayKumar Viswanathan, manager -
product development



15.15: New advantages for use of taper wire in
suspension springs for lightweight design and side
load control
Ahle-Federn – Karsten Landwehr, key account
manager



15.40: TGD as topological geometrodynamics
extended to tire-ground dynamics
S2AB – Magnus Roland, chairman & CEO



16.05: Tyre physical integrity and wear monitoring
system
DUFOURNIER Technologies – Arnaud Dufournier,
president and Damien Gerard, sales engineer



16.30: Electrorheologic semi-active damper for racing
motorcycles
Fludicon GmbH – Dr Joachim Funke, director
automotive



27.6.4 VI-GRADE

27.6.4.1 2017

https://www.vi-grade.com/en/about/users_conferences/2017-vi-grade-users-conference_turin-italy/conference_proceedings/

Présentations intéressantes

- [MdynamiX](#)
- [Magnetti](#)
- [3D Mapping](#)
- [Hyundai](#)
- [Danisi : Optimising passive vehicle dynamics for active safety and autonomous driving](#)
- [Politecnico Torino : Objective Evaluation and Design of a Rear Wheel Steering System with the Help of a VI-CarRealTime Vehicle Model and a HIL Setup](#)

- **Piaggio** : [Virtual Engine for an NVH investigation on a motorbike engine](#)
- **Univ. Firenze** : [Firenze Race Team driverless](#)

27.6.4.2 2016

https://www.vi-grade.com/en/about/users_conferences/2016-vi-grade-users-conference_wiesbaden-germany/conference_proceedings/

27.6.4.3 2015

http://www.vi-grade.com/index.php?pagid=2015uc_program

27.7 LIENS

<http://www.ae.gatech.edu/people/ptsiotra/Papers/vsd03.pdf>

Simulations for the use of GPS compensated sensors for vehicle dynamic systems control ([pdf](#))

Parametric multi-body analysis of kart dynamics ([pdf](#))

27.8 SOCIETES SPECIALISEES

<http://www.danisieng.com/simulation/>

<https://optimumg.com/>

Voir par exemple cette interview de Claude Rouelle : <https://www.youtube.com/watch?v=4urKZh5bonU>

3D Mapping

Horiba Mira

Idiada

Leane

Multimatic

MegaRide

Pertechs : <http://www.pertechs.se/>

<http://www.car-d.fr/> (Gilles Schaefer)

27.9 UNIVERSITES

27.9.1 LIEGE

ULg - LTAS - Automotive Engineering Research Group

<http://www.ingveh.ulg.ac.be/>

avec les cours de J. Duysinx, notamment MECA 0525 :

<http://www.ingveh.ulg.ac.be/index.php?page=MECA0525>

27.9.2 CHALMERS

<https://www.chalmers.se/en/departments/m2/research/veas/Pages/Vehicle-Dynamics.aspx>

27.9.3 GEORGIA TECH

Dynamics and Control Systems Laboratory

<http://dcs.gatech.edu/>

27.9.4 UNIV. WATERLOO

Projet Smart Tires: <https://uwaterloo.ca/mechatronic-vehicle-systems-lab/research/smart-tires>

https://www.researchgate.net/profile/Yanjun_Huang

Alireza Kasaiezadeh ([google scholar](#))

<https://uwaterloo.ca/motion-research-group/chuan-hu>

<https://aanddtech.com/university-of-waterloo-vms/>

Naser Mehrabi

	Vehicle Dynamics Controls Engineer General Motors août 2018 – Aujourd’hui - 6 mois Canada
	University of Washington 1 an 3 mois
	Postdoctoral Researcher juin 2017 – août 2018 - 1 an 3 mois Seattle, Washington
	Course Facilitator janv. 2018 – mars 2018 - 3 mois Greater Seattle Area [Co-Instructor] Human Engineering Seminar (ME 520 F)
	Course Description: Robotic and rehabilitation technologies
	University of Waterloo 6 ans 10 mois
	Postdoctoral Fellow nov. 2014 – juin 2017 - 2 ans 8 mois Canada
	*Significantly contributed to writing of an OCE grant proposal (amount \$110K) on the controller development for autonomous driving in collaboration with Maplesoft and University of Waterloo

Sa thèse : [Dynamics and Model-Based Control of Electric Power Steering Systems](#)

27.10 THESES

Titre : Optimal Coordination of Chassis Systems for Vehicle Motion Control

Auteur : Moad Kissai

Date : 2019

Lien : <https://www.theses.fr/2019SACLY004>

Titre : Application de la méthode de conception robuste "First design" sur un train avant à carrossage piloté

Auteur : E. Koensgen

Date : 2008

Lien : <https://www.theses.fr/137336837>

Titre : Automatic Generation of Real-Time Simulation Code for Vehicle Dynamics using Linear Graph Theory and Symbolic Computing

Auteur : Kevin Morency

Date : 2007

Lien : <https://uwspace.uwaterloo.ca/bitstream/handle/10012/3002/morencymthesis.pdf;sequence=1>

Titre : Contribution à l'étude et à la validation expérimentale d'observateurs appliqués à la dynamique du véhicule

Auteur : Joanny Stephan

Date : 2004

Lien : <https://www.theses.fr/2004COMP1539>

Titre : Identification des paramètres dynamique d'une voiture

Auteur : Gentiane Venture

Date : 2003

Mots-clés : identification

Lien : <https://tel.archives-ouvertes.fr/tel-00696169/document>

Titre : Analyse du comportement dynamique des véhicules routiers légers : développement d'une méthodologie appliquée à la sécurité primaire

Auteur : Daniel Lechner

Date : 2002

Lien : <https://www.theses.fr/2002ECDL0016>

Titre : Sur la modélisation et la commande de suspension de véhicules automobiles

Auteur : Damien Sammier

Date : 2001

Mots-clés : véhicules automobiles – suspension active – commande – Hinf – Skyhook – placement de pôles – découplage – rejet de perturbations

Keywords : automotive – active suspension – Hinf control – Skyhook – pole placement – row by row decoupling – disturbance rejection

Lien : <http://tel.archives-ouvertes.fr/tel-00198474>

28 PERSONNALITÉS

28.1 DUGOFF, HOWARD

Howard Dugoff (1936-2020) was a research engineer at the Highway Safety Research Institute (University of Michigan in Ann Arbor) when he wrote a technical report in which a tire model was defined : [Tire performance characteristics affecting vehicle response to steering and braking control inputs](#)

△ **Tire performance characteristics affecting vehicle response to steering and braking control inputs.** Final report - Dugoff, H. – 1969

<https://deepblue.lib.umich.edu/handle/2027.42/1387>

Dugoff, H., Fancher, P., and Segel, L., "An Analysis of Tire Traction Properties and Their Influence on Vehicle Dynamic Performance," SAE Technical Paper 700377, 1970, <https://doi.org/10.4271/700377>.

Dugoff, H., Segel, L., and Ervin, R., "Measurement of Vehicle Response in Severe Braking and Steering Maneuvers," SAE Technical Paper 710080, 1971, <https://doi.org/10.4271/710080>



Fig. 1A - 1967 Ford station wagon



Fig. 1B - 1970 Toyota 2000 GT



Fig. 1C - 1961 Chevrolet Corvair

28.2 GUIGGIANI, MASSIMO (UNIV. PISA)

<http://www.dimnp.unipi.it/guiggiani-m/>

Auteur de "The Science of Vehicle Dynamics"

28.3 JACOBSON, BENGT (UNIV. CHALMERS)

Head of Research Group at Univ. Chalmers

<https://www.chalmers.se/en/staff/Pages/bengt-jacobson.aspx>

28.4 MINAKER, BRUCE (UNIV. WINDSOR)

<http://www.uwindsor.ca/engineering/mame/321/dr-b-minaker>

Minaker B.P. (2012) **On the Development of an Open-Source Vehicle Dynamics Simulation**. In: Su CY., Rakheja S., Liu H. (eds) Intelligent Robotics and Applications. ICIRA 2012. Lecture Notes in Computer Science, vol 7508. Springer, Berlin, Heidelberg

In an effort to alleviate this situation, an open-source vehicle simulator that could be both freely distributed and dissected was sought. A number of open-source codes were identified; the candidates generally fall into one of three categories: those intended for engineering analysis of the motion of general mechanical systems; codes developed specifically for vehicle dynamics; and ‘physics engines’. Of the open-source dynamics codes intended for engineering analysis, two notable examples are MBDyn[5], developed at the Politecnico di Milano, and DynaMechs[6], developed at The Ohio State University. MBDyn is a time domain multibody dynamics solver, with a command line interface and an impressive array of multi-physics capabilities. It is an active project and has an extensive team of developers. DynaMechs is a C++ library of routines similar in intent to MBDyn. However, in contrast to MBDyn, the code appears to have been unmaintained for a number of years.

28.5 OLLEY, MAURICE

<http://alexandre-schyns.e-monsite.com/pages/rolls-royce-of-america/maurice-olley.html>

28.6 PACEJKA, HANS

Klaus J. PLASTERK (1989) **The End of the First Era: A Farewell to Hans Pacejka as Editor-in Chief**, Vehicle System Dynamics, 18:6, 381-382, <http://dx.doi.org/10.1080/00423118908968929>

On July 16 to 18, 1968, the late Professor Herbert K. Sachs organized the First International Conference on Vehicle Mechanics at Wayne State University in Detroit. In the course of the publication of the Proceedings of this conference, we discussed the desirability of creating a new international journal in this field. Was there a need for a new journal, and if so, what should be its precise scope? It should not duplicate any existing journal, it should be of value for the readers, and it should be viable. When Professor Sachs visited the Netherlands, we discussed our plans with the nestor of Vehicle Mechanics at the Delft University of Technology, Professor H.C.A. van Eldik Thieme. He welcomed our plans, and suggested that we should ask Dr. Ir. Hans Pacejka, at that time Associate Professor, to serve on the Board of Editors. The result was the journal VEHICLE SYSTEM DYNAMICS - International Journal of Vehicle Mechanics and Mobility. As stated in the first issue, the journal was established for the purpose of serving

the scientific community ... by publishing research papers on theoretical and applied mechanics which carry strong implications of their usefulness in the study of vehicular motion. The journal was created in order to facilitate the process of communication between the ever-growing number of engineering scientists and thereby further the development of the transport industry in general. It should serve as a forum for the researcher for the presentation of his ideas and skills in the solution of complex vehicle systems problems.

The first issue was published in May 1972, containing articles by Kailish C. Kapur, P. Lugner and Hans B. Pacejka, with Herbert K. Sachs as the Editor-in-Chief and Hans Pacejka as Associate Editor. That was the beginning of a very close and agreeable cooperation between Hans Pacejka and myself in the publication of the journal. During the first years, Professor Sachs worked actively in the acquisition and reviewing of articles, leaving most of the practical work to Pacejka. He was soon realistic enough to see that Hans Pacejka did most of the job, and suggested that Hans should become an Editor-in-Chief besides himself. This was effected with the publication of Volume 3 in 1973. After the untimely death of Professor Sachs, J. Karl Hedrick became his successor from Volume 17 (1988) onward. Hans Pacejka's doctoral thesis (1966) dealt with 'The Wheel Shimmy Problem.' His main activity concerns the pneumatic tire in relation with vehicle dynamics, and he contributed many important publications on that theme: in periodicals, in conference and symposia proceedings, in chapters in edited books, and last but not least as organizer of scientific conferences. He also was the Secretary-General - and driving force - of the International Association for Vehicle System Dynamics until last September (now succeeded by Robin Sharp). He deserves our gratitude for these activities, which has recently been acknowledged by the fact that the University of Stockholm made him a doctor honoris causa. After 18 years of activity as Editor of our journal, Hans Pacejka has expressed the wish to retire as Editor-in-Chief of the journal and to hand over his task to Peter Lugner. Was it a coincidence that they both published an article in the very first issue, or was that Professor Sachs's experienced foresight? Whatever it was, we regard it, after 18 successful years, as a good omen for the continuation of the journal.

29 REFERENCES

- Aubouet, S. (2010). *Semi-active SOBEN suspensions modeling and control*. Thèse de doctorat.
- Basset, M. (s.d.). *Problématique de l'identification de la liaison véhicule-sol*. Récupéré sur <http://jnrr05.irisa.fr/document/jnrr-010-01-basset.pdf>
- Bennett, L. (2012). *Ride and handling assessment of vehicles using four-post rig testing and simulation*. PhD, Oxford Brookes University. Récupéré sur <https://radar.brookes.ac.uk/radar/file/7fc3dce7-8da4-4362-a5dc-df16a19c1683/1/bennett2012ride.pdf>
- Besselink, I. J. (2010). *An improved Magic Formula/Swift tyre model that can handle inflation*. Récupéré sur <http://www.mate.tue.nl/mate/pdfs/12478.pdf>
- Canudas-de-Wit, C. (2002). *Dynamic Friction Models for Road/Tire Longitudinal Interaction*. Récupéré sur <http://dcsli.gatech.edu/papers/vsd02.pdf>
- Crolla, D. (1999). Olley's "Flat Ride" Revisited. *Vehicle System Dynamics*, 762-774. doi:<https://doi.org/10.1080/00423114.1999.12063128>
- Denoual, T. (2012). *Contribution à l'objectivation des prestations dynamiques sur simulateur de conduite*. PhD. Récupéré sur <https://tel.archives-ouvertes.fr/tel-00756682/>
- Eichstetter, M. (2017). *Design of vehicle system dynamics using solution spaces*. doi:<http://dx.doi.org/10.14279/depositonce-7097>
- Groenendijk, M. (2009). *Improving Vehicle Handling Behaviour with Active Toe-control*.
- Hamrouni, E. (2021). *Amélioration des lois de commande de la suspension par la mutualisation des capteurs mis à disposition par les Aides à la Conduite (ADAS)*. Thèse de doctorat. Récupéré sur <https://www.theses.fr/2021BORD0236>
- Hazare, M. (2014). *An integrated systems engineering methodology for design of vehicle handling dynamics*. PhD, Clemson University. Récupéré sur https://tigerprints.clemson.edu/all_dissertations/1451/
- Kiefer, J. (1996). *Modeling of road vehicle lateral dynamics*. Récupéré sur <https://api.semanticscholar.org/CorpusID:106583745>
- Lugner, P. (2019). *Vehicle Dynamics of Modern Passenger Cars*. Springer.
- Milliken, W., & Milliken, D. (1995). *Race Car Vehicle Dynamics*.
- Pauwelussen, J. (2014). *Essentials of Vehicle Dynamics*. Elsevier.
- Reineh, M. (2012). *Physical Modeling and Simulation Analysis of an Advanced Automotive Racing Shock Absorber using the 1D Simulation Tool AMESim*. Récupéré sur <http://liu.diva-portal.org/smash/get/diva2:620275/FULLTEXT01.pdf>
- Rill, G. (2005). *A Modified Implicit Euler Algorithm for Solving Vehicle Dynamic Equations*. Récupéré sur http://www.usp.br/lds/wp-content/uploads/2014/12/Vehicle_Dyn_Rill_06.pdf
- Sathishkumar, P. (2014). *Mathematical modelling and simulation quarter car vehicle suspension*. Récupéré sur https://www.ijirset.com/upload/2014/icets/274_ME513.pdf
- Savaresi, S., Poussot-Vassal, C., Spelta, C., Dugard, L., & Sename, O. (2010). *Semi-Active Suspension Control Design for Vehicles*. Elsevier.

Siemens Driving Dynamics Seminar. (2017). Récupéré sur
<https://community.plm.automation.siemens.com/t5/Event-Collateral/Driving-Dynamics-Seminar/ta-p/435311>

Tavernini, D. (2013). On the optimality of handbrake cornering. doi:10.1109/CDC.2013.6760213

Velenis, E. (2003). *Dynamic Tire Friction Models for Combined Longitudinal and Lateral Vehicle Motion.* Récupéré sur <http://dcsl.gatech.edu/papers/vsd03.pdf>

30 MISC.

30.1 COMPENDIUM CHALMERS

Dans le compendium de Chalmers il est écrit :

In ISO and Figure 1-20, wheel side slip is defined so that it is positive for positive lateral speed. This means that lateral tyre forces on the wheel will be negative for positive side slip. Some would rather want to have positive force for positive side slip. Therefore, one can sometimes see the opposite definition of wheel side slip, as e.g. in (Pacejka, 2005). It is called the "modified ISO" sign convention.

avec l'illustration suivante :

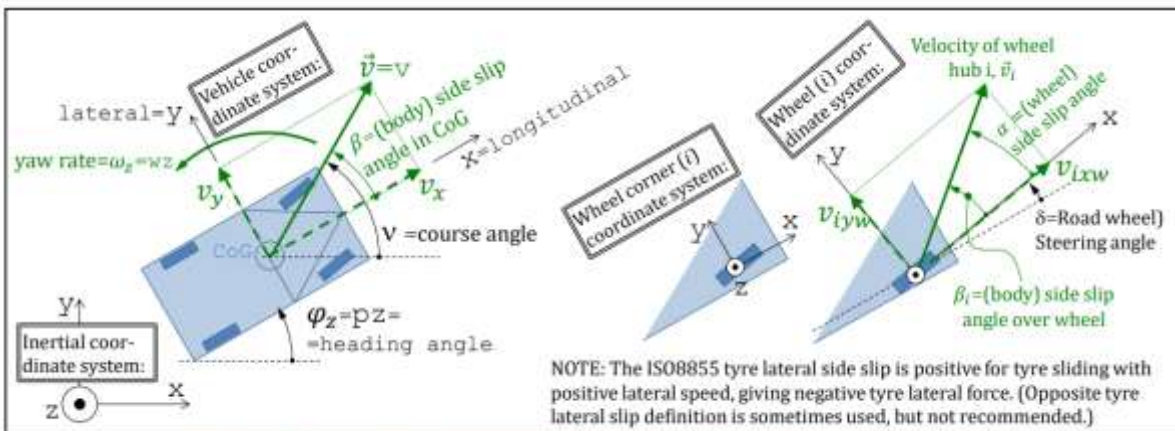


Figure 1-20: Coordinate systems and motion quantities in ground plane.

Je ne comprends pas "This means that lateral tyre forces on the wheel will be negative for positive side slip"

30.2 ACTEURS FRANÇAIS

30.2.1 BASSET, MICHEL

30.2.2 SCHAEFER, GILLES

Fondateur de SERA-CD

Créateur du logiciel CALLAS

30.2.3 LECHNER, DANIEL

30.2.4 M'SIRDI, KOUDER NACER

<https://www.idref.fr/061087823>

<http://nkms.free.fr/>

30.2.5 STEPHANT, JOANNY

<https://sites.google.com/site/joannystephant/>

<https://scholar.google.fr/citations?user=xb9-AOIAAAJ&hl=fr>

30.3 ACTEURS CONTEMPORAINS

30.3.1 DUSINI, LUCA (FIAT, MASERATI)

<https://it.linkedin.com/in/luca-dusini-447b725/>



Maserati
5 ans 7 mois

- **Responsible for vehicle dynamics: testing and simulation**

décembre 2017 – Aujourd’hui • 1 an 6 mois

Modena

- Guidance of the team of Engineers for reaching the target performance in the vehicle dynamics field starting from the beginning of the development until the final delivery for handling, ride, steering feel, braking.
- Sign-off technical reports and presentations to the management.
- Development of the numerical models and validation with the experimental results
- Defining the add-on requirements and vehicle technical specification in order to achieve the target
- Develop new methodologies for improving the prediction of the numerical models and the accuracy of the measurements

- **CAE manager for vehicle dynamics and ride comfort**

novembre 2013 – décembre 2017 • 4 ans 2 mois

Modena Area, Italy

Managing a group of internal and external resources in order to develop the new high performance RWD platform

- Defining the technical specifications of the suspension components, brakes and engine mounts
- Validation of the numerical models with the experimental results
- Defining the add-on on the project in order to achieve the handling and ride-comfort targets
- Technical management of the suppliers, especially the bushing's supplier
- Development from scratch of the methodology for using the simulator tool for the development of the handling performance of the car
- Fast problem solving for the solution of the problems arising during the development using the six sigma approach

30.3.2 GADOLA, MARCO (UNIV. BRESCIA)

<https://orcid.org/0000-0002-5632-590X>

<https://www.linkedin.com/in/marcogadola>



Dept. of Industrial and Mechanical Engineering, University of Brescia

25 ans

Head of Virtual Driving Lab

janv. 2020 – Aujourd’hui · 1 an 3 mois
Brescia, Italy

A VI-grade driving simulator is now active at the University of Brescia. It is dedicated to R&D in the fields of active systems for vehicle dynamics, system integration for IC/hybrid/electric powertrains, and human-vehicle interaction. This is also the very first professional simulator available to engineering students in the whole country.



UniBS driving simulator

Prof @DIMI - Automotive Engineering & Design, Vehicle Dynamics
1996 – Aujourd’hui · 25 ans

Brescia Area, Italy

Head of Automotive Group



Vehicle Dynamics Lab
@DIMI - four poster...



Faculty Advisor

UniBS Motorsport Formula SAE and Motostudent teams

janv. 2013 – Aujourd’hui · 8 ans 3 mois

Brescia Area, Italy



BRX250_Aragon2016_2



BRX250_Aragon2016



Race Engineer

SMP Racing

janv. 2016 – déc. 2016 · 12 mois

2016 FIA WEC - World Endurance Championship

3rd place, 24 Hours of Le Mans 2016, LMP2 class - 7th place overall



#37 BR01 SMP Racing,
Le Mans 2016

30.3.3 GIL GOMEZ, GASPARD (MCLAREN, VOLVO)

Est chez Mathworks depuis 2020

<https://www.linkedin.com/in/phd-gaspar-gil-gomez-2b4140107/>

4 publis à lire sur

<http://kth.diva-portal.org/smash/person.jsf?pid=authority-person%3A32619&dswid=-1149>

https://www.researchgate.net/scientific-contributions/2080240100_Gaspar_L_Gil_Gomez



Senior Technical Account Manager - Automotive

MathWorks - Temps plein

mai 2020 – Aujourd’hui - 5 mois

Gothenburg, Västra Götaland County, Sweden

Shaping the way the automotive industry develops systems and helping it to improve product development processes and workflows, by finding smart solutions, through the use of Technical Computing and Model-Based Design with MATLAB and Simulink.

McLaren Racing

2 ans 2 mois

Acting Project Leader - Simulator Development

janv. 2019 – août 2019 - 8 mois

Woking, United Kingdom

- Planning and development of the simulator environment
 - Ensuring that the simulator is always operational and up-to-date
 - Analysis/improvement of the vehicle model and the cues used to immerse the racing drivers
 - Race support and Simulator-to-Track correlation
- [...voir plus](#)

Simulator Development Engineer

juil. 2017 – janv. 2019 - 1 an 7 mois

Woking



Volvo Car Group

9 ans 4 mois

Senior Analysis Engineer - Vehicle Dynamics Concepts

avr. 2017 – mai 2017 · 2 mois

Gothenburg, Västra Götaland County, Sweden

Industrial PhD Student Vehicle Dynamics

mars 2013 – mars 2017 · 4 ans 1 mois

Gothenburg

This is a PhD thesis at Volvo Car Group (Gothenburg, Sweden) in collaboration with KTH Royal Institute of Technology (Stockholm, Sweden). The project is connected to a FFI project, iCOMSA - Correlation of Objective Measures and Subjective Assessments: efficient vehicle dynamics evaluation and new intelligent concept.... Voir plus



iCOMSA Tests

Function Developer for the Vehicle Dynamics Control Function

août 2011 – févr. 2013 · 1 an 7 mois

Gothenburg, Sweden

- System designing, planning and development of Vehicle Dynamics Control

- Test environments development and testing by simulations and in-vehicle testing

Chassis and Active Safety Hardware in the Loop Simulation Engineer

févr. 2008 – août 2011 · 3 ans 7 mois

Gothenburg, Sweden

- Planning and development of the simulation environment;

- Testing, analysis and evaluation of active safety functions, e.g. "Advance and Roll Stability Control", "City Safety" and "Pedestrian detection with full auto brake"

30.3.4 HAZELHURST JAMES (BENTLEY, LOTUS)

<https://www.linkedin.com/in/james-hazlehurst-9b141948/>



Lead Vehicle Dynamics Engineer

Group Lotus

mars 2019 – Aujourd’hui · 1 an 7 mois

Hethel



Bentley Motors Ltd

8 ans 6 mois

Vehicle Dynamics Engineer

juil. 2012 – mars 2019 · 6 ans 9 mois

Crewe, United Kingdom

Lead Vehicle Dynamics Engineer: New Flying Spur SOP 2019

- Mono-tube Damper, Air Spring, Passive ARB and Bush hardware tuning to meet primary ride, secondary ride and handling targets
- Semi-active Damper, Triple Volume Air Spring, Active Roll Control, Active Centre Differential and Rear Wheel Steering calibration to meet primary ride, secondary ride and handling targets whilst delivering distinct charisma settings for each system
- Collaborative working with Analysis and Objective Test functions to improve digital prototyping capability
- Planning and carrying out vehicle testing at various locations around Europe, including logistics of test vehicles, equipment and personnel

30.3.5 LENZO, BASILIO

Intervenant régulier dans Vehicle Dynamics International

<https://www.shu.ac.uk/about-us/our-people/staff-profiles/basilio-lenzo>

Dr Basilio Lenzo received his MSc in Mechanical Engineering from the University of Pisa (1st cum laude, thesis at Ferrari F1) and Sant'Anna University (1st cum laude, thesis at Ecole Normale Supérieure de Cachan Paris) in 2010. In 2013, he received his PhD in Robotics (1st cum laude) from Sant'Anna University, too.

Basilio joined Sheffield Hallam University in 2016 as a Senior Lecturer in Automotive Engineering with the Materials and Engineering Research Institute and the Centre for Automation and Robotics Research. His current research interests include vehicle dynamics, control, and robotics.

30.3.6 SERRA, LOIC - MERCEDES GP

Head of Vehicle Dynamics at Mercedes GP

<https://www.linkedin.com/in/loic-serra-41819847/>

<http://en.f1i.com/magazine/271296-men-behind-mercedes-design-team.html/6>

Loïc Serra joined Lewis Hamilton and Valtteri Bottas on the podium in Canada. Born in Ivory Coast, the 45 year old engineer has run the Mercedes vehicle dynamics department since 2013.

A graduate from the "École Nationale d'Arts et Métiers de Paris", Serra began his career at Michelin (like his counterpart at Red Bull, Pierre Waché), where he was in charge of tyre-chassis interactions for a decade. In October, 2006 he joined BMW Sauber as head of vehicle performance. Three years later he was promoted to chief dynamic engineer. Ross Brawn was convinced. Sera was brought in four years ago to reinforce the Brackley design office.

McLaren approached him last year but Toto Wolff and Paddy Lowe convinced him to stay.

30.3.7 SYROPOULOS, GEORGIOS (LOTUS, TESLA, FARADAY, PININFARINA)

[Georgios Syropoulos](#)



Chassis Dynamics Manager
Automobili Pininfarina · Temps plein
déc. 2019 – Aujourd’hui · 6 mois
Munich Area, Germany



Vehicle Dynamics Technical Specialist
Faraday Future
juin 2017 – nov. 2019 · 2 ans 6 mois



Vehicle Dynamics
Tesla Motors
mars 2013 – févr. 2017 · 4 ans



Vehicle Dynamics Engineer
Lotus Cars
nov. 2007 – mars 2013 · 5 ans 5 mois
Hethel
Steering Ride & Handling
Test Driving
Competition Car Performance Evaluation
Race Engineering

[...voir plus](#)



Development Engineer
Williams Hybrid Power Limited
avr. 2007 – nov. 2007 · 8 mois
Hingham, Racing Technology Norfolk
Formerly known as Automotive Hybrid Power, participated in the development of the KERS system for Williams F1 car.

30.3.8 TAVERNINI, DAVIDE (UNIV. SURREY)

https://www.researchgate.net/profile/Davide_Tavernini/research

<https://www.linkedin.com/in/davide-tavernini-41b09550/>



University of Surrey

4 ans 5 mois

Lecturer (Assistant Prof) in Advanced Vehicle Engineering

avr. 2018 – Aujourd’hui · 2 ans 2 mois

Guildford, United Kingdom

Research focus activities:

- { Modelling of vehicle systems
- { High and low level vehicle control strategies design
- { Vehicle state estimation
- { Vehicle testing, data acquisition and analysis
- { On- and off-road vehicle dynamics
- { Optimal Control

[...voir plus](#)

Research Fellow in Advanced Vehicle Engineering

janv. 2016 – avr. 2018 · 2 ans 4 mois

Guildford, Regno Unito

Research focus activities:

- { Vehicle systems and subsystems modelling
- { Optimal Control
- { Advanced Control techniques

[...voir plus](#)



SilverStream prototype vehicle completed



SilverStream prototype vehicle completed



Research Fellow in Active Chassis Control for Electric/Hybrid Vehicles

Cranfield University

janv. 2014 – déc. 2015 · 2 ans

Bedford, United Kingdom

Research focus activities:

- { Vehicle systems and subsystems modelling
- { Optimal Control
- { Advanced Control and State Estimation techniques

[...voir plus](#)



Concept_e project vehicle demonstrators



Concept_e project vehicle demonstrator

30.3.9 TSIOTRAS, PANAGIOTIS (GEORGIA TECH.)

Panagiotis Tsiotras

<http://dcsl.gatech.edu/>

- Minimum-Time Travel for a Vehicle with Acceleration Limits: Theoretical Analysis and Receding Horizon Implementation
- Dynamic Friction Models for Road/Tire Longitudinal Interaction
- Dynamic Tire Friction Models for Combined Longitudinal and Lateral Vehicle Motion

<http://www.ae.gatech.edu/people/ptsiotra/Papers/vsd03.pdf>

30.3.10 VELENIS, EFSTATHIOS (CRANFIELD UNIV.)

Voir les publis en §0

<http://www.cranfield.ac.uk/About/People-and-Resources/academic-profiles/satm-ac-profile/dr-efstathios-e-velenis>

Dr Velenis received his PhD in Aerospace Engineering from Georgia Institute of Technology in 2006. His PhD research was honoured with the Georgia Institute of Technology's Luther Long award for the best PhD thesis in the area of Engineering Mechanics.

From 2006 to 2007 he worked as a Postdoctoral Fellow in trajectory optimisation for land vehicles at the Georgia Institute of Technology, and as a visiting researcher at Ford Motor Company in Dearborn, Michigan.

30.4 CHEZ LES CONSTRUCTEURS

30.4.1 PSA

Joaquim Sumarroca



PSA Peugeot Citroën

11 ans 10 mois

Vehicle Dynamics Engineer

avr. 2012 – Aujourd’hui · 6 ans 10 mois
Vélizy

- Vehicle dynamics calculation: ride, handling, active safety, steering...
- Specifying functional requirements for chassis components.
- Chassis pre-setup definition and setup assistance.

Driving Simulation Engineer (Peugeot Sport, 908 of 24h Le Mans)

sept. 2009 – mars 2012 · 2 ans 7 mois
Vélizy

- Adapting a passenger car driving simulator to a motorsport simulator.
- Simulator development.
- Preparation, execution and analysis of simulator tests.

Driving Simulation Engineer

nov. 2007 – sept. 2009 · 1 an 11 mois
Vélizy

- Suppliers validation.
- Simulator development for research projects.
- Integration, reworking and analysis of vehicle dynamics models in the simulator.

Master's Thesis

avr. 2007 – oct. 2007 · 7 mois
Vélizy

Motion cueing algorithm setup of the dynamic driving simulator of PSA Peugeot Citroën R&D department.

30.4.2 LAMBORGHINI

Lorenzo Rinaldi (Head of Vehicle Dynamics)



Automobili Lamborghini S.p.A.

11 ans 3 mois

R&D - Head of Vehicle Dynamics
janv. 2013 – Aujourd’hui · 6 ans 1 mois

Head of Vehicle Dynamics
nov. 2012 – Aujourd’hui · 6 ans 3 mois

Vehicle Dynamics Engineer
nov. 2007 – déc. 2013 · 6 ans 2 mois
R&D Department - Chassis, Suspension and Testing

- Vehicle Dynamics Specialist: car setup, ride & handling test, damper tuning and servo-electric steering system calibration;
- Active Suspension system tuning;
- Virtual Simulation on ACAR & VI-Grade environments;
- Track & Race Engineer Voir moins

Luigi Taraborrelli (Head of Chassis and Vehicle Dynamics)

R&D Head of Chassis and Vehicle Dynamics

janv. 2008 – Aujourd’hui · 11 ans 1 mois

Sant’Agata Bolognese (BO), Italy

I lead the development of Chassis and Vehicle Dynamics for the Lamborghini car’s business.

My responsibilities: Chassis Concept Development, Car Characteristic, Overall vehicle laptime performances, Vehicle Dynamics targets, Handling & ride Characteristic, Suspension elastokinematics, Car Objectivation, Virtual simulation, Software coding and in-vehicle Software parametrization and calibration activities, Functional safety, Product liability.

I steer a unique and phenomenal team of engineers in the Design, Development and Sign-off of: Suspensions components, Rims & Tires, Steering and Brake system, ABS/ESC, Pedal box, Exhaust system, Fuel system, Drive-assistance systems.

We develop Chassis Electronics and calibrate Mechatronic actuators for: semi-active suspensions, active steering and rear-wheel steering, active differentials, TV and TVBB.

Since 2014 we have expanded our responsibility to the electrification of Chassis working on PHEV project.

Since 2015 we have the responsibility and pride for Nurburgring record-breaking laptime of Lamborghini very high performing vehicles: Aventador SV, SVJ, Huracan Performante.

Since 2016 we have the responsibility of dynamic ADAS functions including: Active Cruise Control, Lane keeping, Lane departure warning and Emergency assist.

